Hydrocarbon potential of the Prince Albert Formation, Ecca Group in the main Karoo Basin, South Africa.

By

Haajierah Mosavel

Student number: 2807100

2021

Supervisor: Dr Mimonitu Opuwari

Department of Earth Science

University of the Western Cape

Co-supervisors: Dr Abdi Siad and Dr Douglas Cole

A thesis submitted in fulfilment of the requirements for the degree of

Doctor of Philosophy in Geology in the Department of Earth Sciences, University of the Western Cape

UNIVERSITY of the
WESTERN CAPE

Council for Geoscience

Declaration

I declare that, Hydrocarbon potential of the Prince Albert Formation, Ecca Group in the main Karoo Basin, South Africa, is my own work, that it has not been submitted before for any degree or examination in any other university, and that all the sources I have used or quoted have been indicated and acknowledged by means of complete references.

Haajierah Mosavel Date: August 2021

Outcome of Research

Published journal papers, peer reviewed:

Mosavel, H., Cole, D.I. and Siad, A.M., 2019. Shale gas potential of the Prince Albert Formation: a preliminary study. South African Journal of Geology, 122.4, 541–554.

Mosavel, H. and Cole, D.I., 2019. Lithostratigraphy of the Prince Albert Formation (Ecca Group, Karoo Supergroup). South African Journal of Geology, 122.4, 571–582.

Published conference papers and articles:

Mosavel, H., Cole, D. and Siad, A.M., 2019. Geological Results from the Drilling of Two Deep Percussion Boreholes in the Beaufort West Municipal Area. Council for Geoscience Annual Conference 'Merging maps for an emerging future', 11-12 February 2019, Pretoria, South Africa, p.93

Mosavel, H., Cole, D. and Musetsho, M., 2018. Investigations of deep hydrological targets in the Beaufort West Municipal Commange. Geoclips, 52, 1–2.

Mosavel, H., 2018. Investigating the shale gas potential of the Prince Albert Formation in the southern part of the main Karoo Basin. Geocongress Conference, University of Johannesburg, 18-20 July 2018, South Africa, p. 180.

Mosavel, H., Cole, D. and Nxokwana, N., 2018. Results of a hydrological investigation as part of the Karoo Deep Drilling project in Beaufort West. Geocongress Conference, University of Johannesburg, 18-20 July 2018, South Africa, p.181.

Hydrocarbon potential of the Prince Albert Formation, Ecca Group in the main Karoo Basin, South Africa.

Keywords

Prince Albert Formation

main Karoo Basin

Whitehill Formation

Dwyka Group

Shale

Hydrocarbons

Porosity

Permeability

Acknowledgements

I would like to thank the Almighty who has given me the necessary strength, wisdom and insight to complete this doctoral thesis. I would like to express my sincere gratitude and appreciation to my supervisors, Dr Mimonitu Opuwari, Dr Abdi Siad and Dr Douglas Cole for carefully reading, criticising and correcting all drafts, and making useful suggestions which are integrated into this study to improve its standard. They provided encouragement, enthusiasm, and were my guides when I entered uncharted territory during this study. You willingly shared your knowledge and time, thank you for all your assistance and patience through the years.

I gratefully acknowledge the Council for Geoscience for funding this project and allowing me the opportunity to conduct the technical aspects of this research. I also would like to thank Cimera, the University of Johannesburg and Professor Nic Beukes, for the relevant core data and funds for this research.

My family is my foundation. Grandmother Rukaya, mother Ghyrieya and aunt Tougieda for teaching me the importance of perseverance, self-motivation and hard work. I owe much of my success to you. I am grateful to my three brothers, seeing the confidence you have in me, gave me the strength to become a better role model for you. Furthermore, I wish to thank my husband, Qaabil Dramat for understanding the late nights, stressful moments and words of encouragement. You are my hero.

Abstract

This thesis focusses on the hydrocarbon potential of the Prince Albert Formation in terms of its shale gas potential. Unconventional gas production from hydrocarbon-rich shale formations, known as “shale gas”, is one of the most rapidly expanding trends in onshore oil and gas exploration and exploitation today. In South Africa, the southern portion of the main Karoo Basin is potentially favourable for shale gas accumulation and may become a game changer in the energy production regime of the country. The Prince Albert Formation was selected for research, since previous studies in South Africa have focused on shale from the Whitehill Formation, which together with the underlying Prince Albert Formation, occur within the lower Ecca Group in the main Karoo Basin.

The petrophysical properties and shale gas potential of the Prince Albert Formation was determined using the parameters of mercury porosimetry, total organic carbon (TOC), vitrinite reflectance, Rock-Eval and residual gas measurements. The lithostratigraphy, rock classification, and depositional environment of the Prince Albert Formation, together with the adjacent parts of the overlying Whitehill Formation and underlying Dwyka Group within the southern part of the main Karoo Basin were addressed. Rock types were characterised using X-ray fluorescence (XRF), X-Ray diffraction (XRD) and statistical analysis. Geochemical proxies and stable isotopes ($\delta^{18}O$, $\delta^{13}C$ and $\delta^{15}N$) were used to identify the depositional environment. Additionally, the Dwyka Group, Prince Albert and Whitehill formations were correlated with equivalent Southern Gondwanaland units to understand basin development.

The results of the shale gas study of the Prince Albert Formation showed porosities ranging between 0.08 and 5.6%, permeabilities between 0 and 2.79 micro-Darcy, TOC between 0.2 and 4.9 weight % and vitrinite reflectance values between 3.8 to 4.9%. Rock-Eval analysis

indicated that the kerogen in the shale was Type III and IV and hydrogen indices were less than 65 mg/g. Free or absorbed gas was not detected in the recently drilled boreholes KZF-01 and KWV-01 used in this study. It is probable that the absence of gas is a result of overmaturity due to tectonic duplication in KZF-01 and thermal degassing associated with dolerite intrusions in KWV-01. Although the porosity and TOC values of the Prince Albert Formation shales across the southern part of the main Karoo Basin are comparable with, but at the lower limits of, those of the gas-producing Marcellus shale in the United States (porosities between 1 and 6% and TOC between 1 and 10 weight %), the high vitrinite reflectance values indicate that the shales are overmature with questionable potential for generating dry gas.

A comprehensive rock classification were compiled for the Prince Albert Formation, which consists of shale and minor ferruginous shale ranging between thicknesses of 30 and 168 m based on field work and core descriptions. Mineralogical, geochemical and statistical data, classified collected samples as Fe-shale, phosphatic shale, manganiferous shales, shale, wacke, Fe-sand and litharenite.

In unconventional resources, understanding the depositional environment is important in delineating the depositional process and bottom water conditions. The Prince Albert Formation was interpreted as marine forming under dysoxic to euxinic conditions. $\delta^{13}C$ values range between -17.5 and -23.1 ‰ and $\delta^{15}N$ between 8.5 and 11.1 ‰ reflecting marine conditions. Sediments of the Prince Albert Formation were interpreted as middle to outer continental shelf deposits based on various lithologies identified and XRF data (geochemical proxies).

Compiled literature of the karoo- type basins in Southern Gondwanaland provides a correlation of the Dwyka Group, Prince Albert and Whitehill formations in South Africa. Based

on stratigraphy and radiometric dating, the Dwyka Group, Prince Albert and Whitehill formations have been correlated with lithostratigraphic units in the Falkland Islands, Namibia (Huab, Karasburg and Aranos basins), the Ellsworth Basin of Antarctica and the Sauce Grande and Parana basins of South America. This correlation suggest that the main Karoo foreland system was subjected to very similar tectonic influences present in the other karoo-type basins of Southern Gondwanaland.

In conclusion, results from this research indicate that viable conditions for shale gas might exist within the "sweet spot" areas constrained by formation thickness being > 30 m, relative dolerite intrusion of < 20%, relative total organic carbon content > 4 weight %, and maturity of < 3.5%. It is essential that new exploration boreholes be drilled within the "sweet spot" areas to test whether the lower Ecca Group (Prince Albert and Whitehill formations) has the potential to generate viable shale gas.

Table of Contents

List of figures

List of tables

Chapter 1

Introduction

1.1 Current shale gas research in South Africa

The Council for Geoscience (CGS) has been tasked with conducting a Strategic Environmental Assessment (SEA) in the Karoo by the South African Government. This will assist the South African government with decision-making to establish effective policy, legislation and sustainability conditions under which shale gas development could occur.

The Karoo Deep Drilling project is in response to a growing interest in possible large shale gas resources in the main Karoo Basin. The SEA has several objectives, which focus predominantly on conducting an environmental baseline investigation in the Karoo. This includes projects focussed on geological research and the updating of 1:50 000 scale geological maps, hydrogeological sampling/monitoring and conducting of geophysical investigations. These serve as a preliminary exercise leading and assisting a deep drilling research programme in the Karoo. This deep drilling programme includes drilling of a 4000 m borehole, which will be the first deep borehole drilled since the late 1960's.

The objectives of the CGS deep drilling programme are to determine an environmental baseline, assess the lithologies and the amount of recoverable natural gas in carbonaceous shales, study groundwater dynamics and possible contamination and monitor potential seismic interferences around a deep stratigraphic borehole drilled at a selected pilot site, near Beaufort West (Cole et al., 2016a). It will lead to the collection of new information on the geology of the Ecca Group at depth with the aim of covering various geo-environmental impacts that are of public concern. The drilling site (Fig. 1.1) was selected in the municipal

area east of Beaufort West within “sweet spot areas” defined by both Cole (2014) and Mowzer and Adams (2015).

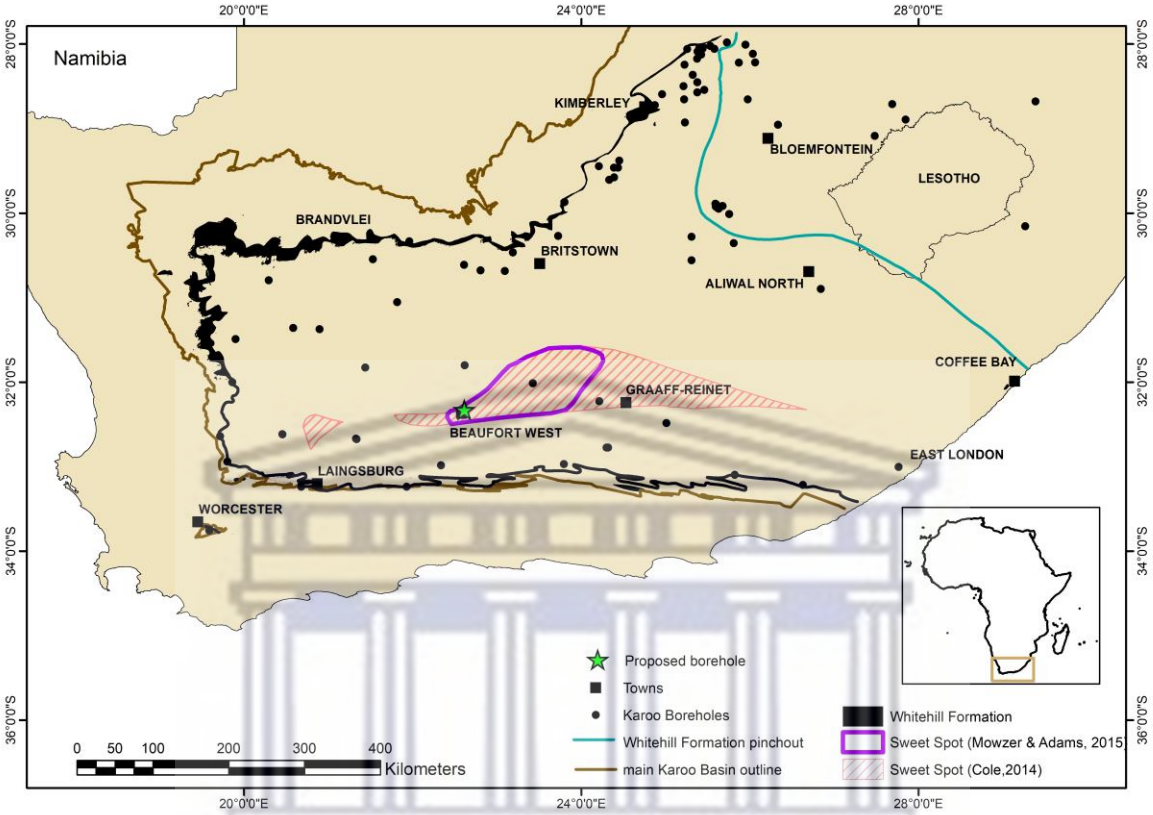

Figure 1.1. Regional and local scale study areas around the proposed 4000 m-deep borehole of the Karoo Deep Drilling project.

The Karoo Deep Drilling project has various tasks at both regional and local scale (Fig. 1.2):

- Geological mapping.
- Seismic studies to locate the depth of the Whitehill Formation.
- Groundwater investigations in a 10 km radius around the planned borehole for baseline record and monitoring programs to identify future changes induced by the deep drilling.
- Seismological monitoring for baseline assessment and changes that might be induced during drilling.

- Shallow ground geophysics: Time Domain Electromagnetics, magnetics, resistivity and seismic refraction surveys.
- Deep ground geophysics: AMT and BMT magnetotellurics to better define the Whitehill Formation at depth and shallow to semi-deep aquifers within the study area.
- High resolution airborne magnetic and radiometric survey over a large area in order to determine regional structures that do not show at surface, i.e. dolerite and tectonic fractures.
- Shallow percussion drilling (150 – 161 m) of five boreholes within the municipal grounds of Beaufort West.
- Deep percussion drilling (516 and 1402 m) of two boreholes in the vicinity of the proposed 4000 m-deep borehole to determine aquifers and monitor groundwater movements over a long period.
- Core drilling of a 4000 m-deep stratigraphic borehole to attain knowledge of the lower Ecca Group shales, the amount and type of natural gas present, and the properties and distribution of deep groundwater.

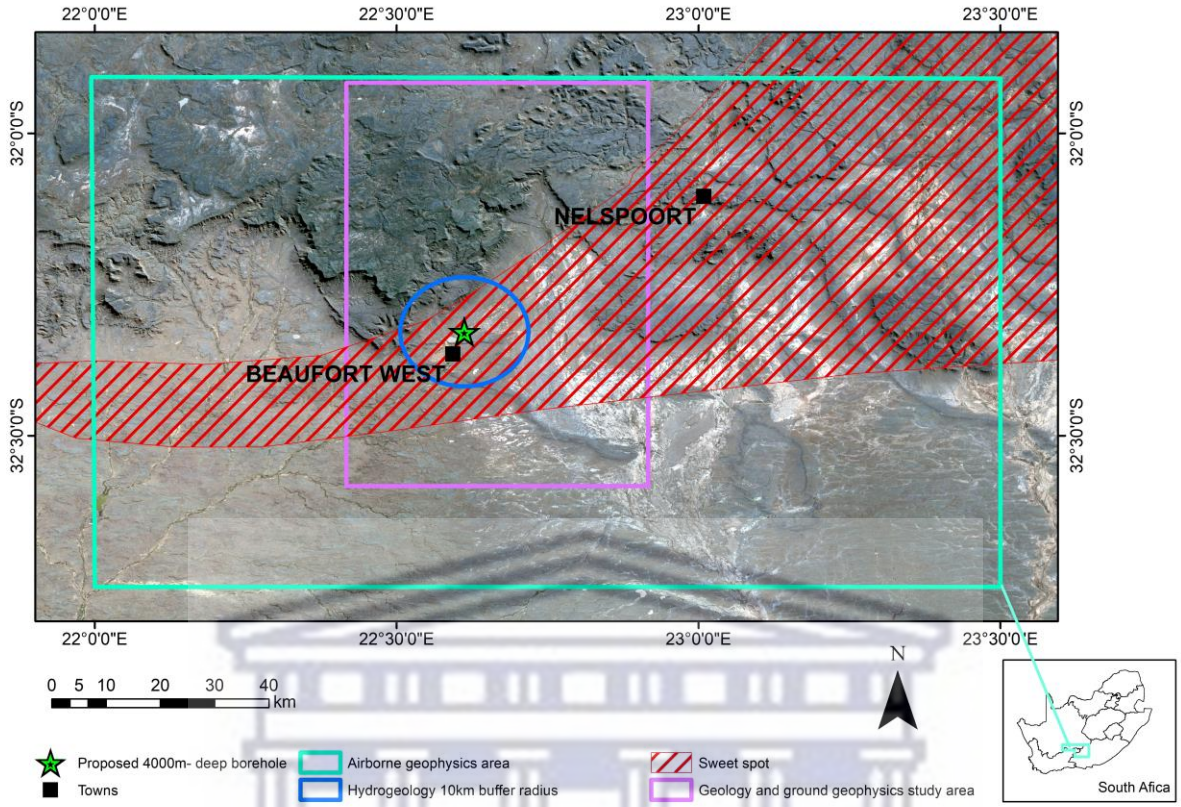

Figure 1.2. Regional and local scale study areas around the proposed 4000 m-deep borehole of the Karoo Deep Drilling project.

The southern portion of the main Karoo basin is known to be potentially favourable for shale gas accumulation and other commodities such as uranium and deep hot waters, all being of strategic importance for the energy demand of South Africa. Varying quantities of gas were obtained by desorbed gas analysis undertaken by Soekor on Ecca Group shale samples retrieved from deep borehole cores in the late 1960s (Rowsell and De Swardt, 1976). Only the lower Ecca Group shales within the dry gas window south of latitude 29°S have comparable total organic carbon (TOC) content to those of producing shales elsewhere in the world. The lower Ecca Group comprises black, organic-rich shale of the Whitehill Formation overlying dark grey shale of the Prince Albert Formation.

A “sweet spot” for shale gas was defined by Cole (2014) and Mowzer and Adams (2015) with the highest gas recovery potential from the carbonaceous Whitehill Formation, using a series

of restrictive parameters namely formation thickness, relative dolerite thickness, relative total organic carbon content, 1500 m-depth contour and maturity .

For shale gas, there is a lack of information regarding the hydrocarbon potential and economic viability of host lithologies in the main Karoo Basin. Presently, quantitative scientifically-based conclusions cannot be drawn on these matters with the current available information. Geological research on the deep Karoo is therefore deemed necessary to be able to competently address these issues by providing the necessary information.

1.2 Significance of Shale gas

Shale gas refers to natural gas trapped within shale formations. It is a combination of flammable hydrocarbons, primarily composed of methane (CH_4), but also containing lesser percentages of butane, ethane, propane, and other gases (Lapidus et al., 2000). The gas is odourless, colourless and when ignited, releases a significant amount of energy (Arthur et al., 2008). Natural gas is environmental friendly in that it burns cleanly and emits much smaller quantities of harmful emissions than either coal or oil (EIA, 1999).

Natural gas is found in rock formations at depth and processed on extraction in order to eliminate other gases, water, sand, and impurities (Arthur et al., 2008). Other hydrocarbon gases, such as butane and propane, are captured and marketed separately which is refined for liquefied petroleum gas from crude oil (Twine et al., 2012). Once the natural gas has been purified, it can be distributed through pipelines to endpoints for residential, commercial, industrial and transportation use. Natural gas is an attractive energy source as it could be used in various economic sectors, to generate residential heat and electricity, and a cleaner fossil fuel to mitigate global warming.

1.3 The role of shale gas in South Africa's energy demand

Coal supplies about 69% of South Africa's primary energy needs, with crude oil, gas, nuclear, hydro, solar and wind which accounts for the remaining 31% of the total energy (Energy Sources, 2020). While the existence of a significant gas resource in the main Karoo Basin would have implications for South Africa's energy supply by reducing national dependence on other fossil fuels. In 2011, the United States Energy Information Administration made a first pass estimate resource of 485 trillion cubic feet (Tcf) of shale gas in the main Karoo Basin that could be technically recoverable using hydraulic fracturing (Kuuskraa et al. 2011). This estimation, based purely on the thickness, the depth and the size of the carbonaceous, organic rich, Whitehill Formation, has since been revised after considering other geological parameters and restricted areas and was brought down to a lower but still very important resource (13 Tcf; Cole, 2014; de Kock et al., 2017). Given that one Tcf is one trillion cubic feet, shale reserves if proven in South Africa could provide heating energy up to 3000 homes, generate 204 billion kilowatt-hours of electricity, or fuel 2 448 000 000 natural gas-powered vehicles for one year (Arthur et al., 2008).

1.4 Scope of this research

This research was undertaken in conjunction with the Karoo Deep Drilling Project of the Council for Geoscience, which focusses on the shale gas potential of the main Karoo Basin. As previously mentioned, South Africa cannot make quantitative, scientifically-based conclusions and recommendations concerning the shale gas potential and its economic value, since critical information is lacking. This research concentrates primarily on the Prince Albert Formation of the Ecca Group, Karoo Supergroup, since most previous studies have focussed

on the overlying, carbonaceous Whitehill Formation, which is a primary target for shale gas (Cole, 2014). In contrast, there has been sparse research into the shale gas potential of the Prince Albert Formation.

1.5 Research aims and objectives

The main Karoo Basin has been identified as a potential resource of shale gas in South Africa. This research forms part of the ongoing research of the main Karoo Basin and as a potential reservoir for shale gas. The following aims and objectives have been undertaken:

1. To assess the shale gas-bearing potential of the Prince Albert Formation of the main Karoo Basin and to compare it against the Barnett and Marcellus shales of the United States of America.
2. To determine the Prince Albert Formation's petrophysical properties as a potential gas reservoir;
3. Characterisation of its depositional environment and rock types. The lithostratigraphic units above and below the Prince Albert Formation, i.e. the Whitehill Formation and the Dwyka Group were also studied in terms of depth, thickness, lithology and depositional environment;
4. Basin development of the main Karoo foreland system of South Africa within the Gondwanaland context. Karoo-type basins across southern Gondwanaland are described and correlated with units equivalent to the Dwyka Group, Prince Albert Formation and Whitehill Formation. This work is substantiated by a comprehensive literature analysis of Karoo-type basins in South America, Namibia, the Falkland Islands and Antarctica.

The aims and objectives mentioned above has direct implications for hydrocarbon exploration. The shale gas potential of the Prince Albert Formation was determined using the following parameters, Rock-Eval, vitrinite reflectance and residual methane gas measurements. These parameters were necessary to understand the generation of hydrocarbons in source rocks. The organic carbon, which gives off hydrocarbons during pyrolysis, is referred to as kerogen (Tissot and Welte, 1984). Hydrocarbon generation only begins after burial of organic- rich sediments to a depth of 2 km (Tissot and Welte, 1984) and in order to preserve organic material from oxidation, a moderate to reducing environment is required. Rock-Eval pyrolysis is used to identify the type and maturity of organic matter and to detect the hydrocarbon potential in sedimentary rocks. Vitrinite reflectance is used as an indicator of thermal maturity in hydrocarbon source rocks. Generally, oil generation is correlated with reflectances of between 0.5 and 1.2% and gas generation between 1.1 and 5% (Tissot and Welte, 1984). Residual gas analysis may represent either gases (methane to pentane) generated in *situ* or those which have migrated.

The petrophysical properties of the Prince Albert Formation is essential to understand the porosity and permeability of a potential hydrocarbon reservoir. Stratigraphical descriptions are important in denoting variations in thicknesses, lithology and depositional age. In unconventional resources, understanding the depositional environment is important in delineating the depositional process and bottom water conditions i.e. successful shale gas plays thus far have been products of anoxic quiet water environments (Arthur et al., 2008). Through the basin development of the main Karoo Basin within the context of Gondwanaland, one can understand the age, stratigraphy and tectonic influences related to the Prince Albert Formation. These factors are important to understand the type of basin (e.g. rift or graben) for hydrocarbon exploration.

The objective is to use the results of this research to formulate a recommendation, which will address the shale gas potential of the Prince Albert Formation and whether exploration or production are viable in South Africa.

1.6 Thesis outline

This thesis comprises of six chapters and structured as follows:

- Chapter one comprises an introduction to the Karoo Deep Drilling project undertaken by the Council for Geoscience, the significance of shale gas, the role of shale gas in South Africa's energy demand as well as the scope and aims of this research.
- Chapter two outlines the literature review of the shale gas potential of the Prince Albert Formation, the geological setting and stratigraphy of the Dwyka and Lower Ecca Groups in the main Karoo Basin, the development of the main Karoo Basin and the description and correlation of units equivalent to the Dwyka Group, Prince Albert and Whitehill formations.
- Chapter three outlines the methodologies employed in this research.
- Chapter four represents the results of the work, as explained below. Section 4.1 presents the rock classification of the various rock types identified in this study as well as their classification after Herron (1988). Section 4.2 deals with the depositional environment of the Prince Albert Formation. Section 4.3 comprises the results of the petrophysical chacterisation by mercury porosimetry. Section 4.4 presents the shale gas potential results of the Prince Albert Formation.
- Chapter five is a discussion and synthesis the results of Chapter four. These data have been used to explain the rock types, depositional environment, shale gas potential

and shale gas shows of the collected samples. Additionally, Chapter five provides a discussion on the correlation of the Dwyka and Lower Ecca Groups of the main Karoo Basin with units across Gondwanaland to understand the development of the main Karoo Basin.

- Chapter six presents the conclusion of this research.

Chapter 2

Literature Review

This chapter discusses the shale gas potential of the Prince Albert Formation, Geological setting of the Cape Supergroup, the Dwyka and Lower Ecca Groups of the Karoo Supergroup, the structural evolution and characterisation of the main Karoo Basin and the description of units equivalent to the Dwyka Group, Prince Albert and Whitehill formations across southern Gondwanaland.

2.1 Review of Shale gas and its occurrence in South Africa

What is shale gas?

Shale is a sedimentary rock comprised predominantly of clay-sized particles. It formed as a result of mud being deposited in a sedimentary environment followed by burial and consolidation over millions of years. The formation of organic-rich shale occurred when organic matter from algae, plants and animals was incorporated into the suspension-settled mud on the basin floor. The organic-rich muds required preservation under anoxic conditions and a carbonaceous shale would have formed with increasing burial pressure and temperature (Geel et al., 2015). The organic material or kerogen generates several types of hydrocarbon with increasing depth and burial (Fig. 2.1). The first stage is the formation of kerogen. As depth, pressure and temperature increases, kerogen converts to crude oil. Once temperatures exceed 120^{o}C, crude oil converts into wet or dry gas depending on depth, pressure, composition and subsurface processes (Tissot and Welte, 1984).

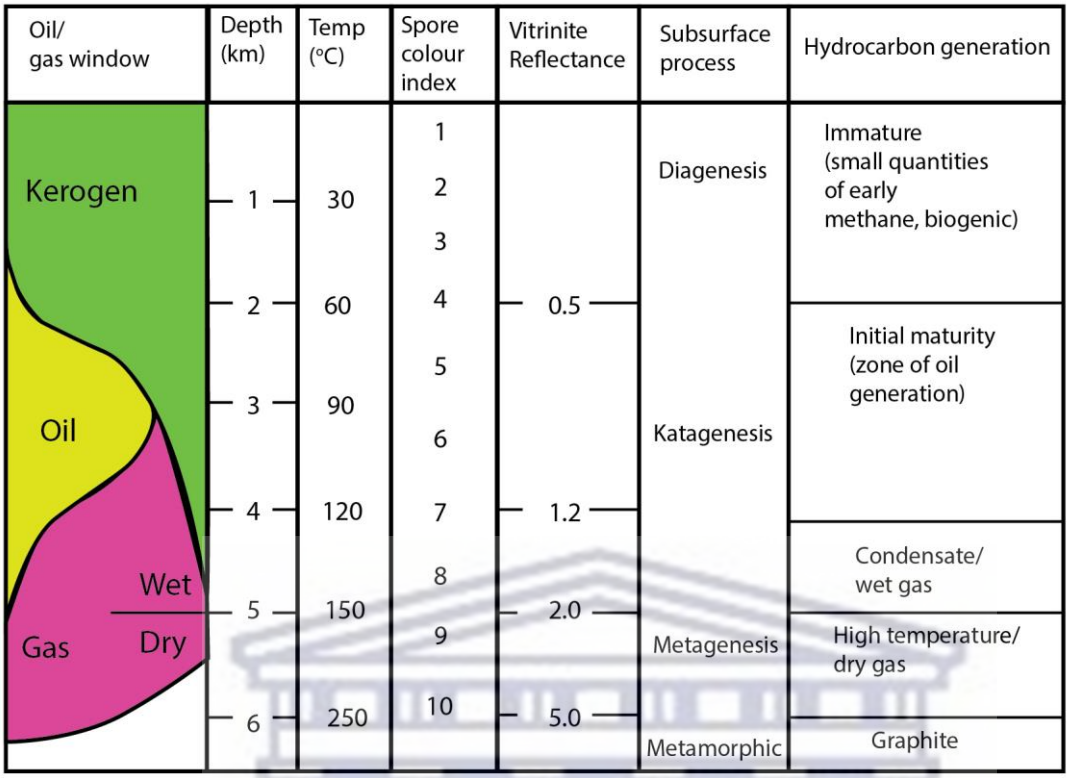

Figure 2.1. Stages of organic matter maturation for hydrocarbons (modified after Tissot and Welte, 1984).

Shale gas falls within the dry gas stage. With a further increase in temperature and pressure, overmaturation and burial metamorphism occur and the organic-rich shale passes into the zone of anchimetamorphism (Smithard et al., 2015). In this zone, kerogen converts to graphite at vitrinite reflectance values exceeding 5, accompanied by a reduction in shale porosity (Laughrey et al., 2011). Shale gas is located predominantly in the pore space of the shale and less commonly within organic material (Mroczkowska- Szerszeń, 2015).

Shale gas is an unconventional source of natural gas and comprises five forms of dry gas, namely methane, butane, ethane, propane and pentane. Only methane, which is highly combustible, is the economic target. Nitrogen and carbon dioxide can also be present (Arthur et al., 2008). Natural gas (methane) is a more eco-friendly source of energy in electricity

power station, in contrast to coal, when used in electricity power stations. Shale gas releases less than 50% carbon dioxide compared with coal, and is more power efficient (Nature, 2009).

In order for a shale unit to host economically-viable quantities of gas, certain properties should be considered, i.e. organic maturity, organic content, porosity, depth of burial, brittleness and unit thickness. Shale gas is extracted by means of hydraulic fracking, which creates fractures in the shale for the release of gas (Fig. 2.2). Hydraulic fracking is normally carried out in a horizontal borehole at depth, with the gas being captured at surface via a vertical borehole (Fig. 2.2). Although shale gas has its advantages to the economy, it can also damage the environment by contaminating shallow groundwater, causing unexpected blowouts, and induced seismicity (Fakir, 2015). Hydraulic fracking is normally carried out at depths greater than 1500 m to avoid shallow tectonic fractures that could provide pathways for the escape of fracking fluids to the surface (Fakir, 2015). Multiple drill casing is installed to avoid contamination of shallow groundwater.

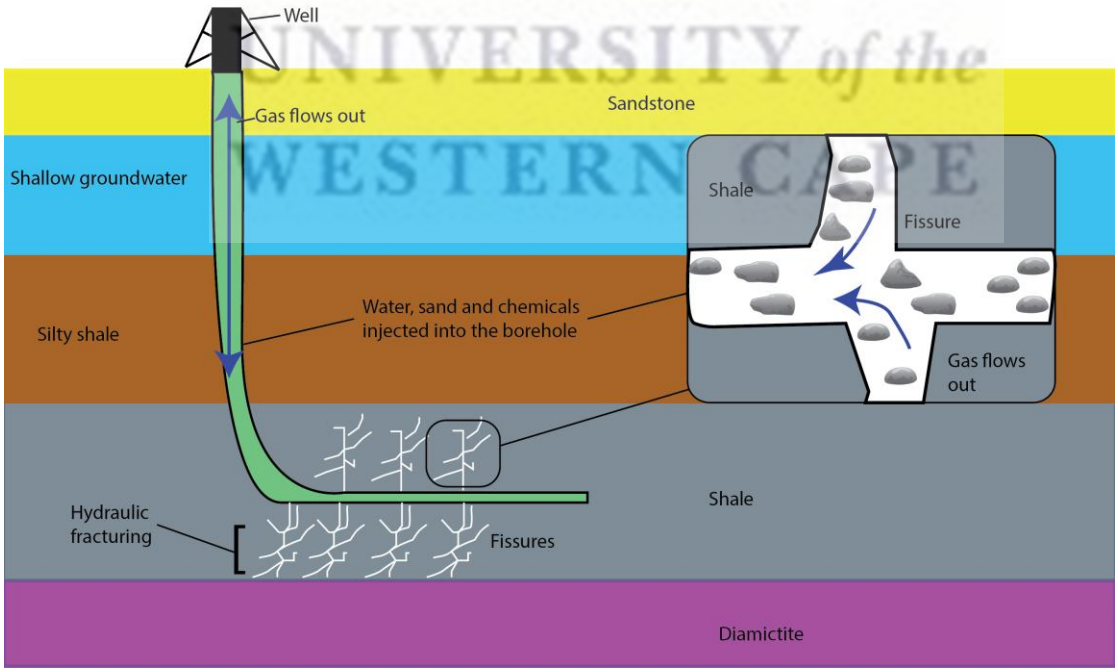

Figure 2.2. Hydraulic fracturing of an impermeable shale layer via horizontal drilling.

2.1.1 The Prince Albert Formation as a target for shale gas

The carbonaceous Whitehill Formation has been of interest for shale gas due to its high total organic carbon content (TOC), thermal maturity, thickness, fine grained lithology and clay content with minimal interest in the underlying Prince Albert Formation (Cole, 2014; Geel et al., 2013; Geel et al., 2015). The United States of America (USA) is well known for its experience in shale gas exploration and hydraulic fracturing, for example the gas-producing, Marcellus and Barnett formation shales. Based upon data from these economically- viable shales, their shale gas potential was compared to that of the Prince Albert Formation (Table 2.1). However, compared with the USA, there is a major contrast in that the shales are unaffected by dolerite intrusions unlike the main Karoo Basin shales. These intrusions are detrimental as they have thermally overmatured the shales. Similarly, the Cape Orogeny has resulted in deep burial and tecto-metamorphism of the shales, with only the Marcellus shales in the USA being similarly affected.

Cole (2014) and Mowzer and Adams (2015) have proposed “sweet spot” areas of shale gas potential for the Prince Albert Formation in the southern part of the main Karoo Basin, based mainly on TOC content and degree of thermal maturity. Also, the strata contain less than 20% dolerite intrusions. This present study of the hydrocarbon potential of the Prince Albert Formation was mostly confined to these “sweet spot” areas.

Table 2.1. Properties of the Prince Albert Formation compared with the Whitehill, Barnett, Fayetteville, Marcellus and Antrim Formation shales in terms of shale gas potential (data from Arthur et al. (2008), Geel et al. (2015), de Kock et al. (2017) and Cole (2014)).

	Prince Albert (main Karoo Basin, S.A)	**Whitehill (main Karoo Basin, S.A)**	**Barnett (Fort Worth Basin, USA)**	**Fayetteville (Arkoma Basin, USA)**	**Marcellus (Appalachian Basin, USA)**	**Antrim (Michigan Basin, USA)**
Thickness range (m)	30 – 320	0.4 – 80	30 – 182	20 – 60	15 – 60	21 – 4
TOC (%)	0.35 – 12.4	0.5 – 14.7	4.5	4 – 9.8	3 – 12	1 – 20
Total porosity (%)	0.53	0.35	4 – 5	2 – 8	10	9
Gas content (scf/ton)	–	–	300 – 350	60 220	60 – 100	40 – 100
Gas resource (Tcf)	72	13 – 49	44	41.6	262	20
Scf= standard cubic feet of gas Tcf= trillions of cubic feet of gas						

2.1.2 Previous studies related to shale gas in South Africa

Investigations of the hydrocarbon potential of the main Karoo Basin have been ongoing since the 1940s, focussing on conventional oil and gas plays and source rocks. In the 1940s, the Geological Survey of South Africa drilled 11 boreholes and concluded that carbonaceous shales of the Whitehill Formation and Bokkeveld Group were potential source rocks for oil, but the low porosities (< 2%) in sandstones of the Ecca and Beaufort Groups mitigated against the presence of oil reservoirs (Haughton et al., 1953).

Soekor (Southern Oil Exploration Corporation (Pty) Ltd) was established in 1965 (Berry, 2018) with a mandate to prove or disprove the existence of economic accumulations of oil or gas in South Africa (Rowsell and De Swardt, 1976). This company drilled some forty-one deep

boreholes in the main Karoo Basin (Rowsell and De Swardt, 1976; Van Vuuren, 1983). Several types of laboratory analyses were made on core samples and percussion chips. These included measurement of organic carbon content, extraction and measurement of the total soluble organic matter, constitution of the extract, C_1-C_5 (methane to pentane) gas analysis, determination of the CR/CT ratio (residual, non-volatile carbon after pyrolysis to total carbon in the kerogen), optical study of organic matter in reflected and transmitted light, clay mineralogy, illite crystallinity (Kübler index), bulk-density, porosity and permeability measurements and vitrinite reflectance determinations. As a result of deep burial of source rocks, together with the effects of dolerite intrusion in the central part of the basin (between latitudes 31°30' and 32°30'S), and diagenesis related to the Cape Fold Belt in the southernmost part of the basin (south of the latitude 32° 30' S), Rowsell and De Swardt (1976) showed that the Ecca Group shales had a low hydrocarbon potential. Minor high-pressure, low-volume gas shows were encountered in most of the wells, predominantly in fractured Ecca Group shale, with the most spectacular show occurring in November 1968 in borehole CR 1/68 located about 50 km east of Graaff-Reinet (Fig. 2.3), which blew 8.8 million cubic feet of methane in one week. This blow out emanated from a gas vug/pocket within the Fort Brown Formation (2532 m to 2612 m depth), although the actual shale of this formation was found to be overmature and in the zone of anchimetamorphism (Rowsell and De Swardt, 1976). Several small conventional oil and gas fields were found in the Mpumalanga, Free State and KwaZulu-Natal provinces (Van Vuuren et al., 1998). Rowsell and De Swardt (1976) delineated a dry gas window from the C1/C5 ratio of Ecca Group shale samples in the area south of latitude 29°S. These authors measured up to 15 ml/kg of desorbed gas from samples of the Whitehill Formation in five deep boreholes namely QU 1/65 (Fraserburg), Vrede 1/66 (Graaff-Reinet), KW 1/67 (Prince Albert), CR 1/68 (Pearston) and OL 1/69 (Calvinia).

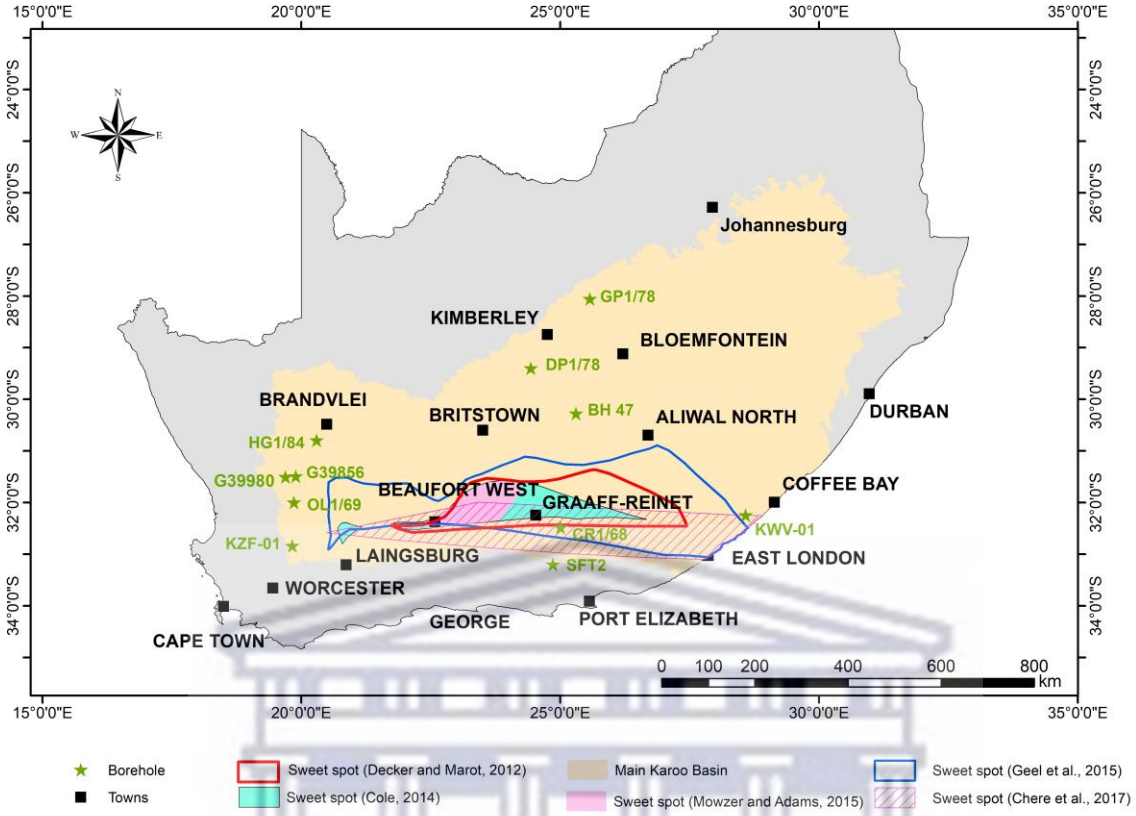

Figure 2.3. "Sweet spots" or potential shale gas areas located in the southern part of the main Karoo Basin and boreholes referred to in the text.

Between 1976 and 1987, the Geological Survey of South Africa and Soekor undertook an investigation of the shale oil potential of the Whitehill Formation, focussing on the area between Hopetown and Hertzogville. Fourteen shallow boreholes were drilled and samples of Ecca Group shales were retrieved for various laboratory analyses (Cole and McLachlan, 1994). Samples were also retrieved from the same stratigraphic unit in five boreholes drilled by the Industrial Development Corporation (IDC), for the same purpose, in the region between Boshof and Hertzogville between 1977 and 1978. Analyses comprised measurement of organic carbon content, Rock-Eval pyrolysis, optical study of organic matter in transmitted light, constitution of organic matter and one measurement of vitrinite reflectance (0.875%) in the Prince Albert Formation (Cole and McLachlan, 1994). The most viable result was

obtained from borehole DP 1/78, 78 km southwest of Kimberley (Fig. 2.3) where a 5.7 m-thick shale interval of the Whitehill Formation yielded an average of 42.7 litres per metric ton of oil (Cole and McLachlan, 1991). This yield was less than the stratigraphically-equivalent Irati Formation in Brazil, which has an average yield of 80 litres per metric ton over 9.7 m (Cole and McLachlan, 1991). No dolerite was present in borehole DP 1/78 and its yield is within the sub-economic category (Cole and McLachlan, 1991). Both Rowsell and De Swardt (1976) and Cole and McLachlan (1991) concluded that the main Karoo Basin has a low economic potential for conventional oil and gas.

More recently, there has been a global interest for the exploitation of unconventional gas resources, i.e. coal bed methane and thermogenic shale gas (Jarvie et al., 2007). In South Africa, interest remained focussed on the Lower Permian Whitehill Formation, which has the highest total organic carbon content. A few studies have shown the impact of dolerite intrusion on shale gas generation and preservation (Aarnes et al., 2011; Smithard et al., 2015; de Kock et al., 2017; Adeniyi et al., 2018). Numerical modelling and field studies by Aarnes et al. (2011), suggest that dolerite sills can generate methane gas by contact metamorphism. However, much of this gas has escaped to the surface via pathways in breccia pipes and hydrothermal vents, examples being boreholes G39980 and G39856 near Calvinia (Fig. 2.3). However, de Kock et al. (2017) and Adeniyi et al. (2018) contradicted these findings from studies made on the core of one borehole, BH 47 near Philippolis (Fig. 2.3), where samples located furthest from a dolerite sill had higher total reflectance measurements, i.e. thermal maturity, than those closer to the sill.

Between 2012 and 2015, three boreholes were drilled partly to investigate the shale gas potential of the Ecca Group, namely SFT2 near Jansenville, KZF-01 near Ceres and KWV-01 near Willowvale (Fig. 2.3). In borehole SFT2, Rock-Eval pyrolysis and vitrinite reflectance measurements showed that the Ecca Group shales were overmature due to tectono-metamorphism associated with the Cape Fold Belt (Geel et al., 2013; Geel et al., 2015). Desorbed and residual gas measurements were made on Ecca Group shales from boreholes KZF-01 and KWV-01, but only very low yields of methane were confined to the Whitehill Formation (de Kock et al., 2017). The TOC content and thermal maturity of the shales were found to be variable within the target Whitehill Formation and de Kock et al. (2017) suggested a new shale gas resource estimate of between 13 and 49 TcF. A later study by Chere et al. (2017) on ten Soekor boreholes estimated a gas resource of 10 – 50 TcF for the Whitehill Formation and 65 – 400 TcF for the Prince Albert Formation. However, these estimates are questionable, as vitrinite reflectance was excluded from the study and the proposed location of the gas resource lies in the southeastern part of the Karoo Basin, where Rowsell and De Swardt (1976) showed the Ecca Group to be overmature using illite crystallinity measurements.

"Sweet spots" identified for shale gas in the Whitehill Formation are found between latitudes 31°00'S and 33°00'S and longitudes 20°30'E and 29°00'E. These "sweet spots" are based on an interpreted paucity of dolerite intrusions, vitrinite reflectance values lying within the dry gas window, total organic carbon content (TOC), formation thickness, and the 1500 m depth contour to avoid groundwater contamination (Fig. 2.3; Decker and Marot, 2012; Cole 2014; Mowzer and Adams, 2015; Geel et al., 2015; Chere et al., 2017; Cole, 2019). The Council for Geoscience is planning to drill a new 4000 m-deep stratigraphic borehole in Beaufort West within these identified "sweet spots".

2.1.3 Exploration potential of the Karoo Basin

Seven technical co-operation permits were approved for Shell, Falcon Oil and Gas, Bundu Gas and Oil, Badimo Gas, Rhino Oil, Afro Energy (Pty) Ltd and Motuoane Energy, in 2020 (Fig. 2.4; Petroleum Agency of SA, 2020). Environmentalists and farmers objected to possible fracking in the Karoo and as a result, the South African government placed a moratorium on exploration rights for shale gas in 2011 until further notice. In 2014, new regulations of environmental impacts of hydraulic fracturing in South Africa were published by the *Centre for Environmental Rights*, resulting in the ban of exploration by means of fracking until the release of final regulations on shale gas.

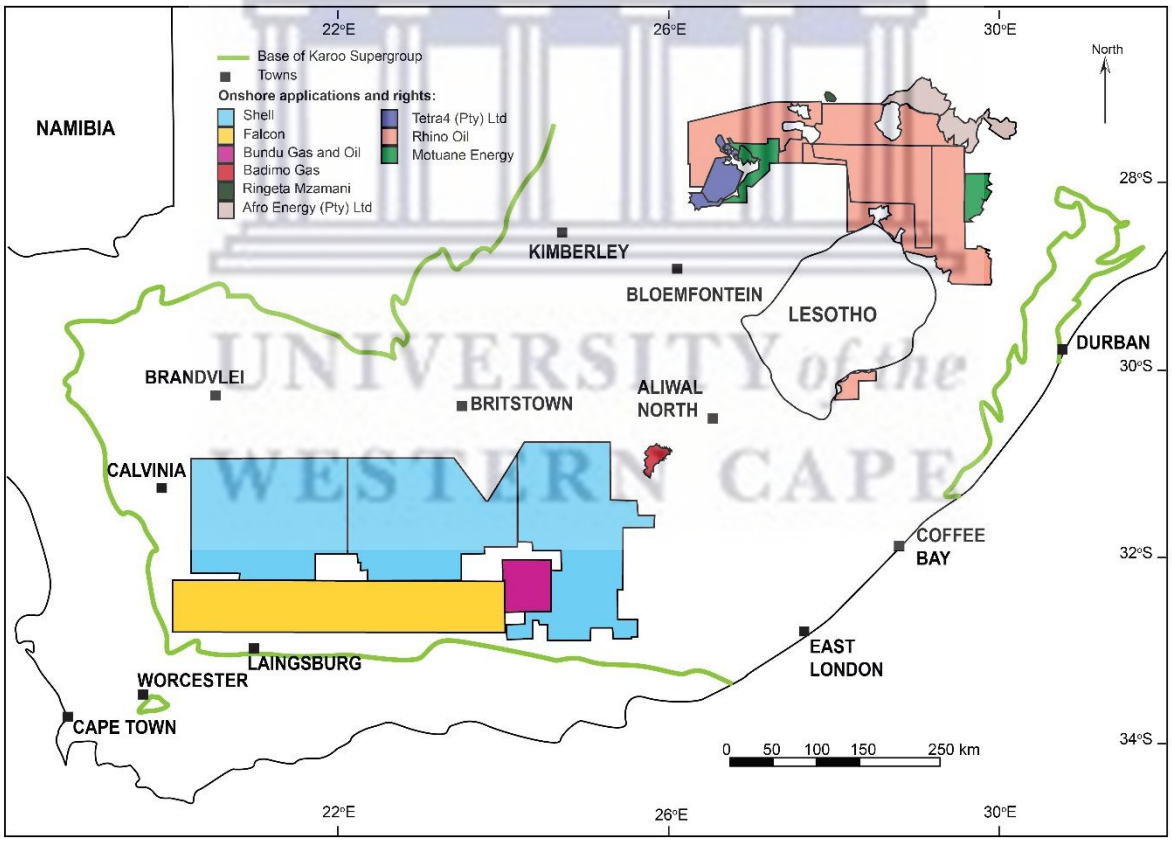

Figure 2.4. Onshore application and right areas in the Karoo Basin of South Africa (2020).

The Petroleum Agency of South Africa (PASA) instructed the applicants to review and change their environmental management plans (EMPs) as a stepping stone towards finalisation of the application process. Due to hydraulic fracturing as the only technique for shale gas extraction in the Karoo, EMP's would have to be aligned with the regulations and approved by PASA. Once this has been achieved and permission for exploration is granted by the Minister of Mineral Resources, exploration may start in the Karoo.

2.2 Previous studies related to the Prince Albert Formation

Until now, the main hydrocarbon target in the Ecca Group has been the Whitehill Formation and much research has focused on this unit, e.g. Geel et al. (2015), de Kock et al. (2017). In contrast, limited studies have been made on the Prince Albert Formation to a lesser degree of focus (Table 2.2). Geel et al. (2013, 2015) selected four core samples from a borehole (SFT2) drilled near Jansenville in the southeastern part of the main Karoo Basin for Rock-Eval analysis, total organic carbon (TOC) content, stable isotope analysis, vitrinite reflectance and porosity. Ferreira (2014) completed an M.Sc. study in the Laingsburg area and selected eleven outcrop samples of the Prince Albert Formation for TOC, Rock-Eval and organic geochemistry. De Kock et al. (2017) studied five core samples from a borehole (KZF-01) drilled near Ceres in the southwestern part of the basin for Rock-Eval and TOC. Chere et al. (2015, 2017) collected five core samples from borehole KL 1/65 (Sutherland) and borehole SP 1/69 (East London) for TOC, vitrinite reflectance and Rock-Eval analyses. Baiyegunhi et al. (2018) selected eleven core samples from four boreholes (KWV-01, SP 1/69, CR 1/68, SC 3/67) and twelve outcrop samples, all in the southeastern part of the main Karoo Basin for TOC, Rock-Eval, vitrinite reflectance and porosity. Schulz et al. (2018) retrieved one core sample from borehole KL1/65 and one from borehole AB 1/65 for TOC and Rock-Eval analysis.

These authors focussed on specific areas of the main Karoo Basin and found that the organic matter was dominated by Type III kerogen. Type III suggests that the Prince Albert Formation is gas prone, but direct or residual gas measurements on their samples were not made. Residual gas constitutes the main parameter of shale gas and is attached to the pores of the shale and organic matter. These measurements should therefore form the first assessment of the shale gas potential of the Prince Albert Formation.

Table 2.2. Previous studies of the Prince Albert Formation related to shale gas in South Africa.

Authors	**Geel et al. (2013, 2015)**	**Ferreira (2014)**	**de Kock et al. (2017)**	**Chere et al. (2015, 2017)**	**Baiyegunhi et al. (2018)**	**Schulz et al. (2018)**
Boreholes	SFT2	–	KZF-01 and KWV-01	KL1/65 and SP 1/69	KWV-01, SP 1/69, CR 1/68, SC 3/67	KL 1/65 and AB 1/65
Location	Near Jansenville, Eastern Cape	Laingsburg, Western Cape	Tankwa and Willowvale	Sutherland and East London	Eastern Cape	Near Sutherland and Loxton, Western Cape
Sample type	Core	Outcrop	Core	Core	Outcrop and core	Core
TOC	0.37 wt.%	0.12 – 0.60 wt.%	0.22 – 3.64 wt.%	0.3 – 7.3 wt.%	0.28 – 7.35	<3 wt. %
Stable isotopes	δ13C is -23.8‰ δ 15N is between 6 and 7‰	–	–	–	–	–
Vitrinite reflectance	~4%	–	–	1.5 – 3.6%	3.12 – 3.84%	–
Porosity	0.53%	–	–	-	0.560%	–
Residual gas	–	–	–	–	–	–
Kerogen	Type III	Type III	Type III or Type IV	Type III	Type III	Type II

In 1965, SOEKOR was established with a mandate to prove or disprove the existence of hydrocarbons in South Africa (Rowsell and De Swardt, 1976). Measurements of desorbed

/residual gas of shale samples of the Ecca Group were taken from the cores of 20 deep boreholes in the main Karoo Basin (Rowsell and De Swardt, 1976). These included samples of the Prince Albert Formation in five boreholes, but obtained only low desorbed gas values dominated by methane (Table 2.3) as compared to active shale gas plays in the USA (Table 2.4). These authors concluded that the low desorbed gas contents were a result of an overmaturity of the shale, which has illite crystallinity (Kübler Index) values between 2.5 and 4.0 corresponding to the zone of anchimetamorphism. Therefore, this thesis brings a more regional approach across the southern part of the main Karoo Basin, including residual gas measurements of fresh core data of the Prince Albert Formation which has been lacking since 1976.

Table 2.3. Prince Albert Formation desorbed gas measurements from five SOEKOR boreholes drilled in the Karoo Basin (from Rowsell and De Swardt, 1976).

Borehole	**Gas contents (m^3/t)**	**Percentage of methane in total gas**
OL1/69	0.2 – 0.000016	89 – 96
KC1/70	0.0001	81 – 82
KW1/67	0.005	92
VR1/66	0.0028	65
SP1/69	0 – 0.0084	99

Table 2.4. Desorbed gas measurements from shale gas basins in the United State (from Arthur et al., 2008).

Shale Gas Basin	**Gas content (m^3/t)**
Barnett Shale	9 – 10
Fayetteville	2 – 6
Haynesville	3 – 9
Marcellus	2 – 3
Woodford	6 – 9
Antrim	1 – 3
New Albany	1 – 2

2.3 Geological Setting

Introduction

The Karoo Supergroup is a component of the Pangean Supersequence of the Gondwanaland province of Pangea (Veevers, 1990). Karoo Supergroup sedimentation started around 310 Ma (Isbell et al., 2008), in an elongate, east-west oriented Karoo Basin that was connected to the Kalahari and Sauce Grande (Sierra Australes) basins (Visser and Praekelt, 1996). Karoo Supergroup sedimentation also occurred in narrow, fault-controlled, Zambezian-type basins in the northern part of South Africa (Veevers et al., 1994). The main Karoo Basin formed as a successor basin to the early Palaeozoic Cape Basin along the south-western margin of Gondwanaland (Veevers et al., 1994).

2.3.1 Cape Basin, South Africa

2.3.1.1 Cape Supergroup

The Cape Supergroup (Fig. 2.5A and B) overlies Precambrian- Cambrian basement and underlies the Karoo Supergroup, which was deposited in a passive margin basin, from Early Ordovician (~ 500 Ma) to Early Carboniferous (~330 Ma) (Thamm and Johnson, 2006). It comprises of three subdivisions namely, Table Mountain, Bokkeveld and Witteberg Groups which extends throughout the 1000 km length of the Cape Fold Belt, forming the southern mountain ranges of the Western and Eastern Cape Provinces (Thamm and Johnson, 2006). The Table Mountain Group comprises of a sandstone-dominated succession ranging from Orovician to Early Devonian (Thamm and Johnson, 2006). The overlying Bokkeveld Group (Fig. 2.5 B) consist of fossiliferous shale and sandstone units of Early to Middle Devonian age (Penn-Clarke, 2017). Deposition of the Bokkeveld Group was associated with a prograding, wave-dominated deltas (Penn-Clarke, 2017). The overlying Late Devonian to Early Carboniferous,

Witteberg Group consists of sandstone and mudrock which was deposited in a shallow marine, paralic and deltaic environment (Thamm and Johnson, 2006). The Cape Supergroup was succeeded by the Karoo Supergroup at the end of the Carboniferous.

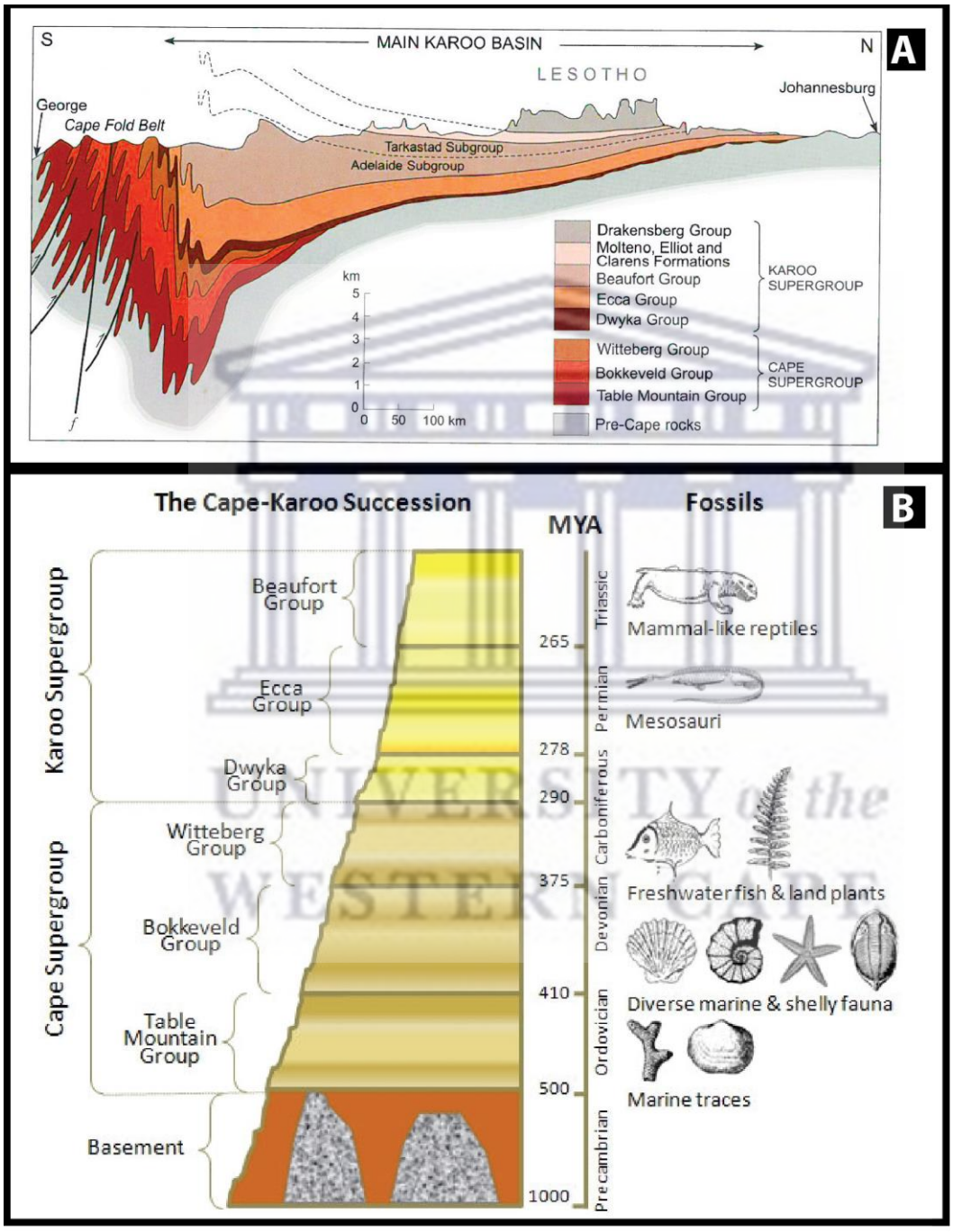

Figure 2.5. (A) Schematic north- south section across the main Karoo Basin (Johnson et al, 2006). (B) The Cape- Karoo succession and its associated fossils (Geocaching, 2021).

2.3.2 main Karoo Basin, South Africa

The main Karoo Basin (Fig. 2.6) is underlain by a stable crust comprising a middle crust of Mesoproterozoic Namaqua-Natal Metamorphic Belt and a lower crust of Palaeoproterozoic Namaqua-Natal Metamorphic Belt and Archean cratonic basement in the northeast (Lindique et al., 2007, 2011). Strata of the Karoo Supergroup form the sedimentary infill in the main Karoo Basin, which has an areal extent of about 700 000km^2. The strata have a maximum cumulative thickness of 12 km in the southeastern part (Fig. 2.5 A; Johnson et al., 1996, 2006), but seismic studies carried out in the southern part by Lindeque et al. (2007, 2011) indicate that the Karoo Basin is about 5 km deep at the frontal margin of the Cape Fold Belt, consistent with earlier interpretations from well data (Rowsell and De Swardt, 1976; Scheiber- Enslin et al., 2014). The high cumulative thickness figure of 12 km for the Karoo Supergroup (Johnson et al., 1996, 2006) is probably a result of tectonic duplication by means of thrusting, as shown for example in borehole SC 3/67, 60 km south of Graaff-Reinet. The Karoo Supergroup ranges in age from Late Carboniferous to Middle Jurassic (Johnson et al., 2006).

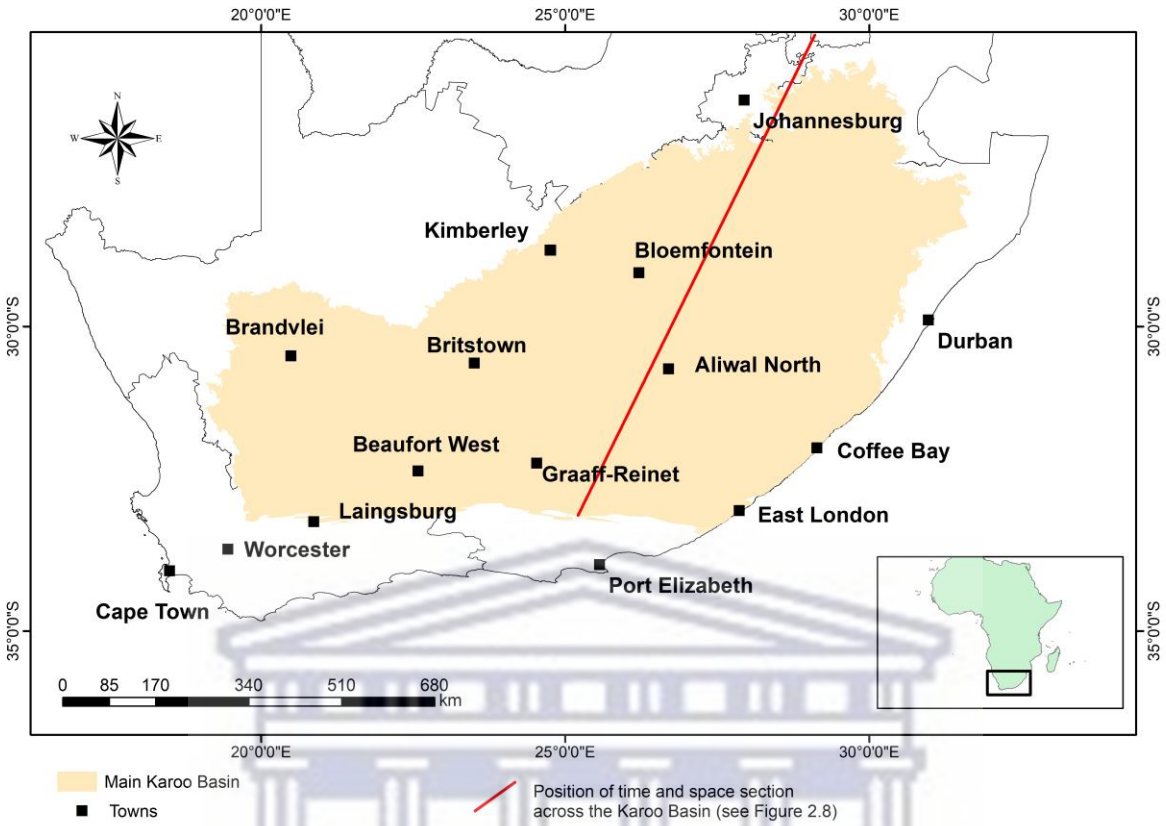

Figure 2.6. Distribution of the Karoo Supergroup in the main Karoo Basin in South Africa.

2.3.2.1 Karoo Supergroup

The Karoo Supergroup is stratigraphically divided into several groups defined by their age and contrasting lithological characteristics. From base up, these groups are the Dwyka, Ecca, Beaufort, Stormberg and Drakensberg Groups (Johnson, 1994). As this thesis is concentrated on the Prince Albert Formation, only this formation and the underlying and overlying units are described in detail, in terms of lithology, age and depositional environment.

2.3.2.1.1 Dwyka Group

The Dwyka Group is the oldest and lowermost unit of the Karoo Supergroup (Fig. 2.5A and B). It consists of a variety of lithofacies (Visser, 1986) dominated by diamictite. Volcanic tuff beds are present in the upper half of the group in the southern part of the main Karoo Basin and

western part of the Kalahari Basin in Namibia and juvenile zircons contained in these beds were used to obtain radiometric dates (Bangert et al., 1999). These ranged in age from 302 to 290 Ma, leading Isbell et al. (2008) to estimate an age of between 312 and 290 Ma for the Dwyka Group, i.e. Late Carboniferous (Moscovian) to Early Permian (Sakmarian) age (International Commission on Stratigraphy, 2017). In the main Karoo Basin, the Dwyka Group becomes younger towards the north and east in the direction of the source areas (Fig. 2.7; Visser, 1987; Bangert et al., 1999). The Dwyka Group rests on glaciated Precambrian bedrock surfaces along the northern basin margin, which display well- developed striated glacial pavements in places (Visser and Loock, 1988; Von Brunn, 1994). In the southern part of the basin, it overlies the Cape Supergroup unconformably or paraconformably, whereas in the eastern part, it unconformably overlies the Natal Group and Masikaba Formation in the east (Johnson et al., 2006).

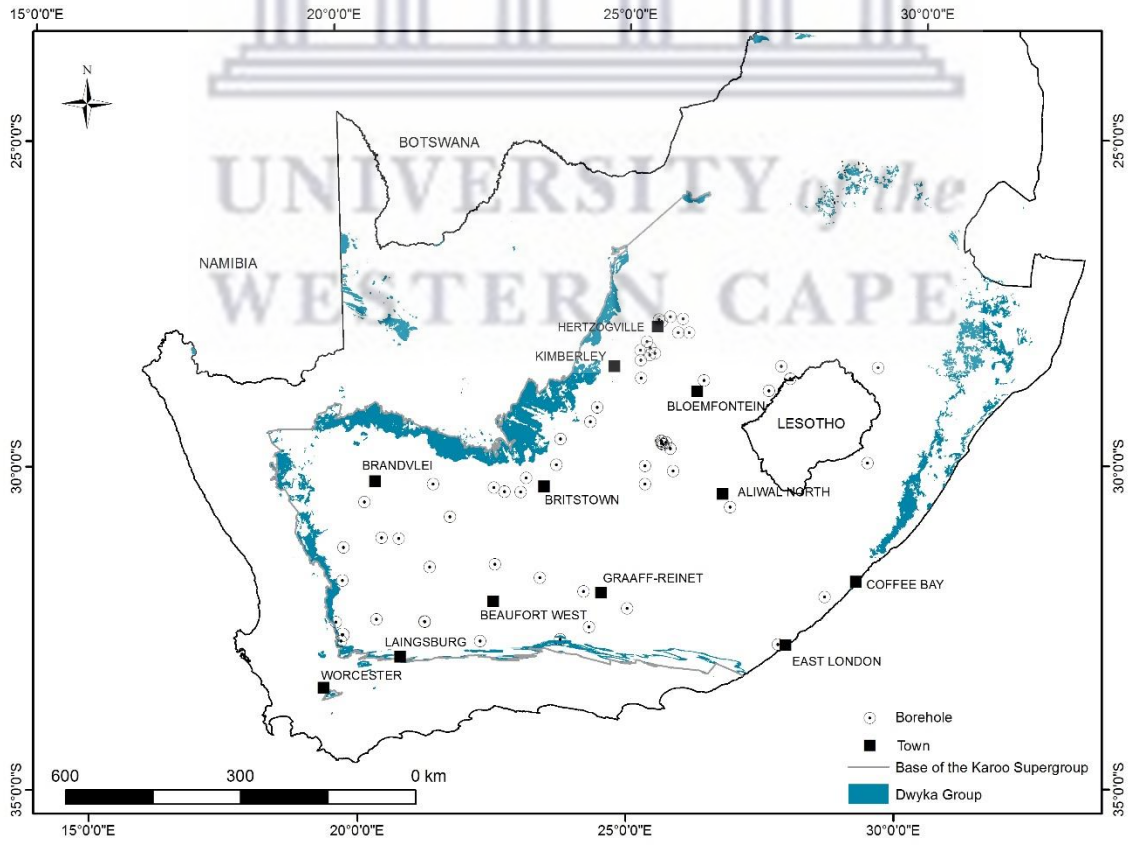

Figure 2.7. Distribution of the Dwyka Group in South Africa south of latitude 24°S.

The Dwyka Group consists of two formations, a diamictite-rich Elandsvlei Formation, and a mixed lithofacies – diamictite, mudstone, sandstone and conglomerate – Mbizane Formation (Visser et al., 1990). The former occurs south of latitude 30°S and the latter north of this latitude with the exception of the northern KwaZulu-Natal region, where both formations are present with the Mbizane Formation overlying the Elandsvlei Formation (Visser et al., 1990).

The Elandsvlei Formation consists of massive diamictite and subordinate stratified diamictite, mudstone with ice-rafted debris, sandstone, silty rhythmite, shale and rare conglomerate (Visser et al., 1997). The massive diamictite is thought to be a rain-out deposit, which was produced by a combination of suspension settling of fines from meltwater plumes and icebergs and the introduction of clasts from debris-laden icebergs or from debris release by basal melting near the grounding line of floating glacial tongues or ice shelves (Isbell et al., 2008). The stratified diamictite, consisting of thin beds of massive diamictite interbedded with dropstone-bearing mudstones and rhythmites, is interpreted as the deposits of sediment gravity flows, suspension settling from underflows and overflows, silty turbidity currents, and ice rafting in an ice-distal setting. Sandstone bodies may have formed as eskers in subglacial tunnels, or as basin slope and/or grounding line fans, some of which slumped into the underlying water-saturated diamicton following deposition (Visser et al., 1997). Thick mudstones with sparse diamictites and sandstones may have formed from suspension settling from meltwater plumes, ice rafting and/or sporadic debris flows (Visser, 1997).

The Mbizane Formation in the northern part of the basin consists of a heterolithic arrangement of massive and stratified diamictite, dropstone-bearing mudstone and rhythmite, sandstone, and conglomerate (Visser and Kingsley, 1982; Visser, 1986). The

massive diamictite was probably deposited as a result of debris rain from melting icebergs and, where stratified, by subaqueous debris flows associated with tidewater glaciers (Cole, 1991; Visser, 1997). The shales represent suspension settling of mud both in a freshwater environment close to the melting glaciers (Cole, 1991) and in a shallow marine environment, as indicated by the fossil fauna (McLachlan and Anderson, 1973). Rhythmites have been interpreted as pelagic mud alternating with silt or sand deposits from underflows/turbidity currents derived from inflowing subglacial meltwater (Cole, 1991). Dropstones in the mudstones are probably a result of iceberg rafting (Visser and Kingsley, 1982; Cole, 1991; Von Brunn, 1996). Sandstone and conglomerate represent proglacial subaqueous outwash and sediment gravity-flow deposits, including turbidity-flow and small delta deposits that accumulated during retreat of the tidewater glaciers (Visser and Kingsley, 1982; Cole, 1991). Visser (1986) delineated a southern platform facies characterised by a fairly uniform diamictite lithology, with thickness ranging from 100 m to 800 m, and a northern valley/inlet facies characterised by rapid thickness changes (up to 200 m variation within short distances), variable lithology, a low massive diamictite content and a high mudrock content. The southern platform facies corresponds with the Elandsvlei Formation and the northern valley/inlet facies with the Mbizane Formation (Visser et al., 1990).

Four deglaciation sequences have been recognised in the Elandsvlei Formation (Theron and Blignault, 1975; Visser, 1997). A deglaciation sequence is defined as an upward-thinning sediment package deposited seaward of the ice-grounding line during a major recessional phase of an extensive ice margin (Visser, 1997). A complete sequence consists of a massive basal diamictite, up to 250 m thick, overlain by a combination, up to 200 m thick, of stratified diamictite, diamictite containing sandstone bodies, rhythmite and shale, with or without ice-rafted material (Visser, 1997). In the northern part of the basin, two sequences have been

recognized in deep palaeovalleys incised into bedrock, but generally, only one sequence is present (Isbell et al., 2008). These sequences probably correspond with sequences 3 and 4 in the south; with sequence 4, the youngest, topmost sequence, representing the single sequence where present.

The Dwyka Group is present in the small Karoo-aged basins north of the main Karoo Basin, namely the Tshipise, Tuli, Ellisras (Lephalale/Waterberg) and Springbok Flats basins (Johnson et al., 2006). Individual informal formation names were applied to each basin (Johnson et al., 2006), but recently, a single, formal name, Tshidzi Formation, has been published, taking into account the lithological similarity of all the basal diamictites and pebbly mudstones in these basins (Bordy, 2018). The name Tshidzi Formation was originally applied to the Tshipise and Tuli basins. Thickness is highly variable ranging from < 1 m to 180 m in the Ellisras Basin and this suggests deposition and preservation in glacially-influenced, localized depressions of a rugged pre-Karoo topography (Bordy, 2018).

Visser (1987) indicated that a highland termed the Cargonian Highlands, separated the main Karoo Basin from the Kalahari Basin. This highland was capped by an ice sheet and was the source of glaciers flowing southwestward into the main Karoo Basin and northwestward into the Kalahari Basin. Glacial sediment thickened away from these highlands and some areas of pre-Karoo basement that build these highlands were overlapped by suspension-settled muds of the Ecca Group, both along the northern margin of the main Karoo Basin and the southern margin of the Kalahari Basin (Veevers et al., 1994). During deposition of glacial sediment in localized depressions in the Tshipise, Tuli, Ellisras (Lephalale/Waterberg) and Springbok Flats basins, which were located directly on the Cargonian Highlands, the predominant glacial

movement direction was southwestwards (Bordy, 2018). This probably occurred during the final phase of glaciation, i.e. deglaciation sequence 4, cf. Isbell et al. (2008).

A sharp to gradational contact separates Dwyka Group strata from the overlying Ecca Group shales of the Prince Albert and Pietermaritzburg Formations (Visser, 1997). This marks the final phase of deglaciation sequence 4 in the form of suspension-settled mud of the Ecca Group and which coincided with the retreat of tidewater glaciers away from the basin margins (Isbell et al., 2008).

2.3.2.1.2 Ecca Group

The Ecca Group consists of stratigraphic units of Permian age that reflect a variety of marine and marginal marine environments (Johnson et al., 2006). This thesis focusses on the Prince Albert Formation and to a lesser extent, the Whitehill Formation, which are located in the lower part of the Ecca Group in the central and southwestern parts of the Karoo Basin (Fig. 2.8; Johnson et al., 2006).

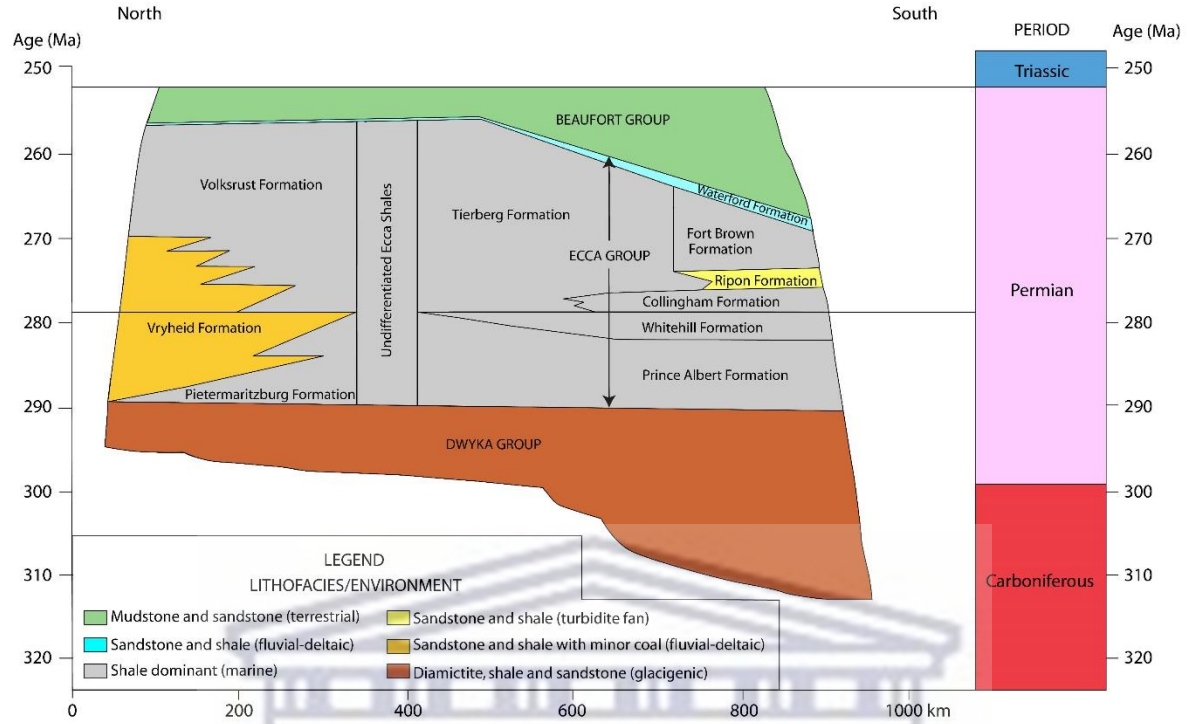

Figure 2.8. Distribution in time and space of Late Carboniferous to latest Permian stratigraphic units including lithology and depositional environment in the main Karoo Basin (Kingsley, 1981; Johnson et al., 2006; Cole, 2018, 2019).

2.3.2.1.2.1 Prince Albert Formation

The Prince Albert Formation conformably overlies the Dwyka Group, but in the northwestern part of the Karoo Basin between Copperton and Hertzogville, it unconformably overlies the pre-Karoo basement where the Dwyka Group is absent (Fig. 2.9; Mosavel and Cole, 2019). The Prince Albert Formation is conformably overlain by the Whitehill Formation. It is Early Permian (Artinskian to early Kungurian) in age (International Commission on Stratigraphy, 2017) based on U-Pb dates of 289.6 ± 3.4Ma and 288 ± 3Ma from juvenile magmatic zircons of tuff beds in the basal part of the formation in the main Karoo Basin (Bangert et al., 1999), dates of 280.5 ± 2.1 Ma from zircons from volcanic tuffs in the overlying Whitehill Formation in the Aranos Basin of southern Namibia (Werner, 2006) and 278.4 ± 2.2 Ma from the

stratigraphic-equivalent Irati Formation in the Paraná Basin at São Mateus do Sul, southern Brazil (Santos et al., 2006).

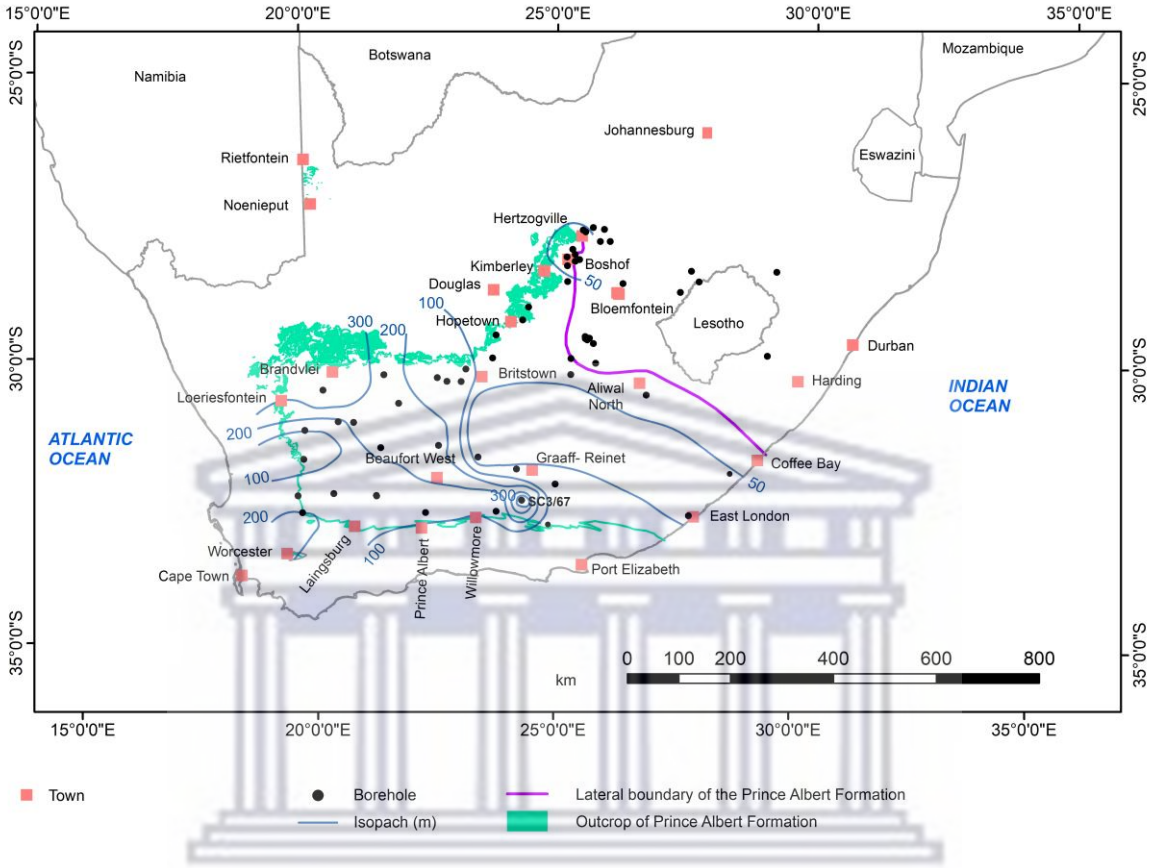

Figure 2.9. Isopach and distribution map of the Prince Albert Formation in the main Karoo Basin of South Africa.

The Prince Albert Formation is restricted to the central and southwestern parts of the main Karoo Basin (Fig. 2.9). The formation thins towards the east and northeast and locally pinches out against basement highs in the Boshof region (Cole and McLachlan, 1994). In outcrop, the Prince Albert Formation along the western and southern margins of the main Karoo Basin (Fig. 2.9), ranges in thickness from 50 to 165 m, whereas borehole data indicate maximum thicknesses of up to 320 m in the northwestern part of the Karoo Basin (Siebrits, 1989; Mosavel and Cole, 2019). In borehole SC 3/67, 60 km south of Graaff-Reinet, the formation attains an anomalous thickness of 497 m, which may be due to tectonic duplication by means

of thrusting (Fig. 2.9). In the northern sector of the basin, the Prince Albert Formation is characterised by greyish to olive- green micaceous shale and grey silty shale, with dark grey to black carbonaceous shale and fine- to medium-grained, feldspathic arenite and wacke occurring locally (Johnson et al., 2006). In both shales and sandstones, brownish calcareous concretions and irregular carbonate bodies are present. In the southern sector of the basin, the formation is characterised by the presence of dark-grey, pyrite-bearing, splintery shale and dark-coloured chert and phosphatic nodules and lenses. In the west, carbonate concretions and irregular bodies with brown encrustation, are spread throughout the Prince Albert Formation. Isolated granule- to cobble-sized clasts (dropstones) occur in the lowermost part of the formation over a maximum thickness of 30 m in the Laingsburg, Loeriesfontein and Boshof-Hertzogville areas (Visser, 1991; Cole and McLachlan, 1994).

Siltstone and very fine- to medium-grained, massive, horizontally laminated, cross-bedded, ripple-laminated, bioturbated or slumped sandstone occur in the area northeast of Kimberley, the Noenieput – Rietfontein area (Fig. 2.9) and in the lower part of the formation in the Laingsburg and Loeriesfontein areas (Mosavel and Cole, 2019). Fining-upward and coarsening-upward sequences are present (Mosavel and Cole, 2019). The Prince Albert Formation merges with the heterolithic Vryheid Formation northeast of Hertzogville with the exception of a basal shale where present, which merges with the Pietermaritzburg Formation (Cole and McLachlan, 1994). Northeast of Kimberley, the overlying Whitehill Formation shows a lateral lithofacies change from black carbonaceous shale into dark grey, silty mudrock and rhythmite (Cole and McLachan, 1994). In borehole GP1/78 near Hertzogville, the carbonaceous shale is only 0.37 m thick and further northeast, it can no longer be differentiated from the Prince Albert Formation (Cole and Basson, 1991; Mosavel and Cole, 2019). The Prince Albert Formation is still present north of Coffee Bay (Fig. 2.9), where the

Whitehill Formation crops out sporadically (Cole and Basson, 1991), but further north it grades into the lower part of the undifferentiated, shale-rich, Ecca Group (Karpeta and Johnson, 1979). This undifferentiated Ecca Group extends northeastwards as far as Harding, where the heterolithic Vryheid Formation pinches out (Johnson et al., 2006). Borehole records indicate that undifferentiated Ecca Group shale occurs northeast of the line of subsurface pinch out of the Prince Albert Formation as far west as Bloemfontein (Fig. 2.9), at which point, the Vryheid Formation merges directly with the heterolithic Prince Albert Formation.

Fossils mostly occur in the lowermost part of the formation. Near Douglas (Northern Cape), the presence of marine fossils, namely cephalopods, lamellibranchs, brachiopods and palaeoniscoid fish, together with coprolites, wood and spores, have been recorded from a section between 10 and 16 m above the base of the Prince Albert Formation (McLachlan and Anderson, 1973). Oelofsen (1986) described a fossil shark from near the base of the formation north of Klaarstroom, while Visser (1994) reported sponge spicules, foraminifera, radiolarian and acritarchs from the basal 5 m of the formation at Laingsburg. Cole and McLachlan (1994) reported the presence of sponge spicules and fossil leaves from borehole core near Hopetown and fossil wood and leaves from core in the Kimberley – Hertzogville area.

Sedimentation occurred in a basin plain to shelf environment within a probable retro-arc foreland basin that opened towards the southwest (Visser, 1994). The presence of marine invertebrates and a shark in the lowermost part of the formation indicates marine conditions that coincided with a major transgression, following collapse of the ice sheets associated with the glacigenic Dwyka Group (Visser, 1994). The precipitation of phosphate indicates that water depth was probably between 250 and 400 m in the southern part of the basin (Bühmann et al., 1989; Visser, 1991), but shallowed towards the north, northeast and east

where phosphate is absent (Visser, 1994). Siliceous and phosphatic rocks could probably have formed by chemical or biological processes under reducing conditions, in areas where upwelling of cold water occurred (Johnson et al., 2006). This upwelling could have resulted in a rich marine life causing organic materials to be trapped in the bottom muds. Enrichment of these deposits was caused by early diagenetic processes, forming nodules and lenses (Johnson et al., 2006).

Mudrocks of the Prince Albert Formation indicate suspension settling of mud, whereas the siltstones and sandstones represent tractional fall-out from turbidity currents (Visser, 1991; Mosavel and Cole, 2019). Cross-bedded and ripple-laminated sandstones were deposited by tractional bottom currents (Visser, 1994) and in the Boshof – Hertzogville area, the sequences of mudrock, rhythmite and sandstone represent deposition in a deltaic environment with the sediments being derived from an adjacent northerly provenance (Cole and McLachlan, 1994). The dispersed granule- to cobble-sized clasts in the lowermost part of the formation are interpreted as iceberg-rafted dropstones (Visser, 1991). Climatic conditions were cool to temperate (Visser, 1991).

2.3.2.1.2.2 Whitehill Formation

The Whitehill Formation conformably overlies the Prince Albert Formation and is overlaid by the Collingham Formation in the southern part of the main Karoo Basin and the Tierberg Formation in the northwestern part. It persists over more than 300 000 km^2 within the main Karoo Basin of South Africa (Fig. 2.10) and the adjacent Karoo basins of Namibia. Various ages have been assigned to the Whitehill Formation, i.e. Early Permian (McLachlan and Anderson, 1973; Anderson, 1977); Late Sakmarian (Oelofsen and Araujo, 1987); Baigendzian (Veevers et al., 1994); and Kungurian (Visser, 1990). However, with the advent of more accurate

radiometric dating of juvenile zircons from volcanic tuffs within the Whitehill and adjacent formations, a middle Kungurian age, i.e. 278 – 282 Ma (International Commission on Stratigraphy, 2017) is indicated, with ages of 280.5 ± 2.1 Ma from the Whitehill Formation in the Aranos Basin of southern Namibia (Werner, 2006), 278.4 ± 2.2 Ma from the stratigraphic-equivalent Irati Formation in the Paraná Basin at São Mateus do Sul, southern Brazil (Santos et al., 2006) and 269.5 ± 1.2 Ma from the Tierberg Formation some 600 metres above the top of the Whitehill Formation in the southwest part of the main Karoo Basin (Belica et al., 2017). The Whitehill Formation mostly consists of a white-weathering, black, carbonaceous shale, which makes it a useful marker unit. In fresh outcrop and in borehole core, the black, carbonaceous shale is characterised by the presence of disseminated pyrite. Shale from core of the Whitehill Formation can be distinguished from the overlying and underlying shales by the fact that it gives a black streak on concrete (D. Cole, 2015, personal communication). The thickness of the Whitehill Formation varies between 10 and 80 m (Cole and Basson, 1991; Smithard et al., 2015) and contains up to 17% organic carbon (Cole and McLachlan, 1991). Northeast of Kimberley, the Whitehill Formation shows a lateral lithofacies change from black carbonaceous shale into dark grey, silty mudrock and rhythmite (Cole and McLachan, 1994).

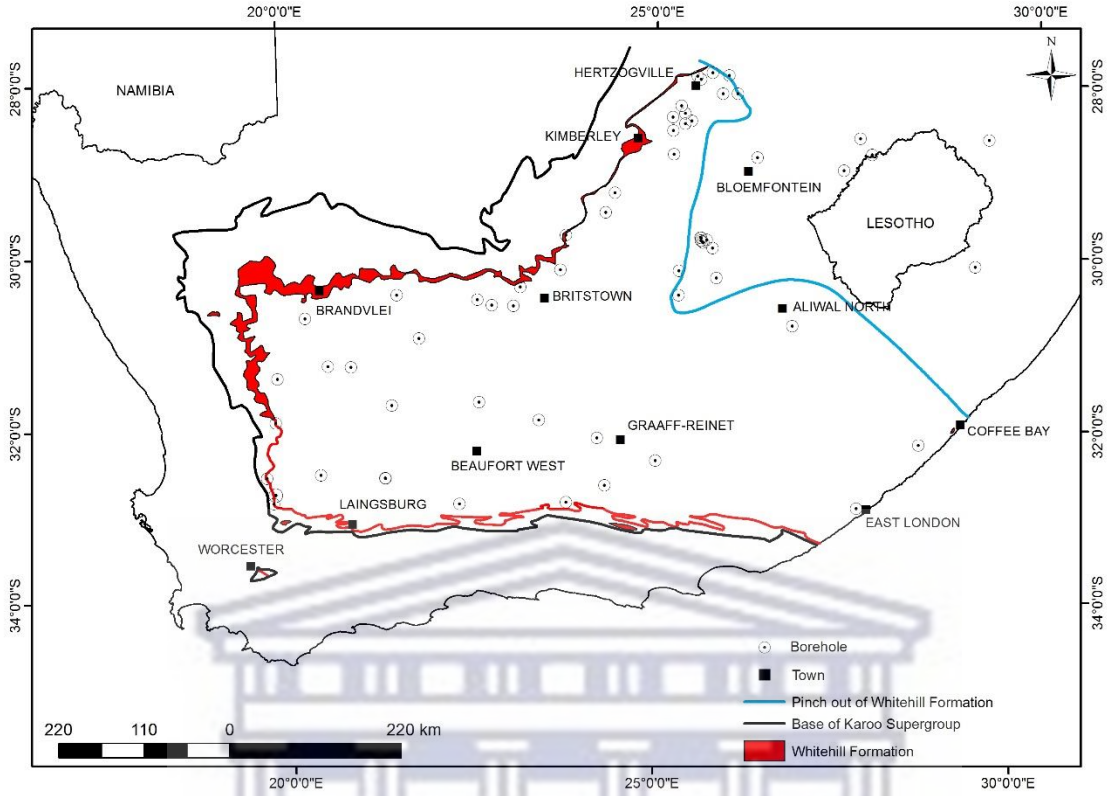

Figure 2.10. Distribution of the Whitehill Formation in the main Karoo Basin and position of the subsurface limit of the Whitehill Formation (D. Cole, 2017, personal communication).

In borehole GP1/78 near Hertzogville, the carbonaceous shale is only 0.37 m thick and further northeast, it can no longer be differentiated from the Prince Albert Formation (Cole and Basson, 1991; Mosavel and Cole, 2019). It is therefore apparent that the Whitehill Formation grades into the upper part of the Prince Albert Formation (Cole and Basson, 1991) with both formations grading into the lithologically-similar Vryheid Formation in the region between Hertzogville and Wesselsbron. Both the combined Whitehill and Prince Albert Formations and the Vryheid Formation have an average thickness of 50 metres, and the relatively thinner Whitehill Formation corresponds to the upper part of the 2nd fluvio-deltaic cycle of the Vryheid Formation (Fig. 2.8). Rarely, thin tuffaceous beds occur in the Whitehill Formation

(McLachlan and Jonker, 1990), whereas ferruginous, carbonate concretions are dispersed throughout the formation (Johnson et al., 2006).

The black carbonaceous shale of the Whitehill Formation was deposited by suspension settling of mud in a young, underfilled foreland basin under anoxic conditions similar to the Black Sea (Cole and McLachlan, 1991; Visser, 1992). According to Johnson et al. (2006) anoxia resulted due to the high concentration of organic matter in the water body and the restricted oceanic circulation in the Karoo Basin. Preservation of organic material was high due to the absence of benthonic fauna. Along the shallow marginal regions of the basin, anoxic conditions were less, allowing for the deposition of very fine-grained sandstone, siltstone and carbonate rocks, interbedded with the black shales (rhythmite). The sand and silt could possibly represent distal turbidites and storm deposits (Johnson et al., 2006). Airborne volcanic ash, deposited with muds, was derived from a magmatic arc in the palaeowest or southwest. The presence of fossils such as rare insect wings (McLachlan and Anderson, 1977), the *Mesosaurus* reptile (Oelofsen and Araujo, 1987), plant remains, fossil wood and leaves (Cole and Basson, 1991), palaeoniscoid fish and arthropods have been reported for the Whitehill Formation, with the mesosaurid reptiles, crustaceans and palaeoniscoid fish occurring in the upper part and the ichnofossils in the central part of the formation (Oelofsen, 1981).

The Whitehill Formation has been considered as an oil shale prospect (Cole, 1978; Cole and McLachlan, 1991) and recently a shale gas prospect due to its correlative in South America, the Irati Formation, which contains the world's second largest reserves (Bruni et al., 1971). However, Roswell and De Swardt (1976), Geel et al. (2015) and de Kock et al. (2017) found that a relatively high grade diagenesis is present due to deep burial in the southern part of

the basin, deformation and metamorphism in the southernmost region associated with the Cape Fold Belt and thermal metamorphism caused by the intrusion of dolerite north of latitude 32°30'S.

2.4 Structural evolution and chacterisation of the main Karoo Basin

There have been various proposals concerning the main Karoo Basin in terms of type and development.

2.4.1 Retroarc foreland basin

The main Karoo Basin was initially interpreted as a retroarc foreland basin that developed behind a magmatic arc and fold-thrust belt (Cape Fold Belt) located south of the basin (Johnson, 1991; Catuneanu et al., 1998; Johnson et al. 2006). Development of the basin was caused by northward subduction of oceanic crust (palaeo-Pacific or Panthalassan Plate of Veevers et al., 1994) beneath the Gondwanaland supercontinent. However, because of the lack of igneous activity and regional metamorphism within the Cape Fold Belt, the distance between the fold belt and the subduction zone was probably in the order of 2000 km leading Lock (1980) to propose a flat plate subduction model. Catuneanu (2004), assigned foreland systems into flexural provinces: foredeep (foreland basin), forebulge (peripheral bulge) and back-bulge (Fig. 2.11). Foreland systems form by the flexural deflection of the lithosphere due to supra- and sublithospheric loads.

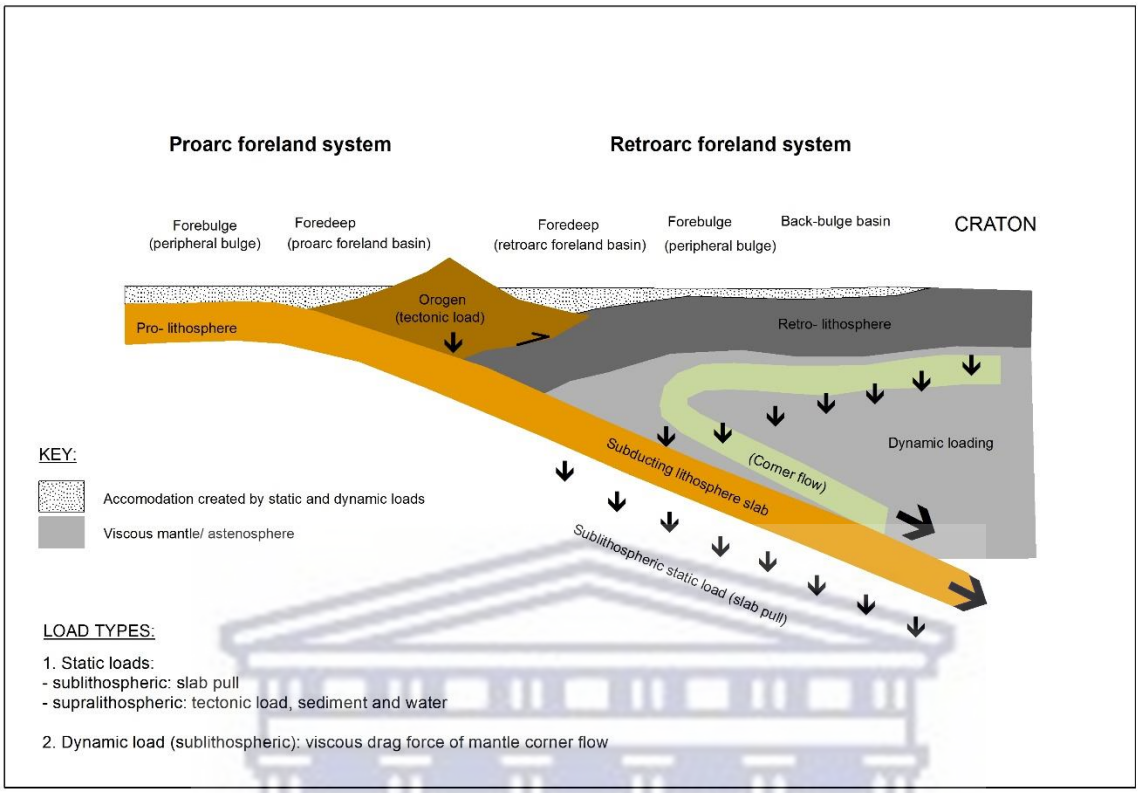

Figure 2.11. Proarc and retroarc foreland systems: tectonic setting and controls on accommodation with subduction towards the north (modified after Catuneanu, 2004).

Tectonic forces control the formation of a retroarc foreland type basin and its accommodation space. In a retroarc foreland system, the subsidence depends on the type of load, whether static or dynamic, with the rate of subsidence increasing towards the orogenic belt. As a result, the basin fill forms an overall wedge-shaped geometry indicating the tectonic control. Flexural tectonics and dynamic subsidence are the two main tectonic controls in a retroarc foreland system (Catuneanu, 2004).

The stratigraphy of the Karoo Basin has been linked to the subduction of the palaeo-Pacific (Panthalassan) plate beneath the Gondwana plate towards the north with four to five different compressional events associated with the Cape Orogeny between ~300 Ma and ~215 Ma. These events were dated using $^{40}Ar/^{39}Ar$ step heating analyses on fine-grained rocks

from the Cape Fold Belt (Hälbich et al., 1983; Gresse et al., 1992) and have been linked to the Late Palaeozoic amalgamation of Gondwanaland. However, Hansma et al. (2016) criticised these studies, since they assessed age clusters and not age plateaux, and completed a similar study on muscovite from samples collected in the Cape Fold Belt between Montagu and George. They found that the thermal or deformational resetting ages clustered into two groups: 276±5 to 261±3 Ma and 254±2 to 248±2 Ma. Taking cognisance of the ages of sedimentation, this indicates that the Cape Supergroup, Dwyka Group and Prince Albert Formation would have been lithified prior to deformation, but deposition of the younger Ecca Group and Beaufort Group would have coincided with the orogenic events. This coincidence is supported by syn-sedimentary deformation within the upper Ecca Group (Oliveira et al., 2011). The initial deformational event was probably deep-seated and resulted in the development of a northeast-trending basin floor swell in the Cape Fold Belt Syntaxis. As a result, and less mud from suspension accumulated over this swell during sedimentation of the Whitehill Formation (De Beer, 1992), and submarine fans of the Skoorsteenberg and Laingsburg Formations were confined to the basin plain northwest and southeast of this swell (Wickens, 1992). The second phase of deformational events between 254 and 248 Ma coincides with deposition of the Late Permian Balfour Formation and Early Triassic Katberg Formation (Rubidge, 2005; Rubidge et al., 2013). Hansma et al. (2016) suggested that it may not have been a deformational episode, but a record of the cooling of exhumed rocks, since the dated samples are from the Cape Supergroup rocks in the south and no syn-sedimentary deformation has been reported in the Balfour and Katberg Formations. Conversely, Turner (1999) argues that evidence in the Upper Karoo succession supports an extensional depositional environment and uplift. According to Turner (1999), the extension resulted from

a thermal anomaly off the current southeast coast of South Africa, which is refuted by Bordy et al. (2005).

2.4.2 Transtensional foreland type basin

Studies by Tankard et al. (2009; 2012) contest the retro-arc foreland basin model of the main Karoo Basin based on the absence of a nearby magmatic arc (geophysical data) and a proposed later start of the Cape Orogeny in the Early Triassic. These statements have since been disputed by Hansma et al. (2016) - see above. Tankard et al. (2009; 2012) suggested that there was a period of regional uplift lasting about 30 million years, following deposition of the Witteberg Group at ~ 330 Ma. This was followed by a dynamic phase of subsidence that pre-dated the Cape Orogeny, with subsidence occurring due to vertical displacement of rigid basement blocks decoupled along major crustal-scale boundary faults, such as the Doringberg Fault. An extensional ramp syncline formed in the southern part of the basin (Fig. 2.12). The transtensional foreland basin only developed during the Triassic Period, as a result of the Cape Orogeny causing subsidence of a northern Natal block relative to a Namaqua block along an east-trending Hartbees-Mbotyi fault zone (Fig. 2.12; Tankard et al., 2009, 2012). Based on supportive evidence, Visser and Praekelt (1996) and Tankard et al., (2009; 2012) interpret the Cape Fold Belt as a sinistral strike-slip orogeny linked to oblique reaction of the southern Namaqua suture.

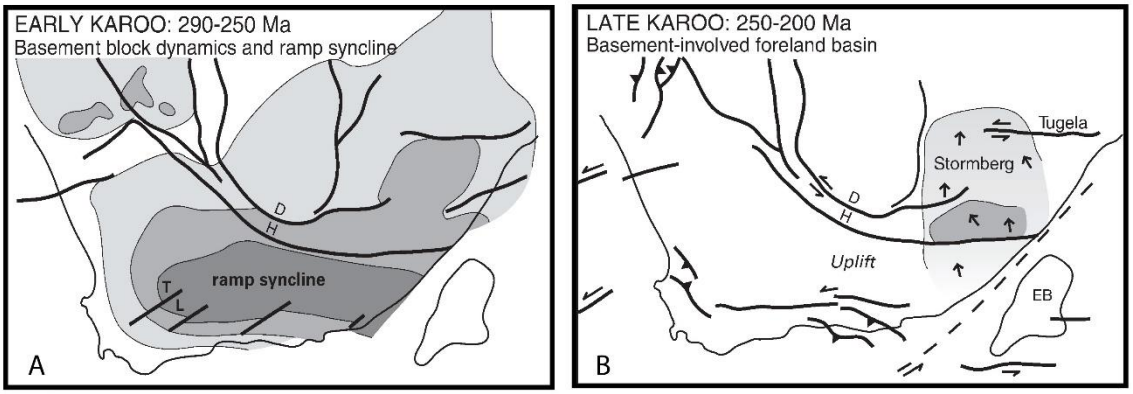

D- Doringberg Fault
H- Hartbees Fault
T- Tanqua fan
L- Laingsburg fan
EB- Ewing Bank

Figure 2.12. A) Early Karoo subsidence involved decoupled basement blocks and an extensional ramp syncline. B) Late Karoo tectonism characterized by Namaqua uplift, transtentional subisidence of the Natal block and transpressional uplift of the Falkland Plateau- Ewing Bank (Tankard et al., 2009).

2.4.3 Jura-type basin

Reflection seismic studies undertaken in the western part of the Karoo Basin (Lindeque et al., 2011) suggest that the Karoo Basin formed in front of a thin-skinned Jura-type fold belt, since there is no significant fore-deep stratigraphic thickening of the Karoo Basin strata (Fig. 2.13) nor a thick crustal root beneath the Cape Fold Belt front. In southern South America, granites aged between 300 and 225 Ma are associated with subduction of the adjacent palaeo-Pacific (Panthalassan) plate beneath the Gondwanaland plate (López-Gamundi et al., 1994). However, there is an absence of similar granites in the Cape Fold Belt along the southern margin of the main Karoo Basin. This absence, together with the absence of a suture zone and palaeoceanic crust below the Karoo Basin, suggest that subduction here, towards the south (Fig. 2.14; Lindeque et al., 2011). The tectonic model (Fig. 2.13) suggests a 2 to 5 km-thick, folded Karoo Supergroup, with deformation along low-angle listric faults along the unconformable contact of the Cape Supergroup with the Mesoproterozoic basement (Fig.

2.13; Lindeque et al., 2011). These listric faults are associated with apparent local décollement surfaces of the Whitehill and Prince Albert Formations.

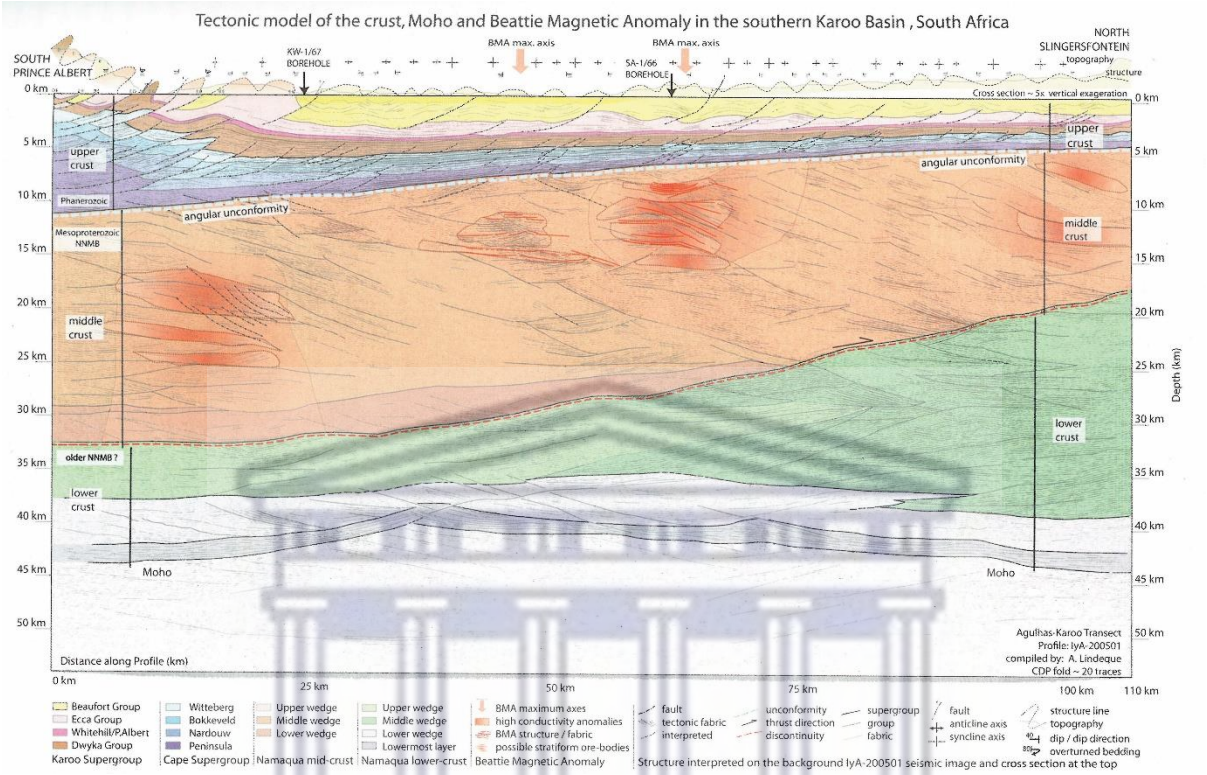

Figure 2.13. Crustal tectonic model with the upper crust comprising the Karoo Supergroup (yellow to brown) and Cape Supergroup (light blue to purple), separated from the basement by an angular unconformity (dashed line) and Namaqua- Natal Metamorphic Belt mid-crust (shades of orange) (Lindeque et al., 2011).

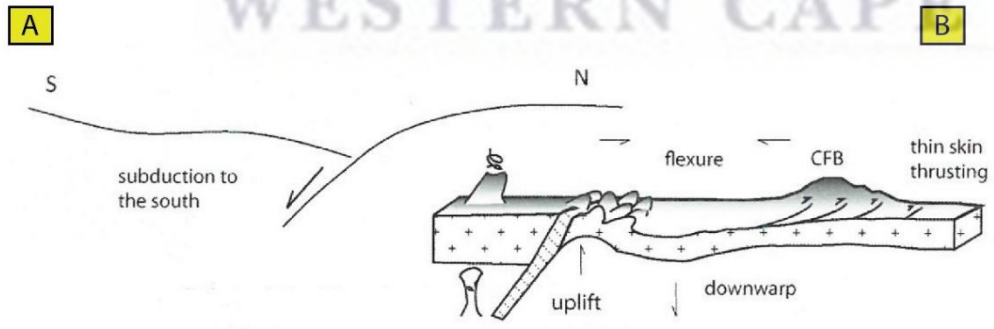

Figure 2.14. Southward model of continent- continent collision and subduction (from Lindeque et al. 2011). A) Simplified model and B) crustal model.

2.5 Description of units equivalent to the Dwyka Group, Prince Albert and Whitehill formations in southern Gondwanaland

During the late Precambrian and early Palaeozoic Era, amalgamated continental crust formed a supercontinent named Pangaea. Pangaea was periodically split into two smaller supercontinents named Laurentia and Gondwanaland, which were partially separated by an ocean called Tethys (Veevers, 2000). Pangaea was finally amalgamated during the Middle Triassic, prior to complete and permanent splitting (Veevers, 2000).

Gondwanaland represents a large continental crustal unit that existed for about 200 million years. Gondwanaland included South America, Africa, Antarctica, Australia, Madagascar, India and various other smaller fragments (Fig. 2.15; de Wit et al., 1988; Veevers, 2000). This section briefly describes the age, lithostratigraphy, depositional history and biostratigraphy of the successions within the various basins of southwestern Gondwanaland, together with possible correlations of the stratigraphic units with the Dwyka Group, Prince Albert and Whitehill formations in the main Karoo Basin (Figs. 2.15 and 2.16).

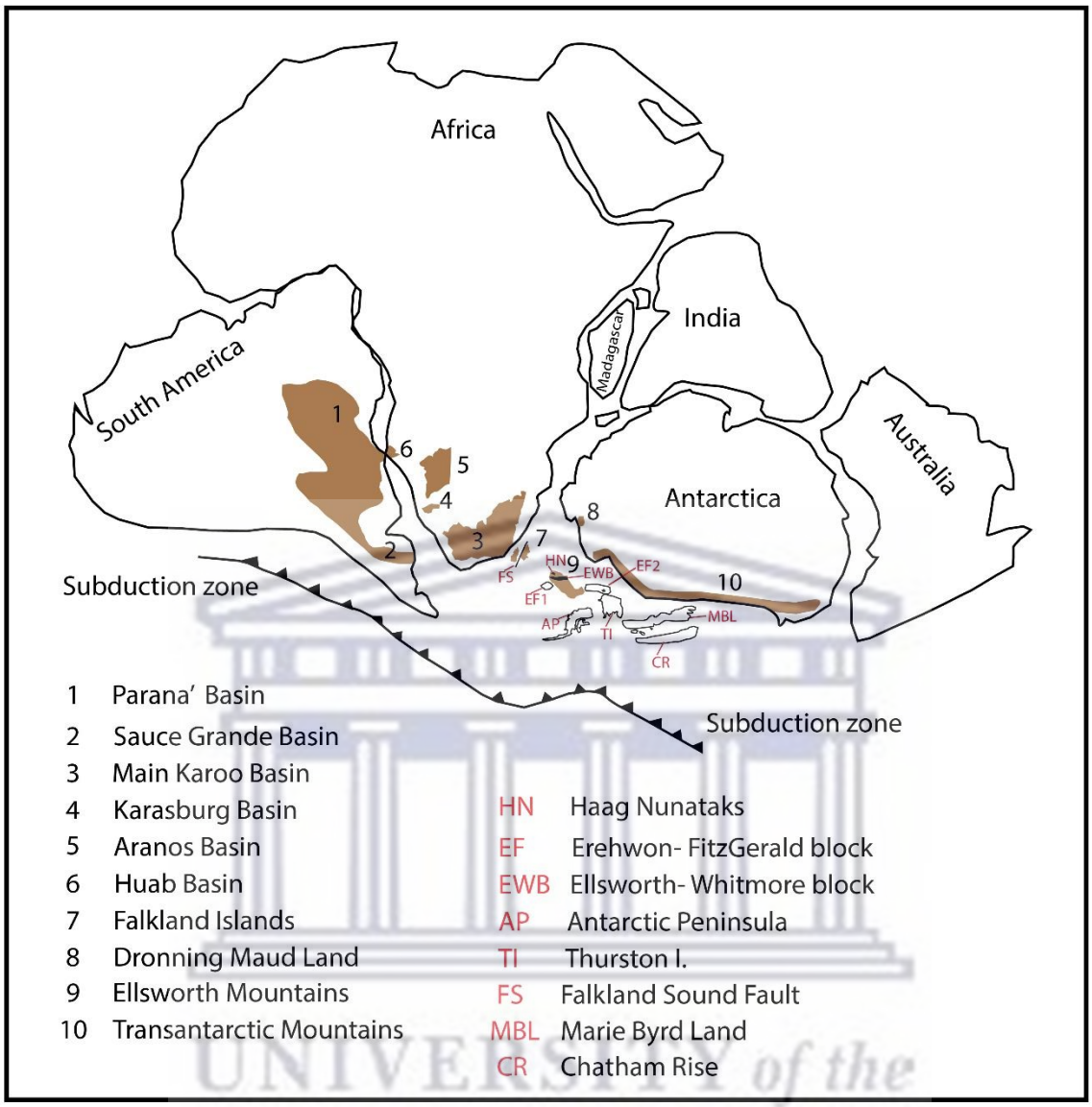

Figure 2.15. Simplified map of Gondwanaland showing the location of basins described in the text (coloured brown). Map modified from de Wit et al. (1988) and Elliot et al. (2016).

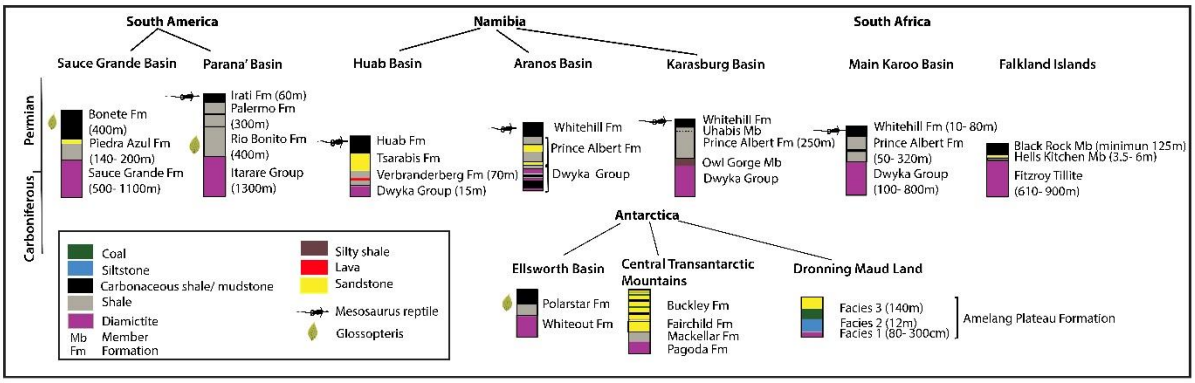

Figure 2.16. Generalised stratigraphic columns of Permian successions in the Sauce Grande, Paraná, Huab, Aranos, Karasburg, Main Karoo, Falkland Islands, Ellsworth Mountains, Central Transantarctic Mountains and Dronning Maud Land basins (modified after Faure and Cole, 1999; Trewin et al., 2002, Bauer, 2009, and Elliot et al., 2016).

2.5.1 South America

2.5.1.1 Sauce Grande Basin

The Late Paleozoic Sauce Grande Basin is located along the Paleo-Pacific margin of southern South America between latitudes 30°S and 40°S (López-Gamundi et al., 1994). The Sauce Grande Basin formed during the Late Carboniferous (290 Ma) on magmatic basement of the Sierras Pampeanas. López- Gamundi et al. (1994) suggest that the final development of the Sauce Grande Basin continued into the south-western part of the Paraná Basin, controlled by Pampean structures (Bracaccini, 1960; Salfity and Gorustovich, 1983). The pre-Carboniferous basement of the Sauce Grande Basin comprises either an igneous- metamorphic basement or a Palaeozoic sedimentary basement depending upon location.

Sedimentation in the Sauce Grande Basin started at approximately 290 Ma with glacigene deposits of the Sauce Grande Formation (Andreis et al., 1987). Sedimentation continued

throughout the Permian Period without major breaks as the basin was not affected by tectonic and magmatic activity along the Gondwanan continental margin.

The Sauce Grande Basin contains only the Pillahincó Group of sedimentary rocks with the Sauce Grande forming the lowermost formation (Harrington, 1947). The Pillahincó Group unconformably overlies the Early Devonian Lolén Formation and is unconformably overlain by Miocene-aged conglomerate in the Sierras Australes of the Buenos Aires Province (López-Gamundi et al., 1994). Isolated exposures of the Pillahincó Group between the Sierras Australes and the Tandilia Range in the northeast and near Mar del Plata define the approximate northeastern margin of the basin (López-Gamundi et al., 1994).

Pillahincó Group

The Pillahincó Group consists of four formations, namely the Sauce Grande, Piedra Azul, Bonete, and Tunas formations (Fig. 2.16). The Pillahincó Group ranges in age from latest Carboniferous to latest Permian, with a thickness of 2000 m to 4500 m (López-Gamundi et al., 1994).

Sauce Grande Formation

The basal Sauce Grande Formation consists of diamictite (74%), sandstone (24%), and shale (2%) with thicknesses ranging between 500 m and 1100 m (Andreis et al., 1987). The lower part of the Sauce Grande Formation consists of massive diamictite with scattered lenses of sandstone near the base and top. The upper part of the formation consists mainly of diamictite with interbeds of rippled sandstone and conglomerate (Amos and López-Gamundi, 1981). Abundant dropstones are present in thin shale intervals of the Sauce Grande Formation. Archangelsky et al. (1987) suggested a latest Carboniferous to earliest Permian

age for the Sauce Grande Formation based on spores found in the diamictite. The Sauce Grande Formation has been interpreted as a glaciomarine deposit with the diamictites being mostly deposited by sediment gravity flows (Coates, 1969; Harrington, 1980; Andreis, 1984). The Sauce Grande Formation is similar to the Dwyka Group in South Africa in terms of stratigraphic age and lithology.

Piedra Azul Formation

The Piedra Azul Formation consists of shale and subordinate cross-bedded, fine-grained sandstone ranging between 140 m and 200 m in thickness (Andreis et al., 1989). The depositional environment for the Piedra Azul Formation has been interpreted as marine.

Bonete Formation

The Bonete Formation consists of bioturbated shale and rippled and cross-bedded sandstone with a Eurydesma fauna of Tastubian (Early Sakmarian (International Commission on Stratigraphy, 2017)) age, together with a Glossopteris flora (Archangelsky and Cúneo, 1984).

Tunas Formation

The Tunas Formation overlies the Bonete Formation and consists of a 1500 m thick succession of fine- to medium-grained sandstone and mudstone deposited in a shallow marine to deltaic environment (López-Gamundi et al., 1994). Tuffaceous layers are also present within the Tunas Formation, which have been interpreted as ash falls by Iñíguez et al. (1988), thereby providing evidence of volcanism in adjacent areas during sedimentation. The less quartzose petrofacies of the Tunas Formation has a northeastward paleocurrent pattern with deposition occurring in a deltaic to non-marine environment (López-Gamundi et al., 1994). Glossopteris

flora, were found in the lower half of the Tunas Formation inferring an Early Permian age (López-Gamundi et al., 1994). New SHRIMP radiogenic isotope dating of zircons in tuffs by López-Gamundi et al. (2013) confirms an Early Permian (280.8 ±1.9 Ma, Kungurian) age of the uppermost section of the Tunas Formation, which coincide with Ar-Ar dates of 282.4 ± 2.8 Ma provided by Tohver et al. (2008). The ages of this uppermost section correspond to the ages of the Whitehill and Irati formations (see above), which suggests that the lower Tunas Formation and the Bonete and Piedra Azul formations correlate with the Prince Albert Formation in the main Karoo Basin, the latter on the basis of similar lithologies (cf. Mosavel and Cole, 2019).

2.5.1.2 Paraná Basin

During the Carboniferous- Permian, the Paraná Basin was located in the southwestern portion of Gondwana (Fig. 2.15 and 2.17). At present, the Paraná Basin is situated in the south-central portion of South America, covering an area of 1 500 000 km^2. Geological evidence has shown that during the Late Carboniferous and Permian, the Paraná Basin was interconnected with the main Karoo Basin in South Africa (Oelofsen and Araujo, 1987).

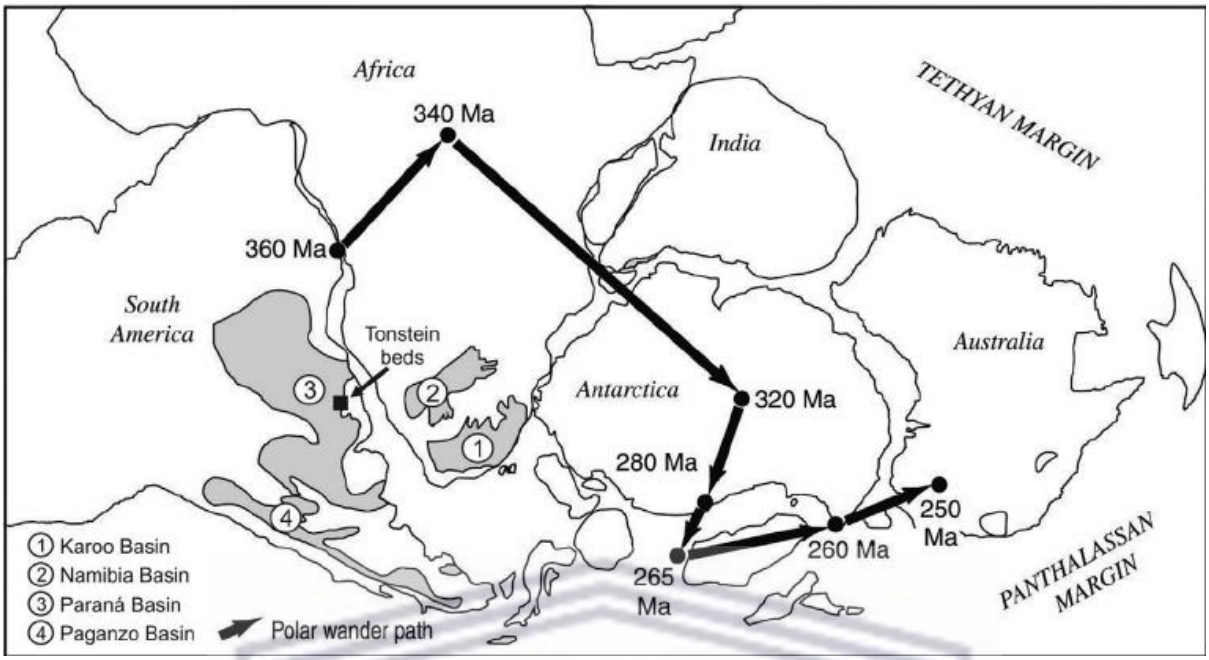

Figure 2.17. Reconstruction of Gondwanaland in the Late Paleozoic showing the Karoo, Namibia, Paraná and Panganzo Basins with polar wander path (after Isbell et al., 2003).

For the Paraná Basin, the Itararé Group, Guatá Group (Rio Bonito and Palermo Formations) and the Irati Formation of the Passa Dois Group will be described (refer Fig. 2.18).

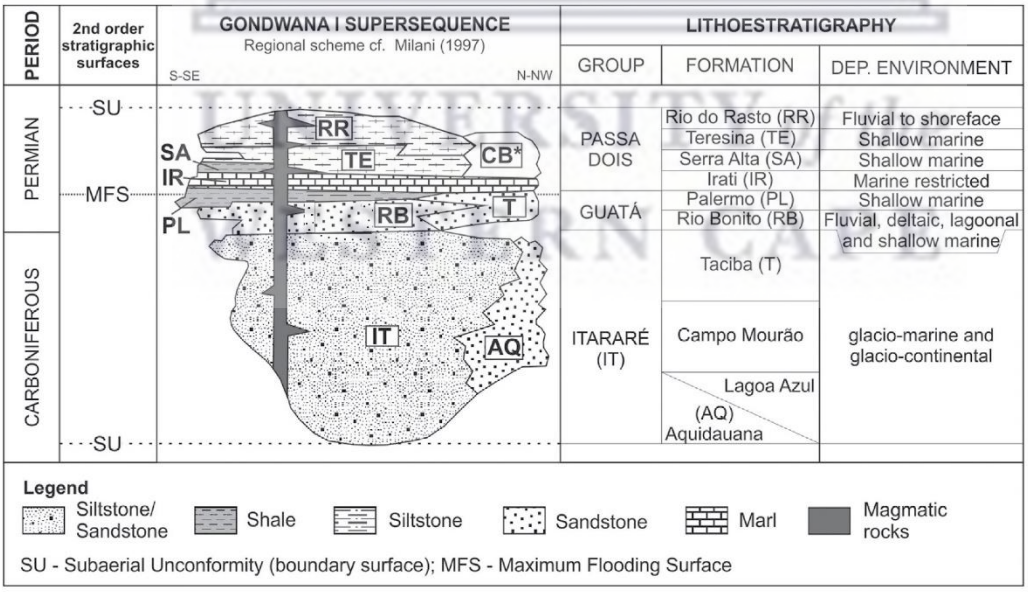

Figure 2.18. Stratigraphic overview of the Carboniferous to Permian Gondwana I Supersequence and lithostratigraphy of the Paraná Basin (after Milani, 1997).

Itararé Group

The Itararé Group lies unconformably on Devonian rocks of the Ponta Grossa and Furnas Formations, and locally over Precambrian basement. It is overlain by Permian glacial sandstones and shales of the Guatá Group.

The maximum thickness of the Itararé Group occurs in the State of São Paulo, where it is about 1300 m (França and Vesely, 2007). Glacial striations are in an N-S or NW - SE direction (Rocha- Campos, 1967; Gesicki et al., 1996), which indicate the direction of glacial movements towards the north and northwest (Veevers, 2004). The Itararé Group is subdivided into three formations namely the basal Lagoa Azul, Campo Mourão, and Taciba Formations (França and Potter, 1991).

Lagoa Azul Formation

This consists of a highly silicified sandstone unit, as well as an extensive pebbly shale known as the Roncador Layer. The Roncador Layer is composed of black to greenish shale and rhythmite containing ice-rafted debris ranging from granule to pebble size. A distinctive brownish colour is seen in outcrop and core suggesting subaerial exposure during the Late Carboniferous (França and Vesely, 2007). Grey to black, slumped and massive diamictites are locally present. Deposition of the Roncador Layer occurred during a maximum flood event that covered basement areas such as São Bento do Sul, where the unit overlies Precambrian granitic rocks. The Lagoa Azul Formation was deposited in a glacio-marine and glacio-continental environment (Cagliari et al., 2014).

Campo Mourão Formation

The Campo Mourão Formation, which overlies the Lagoa Azul Formation, is a sandstone-rich unit interbedded with siltstone, diamictite and rhythmite. Milani (1997) interpreted deposition from a glacio-marine and glacio-continental environment. The Campo Mourão Formation ranges from Stephanian to middle Sakmarian in age. A unique feature of the Campo Mourão Formation is the basal channelized sandstones that fill palaeovalleys, such as the Lapa Channel near the city of Lapa in Paraná State. The lithology of the Lapa Channel consists of massive and stratified sandstone, with conglomerate in the lower sections. This channel is about 65 km long, 2 km wide and 100 m thick (França and Vesely, 2007). Fossil content within the Campo Mourão Formation is poor.

Taciba Formation

The Middle Sakmarian to Artinskian Taciba Formation forms the youngest unit of the Itararé Group. It comprises slumped and massive diamictite throughout the Paraná Basin and interfingers with black shale and rhythmite of the Rio do Sul Member in the south. Gamma ray logs of the Taciba Formation indicate that deposition occurred during a maximum flooding event at the end of the Gondwana glaciation in a glacio-marine and glacio-continental environment (Cagliari et al., 2014).

The Itararé Group is temporally related to the Dwyka Group in the main Karoo Basin (Isbell et al., 2012).

Guatá Group

The Guatá Group overlies the Itararé Group and is considered to be Sakmarian in age (Schneider et al., 1974). The Guatá Group consists of a lower Rio Bonito Formation and an upper Palermo Formation (Fig. 2.18).

Rio Bonito Formation

White (1908) first defined the Rio Bonito Formation as "Rio Bonito layers" but in 1974 a study by Schneider et al. (1974) raised the category to formation. This Formation comprises three members namely, Triúnfo, Paraguaçu, and Siderópolis, which were named by Schneider et al. (1974). Coal layers and post-glacial conglomerates are found at the base of the Triúnfo Member, which has been related to coastal fringes by Christiano-de-Souza and Ricardi-Branco (2015). A wide range of fossil plants, i.e. Glossopteris flora, can be found within the coal layers. The base of the Paraguaçu Member contains fine-grained sandstones associated with calcirudites and the top is predominantly composed of medium- to coarse-grained sandstones alternating with carbonaceous layers (Schneider et al., 1974). The Paraguaçu Member mostly consists of shale and siltstone and some fossil plants have been recorded (Schneider et al., 1974). The Siderópolis Member comprises sandstone, shale and coal.

The Triúnfo Member represents a fluvial-dominated deltaic system, whereas the Siderópolis Member represents a wave-dominated deltaic system with some coastal plain sandstones, shales and coals (Schneider et al., 1974). The intervening Paraguaçu Member coincides with a major regional transgression with the shale and siltstone dominated succession representing deposition in shallow marine, shoreline and lagoonal environments.

The lower boundary of the Rio Bonito Formation represents an erosional surface with the upper boundary being transitional and erosional (Lopes et al., 2003). U-Pb zircon age dating on volcanic tuffs indicates that deposition of the Rio Bonito Formation occurred between latest Sakmarian (290.6 ± 2.8 Ma) and early Kungurian (281.7±3.2 Ma) times (Cagliari, 2014; International Commission on Stratigraphy, 2017). Studies of Carboniferous-Permian deposits in southern Gondwana, including litho-, bio- and sequence-stratigraphy, indicate that the Rio Bonito Formation has been temporally related to the Prince Albert Formation in Namibia (Stollhofen, 1999; Werner, 2006).

Palermo Formation

The Palermo Formation overlies the Rio Bonito Formation and consists of shales, siltstones and silty sandstones, which have been related to the Supersequence Maximum Flooding Surface (Milani, 1997, Fig. 2.18). The Palermo Formation records initially a transgression over the preceding deltas of the Siderópolis Member. The depositional environment has been interpreted as shallow marine, with all lithologies of the Formation, except shales, being intensely bioturbated. The Palermo Formation has a maximum thickness of 300 m.

Passa Dois Group

The Passa Dois Group comprises four formations, namely the Irati, Serra Alta, Teresina and Rio do Rasto formations.

Irati Formation

The Irati Formation conformably overlies the Palermo Formation and consists of abundant organic-rich (carbonaceous) shales and mudstones, which characterize the basal portion of the unit (Taquaral Member). These are overlaid by claystones and siltstones intercalated with

tabular beds of dolomitic limestone (Assistência Member) (Schneider et al., 1974; Araújo et al., 2001; Hachiro et al., 1993; Hachiro, 1996). Sediments of the Irati Formation represents the maximum transgressive flooding event in the Paraná Basin and coincides with its connection to the Panthalassa Ocean (Milani et al., 2007). During deposition of the Irati Formation, the Paraná Basin was a huge (> 1.300 000 km^2), closed, inland, oxic to anoxic body of water (Araújo, 2001), which formed under relatively stable tectonic conditions.

The Irati Formation is of middle Kungurian age, i.e. 278 – 283 Ma (International Commission on Stratigraphy, 2017), based on SHRIMP U- Pb dating of juvenile igneous zircons from volcanic tuffs of 278.4 ± 2.2 Ma (Santos et al., 2006). The Irati Formation is approximately 60 m thick and is correlated with the Whitehill Formation in the Huab, Karasburg and main Karoo Basins and with the Black Rock Member in the Falkland Islands (Faure and Cole, 1999; Fig. 3.4.2) over an area of about 4 million km^2 (Limarino et al., 2014). Fossils such as the impressions of glossoteridales, bivalves and the branches of conifers and trunks permineralized by silica, are present (Schneider et al., 1974). The most important fossils are the mesosaurid reptiles *Mesosaurus brasiliensis* and *Stereosternum tumidum,* which supported correlation of the Irati Formation with the Whitehill Formation (Oelofsen and Araujo, 1987).

2.5.2 Namibia, Africa

The Karasburg, Aranos, Waterberg, Owambo and Huab basins in Namibia have been correlated with the main Karoo Basin of South Africa (Catuneanu et al., 2005). It is beyond the scope of this thesis to review the stratigraphy of all basins in Namibia. However, reliable correlations between the Huab Karasburg and Aranos Basins have been presented in this

thesis. In the Gondwanaland reconstruction, the Huab Basin lies adjacent to the Paraná Basin and probably formed an eastern extension.

2.5.2.1 Huab Basin

The Karoo Supergroup in the Huab Basin attains a maximum thickness of 280 m and is Carboniferous to Permian in age. Strata in of the Huab Basin that are equivalent to the Dwyka Group and lower Ecca Group will be discussed below.

Dwyka Group

Basal Karoo deposits of the Huab Basin consists of rare diamictites in the form of dropstone-bearing shale of lacustrine origin that include thin turbidite units. A matrix-supported diamictite contains clasts ranging in diameter from a few centimetres to several tens of centimetres set in a pelitic to psammitic matrix (Horsthemke et al., 1990). Clasts consist predominantly of quartz, quartzite and schist (Hodgson, 1972). The Dwyka Group attains a maximum thickness of 15 m and unconformably overlies Precambrian basement rocks (Catuneanu et al., 2005).

Verbrandeberg Formation

The Verbrandeberg Formation consists of carbonaceous mudstone, fine-grained sandstone and thin, laterally-restricted coal seams. This succession attains a maximum thickness of 70 m, including a 1.5 m thick basaltic lava (Ledendecker, 1992). Stollhofen (1999) relates the lava to a widespread extensional reactivation of NW-SE to N-S trending basement anisotropy.

Tsarabis Formation

The Tsarabis Formation is characterised by two stacked transgressive cycles; firstly, a laterally-amalgamated, meandering fluvial sandstone unit that grades upwards into a plane bedded foreshore unit containing the marine trace fossil *Siphonichnus* (Jerram et al., 1999). The second transgressive cycle comprises the basal amalgamation of fluvial channel sandstones interfingering with foreshore sandstones. Shoreface sandstones are characterised by hummocky cross stratification and trace fossils.

The Tsarabis Formation contains fossilised wood - *Prototaxoxylon africanum* (Bamford, 2000), which occurs only in the Permian Waterford, Fort Brown and Abrahamskraal Formations of the main Karoo Basin of South Africa (Bamford, 1999). Another species, *Araucarioxylon karooensis,* occurs both within the Tsarabis Formation and the Normandien Formation of the main Karoo Basin (Bamford, 2000).

Huab Formation

The Huab Formation represents shallow marine sediments, i.e. stromatolites, marlstones with microbial mats and flat pebble breccias. Two transgressive cycles have been identified in the Huab Formation (Jerram et al., 1999) with basal shallow water, stromatolite bioherms and overlying kerogeneous multi-coloured marlstones. An extensive fossilised bone bed containing remnants of the *Mesosaurus* reptile is found at the top of the Huab Formation (Oelofsen, 1981). This implies that this unit correlates with the Irati formation in the Paraná Basin and with the Whitehill Formation in the other Namibian basins and the main Karoo Basin of South Africa.

In west Khorixas, Namibia, the fossilised wood *Araucarioxylon africanum* is found within the Huab Formation (Bamford, 2000). This same wood is found within the Normandien Formation (Upper Permian) of the main Karoo Basin.

2.5.2.2 Karasburg Basin

Dwyka Group

The Dwyka Group consists of a basal diamictite overlain by mudstone containing dropstones and fossils. These sediments were deposited during the Late Carboniferous to Early Permian glaciation. In the Karasburg Basin, the Dwyka Group consists of two facies, namely:

1. A red weathering (buff coloured in places) facies, consisting of sandy mudstone, sandstone and siliceous shale with calcareous concretionary masses and lenticular layers of boulder beds. Ripple marks and invertebrate tracks are seen in the sandstones (Anderson, 1975).
2. A dark bluish-grey facies, consisting of dropstone-bearing shale and intercalated layers of boulder-mudstone. Small and large spherical, ellipsoidal phosphatic and calcareous concretions are also present (Werner, 2006).

These two facies were interpreted to originate from two different ice sheets. Facies one was deposited by the Namaland Ice and facies two by the Griqualand/Transvaal Ice (Du Toit, 1921; Haughton and Frommurze, 1927, 1936; Schreuder and Genis, 1975). The thickness of the Dwyka Group in the Karasburg Basin was originally unknown, since the Dwyka-Ecca boundary is not shown on geological maps and the Dwyka Group and Prince Albert Formation are shown as one single unit on these published maps. However, Geiger (1999) mapped the Dwyka-Ecca boundary in a small area opposite Zwartbas, where the Dwyka Group has a total thickness of

145m. SHRIMP U-Pb dating of tuff layers in the basal part of the Dwyka Group yielded an age of 302.3 ± 2.1Ma (Bangert, 2000; Geiger, 2000).

Ecca Group

Prince Albert Formation

In the Karasburg Basin a marker horizon is seen at the Dwyka-Ecca boundary. This horizon comprises several white-weathering, slightly coarser-grained shale units within dark greenish-grey shales. This horizon was termed the 'White Horizon' by Geiger (1999), and is followed by the Owl Gorge Member of Werner (2006).

In the Owl Gorge type locality, the Owl Gorge Member consists of three white weathering shale horizons and attains a thickness of 12.5 m (Werner, 2006). Within this succession are intercalated, thin, diagenetic layers and lenses of bluish-grey to black, phosphatic shale impregnations and light coloured, diagenetic, carbonate concretions and layers. The Owl Gorge Member has been interpreted as a large-scale fining-upward, retrogradational succession (Werner, 2006). Apart from the Owl Gorge Member, the Prince Albert Formation also consists of a bluish- to greenish-grey shale succession at the base. The Prince Albert Formation attains a thickness of about 250 m. The uppermost part of the Prince Albert Formation grades from fissile greenish-grey, silty shales into hard-weathering shales, forming steep cliff-like exposures (Werner, 2006). This coarsening-upward succession is referred to as the Uhabis Member with the Uhabis River Tuff located close to the boundary with the Whitehill Formation.

Werner (2006) dated both the base of the Prince Albert Formation (Owl Gorge tuffs) with a weighted mean $^{206}Pb/^{238}U$ age of 290.0± 1.7 Ma and the uppermost Prince Albert Formation (Uhabis River Tuff) with a weighted mean $^{206}Pb/^{238}U$ age 279.1± 1.5 Ma.

Whitehill Formation

The Whitehill Formation in the Karasburg Basin consists of white-weathering, black carbonaceous shales with a measured thickness of ca. 40 to 45 m (Werner, 2006; Schreuder and Genis, 1975). In outcrop, the Whitehill Formation can be subdivided into three zones. The lower and upper part of the formation has a light, white to bluish-grey weathering colour and the middle part has a dark, olive-green to brownish weathering horizon (Werner, 2006). In the upper 10 metres of the Whitehill Formation, *Mesosaurus* remains were found, with arthropods in the uppermost 1 to 2 metres of fissile shales, and fish remains and plant fragments in the upper part (Werner, 2006). The fissile shales of the uppermost part of the Whitehill Formation are characterised by abundant burrows, which mark the boundary between the Whitehill Formation and overlying Collingham Formation. SHRIMP data for zircons from the Khabus Tuff found in the middle part of the Whitehill Formation, yielded an age of 280.5± 2.1 Ma (Werner, 2006).

2.5.2.3 Aranos Basin

The Aranos Basin is located in the southeastern part of Namibia and forms the westward extension of the Kalahari Basin in Botswana (Johnson et al., 1996; Catuneanu et al., 2005). The Karoo Supergroup is well exposed in the Aranos Basin between Kalkrand and Keetmanshoop and extends eastwards to the border with Botswana along longitude 20°E beneath a cover of Kalahari Group sediments (Fig. 2.19).

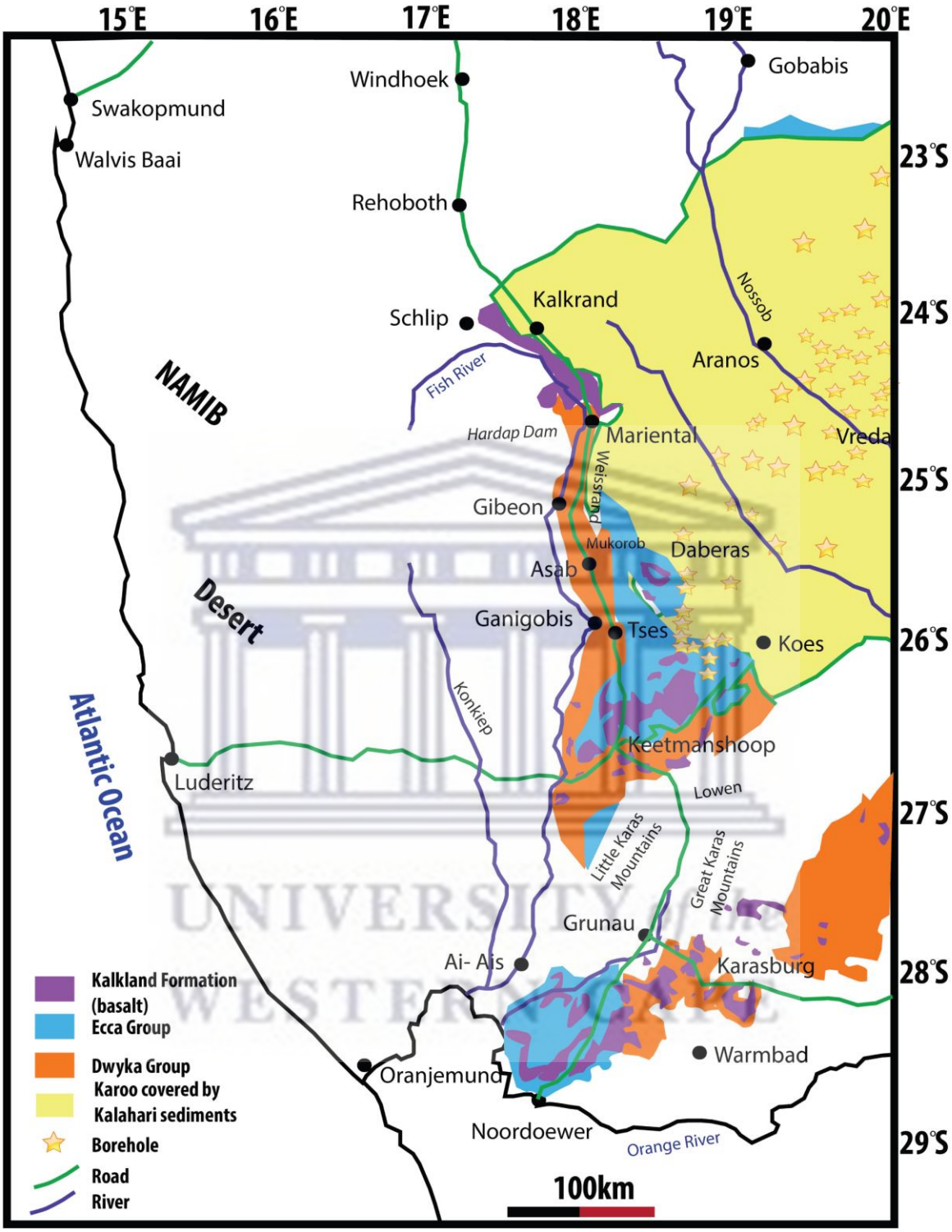

Figure 2.19. Map showing the Karoo Supergroup in the Aranos Basin and in the Karasburg Basin in southern Namibia (from Werner, 2006).

The stratigraphy of the Aranos Basin has been reviewed by Johnson et al. (1996) and Catuneanu et al. (2005), but is described in detail by Werner (2006). There is a westward

lateral change in lithofacies across the basin from a proximal to a distal depositional setting accompanied by a change in lithostratigraphy (Fig. 2.20).

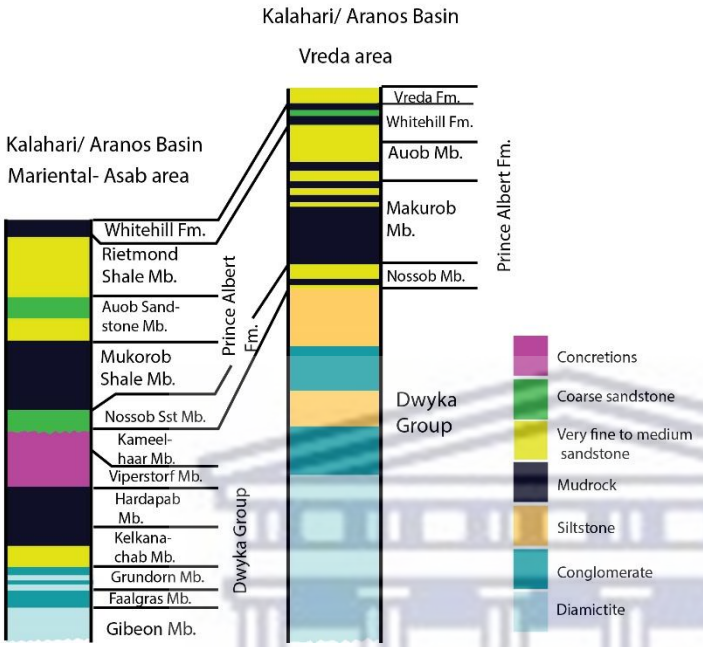

Figure 2.20. Correlation panel of the Kalahari Basin in the Mariental- Asab area and the Vreda area (modified after Johnson et al., 1996).

Dwyka Group

In southern Namibia, sedimentation of the Dwyka Group started in the late Carboniferous (Bangert et al., 1999). The Dwyka Group consists of glaciogenic sediments, which unconformably overlie Cambrian shales and quartzites of the Nama Group (Himmler et al., 2008). The Dwyka Group was deposited in a NW-SE striking, intracontinental rift basin, which developed during the rifting of the South Atlantic margin (Stollhofen, 1999), although Catuneanu et al. (2005) proposed deposition in a sag-type basin that formed due to the release of heat following the formation of Karoo rift basins in eastern Africa. Following Werner (2006), the Dwyka Group has been divided into three members, which from base

upwards are the Gibeon Tillite, the Ganigobis Shale and the Tses Boulder- Mudstone members (Fig. 2.21; Werner, 2006).

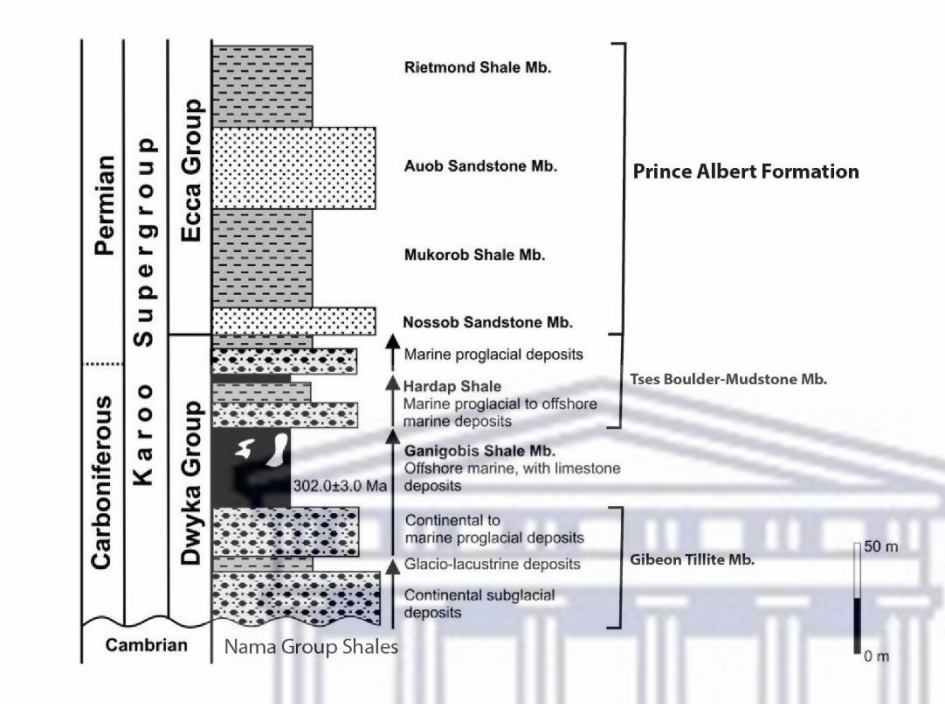

Figure 2.21. Stratigraphic log of the Mariental- Keetmanshoop area showing the Dwyka Group and Prince Albert Formation (modified after Himmler et al., 2008).

Gibeon Tillite Member

In Figure 2.21, the basal unit, the Gibeon Tillite attains a maximum thickness of about 30 m consisting predominately of diamictite with minor sandstone and shale interbeds. The diamictite represents a continental subglacial depositional environment, whereas the sandstone and mudstone represent esker, continental to marine proglacial and glacio-lacustrine environments (Werner, 2006).

Ganigobis Shale Member

The overlying Ganigobis Shale Member is 80 m thick and consists of dark coloured, slightly carbonaceous shale with minor dropstones in places (Himmler et al., 2008). These shales

contain ash-fall tuff layers, which yielded a $^{206}Pb/^{238}U$ age of 302.0 ± 3.0 Ma (Bangert et al., 1999). Phosphatic concretions consisting of minute, spherical radiolarian and palaeoniscoid fish remains, characterise the basal unit of the Ganigobis Shale Member. The top unit is characterised by limestone deposits with abundant tubular-sized (algal mounds) fossils of 1.5 mm in diameter (Himmler et al., 2008).

Tses Boulder- Mudstone Member

The Tses Boulder- Mudstone Member consists of four units (Fig. 2.21). The lowest unit consists of marine proglacial and debris rain-out diamictite and thick, massive or cross bedded sandstone deposited by gravity flow. Overlying this unit, is the 75 m-thick Hardap Shale, characterised by dropstone-rich, sandy mudstone with an upward decrease in sand and dropstone content (Stollhofen et al., 2000). The Hardap Shale unit is also characterised by its marine fossil content and has been related to the Gondwana-wide *Eurydesma* transgression (Bangert et al., 1999). The third unit consists of a basal layer of gravity-flow sandstones and dropstone-bearing mudstones followed by a layer of plane-bedded, offshore, marine mudstones with no dropstones present. The 70 m-thick uppermost unit consists of gravity flow sandstones termed the Tses sandstone (Werner, 2006), dropstone-bearing sandy mudstone overlain by greenish, dropstone-poor mudstone with thin, sandy, turbidite interbeds (Stollhofen et al., 2000). The Tses Boulder- Mudstone Member is conformably overlain by the Prince Albert Formation (Fig. 2.21).

Prince Albert Formation

The Prince Albert Formation is exposed in the Mariental – Keetmanshoop area, where it comprises from base upwards, the Nossob Sandstone, Mukorob Shale, Auob Sandstone and

Rietmond Shale Members (Johnson et al., 1996; Werner, 2006; Himmler et al., 2008). However, there is a lateral lithofacies change between Vreda in the east and Mariental – Asab in the west. The result is that the upper part of the Auob Sandstone Member grades westward into the Rietmond Shale Member.

Nossob Sandstone Member

There is a gradation from the Dwyka Group (Tses Boulder- Mudstone Member) into the Prince Albert Formation, as indicated by the presence, in places, of dropstones in the basal part of the Mukorob Shale Member above the Nossob Sandstone Member (Fig. 2.21; Werner, 2006). Outcrop thicknesses of the Nossob Sandstone Member range from 1 m to 25 m, but in core, they are between 20 m and 40 m. In the northern part of the Aranos Basin, the Nossob Sandstone Member consists of a proximal facies characterised by a fluvially-dominated delta, whereas in the south, a distal facies is present, characterised by storm-wave and basin floor turbidite deposits (Werner, 2006). A conglomeratic base is seen in some places containing *Eurydesma* shells (Grill, 1997). The Nossab Sandstone Member is capped by pebbly, medium- to coarse-grained sandstones with trough and ripple cross-lamination and carbonate concretions in places. These sandstones represent delta-plain, distributary channel deposits (Stollhofen et al., 2000).

Mukorob Shale Member

The argillaceous Mukorob Shale Member consists of laminated, dropstone-free mudstone indicative of offshore marine deposits. Stollhofen et al. (2000) have identified thin tuff layers in the upper part of this member. In the Mariental and Keetmanshoop area, outcrops of the Mukorob Shale Member consist of dark grey to slightly green claystone and siltstone

interbedded with fine-grained sandstone (Werner, 2006). Between Mariental and Asab, a thickness of 60 m to 90 m has been recorded (Heath, 1972). In the Aranos area, the Mukorob Shale Member consists of dark grey to green shales in the lower part of the succession attaining a maximum thickness of 63 m. In the upper part, a thin limestone unit is sandwiched between the lower shale and overlying sandy unit. This sandy unit consists of shale, siltstone and sandstone in a coarsening-upward sequence.

Auob Sandstone Member

The Auob Sandstone Member conformably overlies the Mukorob Shale Member. The lower part of the Auob Sandstone Member comprises a proximal to distal, marine, delta-front, turbiditic sandstone with thin layers of mudstone. This is overlain by plane-bedded to hummocky cross-bedded and bioturbated sandstones deposited in a marine shoreface and longshore environment (Werner, 2006). In the upper part, large lenticular, medium- to coarse-grained, trough cross-bedded sandstones are present, which have been interpreted as delta plain, distributary channel deposits (Stollhofen et al., 2000; Werner, 2006). Dark carbonaceous mudstones interbedded with ripple cross-bedded sandstones are present in the upper unit. In places, above the channel deposits, reddish-coloured, sandy siltstones and lenticular fine-grained sandstones are present (Grill, 1997). The thickness of the Auob Sandstone Member ranges from 14 m to 60 m (Heath, 1972; Grill, 1997; Werner, 2006). In the Aranos - Vreda area, two coal seams have been identified in the Auob Sandstone Member from borehole core (Kingsley, 1985; Werner, 2006). The main coal seam, named the Impala Coal Seam (Kingsley, 1985), lies about 30 m above the base of the member, and the upper coal zone in the Mariental – Koës – Keetmanshoop area (Kingsley, 1985), occurs 50 m higher in the succession (Cairncross, 2001). The coals originated from peat swamps located behind

beach barriers on the lower delta plain (Kingsley, 1985). The upper coal zone grades into carbonaceous shale and limestone of the Whitehill Formation in the vicinity of Koës (Kingsley, 1985).

Rietmond Shale Member

The Rietmond Shale Member is the uppermost member of the Prince Albert Formation and is only present in the Mariental – Koës – Keetmanshoop area (Kingsley, 1985). It attains a maximum thickness of 150 m (Werner, 2006). It consists of a basal mudstone and fine-grained sandstone unit deposited in a prodelta environment, overlain by thin layers of normally graded sandstones interpreted as proximal to distal, marine, delta-front turbidites. These are followed by a 25 m-thick marine shoreface and longshore deposit of typically cross-bedded sandstones (Stollhofen et al., 2000). The latter unit is overlain by a 100 m thick pro-delta mudstone and fine-grained sandstone deposit.

Whitehill Formation

The Whitehill Formation is present in the Mariental – Koës – Keetmanshoop area, both in outcrop and subsurface and is laterally-equivalent to the uppermost part of the Auob Sandstone Member centred on the Upper Coal Seam east of approximately longitude 19°E (Fig. 2.19; Kingsley, 1985; Werner, 2006). *Mesosaurus* remains, arthropods, fish remains, plant fragments and burrows have been found within the Whitehill Formation (Werner, 2006). Werner (2006) identified six different facies for the Whitehill Formation characteristic for individual regions in southern Namibia. These facies will be described from south to north.

Aussenkjer-Noordoewer facies

This facies is found in the southernmost part of Namibia in the Noordoewer-Karasburg area. It consists of black shales and in outcrop, a light white to bluish-grey weathered coloured shale and dark, olive green to brownish weathered shale (Werner, 2006). The Aussenkjer-Noordoewer succession overlies the Prince Albert Formation with a thickness of between 40 and 45 m (Werner, 2006).

Gellap facies

The Gellap facies consists predominantly of carbonaceous, bluish-greenish-grey, silty shales interbedded with cherty layers in places. The Gellap facies overlies the Prince Albert Formation which is the Gellap Plateau, about 25 km eastnortheast of Keetmanshoop (Werner, 2006). A 10 cm-thick sandstone bed is present about 15 m above the basal contact, and *Mesosaurus* remains are found in the upper parts of the succession (Werner, 2006). The Whitehill Formation attains a thickness of about 110 m in the Gellap area.

Goris facies

The Goris Whitehill facies attains a thickness between 55 m and 65 m, and is dominated by black carbonaceous shale. This succession is found in the northeastern area of Keetmanshoop within the upper half of the Whitehill Formation (Werner, 2006). In places, weathering and contact metamorphism with hydrothermal alteration, have decoloured the rock to various lighter shades. Carbonate concretions, thin brownish ferruginous horizons and a mappable limestone horizon are present. Fossils of *Mesosaurus*, *Notocaris tapscotti* and fish remains occur within this facies (Werner, 2006).

Panorama facies

The basal unit of the Panorama facies consists of bluish to greenish grey shale and mudrock, grading upward into light brownish, buff-weathered, slightly coarser-grained siltstone. The upper part of this facies typifies the main characteristic of the Whitehill Formation, i.e. its distinctive white-weathering shales. These grade upward into dark carbonaceous, bluish-grey, weathered shales and tuffaceous beds. In the lower part of this succession, a dolomitic limestone horizon has been linked to the Goris facies (Werner, 2006). A total thickness of 50 to 60 m of the Panorama facies has been measured by Werner (2006).

Mukorob-Daberas facies

In the Mukorob National Monument area, the Mukorob-Dabera facies overlies a siltstone-sandstone succession of the Auob Sandstone Member of the Prince Albert Formation. Werner (2006) observed three lithological units in the Daberas area: 1) An interbedded unit of dark grey shale and black limestone, which weathers to a light bluish-grey colour, followed by: 2) Buff-weathered, laminated, siltstone, and 3) Light grey shale. Brandt et al. (1961) observed carbonaceous, black pyritic shales from boreholes drilled in the Daberas area. *Mesosaurus* remains have been found in parts of this succession (Werner, 2006)

Aranos Whitehill facies

The Aranos Whitehill facies of Werner (2006) is not strictly part of the Whitehill Formation by definition, but marks the transition into the uppermost part of the Auob Sandstone Member of the underlying Prince Albert Formation in the eastern part of the basin. Within the Auob Sandstone Member, the Impala Coal Seam is overlain by a 10 m-thick, shoreface/tidal

succession of sandstones and siltstones, followed by an approximately 23 m-thick succession of channel mouth bar and crevasse splay sandstones. These are capped by an upper coal-bearing zone interbedded with sandstone that is equivalent to the Upper Coal Seam (Kingsley, 1985).

2.5.3 Falkland Islands

Before the break up of Gondwanaland started during the Middle to Late Jurassic and again, in the Early Cretaceous, the Falkland Islands were located off southeast Africa (Ben- Avraham et al., 1993). On structural and stratigraphic grounds, Adie (1952a) fitted an inverted Falkland Islands off the Transkei coast, between latitudes 33° and 34° S, to complete the truncated Karoo Basin and Cape Fold Belt. To match up with the stratigraphic units of the Karoo Supergroup, as well as the Cape Fold Belt, thereby completing the "missing" southeast corner of the main Karoo Basin. This location of an inverted Falkland Islands off southeast Africa was supported from palaeomagnetic studies on Early Jurassic dolerite dykes by Mitchell et al. (1986) and Taylor and Shaw (1989). The presence of abundant dolerite dykes and lack of a fold belt on the inverted West Falkland Island led Hyam (1998) to displace this island about 100 km northeast along the Falkland Sound Fault that separates the two islands, thereby positioning West Falkland north of the "dolerite line" in the adjacent main Karoo Basin.

In this section on the Falkland Islands, only the post- Devonian Fitzroy Tillite and Port Sussex Formation will be discussed and related to the Karoo stratigraphy in the adjacent main Karoo Basin of the Eastern Cape Province of South Africa (Table 2.5).

Table 2.5. Stratigraphic equivalence of lithological units in the Falkland Islands and South Africa (after Trewin et al., 2002).

South Africa, Ecca Pass		**Falklands**	
Formation	*Member*	*Member*	*Formation*
Koonap		Egg Harbour	Bay of Harbours
Fort Brown		Praltos	
		Saladero	Brenton Loch
Ripon	Trumpeters	Cantera	
	Wonderfontein		
	Pluto's Vale	Terra Motas	
Collingham		Shepherds Brook	Port Sussex
Whitehill		Black Rock	
Prince Albert	(basal part only)	Hells Kitchen	
Dwyka Group		(undifferentiated)	Fitzroy Tillite
	Unnamed mud units	Quark Pond and unnamed mud unit	
		(undifferentiated)	

Fitzroy Tillite Formation

The Fitzroy Tillite Formation consists of clast-poor diamictite ranging between 610 m and 900 m thick, with a sandy mudstone matrix comprising 50 – 95% of the entire rock (Aldiss and Edwards, 1999). Clasts are mainly quartzite and granite ranging up to cobble size on East Falkland and up to boulder size on West Falkland (Frakes and Crowell, 1967). Facies on West Falkland include interbedded ribbon-shaped sandstones, which have been interpreted as eskers and a probable terrestrial environment (Trewin et al., 2002). Facies on East Falkland consist of pebbly sandstones, which have been interpreted as subaqueous debris flows. A submarine slope was suggested by Frakes and Crowell (1967) in the vicinity of the present-day Falkland Sound Fault.

The Quark Pond Member (Table 2.5), a mappable unit of the Fitzroy Tillite Formation, up to 7 m thick, consists of bedded diamictite, laminated shale and mudstone with dropstones, and

lies within the upper part of the formation in West Falkland (Scasso and Mendia, 1985; Aldiss and Edwards, 1999). A laminated siltstone unit, containing the trace fossil *Umfolozia,* occurs near the base of the Fitzroy Tillite Formation at Carcass Bay, West Falkland. The Quark Pond Member and the siltstone unit at Carcass Bay are comparable to a thin shale deposit in the Dwyka Group diamictite at Swart Umfolozi in KwaZulu-Natal Province, South Africa (Savage, 1971), from which the trace fossil *Umfolozia* has been described (Anderson, 1976, 1981).

The Fitzroy Tillite Formation has been interpreted as a glacial deposit where its extensive and continuous nature suggests a dominantly subaqueous origin. According to Visser (1989), deposition of the Dwyka Group in South Africa was deposited from a sub-polar marine ice sheet which was primarily grounded and later developed into a floating ice sheet before the disintegration stage. Ice flow was in a westerly direction in the Eastern Cape, which correlates with the direction in the restored, inverted Falklands, where flow was from the east (Fig. 2.22, Visser, 1987). Trewin et al. (2002) suggests that the Quark Pond Member has possible regional significance and represents the *Eurydesma* (Sakmarian) transgression, which was an Early Permian global event. This event could be correlated with a similar mudrock unit in the Dwyka Group in the southern Karoo (Visser, 1993).

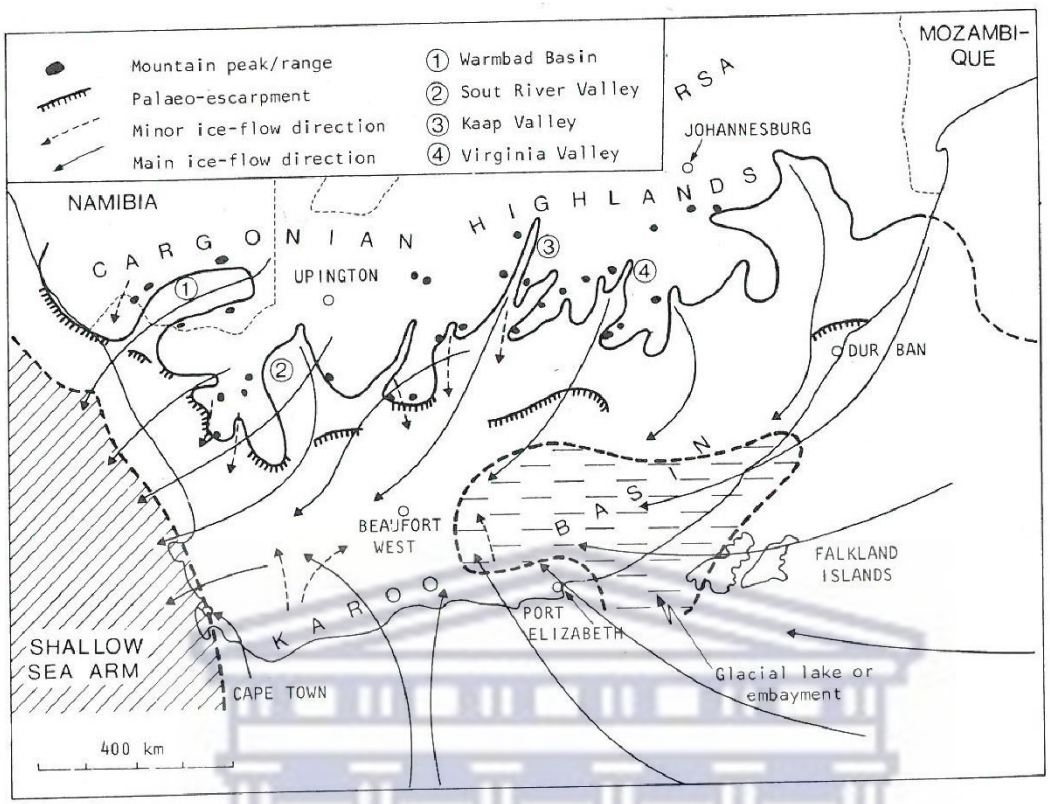

Figure 2.22. Outline of main Karoo Basin during maximum glaciation. Palaeoice-flow directions based on striated pavements, palaeotopography, glacio-tectonic features, and facies changes and clast composition of the glacial deposits (after Visser, 1987).

Port Sussex Formation

In Table 2.5, Port Sussex Formation is subdivided into three members, namely the Hells Kitchen, Black Rock and Shepherds Brook. However, focus will remain on the Hells Kitchen and Black Rock members in this thesis.

Hells Kitchen Member

The Hells Kitchen Member overlies the Fitzroy Tillite on a sharp undulating boundary, with a local relief of 0.25 m. This member consists of thin interbeds of sandy mudstone and laminated fine- to medium-grained sandstone, which contain granules and pebbles that were

deposited as dropstones (Trewin et al., 2002). The Hells Kitchen Member ranges in thickness from about 4.5 m at Port Sussex, 3.5 m to 6 m near Mount Pleasant and possibly 10 m at Shell Point. At Shell Point, the member consists of a coarsening-upwards cycle grading from black fissile mudstone to sandstone with pebbles. Trewin et al. (2002) interprets the Hells Kitchen Member as a subaqueous deposit, which represents a rapid change in depositional environment from glacial conditions. The surface contact between the Hells Kitchen Member and the Fitzroy Tillite Formation represents an erosional event, which probably occurred under very shallow, water conditions. The sandstone unit formed under proglacial conditions in a shallow marine environment, possibly linked to deglaciation (Trewin et al., 2002).

Black Rock Member

This member consists of two alternating facies:

1. A black or very dark grey laminated mudstone weathering to a paper shale and

2. A siliceous mudstone that weathers purple with a sub-conchoidal fracture.

Facies one contains pyrite and weathers to a white colour on inland exposures, similar to the Whitehill Formation. On East Falkland (Fig. 2.23), Facies one is intrafolially deformed everywhere and appears to have acted as a decollement level, which causes difficulty in measuring its thickness (Trewin et al., 2002). Frakes and Crowell (1967), estimated a thickness of 125 m for Facies one, but Trewin et al., (2002) considered thick thickness to be regarded as a minimum.

TOC (total organic carbon) values for the Black Rock Member range from 0.5% to 1.5% in the east to over 40% in the Port Sussex area (Trewin et al., 2002). Facies of the Black Rock Member continue as interbeds into the basal part of the overlying Shepherds Brook

Member and lower parts of the Terra Motas Member (refer Table 2.5). At Port Sussex East Falkland, thin green bentonitic mudstone beds occur within the Black Rock Member and also in the lowermost part within black shales overlying the diamictite in the Carcass Bay area, West Falkland (Fig. 2.23).

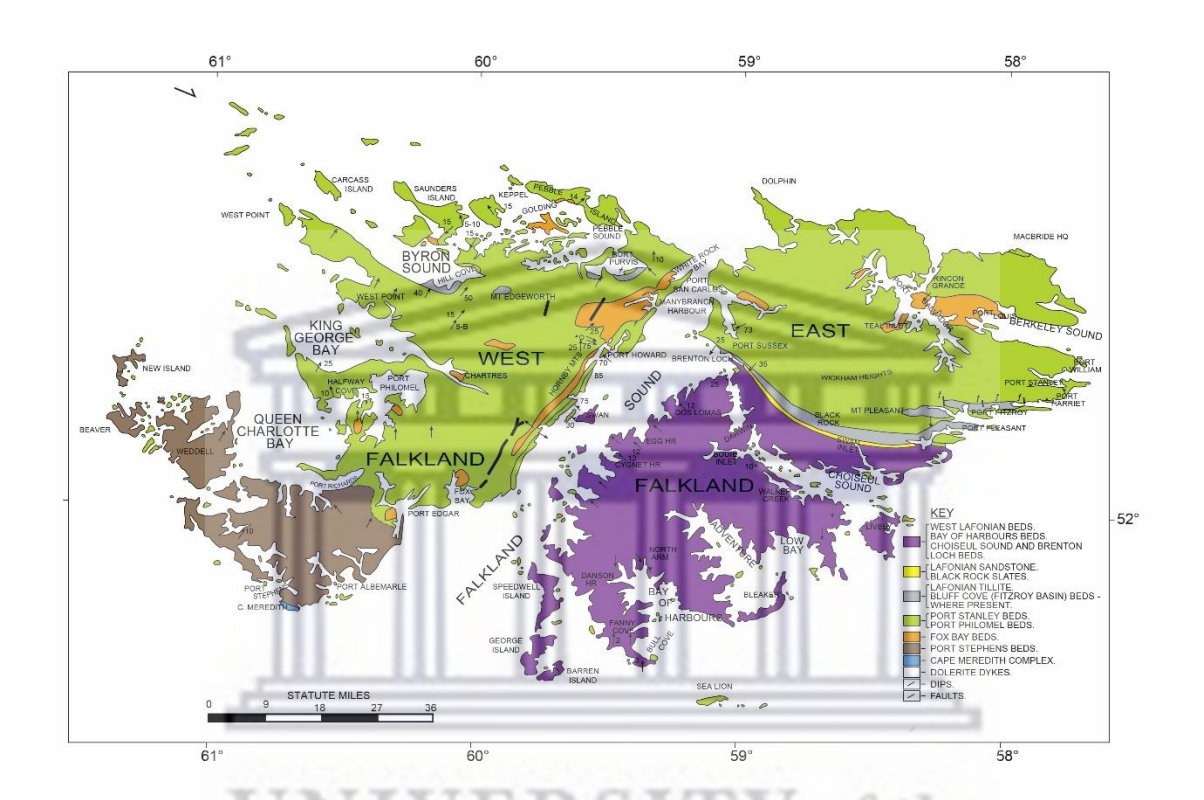

Figure 2.23. Geological map of the Falkland Islands (modified after Adie, 1958).

Deposition of the Black Rock Member occurred under underwent anoxic conditions related to high sea levels. This member has been correlated with the Whitehill Formation in South Africa (Adie, 1952b), as well as the Irati Formation in Brazil (Oelofsen, 1987). In South Africa, there is no evidence that a marine environment existed in at the eastern part of the main Karoo Basin, leading to Trewin et al. (2002) suggesting that the lateral variability of the Black Rock Member is due to its basinal marginal position.

2.5.4 Antarctica

With the formation of Gondwanaland, Antarctica was located southeast of the African continent, occupying both the Panthalassan margin and the East Antarctic craton. Several basins are present, namely the Ellsworth Mountains, Heimefrontfjella- Dronning Maud Land and the Transantarctic Basin. The Permian sedimentary strata of the Ellsworth Mountains (West Antarctica), Heimefrontfjella (East Antarctica) and the Transantarctic Mountains (Central Antarctica) will be discussed in detail, together with their similarities to the main Karoo Basin of South Africa (Fig. 2.24).

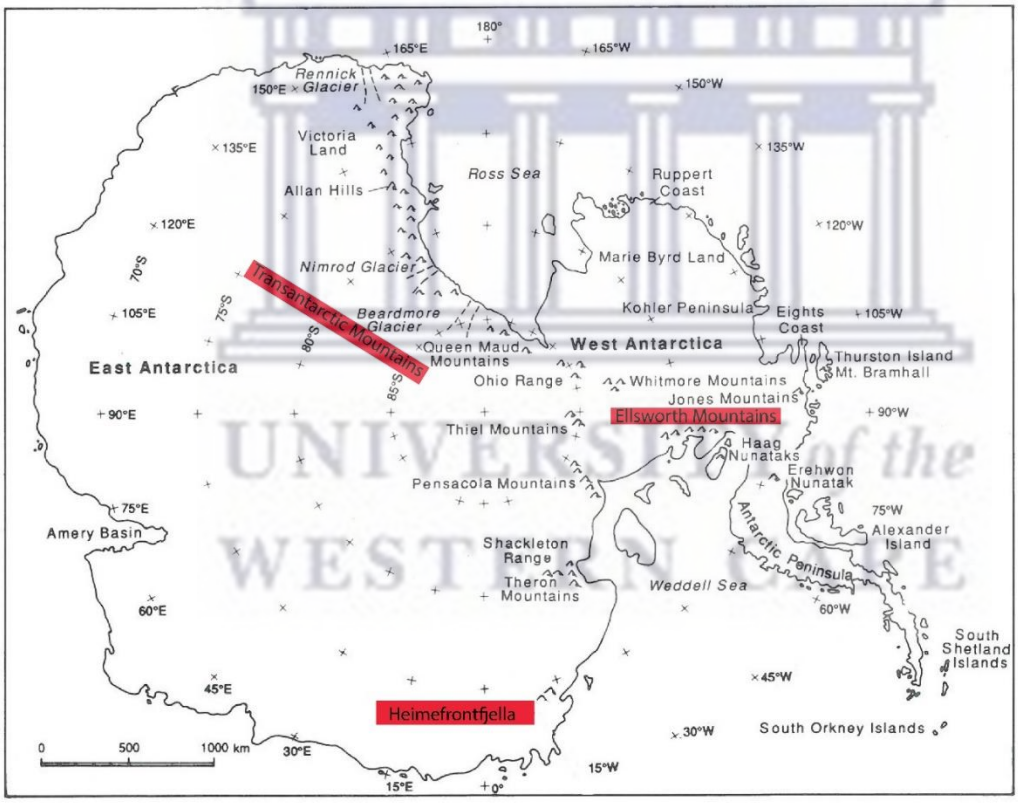

Figure 2.24. Map of Antarctica, highlighting the Ellsworth Mountains, Transantarctic Mountains and Heimefrontfjella in red (after Collinson et al., 1994).

2.5.4.1 Ellsworth Mountains (West Antarctica)

The stratigraphic sequence of the Ellsworth Mountains has a thickness of about 13 km (Fig. 2.25) ranging from Cambrian to Permian in age (Webers et al., 1992). Strata underlying the Permo-Carboniferous, Karoo-equivalent succession comprise the majority of the sequence in the Ellsworth Mountains. These begin with the lowermost Heritage Group, up to 7.6 km thick, consisting of shales, mudstones, siltstones, conglomerates, volcanics and sandstones. The overlying 3 km-thick Crashsite Group comprises quartz- rich sandstones of Upper Cambrian to Devonian age (Webers et al., 1992). Overlying the Crashsite Group is the Mount Wyatt Earp Formation (Fig. 2.25) consisting of sandstone with a brachiopod fauna. The Permo-Carboniferous succession is described below.

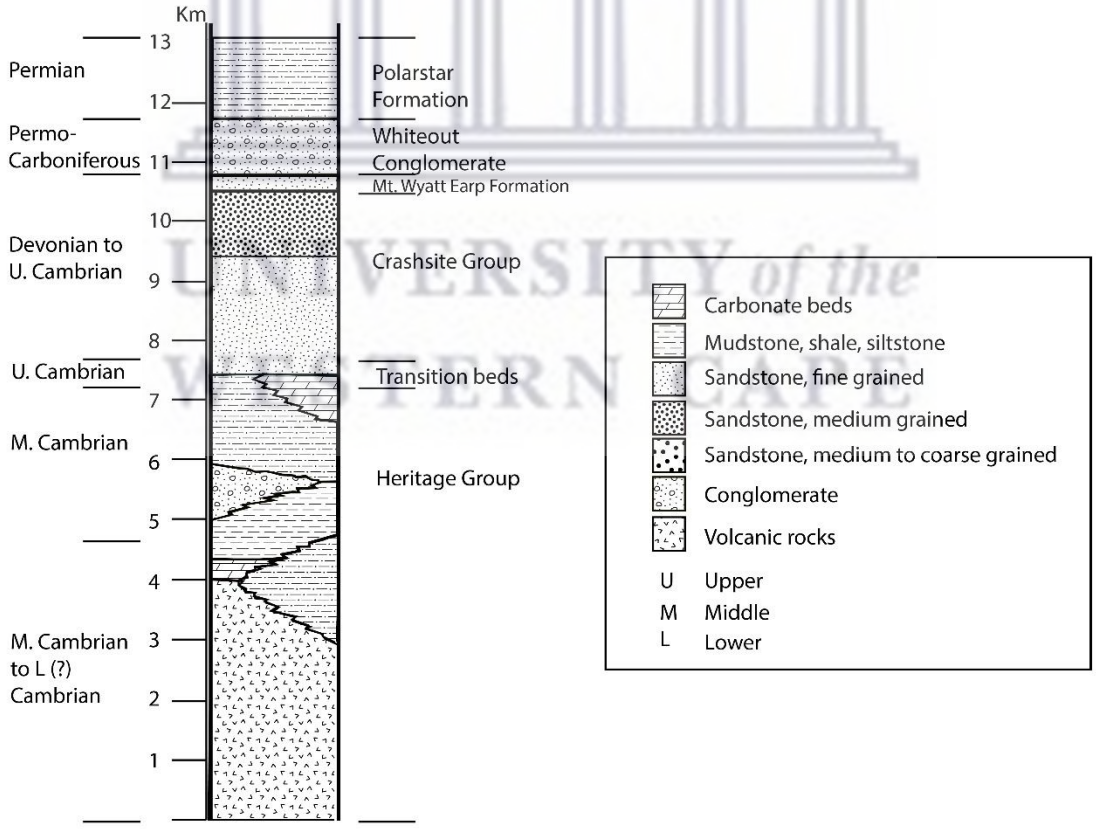

Figure 2.25. Stratigraphic sequence of the Ellsworth Mountains (after Webers et al., 1992).

Whiteout Conglomerate

The Whiteout Conglomerate is up to a 1000 m thick and consists of diamictite with abundant dropstones (Matsch and Ojakangas, 1992). In Figure 2.25, the Whiteout Conglomerate beds are overlain conformably by the Permian Polarstar Formation, containing *Glossopteris* flora in the upper part (Collinson et al., 1992).

Polarstar Formation

The Polarstar Formation is the youngest strata of the Ellsworth Mountains overlying the Whiteout Conglomerate (Fig. 2.25). In the basal part of the Polarstar Formation, fine- grained beds containing granules and pebbles of quartz (dropstones) are present, and were interpreted by Collinson et al. (1992) as residual ice-rafted, debris deposits. Based on several measured sections, Elliot et al. (2016) estimated a minimum thickness of 1.2 km for the Polarstar Formation. Three facies are present within this unit namely:

Facies 1: A basal argillite facies

Facies 2: A mixed sandstone- argillite facies

Facies 3: A *Glossopteris*- bearing coal facies at the top.

Sandstones in this unit are mainly volcaniclastic with tuffs present locally. Detrital zircon grains of sandstone samples indicate a Permian age for the Polarstar Formation (Elliot et al., 2016; Craddock et al., 2017). The most dominant U- Pb zircon age of the Polarstar Formation is about 270 Ma. Craddock et al. (2017) calculated an average depositional age of 263.4 ±1.4 Ma of zircon grains from the Polarstar Formation. Tuff beds within the formation indicate active volcanism of a magmatic arc. Samples taken from Facies 1, yields a depositional age of

268.9 ±1.4 Ma (lowest Guadalupian) and in Facies 2 an age of ~258.0 ±2.1 Ma for a tuff bed and ~260 Ma as a maximum age of deposition for sandstone (Elliot et al., 2016). Collinson et al. (1992) interprets the Polarstar Formation, as a sequence of distal fine-grained deposits merging upward into delta-front deposits and then delta-top deposits.

Structural and paleomagnetic data (Watts and Bramall, 1981; Grunow et al., 1987; Curtis, 2001; Randall and MacNiocaill, 2004) suggest that the Ellsworth- Whitmore block should have been situated adjacent to Coats Land and outboard of the Gondwana structural front observed in the Eastern Cape or Falkland Islands and the Pensacola Mountains (Elliot et al., 2016). Early Paleozoic studies by Curtis (2001), suggest that the Ellsworth Mountains might have been involved in Cambrian back-arc extension during the Gondwana Orogeny. The latter is supported by pre-glacial strata of the Ellsworth Mountains which are more similar to the Cape Supergroup and West Falkland Group. The Polarstar Formation has been linked to the Victoria Group in the central Transantarctic Mountains of the Transantarctic Basin based on paleocurrent data (Collinson et al., 1994).

2.5.4.2 Heimefrontjella, western Dronning Maud Land (East Antarctica)

Permian sedimentary cover is well preserved in northern Heimefrontfjella, East Antarctica. Sedimentary strata of Heimefrontfjella forms part of the Upper Palaeozoic Beacon Supergroup (McKelvey et al., 1970) with equivalents in western Dronning Maud Land. Well preserved micro- and macro-flora found within these sedimentary layers suggests an early Permian age, i.e. Asselian to Artinskian (~290 Ma) (Larsson et al., 1990; Lindström, 1995) as opposed to Proterozoic-Cambrian age detrital zircons dated by Veevers and Saeed (2007).

The early Permian sedimentary cover of Heimefrontfjella has a maximum thickness of 160 m preserved at Schivestolen (Bauer, 2009).

Previously, sedimentary strata in western Dronning Maud Land have been named the Amelang Plateau Formation in Kirwanveggen (Wolmarans and Kent, 1982). The Amelang Plateau Formation has been studied in detailed in the Schivestolen section, with three recognizable facies (Poscher, 1994) mentioned below:

Facies 1: A basal diamictite

Facies 1 consists mainly of sub-angular gneiss boulders ranging up to 50 cm in size with thin silt lenses and sandy layers. This unit ranges between 80 and 300 cm thick depending on the pre-depositional topography (Bauer, 2009). Deposition of Facies 1 has been interpreted as glacial (Larsson and Bylund, 1988; Poscher, 1988, 1992, 1994; Bauer, 2009) based on glacially-abraded contacts with the striated basement and striated and faceted clasts in the diamictites. Palaeo- ice flow measurements (335º± 10º) were measured from striated basement at Haukelandnuten (Bauer, 2009).

Facies 2: An overlying dropstone-bearing siltstone

Facies 2 has a thickness of 12 m consisting of stratified siltstones and pale micaceous sandstones. Deposition seems to change from glacial to periglacial due to a decrease of dropstones and an increase of phytoclasts towards the top of the unit (Bauer, 2009).

Facies 3: The top coal-bearing sandstone facies

A measured section in the Schivestolen area consists of 140 m of light brown to white, feldspar-rich sandstones with thin coal seams (Bauer, 2009). Facies 3 is characterised by

fluvial fining upward sequences of cross bedded sandstones and coaly-shales or coal seams; channel deposits filled with reworked sediments and conglomerates (Poscher, 1988). The coals are sub-bituminous made up of 45% vitrinite, 46% inertinite and 9% liptinite (Bauer et al., 1997). In the vicinity of a Jurassic-aged basalt sill, coal ranks increase to meta-anthracite. Bauer (2009) has interpreted Facies 3 as a fluviatile to marginal marine deposit with coaly-shales or coal seams forming in swamps within an alluvial or outwash plain.

According to Theron and Blignault (1975), the Amelang Plateau Formation relates to glacial withdrawal sequences subsequent to Gondwana glaciation, comparable to cycles of the Dwyka Group in South Africa. Based on the common age (early Permian) and lithofacies of Heimefrontfjella a linkage could be made with the Dwyka Group, Pietemaritzburg and Vryheid Formation of the main Karoo Basin.

2.5.4.3 Transantarctic Basin (Central Antarctica)

Victoria Land

Metschel Tillite

In southern Victoria Land, Early Permian to Carboniferous glacial deposits of the Metschel Tillites are up to 80 m thick (Barrett and Kyle, 1975; Collinson et al., 1994). In northern Victoria Land, a 350 m thick unnamed diamictite- bearing unit is present (Laird and Bradshaw, 1981).

Weller Coal Measures

In Victoria Land Weller Coal Measures overlies the Metschel Tillite comprising of sandstones which are subdivided into two facies, namely 1) coarser braided stream facies and 2) a finer meandering stream facies. Carbonaceous shales and coal within this unit are associated with meandering stream facies which occurs more inland (Collinson et al., 1994). The lower part of

the formation comprises of fining upward cycles of trough cross-bedded, medium- to fine-grained sandstone, carbonaceous siltstone to mudstone and coal. Collinson et al. (1983) characterises these sandstone units based on large- scale lateral accretion and erosional bases. Sandstone units in the upper part of the Weller Coal Measures become coarser and contain sand-filled channels and reactivation surfaces overlain by mudstone drapes characteristic of braided stream deposits (Isbell et al., 1990). This unit is of Early Late Permian age and Late Permian sedimentary rocks are missing in Victoria Land.

Central Transantarctic Mountains

Central Antarctica comprises of 1200 to 1000 Ma cratons set in a matrix of 700 to 500 Ma fold belts which allowed provenance of sediment to take place during the terminal amalgamation of Pangea to provide sediment during the Permian and Triassic (Veevers and Saeed, 2007).

Pagoda Formation

Lower Permian glacial strata of the Pagoda Formation forms the basal unit of the Victoria Group comprising of sequences of diamictite, sandstone and mudstone with thicknesses between 0 and 395 m, but are generally 100 to 200 m thick (Collinson et al., 1994). Diamictites are associated with striated surfaces. In the Beardmore Glacier region, cyclical sequences were interpreted by Miller (1989) as retreats of the ice front in glacial, proglacial- fluvial and glacial- lacustrine environments.

Mackellar Formation

Glacial beds in the Central Transantarctic Mountains are overlain by the Mackellar Formation. This formation consists of one to three coarsening upward cycles of interbedded shale and

fine-grained sandstone, ranging between 60 and 150 m thick. Deposition of Mackellar beds occurred in a brackish to marine environment (Miller and Collinson, 1994; Jackson et al., 2012). Collinson et al. (1994) interpreted upward- fining sandstone beds as turbidites.

Fairchild Formation

The Mackellar Formation is overlain by deltaic to fluvial sandstones of the Fairchild Formation (Elliot et al., 2016). Sandstone packages ranges between 130 to 230 m thick, comprising of medium to coarse grained sandstone with trough cross bedded or fine grained and ripple lamination. This unit becomes unrecognisable in the Ohio Range within the lower Mount Glossopteris Formation.

Buckley Formation

Consists on an upper and lower unit comprising of cyclical sequences of sandstone, carbonaceous siltstone/mudstone and coal extending over 800 km. Coal measures are overlain by lenticular beds of rounded quartz- pebble conglomerate (Collinson et al., 1994). Isbell (1990, 1991) interpreted these coal measures as braided streams and flood plains. In the upper unit, glossopterid-dominated floral assemblages were found (Collinson et al., 1994). Sandstones in the Buckley Formation ranges between coarse- to medium-grained, with coarser units comprised of scour-bounded, fining upward packages ranging between 1 and 5 m. The upper Buckley Formation comprises of volcaniclastic detritus, with two sandstone units yielding detrital zircon U/Pb SHRIMP ages of 253.5 ± 2.0 Ma and 250.3 ± 2.2 Ma (Elliot and Fanning, 2008).

Ohio Range

Buckeye Formation

Comprises of glacial and glacial- marine deposits of up to 310 m thick (Aitchison et al., 1988). Diamictites were deposited at the base of the formation by grounded ices forming striated pavements (Collison et al, 1994). Stratified diamictite, sandstone and mudstone overly the basal diamictite. These sediments reflect a glacial-marine environment together with the presence of hummocky cross- stratification, marine acritarchs and low iron content (Kemp, 1975; Collinson et al, 1994).

Discovery Ridge Formation

Glacial beds in the Ohio Range are succeeded by shales and sandstones of the Discovery Ridge Formation. It consists on a lower and upper unit comprising of Early Permian aged shales and sandstones. This formation ranges up to 170 m thick in the Ohio Range (Long, 1965).

Mount Glossopteris Formation

Mount Glossopteris Formation overlies the Discovery Ridge Formation with a thickness of up to 700 m consisting of 5 to 20 m thick interconnected channel-form sandstones that occur as wide spread sheets (Isbell and Collinson, 1988). Kyle and Schopf (1982) described microfloral assemblages from the lower part and base of the upper part of the formation. The upper part of Mount Glossopteris Formation consists of volcaniclastic debris which were dated at ~270-260 Ma (Elliot and Fanning, 2008).

Chapter 3

Methodology

Fieldwork together with wireline analysis, geochemistry, mineralogy and statistical analysis has been used to characterise rock types of the Dwyka Group, Prince Albert Formation and Whitehill Formation. These investigations were supported by petrographic analysis, XRD and XRF analysis. XRF analysis was further utilised to determine various geochemical proxies to characterise the depositional environment together with stable isotopes. The petrophysical characterisation of the Prince Albert Formation and its shale gas potential was investigated by mercury porosimetry, total organic carbon (TOC) measurements, vitrinite reflectance and residual gas measurements.

The following techniques for each of these investigations are outlined below.

3.1 Field work and sample collection

Rock outcrops and borehole core were sampled and studied across the southern part of the main Karoo Basin and representative samples were collected from the Dwyka Group, Prince Albert Formation and overlying Whitehill Formation. A total of one hundred and thirty-nine samples were collected from various surface and borehole localities (Fig. 3.1).

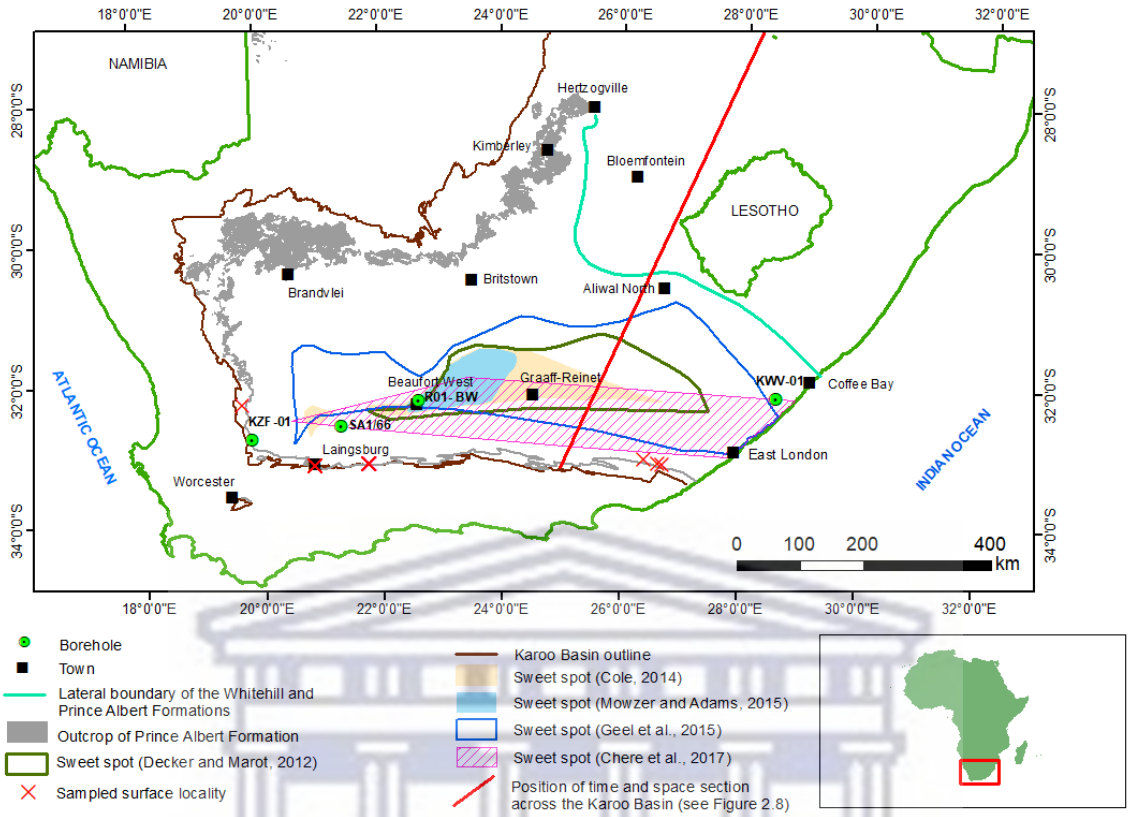

Figure 3.1. Distribution of the Prince Albert Formation and sample localities across the Western and Eastern Cape of South Africa.

3.2 Principles of wireline logging

Wireline logging is a means of measuring the physical, acoustical and electrical properties of rocks penetrated downhole (Mondol, 2015). Wireline logging was carried out by Wireline Alliance for borehole R01-BW. In this study, wireline logs were used to interpret lithological formations downhole and to compare against chip cuttings of borehole R01-BW drilled in Beaufort West. The following wireline logs were utilized:

- Gamma Ray (GR) log: measures the natural radioactivity in formations (in API units) and can be used to identify lithologies and for correlating zones (Asquith and Krygowski, 2004). The radioactivity of the formation is based on the occurrence of uranium, thorium and potassium.

Sandstones and carbonates have low concentrations of radioactive material and has a low gamma ray signature. Shales has a high concentration of radioactive material therefore a high gamma ray signature (Asquith and Krygowski, 2004).

- Density logs: measures the formation's bulk density in g/cm^3. Two separate density values are used, the bulk density (ρb or RHOB) and the matrix density (ρma) (Asquith and Krygowski, 2004). Bulk density represents the density of the entire formation (solid and fluid parts) as measured by the wireline tool. Matrix density is the density of the solid framework of the rock (Asquith and Krygowski, 2004). The density log has also been used to measure the photoelectric-effect (Pe, PE, or PEF). Density logs are best used to determine the lithology of a formation, identify evaporite minerals, detect gas-bearing zones, evaluate shaly-sand reservoirs and determine hydrocarbon density (Asquith and Krygowski, 2004; Darling, 2005).

- Resistivity (LLS and LLD) logs: measure the formation's resistivity in ohms (ohm.m^2/m). These logs are used to determine hydrocarbon-bearing versus water-bearing zones, identify permeable zones and determine porosity (Asquith and Krygowski, 2004).

  Rock materials (matrix or grains) and any hydrocarbons within the pore space are mostly insulators. The ability of a rock to transmit a current is dependent on the presence of water in the pores. As the hydrocarbon saturation increases within the pores (as the water saturation decreases), so does the formation's resistivity (Asquith and Krygowski, 2004). Resistivity also increases as the salinity of the water in the pores decreases (Asquith and Krygowski, 2004). Various resistivity logs are used depending on the borehole diameter, drilling fluid, and salinity of the fluid. Shallow laterolog (LLS) and deep laterolog (LLD) are used to measure the formations resistivity in boreholes

filled with saltwater muds. Induction log deep (ILD), is the only tool to measure resistivity in boreholes drilled with oil-based mud (Asquith and Krygowski, 2004; Darling, 2005).

3.3 X-Ray fluorescence (XRF)

XRF is an analytical technique used for elemental analysis and chemical analysis of rocks (Brouwer, 2010). XRF can also be used to assist in the determination of geological environments, elemental distribution and correlation. The technique ejects an electron from its atomic orbital by the absorption of a light wave (photon), which must be greater than that which the electron is bound to the nucleus of the atom (Craigie, 2018). Once the inner orbital electron has been released, a higher energy level electron will be transferred to a lower energy level orbital. During this transition, a photon may be emitted and this fluorescent light is called the characteristic X-ray of the element (Craigie, 2018). The transition between these two levels always has the same energy, but the element can be determined by measuring the energy (wavelength) of the X-ray light (photon) released by that element. By measuring the intensities of emitted energies of fluorescent light, it is possible to determine the amount of concentration in the sample.

Major and trace elements were determined by X-Ray fluorescence (XRF). A hundred and thirty-nine samples were analysed at the Council for Geoscience laboratories in Silverton.

Sample preparation

For major element analysis, the milled sample (<75 µ fraction) was roasted at 1000°C for at least 3 hours to oxidise Fe^{2+} and S and to determine the loss of ignition (L.O.I.). Glass disks

were prepared by fusing 1.5 g roasted sample and 9 g flux consisting of 49.50% $Li_2B_4O_7$, 49.50 $LiBO_2$ and 1.00% LiBr at 950°C (Willis et al., 2014).

For trace element analysis, 12 g milled sample and 3 g Hoechst wax were mixed and pressed into a powder briquette by a hydraulic press with the applied pressure at 25 tons. The glass disks were analysed by a PANalytical Axios X-ray fluorescence spectrometer equipped with a 4 kW Rh tube, while the powder pellets were analysed by a PANalytical Zetium XRF spectrometer with a 4 kW Rh tube.

3.3.1 Geochemical proxies

Geochemical proxies were derived from XRF data. Certain trace element ratios, namely Th/U, Ni/Co, V/Cr and V/ (V+Ni), provide useful information on the paleoredox conditions (Hatch and Leventhal, 1992; Jones and Manning, 1994; Rimmer et al., 2004). Low Th/U ratios, typically less than two, suggest anoxic conditions with high authigenic uranium (Wignall and Twitchett, 1996). In an oxic environment, concentrated thorium is present in clay sediments and aqueous uranium under organic-rich reducing conditions. High ratios of Ni/Co, V/Cr and V/ (V+Ni) suggest anoxic conditions, as Co and Cr concentrations are not affected by redox conditions (Jones and Manning, 1994). V/Cr ratios <2 indicate oxic conditions, ratios between 2 and 4.25 dysoxic and values >4.25 indicate anoxic/aerobic, bottom water conditions (Scheffler et al., 2006). V/(V+Ni) ratios between 0.46 and 0.60 indicate a weakly stratified dysoxic environment, values greater than 0.80 suggest euxinic conditions, while V/(V+Ni) ratios less than 0.54 suggest oxic conditions at the seafloor (Hatch and Leventhal., 1992).

Phytoplankton decay relates to biogenic barite due to the carbon export from the photic zone in the water column, thus making barium a reliable paleoproductivity indicator (Jeandel et al., 2000; Tribovillard et al., 2004; Riquier et al., 2005). Sr/Ba and Sr/Cu ratios can be related to

climatic conditions and salinity levels. High Sr/Ba ratios reflect high salinity/hot arid conditions while low ratios indicate low salinity/ warm humid conditions (Meng et al., 2012). Sr/Ba ratios greater than 1.0 in a lacustrine environment indicate salty lake water under arid conditions (Zhongsheng et al., 2003; Sheng-ke, 2005). Sr/Cu ratios between 1.3 and 5.0 indicate warm humid conditions and greater than 5.0 reflect a hot arid climate (Lerman, 1978). The nickel and copper ratios Cu/Al and Ni/Al, infer the type of organic matter, as it dissolves under sulphate reducing conditions (Piper and Perkins, 2004; Zhao et al., 2016).

Fresh water, brackish or marine sediments are differentiated by the Rb/K ratio (Campbell and Williams, 1965; Scheffler et al., 2006). In marine waters, the rubidium ion (Rb^{+}) has a concentration of 0.12 ppm compared to 0.0013 ppm in fresh water environments (Taylor and McLennan, 1985). Shales deposited in freshwater to brackish conditions have a Rb/K ratio of less than $4*10^{-3}$, in contrast to marine conditions, where the ratio is greater than $6*10^{-3}$ (Campbell and Williams, 1965).

The chemical index of alteration (CIA) supplies information on chemical weathering, which has been influenced by climate conditions (Scheffler et al., 2006). During normal weathering processes, alkali and alkaline earth elements remain mobile and form soluble cations in an aqueous solution. The latter elements are used to calculate the value of CIA by the following equation (Nesbitt and Young, 1982):

$$\text{CIA} = \frac{Al_2O_3}{Al_2O_3 + Na_2O + K_2O + CaO*} \times 100$$

CaO*= the amount of calcium present in the silicate fraction

CIA identifies the changing proportion of feldspar to clay minerals. Intensive chemical weathering results in high CIA values due to the removal of alkali and alkaline earth elements.

Grain size of sediments affect CIA, whereby coarse-grained, siliciclastic sediments contain higher feldspar/clay mineral ratios than finer sediments, resulting in a lower CIA value (Visser and Young, 1990; Scheffler et al., 2006). CIA values are between 30 and 45 for unaltered basaltic rocks, 50 for granites, between 70 and 75 for shales, 75 and 85 for illite and montmorillonite and about 100 for kaolinite and chlorite (Nesbitt and Young, 1982; Scheffler et al., 2006). Low CIA values relate to cold/arid conditions and high CIA values reflect warm/humid climates.

3.4 X-Ray diffraction (XRD)

XRD data can be used to determine the proportion of different minerals present within a rock. It is a nondestructive technique used to study crystal structures and atomic spacing. The technique is based on constructive interference of monochromatic X-rays and a crystalline sample (Bunaciu et al., 2015). A cathode ray tube produces concentrated monochromatic radiation, which are the generated X-rays. The intensity of the diffracted X-rays are then measured by the rotation of the sample and detector. This interaction between the sample and the incident rays creates a constructive interference and a diffracted ray by using Bragg's law (Bragg and Bragg, 1913):

$$n\lambda = 2d\sin\theta$$

n- Integer

λ- Wavelength of X-rays

d- Interplanar spacing creating the diffraction

θ- Diffraction angle

With Bragg's law, diffracted X-rays are measured by the wavelength of electromagnetic radiation to the diffraction angle (θ) and the lattice spacing in the crystalline sample. Diffraction peaks are then converted to d-spacings in order to detect the mineral compound as each compound has a unique set of d-spacings (Bunaciu et al., 2015).

Sample preparation

A hundred and thirty-nine samples were analysed at the Council for Geoscience laboratories in Silverton to determine the mineralogy of each sample.

Sample Processing: For bulk (whole rock) analysis a representative sample of the rock material was crushed and milled to a fine powder of around 20 μm in size. A sub-sample was pressed into a shallow plastic sample holder against a rough filter paper in order to ensure random orientation.

X-Ray Diffraction measurements were performed on a Bruker D8 Advance (Model: V22.0.28, Bruker, Madison, WI, USA) instrument with a 2.2kW Cu long fine focus tube (Cu Kα, λ=1.54060) and 90 position sample changer. The system is equipped with a Lynx Eye detector with 3.7º active area. Samples are scanned from 2 to 70° 2θ at a speed of 0.02° 2θ steps size/0.5 sec, and generator settings of 40 kV and 40mA.

Data processing and analysis: Phase identification is based on the BRUKER DIFFRAC^{Plus} - EVA evaluation program. Routinely, phase concentrations are determined as semi quantitative estimates (with accuracy ±5%) using the RIR (Reference Intensity Ratio) method and relative peak heights/areas proportions (Brime, 1985).

3.5 Petrographic Analysis

A total of 139 samples were collected throughout the Dwyka Group, Prince Albert and Whitehill formations (Appendix 1 to Appendix 9). Of these samples, twenty were selected as lithological representatives of various rock types identified in this study. The focus of the petrographic analyses was to describe the mineralogy (i.e. identification and quantification of mineral components), diagenetic features, bedding, texture and organic matter of the selected samples.

Samples were prepared through whole-rock block mounts. Samples were mixed with epoxy resin in 3.2 cm diameter phenolic ring form moulds, and placed under a vacuum for 24 hours for the mixture to harden. The hardened petrographic blocks were ground and polished following the standards of ASTM International (2013) and SANS 7404-2 (2015)/ISO 7404-2 (2009), to produce a highly reflective and a scratch free surface. Each petrographic block was studied with the aid of a Leica DM6000 Microscope with Carl Hilgers motorized system. A software called "Hilgus Fossil Diskus" was used to automatically capture the quantified maceral and mineral group composition that was observed under the microscope and the images were automatically saved.

3.6 Statistical Analysis

Univariate analysis

Univariate analysis involves one variable at a time (Reimann et al., 2008). This technique summarises data in order to describe and find patterns in the data. Geochemical variables of samples HM1 to HM139 were analysed using IBM SPSS statistics (IBM SPSS Statistics, 2011). The aim was to examine the normality or skewness of the geochemical data. In SPSS, Frequencies was selected from descriptive statistics to provide information on the minimum,

maximum, mean, standard deviation of the data as well as a graphical display, in the form of a histogram.

Correlation coefficient

Correlation coefficient (CC) analysis establishes a link or relationship between variables and displays them in a matrix form. Covariance measures the relationship amongst variables and is determined by the variability of each variable (Reimann et al., 2008). Covariance ranges from +1.0 to -1.0 and the strength of the relationship is identified by + or -. Covariance greater than zero indicates a positive relationship and less than zero indicates a negative relationship. When the covariance is zero, it indicates no relationship between the two variables. Coefficients closer to +1.0 and -1.0 has a high level of correlation between the variables (Reimann et al., 2008).

The most common methods used to determine a correlation coefficient are the Kendall, Pearson and Spearman correlation (Galton, 1890; Kendal, 1938; Spearman, 1904). Eighteen variables (SiO_2, TiO_2, Al_2O_3, K_2O, MnO, MgO, P_2O_5, CaO, Fe_2O_3, Na_2O, Th, V, Zr, Ni, U, Y, Sr and Rb) from XRF analysis were analysed to determine if there are any element: mineral links that exist using the bivariate correlation method with Pearson correlation coefficient and a two-tailed test of significance using IBM SPSS Statistics 20 software (IBM SPSS Statistics, 2011).

Multivariate statistics

Multivariate statistics is a technique that studies large datasets (Shiker, 2012). It statistically estimates the relationships between different variables in the dataset, correlates how important each variable is and whether dependencies occur between them (Shiker 2012). Three multivariate techniques were used during this study, namely factor analysis, cluster analysis and discriminant analysis. These techniques were used to characterise the rock types

using a geochemical set of major and trace elements from one hundred and thirty-nine samples (HM1 to HM139), and to investigate element associations within the dataset. The statistical methods were performed with IBM SPSS software version 20 (IBM SPSS Statistics, 2011).

Factor analysis

Factor analysis is a technique that reduces a large dataset with several variables to a smaller set of factors that explain the variance in the original dataset without losing important information (Shiker, 2012). Visualization of three or four factors is much easier than an entire data set (Reimann et al., 2008). Factor analysis is an independent technique where there is no dependent variable (Shiker, 2012).

In SPSS, principal component extraction method was selected to find the least number of variables that explain the most variance with factor analysis (Reimann et al., 2008). The first principal component extracted explains the most variance and the second principal component has to be orthogonal to the first component which contains the maximum amount of remaining data (Reimann et al., 2008, Shiker, 2012). The same principal is kept for the succeeding principal components, as long as their eigenvalues are greater than one.

A correlation matrix was first created in order to reduce the original major and trace element dataset. The number of factors were then identified by the total variance explained. Varimax with Kaizer Normalization factor rotation (Davis, 1986) was selected due to the matrix of factor loadings not being unique or easily explained. The next step was interpreting factors by rotated components and structure matrix. Factor scores were saved as variables and compared to sample numbers in order to interpret the rock types. The goal with factor

analysis was to reduce the redundancy among the variables (major and trace elements) by using a smaller number of factors.

Cluster analysis

Cluster analysis is a multivariate method used to identify patterns in a dataset by grouping the data into clusters (Shiker, 2012). Cluster analysis uses distance measure to assign variables, in this case major and trace elements to a number of groups that are similar in nature or behaviour (Reimann et al., 2008). The choice of variables is important as cluster analysis cannot differentiate between relevant and irrelevant variables (Shiker, 2012).

With cluster analysis, no prior information is known about the number of groups or which sample belongs to which group. Hierarchical cluster analysis (Q mode) together with Ward's method and Squared Euclidean distance interval was used (Ward, 1963). With this method, all possible pairs of clusters are combined and the sum of the squared distances within each cluster is calculated. This is then summed over all clusters. The combination that gives the lowest sum of squares is chosen (Shiker, 2012). Squared Euclidean distance was selected as the number of discordant cases where its minimum value is zero, and it has no upper limit. Variables (major and trace elements) were then standardised to z scores prior to clustering as they were measured in wt% and ppm. A dendrogram was produced by agglomerative hierarchical clustering (Kaufman and Rousseeuw, 2005). A cluster dendrogram assess the cohesiveness of the clusters formed and provides information about the number of clusters to keep. The dendrogram displays the clusters graphically where the x-axis represents the distance at which the clusters merge, while the samples and their location were represented against the y-axis. The groups created through cluster analysis were then verified and characterised using discriminant analysis.

Discriminant analysis

Discriminant analysis requires previous classification of data into relatively homogenous subgroups whose characteristics can be described by the statistical distributions of the grouping variables associated with each subgroup (Siad et al., 1994). With discriminant analysis, a grouping variable is required which is obtained from methods like factor analysis and cluster analysis. The aim of using discriminant analysis was to verify and differentiate between Group 1, Group 2 and Group 3.

Stepwise discriminant analysis builds a predictive model for group membership (Shiker, 2012). With this technique the highest correlated independent variable is added followed by successive variables to determine the percentage of correctly classified groups (Siad et al., 1994).

3.7 Stable isotopes

Stable carbon and oxygen isotopes are commonly used to study palaeoclimate, including climate pulses through geological time (Meng et al., 2012; Weissert et al., 2008). Carbon isotopes are used to decipher changes in the global carbon cycle and for chemostratigraphic correlation. Of the two stable carbon isotopes, the abundance of ^{12}C in nature is given as 98.89%, while ^{13}C forms the remaining 1.11% (Craig, 1953). Mass differences of the two isotope species lead to strong fractionation during photosynthetic incorporation of carbon into organic matter, while inorganic carbonate precipitates formed in the aquatic environment are less affected by fractionation processes (Weissert et al., 2008). Stable carbon isotopes ($\delta^{13}C$) and nitrogen isotopes ($\delta\ ^{15}N$) can differentiate between C_3 and C_4 marine and terrestrial organic matter (Khan et al., 2015). C_3 Terrestrial organic material ranges between -

20 ‰ to -30 ‰ (Decker and de Wit, 2006). Marine organic matter ranges between of -25 ‰ to -5 ‰ (Schoeninger and DeNiro, 1983). δ ^{15}N values between 0 ‰ to 5.5 ‰ reflect terrestrial organic matter while values between 4 ‰ to 10 ‰ reflect marine organic matter (Schoeninger and DeNiro, 1983, Geel et al., 2013). Depositional environments can be inferred from various δ^{13}C values (Fig.3.2).

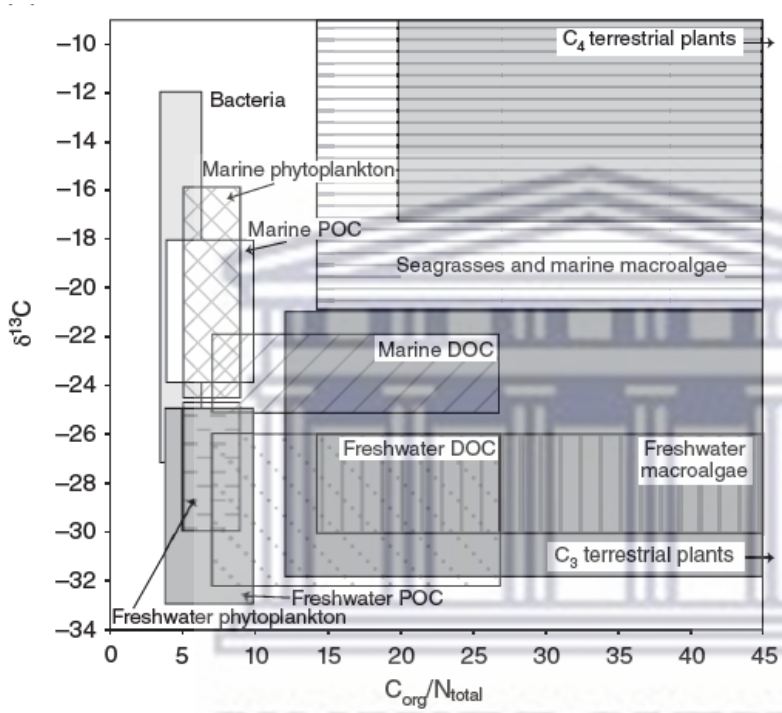

Figure 3.2. The range of δ^{13}C and C/N values for organic matter sources that accumulate in sedimentary environments (Khan et al., 2015).

Oxygen isotopes are useful for chemostratigraphy by reconstructing marine environments and providing information on ice ages (Weissert et al., 2008). In chemostratigraphy, there are two oxygen isotopes, namely, ^{16}O which constitutes 99.8% and ^{18}O the remaining 0.2%. Isotope measurements of ^{18}O/^{16}O are taken according to the Vienna Pee Dee Belemnite Standard (V-PDB) and expressed as per mil notation (‰) due to small variations of the two isotopes.

Sample preparation

Oxygen isotope analyses were made on powdered bulk-rock samples using a conventional extraction method at the University of Cape Town (UCT) Stable Isotope Laboratory. Approximately 10 mg of powder was loaded into nickel tubes, degassed at 200°C for more than 2-3 hours, then reacted with ClF_3 at 550°C for 3 hours. The O_2 gas produced was converted using a hot, platinized carbon rod. In each run of 10, 8 samples and 2 duplicate splits of the internal standard, Murchison line quartz (MQ, $d^{18}O$ = 10.1 ‰) were processed. The CO_2 gas was collected in "break seal" tubes for analysis. The average raw $d^{18}O$ value of MQ (10.1 ‰, calibrated with NBS-28 and assuming a value of 9.64 ‰ for NBS-28) was used to convert raw data to the SMOW scale. The long-term variability of MQ is 0.16 ‰ (2 σ). The $d^{13}C$ and $d^{15}N$ values of the bulk sample were determined using an online continuous flow device described in more detail by Kramers et al. (2013). All stable isotope ratios were determined using a Thermo DeltaXP mass spectrometer in gas-source mode (except for the carbonaceous material) housed in the Department of Archaeology at UCT. Data are reported in d notation, where δ= ((Rsample/Rstandard) —1)1000, where R represents $^{18}O/^{16}O$, D/H, or $^{13}C/^{12}C$. Oxygen, carbon and nitrogen isotope data are referenced against SMOW, PDB and Air, respectively.

3.8 Petrophysical characterisation

3.8.1 Mercury porosimetry

Mercury porosimetry is a technique used to determine the porosity of porous materials, where pore sizes are between 500 µm and 3.5 nm (Giesche, 2006). Unlike other techniques, mercury porosimetry provides a wide range of measurements, i.e. pore size distribution, total

pore area, total pore volume, bulk density skeletal and apparent density. The technique measures the largest entry towards a pore, but not the inner size of the pore (Giesche, 2006).

Total pore volume is calculated by the volume of mercury required to fill all accessible pores divided by the mass of the sample, recorded as total pore volume in units of volume per unit mass (Webb, 2001). Bulk volume (for a collection of samples) is the sum of the volumes of voids within a sample, solids in each sample and voids amongst the samples. Bulk and skeletal densities are determined by dividing the material mass by the volume (Webb, 2001). Porosity is then calculated by dividing total porosity by bulk volume, as shown in the equation below (Rootare and Prenzlow, 1967):

Porosity (%) = $\frac{Total\ porosity\ (Vpt)}{Bulk\ volume\ (VB)}$ x 100%

Permeability is the movement of fluids through a porous material measured in Darcy. Permeability is affected by pressure in a rock, once pressure is increased, mercury enters small and minute pore openings in the rock sample. Once the sample has reached maximum pressure, the mercury spans forming a conduction path equating to the magnitude of permeability (Webb, 2001). Permeability is calculated by the following equation (Katz and Thompson, 1987):

$$\text{permeability} = \frac{1}{226}(L_c)^2\ \sigma/\sigma_0$$

L_c= characteristic length

σ = rock conductivity

σ_0 = conductance of brine in the pore space

Sample preparation

In order to evaluate the physical properties of the Prince Albert Formation shales, porosity, density, bulk density, volume porosity and skeletal density measurements were determined. Twelve core samples were selected from boreholes KZF-01, KWV-01 and SA 1/66 (Table 3.1). Samples were analysed at MCA services in Cambridge, UK. A Micromeritics AutoPore V (9620) instrument was used for the collection of mercury intrusion data using mercury of 99.999 % purity and applying a mercury contact angle of 140 degrees and surface tension of 480 dynes/cm^2. Samples were degassed prior to analysis, for a minimum of two hours under vacuum at a temperature between 25°C and 150°C depending on sample stability. Samples were prepared for the mercury penetrometer, such that sufficient sample mass is provided for analysis or the penetrometer bulb is as full as possible, without causing obstruction to mercury flow. A blank correction was applied using a reference analysis of the actual penetrometer under the same analytical conditions.

Table 3.1. Mercury porosimetry shale samples selected from boreholes KZF-01, KWV-01 and SA 1/66.

Locality	Sample number	Depth (m)
BH KZF-01, Tankwa	HM58	440.81 – 441.17
	HM60	479.72 – 480.10
	HM66	515.36 – 515.69
	HM70	537.14 – 537.44
	HM81	600.48 – 600.70
	HM89	645.45 – 645.76
BH KWV-01, Willowvale	HM95	2311.98 – 2312.36
	HM97	2317.59 – 2317.88
	HM98	2320.40 – 2320.73

	HM100	2326.70 – 2327.00
BH SA 1/66, Merweville	HM125	2785.74 – 2788.78
	HM126	2793.51 – 2798.59

BH = borehole

The penetrometer was previously calibrated in duplicate for volume, using the method detailed by Micromeritics (ASTM International, 2018). For the calculation of density and porosity, the assembled penetrometer is weighed with and without mercury (before and after completion of the low pressure stage of analysis).

Sample evacuation was conducted up to pressures of 50 micrometre of mercury (µmHg). Intrusion data are collected in the approximate applied pressure range 0.3 – 60,000 pounds per square inch (psi) with equilibration occurring after 10 seconds. Maximum mercury intrusion limits are set to 0.01 millilitres per gram (mL/g) or lower to ensure collection of a reasonable number of data points in regions of mercury intrusion. Low pressure analysis is typically conducted to 45 psi, unless sample pore size distribution demands an alternative pressure.

3.9 Shale gas potential

The following techniques below were used to characterise the shale gas potential of the Prince Albert Formation.

3.9.1 Rock-Eval

Rock-Eval pyrolysis is a technique used to determine the hydrocarbon generative potential and thermal maturity of shale samples (Peters and Cassa, 1994). It is the decomposition of organic matter by heating samples in an oven in an inert atmosphere and expressed as a

weight percentage. The type of hydrocarbon a source rock produces depends on the type of kerogen and its thermal maturity. Hydrogen index (HI) and oxygen index (OI) ratios are calculated from Rock-Eval data and plotted on a Van Krevelen diagram, to determine the kerogen types. The main types of kerogen are (Tissot et al., 1974):

- Type I – oil prone
- Type II – mixed oil and gas
- Type III – gas prone
- Type IV – inert gas

The Indian Institute of Technology in Mumbai analysed twelve shale samples selected from boreholes KZF-01 and KWV-01 (Table 3.2). Two samples from borehole SA 1/66 were analysed by Chesapeake Energy in the United States of America (Table 3.2).

Crushed material was analysed by a Rock-Eval 6 pyrolyser, which thermally decomposes organic matter in the sample by means of a step-heating process in an inert atmosphere. During pyrolysis, the amount of hydrocarbons released (S_1 and S_2) was measured with increasing temperature (up to 750°C). S_1 relates to the free hydrocarbons and these are released at temperatures up to 300°C. S_2 are the generated hydrocarbons and hydrocarbon-like compounds and these are released at temperatures of between 300 and 650°C. Generated CO_2 represents the S_3 component and is released at temperatures of 300 and 750°C over a longer period of time. Following completion of pyrolysis, any remaining carbon is residual carbon and is termed S_4.

Table 3.2. Rock-Eval samples selected from boreholes KZF-01, KWV-01 and SA 1/66.

Locality	Sample number	Depth (m)
BH KZF-01, Tankwa	HM58	440.81 – 441.17
	HM68	523.53 – 523.76
	HM69	529.60 – 529.86
	HM79	588.54 – 588.73
	HM82	606.74 – 606.91
	HM85	624.40 – 624.72
	HM88	639.29 – 639.61
	HM90	651.52 – 651.84
BH KWV-01, Willowvale	HM94	2309.05 – 2309.37
	HM96	2315.08 – 2315.37
	HM99	2323.39 – 2323.72
	HM101	2329.56 – 2329.87
BH SA 1/66, Merweville	HM125	2785.74 – 2788.78
	HM126	2793.51 – 2798.59

An important factor for evaluating shale gas resources within a study area depends on the total organic carbon (TOC) content (Kuuskraa et al., 2011). TOC contents were determined from Rock-Eval pyrolysis data using the equation (de Kock et al., 2017):

$$\text{TOC (wt. \%)} = \frac{0.082(S1+S2)+S4}{10}$$

The above equation is subject to error due to the S_1 and S_2 peaks decreasing in very thermally matured sediments. The calculated TOC did not include inorganic carbon as this was measured separately.

3.9.2 Vitrinite reflectance

Vitrinite reflectance is a technique that measures the percentage of incident light reflected from the surface of vitrinite macerals to determine the maturity of the organic matter. Mean values are calculated for the population of vitrinite particles per sample and reflected as percentage reflectance in oil immersion (Dembicki, 2009).

Vitrinite reflectance measurements were analysed at the University of Johannesburg, in order to understand the thermal maturity of the Prince Albert Formation. Twenty dark grey shale samples were selected from outcrop and core of the Prince Albert Formation (Table 3.3). The technique uses microscopical determination of oil polished surfaced blocks to identify vitrinite found within the shale samples. The technique uses the ASTM standard test method D7708 (ASTM International, 2014).

Table 3.3. Vitrinite reflectance samples.

Locality	Sample number	Depth (m)
BH KZF-01, Tankwa	HM57	439.61 – 439.95
	HM58	440.81 – 441.17
	HM69	529.60 – 529.86
	HM79	588.54 – 588.73
	HM82	606.74 – 606.91
	HM85	624.40 – 624.72
	HM88	639.29 – 639.61
	HM90	651.52 – 651.84
BH KWV-01, Willowvale	HM94	2309.05 – 2309.37
	HM96	2315.08 – 2315.37
	HM99	2323.39 – 2323.72
	HM101	2329.56 – 2329.87
Prince Albert outcrop	HM40	61
	HM42	56.7
	HM43	51
	HM48	38.4
Tankwa outcrop	HM24	120
	HM34	135
Laingsburg outcrop	HM3	144
	HM6	121

*Note: BH = borehole. Borehole depths are from surface; outcrop depths are the vertical distance from the Whitehill/ Whitehill Formation boundary.

A petrographic Zeiss microscope (Fig. 3.3) was used with a x500 lens for refractive light and fluorescence intensity measurements and fitted with two digital cameras. The microscope was calibrated to 3.240 cubic zirkonia and 5.20 strontium-titanate (Fig. 3.4), together with immersion oil for a refractive index of 1.518.

"Hilgus Fossil Diskus" software was used to identify vitrinite and bituminite macerals. Random vitrinite reflectance (Ro random) was measured from the organic matter present within the sample (ASTM International, 2014). The mean and standard deviation of each sample was calculated as a reflectance percentage using between 20 and 100 vitrinite counts per shale sample and plotted as a histogram (Fig. 3.5).

Figure 3.3. Petrographic Zeiss microscope at the University of Johannesburg.

Figure 3.4. Strontium- titanate and cubic- zirconia standards were used for calibration of shale samples.

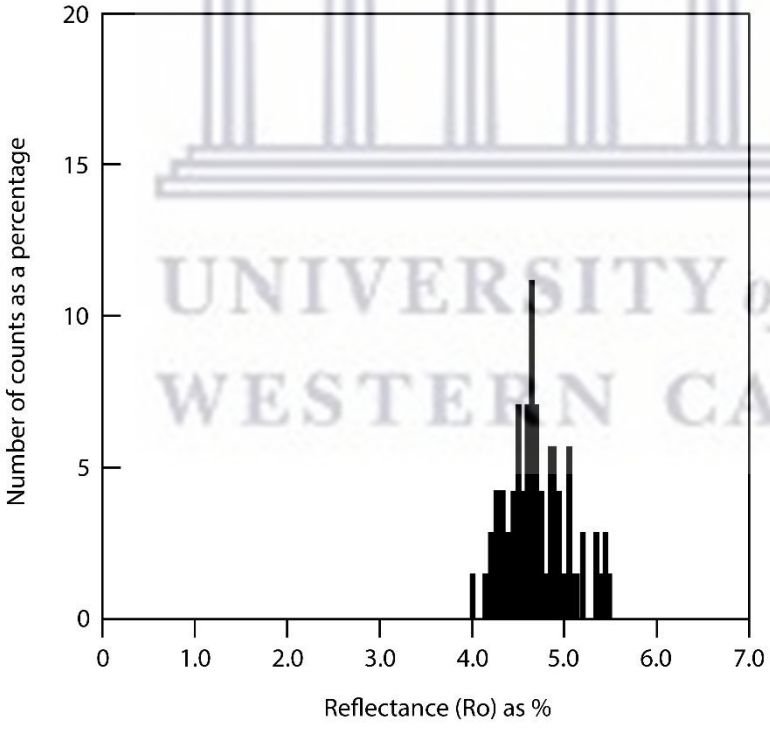

Figure 3.5. Vitrinite reflectance histogram of shale sample HM99 from borehole KWV-01 (Table 3.3) with a reflectance mean of 4.696% and standard deviation of 0.335%.

3.9.3 Residual methane gas measurements

Gas is generated during the maturation of organic matter in carbonaceous shale. Three types of gas may be present in the shale, namely free, desorbed and residual. Free gas is contained within the largest pores and is released when the drill bit intersects the shale and continues to be released until the core is brought to the surface and sealed in a canister. It cannot be directly measured so it has to be estimated. The method used is the USBM graphical method, plotting the cumulative desorbed gas in ml against the square root of time since the canister was closed. This general rule holds as a straight line for about 10 hours after coring, and the straight line is projected backwards before to the time before the canister was sealed to estimate the lost gas (A.P. Cook, Latona Consulting (Pty) Ltd., pers. comm., November 2015). Desorbed gas is attached to the surface of mudstone particles. Core is placed in a canister and measured on site over a period of time for several days (A.P. Cook, Latona Consulting (Pty) Ltd., pers. comm., November 2015). Residual gas is gas that remains trapped in the mudstone, normally within the smaller pores. It is only released after the core has been crushed and milled in the laboratory. Only residual gas measurements were analysed during this study.

Laboratory measurements

Eight shale samples were processed in the Latona methane, rating rod mill at UNISA Florida Campus in Johannesburg (Table 3.4). The rod mill is designed to crush coal samples, and other soft rock samples, and to retain any gas that is released during crushing. The volume of any retained gas can be measured and compared to the mass of crushed sample to determine the residual gas content. The rod mill has dimensions of approximately, 160 mm in diameter and 270 mm in length, and is generally loaded with six steel rods, of which three have a diameter of 20 mm and three a diameter of 30 mm. The rod mill is rotated at approximately 50 rpm.

Shale samples were loaded into a rod mill, which was then closed with a gas-tight seal (Fig. 3.6). An alternating current (AC) electric motor turns the mill by means of a belt pulley, and the motor is switched off at 10 minute intervals to permit any residual gas within the mill to be drained out by means of a ball valve and tube. The tube is connected to an inverted measuring flask, 500 ml or 100 ml, which is filled with water, and gas from the rod mill flows out via the ball valve and tube, into the inverted measuring flask (Fig. 3.6). The gas displaces the water inside the inverted measuring flask and this allows for the volume of gas to be measured. This is repeated every 10 minutes until no further gas is released from the sample. Three consecutive zero readings indicate that the residual gas release has stopped, but a minimum of four readings are always taken. The total volume of gas released from the sample is the sum of all the individual volumes taken at 10 minute intervals.

Table 3.4. Residual methane sample information.

Sample	Locality	Depth (m)	Sample mass crushed (g)	Crushed to
RS1	BH KZF-01	441.54 – 441.84	1215.2	lumps
RS2	BH KZF-01	484.10 – 484.66	1531.4	lumps
RS3	BH KZF-01	507.50 – 507.84	1242.6	mix
RS4	BH KZF-01	554.78 – 555.27	1381.0	lumps
RS5	BH KZF-01	563.57 – 563.94	1549.8	lumps
RS6	BH KZF-01	643.43 – 643.87	974.4	fines
RS7	BH KZF-01	2321.95 – 2322.42	986.8	lumps
RS8	Tankwa outcrop	28	830.8	mix

BH= borehole. Borehole depths are from surface; outcrop depths are the vertical distance from the Prince Albert Formation/Dwyka Group boundary for sample RS8.

Lumps: sample remained mostly as larger pieces of rock.

Mix: sample crushed to a mixture of fines and rock pieces

Fines: sample crushed mostly to fine powder, with few large pieces.

Figure 3.6. Latona's methane rod mill and water displacement measuring flask.

Residual gas calculation:

Residual gas content = $\frac{\text{gas volume released (ml)}}{\text{mass of sample (g)}}$

Example sample mass: 1200 g

Example measured gas volumes:

10 minutes – 50 ml

20 minutes – 80 ml

30 minutes – 120 ml

40 minutes – 60 ml

50 minutes – 20 ml

60 minutes – 0 ml

70 minutes – 0 ml

80 minutes – 0 ml

Total gas volume = 330 ml

Residual gas content = $\frac{330\ (\text{ml})}{1200\ (\text{g})}$ =275 ml/g = 0.275 m^3/t

Modifications for these samples

The first two samples crushed by Latona, RS1 and RS5 (Table 3.4), were hard and not easily broken in the rod mill. It was decided by Latona to perform some pre-crushing of the remaining samples before putting them into the mill, and to extend the minimum crushing times to 60 minutes, and then further to 90 minutes (Fig. 3.7). This resulted in two samples, RS3 and RS8, being crushed to a mixture of fines and rock lumps, but only one sample, RS4, being crushed to fines. All other samples did not produce many fines and remained mostly as rock lumps.

Figure 3.7. View inside mill showing rods and uncrushed samples.

Chapter 4

Results

4.1 Rock classification

4.1.1 Field sections and borehole cores

4.1.1.1 Witbergs River section near Laingsburg

The entire Prince Albert Formation was sampled from outcrops along the Witbergs River some 5 km south of Laingsburg, together with a single sample from the underlying Dwyka Group and two samples from the overlying Whitehill Formation. The geology of the sampling area was derived from the original, unpublished 1:50 000 scale, 3320BB Laingsburg sheet (Geological Survey, 1985), SPOT 5 and Google Earth satellite images. Fieldwork was undertaken along the Witbergs River to obtain lithological descriptions of the nineteen samples taken from the Dwyka Group, Prince Albert Formation and Whitehill Formation (Fig. 4.1). Sample co-ordinates, dip measurements and photograph numbers of each field locality are given in Appendix 1.

The geological boundaries were digitised from the original 1:50 000 scale geological map on ArcMap and edited with field data and SPOT5 imagery.

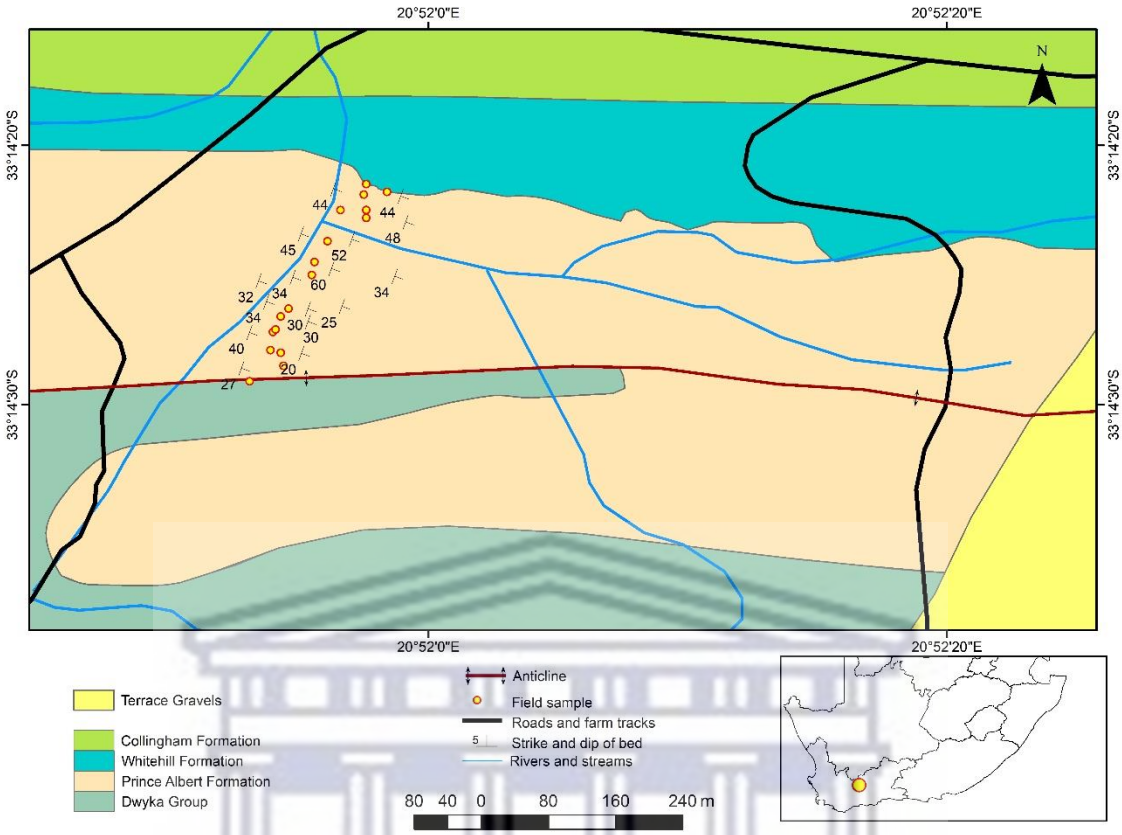

Figure 4.1. Geological map showing positions of field samples in the Witbergs River area, Laingsburg.

Lithostratigraphy

Dwyka Group

The Dwyka Group is located on the southern side of the sampling area and forms the core of an east-plunging anticline (Fig. 4.1). A sample (HM1) was taken on the northern limb of the anticline dipping 008/27 some 2 metres below the contact with the Prince Albert Formation (Fig. 4.1). The Dwyka Group has an estimated thickness of 1000 m in this area and consists predominantly of diamictite (Theron et al., 1991). In the uppermost part, which was sampled, it takes the form of a light olive grey (5Y 6/1) and dark greenish grey (5GY 4/1) diamictite consisting of abundant dropstones set in a silty mudstone matrix (Fig. 4.2). These dropstones are sub-rounded to angular in shape and consist of granite, pegmatite, sandstone and

siltstone up to 70 mm in length. The contact with the overlying Prince Albert Formation is sharp and no dropstones were seen in the basal shales (Fig. 4.2).

Figure 4.2. Dwyka Group (DG) and Prince Albert Formation (PAF) on the eastern side of the Witbergs River (co-ordinates 20.864 E; -33.241 S). GPS is 10cm long.

Prince Albert Formation

In the section sampled along the Witbergs River, the Prince Albert Formation attains a calculated thickness of 159 m based upon ten dip measurements along the section and the distance between each measurement point (Fig. 4.1). The formation consists predominantly of shale that contains isolated, ferruginous beds between 6 cm and 2.2 m thick. The lithological exposures are almost continuous along the eastern side of the Witbergs River where two cliff sections are present. Isolated outcrops also occur in the riverbed, which is mostly covered by scree and gravel. The shale beds dip northwards at between 20 and 60 degrees (Fig. 4.1).

The first shale sample (HM2) was taken from the basal 0.3 m of the formation directly overlying the Dwyka Group and another 16 samples were collected systematically across the succession up to the contact with the overlying Whitehill Formation (Fig. 4.1). Shale of the

Prince Albert Formation ranges in colour from dark to medium dark grey (N3-N4), dark greenish grey (5GY 4/1), olive grey (5Y 4/1), light brown (5 YR 5/6) and moderate brown (5 YR 4/4). The shales display pencil-like weathering with some iron staining in places (Fig. 4.3). The ferruginous beds are dark grey (N3) in colour, hard, and display slickensides and quartz veins in places, e.g. at co-ordinates 20.865E; 33.241S. At co-ordinates 20.866E; 33.239S, approximately 227 m above the base of the formation, a very light grey and light olive grey (N8 and 5Y 6/1) soft clay bed, 9 cm thick, is present interbedded with shale (Fig. 4.4). This is probably a volcanic tuff bed and resembles the tuff beds characteristic of the Collingham Formation in the southern part of the Karoo Basin (Viljoen, 1994).

Figure 4.3. Shale of the Prince Albert Formation displaying pencil-like weathering. A 6cm thick ferruginous bed (FB) is present (co-ordinates 20.865E; -33.241S).

Figure 4.4. A lenticular, light-coloured, clay bed of probable tuffaceous origin within shale of the Prince Albert Formation. Cliff section east of the Witbergs River (co-ordinates 20.865E; -33.239S).

Whitehill Formation

The contact between the Prince Albert Formation and the Whitehill Formation was obscured along the river bank profile. As shown in Figure 4.5, isolated outcrops of weathered Whitehill Formation shale were found 1 m from the inferred contact. The shale is light grey in colour (N7-N8) with abundant iron-staining, coloured light brown (5YR 5/6), moderate brown (5YR 4/4), moderate reddish brown (10R 4/6) and pale reddish brown (10R 5/4) and a sample (HM18) was taken. The actual contact was found on higher ground 25 m east-southeast of the river (Fig. 4.6). Here, the Whitehill Formation is light grey (N7-N8), light to moderate brown (5YR 5/6 - 5 YR 4/4) and pale to moderate reddish brown (10R 5/4 - 10 R 4/6) in colour and another sample (HM19) was retrieved 0.4 m above the Prince Albert / Whitehill Formation contact. These samples were taken in order to identify differences in mineralogy between the two formations.

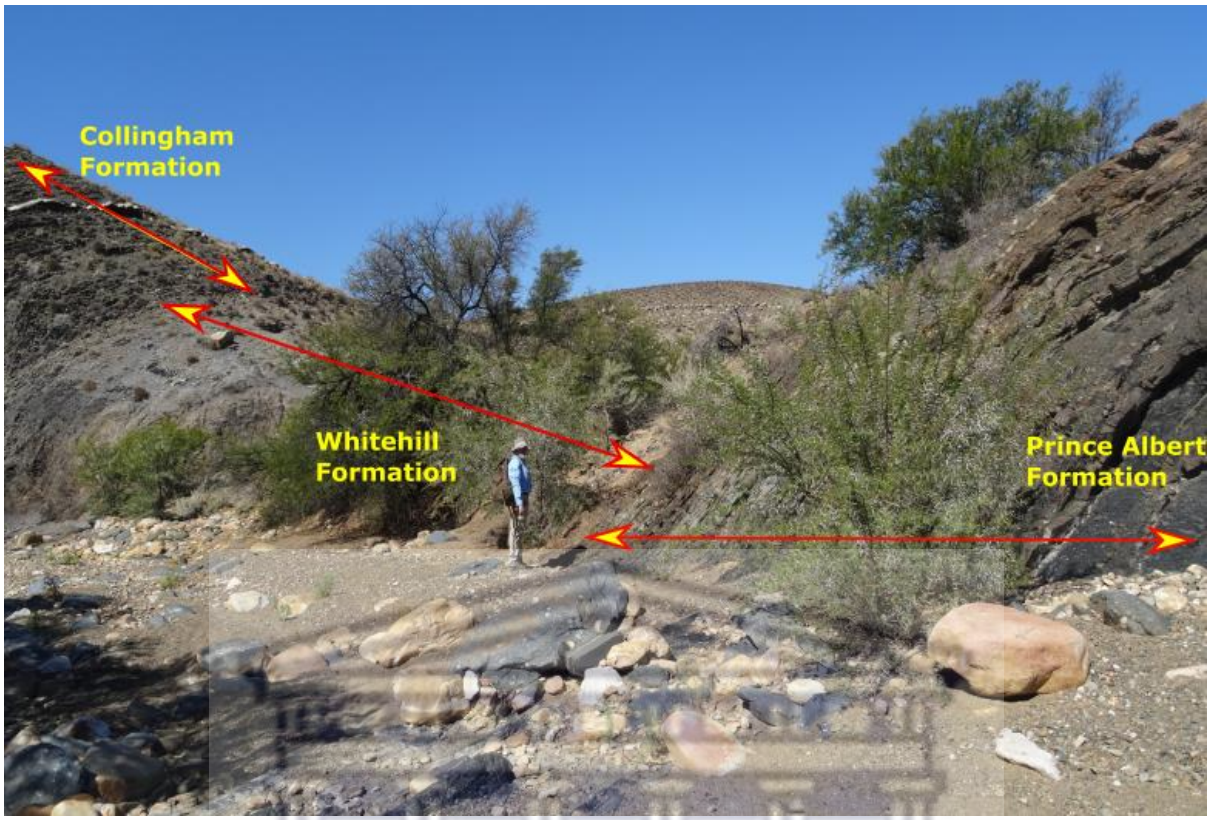

Figure 4.5. Inferred contact between the uppermost part of the Prince Albert Formation and the Whitehill Formation along the Witsberg River. Photograph taken from the northeastern side of the river bed (co-ordinates 20.866E; -33.239S).

Figure 4.6. Contact between the Prince Albert Formation (PAF) and the Whitehill Formation (WF) indicated by the dashed line (co-ordinates 20.866E; -33.239S). Geological hammer is 0.3m long.

4.1.1.2 Tweefontein – Ganskop road section

Twenty samples were collected in the Tankwa Karoo along a gravel road section between the farms Tweefontein and Ganskop, starting 7 km southeast of the R355 provincial road and lying 2 km southwest of the Tankwa River. The section is 100 km south of Calvinia and plots on the remapped and unpublished 1:50 000 scale, 3219BC Elandsvlei geological sheet between latitudes 32°20'S and 32°22'S and longitudes 19°40'E and 19°42'E (Geological Survey, 1986). Fieldwork was undertaken along the gravel road in a southeasterly direction and a total of 20 samples were collected from the Dwyka Group, Prince Albert Formation and Whitehill Formation (Fig. 4.7). Sample co-ordinates, dip measurements and photograph numbers of each field locality are given in Appendix 2.

The geological boundaries were digitised from the original 1:50 000 scale geological map on ArcMap and edited with field data and SPOT5 imagery. According to the remapped 1:50 000 scale geological map, the Prince Albert Formation is subdivided into three units (Pp1, Pp2 and Pp3) based on different colours observed in the field. The map shown here in Figure 4.7 combines these three units, since field observations indicate no major colour contrast throughout the Prince Albert Formation.

The regional dip of the Dwyka and Ecca Groups varies between 2 and 4 degrees with younging of strata towards the east. The very low dip has resulted in exposures of the Prince Albert Formation occurring over a surface width of 1.5 km (Fig. 4.7).

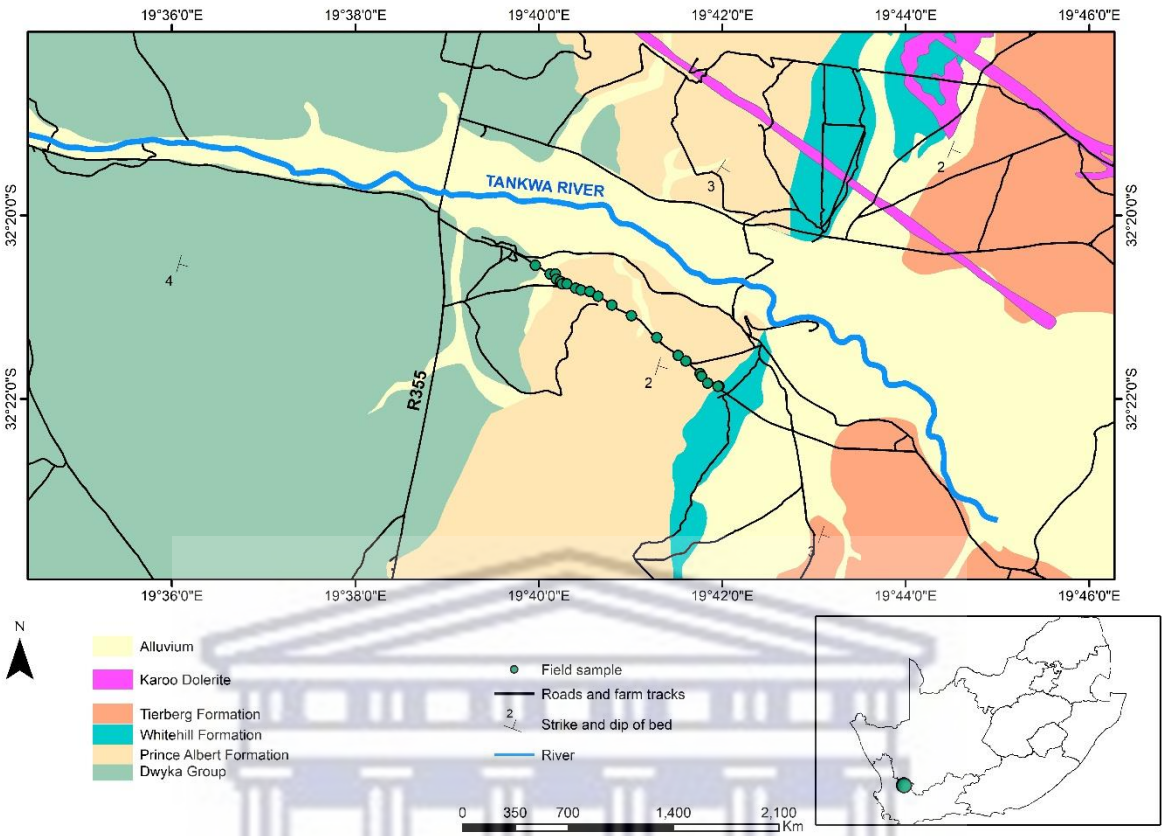

Figure 4.7. Geological map showing positions of field samples along the gravel road section between Tweefontein and Ganskop, Tankwa Karoo.

Lithostratigraphy

Dwyka Group

A single sample (HM20) was collected from the Dwyka Group and consists of silty shale, medium dark grey in colour (N4), containing scattered dropstones of quartzite up to 50 mm in length and isolated dolomite concretions (Fig. 4.8). The Dwyka Group was mostly covered with colluvial gravels and there is a paucity of in-situ outcrops, resulting in an inferred contact between the Prince Albert Formation and the Dwyka Group.

Figure 4.8. Silty shale of the Dwyka Group covered by colluvial gravels (co-ordinates 19.666E; -32.342S). GPS is 10cm long.

Prince Albert Formation

In the Tankwa Karoo, the Prince Albert Formation has an estimated, calculated thickness of 141 m and consists predominantly of shale. Thickness of the Prince Albert Formation was calculated based on outcrop width between samples (HM21 to HM38) and using the regional dip of two degrees east. Since the exposures are flat lying, differences in elevation were not considered.

The lowermost sample (HM21; Appendix 2) of the Prince Albert Formation was collected *in situ* in a small stream bed. It occurs in the lower unit (Pp1) previously mapped (Geological Survey, 1986) and consists of medium grey (N5-N7) and greenish grey (5GY 6/1) shale (Fig. 4.9). Ferruginous beds occur throughout the succession, ranging between 5 and 10 cm thick. They are olive grey (5Y 4/1), light brown (5YR 6/1), moderate yellowish brown (10YR 5/4), brownish black (5YR 2/1) and very dusky red (10R 2/2) in colour with brownish grey (5YR 4/1)

colours rarely present. These ferruginous beds are covered by eluvial and colluvial gravels (Fig. 4.10) and six beds were sampled from the road section.

Figure 4.9. Medium to light grey (N5-N7) shale of the Prince Albert Formation in a dry stream bed overlaid by alluvial/colluvial gravels (co-ordinates 19.669E; -32.343S).

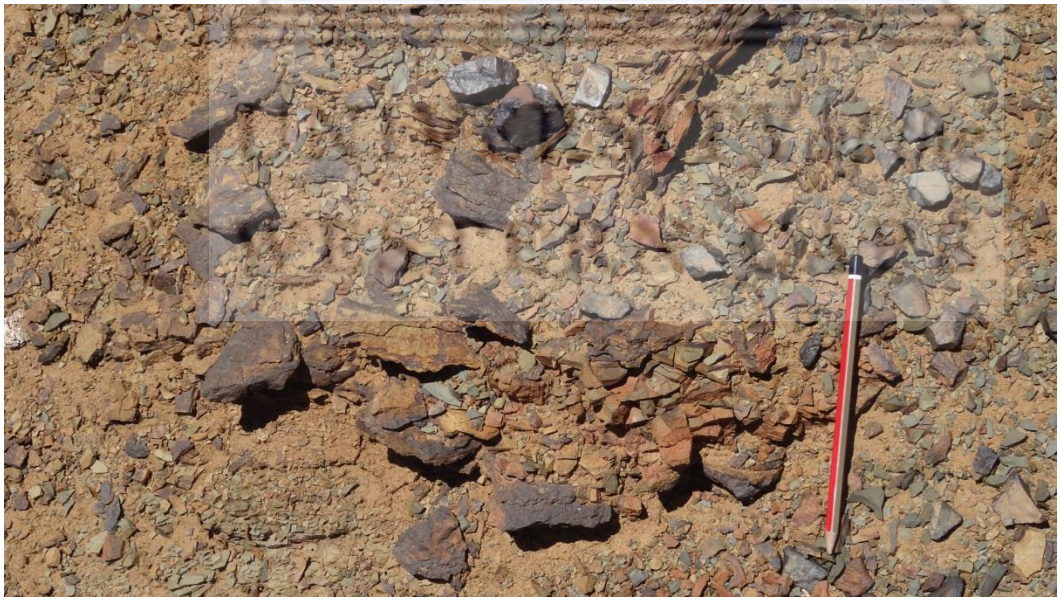

Figure 4.10. Ferruginous shale outcrop 5 Y 4/1 and 5 Y 6/1 in colour and covered by eluvial and colluvial gravels (co-ordinates 19.688E; -32.355S).

A total of 18 Prince Albert Formation shale samples were collected systematically across the succession up to the contact with the overlying Whitehill Formation (Fig. 4.7). Sample HM32 was located in the second unit (Pp2) of the remapped 1:50 000 scale geological map, yet the colours; dark greenish grey (5GY 4/1), olive grey (5Y 4/1) and light olive grey to light brownish grey (5Y 6/1-5YR 6/1) as shown in Figure 4.11, are similar to unit one (Pp1), thereby grouping the units as one succession as discussed earlier. Similar colours occur in unit three (Pp3) of the Prince Albert Formation as shown for example by sample HM35, which consists of greyish olive (10Y 4/2), light olive grey (5Y 5/2) and olive grey (5Y 4/1), slightly silty shale (Fig. 4.12). Shale and slightly silty shale outcrops within the upper part of the Prince Albert Formation display pencil-like weathering.

Figure 4.11. A 0.2m thick shale bed covered by colluvial gravels (co-ordinates 19.683E; -32.351S). Sledge hammer is 0.8m long.

Figure 4.12. Slightly silty shale of unit three (Pp3) covered by colluvial gravels next to the gravel road (co-ordinates 19.695E; -32.362S).

Whitehill Formation

The contact between the Prince Albert Formation and the Whitehill Formation is well-defined (Fig. 4.13), with only 20 cm of the Whitehill Formation being exposed. A light olive grey (5Y 5/2) to moderate olive brown (5Y 4/4), slightly silty shale of the Prince Albert Formation was sampled 0.3 m below the Whitehill Formation contact (Sample HM38). This shale shows iron staining with light brown (5YR 6/4) and dark yellowish orange (10YR 6/6) colours. Sample HM39 was collected from the Whitehill Formation, which comprises a light grey (N7) shale with extensive iron staining coloured light brown (5YR 5/6), moderate yellowish brown (10YR 5/4) and dark yellowish orange (10YR 6/6).

Figure 4.13. Contact between the Prince Albert Formation (PAF) and the Whitehill Formation (WHF), which shows a distinctive white-coloured weathering (co-ordinates 19.699E; -32.364S).

4.1.1.3 Gamka River section, west of Prince Albert

This section across the Prince Albert Formation is the unit holostratotype of the formation and is located along a farm track west of the Gamka River and southwest of the Witpoort homestead on the farm Witte Poort 145, some 25 km west of Prince Albert (Fig. 4.14; Cole, 2005). The strata dip steeply northward at between 63 and 90 degrees and the geology of the section is shown on the original, unpublished 1:50 000 scale, 3321BB Gamkarivier sheet between latitudes 33°13'10"S and 33°13'20"S and longitudes 21°46'15"E and 21°46'30"E (Geological Survey, 1967). Fieldwork was undertaken along the farm track to obtain lithological descriptions of some seventeen samples taken from the Dwyka Group, Prince Albert Formation and Whitehill Formation (Fig. 4.14). Sample co-ordinates, dip measurements and photograph numbers of each field locality are given in Appendix 3.

The geological boundaries were digitised from the original 1:50 000 scale geological map on ArcMap and edited with field data and SPOT5 imagery.

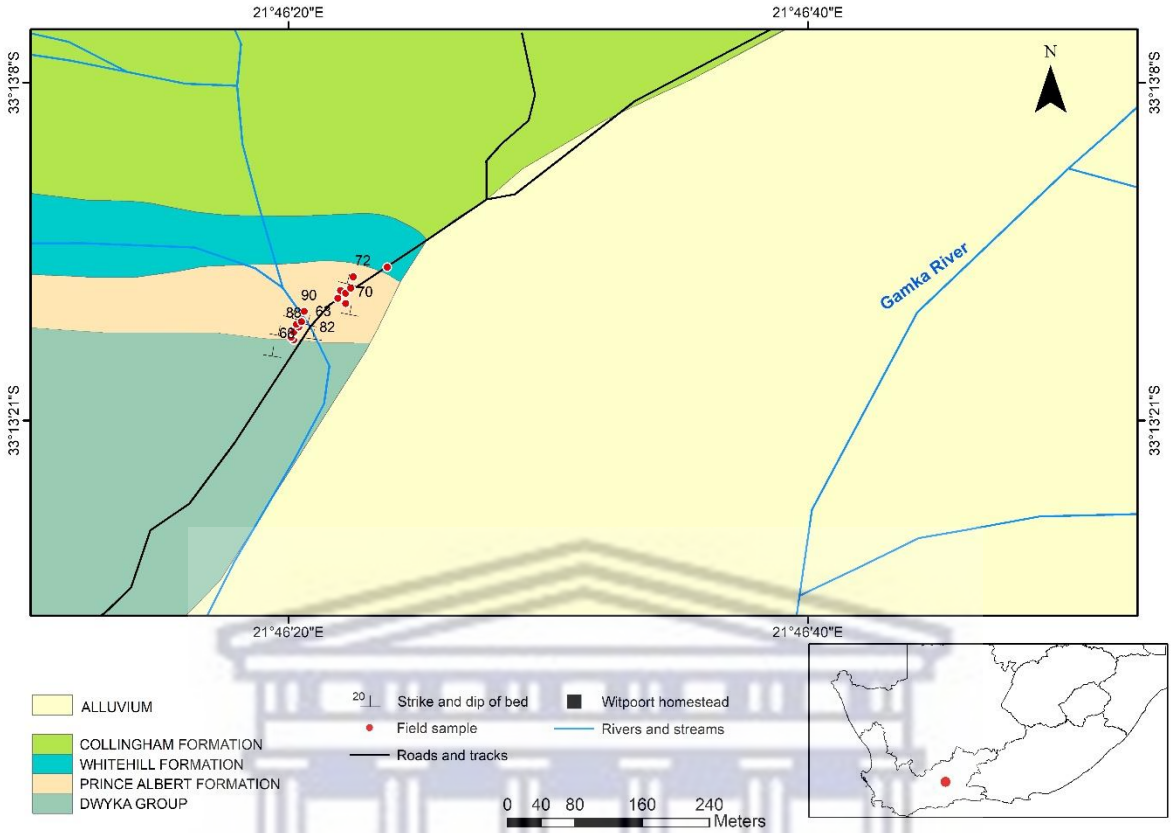

Figure 4.14. Geological map showing positions of field samples in the Gamka River area near Witpoort homestead.

Lithostratigraphy

Dwyka Group

Diamictite of the Dwyka Group is found at the southern end of the field section near the farm track (Fig. 4.14). The diamictite has a siltstone and silty mudstone matrix containing dropstones up to 10 mm long, composed of quartz and sandstone with sporadic vein quartz. A sharp contact is present between the Dwyka Group and Prince Albert Formation (Fig. 4.15). A sample of diamictite (HM40) was collected 1 m south of the contact between the Dwyka Group and the Prince Albert Formation, which is approximately 0.93 m vertically below the contact given a dip of 007/68 (Appendix 3). The matrix of the diamictite is light olive grey (5Y 6/1) and greenish grey (5GY 6/1) in colour (Fig. 4.15).

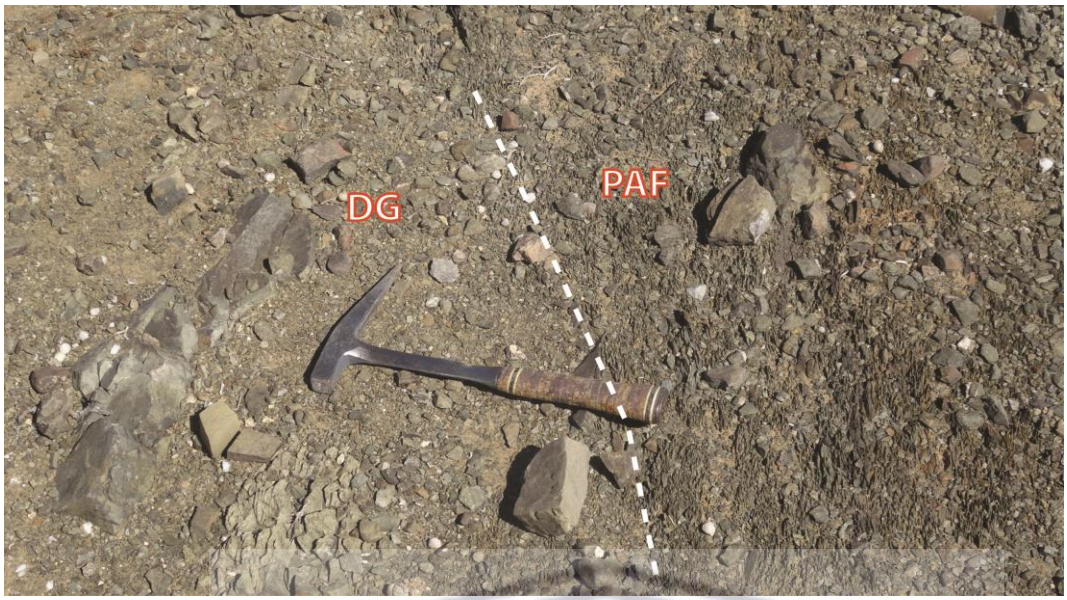

Figure 4.15. Contact between the Dwyka Group (DG) and the Prince Albert Formation (PAF), west of the gravel road to the Witpoort homestead (co-ordinates 21.772E; -33.221S). Geological hammer is 0.4m long.

Prince Albert Formation

The Prince Albert conformably overlies the Dwyka Group and attains a calculated thickness of 57.71 m. Thickness of the Prince Albert Formation was calculated based on outcrop width between samples (HM41 to HM55) and the accompanying fifteen dip measurements along the section (Fig. 4.14; Appendix 3). Since the exposures are flat lying, differences in elevation were not considered.

The Prince Albert Formation consists predominantly of shales, which are medium dark grey (N3-N5), light olive grey (5Y 5/2), greenish grey (5GY 6/1) and dark greenish grey (5 GY 4/1) in colour. Iron staining coloured dark yellowish orange (10YR 6/6), dark to moderate yellowish brown (10YR 4/2- 10YR 5/4), light brown (5YR 5/6) and brownish grey (5YR 4/1) occurs in places. Irregular dark grey (N2-N3), olive black (5Y 2/1) and greyish brown (5YR 3/2) ferruginous beds up to 10 cm thick, occur intermittently and show dusky to dusky yellowish

brown (5YR 2/2 and 10YR 2/2) iron staining (Fig. 4.16). The strata dip between 63 and 90 degrees north (Fig. 4.14) and display pencil-like weathering (Fig. 4.17).

A total of 15 samples were collected across the succession (Appendix 3), but these were not evenly-spaced due to outcrops being discontinuous with areas covered by alluvium and alluvial gravel. The lowermost sample (HM41) was collected at a surface distance of 0.35 m from the basal contact with the Dwyka Group (Fig. 4.15) or approximately 0.32 m vertically above the contact. This sample consists of shale, light olive grey (5Y 6/1) and medium to light grey (N5-N6) in colour with light to moderate brown (5 YR 5/6 and 5YR 4/4) iron staining. The uppermost sample (HM55) of the Prince Albert Formation was collected at co-ordinates 21.773E; 33.221S, approximately 22 m surface distance from the inferred base of the Whitehill Formation or 19.55 m stratigraphically below the contact, given a dip of 002/72 (Appendix 3).

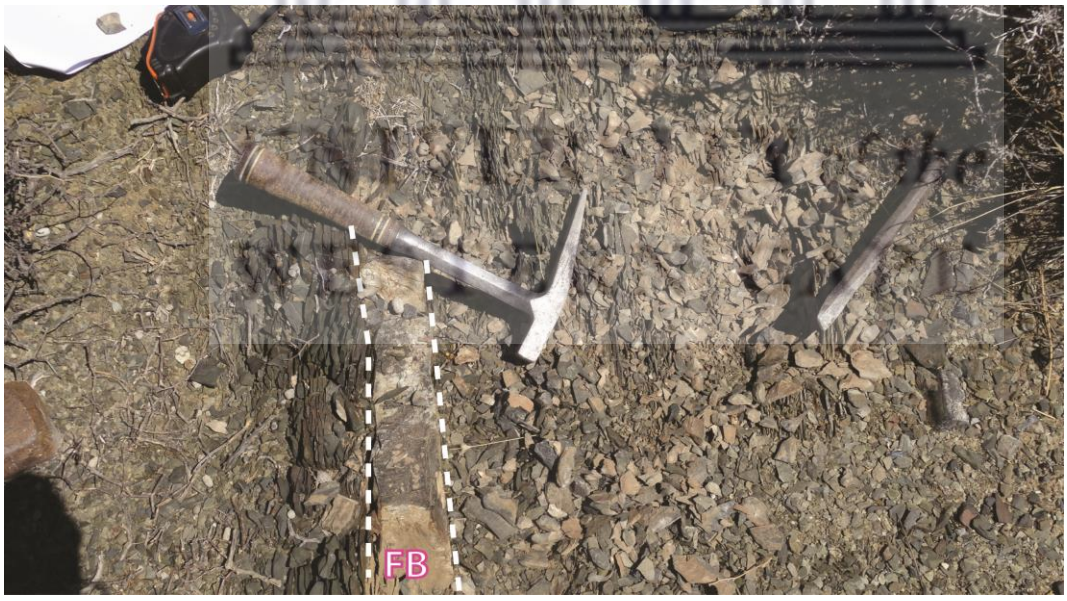

Figure 4.16. Hard ferruginous bed (FB) 6cm thick interbedded with medium dark grey (N3-N5) shales of the Prince Albert Formation (co-ordinates 21.772E; -33.221S).

Figure 4.17. Pencil-like weathering of the Prince Albert Formation shales (co-ordinates 21.772E; -33.221S).

Whitehill Formation

The contact between the Prince Albert and Whitehill Formations was not visible along the gravel road, since the area was covered in scree and alluvium over a distance of 43 m between the uppermost Prince Albert and lowermost Whitehill Formation exposures. The ground west of the farm boundary fence where outcrops may have been present, was not accessed due to the farm-owner being absent from the farm. Typical white weathering shale of the Whitehill Formation was not present and the formation was only identified by the presence of a dolomite concretion within the gravel road (Fig. 4.18). This occurs 23.7 m down dip of sample HM55 and about 8.7 m north of the inferred contact between the Prince Albert and Whitehill Formations. The dolomite concretion is medium to light grey (N4-N6) in colour, 0.5 by 0.8 m in size, and was sampled (HM56).

Figure 4.18. Dolomite concretion within the Whitehill Formation, exposed in the gravel road towards Witpoort homestead (co-ordinates 21.773E; -33.221S).

4.1.1.4 Borehole KZF-01,Tankwa, Ceres

A detailed report by Cole et al. (2016b) describes the entire lithology log and stratigraphy of the core of boreholes KZF-01 and KWV-01 drilled in the Tankwa Karoo and near Willowvale in the Eastern Cape.

Borehole KZF-01 was sited on the farm Zand Fontein 89 in the Tankwa Karoo, which is located 75 km northeast of Ceres in the southwestern part of the main Karoo Basin (Fig 4.19). Borehole KZF-01 was sited by the Karoo Research Initiative (KARIN), which is an academic study of the geology of the Karoo Supergroup and involves researchers from the Universities of Johannesburg, Witwatersrand, Cape Town, Western Cape, Pretoria and Free State in South Africa, the University of Portsmouth in England and the Council for Geoscience, South Africa. KZF-01 was sited south of the dolerite line, which marks the southern limit of Early Jurassic dolerite intrusions and occurs west of the area having a shale gas potential, i.e. the “sweet spot” (Cole, 2014; Mowzer and Adams, 2015).

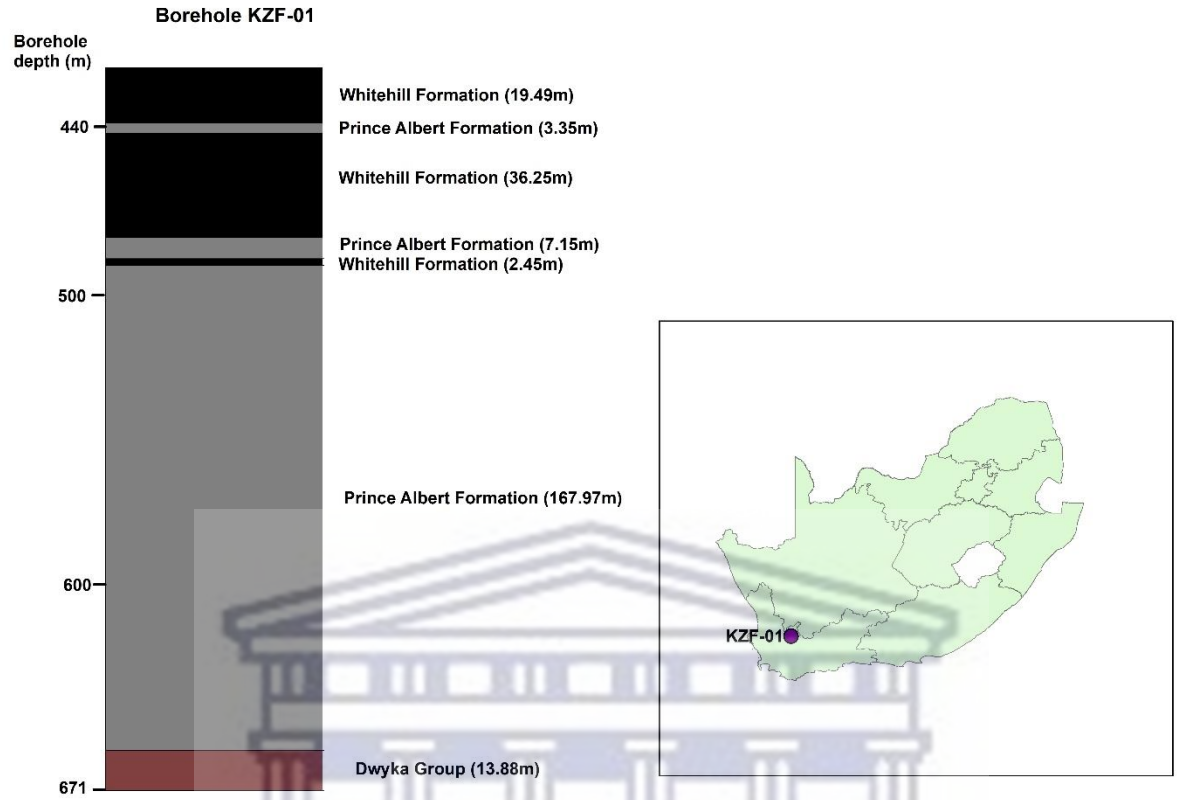

Figure 4.19. Map of borehole location and simplified graphic log of the core of borehole KZF-01 showing the stratigraphy of the Prince Albert Formation and the overlying and underlying units.

Lithostratigraphy

Whitehill Formation

The Whitehill Formation, which is the unit overlying the Prince Albert Formation, is first described. This unit was intersected at three levels in Borehole KZF-01 as a result of low-angle thrusting. The first intersection was between borehole depths of 420.46 m and 439.95 m, giving a thickness of 19.49 metres. Here, the Whitehill Formation consisted of black (N1-N2) shale containing fine pyrite lenses and beds with sparse siltstone beds and laminae, light olive gray (5Y 6/1) in colour and up to 3mm in thickness. One sample (HM57; Fig. 4.20) of carbonaceous shale was taken from between depths 439.61 and 439.95 m (Fig. 4.20). The second intersection of Whitehill Formation was between depths of 443.3 m and 479.55 m,

yielding a thickness of 36.25 metres in thickness. It consists of black (N1-N2), carbonaceous shale and medium grey (N4-N5) silty mudstone. This zone of Whitehill Formation was highly brecciated with quartz veins and rare calcite veins and veinlets. The third intersection (Fig. 4.19) was between depths of 486.7 m and 489.15 m (2.45 metres thick) and comprised black (N1-N2) shale, with very fine-grained pyrite beds and laminae up to 6 cm thick, and quartz veins, some with pyrite. This zone of Whitehill Formation had a gradational base and irregular top (Fig. 4.21). The total thickness of the Whitehill Formation from the three intersections is about 58 metres.

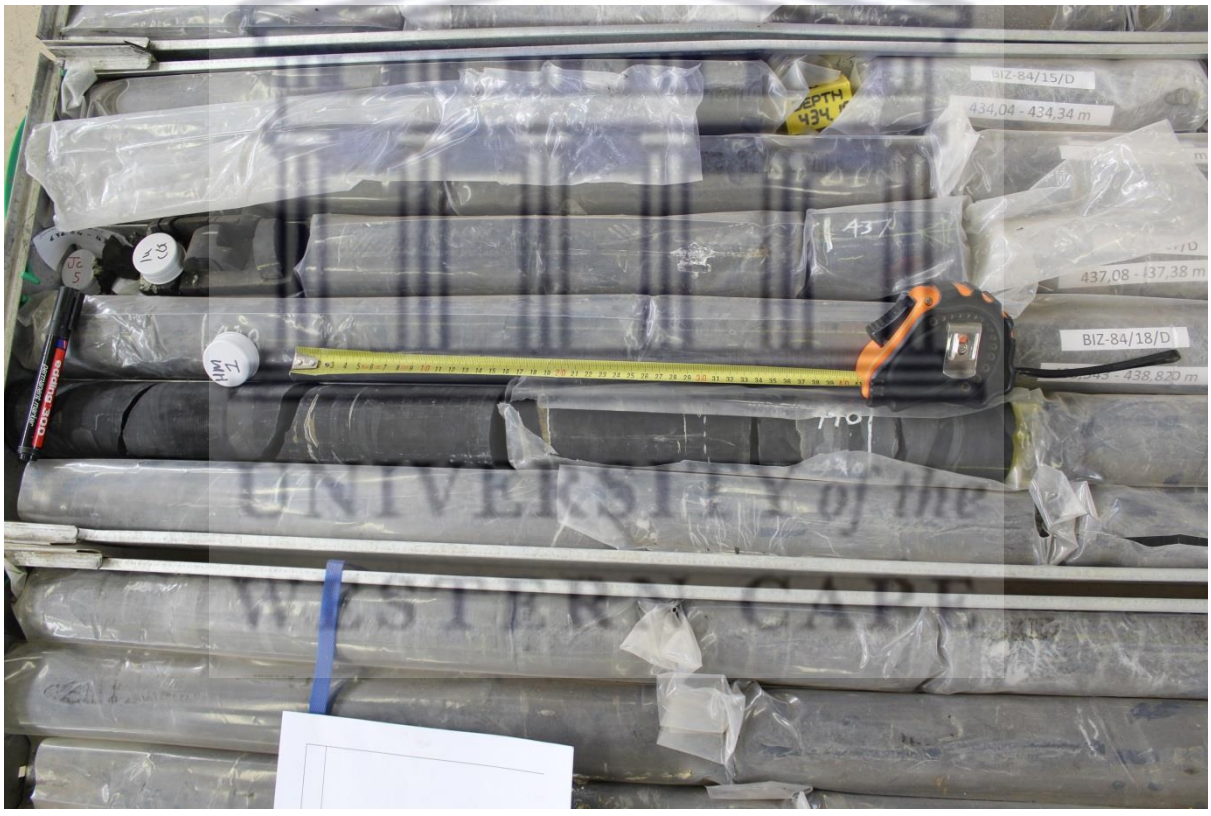

Figure 4.20. Black (N1-N2) carbonaceous shale of the Whitehill Formation of Borehole KZF-01. The tape marks the position of sample HM57 taken from between depths of 439.61 and 439.95 m. Core of the Whitehill Formation has been covered in plastic in order to prevent the oxidation of pyrite contained within the shale.

Figure 4.21. Irregular top (orange dash line) of the Whitehill Formation at 486.7 m below a brecciated contact with the Prince Albert Formation, which has been thrusted over the Whitehill Formation.

Prince Albert Formation

The Prince Albert Formation lies *in situ* between depths of 489.15 m and 657.12 m and is overlaid by the Whitehill Formation with a sharp planar contact. As a result of low-angle thrusting, the Prince Albert Formation was duplicated twice above this *in situ* contact at 489.15 m. The uppermost duplication was between depths of 439.95 m and 443.30 m giving a thickness of 3.35 metres (Fig. 4.19). In this zone, the Prince Albert Formation consists of rhythmite (heterolithic lithofacies) between depths of 439.95 m and 440.58 m, medium dark to light grey (N3-N6) in colour, highly deformed, calcareous and containing sparse lenses of fine-grained pyrite. A massive shale lies between depths of 440.58 m and 440.81 m, greyish black to dark grey (N2-N3) in colour with slightly calcareous, siltstone concretions. Between depths of 440.81 m and 441.44 m, mudstone medium dark to light grey (N4-N6) in colour, slightly calcareous with quartz veins and veinlets up to 10 mm thick, is present (Fig. 4.22).

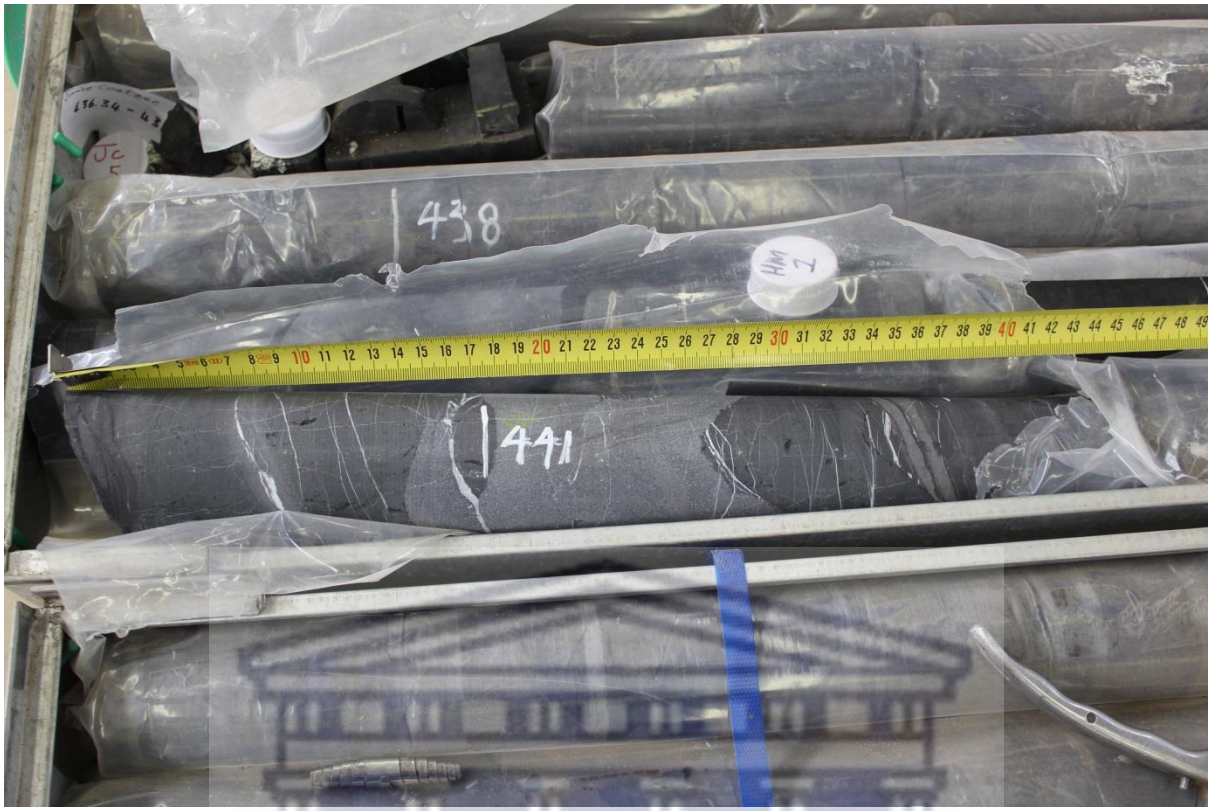

Figure 4.22. Mudstone (N4-N6) between depths 440.81 and 441.17 m with lenticular siltstone concretions (N6), quartz veins and veinlets within the Prince Albert Formation.

Medium light grey (N6), lenticular siltstone concretions occur between depths of 440.73 m and 441.11 m. One sample (HM 58) was taken of the Prince Albert Formation from between depths of 440.81 m and 441.17 m. In the lower part of the duplication, between depths of 441.44 m and 441.73 m, the Prince Albert Formation consists of massive shale, dark to medium grey (N3-N4) in colour with pyrite laminae and lenses. A dark to light grey (N3-N7) rhythmite occurs between depths of 441.73 m and 441.85 m and a light olive grey (5Y 6/1) siltstone between depths of 441.85 m and 441.89 m. A 1 cm thick, very light grey (N8), very fine-grained sandstone overlies a massive shale, medium dark to light grey (N4-N7) in colour between depths of 441.9 m and 441.96 m. A 4 cm-thick siltstone, greenish grey (5 GY6/1) and medium light grey (N6) in colour with shale laminae and lenses occurs between depths of 441.96 m and 442 m. Between depths of 442 m and 443.3 m, a massive shale, greyish black

to medium dark grey (N2-N4) in colour, is present. This was sampled (HM59) between depths of 442.17 m and 442.56 m (Fig. 4.23).

Figure 4.23. A massive shale between depths 442.17 and 442.56m with siltstone beds up to 2cm thick and pyrite lenses up to 2mm thick where sample HM59 was taken.

The lowermost duplication of the Prince Albert Formation was intersected between depths of 479.55 m and 486.70 m, giving a thickness of 7.15 metres (Fig. 4.19). It comprises massive shale, greyish black to medium grey (N2-N5) in colour, with siltstone beds and laminae up to 35 mm thick, abundant quartz veins up to 20 mm thick and rare calcite veins. Dark to medium grey (N3-N4) silty shale, with very fine-grained pyrite occurs between depths of 486.09 m and 486.29 m and is underlain by a 41 cm thick massive shale, which is highly brecciated and contains deformed masses of sandstone with fine-grained pyrite and abundant quartz veins

and veinlets. Two samples (HM60 and HM61) were collected from this lower duplicated zone (Fig. 4.24).

Figure 4.24. Massive shale of the Prince Albert Formation showing positions of samples HM60 and HM61 that were collected respectively from depths 479.72 – 480.10 m and 484.22 – 484.66 m.

The *in situ* Prince Albert Formation extends from depths of 489.15 m to 657.12 m giving a thickness of 167.97 metres (Fig. 4.19). Thirty samples (HM62 - HM91; Appendix 4) of this *in situ* Prince Albert Formation were collected at intervals of 5.6 metres, systematically throughout the formation. The lithology consists of greyish black to medium grey (N2-N5) shale with abundant siltstone and very fine-grained sandstone beds up to 0.43 m in thickness. Numerous quartz veins and isolated volcanic tuff beds up to 0.09 m in thickness, are present. There is a sharp base with the underlying Dwyka Group, with 0.61 m of shale containing dropstones of sandstone and quartzite, up to 4 mm in size, overlying diamictite with a silty mudstone matrix (Fig. 4.25).

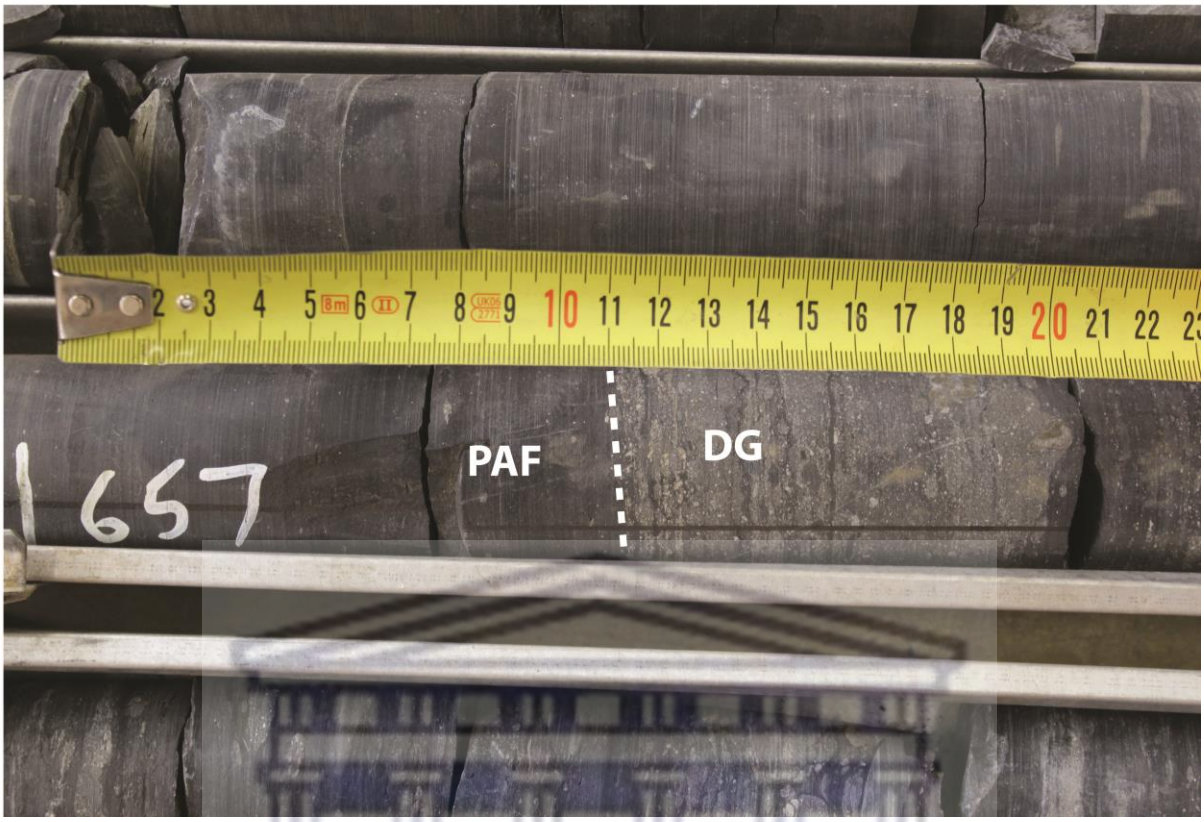

Figure 4.25. Basal contact (white dashed line) at 657.12 m of the Prince Albert Formation (PAF) with the underlying diamictite of the Dwyka Group (DG).

Dwyka Group

The Dwyka Group was intersected at 657.12 m until the end of the borehole at 671 m, giving a thickness of 13.88 metres. The Dwyka Group consists mostly of diamictite, medium dark to medium light grey (N4-N6) in colour. It has a silty mudstone matrix and contains abundant clasts, mostly sandstone and siltstone, up to 30 mm in size (Figs. 4.25 and 4.26). Rare granite and limestone clasts are present and isolated sandstone and siltstone beds and laminae also occur. One sample (HM92) was taken of the Dwyka Group between depths of 657.51 m and 657.80 m.

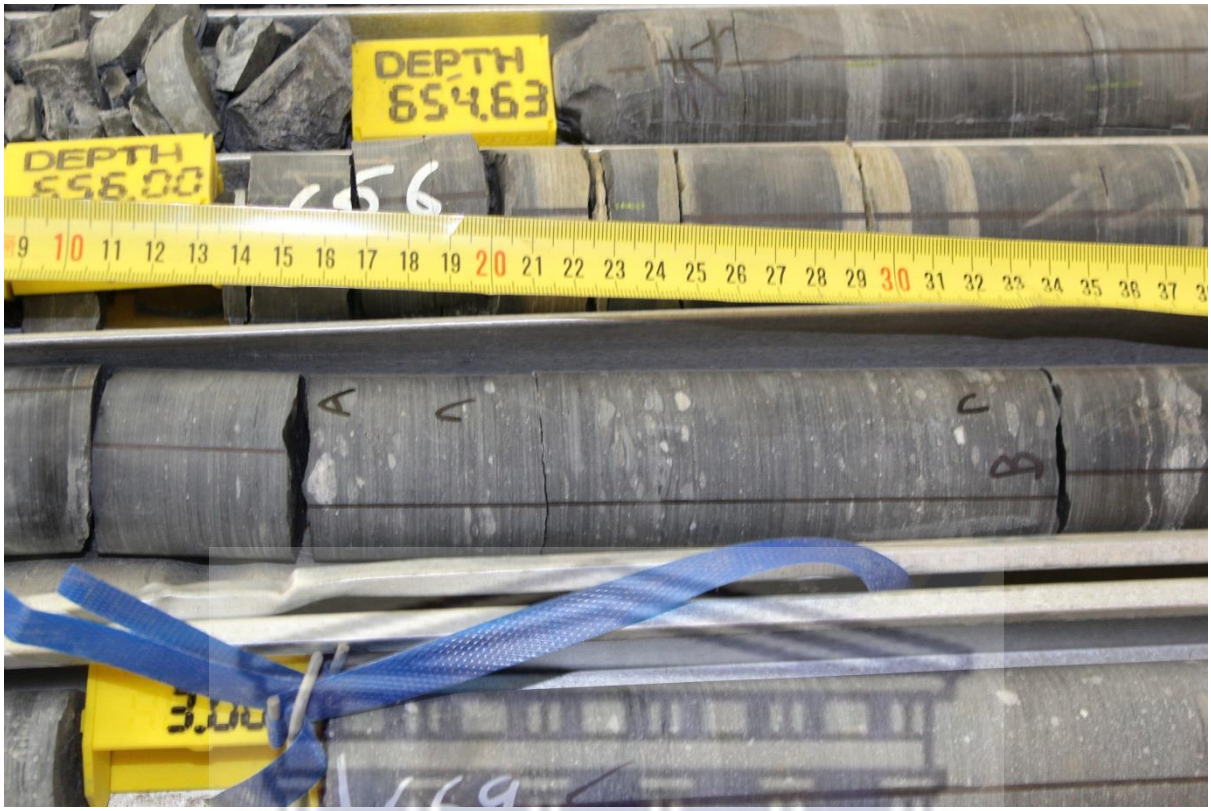

Figure 4.26. Diamictite of the Dwyka Group composed of coarse-grained to pebble size dropstones of sandstone, quartzite, siltstone and limestone set in a silty mudstone matrix.

4.1.1.5 Borehole KWV-01, Willowvale, Eastern Cape

Borehole KWV-01 was sited 7 km northeast of Willowvale (Fig. 4.27), in the southeastern part of the main Karoo Basin by KARIN. KWV-01 was drilled in this part of the basin in order to determine the lithology and stratigraphy of the Ecca Group in an area lacking previous data (closest deep borehole, SP1/69, lies 120 km to the SSW), and to determine the effect of dolerite intrusion on the sedimentary rocks, including the shale gas potential of the Prince Albert Formation.

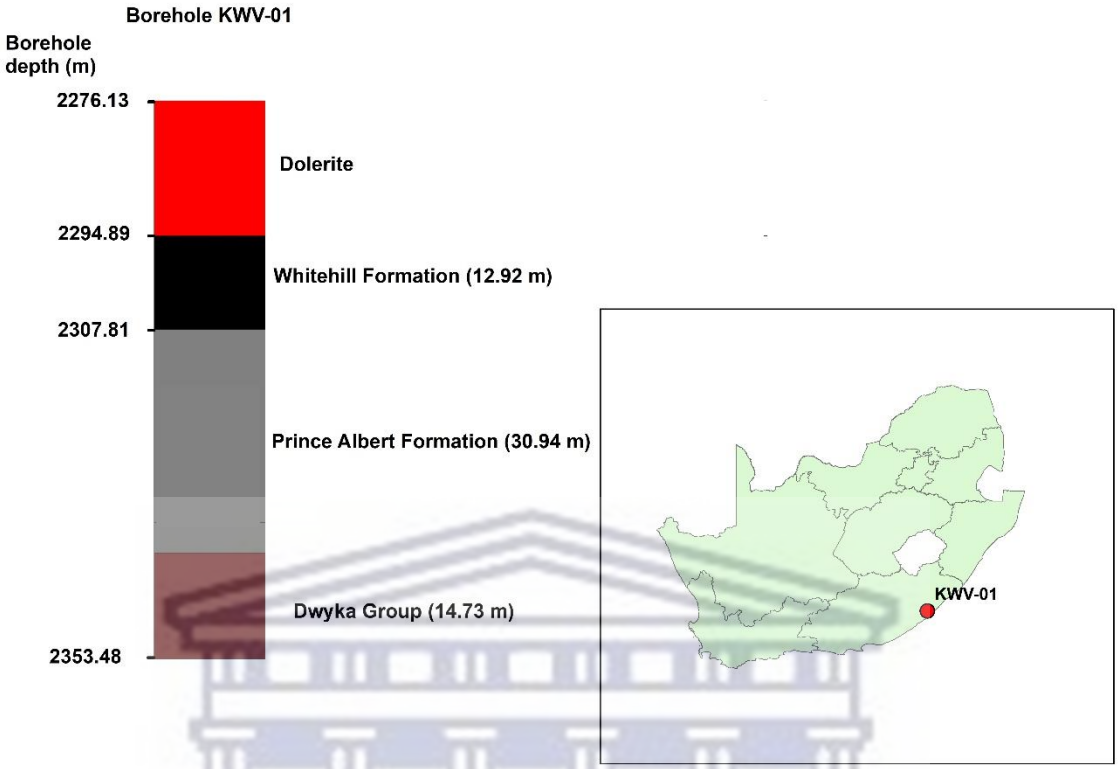

Figure 4.27. Map of borehole location and simplified graphic log of the core of borehole KWV-01 showing the stratigraphy of the Prince Albert Formation and the overlying and underlying units, including dolerite.

Lithostratigraphy

Whitehill Formation

The Whitehill Formation was intersected between depths of 2276.00 m and 2307.81 m with an 18.76 m thick dolerite sill intruding the uppermost part (Fig. 4.27). Black to greyish black (N1-N2) carbonaceous shale, 0.13 m thick occurs above the dolerite sill. The Whitehill Formation below the dolerite sill is 12.92 m thick, giving a total thickness of 13.05 m (Fig. 4.27). Below the sill, the formation consists of black to greyish black (N1-N2), carbonaceous shale containing disseminated pyrite and rare siltstone beds up to 4 cm thick. Light grey (N7-N8) calcareous concretions, beds and laminae, up to 6 mm thick are found in places. One

sample (HM93) was collected from the Whitehill Formation between depths of 2306.96 m and 2307.28 m (Fig. 4.28; Appendix 5). The basal contact with the underlying Prince Albert Formation is sharp and distinctive with black shale overlying dark grey silty shale (Fig. 4.29).

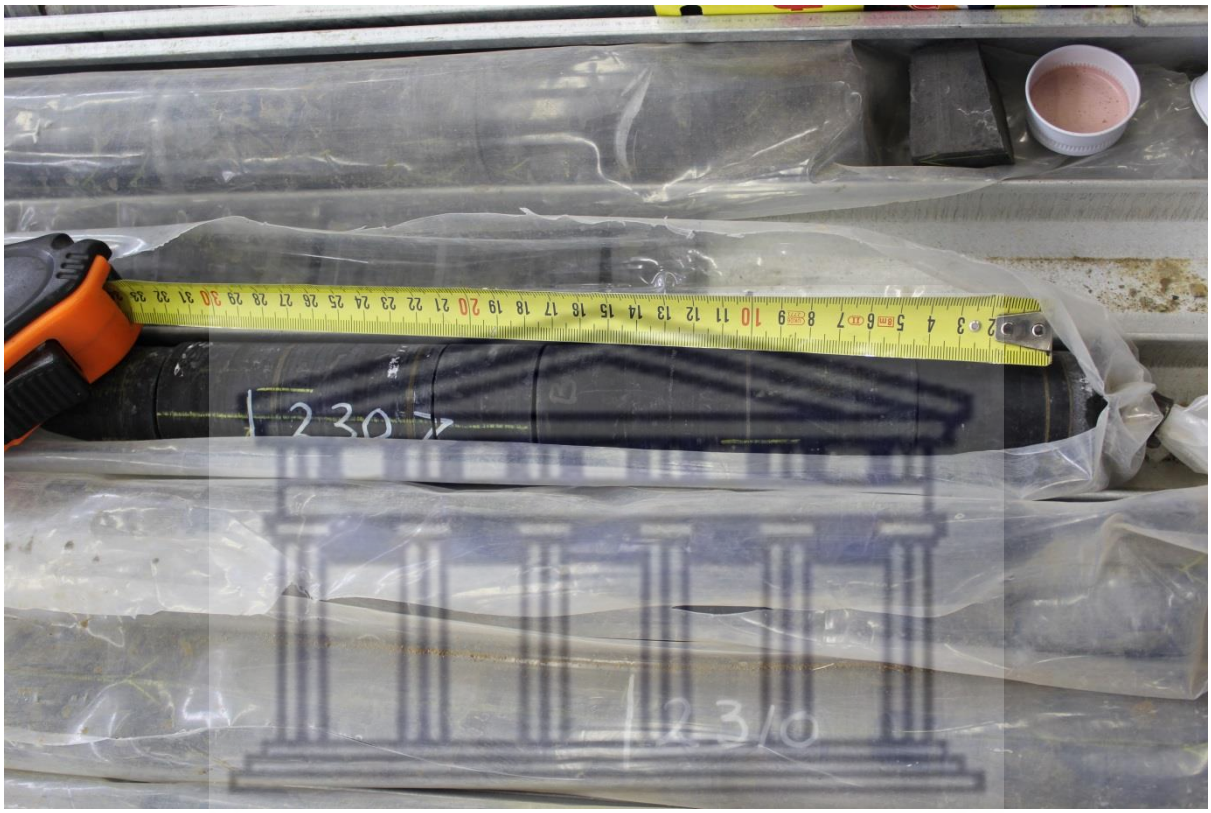

Figure 4.28. Black carbonaceous shale with isolated pyrite laminae forming part of the Whitehill Formation from borehole KWV-01. Sample HM 93 was retrieved from between depths 2306.96 m and 2307.28 m. The core has been covered in plastic in order to prevent the oxidation of pyrite contained within the shale.

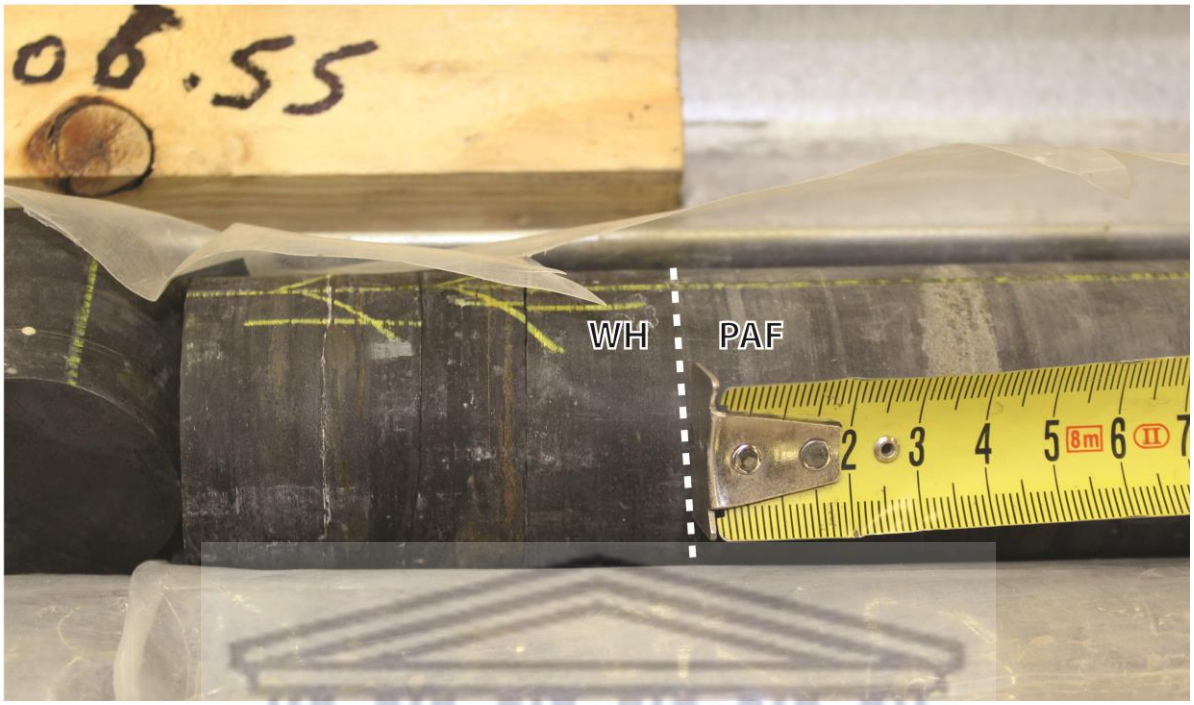

Figure 4.29. Contact between the Whitehill Formation (WHF) and the Prince Albert Formation (PAF) indicated by the white dashed line at a depth of 2307.81 m.

Prince Albert Formation

The Prince Albert Formation extends from depths of 2307.81 m to 2338.75 m having a thickness of 30.94 metres (Fig. 4.27). From depth 2307.81 m to 2323.81 m, the Prince Albert Formation consists of massive silty shale, dark grey to medium grey (N3-N5) in colour, with disseminated fine-grained pyrite and calcite veins. The uppermost sample (HM94; Fig. 4.30) was taken from depths of between 2309.05 m and 2309.37 m and another six samples were collected every three metres throughout the massive silty shale succession (refer Appendix 5). Siltstone beds are present, medium light grey to very light grey (N6-N8) in colour, up to 3 cm thick, and showing soft sediment deformation. Calcareous concretions with shale laminae and lenses, light to very light grey (N7-N8) and light brownish grey (5YR 6/1) in colour, occur locally.

Figure 4.30. Massive silty shale with horizontally laminated siltstone between depths of 2309.50 m and 2309.52 m forming part of the Prince Albert Formation. Sample HM 94 was taken from depths of between 2309.05 m and 2309.37 m.

Rhythmite was intercepted between depths of 2323.81 m and 2338.75 m. It ranges from dark grey to very light grey (N3-N8) in colour and consists of alternations of silty mudstone up to 88 cm thick, siltstone up to 11 cm thick and mudstone up to 6 cm thick. Two samples (HM102 and HM103) of rhythmite were retrieved from depths of between 2332.24 m and 2332.56 m and 2334.14 m and 2334.48 m (Fig. 4.31). Calcareous concretions, medium grey to light grey (N5-N7) in colour, occur between depths of 2327.78 m and 2327.79 m; 2328.64 m and 2328.70 m; and 2329.52 m and 2329.55 m. Shale clasts are present between depths of 2328.64 m and 2328.70 m. A gradational contact is present between the Prince Albert Formation and the Dwyka Group, with rhythmite containing dropstones of very fine-grained sandstone up to 2 mm wide, grading down into clast-poor diamictite with a muddy to silty matrix (Fig. 4.32).

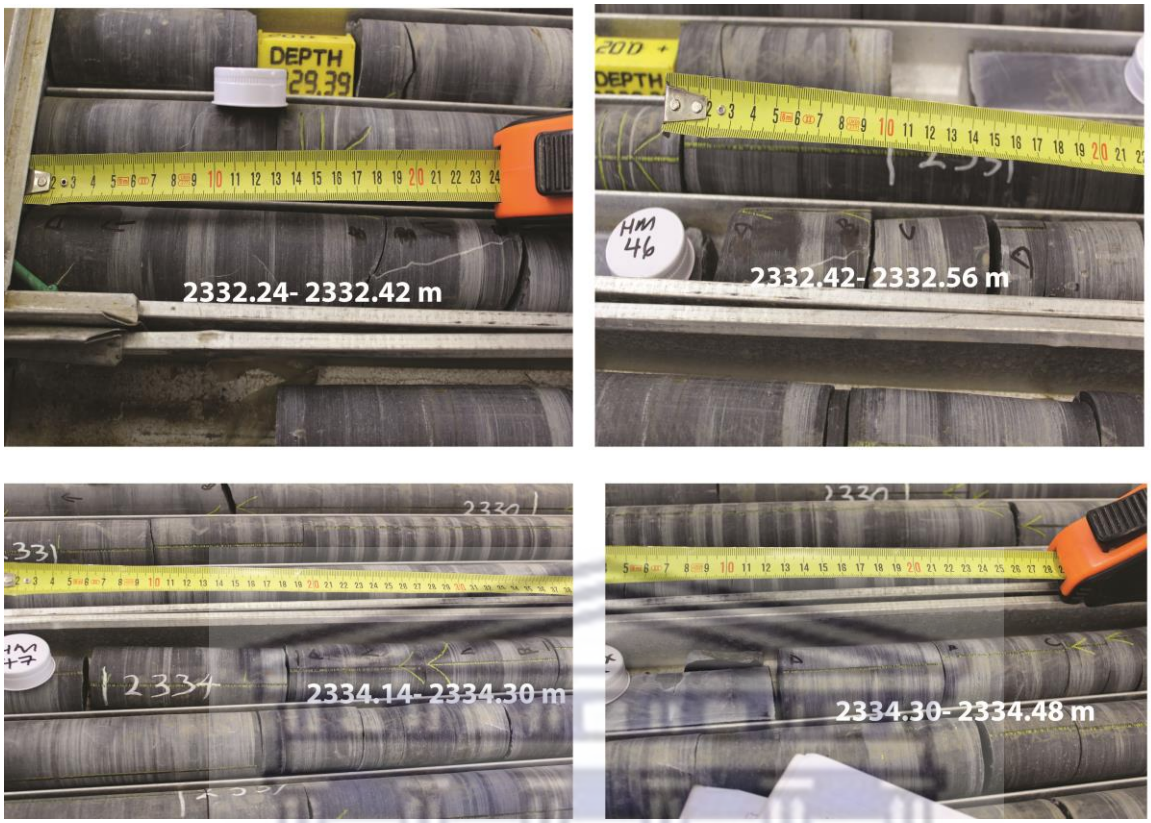

Figure 4.31. Adjoining pictures showing rhythmite of the Prince Albert Formation, from which samples HM102 (2332.24 – 2332.56 m) and HM103 (2334.14 – 2334.48 m) were taken.

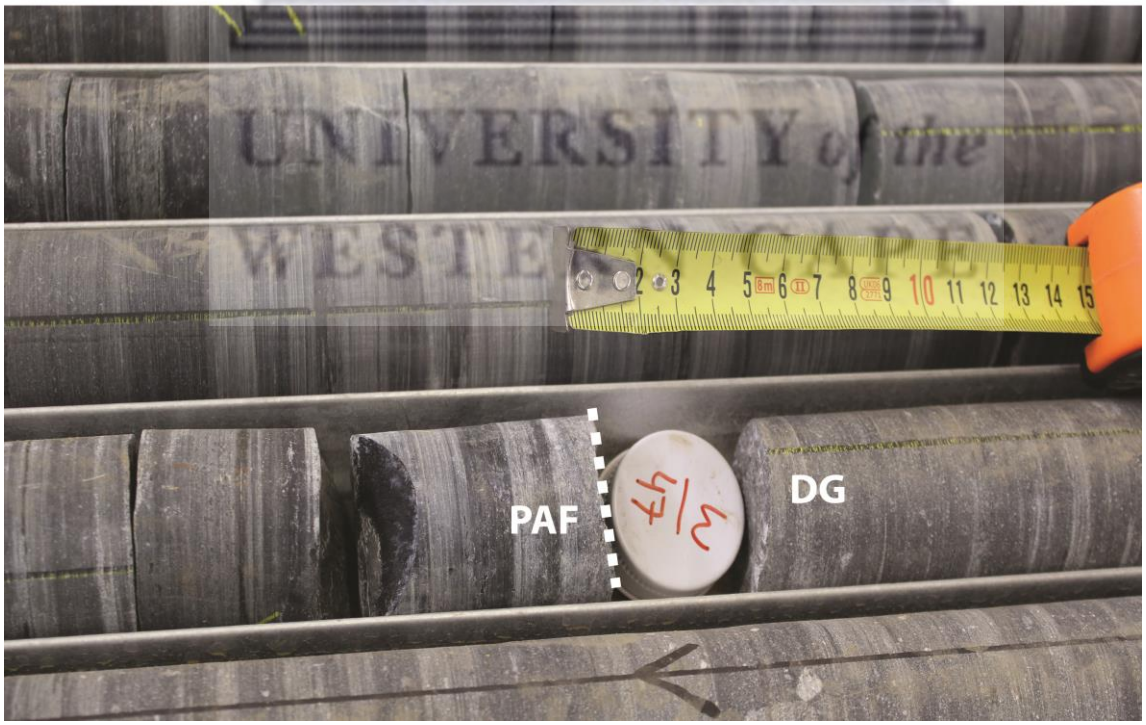

Figure 4.32. Rhythmite of the Prince Albert Formation (PAF), which contains dropstones of very fine-grained sandstone in the basal 36 cm, overlying

diamictite of the Dwyka Group (DG) at 2338.75 m depth (white dash line). A portion of core is missing at the bottle top.

Dwyka Group

The Dwyka Group was intersected at a depth of 2338.75 m in borehole KWV-01 (Fig. 4.32) and was present until the end of the borehole at 2353.48 m, giving a thickness of 14.73 metres (Fig. 4.27). A sample (HM104) of diamicitite was collected 2 cm below the upper contact between depths of 2338.77 m and 2339.18 m (Fig. 4.33). The Dwyka Group consists of massive, clast poor diamictite with a muddy to silty matrix ranging between medium dark grey and medium light grey (N4-N6) in colour (Figs. 4.32 and 4.33). The matrix is sandy and coloured medium light grey to light grey (N6-N7) in places. The lonestones in the diamictite consist mostly of sandstone with some sparse quartz, and are medium-grained to cobble in size (maximum 65 mm).

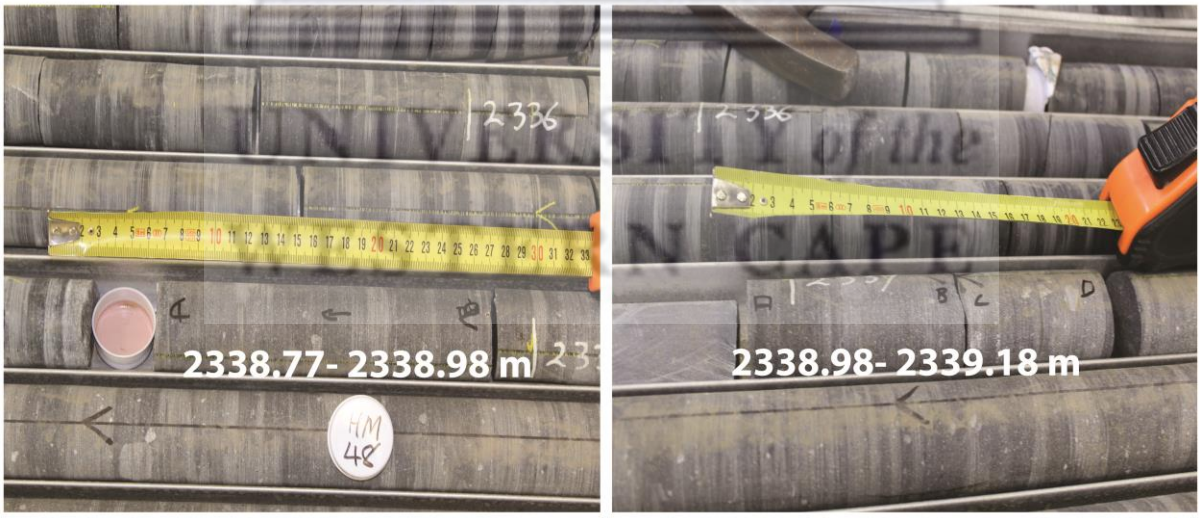

Figure 4.33. Adjoining pictures showing medium dark grey to light grey (N4-N7) diamictite of the Dwyka Group, from which sample HM104 (2338.77 – 2339.18 m) was taken.

4.1.1.6 Grahamstown area, Eastern Cape:

The Prince Albert Formation was sampled from three outcrop sections namely Debruinspoort, Ecca Pass and Pluto's Vale (Kingsley, 1977) north of Grahamstown, Eastern Cape (Fig. 4.34). The geology of the sampled localities was derived from the published 1:250 000 scale, 3326 Grahamstown geology sheet (Geological Survey, 1995) and Google Earth satellite images.

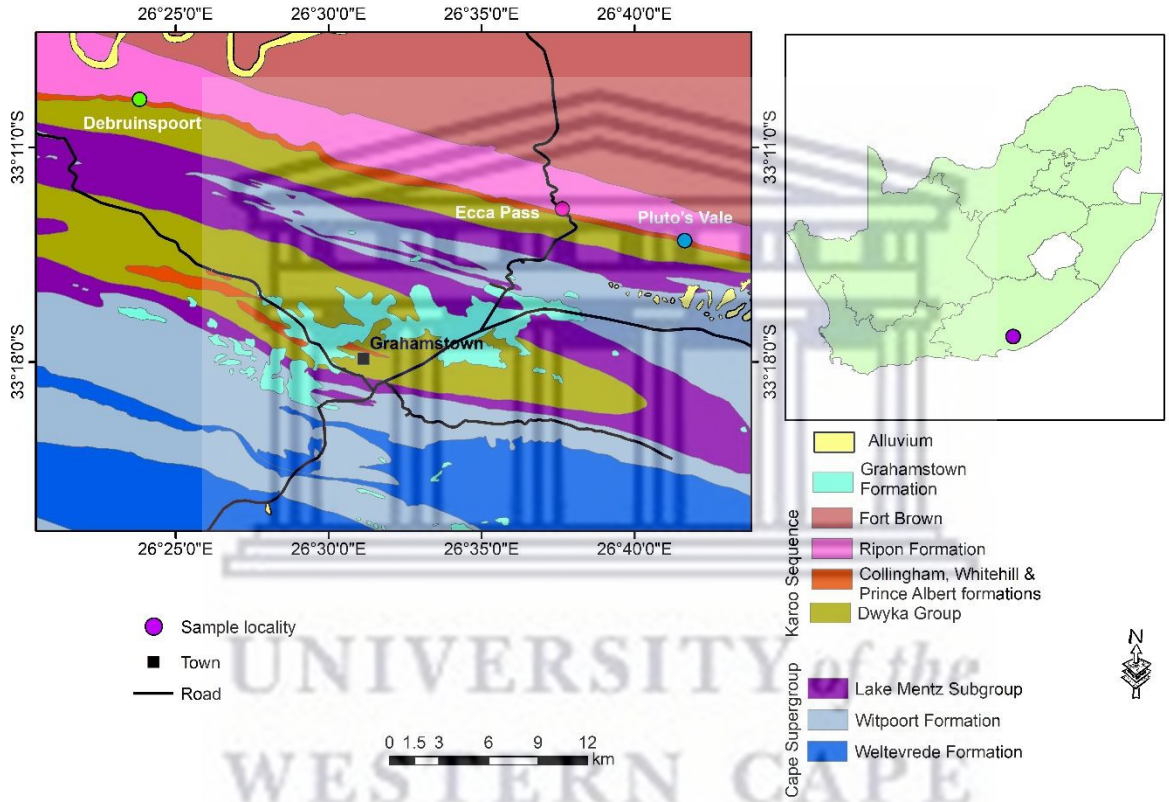

Figure 4.34. Geological map showing positions of sampled outcrop sections near Grahamstown, Eastern Cape (Geological Survey, 1995).

5.1.1.6.1 Debruinspoort

Fieldwork was undertaken along the R344 road to delineate a lithological section and obtain samples of the Prince Albert Formation, as well as the underlying Dwyka Group and overlying Whitehill Formation (Fig. 4.35). However, outcrops were found to be discontinuous and isolated and it was only possible to retrieve five samples and measure an approximate

thickness of the Prince Albert Formation. Sample co-ordinates, dip measurements and photograph numbers of each field locality are given in Appendix 6.

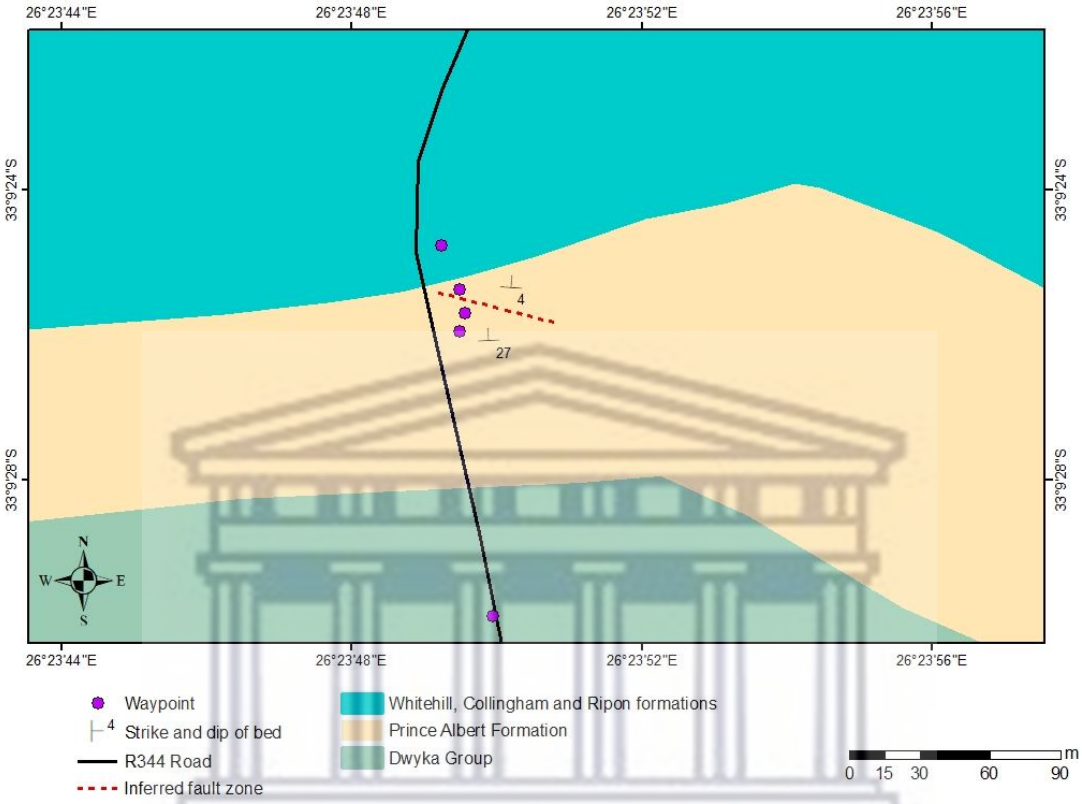

Figure 4.35. Geological map showing positions of field samples at Debruinspoort, Eastern Cape.

Lithostratigraphy

Dwyka Group

A sample (HM105) from the Dwyka Group was collected immediately west of the R344 road about 119 metres south of lowermost Prince Albert Formation sample (Fig. 4.35). The Dwyka Group has an estimated thickness of 630 m in this area and consists predominantly of massive diamictite (Johnson and Le Roux, 1994). In the uppermost part, which was sampled, it takes the form of a light olive grey (5Y 5/2) massive diamictite consisting of dropstones set in a silty mudstone matrix (Fig. 4.36). These dropstones are sub-rounded to angular in shape and

consist of quartz pebbles up to 25 mm in length. The contact with the overlying Prince Albert Formation was not seen due to a cover of scree and vegetation over a distance of 119 m.

Figure 4.36. Diamictite consisting of silty mudstone containing sparse clasts of the Dwyka Group west of the R344 road (co-ordinates 26.397E; -33.158S). Hammer is 30 cm in length.

Prince Albert Formation

In the section at Debruinspoort, the Prince Albert Formation crops out sporadically and there is an extensive cover of scree and vegetation. The formation has a calculated thickness of 57 m based upon the inferred positions of the lower and upper contacts (Fig. 4.35) and the average measured dip (15^{o}) towards the north-northeast. The formation consists predominantly of shaly mudstone (Fig. 4.37).

Figure 4.37. Shaly mudstone of the Prince Albert Formation (co-ordinates 26.397E; -33. 152S).

The lowermost sample of shaly mudstone (HM106) was taken at co-ordinates 26.397E; 33.157S along a road cutting and another two samples were collected systematically across the succession up to the contact with the overlying Whitehill Formation (Fig. 4.35). Shaly mudstone of the Prince Albert Formation ranges in colour from olive grey (5Y 4/1), medium dark grey (N4) and dark greenish grey (5GY 4/1). Abundant quartz veins with some iron staining are present throughout the formation.

At co-ordinates 26. 397E; 33.157S, approximately 5 m down-dip from sample HM107, a fault zone is inferred due to a change in bedding strike with contrasting dip measurements either side of the fault of 4 and 27 degrees (Figs. 4.35 and 4.38).

Figure 4.38. Scree-covered Prince Albert Formation with a fault zone indicated by dashed line.

Whitehill Formation

The contact between the Prince Albert Formation and the Whitehill Formation is not well exposed and isolated outcrops of Prince Albert Formation shale and weathered Whitehill Formation shale (Fig. 4.39) occur 1.3 m apart. The shale is greyish black to dark grey in colour (N2-N3) with abundant quartz veins. Downdip, north of this outcrop of Whitehill Formation, the road section is scree- and vegetation covered over a distance of 90 m, followed by an exposure of *in-situ* Whitehill Formation. This was sampled at co-ordinates 26.397E; 33.157S (sample HM109). This shale ranged in colour from greyish black to dark grey (N2-N3) and weathered very light grey (N8; Fig. 4.40 A). Pyrite staining and ferruginous laminae were present in places (Fig. 4.40 B).

Figure 4.39. Poorly exposed outcrop of the Whitehill Formation close to the contact (covered) with the underlying Prince Albert Formation (co-ordinates 26.396E; -33.157S).

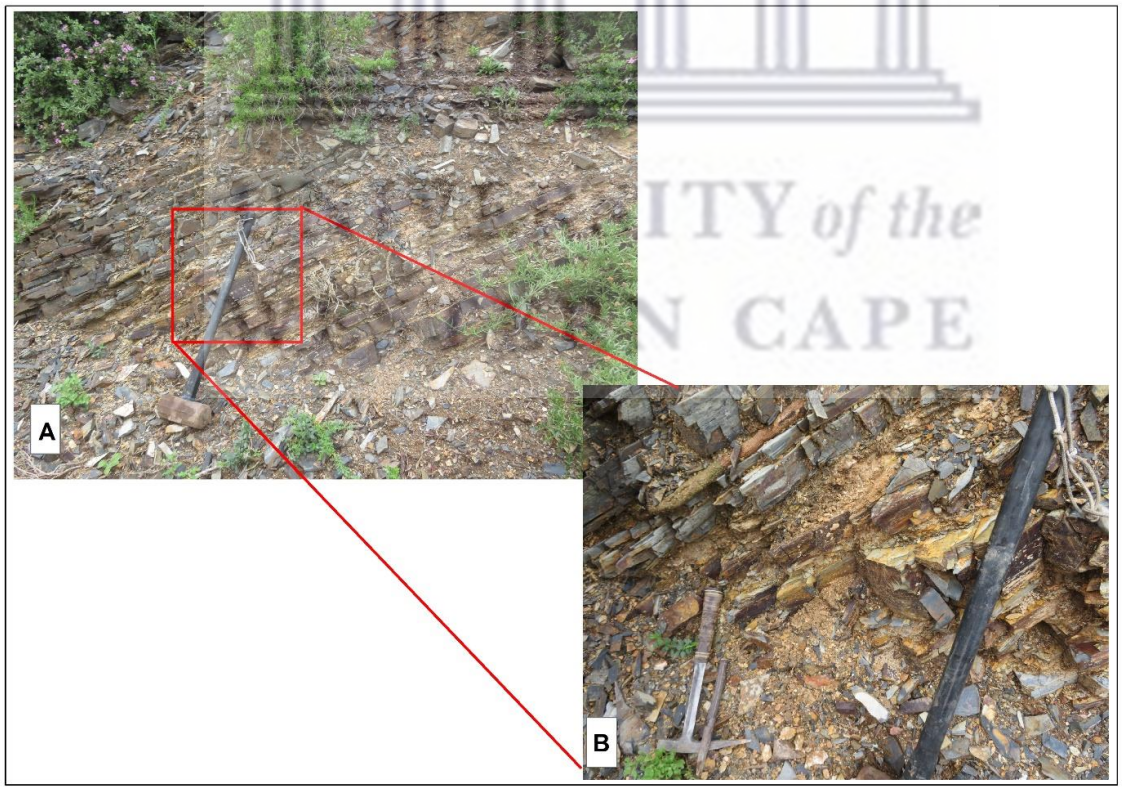

Figure 4.40. (A) Shale of the Whitehill Formation partially covered with vegetation. (B) Beige staining due to oxidation of pyrite in highly weathered shale of the Whitehill Formation.

5.1.1.6.2 Ecca Pass

The Ecca Pass section is located along the R67 road about 14 km northeast of Grahamstown (Fig. 4.34). This section plots on the unpublished 1:50 000 scale, 3326BA Fort Brown geological sheet between latitudes 33°13'S and 33°14'S and longitudes 26°37'E and 26°38'E (Geological Survey, 1960). Fieldwork was undertaken along the R67 road in a northerly, downdip direction from the upper Dwyka Group and traversing the Prince Albert and Whitehill formations (Fig. 4.41). Seven samples were collected and their co-ordinates, dip measurements and photograph numbers of each field locality are given in Appendix 7.

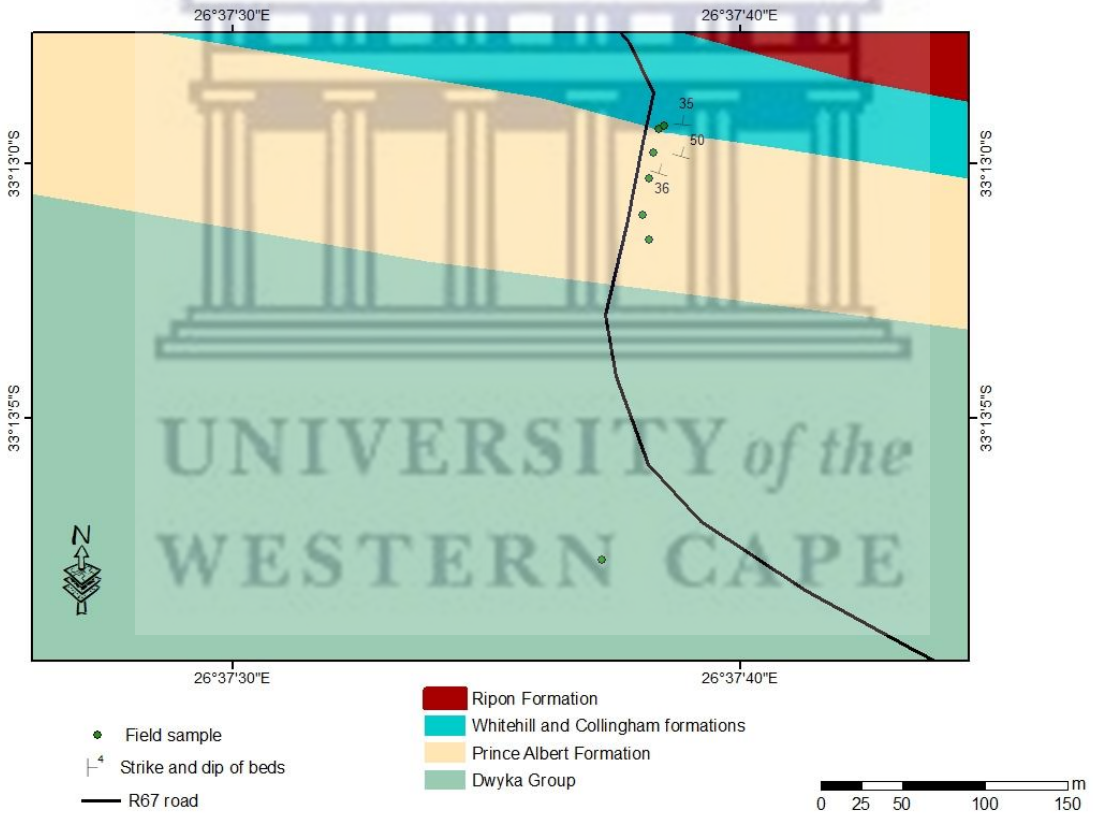

Figure 4.41. Geological map showing positions of field samples along the R67 road section at Ecca Pass, Eastern Cape (modified from 3326BA geological sheet).

Lithostratigraphy

Dwyka Group

A single sample (HM116) was collected from the upper part of the Dwyka Group (Fig. 4.41) and consists of medium dark grey (N4), clast poor, shaly mudstone containing quartzite clasts up to 23 mm in length (Fig. 4.42). The Dwyka Group is mostly covered with vegetation and there is a paucity of *in-situ* outcrops, resulting in an inferred contact between the Prince Albert Formation and the Dwyka Group. The inferred contact was positioned 3.1 m below the lowermost Prince Albert Formation outcrop using a Jacob staff.

Figure 4.42. Diamictite of the Dwyka Group composed of exotic clasts in a mudstone matrix. Site located in a gully about 50 m west of the R67 main road (co-ordinates 26.627E; -33.218S).

Prince Albert Formation

At Ecca Pass, Kingsley (1977) measured a thickness of 58 m for the Prince Albert Formation. It consists predominantly of dark to medium grey (N3-N4), dark greenish grey (5GY 4/1), olive grey (5Y 4/1), dark yellowish brown (10Y 4/2) and light olive grey (5Y 5/2) shaly mudstone, which displays pencil-like weathering (Fig. 4.43). Ferruginous beds occur throughout the succession, ranging between 5 and 50 cm thick (Fig. 4.44). Five samples (HM110 to HM114) were collected systematically across the succession up to the contact with the overlying Whitehill Formation.

Figure 4.43. Light olive grey (5Y 5/2) and dark yellowish brown (10YR 4/2) shaly mudstone of the Prince Albert Formation displaying pencil-like weathering (co-ordinates 26.627E; -33.216S).

Figure 4.44. Ferruginous shale of the Prince Albert Formation weathering into splintery fragments (co-ordinates 26.627E; -33.216S).

Whitehill Formation

The contact between the Prince Albert Formation and the Whitehill Formation is sharp (Fig. 4.45). The Whitehill Formation is characterised by a distinct very light grey (N8), weathered colour due to the oxidisation of pyrite to sulphate with the metabolic waste, sulphuric acid, dissolving calcium carbonate leading to the precipitation of gypsum. Unweathered shale at Ecca Pass is medium dark grey (N4-N5) in colour. Sample HM115 (Appendix 7) was collected 1.2 m above the contact with the Prince Albert Formation.

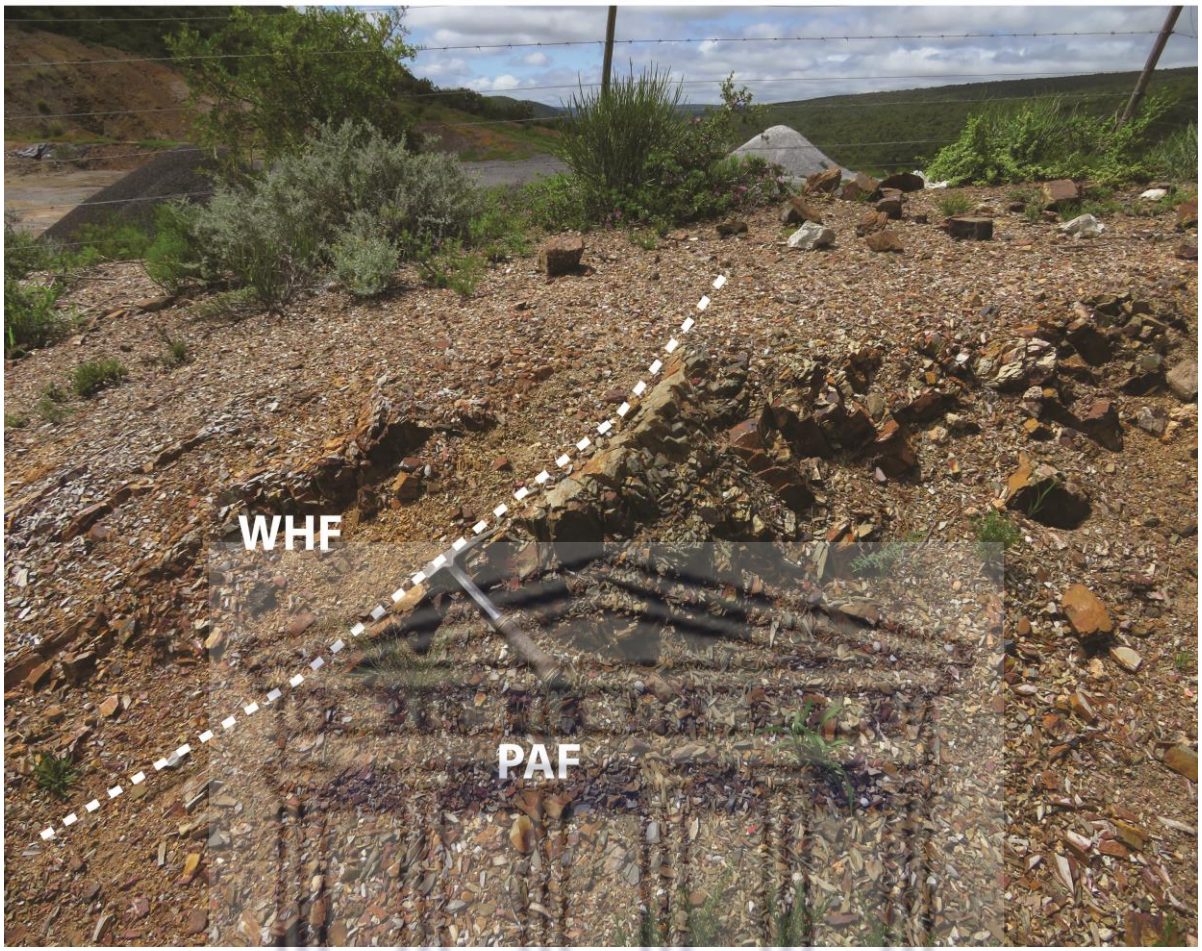

Figure 4.45. Contact between the Prince Albert (PAF) and Whitehill formations (WHF) at Ecca Pass, the latter displaying a distinctive white-weathered colour (co-ordinates 26.627E; -33.216S).

5.1.1.6.3 Pluto's Vale

This section, which traverses the Prince Albert Formation, is about 6.45 km east of Ecca Pass and is located along a gravel road, some 18 km north-east of Grahamstown (Fig. 4.34). The strata dip steeply northward at between 63 and 90 degrees and the geology of the section is shown on the unpublished 1:50 000 scale, 3326BA Fort Brown sheet between latitudes 33°14'S and 33°15'S and longitudes 26°41'E and 26°42'E (Geological Survey, 1960). Fieldwork was undertaken along the gravel road in order to measure a lithological section and obtain samples of the Prince Albert Formation, as well as the underlying Dwyka Group and overlying

Whitehill Formation (Fig. 4.46). However, due to a cover of scree and vegetation, the upper part of the Prince Albert Formation and the Whitehill Formation are not exposed. A total of seven samples were taken from the Prince Albert Formation and one from the Dwyka Group (Fig. 4.46). Sample co-ordinates, dip measurements and photograph numbers of each field locality are given in Appendix 8.

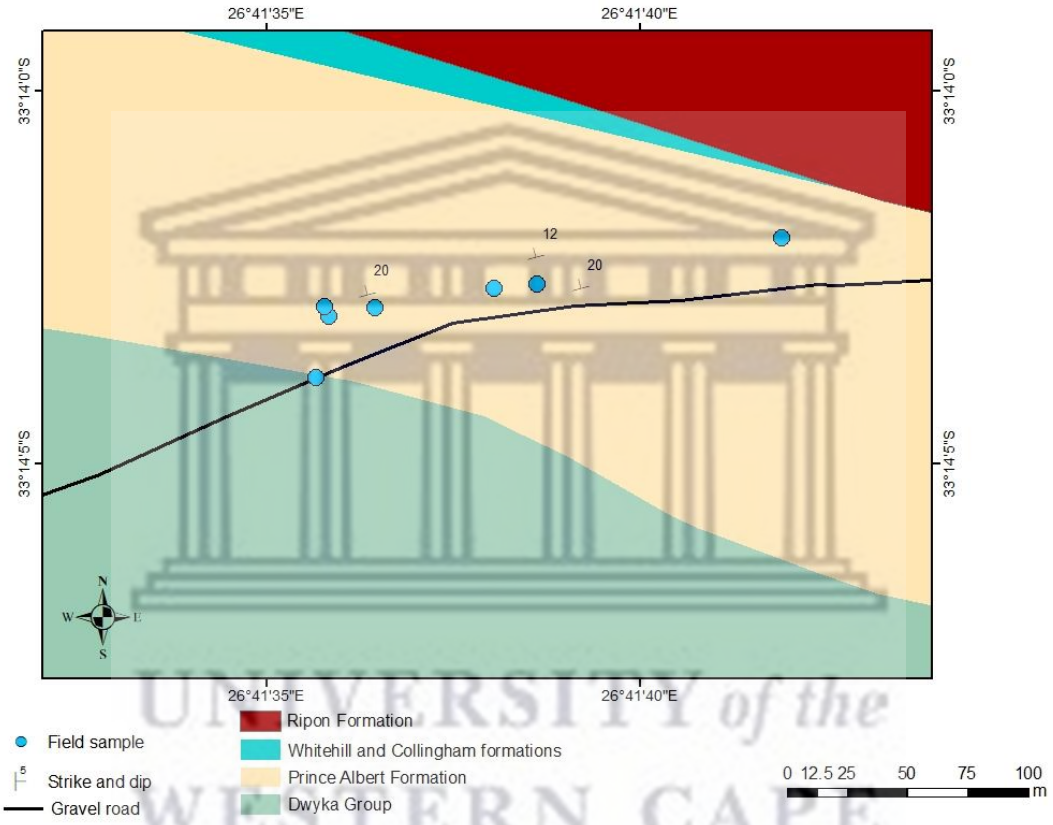

Figure 4.46. Geological map showing positions of field samples collected along the gravel road at Pluto's Vale. (Modified from 3326BA geological sheet).

Lithostratigraphy

Dwyka Group

Diamictite of the Dwyka Group is found at the western end of the field section exposed on the gravel road (Fig. 4.46). The diamictite has a silty mudstone matrix, which contains sparse clasts up to 90 mm in length, composed of quartz and granite. A gradational contact is present

between the Dwyka Group and Prince Albert Formation. The matrix of the diamictite is medium dark grey (N4-N5) in colour (Fig. 4.47). One sample (HM117) was taken.

Figure 4.47. Outcrop of diamictite exposed along the gravel road (co-ordinates 26.693 E; -33.235 S). Geological hammer is 0.3 m long.

Prince Albert Formation

The Prince Albert conformably overlies the Dwyka Group and attains an estimated thickness of 30.64 m, taking into consideration that the upper contact with the Whitehill Formation is covered with scree and vegetation (Fig. 4.48). The thickness of the Prince Albert Formation was determined using measured outcrop thicknesses perpendicular to strike. The strata dip north-northeast at an average of 20 degrees (Fig. 4.46).

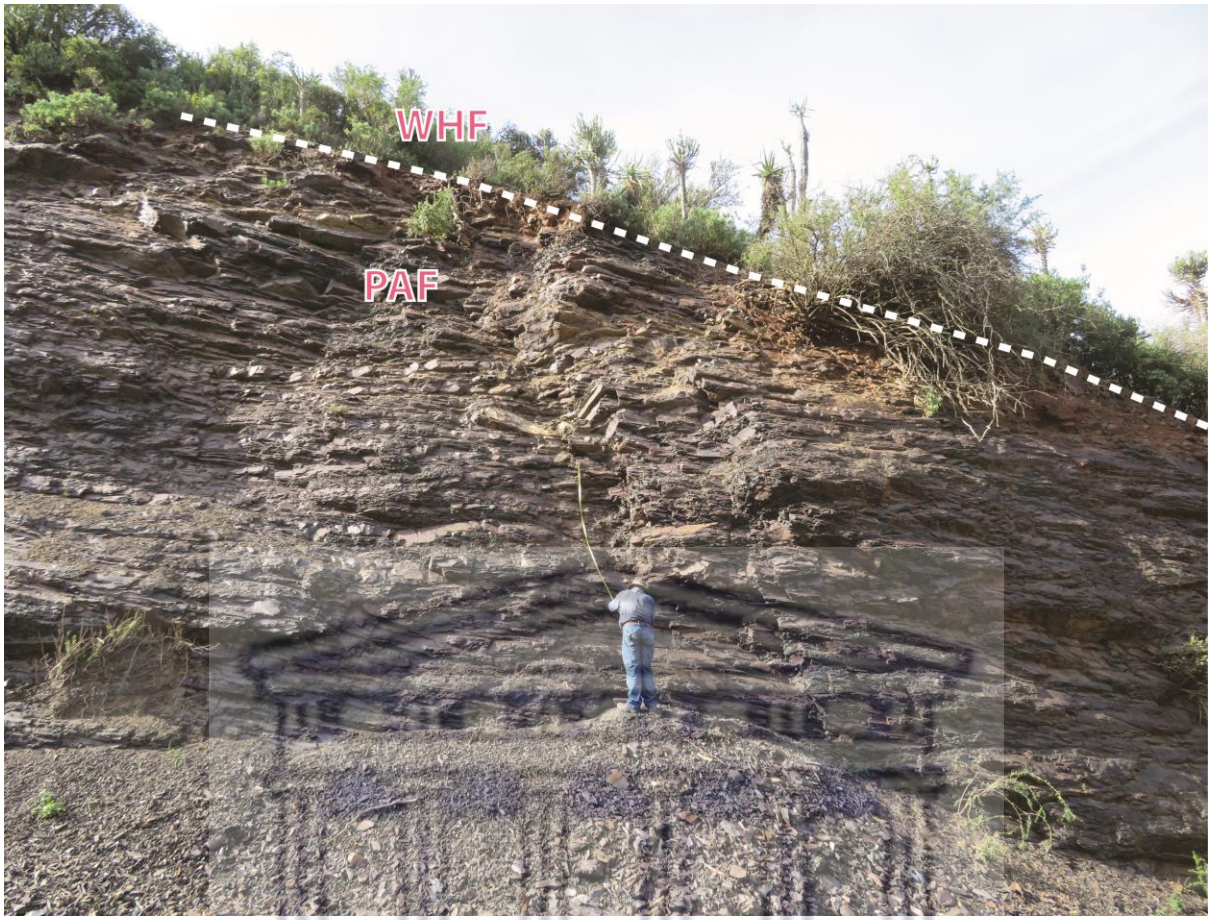

Figure 4.48. Inferred upper contact (covered) between the Prince Albert Formation (PAF) and Whitehill Formation (WHF) (co- ordinates 26.695E; -33.234S).

The Prince Albert Formation consists of silty shale (Figs. 4.48 and 4.49), which is olive grey (5Y 4/1), light olive grey (5Y 5/2), dark yellowish brown (10YR 4/2), dark greenish grey (5GY 4/1) and dark to medium grey (N2-N3) in colour. Ferruginous staining and pencil-like weathering occur in places.

Figure 4.49. Gradational basal contact between the Dwyka Group (DG) and Prince Albert Formation (PAF) indicated by the dashed line with 1.8 m of the Prince Albert Formation being exposed.

A total of seven samples were collected across the succession (Appendix 8), but these were not evenly-spaced due to outcrops being covered by vegetation. Possible tuff beds ranging between 2 cm and 4 cm thick, greyish yellow (5Y 8/4), dusky yellow (5Y 6/4) and greenish grey (5GY 6/1) in colour, were found in places (Fig. 4.50). The uppermost sample (HM124) of the Prince Albert Formation was collected at co-ordinates 26.695E; 33.234S, approximately 3.3 m below the uppermost unit of the Prince Albert Formation (Fig. 4.48). This was the final sample collected as no Whitehill Formation outcrop was present along the gravel road and younger strata occur in an inaccessible steep cliff.

Figure 4.50. Possible tuff bed 2cm thick within mudstone bed of the Prince Albert Formation as indicated below the dashed line (co-ordinates 26.694E; -33.234S).

4.1.1.7 Borehole SA 1/66, Merweville, Western Cape

Borehole SA 1/66 was drilled some 17 km west of Merweville in the late 1960's by Soeker (Fig. 4.51). SA 1/66 was drilled on the farm Hamel Kraal 16 by SA Core Recovery for SOEKOR in the southwestern part of the main Karoo Basin to obtain lithological, stratigraphic and hydrocarbon information.

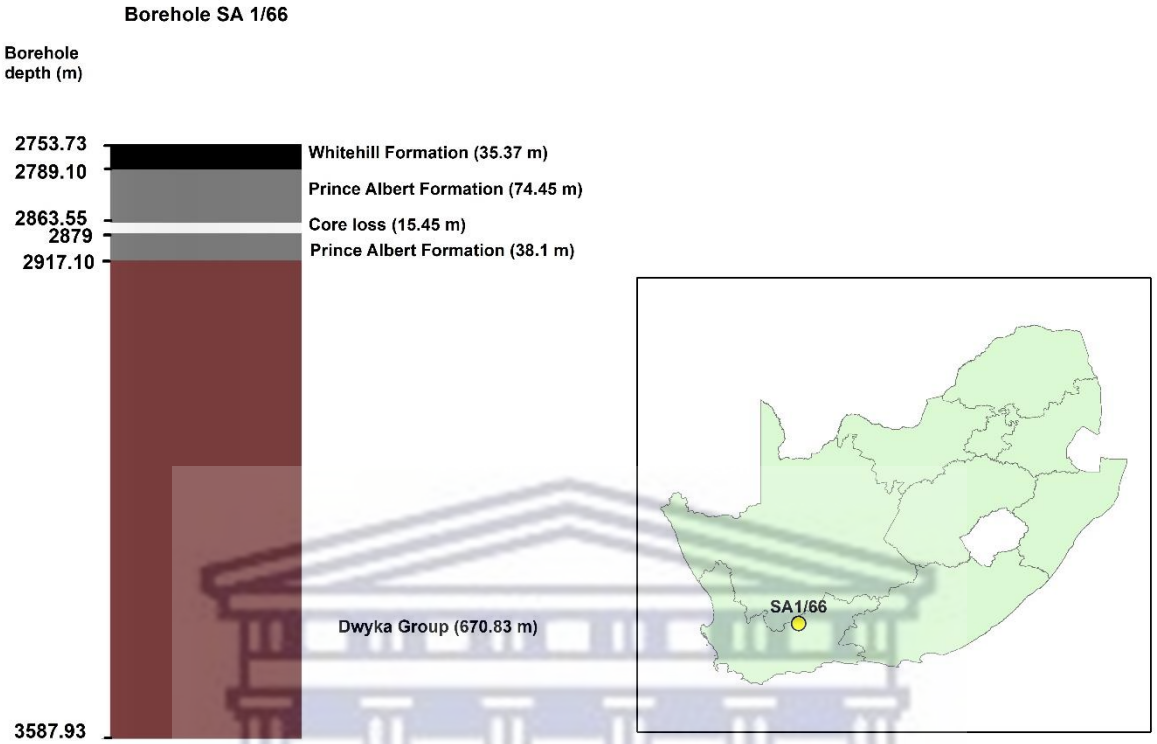

Figure 4.51. Map of borehole location and simplified graphic log of the core of borehole SA 1/66 showing the stratigraphy of the Prince Albert Formation and the overlying and underlying units.

Lithostratigraphy

Whitehill Formation

The Whitehill Formation is first described. The Whitehill Formation has a total thickness of 35.37 m and lies between depths of 2753.73 and 2789.1 m. It consists of black to dark grey (N1-N3), carbonaceous shale chips with pyrite and calcite in places (Fig. 4.52). The basal contact between the Whitehill and Prince Albert Formation is not seen as a result of missing core at depth 2789.08 m (Fig. 4.52). A sample (HM125; Appendix 9) was collected from above this contact between 2785.74 and 2789.08 m.

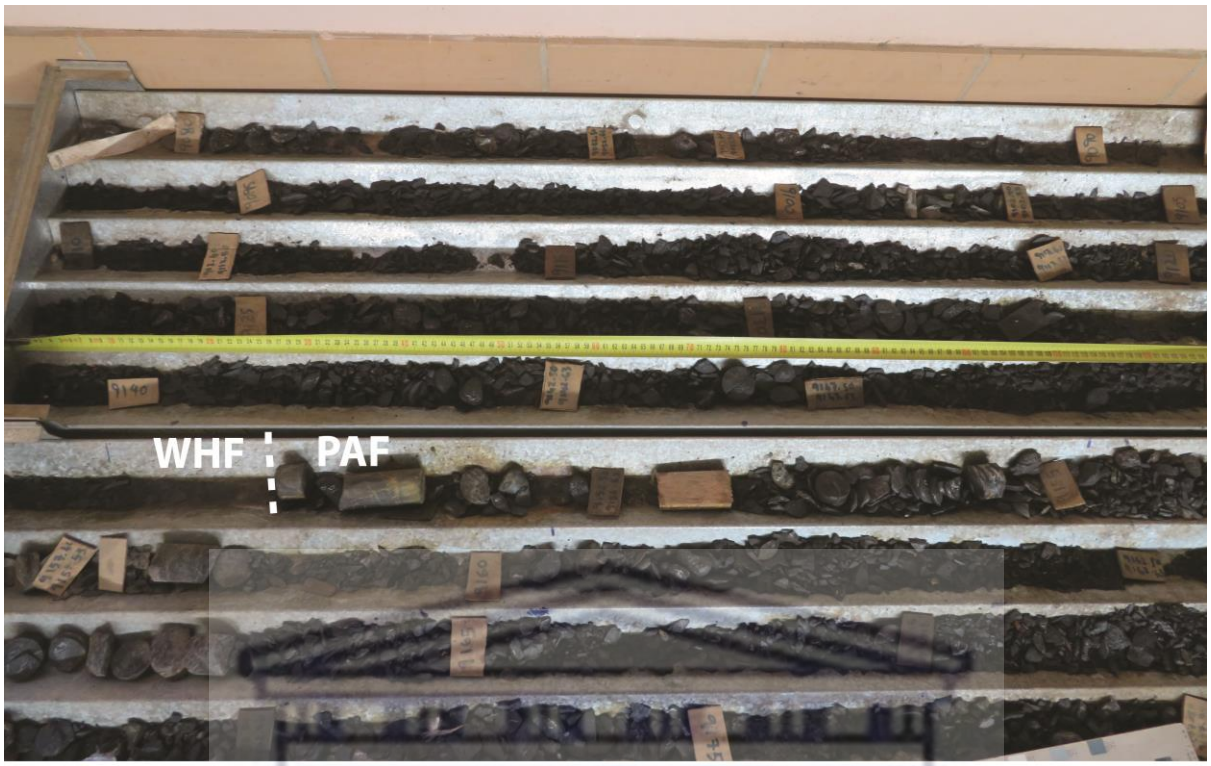

Figure 4.52. N1-N3 carbonaceous shale chips of the Whitehill Formation (WHF) with the underlying contact (white dashed line) of the Prince Albert Formation (PAF) at depth 2789.08 m, not present.

Prince Albert Formation

The Prince Albert Formation extends from 2789.1 m to 2917.1 m having a thickness of 128 metres (Fig. 4.51). From the top of the formation (2789.1 m-depth) down to 2806.47 m-depth, the Prince Albert Formation consists of massive shale, greyish black to medium dark grey (N2-N4) in colour, with isolated calcite veins and calcareous nodules in places. The uppermost sample (HM126; Appendix 9) of the Prince Albert Formation was taken between depths of 2793.54 and 2798.58 m and another twelve samples were retrieved from the underlying Prince Albert succession (refer Appendix 9). Between depths 2806.47 m and 2863.55 m, an interbedded unit of olive grey (5Y 4/1) to medium dark grey (N4) coloured shale and black to

greyish black (N1-N2) coloured shale is present with isolated calcite, pyrite crystals and quartz veins (Fig. 4.53).

Figure 4.53. Interbedded light (5Y 4/1 and N4) and dark grey (N1-N2) shale of the Prince Albert Formation between depths 2806.47m and 2863.55m.

From 2863.55 to 2879 m-depth, no core is available, possibly due to core loss and previous sampling. Below 2879 m-depth, the core diameter increases in size from 3.5 cm to 6.7 cm (Fig. 4.54). Between depths 2879 m and 2916.23 m, a massive shale, greyish black to medium grey (N2-N4) and olive grey (5Y 4/1) in colour with calcite veins and jarosite, occurs locally. A massive medium dark grey (N3-N4), shaley mudstone follows (2916.23 - 2916.82 m) with very rare calcareous concretions and a gradational base. A massive silty mudstone unit lying between 2916.82 m and 2917.1 m marks a gradational boundary between the Prince Albert

Formation and underlying Dwyka Group. This unit is brownish grey (5YR 4/1) and dark to medium grey (N3-N4) in colour, with rare quartz dropstones less than 2 mm in size (Fig. 4.55).

Figure 4.54. Core loss present between depths 2863.55 m and 2879 m underlain by massive shale (Prince Albert Formation) with a core diameter of 6.7cm.

Dwyka Group

The Dwyka Group extends from depths of 2917.1 m to 3587.93 m and consists of a dropstone argillite with a medium to medium light grey (N5-N6), silty mudstone matrix in the upper part. The dropstones are sparse and consists of white quartz, granite and quartzite up to 8 cm in size and increasing in size downwards (Fig. 4.55). One sample (HM139; Appendix 9) was retrieved from near the top of the Dwyka Group between depths of 2919.85 and 2926.24 m.

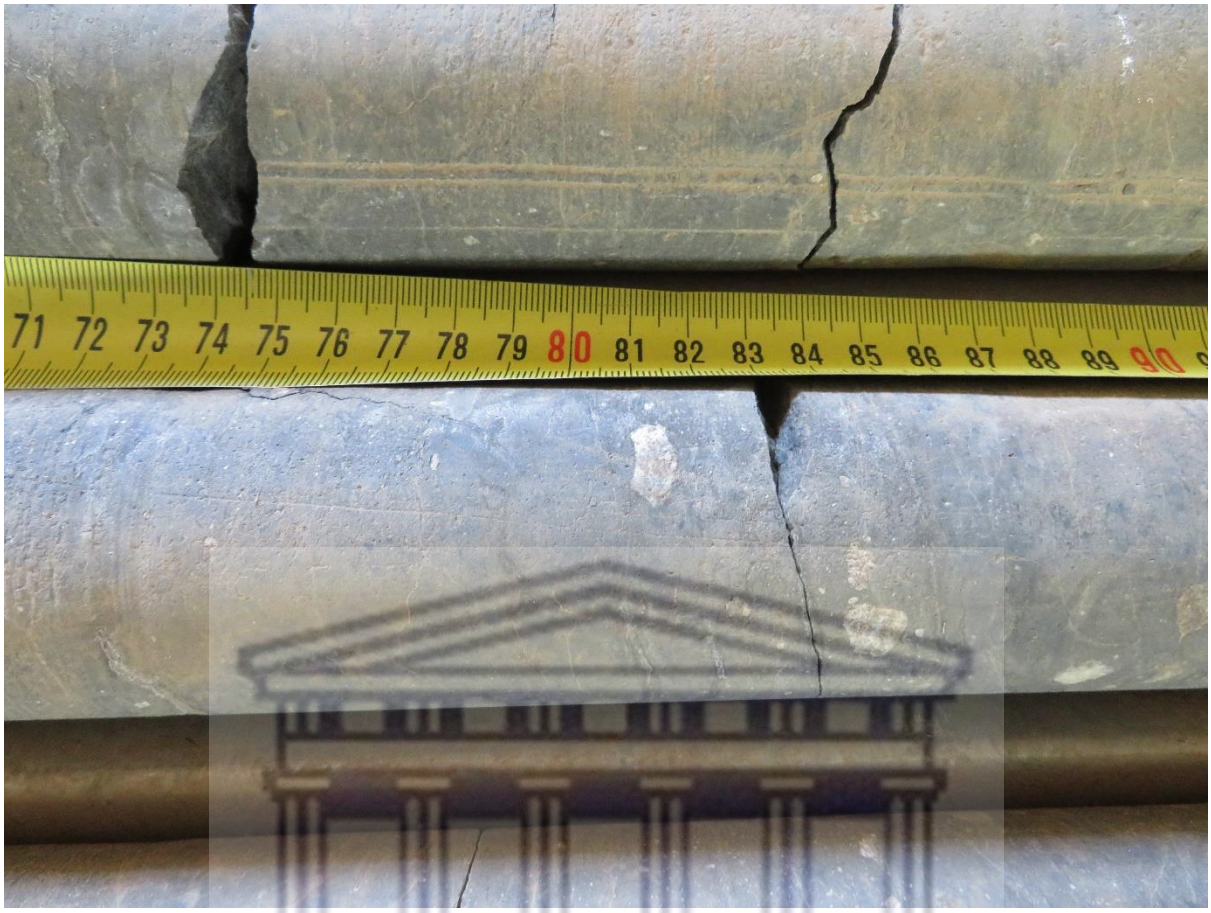

Figure 4.55. Isolated dropstones of granite in diamictite of the Dwyka Group between depths of 3222.34 and 3224.12 m.

4.1.1.8 Beaufort West, Western Cape

4.1.1.8.1 Deep percussion drilling (Borehole R01-BW)

Borehole R01-BW (co-ordinates 22.617E; -32.326S) was drilled at a site located about 490 m northeast of the proposed 4000 m-deep proposed borehole (Fig. 4.56). The borehole was drilled to a depth of 1402 m (Fig. 4.57; Appendix 10) intersecting 57 m of the Poortjie Member of the Middleton Formation. The upper 56 m of shale in the Poortjie Member is silty and calcareous in places. Its colour ranges from medium grey (N4-N6), dark greenish grey (5GY 4/1), light brownish grey (5YR 6/1), brownish grey (5YR 4/1), olive black (5 Y 2/1), dusky brown (5YR 2/2) to greenish grey (5G 6/1). The Poortjie Member normally consists of sandstone units

between 5 and 15 m thick interbedded with subordinate mudstone and siltstone (Cole et al., 2016a). However, the predominance of shale in R01-BW is probably a result of this borehole intersecting a palaeodepositional area of the fluvio-lacustrine Poortjie Member, where low energy, mud settling from suspension was the main sedimentary process (Cole et al., 2016a, c).

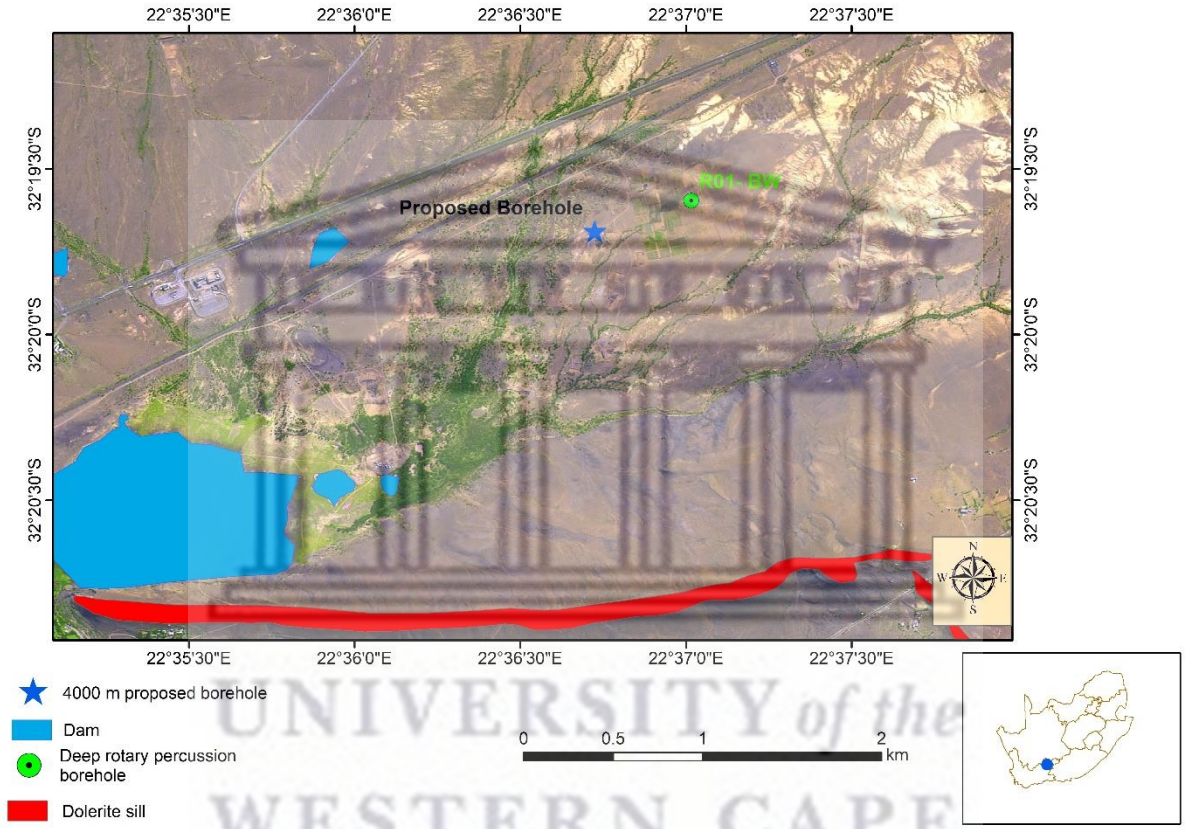

Figure 4.56. Spot 5 satellite imagery showing the position of deep rotary percussion borehole R01-BW and the proposed 4000 m-deep borehole within the municipal grounds of Beaufort West, Western Cape.

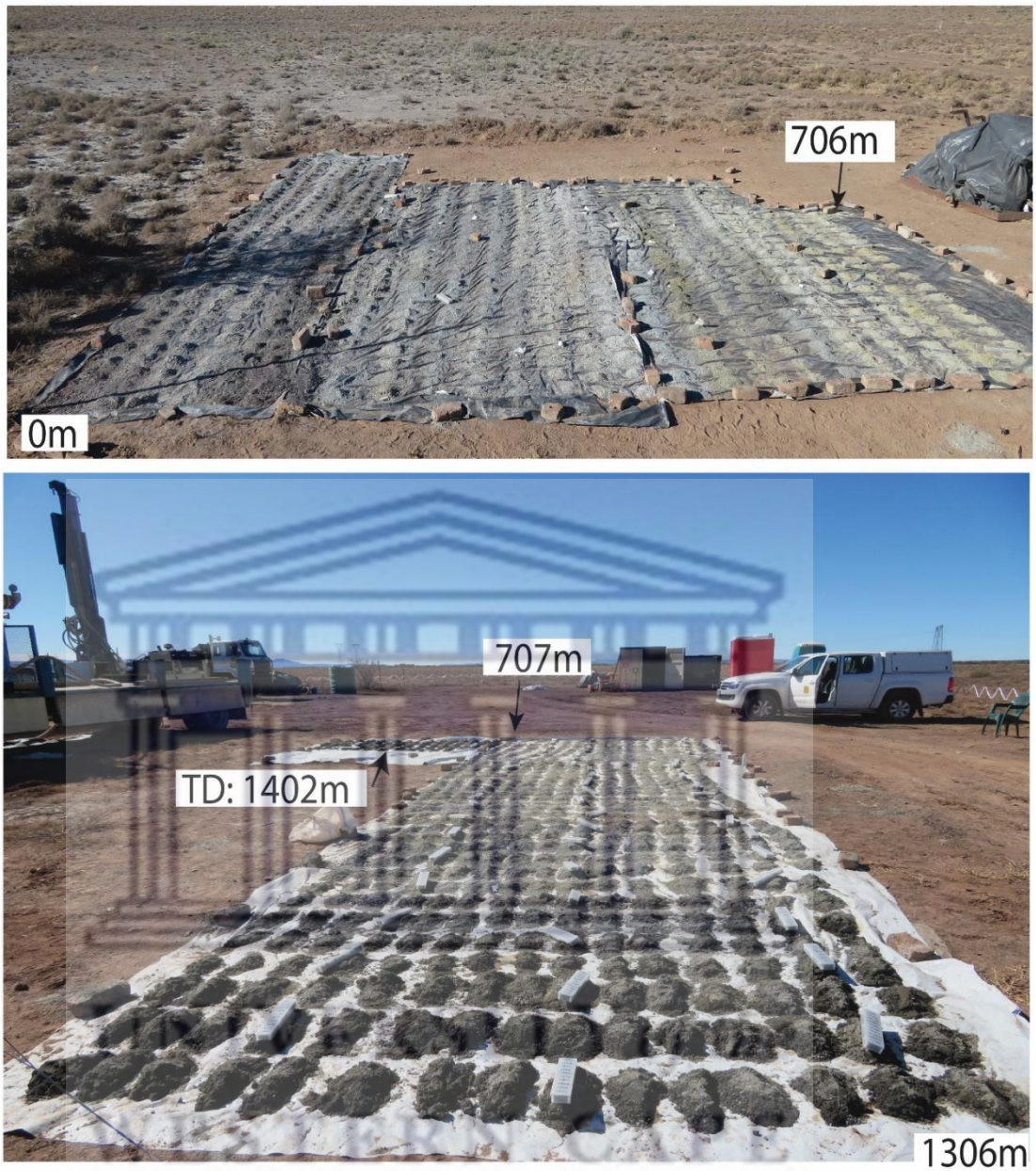

Figure 4.57. Core chips consisting of shale, sandstone, siltstone, dolerite and silty shale from borehole R01-BW laid over the entire drilled interval from 0 to 1402 m.

The Abrahamskraal Formation lies at depths between 57 and 750 m, but is intruded by greyish black to dark grey (N2-N3) dolerite between 492 and 508 m (Fig. 4.58), leaving a true thickness of 677 m for the sedimentary succession. The most abundant lithology is siltstone that is medium grey (N3-N5), olive grey (5Y 4/1), and dark greenish grey (5GY 4/1) in colour.

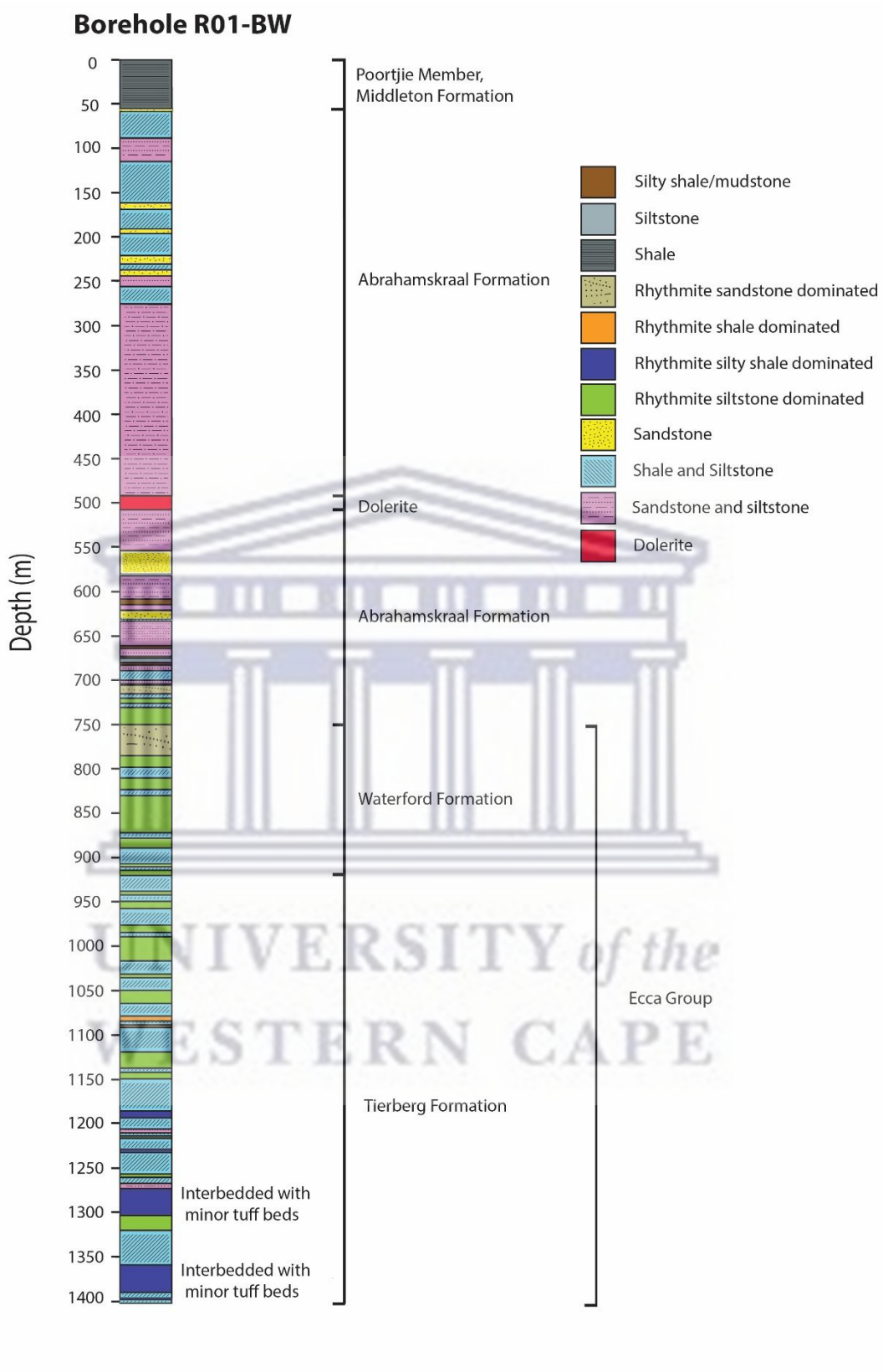

Figure 4.58. Log showing the lithology and stratigraphy of borehole R01-BW.

One occurrence of dusky red (5R 3/4) siltstone was noted between 716 m and 717 m. Silty shale is the next most abundant lithology and is dark greenish grey (5GY 4/1 and 5G 4/1), olive grey (5Y 4/1), dark grey (N2-N4) and brownish black (5YR 2/1) in colour with one occurrence of very dusky red (10R 2/2) silty shale between 743 m and 744 m. Moreover, blackish red (5R 2/2), dark grey (N4), dusky brown (5YR 2/2), olive black (5Y 2/1) and dark greenish grey (5GY 4/1) shale chips were also noted. Sandstone chips are very fine-grained and very fine- to fine-grained and are predominantly grey (N4-N7), dark greenish grey (5GY 4/1) and olive grey (5Y 4/1) coloured. The reddish colours characteristic of the Beaufort Group mudstones (Rubidge et al., 2000) are mostly confined to the upper part of the Abrahamskraal Formation above a depth of 373 m. There is an abundance of calcareous percussion chips, particularly siltstone and shale and some of these could represent calcareous nodules and beds, which are an indicator of subaerial exposure within the flood plain palaeoenvironment (Rubidge et al., 2000).

The lower boundary of the Abrahamskraal Formation was placed at 750 m from the surface (Fig. 4.58), at the base of a 19 m thick siltstone-dominated rhythmite overlying a 35 m thick sandstone-dominated rhythmite of the Waterford Formation (the youngest unit of Ecca Group). The mudrock unit that is normally present at the base of the Abrahamskraal Formation (Cole et al., 2016c) was not apparent with the 19 m thick siltstone-dominated rhythmite containing several one metre thick units of very fine- and very fine- to fine-grained sandstone chips. Certain, large-scale diagnostic features of the Abrahamskraal Formation such as fining-upward successions, cannot be identified from percussion chips, however others, such as the presence of reddish-coloured mudstone (Rubidge et al., 2000), and these were noted as very dusky red (10R 2/2) silty shale chips between depths of 743 and 744 m in

the siltstone-dominated rhythmite unit just six metres above the boundary with the Waterford Formation.

The Waterford Formation is more arenaceous than the Abrahamskraal Formation (Jordaan, 1981) with the sandstone: mudrock ratio reaching 1:1 north of Grahamstown (Rubidge et al., 2012). In borehole R01-BW, the uppermost unit of the Waterford Formation is a 35 m-thick, sandstone-dominated rhythmite that contrasts with the overlying siltstone-dominated rhythmite of the Abrahamskraal Formation. Below the upper sandstone-dominated rhythmite, siltstone- dominated rhythmite and shale as well as siltstone units are present with interbedded, 1 m-thick very fine-grained sandstone. The lower boundary of the Waterford Formation with the underlying Tierberg Formation is defined as the base of the first prominent sandstone above a shale-dominated succession (Johnson, 1994; Viljoen, 2005). Individual sandstone beds were not identified from the percussion chips and the lower boundary was placed at the base of a siltstone-dominated rhythmite unit 6 m thick at a depth of 919 m. This unit contains very fine-grained sandstone chips and overlies a 18-m-thick siltstone and silty shale unit. All in all, in borehole R01-BW, the total thickness of the Waterford Formation is therefore 169 m. Sandstones of the Waterford Formation are very fine-grained and very fine- to fine-grained and dark grey to medium light grey (N3-N6), dark greenish grey (5G 4/1 and 5GY 4/1), medium bluish grey (5B 5/1) and light olive grey (5Y 5/2) in colour. The more abundant siltstones are dark grey to medium light grey (N3-N6), dark greenish grey (5G 4/1 and 5GY 4/1), medium bluish grey (5B 5/1) and olive grey (5Y 4/1). Shale and silty shale, which become more prominent in the lower part of the Waterford Formation, are greyish black to medium dark grey (N2-N4), dark greenish grey (5G 4/1 and 5GY 4/1), medium bluish grey (5B 5/1), brownish grey (5YR 4/1) and moderate brown (5YR 3/4) in colour.

Siltstone-dominated rhythmite is the most abundant unit in the upper part of the Tierberg Formation in borehole R01-BW with shale/siltstone and silty shale-dominated rhythmite becoming the most abundant units at depths below 1148 m. Percussion chips of very fine-grained sandstone and, rarely, very fine- to fine-grained sandstone, are present throughout the Tierberg Formation. Percussion chips of tuffaceous mudstone are found between depths of 1281 and 1282 m, 1291 and 1292 m, 1301 and 1302 m, and 1374 and 1376 m. These are medium grey (N5), medium light grey (N6) and light blush grey (5B 7/1) in colour and are probably similar to the thin (< 5 cm), light grey to yellowish grey, tuffs that occur elsewhere in the Tierberg Formation (Viljoen, 2005). The siltstone is dark grey to medium light grey (N3-N6), dark greenish grey (5G 4/1 and 5GY 4/1) and olive grey (5Y 4/1) in colour. The shale is black to greyish black (N1-N2) and brownish black (5YR 2/1), the silty shale is predominantly greyish black to medium dark grey (N2-N4), dark greenish grey (5GY 4/1), olive black (5Y 2/1) and brownish black (5YR 2/1). The very fine-grained sandstone is medium dark grey to light grey (N4-N7), and the very fine- to fine-grained sandstone is medium grey to medium light grey (N5-N6). Percussion chips of black to greyish black (N1-N2) and brownish black (5YR 2/1) carbonaceous shale are found between depths of 1075 and 1083 m, 1086 and 1089 m, 1097 and 1098 m, 1101 and 1102 m, 1178 and 1179 m, and 1314 and 1315 m, respectively. In borehole R01-BW, the Tierberg Formation is at least 483 m thick.

4.1.1.8.2 Lithology identified from wireline logs (Borehole R01-BW)

In wireline logs, dolerite could be more accurately identified than sandstones. In borehole R01-BW, the dolerite identified from the percussion chips lies between depths of 492 and 508 m (Fig. 4.59), and in the wireline log, corresponds to an interval characterised by very low gamma ray values, high density values and high resistivity values between depths of 489 and 508 m. The resistivity increases and decreases over about 15 m above and below the dolerite, possibly due to contact metamorphism of the intruded sedimentary rocks (cf. Smithard et al, 2015). Although the wireline logs indicate dolerite between depths of 489 and 492 m, the percussion chips from this interval consisted of very fine-grained sandstone with no dolerite. The absence of dolerite could be due to the percussion chips not reaching the surface immediately or missed during sampling. Another dolerite characterised by very low gamma ray, high density and high resistivity values is apparently present between depths of 690 and 692 m in R01-BW (Fig. 4.60). However, no dolerite was found in the percussion chips, which, over this same interval, consisted of silty shale and siltstone. It is probable that the dolerite chips were missed during sampling.

The only other lithology that could be identified in the wireline logs was sandstone, but such identification was not always of high fidelity. Sandstone is characterised by a low gamma ray value and a high resistivity value, and based on this, a correlation of 13 sandstones as determined from the percussion chips, was made. However, at depths below 500 m, there was an overlap of depths between the wireline and percussion chip log, e.g. 621 to 631 m on the percussion log and 619 to 628 m on the wireline log. This was probably a result of the percussion chips not reaching the surface timeously. Some sandstone units identified from

the percussion chips did not give the low gamma ray and high resistivity signature on the wireline log, e.g. between depths of 646 – 649 m.

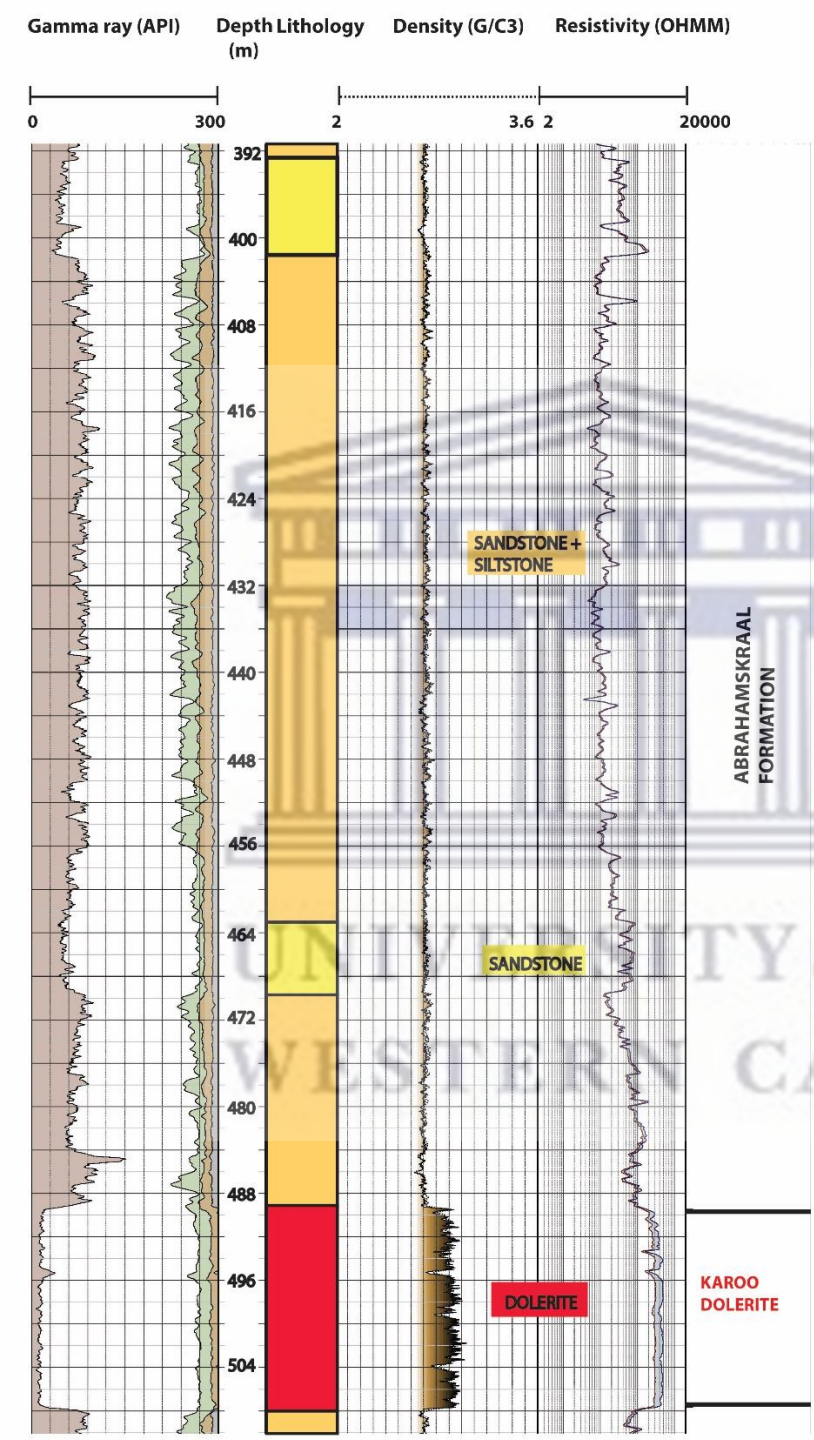

Figure 4.59. Log of borehole R01-BW between depths of 392 and 510 m showing from left side, gamma-ray values, lithology, density values and resistivity values (modified from Wireline Alliance, 2018).

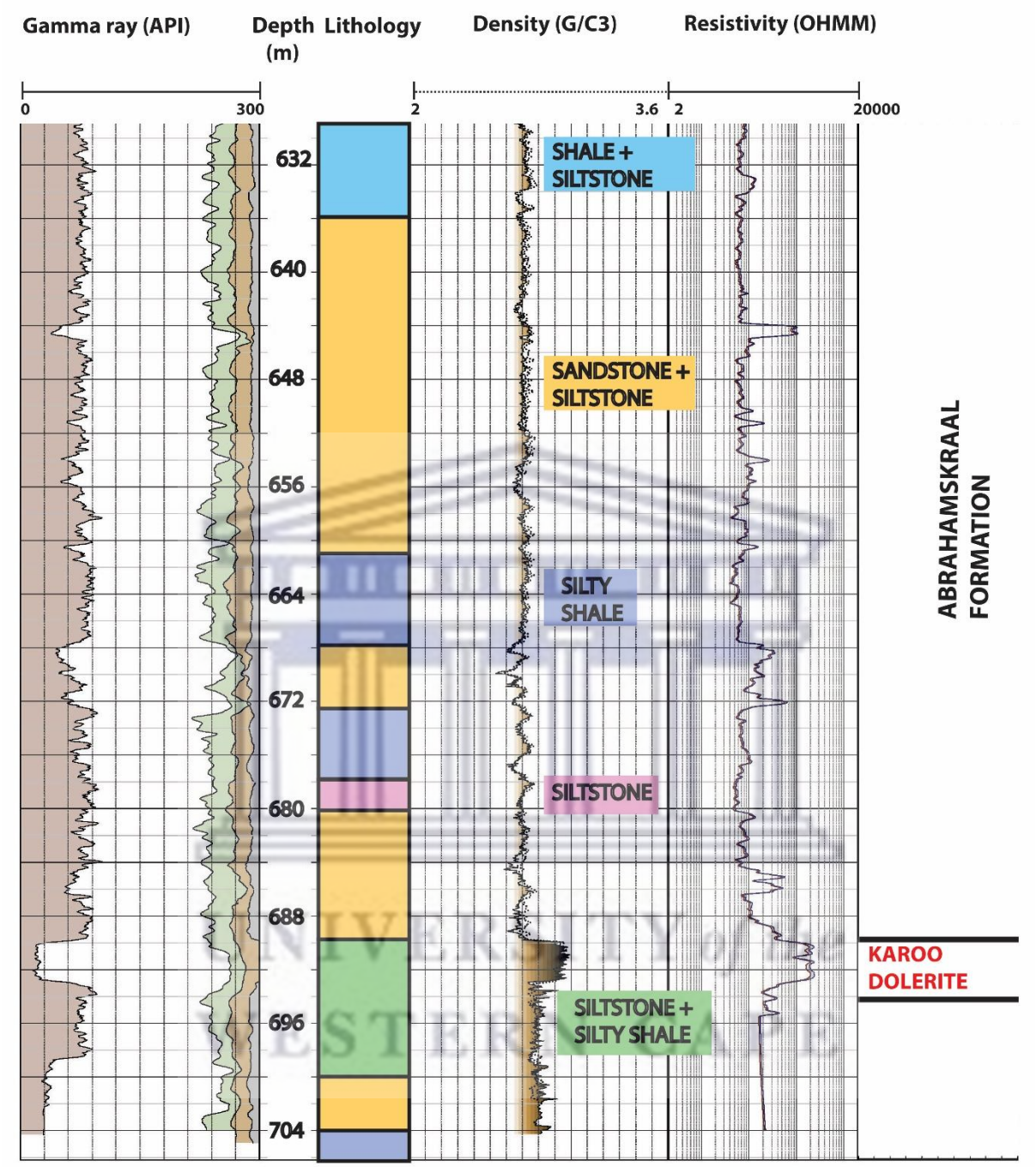

Figure 4.60. Log of borehole R01-BW between depths of 631 and 704 m showing from left side, gamma-ray values, lithology, density values and resistivity values (modified from Wireline Alliance, 2018).

4.1.1.8.3 Concluding remarks for borehole R01-BW

In Beaufort West's region, drilling results of borehole R01-BW indicate that the Abrahamskraal and Waterford Formations attain a thickness of 677 and 169 m, respectively.

The Abrahamskraal Formation thickens towards the south with an outcrop thickness of 2532 m at the holostratotype (Farm Blaauwkranse 30 and Combrinkskraal 93/1) and 2400 m in borehole KW1/67, some 100 km south of Beaufort West (Cole et al., 2016c). The thickness of the Waterford Formation lies within the thickness range of 70 to 350 m in the southern part of the main Karoo Basin (Rubidge et al., 2000, 2012; Cole and Smith, 2008), including 107 m in borehole AB1/65, some 60 km north of Beaufort West (Cole and Wipplinger, 2001), 241 m in borehole SA1/66, some 120 km WSW of Beaufort West and 229 m in borehole KW1/67.

The argillaceous Tierberg Formation was identified in borehole R01-BW, located at latitude 32°19'36"S, below the Waterford Formation at a depth of 919 m. This argillaceous unit could not be assigned to the Fort Brown Formation, because this unit and the underlying Ripon or Laingsburg Formations do not extend in the subsurface north of latitude 32°29'S, as shown in the interpretation of the deep Soekor boreholes SA1/66, AB1/65, KW1/67, CR1/68, SC3/67, KA1/66 and VR1/66 (Winter and Venter, 1970; Viljoen, 1992; Johnson and Kingsley, 1993). . On average, the argillaceous Tierberg Formation is composed of 90 to 95% shale and 5 to 10% siltstone and sandstone, the latter being concentrated in the upper part of the formation (Viljoen, 2005). A thickness of 1252 m was recorded in borehole SA1/66, 120 km WSW of Beaufort West (Viljoen, 2005) and 573 m in borehole AB1/65, 60 km north of Beaufort West, corresponding with the northward decrease in thickness of the formation (Viljoen, 2005).

The intersection of the Tierberg Formation at a relatively shallow depth of 919 m with a thickness exceeding 484 m, suggest that the proposed, ~4000-m-deep borehole would intersect the target Prince Albert Formation at a depth of ~2560 m, assuming thicknesses of 60 m, 40 m and 1500 m for the overlying Whitehill, Collingham and Tierberg formations, respectively (Viljoen, 1992, 2005).

4.1.2 Mineralogical and Geochemical data

Petrographic images of the Prince Albert Formation shales display horizontal lamination and pyrite nodules within a fine-grained matrix (Figs. 4.61 and 4.62). From XRD analysis, the principal minerals in the shales are pyrite (3 – 25%), calcite (2 – 95%), plagioclase (2 – 45%), quartz (5 – 89%), mica (up to 27%) and chlorite (2 – 53%) with minor calcite (up to 95%), apatite (53 – 80%), kaolinite (4 – 40%), and in some cases, up to 88% dolomite and up to 9% gypsum (Appendix 11, 12 and 13). In sample HM57 of borehole KZF-01, a possible algal mat feature was observed (Fig. 4.61 (d)).

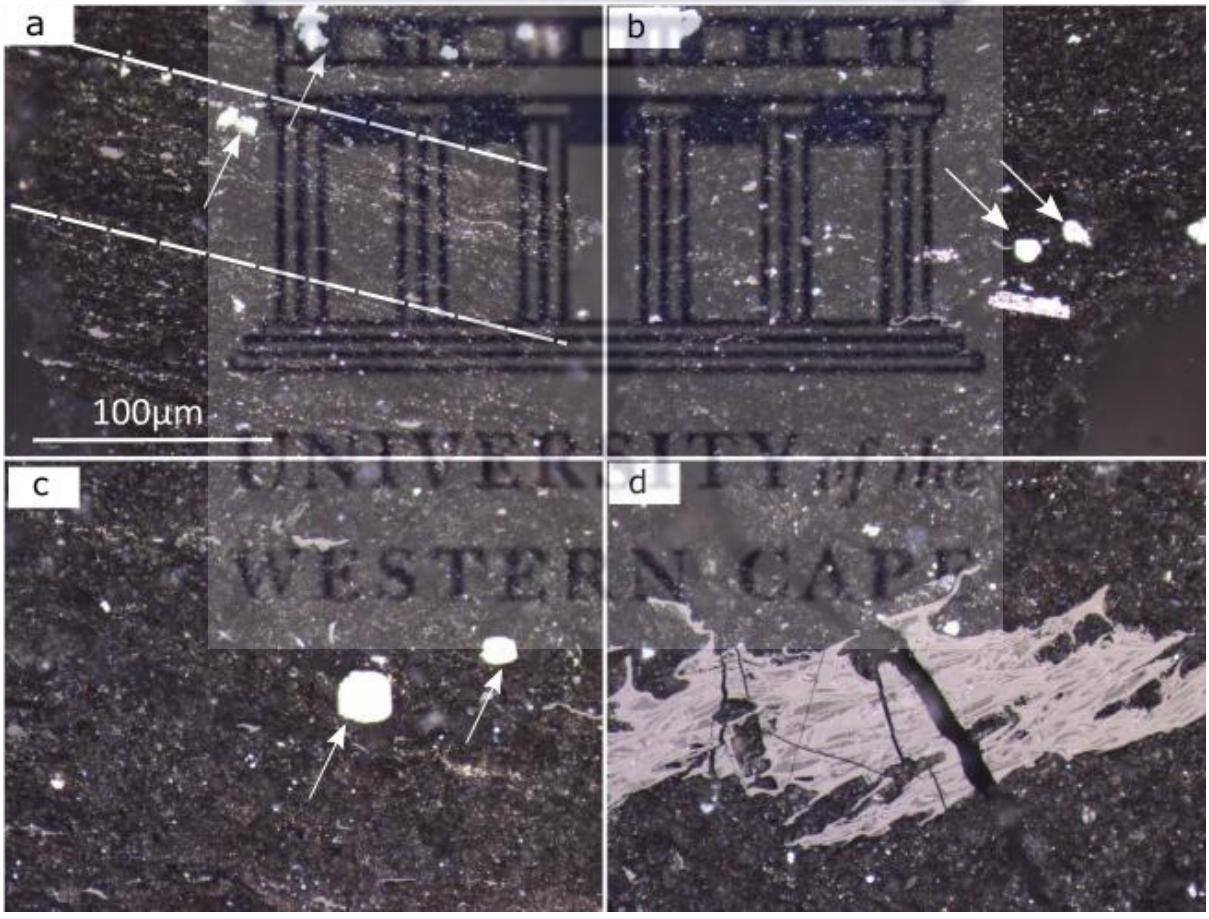

Figure 4.61. Petrographic images of Prince Albert Formation core (sample HM57) of borehole KZF-01. (a) and (b) show laminated shale with large pyrite crystals (arrows). (c) Shows rare organic fragments with pyrite (arrows) and (d) shows a possible algal mat feature within a fine-grained matrix.

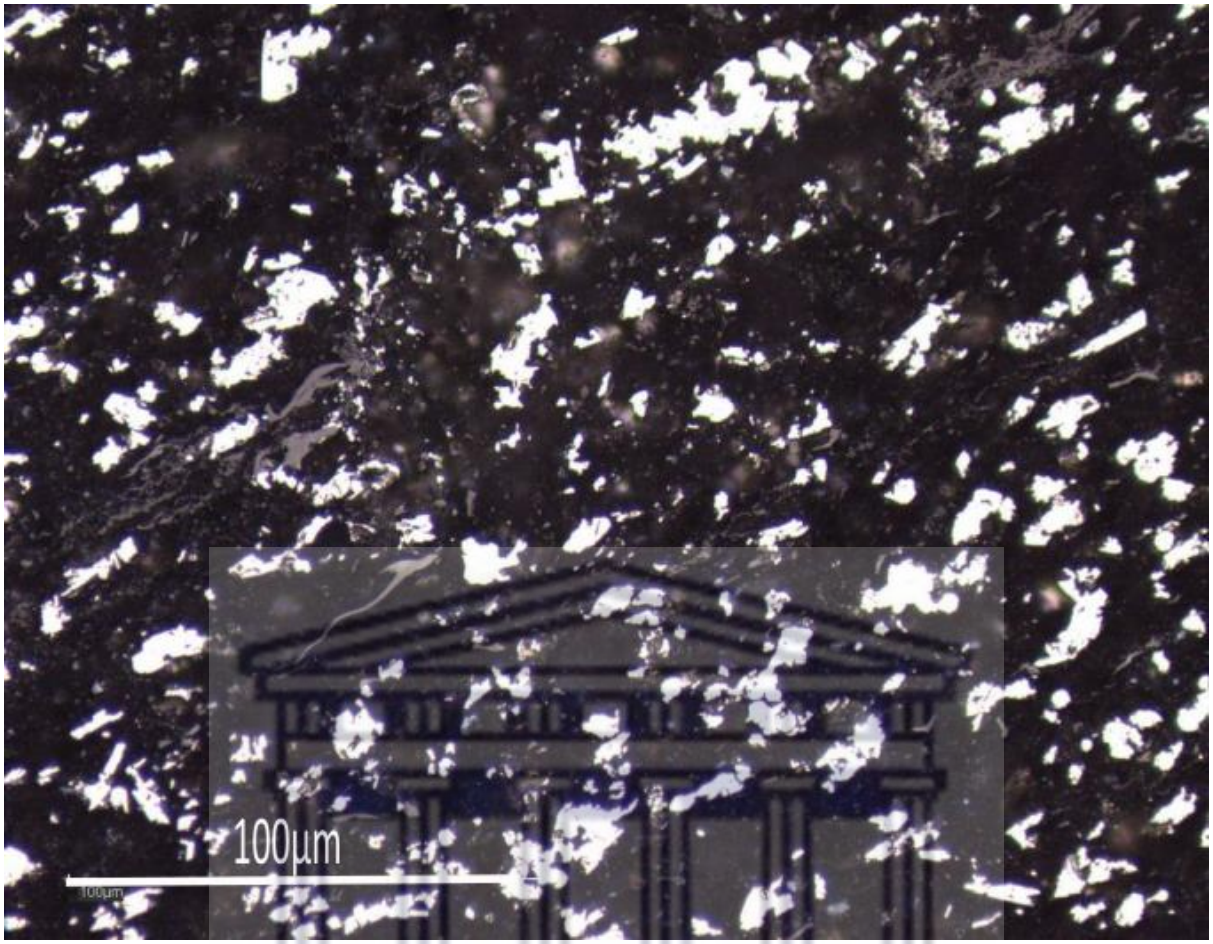

Figure 4.62. Abundant pyrite crystals (shown in white) of sample HM62 from borehole KZF-01.

One hundred and thirty-nine samples from the Dwyka Group, Prince Albert Formation and Whitehill Formation, retrieved from across the southern part of the main Karoo Basin were, analysed chemically (Appendix 14). The chemistry data is plotted in a SandClass scheme (Herron, 1988) which geochemically classifies terrigenous sands and shales based on the SiO_2/ Al_2O_3 and Fe_2O_3/K_2O ratios (Fig. 4.63). These ratios allow one to distinguish between quartz-rich, high ratio sandstones and clay-rich, low ratio shales. Intermediate SiO_2/ Al_2O_3 ratios reflect wackes, feldspathic and lithic sandstones. The Fe_2O_3/K_2O ratio differentiates between lithic fragments and feldspars and can be used as a mineralogical stability indicator (Herron, 1988). Samples with very high Fe_2O_3/K_2O ratios (> 7) are classified as iron-rich or ferruginous

shales or sands. Prince Albert Formation samples taken from borehole KZF-01, Laingsburg and Prince Albert, together with a single sample from borehole KWV-01, reflect an Fe-rich shale containing abundant pyrite (Fig. 4.63). Prince Albert Formation samples taken from Tankwa, Laingsburg, Prince Albert and one sample from Ecca Pass outcrop reflect Fe-rich sand (Fig. 4.63). The majority of the samples have a low Fe_2O_3/K_2O ratio, which lies within the shale and wacke windows for the Dwyka Group, Prince Albert and Whitehill Formations, where there is a stable mineral assemblage of quartz (Fig. 4.63). Litharenite is identified for the Prince Albert and Whitehill Formation samples from Laingsburg, Tankwa, Prince Albert and Debruinspoort, respectively. One sample from the Prince Albert outcrop locality in Figure 4.63, was classified as a sublitharenite.

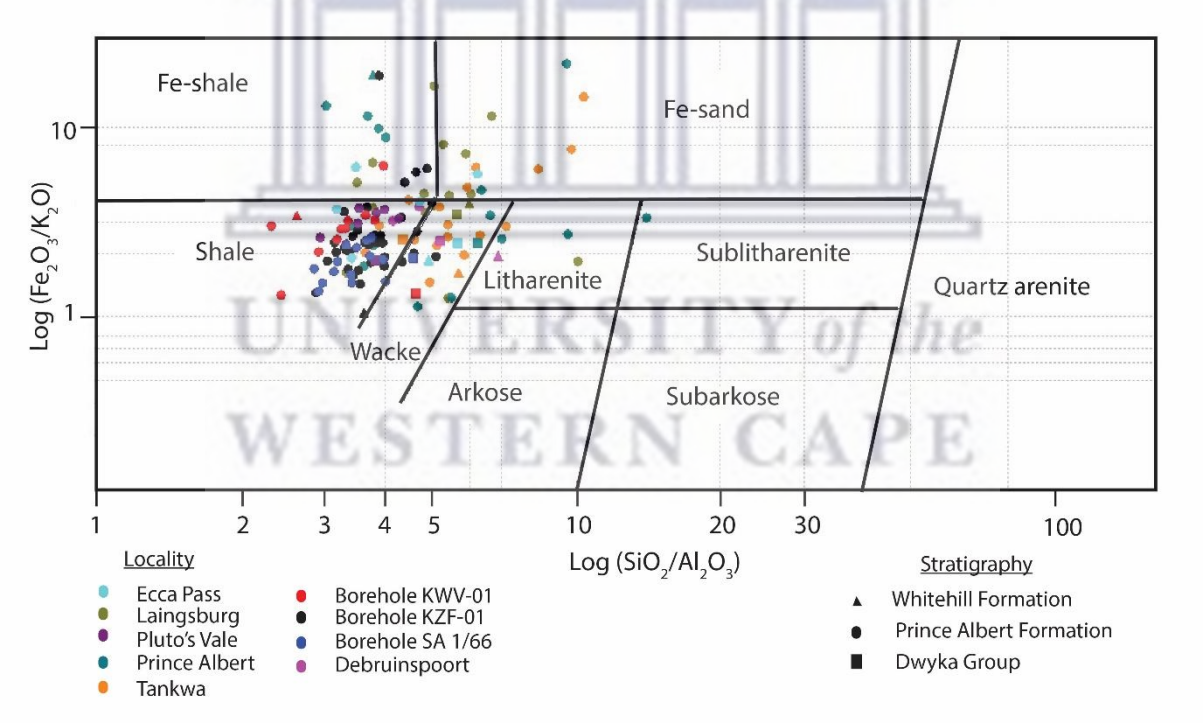

Figure 4.63. Geochemical classification of samples taken from the Whitehill Formation, Prince Albert Formation and Dwyka Group (after Herron, 1988).

A ternary diagram was used as a means to relate geochemical concentrations based on the SiO_2, Al_2O_3 and the CaO ratios (Appendix 14). In Figure 4.64, SiO_2 and Al_2O_3 separate quartz-rich silty shales or siltstones from clay- rich shales. The CaO ratio was used to distinguish calcareous from non-calcareous shales. In Figure 4.64, the majority of the samples are quartz-rich (65% < SiO_2 < 96%), whereas the Laingsburg, Prince Albert, Tankwa, Debruinspoort and Pluto's Vale outcrop samples, as well as borehole KZF-01 samples of the Prince Albert Formation, plot within the calcareous field (10 % < CaO < 75%). One carbonate sample of the Whitehill Formation taken from the Prince Albert outcrop locality was highly calcareous (CaO = 90%), being sourced from a dolomite concretion (Herron, 1988).

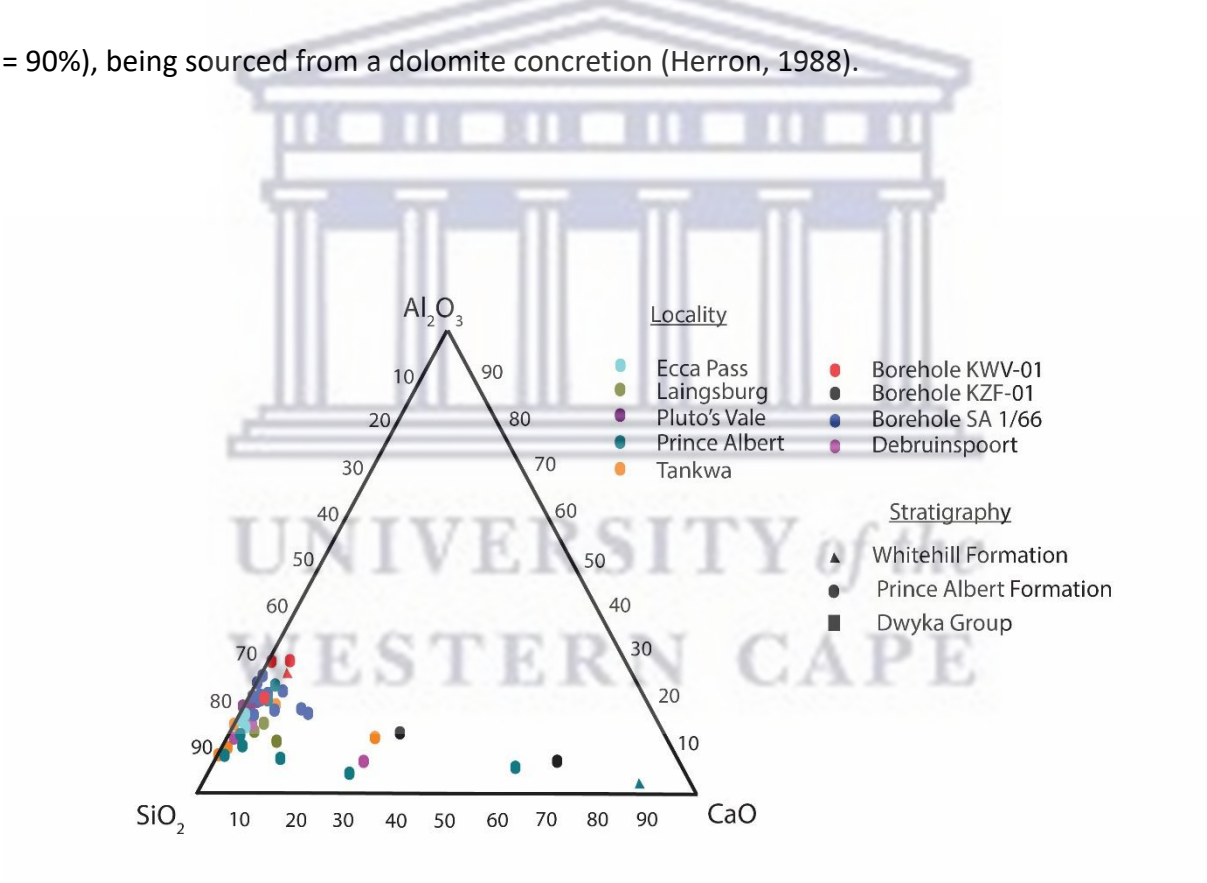

Figure 4.64. Ternary diagram showing the relative proportions of SiO_2, Al_2O_3 and CaO of samples taken from the Tankwa outcrop, Laingsburg, Prince Albert, Debruinspoort, Pluto's Vale, Ecca Pass, and boreholes KZF-01, KWV-01 and SA 1/66.

4.1.3 Statistical techniques

4.1.3.1 Univariate analysis

Major and trace elements (Appendix 14, 15 and 16) from boreholes KZF-01, KWV-01, SA 1/66 and surface outcrops of Laingsburg, Tankwa, Prince Albert, Ecca Pass, Debruinspoort and Pluto's Vale were tested for normality as it is a requirement prior to performing any multivariate statistical analysis. All the variables in the dataset indicate a normal distribution or bell-shaped curve with a few shown in Figure 4.65. With a normal distribution, data points occur either side of the mean value (Fig. 4.65). Therefore the data was assumed to be normally distributed.

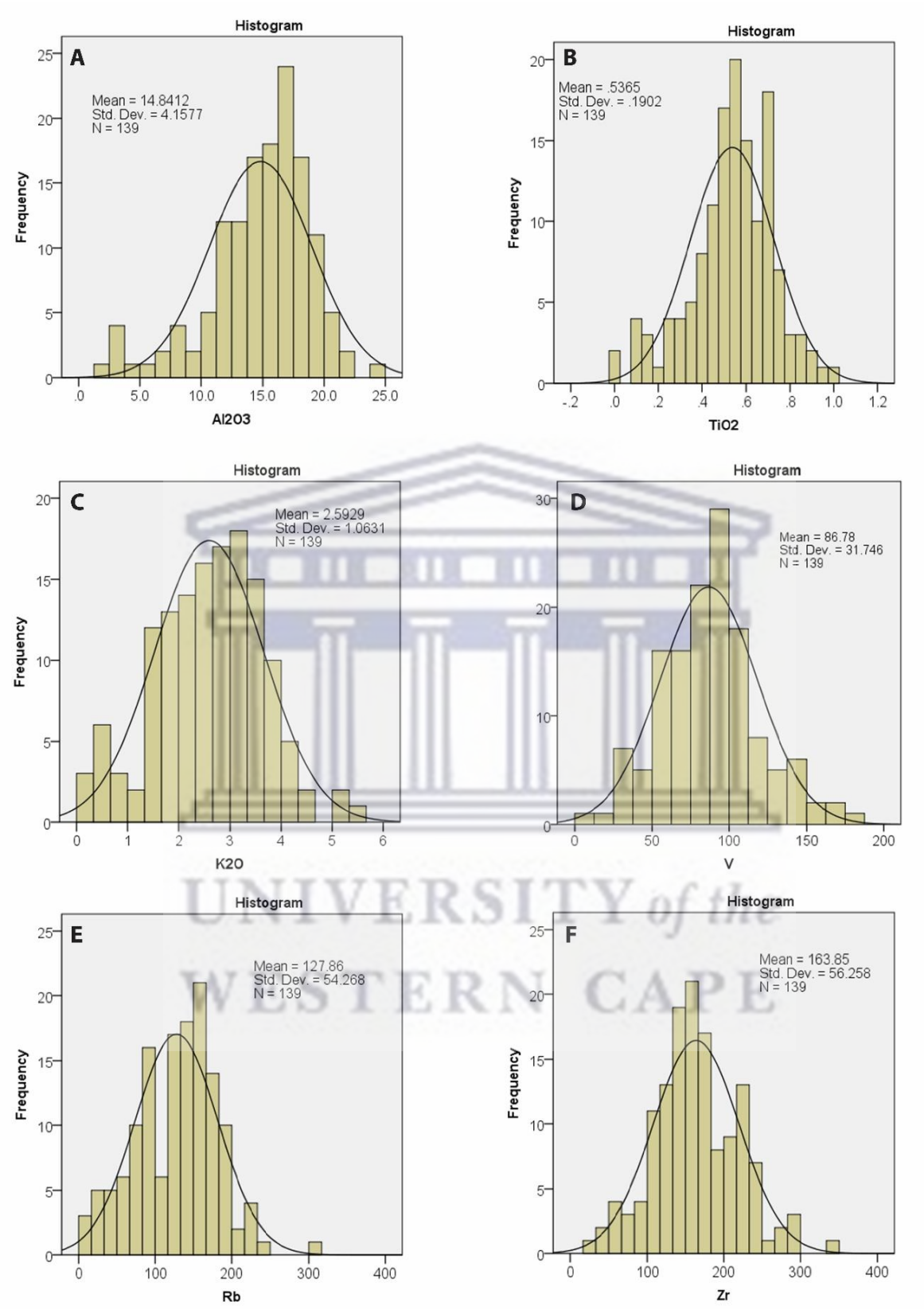

Figure 4.65. Histogram plot of (A) Al_2O_3, (B) TiO_2, (C) K_2O, (D) V, (E) Rb and (F) Zr.

4.1.3.2 Correlation coefficient

To establish element: mineral links, correlation coefficient (CC) techniques were used during this study. Correlation Coefficient scores greater than 0.7 infer a high level of correlation between two elements, between 0.6 and 0.7 they are considered moderate to high and a score less than 0.5 is considered low (Craigie, 2018). With negative correlation coefficient scores, elements would have strong negative associations.

Table 4.1 shows the results of CC applied to samples of the Dwyka Group, Prince Albert Formation and Whitehill Formation across the southern part of the main Karoo Basin. In total, one hundred and thirty-nine samples were used from HM1 to HM139 (Appendix 14, 15 and 16). CC analysis was applied to major and trace elements obtained from XRF-analysis (Appendix 14, 15 and 16), but only a select group is shown in Table 4.1 to show their positive mineral affinities from the dataset.

In Table 4.1, CC values greater than 0.6 are highlighted in bold. A high CC value of 0.79 is shown between major elements TiO_2 and Al_2O_3 indicating element association with clay minerals (Craigie, 2016). MnO and Fe_2O_3 has a CC score of 0.71 which suggests that these major elements are associated with heavy minerals such as hematite. K_2O has a high CC score of 0.73 and 0.87 with TiO_2 and Al_2O_3 respectively indicating a positive relationship between K-feldspars and clay minerals (Borchers et al., 2005). P_2O_5 and CaO displays a positive CC, which may be taken as evidence that these elements have similar mineralogical affinities, being mainly concentrated in carbonate minerals. Ni is positively correlated to TiO_2 with CC scores of 0.60 suggesting heavy mineral association (Table 4.1). A highly positive CC trend is seen between Rb, TiO_2, Al_2O_3 and K_2O with CC scores of 0.67, 0.87 and 0.97 respectively. These scores suggest that Rb is mainly concentrated in clay minerals, micas and K-feldspars (Table

4.1; Craigie, 2016). Sr is positively correlated with CaO which indicates that Sr has mineral affinities towards carbonate minerals. Th has high CC scores of 0.64, 0.87, 0.78 and 0.81 with TiO_2, Al_2O_3, K_2O and Rb respectively, suggesting mineral association with clay minerals, micas and K-feldspars (Table 4.1; Craigie, 2016). A positive association exists between Y and P_2O_5 which suggest that these elements are associated with heavy minerals and/ or biogenic phosphate (Craigie, 2016). Zr has a positive correlation with Al_2O_3, K_2O and Th (Table 4.1), which suggests that Zr is mainly concentrated in clay minerals, with lessor amounts in K-feldspars and heavy minerals (Ahrens, 1945; Craigie, 2018).

Table 4.1. Results of correlation coefficient analysis of major and trace elements taken from the Tankwa, Laingsburg, Prince Albert, Debruinspoort, Ecca Pass and Pluto's Vale outcrops and from boreholes SA 1/66, KZF-01 and KWV-01.

	SiO_2	TiO_2	Al_2O_3	Fe_2O_3	MnO	MgO	CaO	Na_2O	K_2O	P_2O_5	Ni	Rb	Sr	Th	U	V	Y	Zr
SiO_2	1																	
TiO_2	0.23	1																
Al_2O_3	0.29	**0.79**	1															
Fe_2O_3	-0.40	-0.13	-0.18	1														
MnO	-0.52	-0.37	-0.44	**0.71**	1													
MgO	-0.46	-0.09	-0.20	-0.02	0.03	1												
CaO	-0.73	-0.48	-0.58	-0.12	0.21	0.30	1											
Na_2O	0.28	0.29	0.22	-0.26	-0.18	-0.12	-0.24	1										
K_2O	0.16	**0.73**	**0.87**	-0.24	-0.38	-0.13	-0.41	0.09	1									
P_2O_5	-0.37	-0.29	-0.33	-0.10	0.11	-0.08	**0.60**	-0.13	-0.21	1								
Ni	0.09	**0.60**	0.37	-0.02	-0.19	0.00	-0.24	0.05	0.49	-0.13	1							
Rb	0.16	**0.67**	**0.87**	-0.26	-0.39	-0.14	-0.39	0.09	**0.97**	-0.21	0.37	1						
Sr	-0.75	-0.41	-0.47	0.02	0.24	0.28	**0.88**	-0.16	-0.34	0.32	-0.27	-0.30	1					
Th	0.13	**0.64**	**0.87**	-0.13	-0.33	-0.15	-0.40	0.19	**0.78**	-0.24	0.30	**0.81**	-0.28	1				
U	-0.38	-0.04	0.19	-0.02	0.00	-0.09	0.33	-0.09	0.21	0.37	-0.13	0.26	0.37	0.43	1			
V	-0.02	0.59	0.55	0.18	-0.13	0.03	-0.33	-0.04	0.42	-0.21	0.39	0.42	-0.30	0.44	0.05	1		
Y	-0.31	-0.17	-0.13	-0.13	0.05	-0.16	0.49	-0.07	-0.07	**0.92**	-0.12	-0.07	0.24	-0.07	0.51	-0.12	1	
Zr	0.29	0.51	**0.73**	-0.23	-0.30	-0.22	-0.42	0.26	**0.60**	-0.28	0.08	0.64	-0.35	**0.62**	0.21	0.21	-0.04	1

4.1.3.3 Multivariate statistics

4.1.3.3.1 Factor analysis

Factor analysis was used to extract element associations in order to characterise rock types or geochemical process. It was done using a selected set of major and trace elements (Appendix 14, 15 and 16). The number of factors extracted was based on eigenvalue greater than 1 as well as using the total variance explained (Table 4.2), with a cut off of 79.9% explained variance, including the first five factors. Factor scores were then saved as variables and compared to sample numbers in order to interpret the various rock types. Factor one is most dominant and describes 36.7% (Table 4.2) of total data variability. This factor is highly positively loaded with TiO_2, Al_2O_3, K_2O, Rb, Th, U and Zr elements (Table 4.3) which was interpreted as shale (Craigie, 2016). Factor two describes 16.6% (Table 4.2) of the total data variability which is highly negatively loaded with SiO_2 and highly positively loaded with MgO, CaO and Sr (Table 4.3). Factor two was interpreted as diamictite based on the negative loading of SiO_2 or dolomite based on the positive loading of MgO, CaO and Sr (Borchers et al., 2005). Factor three is positively loaded with CaO, P_2O_5, U and Y which was classified as phosphatic shale (Craigie, 2016; Table 4.3). Factor analysis loading plots using the first three factors are shown in Figure 4.66. On the factor loading plot the y-axis represents the communality of a variable, on a scale of -1 to 1. Factor four is highly positively loaded with Fe_2O_3 and MnO and factor five with TiO_2, Ni and V (Table 4.3). Element associations of factor four was interpreted as ferruginous and manganiferous shales. Factor five was interpreted as shale interbedded with tuff. Rhythmite was interpreted as being positive in factors one, two, three and four. A combination of negatively loaded factors (factors 1, 2, 3, 4 and 5) were interpreted as silty shale.

Table 4.2. Total variance described by each factor for samples HM1 to HM139.

Total Variance Explained									
Component	Initial Eigenvalues			Extraction Sums of Squared Loadings			Rotation Sums of Squared Loadings		
	Total	% of Variance	Cumulative %	Total	% of Variance	Cumulative %	Total	% of Variance	Cumulative %
1	6.609	36.716	36.716	6.609	36.716	36.716	4.767	26.485	26.485
2	2.986	16.588	53.304	2.986	16.588	53.304	2.682	14.900	41.385
3	2.076	11.531	64.835	2.076	11.531	64.835	2.651	14.727	56.112
4	1.497	8.315	73.150	1.497	8.315	73.150	2.180	12.113	68.225
5	1.223	6.793	79.943	1.223	6.793	79.943	2.109	11.718	79.943
6	.921	5.117	85.059						
7	.666	3.703	88.762						
8	.567	3.151	91.912						
9	.423	2.352	94.265						
10	.348	1.933	96.197						
11	.225	1.251	97.449						
12	.157	.875	98.323						
13	.135	.752	99.076						
14	.056	.310	99.385						
15	.045	.249	99.634						
16	.038	.208	99.842						
17	.020	.109	99.952						
18	.009	.048	100.000						
Extraction Method: Principal Component Analysis.									

Table 4.3. Rotated component matrix.

Rotated Component Matrix					
	Component				
	Factor 1- Shale	Factor 2- Diamictite and dolomite	Factor 3- Phosphatic shale	Factor 4- Ferruginous and manganiferous shale	Factor 5- Shale interbedded with tuff
SiO_2		-.794			
TiO_2	.608				.599
Al_2O_3	.873				
Fe_2O_3				.937	
MnO				.824	
MgO		.736			
CaO		.737	.494		
Na_2O					
K_2O	.826				
P_2O_5			.931		
Ni					.831
Rb	.865				
Sr		.795			
Th	.910				
U	.536		.550		
V					.618
Y			.957		
Zr	.768				

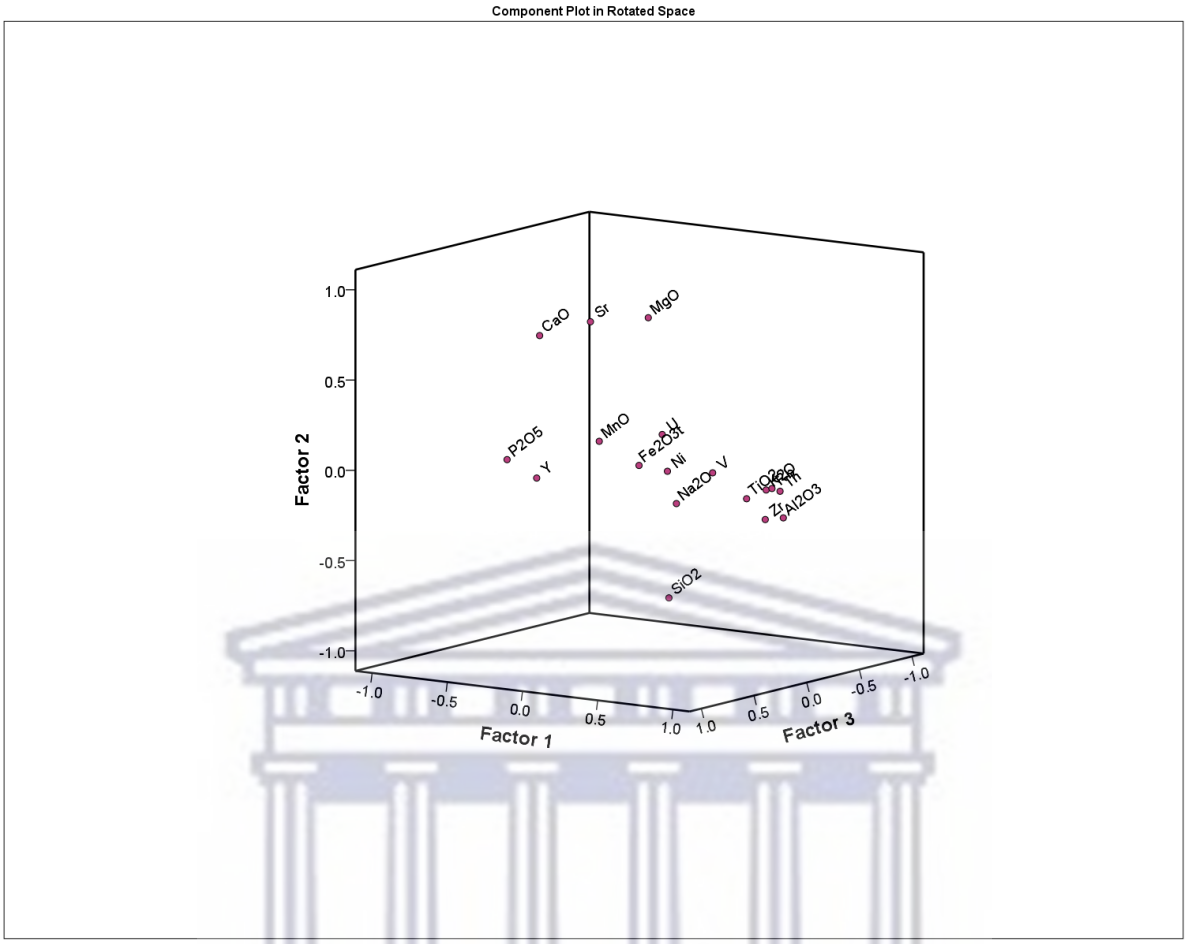

Figure 4.66. Factor Analysis loading plots for selected elements.

4.1.3.3.2 Cluster analysis

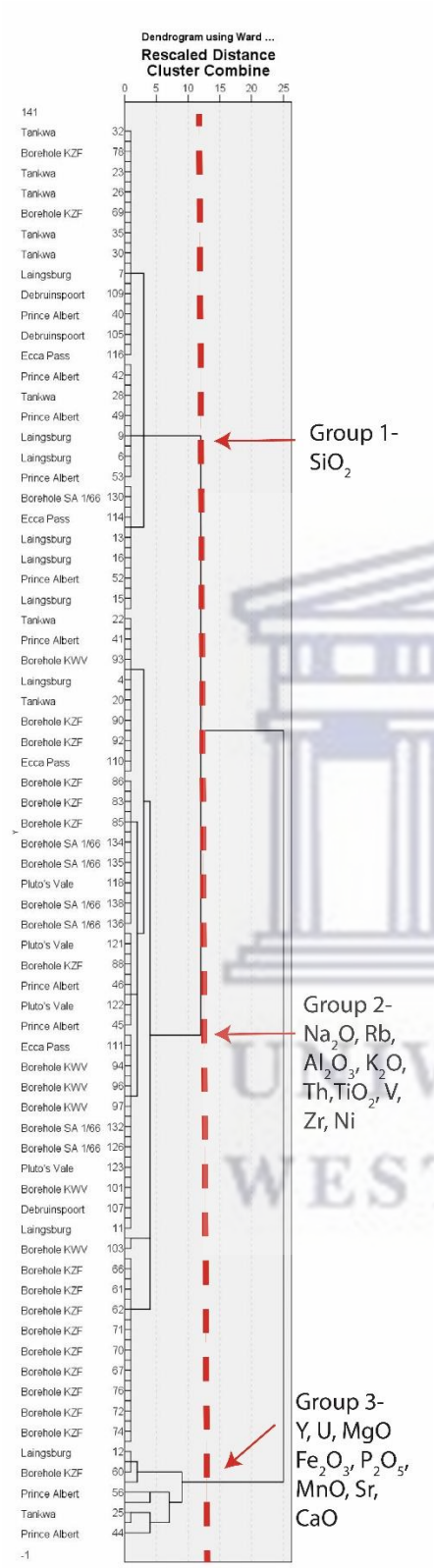

Figure 4.67 Dendrogram from hierarchical cluster analysis using XRF mineralogy data showing three distinct element associations (Group 1 to Group 3).

Cluster analysis was used to classify various rock types from available XRF data from nine sampled localities. With this technique, hierarchical Q-mode cluster analysis was applied using Ward's method with squared Euclidean distance as a measure of distance. This approach helps to determine the best number of clusters to work with as a dendrogram.

In the dendrogram (Fig. 4.67) three major groups were identified. Discriminant function analysis followed which was used to characterise and classify geochemically the three groups. Discriminant function analysis is a method use to characterise and enhance the geochemical distinction between groups (Siad et al., 1994). The groups were created through cluster analysis. The number of functions is always one less than the groups or equal to the number of geochemical variables. Hence two discriminant functions resulted (Table 4.4). Tables 4.4 and 4.5 display the structure matrix (relation between variables and discriminant function) and functions at group centroids (related to groups and discriminant functions).

Function 1 is positively loaded with CaO, Sr, MnO, P_2O_5, Fe_2O_3 and MgO (Table 4.4) which characterises dolomite, phosphatic shale, ferruginous and manganiferous shales (Table 4.5). Function 2 is negatively loaded with Rb, Al_2O_3, K_2O, Th, TiO_2, U, V, Zr, Ni and Y which is interpreted as shale while SiO_2 is positively loaded and interpreted as diamictite (Tables 4.4 and 4.5).

Table 4.4. Structure matrix from cluster membership.

Structure Matrix		
	Function	
	1	2
CaO	.281*	-.093
Sr	.215*	-.152
MnO	.190*	-.075
P_2O_5	.143*	-.075
Fe_2O_3	.066*	-.035
MgO	.061*	-.004
Na_2O	-.054*	-.015
Rb	-.212	-.744*
Al_2O_3	-.322	-.734*
K_2O	-.210	-.695*
Th	-.182	-.627*
SiO_2	-.279	.496*
TiO_2	-.185	-.365*
U	.040	-.319*
V	-.102	-.271*
Zr	-.146	-.265*
Ni	-.078	-.220*
Y	.085	-.118*

Table 4.5. Functions at group centroids.

Functions at Group Centroids		
Geochemical group	Function	
	1	2
Group 1-diamictite	-0.360	1.799
Group 2- shale	-1.671	-0.980
Group 3- dolomite, phosphatic shale, ferruginous and manganiferous shales	17.145	-0.669

4.1.3.3.2.1 Combination of cluster and discriminant function analysis

Discriminant analysis was then selected to reclassify those samples which was misclassified with cluster analysis. Only forty-six samples were classified as Group 1- diamictite, seventy-seven as Group 2- shale and nine samples as Group 3- dolomite, phosphatic shale, ferruginous and manganiferous shale (Table 4.6). The number of samples for Groups 1 to 3 were 95.0% correctly classified with seven misclassified samples. However, the classification was further improved by creating a predicted group membership that classifies the incorrectly classified samples (Table 4.6) into their predicted geochemical group. This resulted in 99.3% samples being correctly classified (Table 4.7).

Table 4.6. Classified samples together with misclassified samples in Groups 1 and 2.

Classification Results						
		Geochemical Group	Predicted Group Membership			Total
			Group 1- diamictite	Group 2- shale	Group 3- dolomite, phosphatic shale, ferruginous and manganiferous shale	
Original	Count	Group 1-diamictite	46	2	0	48
		Group 2- shale	5	77	0	82
		Group 3- dolomite, phosphatic shale, ferruginous and manganiferous shales	0	0	9	9
	%	Group 1-diamictite	95.8	4.2	.0	100.0
		Group 2- shale	6.1	93.9	.0	100.0
		Group 3- dolomite, phosphatic shale, ferruginous and manganiferous shales	.0	.0	100.0	100.0
a. 95.0% of original grouped cases correctly classified.						

Table 4.7. Classification of samples containing Groups 1, 2 and 3.

Classification Results						
		Geochemical Group	Predicted Group Membership			Total
			Group 1- diamictite	Group 2- shale	Group 3- dolomite, phosphatic shale, ferruginous and manganiferous shale	
Original	Count	Group 1-diamictite	51	0	0	51
		Group 2- shale	1	78	0	79
		Group 3- dolomite, phosphatic shale, ferruginous and manganiferous shales	0	0	9	9

	%	Group 1-diamictite	100.0	.0	.0	100.0
		Group 2- shale	1.3	98.7	.0	100.0
		Group 3- dolomite, phosphatic shale, ferruginous and manganiferous shales	.0	.0	100.0	100.0
a. 99.3% of original grouped cases correctly classified.						

In order to find the best discriminating major and trace element, stepwise discriminant analysis was considered. In Table 4.8, Al_2O_3, SiO_2 and Rb were the best discriminating variables between shale and diamictite. Al_2O_3 is the best variable classifying correctly up to 87.1% followed by SiO_2 which improves the classification up to 89.9% and Rb classifying correctly up to 97.1% (Table 4.8).

Table 4.8. Stepwise classification results of Predictors Al_2O_3, SiO_2 and Rb.

Variables	Classification
Al_2O_3	87.1%
SiO_2	89.9%
Rb	97.1%

4.2 Depositional environment

4.2.1 Geochemical proxies:

Geochemical proxies were used to reconstruct the depositional history and climate evolution of the Prince Albert Formation (Scheffler et al., 2006). Shales of the Prince Albert Formation, can either be enriched or depleted in environmental-sensitive elements depending on its redox conditions (Scheffler et al., 2006). Ratios that were used were: SiO_2/Al_2O_3, P_2O_5/Al_2O_3, CIA, Rb/K, V/Cr, V/V+Ni and Sr/Cu.

SiO_2/Al_2O_3 ratio is used as a relative index between quartz-rich and clay-rich sediments (Herron, 1988). A high SiO_2/Al_2O_3 reflects a quartz-rich unit and a low ratio reflects a clay-rich unit. P_2O_5/Al_2O_3 is used as a proxy for palaeoproductivity (Chere, 2015). The chemical index of alteration (CIA) provides information about chemical weathering processes. Low CIA values reflect cold/arid conditions and high CIA values indicate warm/humid climates (Scheffler et al., 2006). Shales reflect CIA weathering indices from between 70 and 75 (Nesbitt and Young, 1982). Rb/K ratios are used to distinguish between fresh water sediments, brackish or marine environments (Campbell and Williams, 1965). Rb/K ratios less than $4*10^{-3}$ in shale reflect fresh water to brackish conditions and ratios greater than $6*10^{-3}$ reflect marine environments (Campbell and Williams, 1965). V/Cr and V/V+Ni ratio reflects changes in redox conditions. V/Cr ratios less than 2 indicate oxic conditions, values between 2 and 4.25 dysoxic and values greater than 4.25 reflect anoxic/aerobic bottom water conditions (Scheffler et al., 2006). V/(V+Ni) ratios between 0.46 and 0.60 indicate a weakly stratified dysoxic environment, values greater than 0.80 suggest euxinic conditions, while V/(V+Ni) ratios less than 0.54 suggest oxic conditions at the seafloor (Hatch and Leventhal., 1992). Sr/Cu ratio can be related

to climatic conditions and salinity levels. Sr/Cu ratios between 1.3 and 5.0 indicate warm humid conditions and greater than 5.0 reflect a hot arid climate (Lerman, 1978).

4.2.1.1 Laingsburg outcrop

SiO_2/Al_2O_3 values generally range between 3.32 and 6.67, with the exception of a single peak of 10.10 in sample 8 from the lower Prince Albert Formation (Table 4.9; Fig. 4.68). These low SiO_2/Al_2O_3 values suggest a clay-rich formation (Chere, 2015). Low paleoproductivity occurs throughout the Dwyka Group and lower Ecca Group as shown by P_2O_5/Al_2O_3 values being less than 0.03 with a single outlier peak of 0.36 from the central part of the Prince Albert Formation in sample 12 (Table 4.9; Fig. 4.68). Increasing CIA values from the Dwyka Group (sample 1) into the overlying Prince Albert Formation (sample 11) indicate increasing warm-humid conditions, as supported by low Sr/Cu values (Scheffler et al., 2006). The CIA value of sample 12 in the central part of the Prince Albert Formation is anomalously low (53), which suggests that a coarser-grained sediment containing a higher feldspar/clay mineral ratio is present (Visser and Young, 1990). Sample 12 also has a Sr/Cu peak of 62.19 (Table 4.9; Fig. 4.68), which reflects hot/arid conditions (Lerman, 1978). From sample 13 towards sample 19 in the upper Prince Albert and Whitehill Formations, warm-humid conditions prevailed, with Rb/K and V/Cr ratios indicating marine and dysoxic bottom water conditions (Campbell and Williams, 1965; Scheffler et al., 2006).

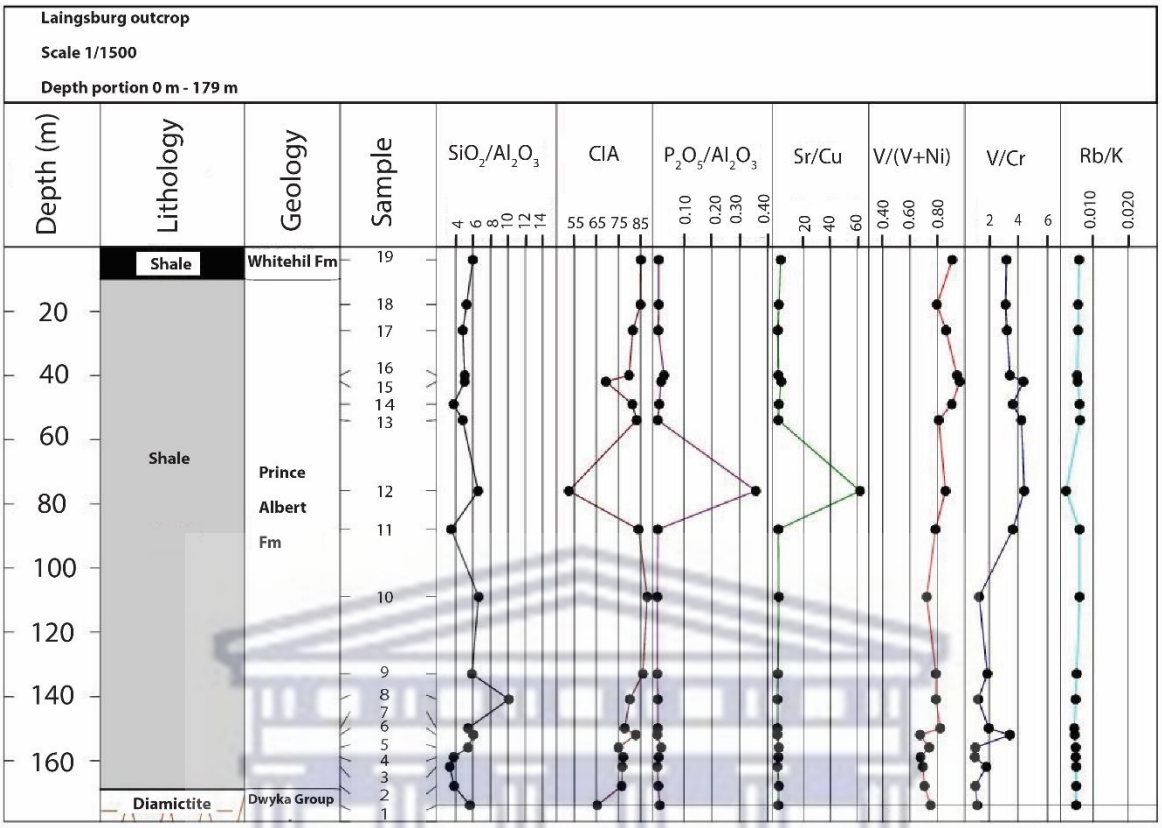

Figure 4.68. Laingsburg outcrop profiles of SiO_2/Al_2O_3, CIA, P_2O_5/Al_2O_3, Sr/Cu, V/(V+Ni), V/Cr and Rb/K.

Table 4.9. Selected geochemical proxies taken from the Prince Albert outcrop, Ecca Pass, Debruinspoort, Pluto's Vale, Laingsburg, Tankwa, and boreholes KZF-01, KWV-01 and SA 1/66. WHF= Whitehill Formation, PAF= Prince Albert Formation, DWY= Dwyka Group.

Locality	Stratigraphy	Sample	SiO_2/Al_2O_3	CIA	P_2O_5/Al_2O_3	Sr/Cu	V/(V+Ni)	V/CR	Rb/K
Laingsburg outcrop	DWY	1	5.63	65.43	0.01	1.56	0.75	1.17	0.0052
Laingsburg outcrop	PAF	8	10.10	80.23	0.01	0.83	0.79	1.25	0.0051
Laingsburg outcrop	PAF	11	3.49	84.29	0.01	1.35	0.78	3.62	0.0062
Laingsburg outcrop	PAF	12	6.60	52.66	0.36	62.19	0.86	4.40	0.0023
Tankwa outcrop	PAF	25	4.60	27.92	1.76	21.57	0.73	1.20	0.0055
Tankwa outcrop	PAF	33	3.89	66.42	0.31	188.20	0.93	6.58	0.0040
Prince Albert outcrop	DWY	40	6.23	72.05	0.01	2.25	0.77	1.41	0.0057
Prince Albert outcrop	WHF	56	3.77	2.91	0.02	668.60	0.33	0.63	0.0268
Debruinspoort outcrop	PAF	106	8.70	19.11	0.08	44.11	0.83	3.38	0.0022
Debruinspoort outcrop	WHF	109	6.88	77.31	0.01	1.95	0.70	2.50	0.0052
Ecca Pass outcrop	DWY	116	5.66	64.59	0.01	10.20	0.73	1.15	0.0051
Pluto's Vale outcrop	PAF	118	3.50	78.95	0.04	0.51	0.77	1.41	0.0060
Borehole KZF-01	WHF	57	3.61	74.27	0.01	2.83	0.70	2.00	0.0061
Borehole KZF-01	PAF	58	3.28	9.48	0.25	311.20	0.89	4.56	0.0077
Borehole KZF-01	DWY	92	3.84	76.21	0.01	2.57	0.78	1.32	0.0057
Borehole KWV-01	PAF	100	2.31	74.08	0.07	2.85	0.84	3.73	0.0057
Borehole KWV-01	PAF	103	2.42	79.83	0.00	2.42	0.80	4.83	0.0067
Borehole SA1/66	WHF	125	3.32	72.53	0.03	4.35	0.85	2.44	0.0058
Borehole SA1/66	WHF	126	3.65	73.68	0.01	4.65	0.85	2.37	0.0060
Borehole SA1/66	PAF	135	3.39	72.00	0.08	3.41	0.77	2.41	0.0055
Borehole SA1/66	DWY	139	4.57	69.37	0.01	6.78	0.73	1.17	0.0057

4.2.1.2 Tankwa outcrop

Low Sr/Cu values (less than 3) in the upper Dwyka Group to lower Whitehill Formation shales, infer deposition under warm-humid conditions (Lerman, 1978). The anomalously low CIA value of 28 in sample 25 from the lower Prince Albert Formation (Table 4.9; Fig. 4.69) suggests a decreased chemical alteration process and reduced leaching of mobile elements during hot/arid conditions (Scheffler et al., 2006). The change from cold, glacial conditions of the upper Dwyka Group Group to a rise in sea-level and marine conditions during the deposition of the Prince Albert and Whitehill Formations (Visser, 1993) is reflected in an increase in the Rb/K ratio from 4.8* 10^{-3} to a mean of 5.5*10^{-3} for the Ecca Group (Appendix 17; Fig. 4.69). Sample 33 from the upper part of the Prince Albert Formation is anomalous with a high Sr/Cu (188), a high V/Cr (6.58) and low Rb/K (4.0*10^{-3}) ratio (Table 4.9; Fig 4.69). This suggests a fresh water pulse induced by the final meltdown of the glaciers causing a temporary return to brackish conditions during the deposition of sample 33 and returning to marine conditions from sample 34 to 39 (Fig. 4.69). Furthermore, V/(V+Ni) and V/Cr ratios indicate that dysoxic and euxinic conditions persisted during the upper Dwyka Group and lower Ecca Group (Prince Albert and Whitehill Formations).

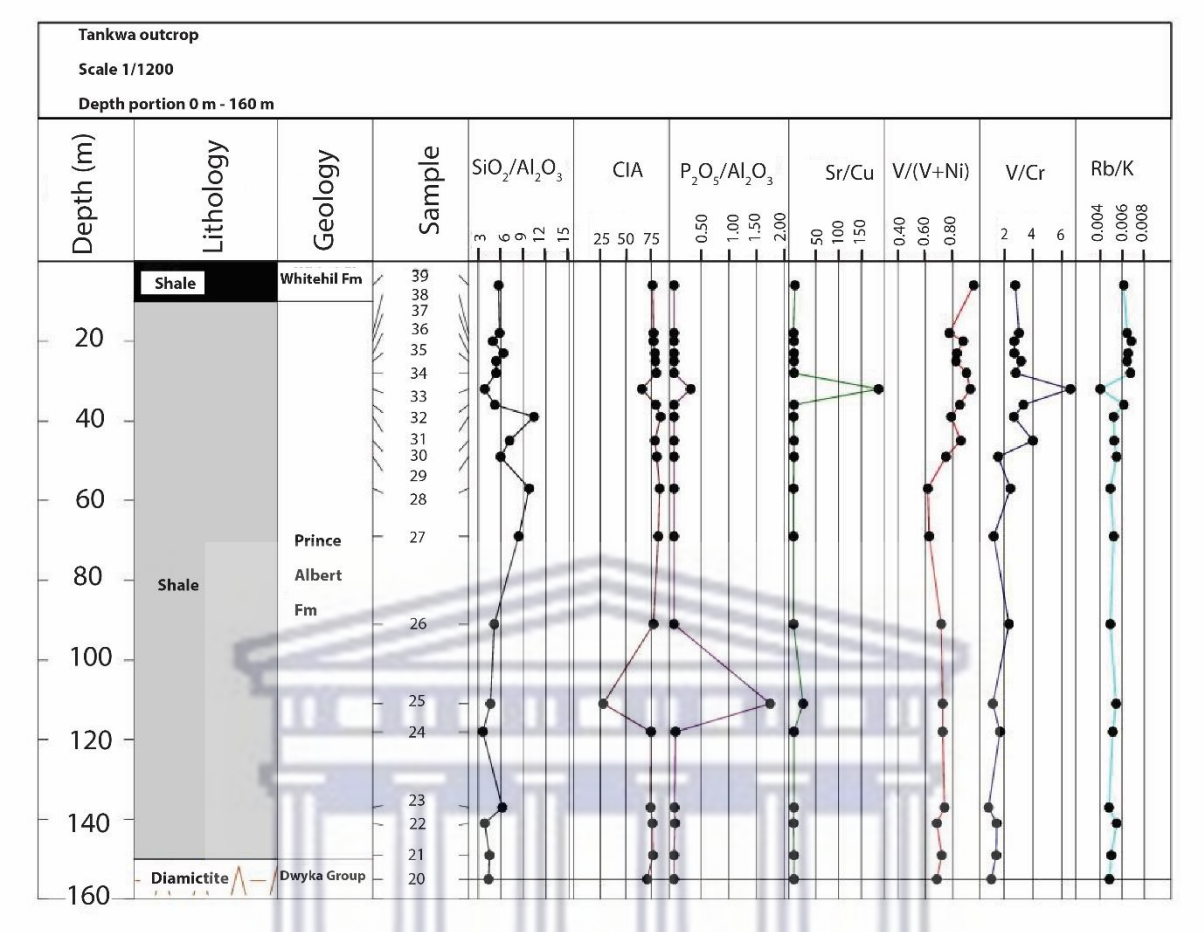

Figure 4.69. Tankwa outcrop profiles of SiO_2/Al_2O_3, CIA, P_2O_5/Al_2O_3, Sr/Cu, V/(V+Ni), V/Cr and Rb/K.

4.2.1.3 Prince Albert outcrop

Low SiO_2/Al_2O_3 ratios of around 6 (sample 40; Table 4.9) in the upper Dwyka Group sediments suggests an arkosic provenance (Scheffler et al., 2006). SiO_2/Al_2O_3 ratios in the Prince Albert Formation have a mean value of 5.92 and a maximum of value of 14.05, which indicates an influx of quartz-rich sediment (Scheffler et al., 2006). Sample 56 (dolomite concretion) of the Whitehill Formation has a SiO_2/Al_2O_3 value of 3.77 having a low quartz content (Fig. 4.70). High CIA (chemical index of alteration; see Section 3.2.1) and low Sr/Cu values from the transition of the upper Dwyka Group to the Prince Albert Formation point to rising temperatures and humid climate conditions which favoured element mobilization during

weathering processes. Sample 56 of the Whitehill Formation has low CIA and high Sr/Cu values (Table 4.9; Fig. 4.70) indicating a hot arid climate (Scheffler et al., 2006). Due to increasing temperatures following the Dwyka glaciation, melting of glaciers and icecaps in the northern mountainous highlands (Cargonian Highlands) of the main Karoo Basin caused sea-level to rise (Visser, 1993). Based on the Rb/K, V/Cr and V/ (V+Ni) ratios in the Prince Albert Formation (Appendix 17; Fig 4.70), marine sedimentary conditions prevailed ranging between dysoxic and euxinic (Scheffler et al., 2006).

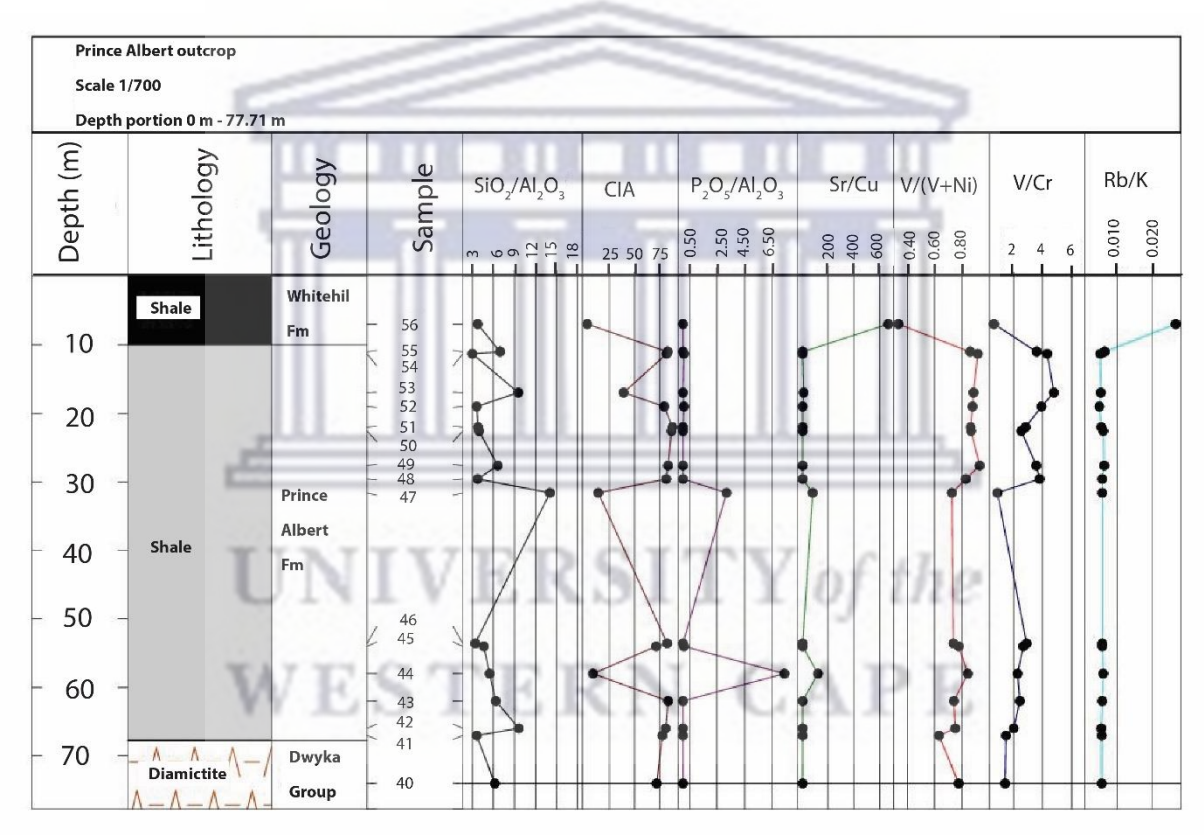

Figure 4.70. Prince Albert outcrop profiles of SiO_2/Al_2O_3, CIA, P_2O_5/Al_2O_3, Sr/Cu, V/ (V+Ni), V/Cr and Rb/K.

4.2.1.4 Debruinspoort outcrop

SiO_2/Al_2O_3 range between 4.14 and 8.70 with the highest quartz-rich shale being sample 106 and 109 of the Prince Albert and Whitehill Formation (Table 4.9; Appendix 17; Fig. 4.71). With

a freshwater pulse induced at sample 106 in the central part of the Prince Albert Formation, has a low CIA (19.11), low Rb/K (0.002) and high Sr/Cu value (44.11, Table 4.9; Fig. 4.71), which suggests cold/arid and freshwater conditions (Scheffler et al., 2006). The transition from cold-arid to warm-humid climatic conditions was accompanied by a sea-level rise, confirmed by high Rb/K ratios from samples 107 to 109 from the upper Prince Albert and Whitehill Formations (Appendix 17; Fig. 4.71). Paleoproductivity (P_2O_5/Al_2O_3) peaks in sample 106 in the central part of the Prince Albert Formation with a value of 0.08, which also indicates dysoxic conditions (Chere, 2015).

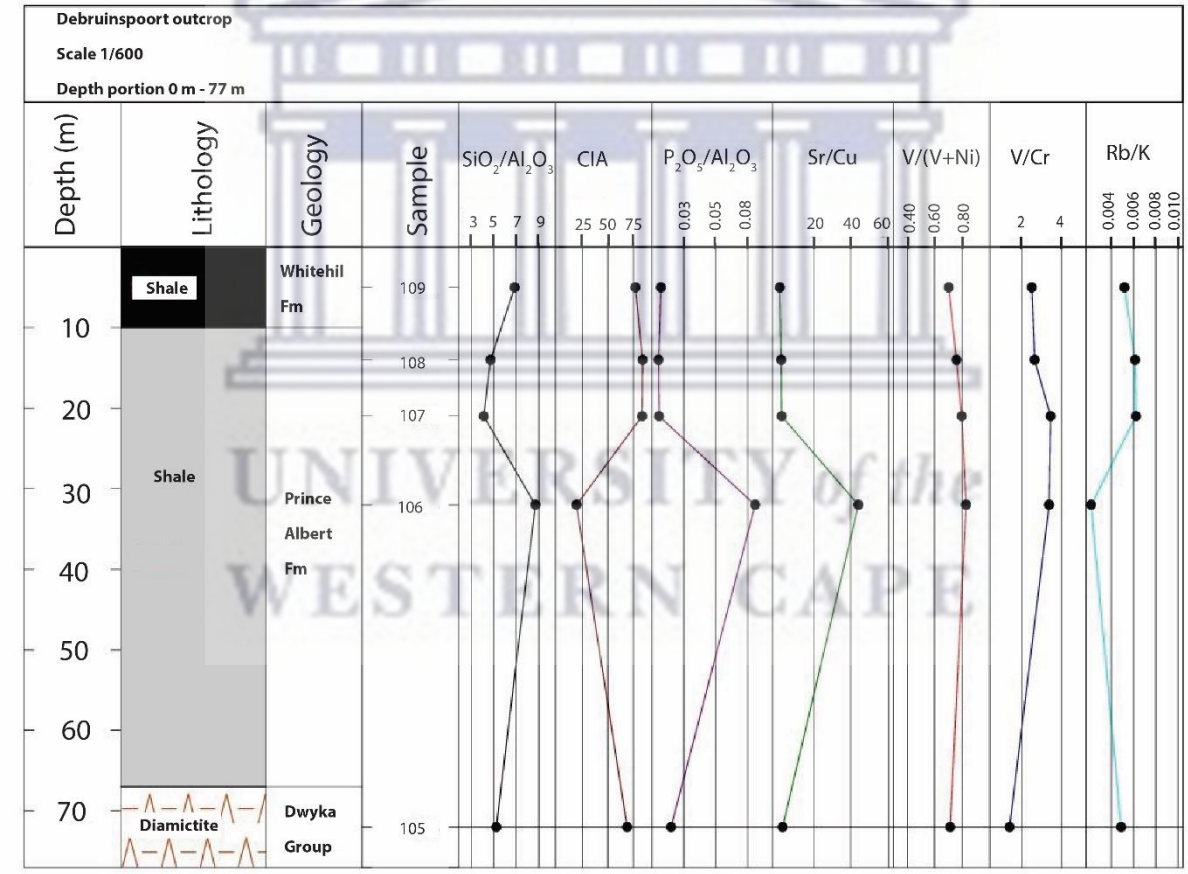

Figure 4.71. Debruinspoort outcrop profiles of SiO_2/Al_2O_3, CIA, P_2O_5/Al_2O_3, Sr/Cu, V/ (V+Ni), V/Cr and Rb/K.

4.2.1.5 Ecca Pass outcrop

Sample 116 of the upper Dwyka Group at Ecca Pass (Table 4.9) has a SiO_2/Al_2O_3 ratio of 5.66 indicating a high quartz-rich diamictite (Herron, 1988). The SiO_2/Al_2O_3 ratio fluctuates throughout the Prince Albert Formation attaining a maximum value of 6.23 and a minimum of 3.16, with a value of 4.93 in the lower Whitehill Formation (Appendix 17; Fig. 4.72). Arid conditions occurred during the deposition of the upper Dwyka Group, as shown by a lower CIA value (65 in contrast to greater than 74 in the Prince Albert Formation) and a high Sr/Cu value of 10 (Appendix 17; Fig. 4.72), which suggest decreasing weathering processes and reduced leaching of mobile elements (Scheffler et al., 2006). The low CIA value could also be attributed to the grain size of the sediment. Warm-humid conditions prevailed during deposition of the Prince Albert and Whitehill Formations with P_2O_5/Al_2O_3 values lying below 0.03 (Appendix 17; Fig. 4.72). Increasing CIA and Rb/K (up to $6.8^* 10^{-3}$) values following deposition of the glacigenic Dwyka Group (Appendix 17; Fig 4.72), suggest increasing temperatures and relatively constant marine conditions accompanied by dysoxic and euxinic conditions (Campbell and Williams, 1965).

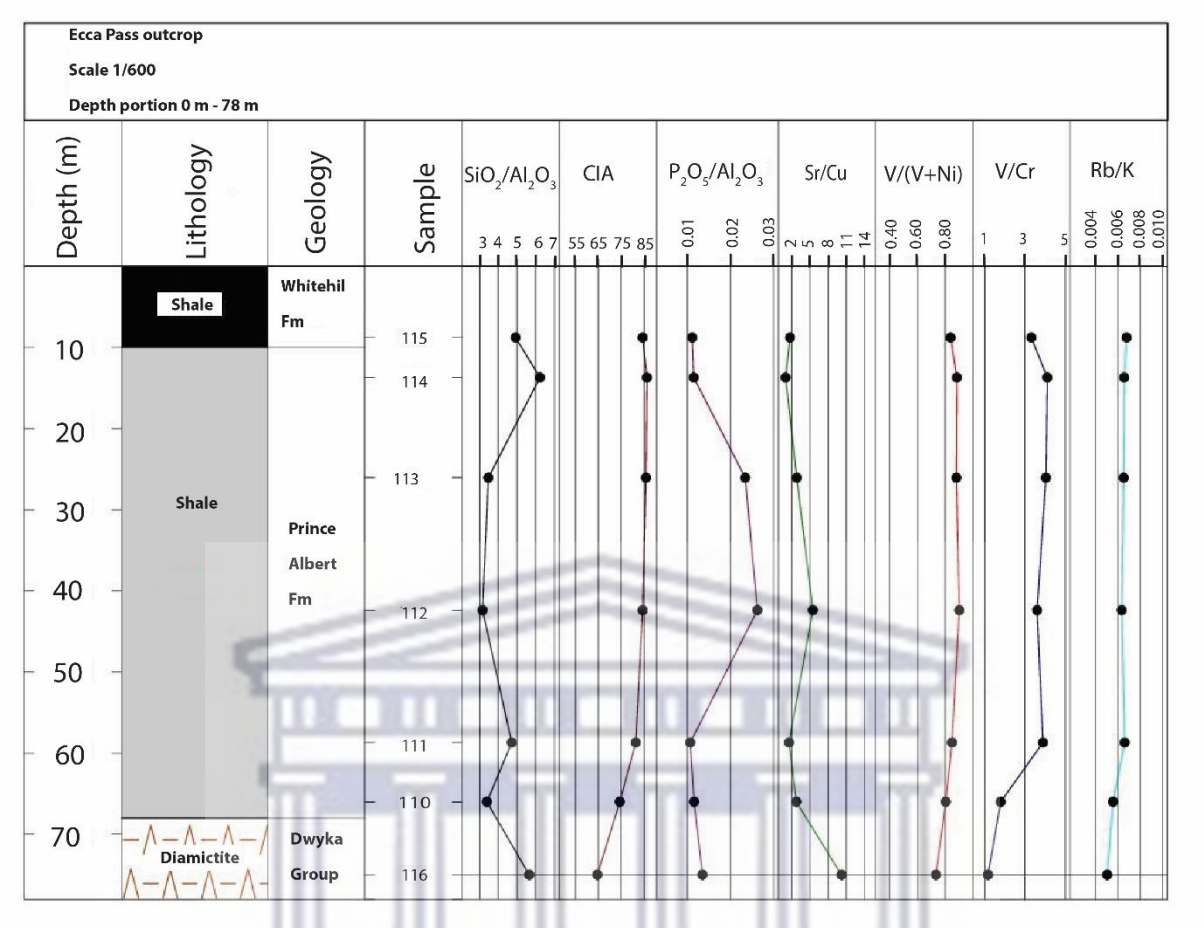

Figure 4.72. Ecca Pass outcrop profiles of SiO_2/Al_2O_3, CIA, P_2O_5/Al_2O_3, Sr/Cu, V/(V+Ni), V/Cr and Rb/K.

4.2.1.6 Pluto's Vale outcrop

Samples of the Dwyka Group and Prince Albert Formation from the Pluto's Vale outcrop in the Eastern Cape, indicate a warm-humid, climatic conditions based upon the high CIA values ranging between 74 and 85 and Sr/Cu values less than 2 (Appendix 17; Fig. 4.73). Low P_2O_5/Al_2O_3 ratios exist throughout the Prince Albert Formation with the exception of sample 118 (0.04). These low peaks suggest a low paleoproductivity (Chere, 2015). Increasing V/(V+Ni) ratios from the top of the Dwyka Group towards the top of the Prince Albert Formation (Appendix 17; Fig. 4.73) indicate the gradual development of euxinic bottom water conditions in a deep water environment (Hatch and Leventhal., 1992).

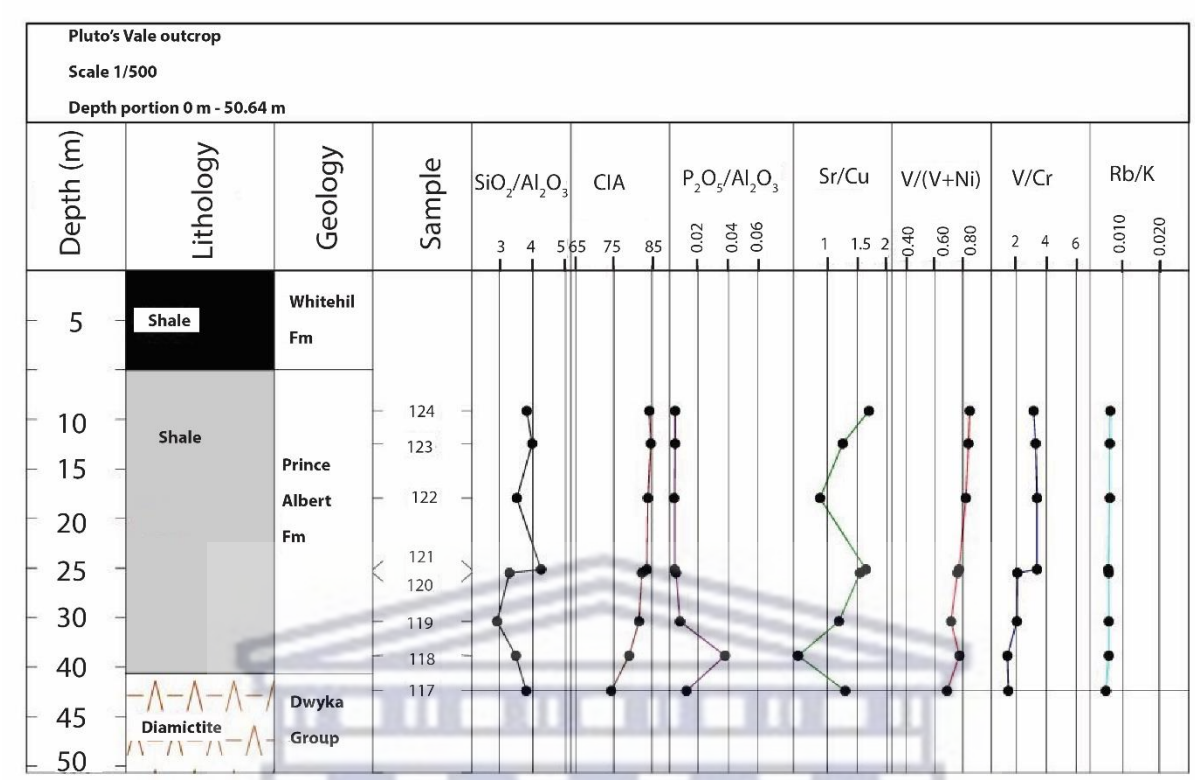

Figure 4.73. Pluto's Vale outcrop profiles of SiO_2/Al_2O_3, CIA, P_2O_5/Al_2O_3, Sr/Cu, V/ (V+Ni), V/Cr and Rb/K.

4.2.1.7 Borehole KZF-01

Diamictite (sample 92; Fig. 4.74) of the upper Dwyka Group of borehole KZF-01 has a SiO_2/Al_2O_3 ratio of 3.84. There is no significant change upwards into the Prince Albert Formation with a mean value of 3.86 (Appendix 17; Fig. 4.74). The lower Whitehill Formation (sample 57) has a lower SiO_2/Al_2O_3 ratio of 3.61, which indicates a low quartz content (Scheffler et al., 2006). Between depths 442.71 and 657.51 m, low P_2O_5/Al_2O_3 (less than 0.03) ratios exist in borehole KZF-01 with a single peak of 0.25 (sample 58) in thrusted Prince Albert Formation (Table 4.9; Fig. 4.74), suggesting a brief period of high paleoproductivity (Chere, 2015). Increasing Rb/K ratios from the top of the Dwyka Group approach a maximum value of $7.7 * 10^{-3}$ in sample 58 from thrusted Prince Albert Formation (Appendix 17; Fig. 4.74). This infers increasing marine conditions (Campbell and Williams, 1965).

Based on the low CIA and Sr/Cu ratios within the Prince Albert Formation (Appendix 17; Fig. 4.74), constant marine conditions accompanied by warm-humid climate conditions are inferred in the hinterland (Scheffler et al., 2006). The anomalously high Sr/Cu ratio of 311 in thrusted Prince Albert Formation (sample 58; Fig. 4.74) probably reflects a short period of hot/arid conditions (Lerman, 1978).

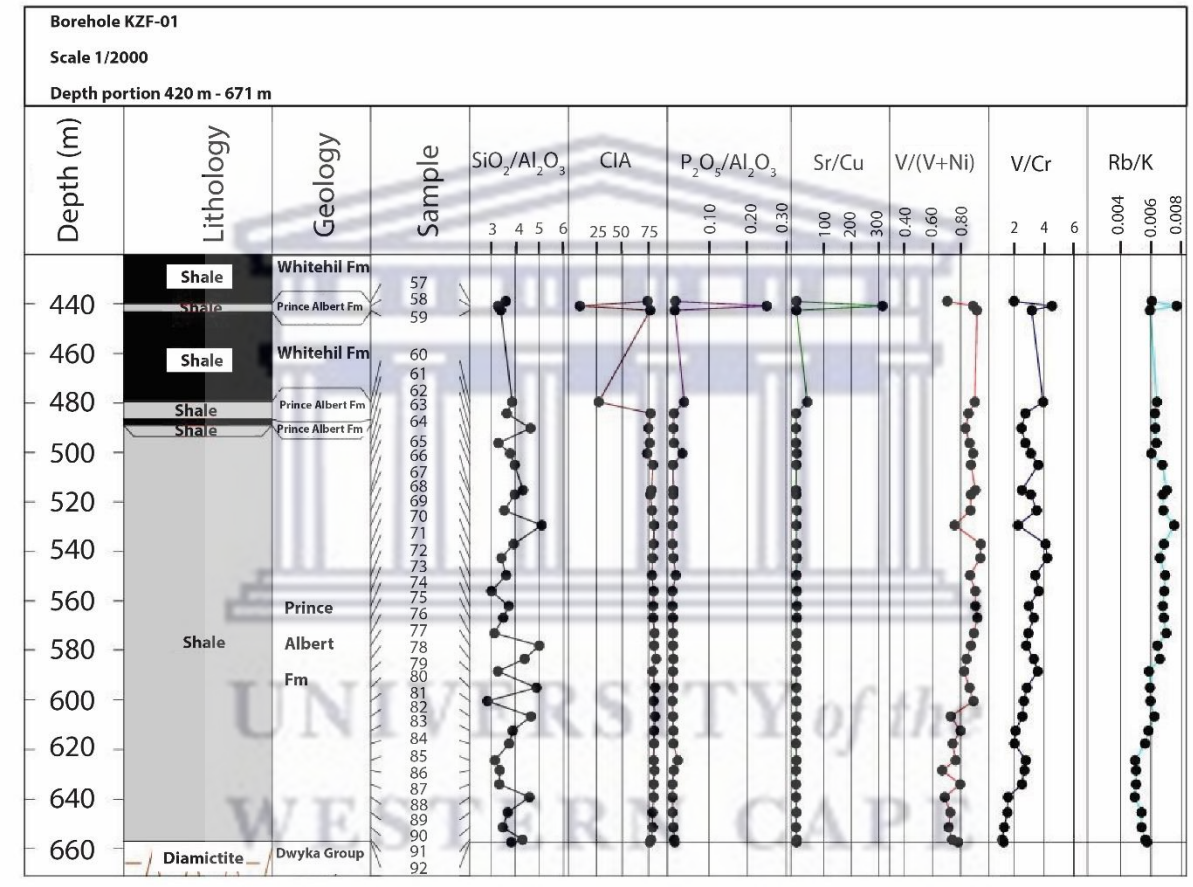

Figure 4.74. Borehole KZF-01 profiles of SiO_2/Al_2O_3, CIA, P_2O_5/Al_2O_3, Sr/Cu, V/(V+Ni), V/Cr and Rb/K.

4.2.1.8 Borehole KWV-01

In borehole KWV-01, V/ (V+Ni) values range between 0.71 and 0.92 (Appendix 17; Fig. 4.75) suggesting euxinic conditions (Hatch and Leventhal, 1992). For the Prince Albert Formation, the V/Cr ratio lies mostly between 3 and 4 (Appendix 17; Fig. 4.75), which indicates dysoxic conditions (Scheffler et al., 2006). However, sample 103 in the basal Prince Albert Formation has a V/Cr value of 4.83 (Table 4.9; Fig. 4.75), suggesting anoxic bottom water conditions (Scheffler et al., 2006). The low P_2O_5/Al_2O_3 values (< 0.01) within the Prince Albert Formation (Appendix 17; Fig. 4.75) indicates a low paleoproductivity (Chere, 2015). However, one sample (sample 100) is anomalous with a peak of 0.07 (Table 4.9; Fig. 4.75), which implies a short period of high paleoproductivity (Chere, 2015). The Prince Albert Formation shows a high chemical index of alteration (CIA) with values between 74 and 82 (Appendix 17; Fig. 4.75). This suggests increasing chemical weathering conditions under a humid climate (Scheffler et al., 2006). Rb/K ratios between $5.7*10^{-3}$ and $7.1*10^{-3}$ (Appendix 17; Fig. 4.75) mark the onset of constant marine conditions throughout the Prince Albert Formation (Campbell and Williams, 1965).

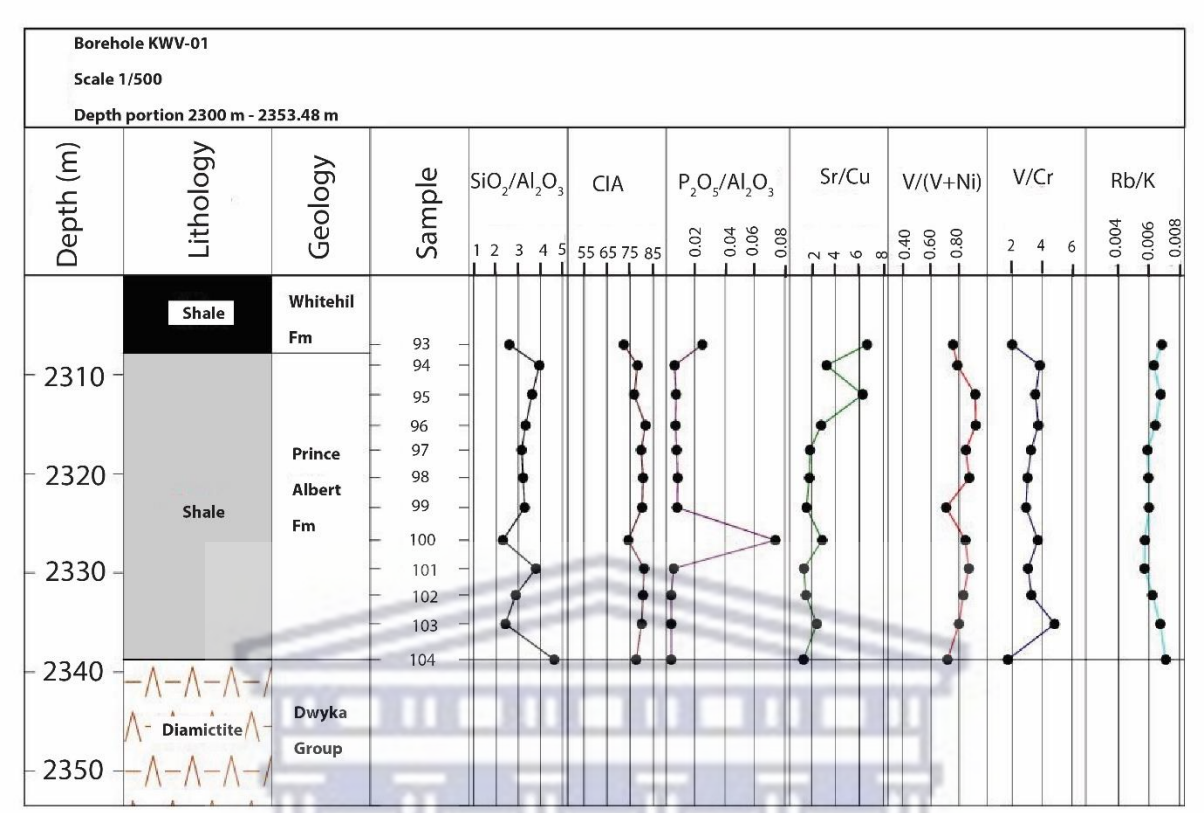

Figure 4.75. Borehole KWV-01 profiles of SiO_2/Al_2O_3, CIA, P_2O_5/Al_2O_3, Sr/Cu, V/(V+Ni), V/Cr and Rb/K.

4.2.1.9 Borehole SA 1/66

In the upper Dwyka Group of borehole SA 1/66, sample 139 has the highest SiO_2/Al_2O_3 ratio of 4.57 (Table 4.9; Fig. 4.76), indicating a high quartz content (Scheffler et al., 2006). This sample also has a high CIA and Sr/Cu ratio (Table 4.9; Fig. 4.76), suggesting that humid conditions prevailed during deposition of the upper Dwyka Group (Scheffler et al., 2006). These climatic led to glacier retreatment, sea-level rise and full marine conditions during deposition of the Prince Albert and Whitehill Formations (Visser, 1993). This is supported by the high Rb/K ratios of the upper Dwyka Group ($5.7*10^{-3}$) and mean for the lower Ecca Group ($5.8*10^{-3}$). In the Prince Albert Formation SiO_2/Al_2O_3 ratios vary between 2.8 and 4.0, suggesting a variable quartz content. Low P_2O_5/Al_2O_3 values, indicate low paleoproductivity, except in sample 135 peaking at 0.08 in the lower Prince Albert Formation (Table 4.9; Fig.

4.76), implying a short period of high paleoproductivity (Chere, 2015). Warm-humid conditions prevailed in the lower Prince Albert Formation with rapidly rising temperatures and a shift from humid to arid conditions, as recorded by a mean CIA value of 77 and a mean Sr/Cu ratio of 2.83 (Appendix 17; Fig. 4.76). In contrast, the upper Prince Albert Formation has a mean CIA value of 59 and a mean Sr/Cu ratio of 10.85, which suggests a hot arid climate (Lerman, 1978). The V/ (V+Ni), V/Cr and Rb/K ratios of the lower Whitehill Formation shale samples (125 and 126; Table 4.9; Fig. 4.76) indicate a deep-water environment and euxinic conditions (Scheffler et al., 2006; Campbell and Williams, 1965).

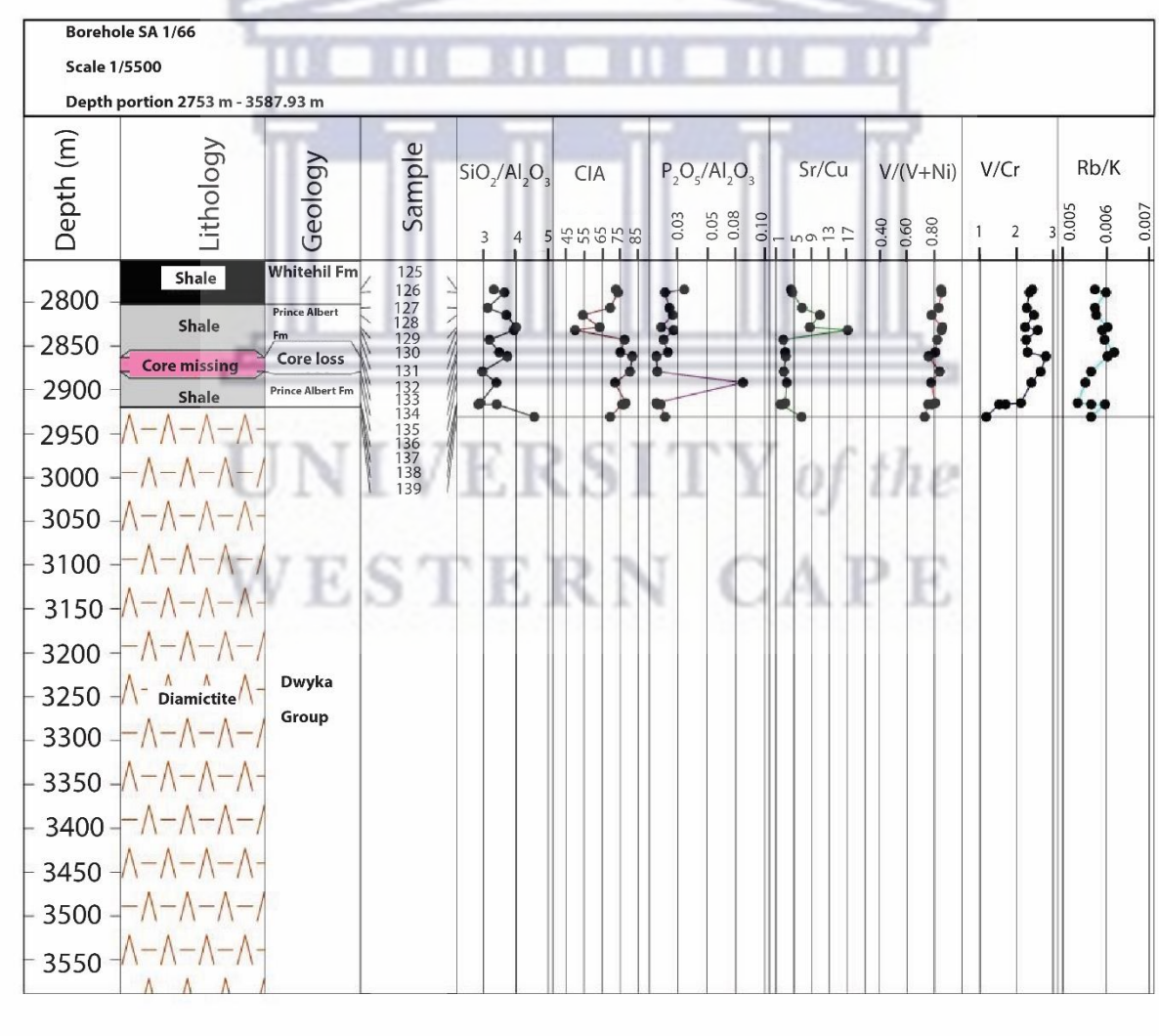

Figure 4.76. Borehole SA 1/66 profiles of SiO_2/Al_2O_3, CIA, P_2O_5/Al_2O_3, Sr/Cu, V/ (V+Ni), V/Cr and Rb/K.

4.2.2 Stable isotopes

Oxygen, carbon and nitrogen isotopes were investigated and the analytical methods are described in Section 3.7. These stable isotopes were analysed using unweathered shale from core from for fresh boreholes KZF-01 and KWV-01. The isotope data, including wt.%C and wt.%N, are given in Table 4.10. Seven samples were retrieved from the Prince Albert Formation and two (HM57 and HM93) from the Whitehill Formation (Table 4.10). Values of $\delta^{18}O$ range from 6.1 to 7.8 ‰, $\delta^{13}C$ between -17.5 and -23.1 ‰ and $\delta^{15}N$ between 8.5 and 11.1 ‰ (Table 4.10). Carbon and nitrogen isotopes were analysed on the darkest powders, i.e. HM57, HM62 and HM93 (Table 4.10). The positive values of $\delta^{18}O$, including the Whitehill Formation (Table 4.10), indicate colder temperatures, possibly associated with ice sheets or glaciers at the time of deposition when the basin was situated near the South Pole at about 289 Ma (Zachos et al., 2001; Schulz et al., 2018).

$\delta^{13}C$ values between -24 to -18 ‰ reflect deeper water deposits with an increase rate of plant burial and the formation of peat, coal and oil (Geel et al.,2015; De Wit, 2016). In Table 4.10, $\delta^{13}C$ values of the Prince Albert Formation agree with typical isotope values of plant wax derived n-alkanes of C_3 plant and heavier $\delta^{13}C$ isotope values indicate contributions from C_3 algae or cyano bacteria (Schouten et al., 2000; Hu et al., 2002; Schwab and Spangenberg, 2007; Adedosu et al., 2014). $\delta^{15}N$ values are important to understand biological processes of plants including marine algae (White, 2013). The nitrogen isotopic composition values are between 8.5 and 11.1 ‰ (Table 4.10) and probably indicate plankton material present in a marine environment (White, 2013).

Table 4.10. Stable isotope data from boreholes KZF-01 and KWV-01.

Borehole	Sample	Depth (m)	$\delta^{18}O$	$\delta^{13}C$	wt.%C	$\delta^{15}N$	wt.%N
KZF-01	HM57	439.61 – 439.95	6.7	-17.5	4.2	10.4	0.35
KZF-01	*HM62	490.39 – 490.91	6.9	-22.1	0.5	8.5	0.19
KZF-01	*HM63	496.30 – 496.84	6.7				
KZF-01	*HM64	500.50 – 500.82	6.5				
KZF-01	*HM78	583.50 – 583.69	6.5				
KWV-01	HM93	2306.96 – 2307.28	6.1	-23.1	7.9	11.1	0.27
KWV-01	*HM94	2309.05 – 2309.37	7.8				
KWV-01	*HM96	2315.08 – 2315.37	7.3				
KWV-01	*HM101	2329.56 – 2329.87	6.7				

*HM - Prince Albert Formation

The d18O values are relative to SMOW (d18O), PDB (d13C) and Air (d15N).

4.3 Petrophysical characterisation

4.3.1 Mercury porosimetry

The methods and calculations are described in Section 3.8.1. Mercury porosimetry measures the largest entry towards a pore, but not the inner size of the pore (Giesche, 2006). Shale samples from boreholes KZF-01, KWV-01 and SA 1/66 were investigated.

In borehole KZF-01, the Prince Albert Formation shale sample HM81 from a depth of 600.48 m (Table 3.1), yielded the highest porosity of 3.345% (Table 4.11). This sample also has the highest permeability (2.79 mD), but the relatively low permeability values in most of borehole KZF-01 (0.13 – 2.79 mD; Table 4.11), suggest compaction and cementation of the shale with minor pore interconnectivity (Cao et al., 2015). Porosity measurements in borehole KWV-01 are lower than those in borehole KZF-01, ranging between 0.078% (HM100) and 0.154% (HM95) for depths between 2311.98 m and 2327 m (Tables 3.1 and 4.11). These volumes are too low to allow for the identification of permeability parameters and the further calculation of permeability. Although the two samples, HM125 and HM126, from borehole SA 1/66, yielded higher, but variable porosities, i.e. 1.9% and 5.6% respectively, the measured permeabilities are very low, being 0.000066 and 0.000138 mD respectively (Table 4.11).

Rowsell and De Swardt (1976) found that in deep borehole cores from the main Karoo Basin, the porosity of shales decreases rapidly with burial and subsequent depletion of interstitial pore water. Hence, porosity measurements of the Prince Albert Formation in borehole KWV-01 are lower than in borehole KZF-01 due to deeper burial and the presence of a 19 m-thick dolerite sill 12 m above the Prince Albert Formation (Fig. 4.77). Porosity measurements of KWV-01 (Table 4.11) decrease with increasing distance from the dolerite sill. This is because

contact metamorphism of shale adjacent to the dolerite increases the porosity by potential fracturing associated with the emplacement of the dolerite sill (Chevallier et al., 2001).

In boreholes KZF-01 and KWV-01, bulk densities, which includes the pore space within the shale, range between 2.185 and 2.400 g/mL, whereas the skeletal densities, which excludes the pore space, range between 2.227 and 2.402 g/mL (Table 4.11). Bulk density measurements for borehole SA 1/66 range between 2.521 and 2.686 g/mL, but no skeletal density measurements were recorded. In addition, the higher porosity shales of borehole KZF-01 display lower bulk densities compared to the low porosity shales of borehole KWV-01 (Table 4.11). The average pore diameters of borehole KZF-01 (0.021 to 0.332 µm) are also lower than those of borehole KWV-01 (0.56 to 2.809 µm.

Table 4.11. Porosity, permeability, bulk density, skeletal density, median pore diameter and average pore diameter of samples of the Prince Albert Formation from boreholes KZF-01, KWV-01 and SA 1/66.

Borehole	Sample number	Median pore diameter (µm) using volume	Median pore diameter (µm) using area	Average pore diameter (µm)	Bulk density (g/mL)	Skeletal density (g/mL)	Porosity (%)	Permeability (micro-Darcy)
KZF-01	HM58	0.291	0.004	0.021	2.325	2.332	0.270	<0.05
	HM60	229.913	0.007	0.332	2.256	2.291	3.131	0.396
	HM66	283.146	0.007	0.143	2.205	2.236	3.05	1.159
	HM70	209.419	0.005	0.056	2.199	2.227	2.447	0.438
	HM81	149.785	0.004	0.052	2.185	2.228	3.345	2.791
	HM89	160.999	0.015	0.168	2.267	2.280	1.014	0.126
KWV-01	HM95	12.907	0.363	2.378	2.298	2.301	0.154	*SNB
	HM97	7.022	0.948	2.809	2.308	2.311	0.134	*SNB
	HM98	1.833	0.178	0.560	2.321	2.324	0.120	*SNB
	HM100	8.108	0.556	1.912	2.400	2.402	0.078	*SNB
SA 1/66	HM125	-	-	-	2.686	-	1.9	0.000066
	HM126	-	-	-	2.521	-	5.6	0.000138

*SNB: Samples HM95, HM97, HM98 and HM100 have insufficient porosity (pore volume and pore size distribution).

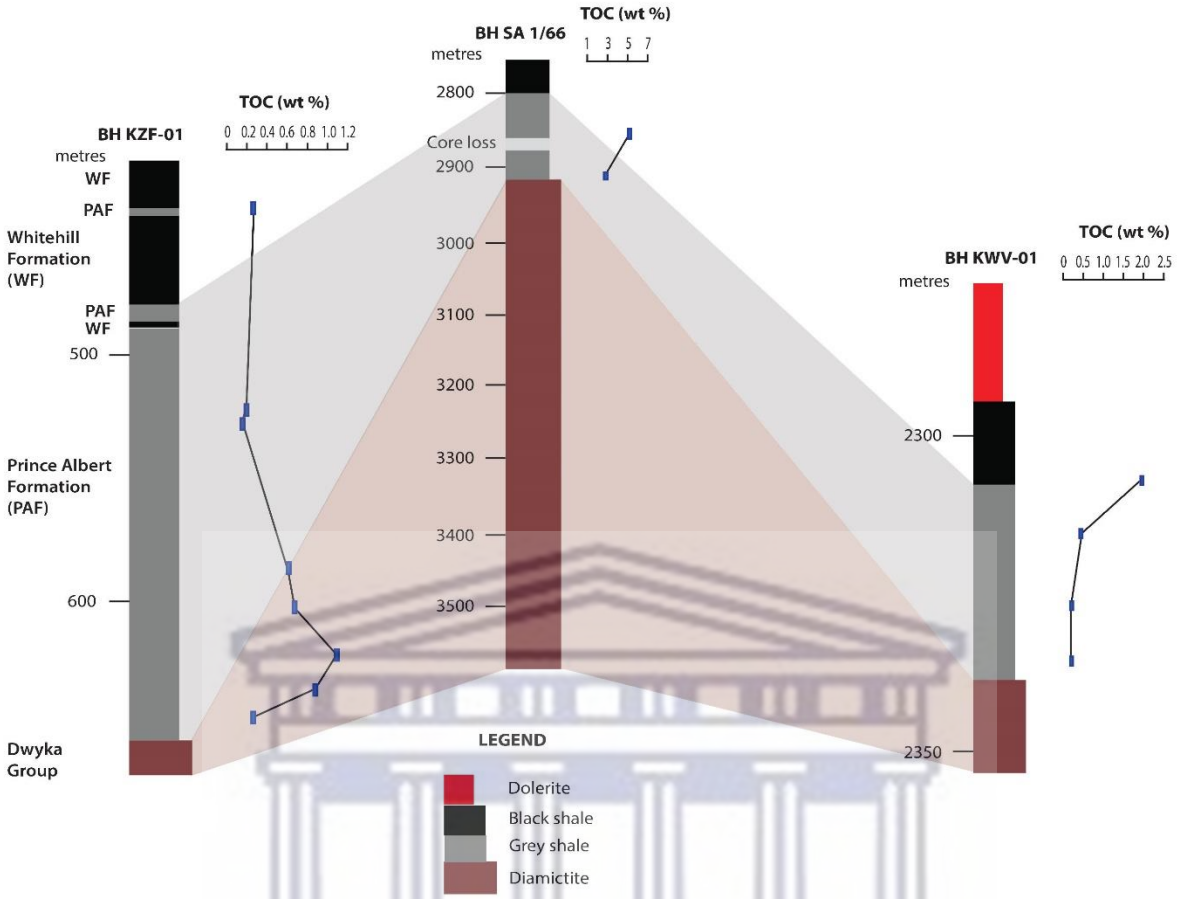

Figure 4.77. Lithological logs of boreholes KZF-01, SA 1/66 and KWV-01 showing the total organic carbon (TOC) content of the Prince Albert Formation.

4.4 Shale gas potential

4.4.1 Rock-Eval and TOC

The type of hydrocarbon generation potential was assessed using a plot of S_2 values against TOC measurements (Prezbindowski, 2010) and the type of kerogen was determined from a plot of hydrogen index (HI) against oxygen index (OI) (Prezbindowski, 2010). The results are listed in Table 4.12 and displayed in Figure 4.78, which indicates that the kerogen is type IV and only has a potential to generate inert gases. The production of inert gases depends on overburden thickness, tectonic processes such as uplift, fractures and faults, which cause the migration and accumulation of these inert gases (Nazeer et al., 2018).

However, $\delta^{13}C$ and $\delta^{15}N$ isotope results (Section 4.2.2) showed evidence of terrestrial algae organic matter input, which is a signature of Type III kerogen. It was observed that TOC values for majority of the samples were very low (Table 4.12) indicating lean organic matter. It has been reported in previous studies (Hunt et al., 2002; Peters et al., 2005; Adedosu et al., 2015), that Rock-Eval pyrolysis data becomes unreliable in organic lean source rock and this might be responsible for the extremely low HI and erratic Tmax values. From the available data, the organic matter could be classified as Type III and IV kerogen.

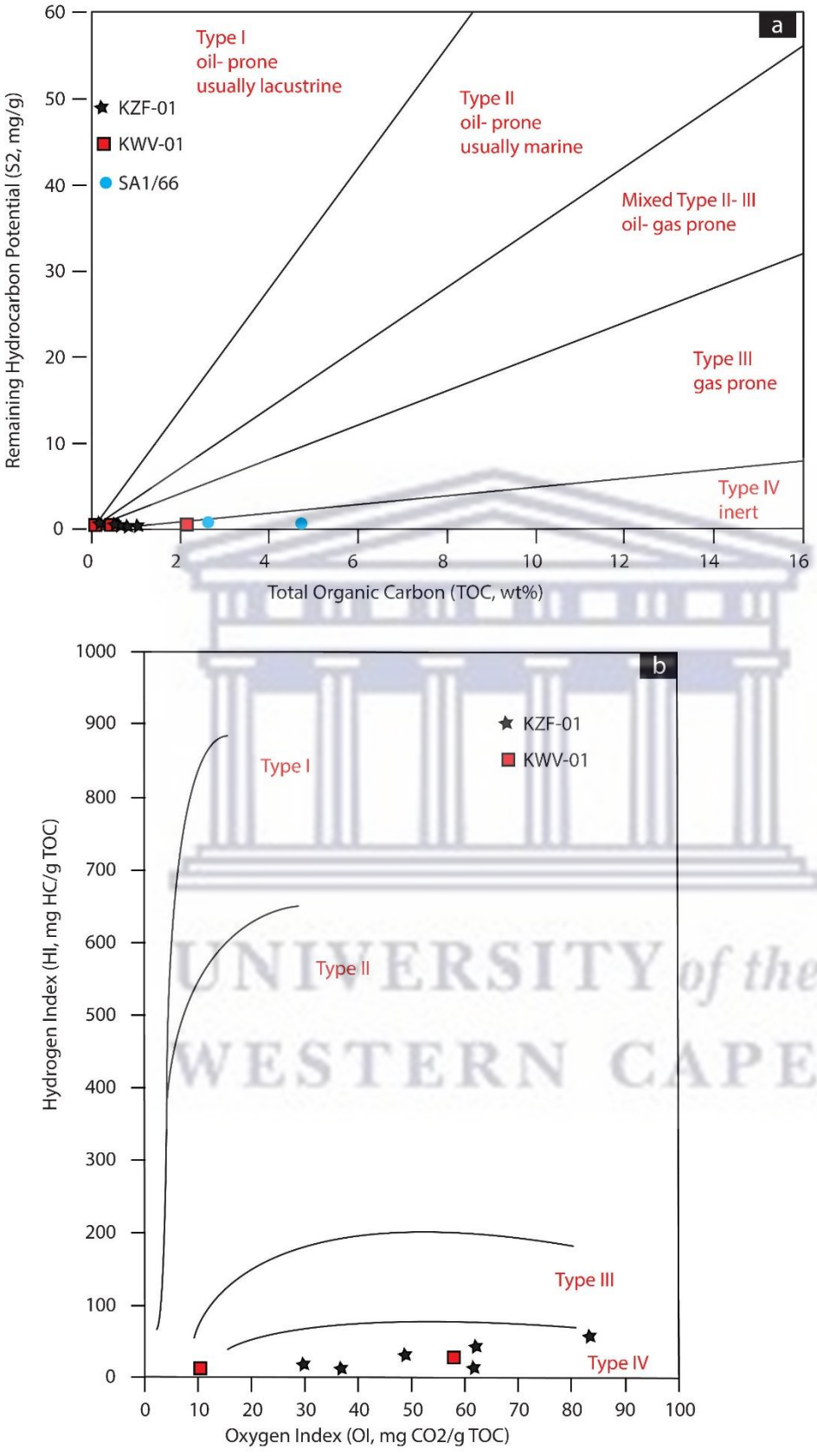

.

Figure 4.78. (a) Kerogen potential plot and (b) HI versus OI plots on the modified Van Krevelen diagram (Dembicki, 2009) of samples indicating the kerogen type.

In borehole KZF-01, TOC ranges between 0.18 and 1.12 wt%, in KWV-01 between 0.2 and 2.27 wt% and in SA 1/66 between 2.76 and 4.87 wt% (Table 4.12). Some of these values exceed the minimum qualifying value of 2 wt% for economically-viable shale gas resources, as defined by Kuuskraa et al. (2011). However, for organic matter to generate hydrocarbons, the carbon has to be associated with hydrogen, normally with a hydrogen index exceeding 150 mg/g (Dembicki, 2009). None of the samples exceed this value (Table 4.12). Tmax values range between 298°C and 453°C (Table 4.12). Twelve of these samples are less than 435°C, which indicates immaturity and the remaining two are between 435°C and 470°C reflecting maturity (Peters and Cassa, 1994). These results are in disagreement with the above findings concerning maturity and are probably dubious values mainly because of very weak S_2 peaks in overmature samples (Dellisanti et al., 2010).

Table 4.12. Results of Rock-Eval analysis and vitrinite reflectance of borehole samples.

Sample and borehole	S_1 - (mg/g)	S_2 - (mg/g)	S_3 - (mg/g)	S_4 (mg/g)	Tmax (°C)	TOC (wt %)	HI	OI	Vitrinite Reflectance (%)
KZF-01									
HM57	-	-	-	-	-	-	-	-	3.58
HM58	0.08	0.14	0.74	2.61	304	0.28	50	264.30	4.32
HM68	0.04	0.09	0.13	1.99	310	0.21	42.90	61.90	-
HM69	0.07	0.11	0.15	1.65	302	0.18	61.10	83.30	4.53
HM79	0.07	0.08	0.23	6.18	304	0.63	12.70	36.50	4.57
HM82	0.14	0.24	0.34	6.68	453	0.70	34.30	48.60	4.25
HM85	0.18	0.19	0.69	10.90	299	1.12	17	61.60	4.61
HM88	0.15	0.17	0.27	8.74	436	0.90	18.90	30	4.48
HM90	0.07	0.11	0.36	2.55	298	0.27	40.70	133.30	4.32
KWV-01									
HM94	0.27	0.28	0.23	22.25	301	2.27	12.30	10.10	3.97
HM96	0.09	0.15	0.30	5.00	302	0.52	26.80	57.70	5.10
HM99	0.10	0.13	0.38	1.81	307	0.20	65	190	4.69
HM101	0.08	0.12	0.37	1.84	303	0.20	60	185	4.91
SA 1/66									
HM125	0.12	0.09	-	48.53	305	4.87	1.90	-	-
HM126	0.12	0.72	-	26.91	320	2.76	26.10	-	-

4.4.2 Vitrinite reflectance

The vitrinite reflectance values of outcropping shale samples of the Prince Albert Formation in the Tankwa and Prince Albert areas are all less than 3% (Fig. 4.79), possibly in the dry gas window (Fig. 4.80; Tissot and Welte, 1984). This contrasts with core samples from boreholes KZF-01 and KWV-01, where the reflectance values are between 3.6 and 5.1% (Table 4.12; Fig. 4.79), which lies within the epimetamorphic zone (Fig. 4.80; Tissot and Welte, 1984). However, the low reflectance values of outcrop samples are probably a result of alteration by surficial weathering and erosion. Reflectance values >3.5% should be not always be considered as areas having a high thermal maturity, since the Marcellus and Utica shales in the U.S.A both produce gas with higher reflectance values (Popova, 2017a, 2017b). Geel et al. (2015) reported reflectance values of between 3.08 and 4.90% and Baiyegunhi et al. (2018) values of between 3.12 and 3.84% for borehole samples of the Prince Albert Formation in the southeastern part of the main Karoo Basin.

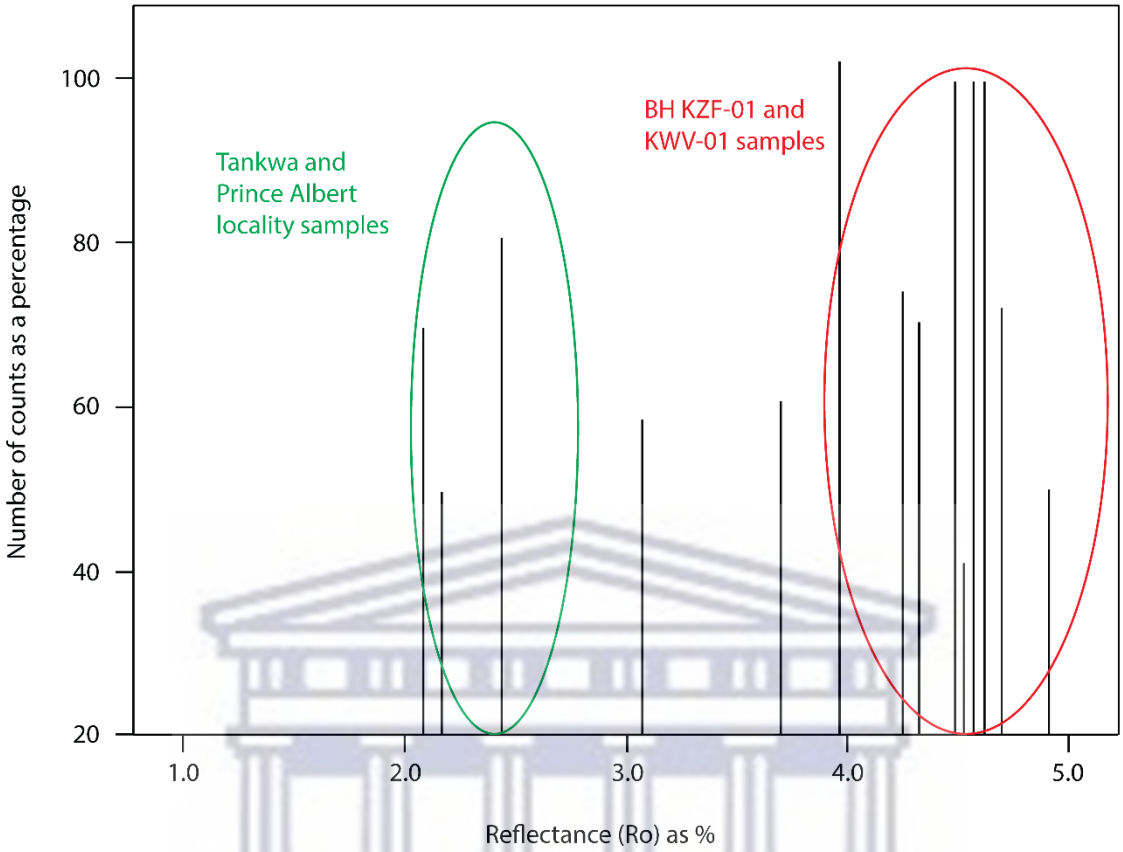

Figure 4.79. Histogram of vitrinite reflectance data of Prince Albert shales from boreholes KZF-01 and KWV-01 and outcrops in the Tankwa and Prince Albert areas.

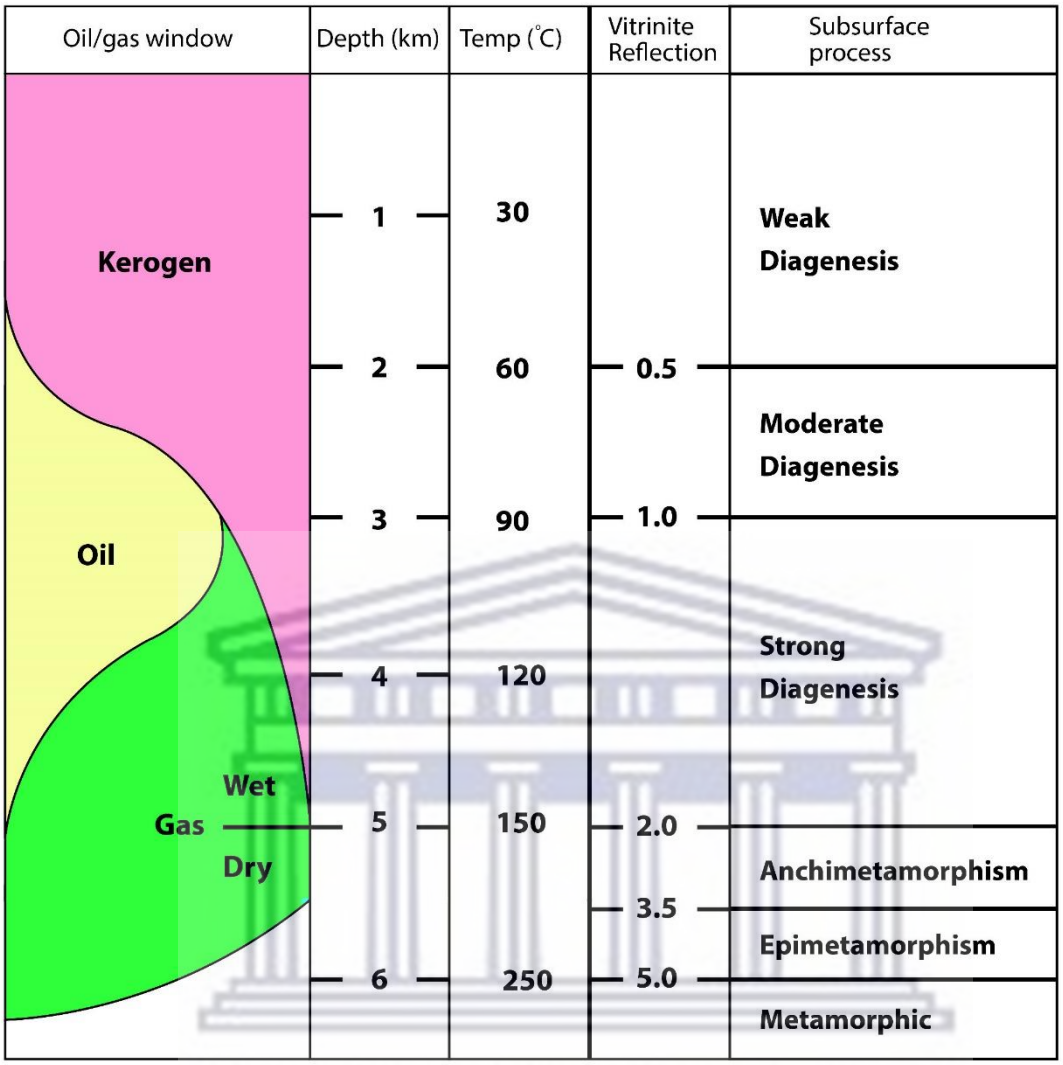

Figure 4.80. Hydrocarbon generation and vitrinite reflectance indices plotted against depth of burial (Tissot and Welte, 1984).

4.4.3 Residual gas

Residual gas is gas that remains trapped in the mudstone, normally within the smaller pores. Measurement techniques are described in Section 3.9.3. It was found that the residual gas content of all the samples was too low to measure, resulting in zero yield (Table 4.13).

Free gas was not measured, since it had to be monitored on the drill site while drilling was taking place. Zero amounts of residual gas volumes suggest that if shale gas was generated in the Prince Albert Formation, it was not preserved in boreholes KZF-01 and KWV-01 possibly due to tectonic thrusting in KZF-01 or thermal degassing related to intrusion of the dolerite sill some 12 m above the Prince Albert Formation in KWV-01.

Table 4.13. Residual gas content of borehole and outcrop samples.

Sample number	Origin	Depths (m)	Sample mass crushed (g)	Residual Gas content (m^3/t)
RS1	BH KZF-01	441.54 – 441.84	1215.2	0
RS2	BH KZF-01	484.10 – 484.66	1531.4	0
RS3	BH KZF-01	507.50 – 507.84	1242.6	0
RS4	BH KZF-01	554.78 – 555.27	1381.0	0
RS5	BH KZF-01	563.57 – 563.94	1549.8	0
RS6	BH KZF-01	643.43 – 643.87	974.4	0
RS7	BH KWV-01	2321.95 – 2322.42	986.8	0
RS8	Tankwa outcrop	25	830.8	0

BH = borehole. Borehole depths are from surface, outcrop depths are the vertical distance from the Prince Albert Formation/Dwyka Group boundary for sample RS8.

Chapter 5

Discussion

The main aim of this thesis was to assess the shale gas potential of the Prince Albert Formation, its petrophysical properties as a potential gas reservoir, rock classification, characterisation of its depositional environment and correlating the Dwyka Group, Prince Albert Formation and Whitehill Formation with equivalent Gondwanaland units.

Rock classification

Rock types of the Prince Albert Formation were classified based on field and core samples, geochemical data and multivariate statistical analysis. The Prince Albert Formation consists of shale, ferruginous shale, rhythmite and silty shale based on field descriptions, borehole core and samples collected. Rock samples were geochemically classified based on geochemical data which reflected Fe-shale, shale, wacke, Fe-sand and litharenite samples (Fig. 4.63).

Elemental ratios taken from geochemical data, was further classified in the form of a ternary diagram (see Fig. 4.64). Elemental ratios concluded that samples (HM1- HM139) were predominantly composed of SiO_2 with subordinate amounts of Al_2O_3, K_2O, Fe_2O_3 and CaO. It was interpreted that elemental ratios of SiO_2 and Al_2O_3 separates quartz-rich silty shales, rhythmite and diamictite from clay- rich shales. Samples comprising of the elemental ratio CaO (Fig. 4.64), was interpreted as consisting of ten calcareous shales with one dolomite sample (HM56) having a high CaO concentration of 90%. Majority of the samples were SiO_2 - rich, whereas samples from Laingsburg, Prince Albert, Tankwa, Debruinspoort and Pluto's

Vale outcrop samples, as well as borehole KZF-01 and SA 1 /66 samples of the Prince Albert Formation, plot within the CaO field (Fig. 4.64).

Additionally, geochemical data was evaluated by multivariate statistics, in the form of factor, cluster and discriminant analysis to identify important element associations and their relationship to various rock types. With factor analysis, eight rock types were identified as shale, diamictite, dolomite, phosphatic shale, ferruginous and manganiferous shale, rhythmite, silty shale and shale interbedded with tuff. These rock types corroborate with field samples (see Section 4.1.1) of the Dwyka Group (diamictite), Prince Albert Formation (shale, silty shale, ferruginous and manganiferous shale, rhythmite and shale interbedded with tuff) and Whitehill Formation (dolomite and shale).

Cluster analysis identified three geochemical groups with distinct element associations (see the dendogram, Fig. 4.67). Linear discriminant function analysis followed which was used to characterise and classify geochemically the three groups. The combination of the two methods resulted in fifty-one samples classified as diamictite (Group 1), seventy-eight samples as shale (Group 2) and nine samples as dolomite, phosphatic, ferruginous or manganiferous shale (Group 3, Table 4.7). Location of each sample was compared to each group which resulted in Group 1 comprising mainly of samples from Laingsburg, Ecca Pass, Prince Albert, Tankwa and Debruinspoort while Group 2 consisted mainly of samples from boreholes KZF-01, KWV-01 and SA 1/66. Group 3 had mixed samples from borehole KZF-01, Prince Albert and Tankwa (Fig. 4.67). Samples were then compared to the stratigraphy, which lead to Groups 1 and 2 being dominated by samples of the Dwyka Group, Prince Albert Formation and Whitehill Formation while Group 3 with samples of the Prince Albert and Whitehill formations. These localities and stratigraphic units identified by the combination of

cluster and linear discriminant analysis corroborate with samples in the ternary diagram classification scheme (Fig. 4.64) in Section 4.1.2 as well as with field observations and samples taken in Section 4.1.1.

In summary, multivariate statistical analysis enhances conventional rock classification methods as a quick and effective technique best used for large datasets. However, it should be taken into account the fact that the technique cannot be used blindly as major and trace elements were carefully selected as they were the criteria of discrimination.

Depositional environment

Lithology, geochemical proxies, stable isotope data and TOC were used to reconstruct the depositional environment and climate conditions during the time of deposition of the Prince Albert Formation.

In the southwestern part of the main Karoo Basin, grey shales of the Prince Albert Formation extend from surface outcrops (Tankwa) to shallow depths of almost 500 m in borehole KZF-01. Tectonic movement is evident by the presence of quartz and calcite veins found in three brecciated/faulted zones of the Prince Albert Formation related to close proximity of the Cape Fold Belt and this has resulted in thrusting and duplication in borehole KZF-01.

In the central southern Karoo Basin, the Prince Albert Formation outcrops at surface (Laingsburg and Prince Albert) and was intersected at a depth of 2789.1 m in borehole SA 1/66 (Fig. 4.51). In the southeastern parts of the basin, surface outcrops of the Prince Albert Formation were sampled near Grahamstown at Debruinspoort, Ecca Pass and Pluto's Vale, whereas deeply buried shale intruded by dolerite, was sampled in borehole KWV-01 near Willowvale (Fig. 3.1). Surface outcrops (Tankwa, Laingsburg, Prince Albert, Debruinspoort,

Ecca Pass and Pluto's Vale) consisted of weathered shale, mudstone and interbedded ferruginous beds, which were tectonically affected by the Cape Orogeny, and, more recently, by weathering. The shales and mudstones represent suspension-settling of mud in a relatively quiet water body, largely unaffected by traction currents and waves (Pettijohn, 1975). Ferruginous beds are mixed sediment produced by co-sedimentation of fine argillaceous sediment and iron bearing minerals (Pettijohn, 1975). The presence of shale, rhythmite units and calcareous concretions in boreholes KZF-01 and KWV-01 supports the basin plain to continental shelf depositional model of Kingsley (1981), Wickens (1984) and Visser (1994). Sands generally occur on the inner shelf and shoreline (Clifton et al., 1971), muds occur on the middle and outer shelf, and heterolithic facies are found either between areas of sand and mud or on the outer shelf (Reading, 1978). Shales dominate on the middle shelf and parts of the outer shelf in relatively quiet waters, with sediment thicknesses ranging between 10 and 40 cm.

The presence of pyrite crystals in boreholes KZF-01 and KWV-01 reflect reducing conditions. The occurrence of algal mat features (borehole KZF-01, Fig. 4.61 (d)), Rb/K ratios and $\delta\ ^{13}C$ stable isotope values infer a prevalence of marine conditions. Rb/K ratios range between $4*10^{-3}$ to $2*10^{-2}$ indicative of a marine environment (Scheffler et al., 2006), while $\delta\ ^{13}C$ values between -26 and -35 ‰ indicate the presence of marine plankton (Schoell, 1984). $\delta^{13}C$ isotope value is characteristics of plant wax derived *n*-alkanes of C_3 plant and heavier $\delta^{13}C$ isotope values observed indicate contributions from C_3 algae or cyano bacteria (Schouten et al., 2000; Hu et al., 2002; Schwab and Spangenberg, 2007; Adedosu et al., 2014). All available evidences support Type III/IV.

Low TOC values (Table 4.12), with very low HI (Hydrogen Index) and high OI (Oxygen Index) ratios of the Prince Albert Formation (Fig. 4.78 (b)) suggests it cannot generate any hydrocarbons, and this is referred to as “dead carbon” (Tissot and Welte, 1984; de Kock et al.,2017). “Dead carbon” could also be referred to as “inertinite” or inert as shale samples were non-reactive (Fig. 4.78). According to Tissot and Welte (1984) and Dembicki (2009), inert samples from Table 4.12 could be from various sources such as recycled/reworked source material, oxidized organic material, inert material from subaerial weathering or biological oxidation in swamps and soils. Thus TOC and HI/OI ratios are not good parameters for determining source material and depositional environment.

Based on various geochemical ratios and palaeoenvironment indicators such as CIA (chemical index of alteration) and Sr/Cu, it was concluded that the Prince Albert Formation was deposited under warm-humid conditions in a marine environment and that a moderate to intense degree of chemical weathering took place during deposition. These results are consistent with that of Scheffler et al. (2006) and Geel et al. (2015). V/(V+Ni) and V/Cr values of the Prince Albert Formation range respectively between 0.33 and 0.95 and 0.62 and 4.83, supporting the concept that the Prince Albert Formation was deposited under dysoxic to euxinic conditions.

Rock types and depositional environments are considered essential factors in determining hydrocarbon reserves of the Prince Albert Formation. The thickness and depth of the formation is important to understand the maturity of the sedimentary rock and the thickness of dolerite intrusions (i.e. in borehole KWV-01). The depositional environment links directly to the TOC of the formation. The high TOC of the Prince Albert Formation (4.87 wt % in borehole SA 1/66) was deposited under dysoxic/ euxinic bottom water conditions to allow for

the preservation of organic matter. The position of the study areas, shallow depths and dolerite intrusions have affcted the ability of the shale of the Prince Albert Formation to retain shale gas.

Shale gas potential

Results of this thesis indicate that samples located outside the "sweet spots" for shale gas in the southern part of the main Karoo Basin (Fig. 3.1) are overmature with low S_2 and hydrogen index values and thus indicate no potential for shale gas (Fig. 4.78). In borehole KZF-01, which is located close to the Cape Fold Belt, tectonism may have resulted in the destruction of porosity and permeability within shales of the Prince Albert Formation affecting the storage and migration properties of the shale. Borehole KWV-01 is located in the region of the Karoo Basin, where dolerite intrusions are prevalent within the Karoo Supergroup, including the Prince Albert Formation (Duncan and Marsh, 2006). Dolerite sills (19 m- and 149 m- thick respectively) occur some 13 m and 122 m above the Prince Albert Formation in borehole KWV-01 and have reduced the shale gas potential as a result of contact metamorphism. In KWV-01 the top of the Prince Albert Formation lies at a depth of 2307.81 m and at least another 5000 m of overburden comprising the Beaufort, Stormberg and Drakensberg Groups was probably present before erosion took place (Fig. 5.1 section D, Johnson et al., 2006; Fig. 5.2, Duncan and Marsh, 2006). This would place the Prince Albert Formation in the metamorphic zone with no potential for generating dry gas, together (Fig. 4.80), with the destruction of temporarily-generated hydrocarbon (Rowsell and De Swardt, 1976).

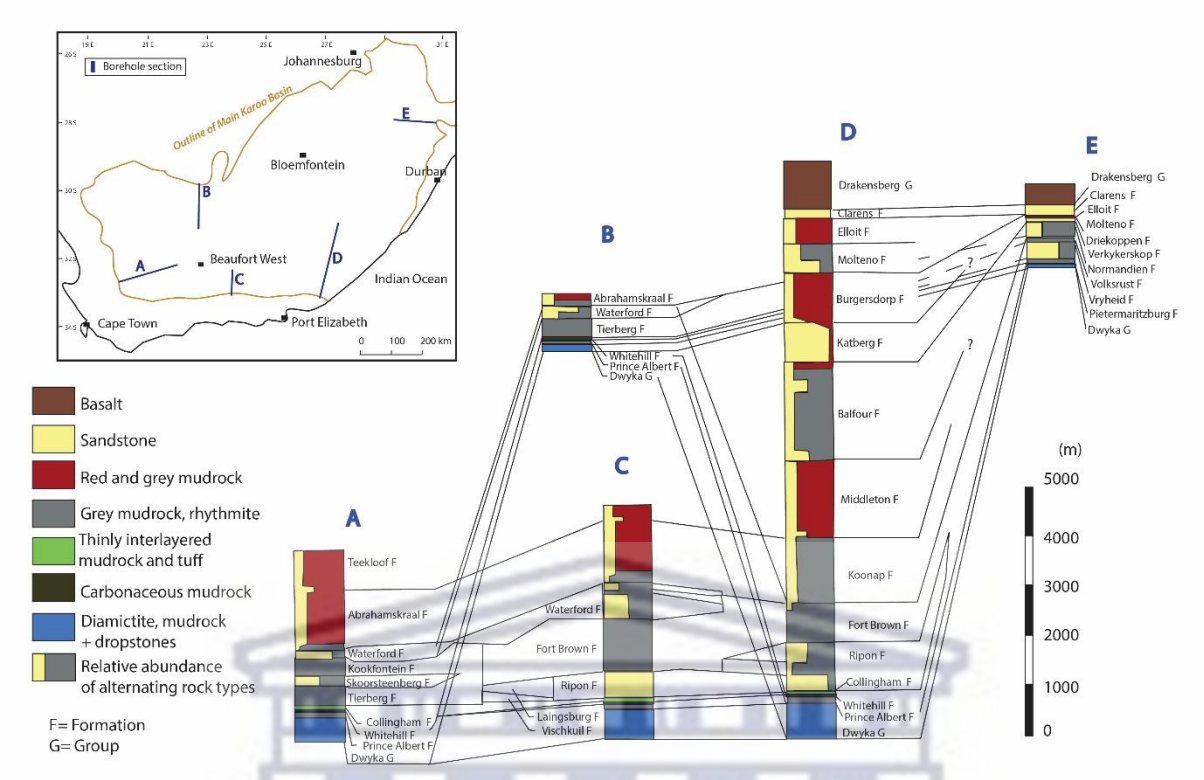

Figure 5.1. Generalised stratigraphy and lithology of the Karoo Supergroup in the main Karoo Basin (modified after Johnson et al., 2006).

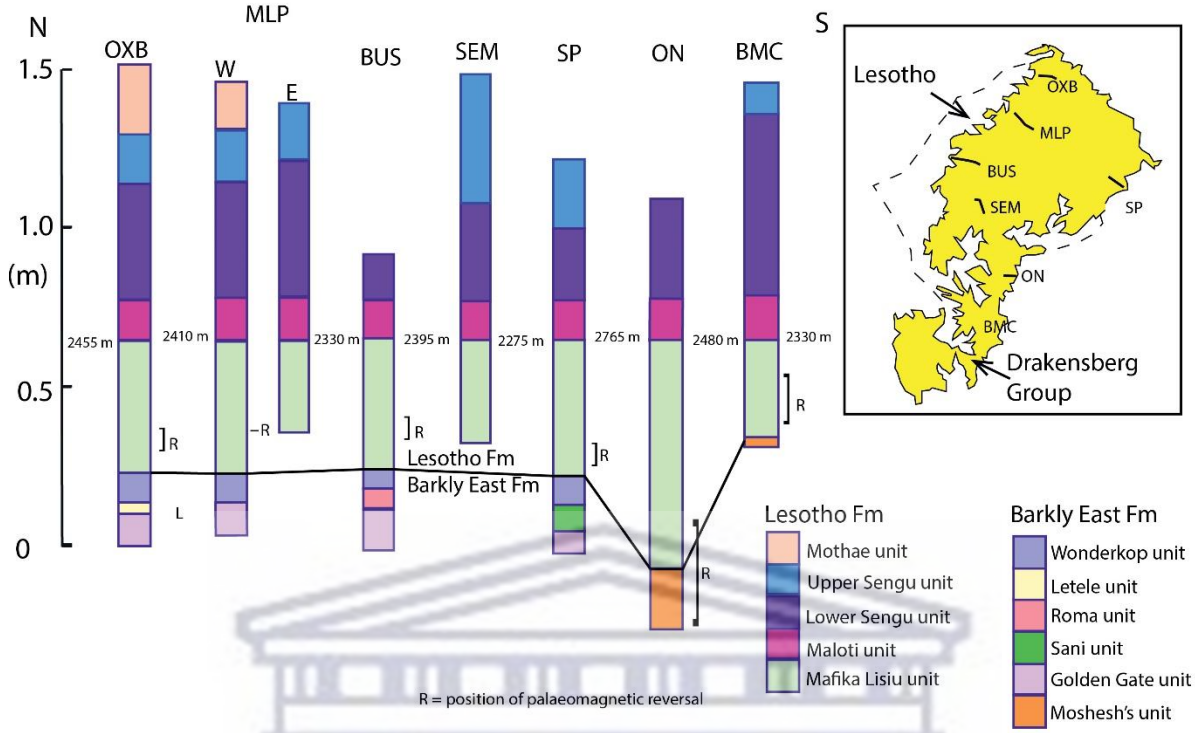

Figure 5.2. Summary of the stratigraphic subdivisions in sections in and around Lesotho based on geochemical composition, showing the elevations for the base of the early Jurassic Maloti unit. Abbreviations for section names on the map are: **OXB**- Oxbow, **MLP**- Mafika Lisiu Pass, **BUS**- Bushman's Pass, **SEM**- Semonkong, **SP**- Sani Pass, **ON**- Ongeluksnek, **BMC**- Ben Macdhui (after Duncan and Marsh, 2006).

This is supported by vitrinite reflectance values between 3.97 and 5.10%, which fall within the epimetamorphic and metamorphic zones (Fig. 4.80). Fresh unweathered core was required for TOC and Rock-Eval measurements, therefore no surface outcrop was used. TOC values are relatively low in boreholes KZF-01 and KWV-01, but in borehole SA 1/66, the TOC and porosity values are comparable with those of the gas-producing Marcellus and Barnett shales in the United States (Table 5.1; Bruner and Smosna, 2011). However, the results of Rock-Eval pyrolysis indicate a low hydrogen index and a Type III and IV kerogen (Fig. 4.78). The low hydrogen index implies that much of the organic matter is not bound to hydrogen and that much of the organic carbon is classified as "dead carbon" (de Kock et al., 2017). The poor

hydrocarbon generation potential is also shown by the low value of S_1 and S_2 combined, which do not exceed 0.84 mg/g (Table 4.12), and fall within the poor quality range of Dembicki (2009).

Table 5.1. Shale-gas potential parameters of the Prince Albert Formation and the gas-producing Barnett and Marcellus shales in the USA.

	Prince Albert Formation, main Karoo Basin S.A (this thesis)			**USA (Bruner and Smosna, 2011)**	
Parameters	**KZF-01**	**KWV-01**	**SA 1/66**	**Barnett (Fort Worth Basin)**	**Marcellus (Appalachian Basin)**
TOC (wt %)	0.53	0.79	3.81	2 – 6	1 – 10
Kerogen type	Type III and IV	Type III and IV	Type III and IV	Type II	Type II and/or Type III
Vitrinite reflectance (%)	4.33	4.67	–	1 – 2%	1 – 4%
Tmax (°C)	338	303	313	465	475
Shale porosity (%)	2.01	0.12	3.75	1 – 6	1 – 6

Variable porosity values ranging between 0.078 and 5.6% (Table 4.11) suggest that the storage capacity for gas might exist in the "sweet spot" areas. The highest porosity of 5.6% in the Prince Albert Formation was found in sample HM 126 of borehole SA 1/66. However, permeability values are quite low ranging from $6.6*10^{-5}$ to 2.791 mD in boreholes KZF-01 and

SA 1/66 (Table 4.11), thus preventing migration of potential hydrocarbons (Baiyegunhi et al., 2018).

Shale gas shows

During drilling of recent boreholes KZF-01 and KWV-01, shale gas was not encountered on site in the form of blow-outs or gas kicks. Once fresh core was retrieved from these two boreholes, the Prince Albert Formation had no gas shows (free or absorbed). However, during this research, residual gas measurements on shale samples of the Prince Albert Formation were completed, but no residual gas was detected. This suggests that either no gas was generated or if generated, it was not preserved in KZF-01 and KWV-01 due to tectonic deformation (thrusting) in KZF-01 forming pathways for gas to escape or thermal degassing due to dolerite intrusions in KWV-01. The low content of clay minerals and high content of brittle minerals, such as quartz and plagioclase, makes shales of the Prince Albert Formation more brittle. High SiO_2/Al_2O_3 ratios in the Prince Albert Formation and mineralogical data indicate the dominance of quartz-rich shale (Figs. 4.68 to 4.76). These minerals create natural fractures allowing gas to escape by migrating horizontally, or possibly being trapped higher up in the stratigraphic sequence, e.g. 8.8 million cubic feet of gas escaped from fractured shale of the Fort Brown Formation in borehole CR 1/68 in one week during November 1968 from a depth of 2532 m (Rowsell and De Swardt, 1976). The brittleness of the Prince Albert Formation (based on brittle minerals present i.e. high quartz, calcite and dolomite) also suggests that it could be stimulated by hydraulic fracturing if exploration takes place.

Correlation of Southern Gondwanaland units equivalent to the Dwyka Group, Prince Albert and Whitehill formations in South Africa

Glacial diamictite of the Fitzroy Tillite Formation has been correlated with the Dwyka Group of South Africa. This is based on the trace fossil *Umfolozia* found both within South Africa and the Falkland Islands, and its westerly-directed glacial striations and Sakmarian age. The Dwyka Group in the Aranos Basin has been linked to the Dwyka Group in the main Karoo Basin and the Sauce Grande Formation in the Sauce Grande Basin based on radiometric dates of 302.0±3.0 Ma and Eurydesma remains (Harrington, 1955). The Itararé Group of the Paraná Basin has been temporally related to the Dwyka Group of South Africa although no radiometric dates or fossil linkage has been made. Lithologically the Itararé Group is similar to the Dwyka Group of the main Karoo Basin with the glacial events ranging between 299 and 325 Ma (Isbell et al., 2012). The Carboniferous-Permian Whiteout Conglomerate of the Ellsworth Mountains has lithologically been linked to the Dwyka diamictite and Fitzroy Tillite Formation (Elliot et al., 2016). However, no available age data for the Whiteout Conglomerate is given and a definite linkage cannot be made. Correlatives of the Dwyka Group deposits in the Karoo Basin can be found in southern Namibia, the Itarare' Group of the Paraná Basin, Sauce Grande Formation of the Sauce Grande Basin, the Fitzroy Tillite Formation on the Falkland Islands and in Antarctica the Whiteout Conglomerate. Sedimentation of the Sauce Grande Basin started with glaciogenic deposits by Late Carboniferous which is approximately the same time interval when sedimentation of the Dwyka Group started in the main Karoo Basin. Linkage between the Sauce Grande and Karoo Basin can be seen by the transgressive phase (Piedra Azul and Prince Albert Formations) immediately above the glacial deposits, interbeds of tuff-rich beds in the upper portion and the presence of clast-rich diamictites of the Sauce Grande Formation, Dwyka Group and Fitzroy Tillite Formation.

Prince Albert Formation shale at Ecca Pass in the Eastern Cape, has a thickness of 58 m (Kingsley, 1977) and lacks both coarse debris and any marine fauna. The basal strata of the Prince Albert Formation (main Karoo Basin) have been correlated with the Hells Kitchen Member of the Falkland Islands, with both showing a similar transition from mudrock containing ice-rafted debris less than a meter thick, into rhythmites up to 80 m thick (Visser, 1989). The base of the Prince Albert Formation has been interpreted by Visser (1989) as a marine condensed section and by Veevers et al., (1994) as a stepped rise in sea level. As no age data is available for the Hells Kitchen Member, a chronostratigraphic linkage cannot be made with the Prince Albert Formation of South Africa. In the Paraná Basin, the coal-bearing Rio Bonito Formation and the overlying Palermo Formation are basically age-equivalents of to the Prince Albert Formation in Namibia (Stollhofen, 1999). Facies of the Polarstar Formation are apparently similar to the Prince Albert and Whitehill Formations of the main Karoo Basin, as well as the Port Sussex Formation of the Falkland Islands, being organic-rich, but lacking distinctive pyrite-rich beds. Zircon ages for the Polarstar Formation indicate a maximum depositional age of ~269 Ma (Fig. 5.3). However, tuff beds of the Dwyka Group have been dated at ca. 297 Ma and tuffs of the Prince Albert Formation at ca. 288 – 289 Ma (Fig. 5.3; Bangert et al., 1999). Elliot et al. (2016) suggests that the Polarstar Formation was deposited in a different sub-basin to that of the Karoo and Falkland Islands strata, with no connection between the basins based on regional paleocurrent data and timing of events. In the Western Cape Province of South Africa, Karoo strata were deposited in a marine environment, comparable to the Polarstar Formation, where there was access to the open sea, as well as a developing magmatic arc (Elliot et al., 2016). The proposed Polarstar sub-basin of Elliot et al. (2016) has been supported by paleoflow measurements of the Karoo/Falkland, Permian strata, which suggest that the Ellsworth Mountains were located

some distance from the Falkland Islands to accommodate the source region (Fig. 2.24). In NW Namibia, the Verbrandeberg Formation, as well as the Tsarabis Formation, correlate with the Prince Albert Formation in southern Namibia (Holzförster et al., 2000).

Lithologically, the Black Rock Member in the Falkland Islands could be considered as an equivalent to the Whitehill Formation, based on the pyrite and TOC content, and the white-weathered exposures (Faure and Cole, 1999). The Black Rock Member underwent anoxic conditions related to deep sea levels which have been compared to equivalent conditions for the Whitehill Formation (main Karoo Basin) and Irati Formation (Paraná Basin). López-Gamundi et al. (2013) used tuff dates of 280.8± 1.9 Ma (Artinskian) for the Tunas Formation in the Sauce Grande Basin to correlate with the Irati Formation in the Parana Basin dated at 278± 2.2 Ma (Santos et al., 2006), which seems to favour a correlation with the Whitehill Formation in the main Karoo Basin. Beds equivalent to the uppermost Prince Albert Formation in Namibia have yielded an Artinskian age. In the western part of the main Karoo Basin of South Africa, the Whitehill Formation is similar to that of the Karasburg Basin in southernmost Namibia. In northwestern Namibia, Mesosaurus bones are found in the upper part of the Huab Formation providing evidence of the time-equivalent Whitehill Formation.

The three facies of Western Dronning Maud Land could be linked with the Dwyka Group, Pietermaritzburg and Vryheid Formations of the main Karoo Basin based on the early Permian age and comparable lithofacies. In the Central Transantarctic Mountains, U/Pb SHRIMP ages of 253.5 ± 2.0 Ma and 250.3 ± 2.2 Ma of the Buckley Formation yield Late Permian to Lower Triassic ages and ~270 – 260 Ma age (Guadalupian) for the Mount Glossopteris Formation of the Ohio Range which is younger than the Whitehill Formation of the main Karoo Basin. Hence

the Transantarctic Basin cannot be correlated with the lower Ecca Group of the main Karoo Basin in South Africa.

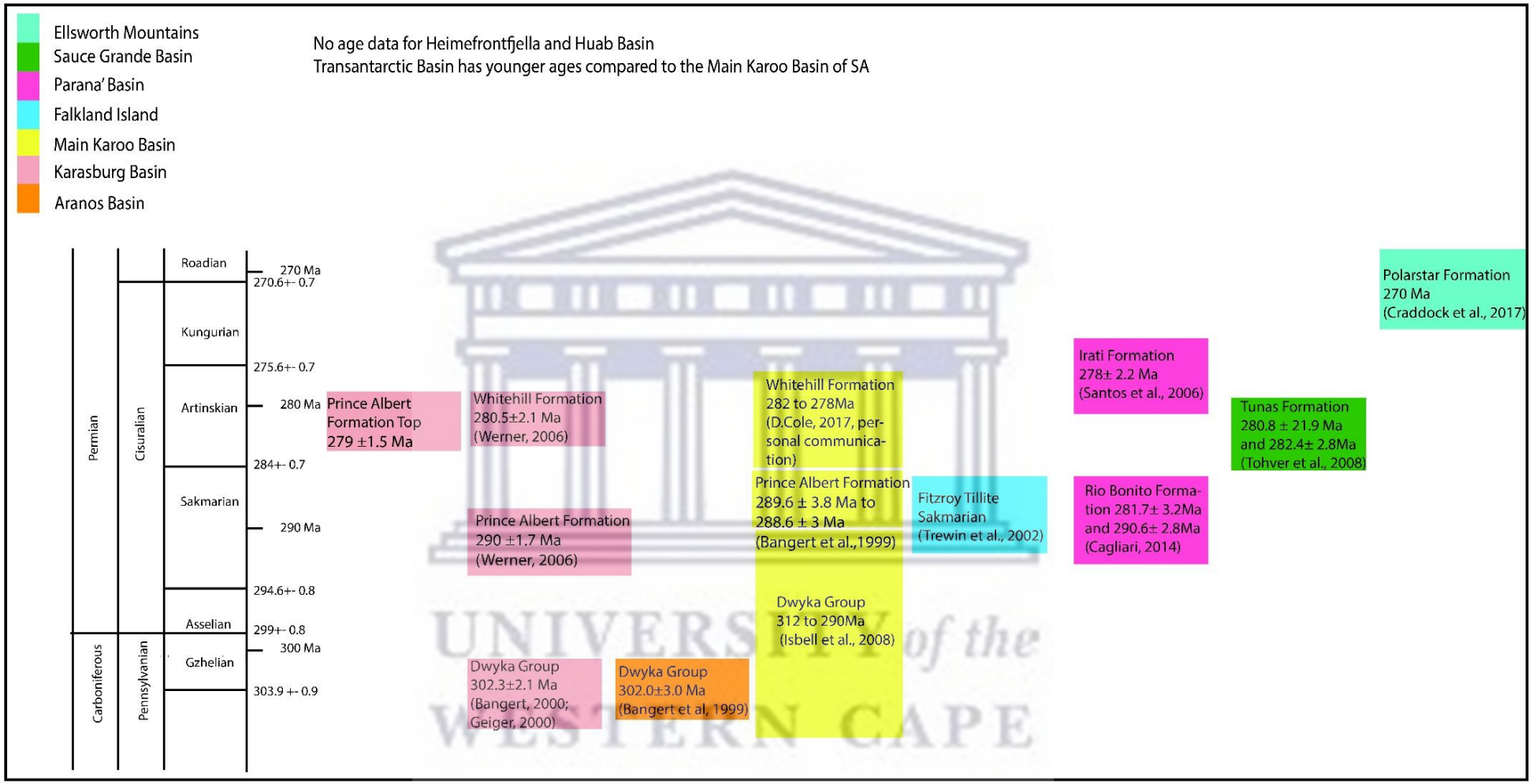

Figure 5.3. Compilation of available radiometric age data for the Dwyka Group, Prince Albert Formation and Whitehill Formation and equivalents in southern Gondwanaland. Chronostratigraphic units after Gradstein et al. (2005).

The following details were noted for the Prince Albert Formation across the south-western, central and south-eastern parts of the main Karoo Basin:

- Rock-Eval pyrolysis is a cost effective means to evaluate hydrocarbon generation/ potential in sedimentary rocks by evaluating its type and maturity of organic matter. However it becomes unreliable in organic lean source rock and this might affect the HI and Tmax values.
- The majority of the fresh cored shale samples of the Prince Albert Formation have a poor generative potential with an average TOC of 0.62 wt% (range 0.18 – 2.27), with the exception of borehole SA 1/66, which has a range of 2.76 to 4.87 wt%.
- Shales of the Prince Albert Formation show variations in thickness, depth, TOC and geochemical composition laterally across the southern sector of the main Karoo Basin.
- Geochemical proxies suggest variable climatic conditions, such as cold arid or warm humid, and there is a lack of agreement between CIA and Sr/Cu ratios and V/(V+NI) and V/Cr ratios, probably due to different geochemical behavior of these elements. Nevertheless, geochemical proxies still provide the bases for provenance and climate.
- Geochemical proxies of this research suggest temperatures were relatively warm during the deposition of the Prince Albert Formation shales.
- Similarity of equivalent stratigraphic successions to the Dwyka Group, Prince Albert and Whitehill formations suggest that the main Karoo Basin were subjected to very similar tectonic influences via stratigraphy and radiometric dating. These successions are proposed to represent deposition within a retroarc foreland basin (Catuneanu, 2004). Johnson (1991), Catuneanu et al. (1998), Johnson et al. (2006) interpreted a foreland basin developed behind a magmatic arc and fold-thrust belt (Cape Fold Belt)

related to Gondwanaland. The foreland basin evolved to a rift system during the Permian as the Pacific Plate subducted beneath western Gondwana (Veevers, 2004).

Chapter 6

Conclusion

Results from analyses undertaken during this research on the hydrocarbon potential of the Prince Albert Formation in the main Karoo Basin, have been assessed in terms of its shale gas potential. It is concluded that between latitudes 31°05'0"S and 33°0'0"S and longitudes 21°E and 26°E within the "sweet spots" of Cole (2014) and Mowzer and Adams (2015), the Prince Albert Formation has the potential for exploitable shale gas. The Prince Albert Formation in the southwestern and southeastern parts of the basin has been excluded as a potential shale-gas producer due to its location in the epimetamorphic stage, as a result of burial, tectonism of the Cape Fold Belt and heating effects of dolerite intrusion. Epimetamorphism in the Prince Albert Formation was found at depth in the newly drilled boreholes KZF-01 and KWV-01 from vitrinite reflectance measurements and Rock-Eval pyrolysis.

Dolerite intrusions have a major role in the generation of shale gas. In borehole KWV-01, dolerite sills (19 m- and 149 m- thick respectively) occur some 12 m and 122 m above the Prince Albert Formation and have reduced the shale gas potential, as a result of contact metamorphism. The amount of shale gas destroyed is proportional to the sill thickness and thus dolerites should be avoided in exploring for viable shale gas.

Shales containing high organic carbon contents have the best potential for shale gas generation. In borehole SA 1/66, the Prince Albert Formation consists of black to greyish black shale with a TOC ranging from 2.76 to 4.87 wt%, a thickness of 128 m and an absence of dolerite. Borehole SA 1/66 has bulk densities ranging between 2.521 and 2.686 g/mL and shale porosities between 1.9 and 5.6%, which has a positive effect on hydraulic fracturing should exploitation take place. Therefore, it is concluded that variable porosity values,

permeability measurements between 10 and 100 mD, overburdern of less than 3500 m, TOC greater than 3 wt%, less than 20% dolerite intrusion and high hydrogen indices are required for a potential shale gas reservoir. In view of this, the Prince Albert Formation has a sparse economic shale gas potential. However, it is important that new exploration boreholes should be drilled within the “sweet spots” of Cole (2014) and Mowzer and Adams (2015), in order to test whether the lower Ecca Group (Prince Albert and Whitehill formations) has the potential to generate viable shale gas.

References:

Aarnes, I., Svensen, H., Polteau, S. and Planke, S., 2011. Contact metamorphic devolatilization of shales in the Karoo Basin, South Africa, and the effects of multiple sill intrusions. Journal of Chemical Geology, 281, 181–194.

Adedosu, T.A., Ajayi, T.R., Xionga, Y., Lia, Y., Fanga, C., Chena, Y. and Akinlua, A., 2014. Geochemical evaluation of Kolmani River-1 well, Gongola Basin, Upper Benue Trough, Nigeria. Nigerian Association of Petroleum Explorationists Bulletin, 26, 51–79.

Adedosu, T. A., Sonibare, O., Ehinola, O., Tuo, J. and Ekundayo, O., 2015. Petroleum Potential of Awgu Shale Benue Trough, Nigeria. Energy Sources, Part A: Recovery, Utilization and Environmental Effects, 37, 1853–1860.

Adeniyi, E.O., Ossa, F., Kramers, J.D., de Kock, M.O., Belyanin, G. and Beukes, N.J., 2018. Cause and timing of the thermal over-maturation of hydrocarbon source rocks of the Ecca Group (main Karoo Basin, South Africa). Marine and Petroleum Geology, 91, 480–500.

Adie, R.J., 1952a. The position of the Falkland Islands in a reconstruction of Gondwanaland. Geological Magazine, 89, 401–410.

Adie, R.J., 1952b. Representatives of the Gondwana System in the Falkland Islands. In: C. Teichert (Editor). Symposium sur les Séries de Gondwana: Algiers. 19th International Geological Congress, 385–392.

Adie, R.J., 1958. Falkland Islands. (Iles Malouines ou Falkland; Islas Malvinas). Lexique Stratigraphique International 5 (Amerique Latine), 35–55.

Ahrens, L.H., 1945. The geochemical relationship between Thallium and Rubidium in minerals of igneous origin. Transactions of the Geological Society of South Africa, 48, 207–231.

Aitchison, J.C., Bradshaw, M.A. and Newman, J., 1988. Lithofacies and origin of the Buckeye Formation: Late Paleozoic glacial and glaciomarine sediments, Ohio Range, Transantarctic Mountains, Antarctica. Palaeogeography, Palaeoclimatology, Palaeoecology, 64, 93–104.

Aldiss, D.T. and Edwards, E.J., 1999. Geology of the Falkland Islands. British Geological Survey Technical reports, WC/99/10.

Amos, A.J. and López-Gamundi, O.R., 1981. Late Paleozoic tillites and diamictites of the Calingasta- Uspallata and Panganzo basins, San Juan and Mendoza provinces, western Argentina. In: M. Humbrey and W. Harland (Editors). Earth's Pre- Pleistocene glacial record. Cambridge, Cambridge University Press, 859–868.

Anderson, A.M., 1975. Turbidites and arthropod trackways in the Dwyka glacial deposits (Early Permian) of southern Africa. Transactions of the Geological Society of South Africa, 78, 265–273.

Anderson, A., 1976. Fish trails from the Early Permian of South Africa. Palaeontology, 19, 397–409.

Anderson, J.M., 1977. The biostratigraphy of the Permian and Triassic. Part 3. A review of the Gondwana Permian palynology with particular reference to the northern Karoo Basin, South Africa. Memoirs of the Botanical Survey of South Africa, 41, 133pp.

Anderson, A., 1981. The Umfolozia arthropod trackways in the Permian Dwyka and Ecca series of South Africa. Journal of Palaeontology, 55, 84–108.

Andreis, R.R., 1984 Lithofacial analysis of the Sauce Grande Formation (Upper Carbonic?), Sierras Australes, Province of Buenos Aires. Annual Meeting IUGS- IGCP Project 211 Late Paleozoic of South America, Bariloche, Abstracts, 28–29.

Andreis, R.R., Amos, A.J., Archangelsky, S. and González, C.R., 1987. Sauce Grande Basins (Southern Sierras) - Colorado. In: S. Archangelsky (Editor). El Sistema Carbonífero en la República Argentina: Córdoba, Academia Nacional de Ciencias, 213–233.

Andreis, R.R., Iñíguez, A.M., Lluch, L.L. and Rodríguez, S., 1989. Palaeozoic Basin of Ventania, Sierras Australes, Province of Buenos Aires. In: G.A. Chebli and L.A. Spalletti (Editors). Las Cuencas Sedimentarias Argentinas. Geological Correlation Series, No. 6, 265–289.

Araújo, L.M., 2001. Analise da Expressao Estratigrafica dos Parametros de geoquimica Organica nas Sequencias Deposicionais Irati. Unpublished PhD thesis, Federal University of Rio Grande do Sul, Brazil, 307pp.

Araújo, L.M., Rodrigues, R. and Scherer, C.M.S., 2001. Irati depositional sequences: chemo-stratigraphic framework and paleoenvironmental inferences. Ciência- Técnica-Petróleo, 20, 193–202.

Archangelsky, S. and Cúneo, R., 1984. Continental Permian Zoning of Argentina based on its fossil plants. Memoria III Congreso Latinoamericano de Paleontología, 143–153.

Archangelsky, S., Azcuy, C.L., González, C.R. and Sabattini, N., 1987. Age of the biozones. In: S. Archangelsky (Editor). El Sistema Carboníferode la República Argentina: Córdoba, National Academy of Sciences, 293–301.

Arthur, J.D., Langhus, B. and Alleman, D., 2008. An overview of modern shale gas development in the United States. ALL Consulting, US, 21pp. Available at: http://www.all.llc.com/publicdownloads/ALLShaleOverviewFinal.pdf.

Asquith, G. and Krygowski, D., 2004. Basic well log analysis (Second Edition). AAPG Methods in Exploration 16, 248pp.

ASTM International., 2013. D2797-13 Standard practice for preparing coal samples for microscopical analysis by reflected light. Annual Book of ASTM Standards: Petroleum Products, Lubricants, and Fossil Fuels; Gaseous Fuels; Coal and Coke, 5, 5.06. ASTM International, West Conshohocken, PA, 469–473.

ASTM International., 2014. Standard Test Method for Microscopical determination of the vitrinite dispersed in sedimentary rocks (D7708-14). ASTM International, West Conshohocken, Pennsylvania, 2014, www.astm.org

ASTM International., 2018. Standard Test Method for Determination of Pore Volume and Pore Volume Distribution of Soil and Rock by Mercury Intrusion Porosimetry (D4404-18). ASTM International, West Conshohocken, Pennsylvania, 2018, www.astm.org

Baiyegunhi, C., Liu, K., Wagner, N., Gwavava, O. and Oloniniyi, T.L., 2018. Geochemical evaluation of the Permian Ecca shale in Eastern Cape Province, South Africa: Implications for shale gas potential. Acta Geologica Sinca (English Edition), 92(3), 1193–1217.

Bamford, M.K., 1999. Permo- Triassic fossil woods from the South African Karoo Basin. Palaeontologia Africana, 35, 25–40.

Bamford, M.K., 2000. Fossil woods of Karoo age deposits in South Africa and Namibia as an aid to biostratigraphical correlation. Journal of African Earth Science, 31 (1), 119–132.

Bangert, B., Stollhofen, H., Lorenz, V. and Armstrong, R., 1999. The geochronology and significance of ash- fall tuffs in the glaciogenic Carboniferous- Permian Dwyka Group of Namibia and South Africa. Journal of African Earth Science, 29, 33–49.

Bangert, B., 2000. Tephrostratigraphy, petrography, geochemistry, age and fossil record of the Ganigobis Shale Member and associated glaciomarine deposits of the Dwyka Group, Late Carboniferous, southern Africa. Unpublished PhD thesis, University of Würzburg, Germany, 260pp. [URL:http://opus.bibliothek.uni-wuerzburg.de/opus/volltexte/2002/223/]

Barrett, P.J. and Kyle, R.A., 1975. The Early Permian glacial beds of south Victoria Land and the Darwin Mountains, Antarctica. In: K.S.W. Campbell (Editor). Gondwana Geology. Canberra, Australian National University Press, 333–346.

Bauer, W., Hagemann, H.W., Poscher, G., Sachsenhofer, R.F. and Spaeth, G., 1997. Permian coals from western Dronning Maud Land composition, environment, and the influence of Jurassic magmatism on their maturity. In: C.A. Ricci (Editor). The Antarctic Region: Geological Evolution and Processes. Siena, 945–951.

Bauer, W., 2009. Permian sedimentary cover, Heimefrontfjella, western Dronning Maud Land (East Antarctica). Polarforschung, 79, 39–42.

Belica, M.E., Tohver, E., Poyatos-More'. M., Flint, S., Parra-Avila, L.A., Lanci, L., Denyszyn. S. and Pisarevsky, S., 2017. Refining the chronostratigraphy of the Karoo Basin, South

Africa: Magnetostratigraphic constraints support an early Permian age for the Ecca Group. Geophysical Journal International, 211(3), 1354–1374.

Ben- Avraham, Z., Hartnady, C.J.H. and Malan, J.A., 1993.Early tectonic extension between the Agulhas Bank and the Falkland Plateau due to rotation of the Lafonia microplate. Earth and Planetary Science Letters, 117, 43–58.

Berry, B., 2018. Soekor (South Africa) Southern Oil Exploration Corporation (Pty) Ltd. Available at: https://www.crwflags.com/fotw/flags/za$soek.html (viewed 3/9/2020).

Borchers, S.L., Schnetger, B., Böning, P. and Brumsack, H.-J., 2005. Geochemical signatures of the Namibian diatom belt: Perennial upwelling and intermittent anoxia. Geochemistry, Geophysics, Geosystems, 6(6), 1–20.

Bordy, E.M., 2018. Lithostratigraphy of the Tshidzi Formation (Dwyka Group, Karoo Supergroup), South Africa. South African Journal of Geology, 121 (1), 109–118.

Bordy, E.M., Hancox, P.J. and Rubidge, B.S., 2005. Turner, B.R. and Thomson, K., Discussion on 'Basin development during deposition of the Elliot formation (Late Triassic- Early Jurassic), Karoo Supergroup, South Africa' (South African Journal of Geology, 107, 397–412) - A Reply. South African Journal of Geology, 108, 454–461.

Bracaccini, O.I., 1960. Main guidelines of the structural evolution of Argentina: Buenos Aires. Petrotecnia, 10, 57–69.

Bragg, W.H. and Bragg, W.L., 1913. The reflection of X-rays by crystals". Proceedings of the Royal Society of London. 88 (605), 428–38.

Brandt, J.W., Martin, H. and Kirchner, J.G., 1961. Interim report of the Coal Commission of

South West Africa. Economic Geology Series, Geological Survey of Namibia, EG 035, 125pp.

Brime, C., 1985. The accuracy of X-ray diffraction method for determining mineral mixtures. Mineralogical Magazine, 49, 531–538.

Brouwer, P., 2010. Theory of XRF: Getting acquainted with the principles. PANalytica BV, Netherlands, 59pp.

Bruner, K.R. and Smosna, R., 2011. A comparative study of the Mississipian Barnett Shale, Fort Worth Basin, and Devonian Marcellus Shale, Appalachian Basin. U.S. Department of Energy. National Energy Technology Laboratory, 118pp.

Bruni, C.E., Vasconcelos, D. and Padula, V.T., 1971. Brazilian oil shale development. In: Proceedings, Eighth World Petroleum Congress, Moscow. The Permanent Council of World Petroleum Congress, 2, 13–24.

Bühmann, D., Bühmann, C. and Von Brunn, V., 1989. Glaciogenic banded phosphorites from Permian sedimentary rocks. Economic Geology, 84, 741–750.

Bunaciu, A.A., Udristioiu, E.G. and Aboul-Enein, H.Y., 2015. X-ray diffraction: Instrumentation and applications. Critical reviews in Analytical Chemistry, 45, 289–299.

Cagliari, J., Lavina, E.L.C., Philipp, R.P., Tognoli, F.M.W., Basei, M.A.S. and Faccini, U.F., 2014. New Sakmarian ages for the Rio Bonito Formation (Paraná Basin, southern Brazil) based on LA- ICP- MS U-Pb radiometric dating of zircon crystals. Journal of South American Earth Sciences, 56, 265–277.

Cairncross, B., 2001. An overview of the Permian (Karoo) coal deposits of southern Africa. Journal of African Earth Sciences, 33, 529–562.

Campbell, F.A. and Williams, G.D., 1965. Chemical composition of shales of Mannville Group Lower Cretaceous of Central Alberta, Canada. AAPG Bulletin, 49, 81–87.

Cao, T., Song, Z., Wang, S., Cao, X., Li, Y. and Xia, J., 2015. Characterizing the pore structure in the Silurian and Permian shales of the Sichuan Basin, China. Journal of Marine and Petroleum Geology, 61, 140–150.

Catuneanu, O., 2004. Retroarc foreland systems- evolution through time. Journal of Earth Sciences, 38, 225–242.

Catuneanu, O., Hancox, P.J. and Rubidge, B.S., 1998. Reciprocal flexural behaviour and contrasting stratigraphies: a new basin development model for the Karoo retroarc foreland system, South Africa. Basin Research, 10, 417–439.

Catuneanu, O., Wopfner, H., Eriksson, P.G., Cairncross, B., Rubidge, B.S. and Smith, R.M.H., 2005. The Karoo Basins of south- central Africa. Journal of African Earth Sciences, 42, 211–253.

Chere, N., 2015. Sedimentological and geochemical investigations on borehole cores of the Lower Ecca Group black shales, for their gas potential- Karoo Basin, South Africa. Unpublished MSc thesis, Nelson Mandela Metropolitan University, Port Elizabeth, 268pp.

Chere, N., Linol, B., de Wit, M. and Schulz, H.M., 2017. Lateral and temporal variations of black shales across the southern Karoo Basin - Implications for shale gas exploration. South African Journal of Geology, 120, 541–564.

Chevallier, L., Goedhart, M. and Woodford, A.C., 2001. The influences of dolerite sill and ring complexes on the occurrence of groundwater in Karoo fractured aquifers: A morpho-tectonic approach. Water Research Commission Report No 937/1/01, 146pp.

Christiano-de-Souza, I, C. and Ricardi-Branco, F.S., 2015. Study of the West Gondwana Floras during the Late Paleozoic: A paleographic approach in the Paraná Basin- Brazil. Journal of Palaeography, Palaeoclimatology, Palaeoecology, 426, 159–169.

Clifton, H.E., Hunter, R.E. and Phillips, R.L., 1971. Depositional structures and processes in the non-barred, high energy nearshore. Journal of Sedimentary Petrology, 41, 651–670.

Coates, D.A., 1969. Stratigraphy and sedimentation of the Sauce Grande Formation, Sierra de la Ventana, southern Buenos Aires Province. Argentina: 1st Symposium on Geology and Paleontology of Gondwana, 2, 799–816.

Cole, D.I., 1978. Preliminary report on the oil potential of the Whitehill Formation between Strydenburg (Cape Province) and hertzogville (Orange Free State). Geological Survey of the Republic of South Africa, No.1978-0304 unpublished.

Cole, D.I., 1991. Depositional environment of the Dwyka Group in the Boshof-Hertzogville area, Orange Free State. South African Journal of Geology, 94, 272–287.

Cole, D.I., 2005. Prince Albert Formation. Catalogue of South African lithostratigraphic Units 8, South African Committee for Stratigraphy, South Africa, 8–33.

Cole, D.I., 2014. Geology of Karoo shale gas and how this can influence economic gas recovery. Fossil Fuel Foundation Gas Conference, 21 May 2014. Slide presentation. Ref: www.fossilfuel.co.za/ conferences/2014/GAS-SA.

Cole, D.I., 2018. New insights into the stratigraphy of the lower Ecca Group using recent data from deep borehole logs in the central and southern parts of the main Karoo Basin. Abstracts, Geocongress 2018, 18-20 July 2018, Geological Society of South Africa, University of Johannesburg, Johannesburg, South Africa, 51.

Cole, D.I., 2019. Review of shale gas potential of the Whitehill Formation in the main Karoo Basin, South Africa. Abstracts, Council for Geoscience Conference, 11-12 February 2019, Pretoria, South Africa, 53.

Cole, D. I. and Basson, W. A., 1991. Whitehill Formation. In: M.R. Johnson (Editor). Catalogue of South African Lithostratigraphic Units. South African Committee for Stratigraphy, 3–52.

Cole, D.I. and McLachlan, I.R., 1991. Oil potential of the Permian Whitehill Shale Formation in the main Karoo Basin, South Africa. Pp. 379-390. In: H. Ulbrich and A.C. Rocha Campos (Editors). Gondwana Seven proceedings. Geosciences Institute, University of Sao Paulo, Sao Paulo, Brazil, 714pp.

Cole, D.I. and McLachlan, I.R., 1994. Oil shale potential and depositional environment of the Whitehill Formation in the main Karoo Basin. Republic Geological Survey of South Africa, 1994–0213.

Cole, D., Mosavel, H., Browning, C., Chevallier, L., Mitha, V., Dhansay, T., Musekiwa, C. and Maya, M., 2016a. Environmental baseline modelling and observed changes during drilling of a deep stratigraphic borehole in the Karoo: Results of a geological investigation around Beaufort West. CGS report Number: 2016-0093.

Cole, D.I., Robey, K. and Mosavel, H., 2016b. Karoo research initiative (KARIN): Shale gas potential and groundwater study: Project ST-2016-1260. Report, Council for Geoscience, No. 2016-0098.

Cole, D.I., Johnson, M.R. and Day, M.O., 2016c. Lithostratigraphy of the Abrahamskraal Formation (Karoo Supergroup), South Africa. South African Journal of Geology, 119.2, 415–424.

Cole, D.I. and Smith, R.M.H., 2008. Fluvial architecture of the Late Permian Beaufort Group deposits, S.W. Karoo Basin: Point bars, crevasse splays, palaeosols, vertebrate fossils and uranium. Field Excursion Guidebook, American Association of Petroleum Geologists International Conference, Cape Town, FT02: 1–110.

Cole, D.I. and Wipplinger, P.E., 2001. Sedimentology and molybdenum potential of the Beaufort Group in the main Karoo Basin. Memoir, Council for Geoscience, South Africa, 80, 225pp.

Collinson, J.W., Pennington, D.C. and Kemp, N.R., 1983. Sedimentary petrology of Permian-Triassic fluvial rocks in Allan Hills, central Victoria Land. Antarctic Journal of the United States, 18 (5), 20–22.

Collinson, J.W., Vavra, C.L. and Zawiskie, J.M., 1992. Sedimentology of the Polarstar Formation, (Permian), Ellsworth Mountains, West Antarctica. In: G.F. Webers, C. Craddock and J.F. Splettstoesser (Editors). Geology and Paleontology of the Ellsworth Mountains, West Antarctica. The Geological Society of America, Boulder, Memoir 170, 63–79.

Collinson, J.W., Elliot, D.H., Isbell, J.L. and Miller, J.M.G., 1994. Permian- Triaassic Transantarctic Basin. In: J.J. Veevers and C. McA. Powell (Editors). Permian-Triassic Pangean Basins and Foldbelts along the Panthalassan Margin of Gondwanaland: Boulder, Colorado. Geological Society of America, Memoir 184, 173–222.

Craddock, J.P., Fitzgerald, P., Konstantinou, A., Nereson, A. and Thomas, R.J., 2017. Detrital zircon provenance of upper Cambrian- Permian strata and tectonic evolution of the Ellsworth Mountains, West Antarctica. Gondwana Research, 45, 191–207.

Craig, H., 1953. The Geochemistry of the Stable Carbon Isotopes. Geochimica et Cosmochimica Acta, 3, 53–92.

Craigie, N.W., 2016. Chemostratigraphy of the Silurian Qusaiba Member, Eastern Saudi Arabia. Journal of African Earth Sciences, 113, 12–34.

Craigie, N.W., 2018. Principles of elemental chemostratigraphy: A practical user guide. Springer Nature, Switzerland, 189pp.

Curtis, M.L., 2001. Tectonic history of the Ellsworth Mountains, West Antarctica: reconciling an Antarctic enigma. Geological Society of America Bulletin, 113, 939–958.

Darling, T., 2005. Well logging and Formation Evaluation. Gulf Professional Publishing, 326pp.

Davis, J.C., 1986. Statistics and Data Analysis in Geology, 2nd edn. Wiley, New York, 646pp.

De Beer, C.H., 1992. Structural evolution of the Cape Fold Belt syntaxis and its influence on syntectonic sedimentation in the SW Karoo Basin. In: M.J. de Wit and I. Ransome (Editors). Inversion Tectonics of the Cape Fold Belt, Karoo and Cretaceous Basins of Southern Africa. Balkema, Rotterdam, 197–206.

Decker, J.E. and de Wit, M.J., 2006. Carbon isotope evidence for CAM photosynthesis in the Mesozoic. Terra Nova, 18, 9–17.

Decker, J. and Marot, J., 2012. Investigation of hydraulic fracturing in the Karoo of South Africa. Annexure A: Resource Assessment. Petroleum Agency of South Africa, 8pp.

De Kock, M.O., Beukes, N.J., Adeniyi, E.O., Cole. D., Götz, A.E., Geel, C. and Ossa, F-G., 2017. Deflating the shale gas potential of South Africa's main Karoo Basin. South African Journal of Science, 113, 1–12. http://dx.doi.org/10.17159/sajs.2017/20160331

Dellisanti, F., Pini, G.A. and Baudin, F., 2010. Use of Tmax as a thermal maturity indicator in orogenic successions and comparison with clay mineral evolution. Clay Minerals, 45, 115–130.

Dembicki, H., 2009. Three common source rock evaluation errors made by geologist during prospect or play appraisals. American Association of Petroleum Geologists Bulletin, 93, 341–356.

De Wit, M.J., Jeffery, M., Bergh, H. and Nicolaysen, L., 1988. Geological map of sectors of Gondwana reconstructed to their disposition- 150Ma. American Association of Petroleum Geologists.

De Wit, M.J., 2016. Organic carbon isotope stratigraphy of the Karoo Supergroup. In: L. Bastien and M.J. De Wit (Editors). Origin and Evolution of the Cape Mountains and Karoo Basin. Springer, 17, 169–179.

Duncan, A.R. and Marsh, J.S., 2006. The Karoo Igneous Province. In: M.R. Johnson, C.R. Anhaeusser and R.J. Thomas (Editors). The Geology of South Africa. Geological Society of South Africa, Council for Geoscience, Pretoria, 501–520.

Du Toit, A.L., 1921. The Carboniferous glaciation of South Africa. Transactions of the Geological Society of South Africa, 24, 188–227.

EIA., 1999. Natural Gas 1998: Issues and Trends. https://digital.library.unt.edu/ark:/67531/metadc675165/. [Accessed: 9/8/2021].

Elliot, D.H. and Fanning, C.M., 2008. Detrital zircons from upper Permian and lower Triassic Victoria Group sandstones, Shackleton Glacier region, Antarctica: evidence for multiple sources along the Gondwana plate margin. Gondwana Research 13, 259–274.

Elliot, D.H., Fanning, C. M. and Laudon, T.S., 2016. The Gondwana Plate margin in the Weddell Sea sector: Zircon geochronology of Upper Paleozoic (mainly Permian) strata from the Ellsworth Mountains and eastern Ellsworth Land, Antarctica. Gondwana Research 29, 234– 247.

Energy Sources., 2020. Coal Department: Energy. Republic of South Africa. https://www.energy.gov.za. [Retrieved: 8/8/2021].

Fakir, S., 2015. Framework to assess the economic reality of shale gas in South Africa. Climate and Energy. WWF Technical report, 60pp.

Faure, K. and Cole. D., 1999. Geochemical evidence for lacustrine microbial blooms in the vast Permian Main Karoo, Paraná, Falkland Islands and Huab basins of southwestern Gondwana. Palaeogeography, Palaeoclimatology, Palaeoecology 152, 189–213.

Ferreira, J.C., 2014. Characterization of potential source rocks of the Prince Albert, Whitehill and Collingham Formations in the Laingsburg sub- basin, South Africa. Unpublished MSc thesis, University of the Western Cape, Cape Town, 157pp.

Frakes, L.A. and Crowell, J.C., 1967. Facies and paleogeography of Late Palaeozoic diamictite, Falkland Islands. Geological Society of America Bulletin, 78, 37–58.

França, A.B. and Potter, P.E., 1991. Stratigraphy and reservoir potential of glacial deposits of the Itarare Group (Carboniferous- Permian), Parana Basin, Brazil. American Association of Petroleum Geologists Bulletin. Tulsa, Estados Unidos, 75, 62–85.

França, A.B. and Vesely, F.F., 2007. Stratigraphy and sedimentology of the Late Paleozoic glacial record of the Panará Basin: Brazil. In: R. Lannuzzi and D.R. Boardman (Editors). Problems in Western Gondwana geology. Workshop Extended abstracts, 46–50.

Galton, F., 1890. Kinship and correlation. North American Review, 150, 419–431.

Geel, C., Schulz H.-M., Booth, P., de Wit. M. and Horsfield, B., 2013. Shale gas characteristics of Permian black shales in South Africa: results from recent drilling in the Ecca Group (Eastern Cape). Energy Procedia, 40, 256–265.

Geel, C., de Wit, M.J., Booth, P., Schulz, H.M. and Horsfield, B., 2015. Palaeo-environment, diagenesis and characteristics of Permian black shales in the Lower Karoo Supergroup flanking the Cape Fold Belt near Jansenville, Eastern Cape, South Africa: Implications for the shale gas potential of the Karoo Basin. South African Journal of Geology, 118, 249–274.

Geiger, M., 1999. An explanation of the Geological Map 1:10000 of the Namibian borderland along the Orange River at Zwartbas, Warmbad District, Karas Region, Namibia. Unpublished. Diplomkartierung, University of Würzburg, 80pp.

Geiger, M., 2000. The geology of the southern Warmbad basin margin – tephrostratigraphy,

age, fossil record and sedimentary environment of Carboniferous-Permian glacigenic deposits of the Dwyka Group, Zwartbas, southern Namibia. Unpublished Diploma thesis, University of Würzburg, Germany, 79pp.

Geocaching., 2021. Bokkeveld fossils. https://www.geocaching.com/geocache/GC336KY_bokkeveld-fossils?guid=8b278538-472c-4ade-9387-d8b173a9039f. [Accessed: 2/8/2021]

Geological Survey., 1960. Geological map of sheet 3326BB (Fort Brown): Scale 1:50 000. Compiler: E.D. Mountain. Government Printer, Pretoria.

Geological Survey., 1967. Geological map of sheet3321BB (Gamkarivier): Scale 1:50 000. Compilers: J.N. Theron., H.de V. Wickens and P. Grey. Government Printer, Pretoria.

Geological Survey., 1985. Geological map of sheet 3320BB (Laingsburg): Scale 1:50 000. Compiler: H.de V. Wickens. Government Printer, Pretoria.

Geological Survey., 1986. Geological map of sheet3219BC (Elandsvlei): Scale 1:50 000. Compiler: J.N. Theron. Government Printer, Pretoria.

Geological Survey., 1995. Geological map of sheet 3326 (Grahamstown): Scale 1:250 000. Compilers: E.D. Mountain, D.J. Roby and M.R. Johnson. Government Printer, Pretoria.

Gesicki, A.L.D., Ricominni, C., Boggiani, P.C. and Coimbra, A.M., 1996. Evidence of glacial advance in the Aquidauna Formation (Neopaleozoic of the Paraná Basin) in the state of Mato Grosso do Sul. Brazilian Congress of Geology, 39; Salvador. Anais do, São Paulo: Brazilian Society of Geology, 1, 124–127.

Giesche, H., 2006. Mercury porosimetry: a general (practical) overview. Particle & Particle Systems Characterization, 23, 1–11.

Gradstein, F.M., Ogg, J.G., Smith, A.G., and with contributions of Agterberg, F.P., Bleeker,W., Cooper, R.A., Davydov, V., Gibbard, P., Hinnov, L., House, M.R., Lourens, L.,Luterbacher, H-P., McArthur, J., Melchin, M.J., Robb, L.J., Shergold, J., Villeneuve, M.,Wardlaw, B.R., Ali, J., Brinkhuis, H., Hilgen, F.J., Hooker, J., Howarth, R.J., Knoll, A.H.,Laskar, J., Monechi, S., Powell, J., Plumb, K.A., Raffi, I., Röhl, U., Sanfilippo, A., Schmitz,B., Shackleton, N.J., Shields, G.A., Strauss, H., van Dam, J., Veizer, J., van Kolfschoten,Th., Wilson, D., 2005. A Geologic Time Scale 2004. Cambridge University Press, 610pp.

Gresse, P.G., Theron, J.N., Fitch, F.J. and Miller, J.A., 1992. Tectonic inversion and radiometric resetting of the basement in the Cape Fold Belt. In: M.J. de Wit and I.G.D. Ransome (Editors). Inversion Tectonics of the Cape Fold Belt, Karoo and Cretaceous Basins of Southern Africa. A.A. Balkema, Rotterdam, 217–228.

Grill, H., 1997. The Permo-Carboniferous glacial to marine Karoo record in southern Namibia: sedimentary facies and sequence stratigraphy. Beringeria, 19, 98pp.

Grunow, A.M., Kent, D.V. and Dalziel, I.W.D., 1987. Mesozoic evolution of West Antarctica and the Weddell Sea Basin: new paleomagnetic constraints. Earth and Planetary Science Letters 86, 16–26.

Hachiro, J., 1996. The Irati (Neopermian) Subgroup of the Paraná Basin. Unpublished PhD thesis, University of São Paulo, Brazil, 196pp.

Hachiro, J., Coimbra, A.M. and Matos, S.L.F., 1993. The chronostratigraphic character of the Irati unit. 1st Symposium on chronostratigraphy of the Paraná Basin, Rio Claro. Abstract, 62–63.

Hälbich, I.W., Fitch F.J. and Miller, J.A., 1983. Dating the Cape Orogeny. In: A.P.G. Söhnge and I.W. Hälbich (Editors). Geodynamics of the Cape Fold Belt. Geological Society of South Africa. Special Publication, No 12, 149–164.

Hansma, J., Tohver, E., Schrank, C., Jourdan, F. and Adams, D., 2016. The timing of the Cape Orogeny: New 40Ar/39Ar age constraints on deformation and cooling of the Cape Fold Belt, South Africa. Gondwana Research, 32, 122–137.

Harrington, H.J., 1947. Explanation of the geological leaves 33 m (Sierra de Curamalal) and 34 m (Sierra de la Ventana). Bulletin, National Directorate of Geology and Mining, No. 61.

Harrington, H.J., 1955. The Permian Eurydesma fauna of the eastern Argentina. Journal of Paleontology, 29, 112–128.

Harrington, H.J., 1980 Southern Sierras of the province of Buenos Aires. Geología Regional Argentina, Academia Nacional de Ciencias, 2, 967–983.

Hatch, J.R. and Leventhal, J.S., 1992. Relationship between inferred redox potential of the depositional environment and geochemistry of the Upper Pennsylvanian (Missourian) stark shale member of the Dennis Limestone, Wabaunsee County, Kansas, USA. Journal of Chemical Geology, 99, 65–82.

Haughton, S.H. and Frommurze, H.F., 1927. The Karroo beds of the Warmbad District, South-West Africa. Transactions of the Geological Society of South Africa, 30, 133–142.

Haughton, S.H. and Frommurze, H.F., 1936. The geology of the Warmbad district, South West Africa. An explanation of geological sheets Amib (H-33-F), Umeis (H-34-A) and Nakop (H-34-B). SWA Department of Mines, Memoir 2, 64pp.

Haughton, S.H., Blignaut, J.J.G., Rossouw, P.J., Spies, J.J. and Zagt, S., 1953. Results of an investigation into the possible presence of oil in Karroo rocks in parts of the Union of South Africa., Geological Survey of South Africa, Memoir 45, 130pp.

Heath, D.C., 1972. Die geologie van die Sisteem Karoo in die gebied Mariental-Asab, Suidwes-Afrika., Geological Survey of South Africa, Memoir 61, 36pp.

Herron, M.M., 1988. Geochemical classification of terrigenous sands and shales from core or log data. Journal of Sedimentary Research, 58(5), 820–829.

Himmler, T., Freiwald, A., Stollhofen, H. and Peckmann, J., 2008. Late Carboniferous hydrocarbon- seep carbonates from the glaciomarine Dwyka Group, southern Namibia. Palaeogeography, Palaeoclimatology, Palaeoecology, 257, 185–197.

Hodgson, F.D.I., 1972. The geology of the Brandberg- Aba Huab area. South West Africa.Unpublished DSc thesis, University of Orange Free State, Bloemfontein, 174pp.

Horsthemke, E., Ledendecker, S. and Porada, H., 1990. Depositional environments and stratigraphic correlation of the Karoo Sequence in northwestern Damaraland. Communication of the Geological Survey of Namibia, 6, 67–77.

Holzförster, F., Stollhofen, H. and Stanistreet, I.G., 2000. Lower Permian deposits of the Huab area, NW Namibia: a continental to marine transition. Communication of the Geological Survey of Namibia, 12, 247–257.

Hu, R.Z., Su, W.C., Bi, X.W., Tu, G.Z. and Hofstra, A.H., 2002. Geology and geochemistry of Carlin-type gold deposits in China. Mineralium Deposita, 37, 378–392.

Hunt, J.M., Philp, R.P. and Kvenvolden, K.A., 2002. Early developments in petroleum geochemistry. Organic Geochemistry, 33, 1025–1052.

Hyam, D.M., 1998. Structural evidence for the fit of the Falkland Islands in pre break-up Gondwana. Geoscientist, 8, 4–7.

IBM SPSS Statistics., 2011. IBM ®SPSS ® Statistics 20. ©Copyright IBM Corporation 1989, 2011.

Iñíguez, A.M., Andreis, R.R. and Zalba, P., 1988. Pyroclastic events in Aires, Argentinian republic. 2nd Jornasdas Geológicas Bonaerenses, Actas, 383–395.

International Commission on Stratigraphy., 2017. International Chronostratigraphic Chart, Volume 2017/02. http://www.stratigraphy.org/index.php/ics-chart-timescale

Isbell, J.L., 1990. Permian fluvial sedimentology of the Transantarctic basin. Unpublished PhD thesis, Ohio State University, Columbus, Ohio, 306pp.

Isbell, J.L., 1991. Evidence for a low- gradient alluvial fan from the palaeo-Pacific margin in the Upper Permian Buckley Formation, Beardmore Glacier region, Antarctica. In: M.R.A. Thomson, J.A. Crame and J.W. Thomson (Editors). Geological evolution of Antarctica. Cambridge, Cambridge University Press, 215–217.

Isbell, J.L. and Collinson, J.W., 1988. Fluvial architecture of the Fairchild and Buckley Formations (Permian), Beardmore Glacier area. Antarctic Journal of the United States, 23 (5), 3–5.

Isbell, J.L., Taylor, T.N., Taylor, E.L., Cuneo, N.R. and Meyer- Berthaud, B., 1990. Depositional setting of Permian and Triassic fossil plants in the Allan Hills, southern Victoria Land. Antarctic Journal of the United States, 25 (5), 28–29.

Isbell, J.L., Miller, M.F., Wolfe, K.L. and Lenaker, P.A., 2003. Timing of late Paleozoic glaciations in Gondwana: was glaciation responsible for the development of Northern Hemisphere cyclothems? In: M.A Chan and A.W. Archer (Editors). Extreme Depositional Environments: Mega End Members in Geologic Time. Boulder, Colorado. Geological Society of America Special Paper, 370, 5–24.

Isbell, J.L., Cole, D.I. and Catuneanu, O., 2008. Carboniferous - Permian glaciation in the main Karoo Basin, South Africa: Stratigraphy, depositional controls, and glacial dynamics. In: C.R. Fielding, T.D. Frank and J.L. Isbell (Editors). Resolving the Late Paleozoic Ice age in Time and Space. Geological Society of America Special Paper, 441, 71–82.

Isbell, J.L., Henry, L.C., Gulbranson, E.L., Limarino, C.O., Fraiser, M.L., Koch, Z.J., Ciccioli, P.L. and Dineen, A.A., 2012. Glacial paradoxes during the late Paleozoic ice age: Evaluating the equilibrium line altitude as a control on glaciation. Gondwana Research, 22, 1–19.

Jackson, A., M., Hasiotis, S.T. and Flaig, P.P., 2012. Preliminary report of trace fossils and sedimentology indicating a shallow marine deltaic environment for the lower Permian Mackellar Formation at Turnabout Ridge and Buckley Island, Beardmore glacier, central Transantarctic Mountains (CTAM), Antarctica. Geological Society of America, Abstracts with Programs, 44(7), 289.

Jarvie, D.M., Hill, R.J., Ruble, T.E. and Pollastro, R.M., 2007. Unconventional shale- gas systems: The Mississippian Barnett Shale of north- central Texas as one model for thermogenic shale- gas assessment. AAPG Bulletin, 91 (4), 475–499.

Jeandel, C., Tachikawa, K., Bory, A. and Dehairs, F., 2000. Biogenic barium is suspended and trapped material as a tracer of export production in tropical NE Atlantic (EUMELI sites). Marine Chemistry, 71, 125–142.

Jerram, D., Mountney, N., Holzförster, F. and Stollhofen, H., 1999. Internal stratigraphic relationships in the Etendeka Group in the Huab Basin, NW Namibia: understanding the onset of flood volcanism. Journal of Geodynamics 28, 393–418.

Johnson, M.R., 1991. Sandstone petrography, provenance and plate tectonic setting in Gondwana context of the southeastern Cape-Karoo Basin. South African Journal of Geology, 94, 137–154.

Johnson, M.R., 1994. Lexicon of South African Stratigraphy. Part 1: Phanerozoic Units. South African Committee for Stratigraphy, Council for Geoscience, South Africa, 56pp.

Johnson, M.R. and Kingsley, C.S., 1993. Lithostratigraphy of the Ripon Formation (Ecca Group), including the Pluto's Vale, Wonderfontein and Trumpeters Members. Lithostratigraphic Series, South African Committee for Stratigraphy, 26, 8pp.

Johnson, M.R. and Le Roux, F.G., 1994. The Geology of the Grahamstown area. Explanation of Sheet 3326: Scale 1: 250 000. Government Printer, Pretoria.

Johnson, M.R., van Vuuren, C.J., Hegenberger, W.F., Key, R. and Shoko, U., 1996. Stratigraphy of the Karoo Supergroup in southern Africa. An overview. Journal of African Earth Science, 23 (1), 3–15.

Johnson, M.R., van Vuuren, C.J., Visser, J.N.J., Cole, D.I., Wickens, H. de V., Christie, A.D.M., Roberts, D.L. and Brandl, G., 2006. Sedimentary rocks of the Karoo Supergroup. In: M.R. Johnson, C.R., Anhaeusser and R.J. Thomas (Editors). The geology of South

Africa. Geological Society of South Africa, Johannesburg, Council for Geoscience, 461–467.

Jones, B. and Manning, D.A.C., 1994. Comparison of geochemical indices used for the interpretation of palaeoredox conditions in ancient mudstones. Chemical Geology. 111, 111–129.

Jordaan, M.J., 1981. The Ecca-Beaufort transition in the western parts of the Karoo Basin. Transactions of the Geological Society of South Africa, 84, 19–25.

Karpeta, W.P. and Johnson, M.R., 1979. The geology of the Umtata area: Explanation sheet 3128 (Umtata). Geological Survey of South Africa, 16pp.

Katz, A.J. and Thompson, A.H., 1987. Prediction of rock electrical conductivity from mercury injection measurements. Journal of Geophysical Research, 92, No. B1, 599–607.

Kaufman, L. and Rousseeuw, P.J., 2005. Finding Groups in Data. John Wiley & Sons, Inc., New York. 369pp.

Kemp, E.M., 1975. The palynology of late Palaeozoic glacial deposits of Gondwanaland. In: K.S.W. Campbell (Editor). Gondwana geology: Canberra, Australian National University Press, 397–413.

Kendal, M., 1938. A new measure of rank correlation. Biometrika, 30, 81–89.

Khan, N.S., Van, C.H. and Horton, B.P., 2015. Stable carbon isotope and C/N geochemistry of coastal wetland sediments as a sea-level indicator. In: I. Shenna, A.J. Long, B.P Horton (Editors). Handbook of sea-level research, John Wiley & Sons Ltd, 20, 295–311.

Kingsley, C. S., 1977. Stratigraphy and sedimentology of the Ecca Group in the Eastern Cape Province, South Africa. Unpublished PhD thesis, University of Port Elizabeth, Port Elizabeth, 286pp.

Kingsley, C.S., 1981. A composite submarine fan-delta-fluvial model for the Ecca and lower Beaufort groups of Permian age in the Eastern Cape Province, South Africa. Transactions of the Geological Society of South Africa, 84, 27–40.

Kingsley, C.S., 1985. Sedimentological aspects of the Ecca Sequence in the Kalahari basin, South West Africa/Namibia. CDM Mineral Surveys, Open File Report, 13/175/510/85/277. Geological Survey of South Africa, 1, 29–34.

Kramers, J.D., Andreoli, M.A.G., Atanasova, M., Belyanin, G.A., Block, D.L., Franklyn, C., Harris, C., Lekgoathi, M., Montross, C.S., Ntsoane, T., Pischedda, V., Segonyane, P., Viljoen, K.S. and Westraadt, J.E., 2013. Unique chemistry of a diamond-bearing pebble from the Libyan Desert Glass strewnfield, SW Egypt: Evidence for a shocked comet fragment. Earth and Planetary Science letters, 382, 21–31.

Kuuskraa, V., Stevens, S., Van Leeuwen, T. and Moodhe, K., 2011. World shale gas resources: An initial assessment of 14 regions outside the United States. Prepared for: United States Energy Information Administration, 2011. Available at: http://www.eia.doe.gov/analysis/studies/worldshalegas.

Kyle, R.A. and Schopf, J.M., 1982. Permian and Triassic palynostratigraphy of the Victoria Group, Transantarctic Mountains. In: C. Craddock (Editor). Antarctic geoscience: Madison. University of Wisconsin Press, International Union of Geological Sciences, series B-4, 649–659.

Laird, M.G. and Bradshaw, J.D., 1981. Permian tillites of north Victoria Land. In: J.J. Hambrey and W.B. Harland (Editors). Earth's pre-Pleistocene glacial record. Cambridge University Press, 237–240.

Lapidus, A.L., Krylova, A. Yu. and Tokonogov, B.P., 2000. Gas chemistry: Status and prospects for development. In: B.P. Tumanyan (Editor). Chemistry and Technology of Fuels and Oils. 36, 2, 82–88.

Larsson, K. and Bylund, G., 1988. Sedimentology, stratigraphy and paleomagnetism in the Heimefrontjella Range. Ber. Polarforsch. 58, 174–180.

Larsson, K., Lindström, S. and Guy-Ohlson, D., 1990. An Early Permian palynoflora from Milordfjella, Dronning Maud Land, Antarctica. Antarctic Science, 2,331–334.

Laughrey, C.D., Ruble, T.E., Lemmens, H., Kostelnik, J., Butcher, A.R., Walker, G. and Knowles, W., 2011. Black Shale Diagenesis: Insights from Integrated High-Definition Analyses of Post-Mature Marcellus Formation Rocks, Northeastern Pennsylvania. Paper presented at: AAPG Annual Convention and Exhibition; April 10-13; Houston, Texas, USA.

Lendendecker, S., 1992. Stratigraphie der Karoosedimente der Huabregion (NW- Namibia) und deren correlation mit zeitaquivalenten sedimenten des Paranábeckens (Südamerika) und des groben Karoobeckens (Südafrika) unter besonderer berücksichtigung der überregionalen geodynamischen und klimatischen entwicklung westgondwanas. Göttinger Arb. Geol. Paläont 54, 87.

Lerman, A., 1978. Lakes chemistry and geology physics. Springer, Berlin, 363pp.

Limarino, C.O., Césari, S.N., Spalletti, L.A., Taboada, A.C., Isbell, J.L., Geuna, S. and Gulbreanson, E.L., 2014. A paleoclimatic review of southern South America during the late Paleozoic: a record from icehouse to extreme greenhouse conditions. Gondwana Research, 25, 1396–1421. http://dx.doi.org/doi:10.1016/j.gr.2012.12.022.

Lindeque, A., Ryberg, T., Stankiewicz, J., Weber, M. and de Wit, M., 2007. Deep crustal reflection experiment across the Southern Karoo Basin, South Africa. South Africa Journal of Geology, 110, 419–438.

Lindeque, A., de Wit, M.J., Ryberg, T., Weber, M. and Chevallier, L., 2011. Deep crustal profile across the southern Karoo Basin and Beattie magnetic anomaly, South Africa: An integrated interpretation with tectonic implications. South Africa Journal of Geology, 114, 265–292.

Lindström, S., 1995. Early Permian palynostratigraphy of the northern Heimefrontfjella mountain- range, Dronning Maud Land, Antarctica. Review of Palaeobotany and Palynology, 89, 359–415.

Lock, B.E., 1980. Flat- plate subduction and the Cape Fold Belt of South Africa. Geology, 8, 35–39.

Long, W.E., 1965. Stratigraphy of the Ohio range, Antarctica. In: J.B. Hadley (Editor). Geology and paleontology of the Antarctic. Washington, D.C., Antarctic Research Series, American Geophysical Union, 6, 71–116.

Lopes, R. da C., Lavina, E.L., Paim, P.S.G. and Goldberg, K., 2003. Stratigraphic and depositional control of coal genesis in the Rio Jacuí region (RS). In: P.S.G. Paim, U.F. Faccini and

R.G. Netto (Editors). Geometria, arquitetura e heterogeneidade de corpos sedimentares: estudo de casos. Unisinos, São Leopoldo, 187–206.

López-Gamundi, O.R., Espejo, I.S., Conaghan, P.J. and Powell, C. McA., 1994. Southern South America. In: J.J. Veevers and C. McA. Powell (Editors). Permian-Triassic Pangean Basins and Foldbelts along the Panthalassan Margin of Gondwanaland: Boulder, Colorado. Geological Society of America, Memoir 184, 281–329.

López-Gamundi, O.R., Fildani, A., Weislogel, A. and Rossello, E., 2013. The age of the Tunas formation in the Sauce Grande basin- Ventana foldbelt (Argentina): Implications for the Permian evolution of the southwestern margin of Gondwana. Journal of South American Earth Sciences, 45, 250–258.

Matsch, C.J. and Ojakangas, R. W., 1992. Stratigraphy and sedimentology of the Whiteout Conglomerate; an Upper Paleozoic glacigenic unit, Ellsworth mountains, West Antarctica. In: G.F. Webers, C. Craddock and J.F. Splettstoesser (Editors). Geology and Paleontology of the Ellsworth Mountains, West Antarctica. The Geological Society of America, Memoir 170, 37–62.

McKelvey, B.C., Webb, P.N., Gorton, M.P. and Kohn, B.P., 1970. Stratigraphy of the Beacon Supergroup between Olympus and Boomerang Ranges, Victoria Land, Antarctica. Nature, 227, 1126–1128.

McLachlan, I. R. and Anderson, A. M., 1973. A review of the evidence for marine conditions in southern Africa during Dwyka times. Palaeontologica Africana, 15, 37–64.

McLachlan, I. R. and Anderson, A. M., 1977. Fossil insect wings from the Early Permian White Band Formation, South Africa. Palaeontologica Africana, 20, 83–86.

McLachlan, I.R. and Jonker, J.P., 1990. Tuff beds in the northwestern part of the Karoo Basin. South African Journal of Geology, 93, 329–338.

Meng, Q., Liu, Z., Bruch, A.A., Liu, R. and Hu, F., 2012. Palaeoclimatic evolution during Eocene and its influence on oil shale mineralisation, Fushun basin, China. Journal of Asian Earth Sciences, 45, 95–105.

Milani E.J., 1997. Tectonic-stratigraphic evolution of the Paraná Basin and its relationship with the Phanerozoic geodynamics of south-western Gondwana. Unpublished PhD thesis, University of Federal do Rio Grande do Sul, Porto Alegre.

Milani E.J., Melo, J.H.G., Souza, P.A., Fernades, L.A. and e França, A.B., 2007. Paraná Basin. Petrobrás Geosciences Bulletin, 15 (2), 265–287.

Miller, J.M.G., 1989. Glacial advance and retreat sequences in a Permo- Carboniferous section, central Transantarctic Mountains. Sedimentology, 36, 419–430.

Miller, M.F. and Collinson, J.C., 1994. Late Paleozoic post-glacial inland sea filled by fine-grained turbidites: Mackellar Formation, central Transantarctic Mountains. In: M. Deymoux, J.M.G. Miller, E.W. Domack, N. Eyles, I.J. Fairchild and G.M. Young (Editors). The Earth's Glacial Record. Cambridge University Press, Cambridge, 215–233.

Mitchell, C., Taylor, G.K., Cox, K.G. and Shaw, J., 1986. Are the Falkland Islands a rotated microplate? Nature, 319, 131–134.

Mondol, N.H., 2015. Well logging: Principles, Applications and Uncertainties. In: K. Bjorlykke (Editor). Petroleum Geoscience: From sedimentary environments to rock physics. Springer, 16, 385–426.

Mosavel, H. and Cole, D.I., 2019. Lithostratigraphy of the Prince Albert Formation (Ecca Group, Karoo Supergroup). South African Journal of Geology, 122.4, 571–582.

Mowzer, Z. and Adams, S., 2015. Shale gas prospectivity analysis of the southern main Karoo Basin. Petroleum Agency South Africa contribution to the strategic environmental assessment, Agency Report FG 2015, 1–57.

Mroczkowska- Szerszeń, M., 2015. The analysis of pore space parameters of shale gas formations rocks within the range of 50 to 2 nm. Nafta-Gaz 2015, 12, 983–991.

DOI: 10.18668/NG2015.12.06

Nature., 2009. 'The shale revolution'. Nature 460, (7255), 551–552.

Nazeer, A., Shah, S.H., Murtaza, G. and Solangi, S.H., 2018. Possible origin of inert gases in hydrocarbon reservoir pools of the Zindapir Anticlinorium and its surroundings in the Middle Indus Basin, Pakistan. Geodesy and Geodynamics, 9, 456–473.

Nesbitt, H.W. and Young, G.M., 1982. Early Proterozoic climates and plate motions inferred from major element chemistry of lutites. Nature, 299, 715–717.

Oelofson, B. W., 1981. An anatomical and systematical study of the family Mesosauridae (Reptilia; Proganosauria) with special reference to its associated fauna and palaeoecological environment in the Whitehill Sea. Unpublished PhD thesis, University of Stellenbosch, South Africa. 164pp.

Oelofsen, B. W., 1986. A fossil shark neurocranium from the Permo-Carboniferous (lowermost Ecca Formation) of South Africa. In: T. Uyeno, R. Arai, T. Taniuchi and K. Matsuura (Editors). Indo-Pacific Fish Biology. Proceedings 2nd International Conference on Indo-Pacific Fishes. Ichthyological Society of Japan, Tokyo, 107–124.

Oelofsen, B. W., 1987. The biostratigraphy and fossils of the Whitehill and Irati shale Formations of the Karoo and Paraná Basins. In: G.C. McKenzie (Editor). Gondwana Six: Stratigraphy, Sedimentology and Palaeontology. American Geophyscial Union. Geophysical Monograph, 41, 131–138.

Oelofsen, B. W. and Araujo, D., 1987. Mesosaurus tenuidens and Stereosternum tumidum from the Permian Gondwana of both southern Africa and South America. South African Journal of Science. 83, 370–372.

Oliveira, C.M.M., Hodgson, D.M. and Flint, S.S., 2011. Distribution of soft-sediment deformation structures in clinoform successions of the Permian Ecca Group, Karoo Basin, South Africa. Sedimentary Geology, 235, 314–330.

Penn-Clarke, C. R., 2017. Pallaeoenvironmental successions and sequence stratigraphy of the Early to Middle Devonian Bokkeveld Group in the Clanwilliam sub-basin, Western Cape Province, South Africa. Ph.D thesis (unpublished), University of the Witwatersrand, 641pp.

Peters, K.E. and Cassa, M.R., 1994. Applied source-rock geochemistry. American Association of Petroleum Geologists. Memoir, 60, 93–120.

Peters, K.E., Walters, C.C. and Moldowan, J.M., 2005.The Biomarker Guide. Second edition. Biomarkers and Isotopes in petroleum systems and Earth History (II). Cambridge University Press. Doi:10.1017/CBO9781107326040

Pettijohn, E.J., 1975. Sedimentary Rocks. Harper and Row Publishers, Inc, 627pp.

Petroleum Agency of South Africa., 2020. Map of Petroleum Exploration and Production activities in South Africa. Available at:

http://www.petroleumagencysa.com/images/pdfs/Hubmap0220.pdf (viewed 9-03-20).

Piper, D.Z. and Perkins, R.B., 2004. A modern vs. Permian black shale- the hydrography, primary productivity, and water- column chemistry of deposition. Chemical Geology, 206, 177–197.

Popova, O., 2017a. Marcellus Shale Play Geology review. Independent Statistics & analysis. Report, United States Energy Information Administration. U.S. Department of Energy, Washington DC, 12pp.

Popova, O., 2017b. Utica Shale Play Geology review. Independent Statistics & analysis. Report, United States Energy Information Administration. U.S. Department of Energy, Washington DC, 21pp.

Poscher, G., 1988. Fazielle Untersuchungen in den jungpaläozoischen Sedimenten der Heimefrontfjella und der Kraulberge. Berlin. Polarforsch, 58, 180–183.

Poscher, G., 1992. Microtextural, sedimentological and geochemical investigations comparing Upper Paleozoic diamictites of Eastern Antarctica, Pre-Cambrian diamictites of Scotland and glacial sediments of the Eastern Alps. Jahrbuch der Geologischen Bundesanstalt, 135, 493– 511.

Poscher, G., 1994. Permokarbone glaziale und periglaziale Sedimentation in den Kottas-Bergen der Heimefrontfjella, Dronning Maud Land, Antarktis. Zentralblatt für Geologie und Paläontologie 1, 1992, 1373–1386.

Prezbindowski, D., 2010. Vitrinite reflectance report. Weatherford Project: HH-47677. Geochemical Services Group, Texas, 69pp.

Randall, D.E. and MacNiocaill, C., 2004. Cambrian paleomagnetic data confirm a Natal Embayment location for the Ellsworth- Whitmore Mountains. Geophysical Journal International 157, 105–116.

Reading, H.G., 1978. Sedimentary environments and facies. Blackwell Scientific Publications, Oxford, 557pp.

Reimann, C., Filzmoser, P., Garrett, R.G. and Dutter, R., 2008. Statistical Data Analysis Explained: Applied Environmental Statistics with R. John Wiley & Sons, Ltd, 181–270.

Rimmer, S.M., Thompson, J.A., Goodnight, S.A. and Robl, T.L., 2004. Multiple controls on the preservation of organic matter in Devonian- Mississippian marine black shales: geochemical and petrographic evidence. Palaeogeography, Palaeoclimatology, Palaeoecology, 215, 125–154.

Riquier, L., Tribovillard, N., Averbuch, O., Joachimski, M.M., Racki, G., Devleeschouwer, X., El Albani, A. and Riboulleau, A., 2005. Productivity and bottom water redox conditions at the Frasnian–Famennian boundary on both sides of the Eovariscan Belt: constraints from trace-element geochemistry. In: D. J. Over, J.R. Morrow and P.B. Wignall (Editors). Understanding Late Devonian and Permian- Triassic Biotic and Climatic events: Towards an integrated approach: Developments in palaeontology and stratigraphy. Elsevier Publication Corporation, 199–224.

Rocha- Campos, A.C., 1967. The Tubarão Group in the Brazilian portion of the Paraná Basin. In: J.J. Bigarella (Editor). Problems in Brazilian Devonian geology. Universidade Federal do Paraná, Curitiba, 27–102.

Rootare, H.M. and Prenzlow, C.F., 1967. Surface areas from mercury porosimeter measurements. Journal of Physical Chemistry, 71, 2733–2736.

Rowsell, D.M. and De Swardt, A.M.J., 1976. Diagenesis in Cape and Karroo sediments, South Africa, and its bearing on their hydrocarbon potential. Transactions, Geological Society of South Africa, 79, 81–145.

Rubidge, B.S., 2005. Re-uniting lost continents – Fossil reptiles from the ancient Karoo and their wanderlust. South African Journal of Geology, 108, 135–172.

Rubidge, B.S., Hancox, P.J. and Catuneanu, O., 2000. Sequence analysis of the Ecca-Beaufort contact in the southern Karoo of South Africa. South African Journal of Geology, 103, 81–96.

Rubidge, B.S., Hancox, P.J. and Mason, R., 2012. Waterford Formation in the south-eastern Karoo: Implications for basin development. South African Journal of Science, 108, 119–123.

Rubidge, B.S., Erwin, D.H., Ramezani, J., Bowring, S.A. and de Klerk, W.J., 2013. High- precision temporal calibration of Late Permian vertebrate biostratigraphy: U-Pb zircon constraints from the Karoo Supergroup, South Africa. Geology, 41, 363–366.

Salfity, J. and Gorustovich, S., 1983. Paleogeography of the Paganzo Group Basin (Upper Paleozoic). Magazine of the Argentine Geological Association, 38, 437–453.

SANS 7404-2, 2015/ISO 7404-2., 2009. Methods for the petrographic analysis of bituminous coal and anthracite. Part 2: Preparation of coal samples. International Organization of Standardization, Geneva, Switzerland, 12pp.

Santos, R.V., Souza, P.A., Oliveira, C.G., Dantas, E.L., Pimentel, M.M., Araújo, L.M. and Alvarenga, C.J.S., 2006. SHRIMP U-Pb zircon dating and palynology of bentonitic layers from the Permian Irati Formation, Paraná Basin, Brasil. Gondwana Research, 9,456–463.

Savage, N.M., 1971. A varvite ichnocoenosis from the Dwyka Series of Natal. Lethaia, 4. 217–233.

Scasso, R.A. and Mendia, J.E., 1985 Stratigraphic and paleoenvironmental features of the Paleozoic Islands of the Falkland Islands. Association Geologico Argentina Revista, 40, 26–50.

Scheffler, K., Buehmann, D. and Schwark, L., 2006. Analysis of late Palaeozoic glacial sedimentary successions in South Africa by geochemical proxies- Response to climate evolution and sedimentary environment. Palaeogeography, Palaeoclimatology, Palaeoecology, 240, 184–203.

Scheiber- Enslin, S. E., Webb, S.J. and Ebbing, J., 2014. Geophysically plumbing the main Karoo Basin, South Africa. South African Journal of Geology, 117, 275–300. doi:10.2113/gssajg.117.2.275.

Schneider, R.L., Muhlmann, H., Tommasi, E., Medeiros, R.A., Daemon, R.F. and Nogueira, A. A., 1974. Stratigraphic review of the Paraná Basin. Brazilian Congress of Geology, XXVIII, Porto Alegre, 1974 1. Anais, Porto Alegre, 41–65.

Schoell, M., 1984. Recent advances in petroleum isotope geochemistry. Organic Geochemistry, 6, 645–663.

Schoeninger, M. and DeNiro, M.J., 1983. Nitrogen and carbon isotopic composition of bone collagen from marine and terrestrial animals. Geochimica et Cosmochimica Acta, 48, 625–639

Schouten, S., Hoefs, M.J.L. and Damsté, J.S., 2000. A molecular and stable carbon isotopic study of lipids in late Quaternary sediments from the Arabian Sea. Organic Geochemistry, 31,509–521.

Schreuder, C.P. and Genis, G., 1975. Die Geologie van die Karasburgse Karookom. Annals, Geological Survey of South Africa, 10, 7–22.

Schulz, H.M., Linol, B., de Wit. M., Schuck, B., Schaepan, I. and Wirth, R., 2018. Early diagenetic signals archived in black shales of the Dwyka and Lower Ecca Groups of the southern Karoo Basin (South Africa): Keys to the deglaciation history of Gondwana during the Early Permian, and its effect on potential shale gas storage. South African Journal of Geology, 121.1, 69–94.

Schwab, V.F. and Spangenberg, J.E., 2007. Molecular and isotopic characterization of biomarkers in the Frick Swiss Jura sediments: A palaeoenvironmental reconstruction on the northern Tethys margin. Organic Geochemistry, 38, 3, 419–439.

Sheng-ke, Y., 2005. Recovery paleosalinity in sedimentary environment – an example of mudstone in Shuixigou group, southwestern margin of Turpan- Hami basin. Xin Jiang Petroleum Geology, 12 (6), 719–722.

Shiker, M.A.K., 2012. Multivariate Statistical Analysis. British Journal of Science, 6(1), 55–66.

Siad, A., Matheis, G., Utke, A. and Burger, H., 1994. Discriminant analysis as a geochemical mapping technique for lateritic covered area of South Western and Central Nigeria. ITC Journal 1994-1, Special CODATA Issue, 7–12.

Siebrits, L. B., 1989. Die sedimentology van die Formasie Carnarvon in die omgewing van Carnarvon. Unpublished MSc thesis, University of Port Elizabeth, Port Elizabeth, 92pp.

Smithard, T., Bordy, E.M. and Reid, D., 2015. The effect of dolerite intrusion on the hydrocarbon potential of the Lower Permian Whitehill Formation (Karoo Supergroup) in South Africa and southern Namibia: A preliminary study. South African Journal of Geology, 118, 489–510.

Spearman, C.E., 1904. "General Intelligence" objectively determined and measured. American Journal of Psychology, 15,201–293.

Stollhofen, H., 1999. Karoo Synrift- sedimentation und ihre tektonische kontrolle am entstehenden kontinentalrand Namibias {Karoo synrift deposition and their tectonic at the evolving continental margin of Namibia}. Zeitschrift der deutschen Geologischen Gesellschaft 149, 519–632.

Stollhofen, H., Stanistreet, I.G., Bangert, B. and Grill, H., 2000. Tuffs, tectonism and glacially related sea-level changes, Carboniferous- Permian, southern Namibia. Palaeogeography, Palaeoclimatology, Palaeoecology, 161, 127–150.

Tankard, A., Welsink, H., Aukes, P., Newton, R. and Stettler, E., 2009. Tectonic evolution of the Cape and Basins of South Africa. Marine and Petroleum Geology, 26, 1379–1412.

Tankard, A., Welsink, H., Aukes, P., Newton, R. and Stettler, E., 2012. Geodynamic interpretation of the Cape and the Karoo basins, South Africa. Phanerozoic Passive Margin, Cratonic Basins and Global Tectonics Maps. USA and UK: Elsevier, 869pp.

Taylor, S.R. and McLennan, S.M., 1985. The Continental Crust. Its composition and evolution. Blackwell Science, 312pp.

Taylor, G.K. and Shaw, J., 1989. The Falkland Islands: new palaeomagnetic data and their origin as a displaced terrane from southern Africa. American Geophysical Union monograph, 50, 59–72.

Thamm, A.G. and Johnson, M.R., 2006. The Cape Supergroup. In: M.R. Johnson, C.R., Anhaeusser and R.J. Thomas (Editors). The geology of South Africa. Geological Society of South Africa, Johannesburg, Council for Geoscience, 443–460.

Theron, J.N. and Blignault, H.J., 1975. A model for the Sedimentation of the Dwyka glacials in the southwestern Cape. In: C.J. Campbell (Editor). Gondwana Geology. National University. Press, Canberra, 347–356.

Theron, J.N., Wickens, H.de V. and Gresse, P.G., 1991. Die geologie van die gebied Ladismith. Explanation of Sheet 3320 (1: 250 000). Geological Survey, Republic of South Africa, 99pp.

Tissot, B., Durand, B., Espitalie, J. and Combaz, A., 1974. Influence of the nature and diagenesis of organic matter in the formation of petroleum. AAPG bulletin, 58, 499–506.

Tissot, B.P. and Welte, D.H., 1984. Petroleum formation and occurrence. Second revised and enlarged edition. Springer-Verlag Berlin, 699pp.

Tohver, E., Cawood, P.A., Rossello, E., Lopez de Luchi, M.G., Rapalini, A. and Jourdan, F., 2008. New SHRIMP U- Pb and 40Ar/39 Ar constraints on the crustal stabilization of southern South America, from the margin of the Rio de Plata (Sierra de Ventana) craton to northern Patagonia. America Geophysical Union. Fall Meeting, EOS (Abstract), T23C-2052.

Trewin, N.H., Macdonald, D.I.M. and Thomas, C.G.C., 2002. The stratigraphy and sedimentology of the Permian of the Falkland Islands: lithostratigraphic and palaeoenvironment links with South Africa. Journal of the Geological Society, London, 159, 5–19.

Tribovillard, N., Riboulleau, A., Lyons, T. and Baudin, F., 2004. Enhanced trapping of molybdenum by sulfurized organic matter of marine origin as recorded by various Mesozoic formations. Chemical Geology, 213, 385–401.

Turner, B.R., 1999. Tectonostratigraphic development of the upper Karoo foreland basin: orogenic unloading versus thermally induced Gondwana rifting. Journal of African Earth Sciences, 28, 215–238.

Twine B.A., Jackson M., Potgieter, R., Anderson, D. and Soobyah, L., 2012. Karoo shale gas report. Econometrix (Pty) Ltd, South Africa, 76pp.

Van Vuuren, C.J., 1983. A basin analysis of the northern facies of the Ecca Group. Unpublished PhD thesis, University of the Orange Free State, South Africa, 249pp.

Van Vuuren, C.J., Broad, D.S., Jungslager, E.H.A., Roux, J. and McLachlan, I.R., 1998. Oil and gas. In: M.G.C Wilson and C.R Anhaeusser (Editors). Mineral Resources of the Republic of South Africa: Handbook. Geological Survey of South Africa, 16, 483–494.

Veevers, J.J., 1990. Tectonic- climatic supercycle in the billion- year plate tectonic eon: Permian Pangean icehouse alternates with cretaceous dispersed continents greenhouse. Sedimentary Geology, 68, 1–16.

Veevers, J.J., 2000. Billion-year earth history of Australia and neighbours in Gondwanaland. Gemoc Press, Sydney, 388pp.

Veevers, J.J., 2004. Gondwanaland from 650–500 Ma assembly through 320 Ma merger in Pangea to 185–100 Ma breakup: supercontinental tectonics via stratigraphy and radiometric dating. Earth-Science Reviews, 68, 1–132.

Veevers, J.J., Cole, D.I. and Cowan, E., 1994. Southern Africa: Karoo Basin and Cape Fold Belt. In: J.J. Veevers and C. McA Powell (Editors). Permian-Triassic Pangean Basins and Foldbelts along the Panthalassan Margin of Gondwanaland. Geological Society of America, Memoir 184, 223–280.

Veevers, J.J. and Saeed, A., 2007. Central Antarctic provenance of Permian sandstones in Dronning Maud Land and the Karoo Basin: Integration of U-Pb and TDM ages and host- rock affinity from detrital zircons. Sedimentary Geology, 202, 653–676.

Viljoen, J.H.A., 1992. Lithostratigraphy of the Collingham Formation (Ecca Group), including the Zoute Kloof, Buffels River and Wilgehout River Members and the Matjiesfontein Chert Bed. Lithostratigraphic Series, South African Committee for Stratigraphy, Geological Survey of South Africa, Pretoria, 22, 10pp.

Viljoen, J.H.A., 1994. Sedimentology of the Collingham Formation, Karoo Supergroup. South African Journal of Geology, 97, 167–183.

Viljoen, J.H.A., 2005. Tierberg Formation. Lithostratigraphic Catalogue Series, South African Committee for Stratigraphy, Council for Geoscience, Pretoria, 8, 8-37–8-40.

Visser, J.N.J., 1986. Lateral lithofacies relationships in the glacigene Dwyka Formation in the western and central parts of the Karoo Basin. Transactions of the Geological Society of South Africa, 89, 373–383.

Visser, J.N.J., 1987. The palaeogeography of part of southwestern Gondwana during the Permo-Carboniferous glaciation. Palaeography, Palaeoclimatology, Palaeoecology, 61, 205–219.

Visser, J.N.J., 1989. The Permo- Carboniferous Dwyka Formation of Southern Africa: deposition by a predominantly subpolar marine ice sheet. Palaeography, Palaeoclimatology, Palaeoecology, 70, 377–391.

Visser, J. N. J., 1990. The age of the late Palaeozoic glacigene deposits in southern Africa. South African Journal of Geology, 93, 366–375.

Visser, J.N.J., 1991. Self-destructive collapse of the Permo-Carboniferous marine ice sheet in the Karoo Basin: evidence from the southern Karoo. South African Journal of Geology, 94, 255–262.

Visser, J. N. J., 1992. Deposition of the Early to Late Permian Whitehill Formation during a sea-level highstand in a juvenile foreland basin. South African Journal of Geology, 95, 181–193.

Visser, J.N.J., 1993. Sea-level changes in a back-arc - foreland transition: the late Carboniferous - Permian Karoo Basin of South Africa. Sedimentary Geology, 83, 115–131.

Visser, J.N.J., 1994. A Permian argillaceous syn- to post- glacial foreland sequence in the Karoo Basin, South Africa. In: M. Deynoux, J.M.G. Miller, E.W. Domack, N. Eyles, I.J. Fairchild and G.W. Young (Editors). Earth's Glacial Record. Cambridge University Press, Cambridge, 193–203.

Visser, J.N.J., 1997. Deglaciation sequences in the Permo-Carboniferous Karoo and Kalahari basins of southern Africa: a tool in the analysis of cyclic glaciomarine basin fills. Sedimentology, 44, 507–521.

Visser, J.N.J. and Kingsley, C.S., 1982. Upper Carboniferous glacial valley sedimentation in the Karoo Basin, Orange Free State. Transactions, Geological Society of South Africa, 85, 71–79.

Visser, J.N.J. and Loock, J.C., 1988. Sedimentary facies of the Dwyka Formation associated with the Nooitgedacht glacial pavements, Barkly West District. South African Journal of Geology, 91, 38–48.

Visser, J. N.J. and Praekelt, H.E., 1996. Subduction, meg- shear systems and Late Palaeozoic basin development in the African segment of Gondwana. Geologische Rundschau, 85, 632–646.

Visser, J.N.J., Van Niekerk, S.W. and Van der Merwe, S.W., 1997. Sediment transport of the Late Palaeozoic glacial Dwyka Group in the southwestern Karoo Basin. South African Journal of Geology, 100, 223–236.

Visser, J.N.J., Von Brunn, V. and Johnson, M.R., 1990. [Carboniferous- Permian] [Karoo Sequence] Dwyka Group. Catalogue of South African Lithostratigraphic Units. South Africa Committee for Stratigraphy, 2–17.

Visser, J.N.J. and Young, G.M., 1990. Major element geochemistry and paleoclimatology of the Permo- Carboniferous glacigene Dwyka Formation and post-glacial mudrocks in southern Africa. Palaeogeography, Paleoclimatology, Palaeoecology, 81, 49–57.

Von Brunn, V., 1994. Glaciogenic deposits of the Permo- Carboniferous Dwyka Group in the eastern region of the Karoo Basin, South Africa. In: M. Deynoux, J.M.G. Miller, E.W. Domack, N. Eyles, I.J. Fairchild and G.W. Young (Editors). Earth's glacial record. Cambridge University Press, Cambridge, 60–69.

Von Brunn, V., 1996. The Dwyka Group in the northern part of KwaZulu-Natal, South Africa: sedimentation during late Palaeozoic deglaciation. Palaeogeography, Palaeoclimatology, Palaeoecology, 125, 141–163.

Ward, J.H., 1963. Hierarchical grouping to optimize an objective function. Journal of the American Statistical Association, 58 (301), 236–244.

Watts, D. R. and Bramall, A.M., 1981. Paleomagnetic evidence for a displaced terrain in western Antarctic. Nature, 293, 638–641.

Webb, P.A., 2001. An introduction to the physical characterization of materials by mercury intrusion porosimetry with emphasis on reduction and presentation of experimental data. Micrometrics Instrument Corporation, Norcross, 22pp.

Webers, G.F., Craddock, C. and Splettstoesser, J.F., 1992. Geologic history of the Ellsworth Mountains, West Antarctica. In: G.F. Webers, C. Craddock and J.F. Splettstoesser (Editors). Geology and Paleontology of the Ellsworth Mountains, West Antarctica. The Geological Society of America, Memoir 170, 1–8.

Weissert, H., Joachimski, M. and Sarnthein, M., 2008. Chemostratigraphy. Newsletters on Stratigraphy, 42(3), 145–179.

Werner, M., 2006. The stratigraphy, sedimentology, and age of the Late Palaeozoic Mesosaurus Inland Sea, SW- Gondwana: new implications from studies on sediments and altered pyroclastic layers of the Dwyka and Ecca Group (lower Karoo Supergroup) in southern Namibia. Unpublished PhD thesis, University of Würzburg, Germany, 428pp.

White, I.C., 1908. Relatório sobre as Coal Measures e rochas associadas ao sul do Brasil. Rio de Janeiro, Com. Est. Minas Carvão de Pedra Brasil, Pt.1, 300pp.

White, W.M., 2013. Geochemistry. Chapter 9: Stable Isotope Geochemistry. John Wiley & Sons, Ltd, U.S. A., 361–420.

Wickens, H. de V., 1984. Die stratigrafie en sedimentology van die groep Ecca wes van Sutherland. Unpublished MSc thesis, University of Port Elizabeth, Port Elizabeth, 86pp.

Wickens, H. de V., 1992. Submarine fans of the Permian Ecca Group in the SW Karoo Basin: Their origin and reflection on the tectonic evolution of the basin and its source areas. In: M.J. de Wit and I. Ransome (Editors). Inversion Tectonics of the Cape Fold Belt, Karoo and Cretaceous Basins of Southern Africa. Balkema, Rotterdam, 117–125.

Wignall, P.B. and Twitchett, R.J., 1996. Oceanic anoxia and the end Permian mass extinction. Science, 272, 1155–1158.

Willis. J., Feather. C. and Turner. K., 2014. Guidelines for XRF analysis. Setting up programmes for WDXRF and EDXRF. South Africa by Shumani Mills Communications, 544pp.

Winter, H. de la R. and Venter, J.J., 1970. Lithostratigraphic correlation of recent deep boreholes in the Karroo-Cape sequence. In: S.H. Haughton (Editor). Proceedings of the Second Gondwana Symposium. Council for Scientific and Industrial Research, 197–204.

Wireline Alliance., 2018. Wireline lithology log (Borehole R01-BW). Torque Africa Exploration. Unpublished data, South Africa, 7pp.

Wolmarans, L.G. and Kent, L.E., 1982. Geological investigations in Western Dronning Maud Land, Antarctica- a synthesis. South African Journal of Antarctic Research, Supplement, 2, 1–93.

Zachos, J., Pagani, M., Sloan, L., Thomas, E. and Billups, K., 2001. Trends, rhythms, and aberrations in global climate 65 Ma to present. Science, 292 (5517), 686–693.

Zhao, J., Jin, Z., Jin, Z., Geng, Y., Wen, X. and Yan, C., 2016. Applying sedimentary geochemical proxies for paleoenvironment interpretation of organic- rich shale deposition in the Sichuan Basin, China. International Journal of Coal Geology, 163, 52–71.

Zhongsheng, S., Kaiyuan, C., Jun, S., Baojun, L., Hujun, H. and Gang, L., 2003. Feasibility analysis of the application of the ratio of strontium to barium on the identifying sedimentary environment. Fault- Block Oil & Gas Field, 10 (20), 12–16.

Appendices

Appendix 1: Field locality information of samples collected along the Witbergs River section near Laingsburg.

Date	Sample No.	Lithology/Stratigraphy	X	Y	Photo Number	Dip of Beds
2017/02/02	None	Dwyka Group/ Prince Albert Formation contact	20.86475	-33.24142	2252-2255	
2017/02/02	HM1	Diamictite (Dwyka Group)	20.86475	-33.24142		
2017/02/02	HM2	Shale (Prince Albert Fm)	20.86475	-33.24142		008/27
2017/02/02	HM3	Shale (Prince Albert Fm)	20.86511	-33.24125	2256-2257	008/20
2017/02/02	HM4	Ferruginous bed (Prince Albert Fm)	20.86511	-33.24125	2258-2261.	
2017/02/02	HM5	Ferruginous bed (Prince Albert Fm)	20.86508	-33.24111	2262-2263	002/40
2017/02/02	None	Continuous outcrop (Prince Albert Fm)	20.86497	-33.24108		005/30
2017/02/02	HM6	Shale (Prince Albert Fm)	20.865	-33.24089	2264-2266	004/34
2017/02/02	HM7	Shale (Prince Albert Fm)	20.86503	-33.24086		010/25
2017/02/02	HM8	Shale (Prince Albert Fm)	20.86508	-33.24072	2267-2268	008/30
2017/02/02	HM9	Continuous outcrop (Prince Albert Fm)	20.86517	-33.24064	2269-2270	012/32
2017/02/02	HM10	Shale (Prince Albert Fm)	20.86542	-33.24028	2271-2272	005/34
2017/02/02	HM11	Shale (Prince Albert Fm)	20.86544	-33.24014	2273-2274	002/60

2017/02/02	HM12	Ferruginous bed (Prince Albert Fm)	20.86558	-33.23992	2277-2278	004/45
2017/02/02	None	Ferruginous bed (Prince Albert Fm)	20.86572	-33.23958		
2017/02/02	HM13	Shale (Prince Albert Fm)	20.866	-33.23967	2279-2280	005/52
2017/02/02	HM14	Shale (Prince Albert Fm)	20.866	-33.23958	2282-2283	
2017/02/02	HM15	Ferruginous bed (Prince Albert Fm)	20.866	-33.23958		010/48
2017/02/02	None	Tuff? (Prince Albert Fm)	20.86597	-33.23942	2284-2285	
2017/02/02	HM16	Shale (Prince Albert Fm)	20.86597	-33.23942		020/40
2017/02/02	HM17	Shale (Prince Albert Fm)	20.866	-33.23931	2286, 2289-2291	005/44
2017/02/02	None	Prince Albert/Whitehill Formation contact	20.86622	-33.23939	2292-2294	
2017/02/02	HM18	Shale (Whitehill Formation)	20.86622	-33.23939		014/44
2017/02/02	HM19	Shale (Whitehill Formation)	20.86622	-33.23939		

Appendix 2: Field locality information of samples collected along the Tweefontein – Ganskop road section, Tankwa Karoo.

Date	Sample No	Lithology/Stratigraphy	X	Y	Photo Number	Dip of Beds
2017/09/02	HM20	Diamictite (Dwyka Group)	19.66606	-32.34239	2295-2296	
2017/09/02	none	Shale (Prince Albert Fm)	19.66872	-32.34397		
2017/09/02	HM21	Shale (Prince Albert Fm)	19.66967	-32.34397		
2017/09/02	HM22	Shale (Prince Albert Fm)	19.66986	-32.34492	2300-2301	
2017/09/02	HM23	Ferruginous bed (Prince Albert Fm)	19.67061	-32.34533	2302-2303	
2017/09/02	HM24	Shale (Prince Albert Fm)	19.67092	-32.34575	2304-2307	
2017/09/02	HM25	Shale (Prince Albert Fm)	19.67178	-32.34575	2308-2309	
2017/09/02	HM26	Slightly silty shale (Prince Albert Fm)	19.67333	-32.34656	2310-2311	120/4
2017/09/02	HM27	Ferruginous bed (Prince Albert Fm)	19.67431	-32.34689	2312-2313	
2017/09/02	HM28	Ferruginous bed (Prince Albert Fm)	19.67594	-32.34717	2314-2315	135/3
2017/09/02	HM29	Ferruginous bed (Prince Albert Fm)	19.67742	-32.34803	2316-2317	
2017/09/02	HM30	Shale (Prince Albert Fm)	19.67994	-32.34964	2318	
2017/09/02	HM31	Ferruginous bed (Prince Albert Fm)	19.6835	-32.35153	2319-2320	

2017/09/02	HM32	Shale (Prince Albert Fm)	19.68811	-32.3555	2321-2322	
2017/09/02	HM33	Ferruginous bed (Prince Albert Fm)	19.692	-32.35875	2323-2324	
2017/09/02	HM34	Shale (Prince Albert Fm)	19.69339	-32.35978	2325	
2017/09/02	HM35	Slightly silty shale (Prince Albert Fm)	19.69594	-32.36206	2326-2327	
2017/09/02	HM36	Shale (Prince Albert Fm)	19.69625	-32.36253	2328-2329	
2017/09/02	HM37	Shale (Prince Albert Fm)	19.69733	-32.36378	2330-2331	
2017/09/02	HM38	Slightly silty shale (Prince Albert Fm)	19.69939	-32.36433	2332-2336	
2017/09/02	HM39	Shale (Whitehill Fm)	19.69919	-32.36436	2332-2336	

Appendix 3: Field locality information of samples collected along the Gamka River section west of Prince Albert.

Date	Sample No	Lithology/Stratigraphy	X	Y	Photo Number	Dip of Beds
17/03/2017	HM40	Siltstone and silty mudstone (Dwyka Group)	21.77228	-33.2216	2390-2391	007/68
17/03/2017	HM41	Shale (Prince Albert Fm)	21.77225	-33.2216	2390-2391	007/68
17/03/2017	HM42	Shale (Prince Albert Fm)	21.77225	-33.2216	2392-2393	005/88
17/03/2017	HM43	Shale (Prince Albert Fm)	21.77228	-33.2216	2394-2395	008/82
17/03/2017	HM44	Ferruginous bed (Prince Albert Fm)	21.77233	-33.2215	2396-2397	002/90
17/03/2017	HM45	Shale (Prince Albert Fm)	21.77233	-33.2215	2396-2397	002/90
17/03/2017	HM46	Shale (Prince Albert Fm)	21.77231	-33.2215	2398-2399	002/63
17/03/2017	HM47	Ferruginous bed (Prince Albert Fm)	21.77236	-33.2214	2400-2401	002/63
17/03/2017	HM48	Shale (Prince Albert Fm)	21.77239	-33.2213	2402-2403	002/63
17/03/2017	HM49	Shale (Prince Albert Fm)	21.77283	-33.2213	2406	005/70
17/03/2017	HM50	Shale (Prince Albert Fm)	21.77275	-33.2212	2404-2405	005/70
17/03/2017	HM51	Shale (Prince Albert Fm)	21.77278	-33.2211	2407-2408	014/70
17/03/2017	HM52	Shale (Prince Albert Fm)	21.77283	-33.2211	2409-2410	014/70

17/03/2017	HM53	Ferruginous bed (Prince Albert Fm)	21.77289	-33.2211	2411	002/72
17/03/2017	HM54	Shale (Prince Albert Fm)	21.77289	-33.2211	2412-2413	002/72
17/03/2017	HM55	Shale (Prince Albert Fm)	21.77286	-33.2210	2414-2415	002/72
17/03/2017	HM56	Dolomite concretion (Whitehill Fm)	21.77328	-33.2209	2416-2417	

Appendix 4: Borehole KZF-01: Locality information of samples collected in the Tankwa Karoo, northeast of Ceres.

Date	Sample No	Lithology/ Stratigraphy	X	Y	Depth of sample taken (m)	Photo Number
5/08/2017	HM57	Shale (Whitehill Fm)	19.825839	-32.841786	439.61-439.95	022-023
5/08/2017	HM58	Shale (Prince Albert Fm)	19.825839	-32.841786	440.81-441.17	026
5/08/2017	HM59	Shale and siltstone (Prince Albert Fm)	19.825839	-32.841786	442.17-442.56	0027- 0028
5/08/2017	HM60	Shale (Prince Albert Fm)	19.825839	-32.841786	479.72-480.10	0032-0034
5/08/2017	HM61	Shale (Prince Albert Fm)	19.825839	-32.841786	484.22-484.66	0034-0037
5/08/2017	HM62	Shale (Prince Albert Fm)	19.825839	-32.841786	490.39-490.91	0042- 0043
5/08/2017	HM63	Shale (Prince Albert Fm)	19.825839	-32.841786	496.30-496.84	0044-0045
5/08/2017	HM64	Shale (Prince Albert Fm)	19.825839	-32.841786	500.50-500.82	0046- 0047
5/08/2017	HM65	Shale (Prince Albert Fm)	19.825839	-32.841786	505.10-505.47	0048- 0049
5/08/2017	HM66	Shale (Prince Albert Fm)	19.825839	-32.841786	515.36-515.69	0050-0051
5/08/2017	HM67	Shale (Prince Albert Fm)	19.825839	-32.841786	517.10-517.39	0052-0053
5/08/2017	HM68	Shale (Prince Albert Fm)	19.825839	-32.841786	523.53-523.76	0054- 0055

5/08/2017	HM69	Shale (Prince Albert Fm)	19.825839	-32.841786	529.60-529.86	0056- 0057
5/09/2017	HM70	Shale (Prince Albert Fm)	19.825839	-32.841786	537.14-537.44	0060- 0061
5/09/2017	HM71	Shale (Prince Albert Fm)	19.825839	-32.841786	542.61-542.89	0062- 0063
5/09/2017	HM72	Shale (Prince Albert Fm)	19.825839	-32.841786	549.62-549.92	0064- 0065
5/09/2017	HM73	Shale (Prince Albert Fm)	19.825839	-32.841786	556.08-556.40	0066-0067
5/09/2017	HM74	Shale (Prince Albert Fm)	19.825839	-32.841786	562.14-562.35	0068- 0069
5/09/2017	HM75	Shale (Prince Albert Fm)	19.825839	-32.841786	566.96-567.14	0070- 0071
5/09/2017	HM76	Shale (Prince Albert Fm)	19.825839	-32.841786	573.15-573.45	0072- 0073
5/09/2017	HM77	Shale (Prince Albert Fm)	19.825839	-32.841786	578.04-578.26	0074- 0075
5/09/2017	HM78	Shale (Prince Albert Fm)	19.825839	-32.841786	583.50-583.69	0076- 0077
5/09/2017	HM79	Shale (Prince Albert Fm)	19.825839	-32.841786	588.54-588.73	0078- 0079
5/09/2017	HM80	Shale (Prince Albert Fm)	19.825839	-32.841786	595.08-595.32	0080- 0081
5/09/2017	HM81	Shale (Prince Albert Fm)	19.825839	-32.841786	600.48-600.70	0082- 0083
5/09/2017	HM82	Shale (Prince Albert Fm)	19.825839	-32.841786	606.74-606.91	0084- 0085
5/09/2017	HM83	Shale (Prince Albert Fm)	19.825839	-32.841786	612.45-612.69	0086- 0087, 0150- 0157

5/09/2017	HM84	Shale (Prince Albert Fm)	19.825839	-32.841786	617.79-618.16	0088- 0089, 0152
5/09/2017	HM85	Shale (Prince Albert Fm)	19.825839	-32.841786	624.40-624.72	0090- 0091, 0153
5/09/2017	HM86	Shale (Prince Albert Fm)	19.825839	-32.841786	628.54-628.94	0092- 0093, 0154
5/09/2017	HM87	Shale (Prince Albert Fm)	19.825839	-32.841786	634.09-634.53	0094- 0095, 0155
5/09/2017	HM88	Shale (Prince Albert Fm)	19.825839	-32.841786	639.29-639.61	0096- 0097, 0156
5/09/2017	HM89	Shale (Prince Albert Fm)	19.825839	-32.841786	645.45-645.76	0098- 0099, 0157
5/09/2017	HM90	Shale (Prince Albert Fm)	19.825839	-32.841786	651.52-651.84	0100- 0101, 0158
5/09/2017	HM91	Shale (Prince Albert Fm)	19.825839	-32.841786	656.60-656.84	0102- 0103
5/09/2017	HM92	Diamictite (Dwyka Group)	19.825839	-32.841786	657.51-657.80	0106- 0107, 0159

Appendix 5: Borehole KWV-01: Locality information of samples collected near Willowvale, Eastern Cape.

Date	Sample No	Lithology/ Stratigraphy	X	Y	Depth of sample taken	Photo Number
5/10/2017	HM93	Shale (Whitehill Fm)	28.585820	-32.244247	2306.96-2307.28	0110-0112, 0138
5/10/2017	HM94	Shale (Prince Albert Fm)	28.585820	-32.244247	2309.05-2309.37	0113-0114, 0139
5/10/2017	HM95	Shale (Prince Albert Fm)	28.585820	-32.244247	2311.98-2312.36	0115-0116, 0140
5/10/2017	HM96	Shale (Prince Albert Fm)	28.585820	-32.244247	2315.08-2315.37	0117-0118, 0141
5/10/2017	HM97	Shale (Prince Albert Fm)	28.585820	-32.244247	2317.59-2317.88	0119-0120, 0142
5/10/2017	HM98	Shale (Prince Albert Fm)	28.585820	-32.244247	2320.40-2320.73	0121-0122, 0143
5/10/2017	HM99	Shale (Prince Albert Fm)	28.585820	-32.244247	2323.39-2323.72	0123-0124, 0144
5/10/2017	HM100	Shale (Prince Albert Fm)	28.585820	-32.244247	2326.70-2327.00	0125-0126, 0145

5/10/2017	HM101	Shale (Prince Albert Fm)	28.585820	-32.244247	2329.56-2329.87	0127-0128, 0146
5/10/2017	HM102	Rhythmite (Prince Albert Fm)	28.585820	-32.244247	2332.24-2332.56	0129-0130, 0147
5/10/2017	HM103	Rhythmite (Prince Albert Fm)	28.585820	-32.244247	2335.14-2335.48	0131-0132, 0148
5/10/2017	HM104	Diamictite (Dwyka Group)	28.585820	-32.244247	2338.77-2339.18	0135-0137, 0149

Appendix 6: Field locality information of samples collected along the R344 Debruinspoort section near Grahamstown.

Date	Sample No.	Lithology/Stratigraphy	X	Y	Photo Number	Dip of Beds
21/02/2018	HM105	Silty mudstone with sparse clasts (Dwyka Group)	20.86475	-33.24142	2252-2255	
21/02/2018	HM106	Shaly mudstone (Prince Albert Fm)	20.86475	-33.24142		017/27
21/02/2018	HM107	Shaly mudstone (Prince Albert Fm)	20.86475	-33.24142		
21/02/2018	HM108	Shaly mudstone (Prince Albert Fm)	20.86511	-33.24125	2256-2257	010/04
21/02/2018	CONTACT	Black carbonaceous shale (Whitehill Fm)	20.86511	-33.24125	2258-2261	
21/02/2018	HM109	Carbonaceous shale (Whitehill Fm)	20.86508	-33.24111	2262-2263	

Appendix 7: Field locality information of samples collected along the R67 Grahamstown to Fort Beaufort main road, Ecca Pass.

Date	Sample No	Lithology/Stratigraphy	X	Y	Photo Number	Dip of Beds
22/02/18	Inferred Dwyka contact measured to first PAF outcrop	Diamictite (Dwyka Group)	26.62724	-33.21746		
22/02/18	HM116	Shaly mudstone (Dwyka Group)	26.62702	-33.21883		
22/02/18	HM110	Shaly mudstone (Prince Albert Fm)	26.62728	-33.21708	0996-0998	
22/02/18	HM111	Shaly mudstone (Prince Albert Fm)	26.62724	-33.21695	0969-0970	
22/02/18	HM112	Shaly mudstone (Prince Albert Fm)	26.62728	-33.21675	0971-0972	
22/02/18	HM113	Shaly mudstone (Prince Albert Fm)	26.6273	-33.21661	0973-0976	024/36
22/02/18	HM114	Shaly mudstone (Prince Albert Fm)	26.62733	-33.21648	0977-0979	026/50
22/02/18	HM115	Shale (Whitehill Fm)	26.62736	-33.21646	0980-0987	036/35

Appendix 8: Field locality information of samples collected along Pluto's Vale section northeast of Grahamstown, Eastern Cape.

Date	Sample No	Lithology/Stratigraphy	X	Y	Photo Number	Dip of Beds
22/2/18	HM117	Diamictite (Dwyka Group)	26.69349	-33.23469	0999-1000	
22/2/18	HM118	Silty mudstone (Prince Albert Fm)	26.69349	-33.23469	1001-1005	
22/2/18	HM119	Shale (Prince Albert Fm)	26.69349	-33.23469	1006-1008	010/20
22/2/18	No sample	Shale (Prince Albert Fm)	26.69351	-33.23425	1009-1011	010/12
22/2/18	HM120	Shaly mudstone (Prince Albert Fm)	26.6939	-33.23407	1012-1013	
22/2/18	HM121	Silty mudstone (Prince Albert Fm)	26.69404	-33.23419	1017-1019	000/20
22/2/18	HM122	Shaly mudstone(Prince Albert Fm)	26.69404	-33.23419	1021-1020	
22/2/18	HM123	Shaly mudstone (Prince Albert Fm)	26.69404	-33.23419	1022-1024	
22/2/18	HM124	Shaly mudstone (Prince Albert Fm)	26.69497	-33.23388	1025-1031	

Appendix 9: Borehole SA 1/66: Locality information of samples collected near Merweville, Western Cape.

Date	Sample No	Lithology/Stratigraphy	X	Y	Depth of sample interval (m)	Photo Number
14/03/2018	HM125	Shale (Whitehill Fm)	21.33352	-32.67475	2785.74-2789.08	1043- 1046
14/03/2018	HM126	Massive shale (Prince Albert Fm)	21.33352	-32.67475	2789.08-2802.16	1049- 1051
14/03/2018	no sample	Massive shale (Prince Albert Fm)	21.33352	-32.67475	2802.16-2806.59	1052- 1053
14/03/2018	HM127 and HM128	Interbedded light and dark grey shale (Prince Albert Fm)	21.33352	-32.67475	2806.59-2828.78	1054-1055
14/03/2018	HM129	Massive shale (Prince Albert Fm)	21.33352	-32.67475	2828.78-2832.05	1056- 1057
14/03/2018	HM130	Massive shale (Prince Albert Fm)	21.33352	-32.67475	2832.05-2843.16	1058- 1059
14/03/2018	HM131	Massive shale (Prince Albert Fm)	21.33352	-32.67475	2843.16-2857.23	1060-1062
14/03/2018	HM132	Interbedded light and dark grey shale (Prince Albert Fm)	21.33352	-32.67475	2857.23-2861.93	1063- 1065
14/03/2018	HM133	Massive shale (Prince Albert Fm)	21.33352	-32.67475	2861.93-2863.55	1066- 1068
		CORE MISSING/CORE LOSS	21.33352	-32.67475	2863.55-2879	

14/03/2018	HM134	Massive shale (Prince Albert Fm)	21.33352	-32.67475	2879-2891.95	1069- 1072
14/03/2018	no sample	Massive shale (Prince Albert Fm)	21.33352	-32.67475	2891.95-2892.17	1073
14/03/2018	HM135	Massive shale (Prince Albert Fm)	21.33352	-32.67475	2892.17-2915.09	1076- 1078
14/03/2018	no sample	Massive shale (Prince Albert Fm)	21.33352	-32.67475	2915.09-2915.11	1079-1080
14/03/2018	HM136	Massive shale (Prince Albert Fm)	21.33352	-32.67475	2915.12-2915.62	1081- 1083
14/03/2018	no sample	Massive shale (Prince Albert Fm)	21.33352	-32.67475	2916.13-2916.23	1084- 1085
14/03/2018	HM137	Massive shaley mudstone (Prince Albert Fm)	21.33352	-32.67475	2916.52-2916.82	1086- 1087
14/03/2018	HM138	Massive silty mudstone (Prince Albert Fm)	21.33352	-32.67475	2916.82-2917.10	1088- 1090
14/03/2018	HM139	Dropstone Argillite (Dwyka Group)	21.33352	-32.67475	2919.85-2926.24	1091- 1094

Appendix 10: Borehole R01-BW log (logged by D. Cole and H. Mosavel)

Depth top (m)	Depth bottom (m)	Water Strike Depths	Photo (DRY chips)	Colour (Munsell colour)	Lithology	Description	Radioactivity
0	1		105-1095	N7, 5YR 2/1	Shale		None
1	2		105-1095	5YR 6/1	Shale		None
2	3		105-1095	5YR 6/1; N7	Shale and siltstone	Shale 5YR 6/1 (2-2.5m) and siltstone N7 (2.5- 3m)	None
3	4		105-1095	N7, 5B 9/1	Silty shale	Calcareous	None
4	5		105-1096	N4- N5, 5YR 6/1	Shale		None
5	6		105-1096	N5- N6, 5YR 4/1	Shale		None
6	7		105-1096	N5- N6, 5YR 4/1	Shale		None
7	8		105-1096	N4- N5, 5GY 4/1	Shale	Slightly calcareous	None
8	9		105-1096	N5, 5GY 4/1, 5YR 6/1	Shale		None
9	10		105-1097	N5- N6, 5YR 3/2	Shale		None
10	11		105-1097	N4, 5Y 4/1	Shale		None

11	12		105-1097	N5- N6, 5GY 4/1	Shale		None
12	13		105-1097	N5- N6, 5GY 4/1	Shale		None
13	14		105-1097	5YR 4/1, N4- N5	Shale		None
14	15		105-1098	N5, 5Y 4/1	Shale		None
15	16		105-1098	N5	Shale		None
16	17		105-1098	N4- N5, 5YR 4/1	Shale		None
17	18		105-1098	N5- N6	Shale	Slightly silty	None
18	19		105-1098	N5-N6, 5YR 6/1	Shale		None
19	20		105-1099	N5-N6, 5YR 4/1	Shale		None
20	21		105-1099	N5-N6	Shale	Silty	None
21	22		105-1099	N5- N6	Shale	Silty	None
22	23		105-1099	N5, 5YR 4/1	Shale	N5 (22- 22.5m) and 5YR 4/1 (22.5- 23m)	None
23	24		105-1099	5YR 4/1; N5- N6	Shale and silty shale	5YR 4/1 (23- 23.3m) and N5- N6 (23.3- 24m)	None
24	25		105-1100	N5- N6, 5Y 4/1	Shale	Silty, slightly calcareous	None
25	26		105-1100	N5- N6	Shale	Slightly silty	None

26	27		105-1100	N5- N6, 5YR 6/1	Shale		None
27	28		105-1100	N5- N6	Shale	Silty	None
28	29		105-1100	N5- N6	Shale	Silty	None
29	30		105-1101	N5	Shale	Silty	None
30	31		105-1101	N5- N6, 5YR 4/1	Shale		None
31	32		105-1101	N5, 5YR 4/1, 5GY 4/1	Shale		None
32	33		105-1101	N5- N6, 5Y2/1	Shale	Silty	None
33	34		105-1101	N5, 5YR 4/1	Shale		None
34	35		105-1101	N5- N6, 5YR 4/1	Shale	Silty	None
35	36		105-1101	N5, 5YR 4/1	Shale	Silty	None
36	37		105-1102	5YR 4/1, N4-N5	Shale		None
37	38		105-1102	N4- N5, 5YR4/1	Shale		None
38	39		105-1102	N4- N5, 5YR4/1	Shale		None
39	40		105-1103	N4, 5GY 4/1	Shale	Slightly calcareous	None

40	41		105-1103	N4, 5YR 4/1	Shale	Calcareous	None
41	42		105-1103	5YR 4/1, N5	Shale	Silty	None
42	43		105-1103	N5, 5GY 4/1	Shale		None
43	44		105-1103	5GY 4/1, 5YR 4/1	Shale	Calcareous	None
44	45		105-1105	5GY 4/1, 5YR 4/1	Shale		None
45	46		105-1105	5YR 4/1, N4	Hale		None
46	47		105-1105	5YR 4/1, N4	Shale		None
47	48		105-1105	5GY 4/1, N4	Shale	Silty, calcareous	None
48	49		105-1105	5YR 4/1	Shale	Silty, calcareous	None
49	50		105-1106	5YR 4/1	Shale	Calcareous	None
50	51		105-1106	5YR 2/2	Shale		None
51	52		105-1106	5Y 4/1	Shale	Silty	None
52	53		105-1106	5YR 2/2	Shale	Silty	None
53	54		105-1106	5YR 4/1, 5GY4/1	Shale		None
54	55		105-1107	N4, 5GY4/1	Shale	Silty, slightly calcareous	None

55	56		105-1107	5Y 4/1, 5G 6/1	Shale	Silty, calcareous	None
56	57		105-1107	5Y 3/2	Very fine to fine grained sandstone	Calcareous	None
57	58		105-1107	5YR 3/4; 5GY 4/1	Shale and silty shale		None
58	59		105-1107	5YR 3/4, 5Y 2/1	Shale		None
59	60		105-1107	5YR 4/1, 5Y 4/1	Shale	Silty	None
60	61		105-1108	N4, 5YR 4/1	Shale	Silty	None
61	62		105-1108	5Y4/1, 5GY 4/1	Shale	Silty	None
62	63		105-1108	5GY 4/1, 5YR 4/1, 5YR 3/2	Shale	With sparse clay	None
63	64		105-1108	5YR4/1, 5Y 4/1	Shale	With sparse clay, silty calcareous	None
64	65		105-1108	5YR 4/1, 5YR 3/4	Shale	With sparse clay, silty calcareous	None
65	66		105-1110	5 YR 3/2, 5Y4/1, 5Y 2/1	Shale	With sparse clay, slightly silty, silty calcareous	None
66	67		105-1110	5YR 3/2, 5Y 2/1	Shale and clay	Sparse fine grained sandstone, horizontal laminae, 10YR 6/2	None
67	68	WATER STRIKE	105-1110	5 Y4/1, 5GY 4/1	Clay with rock chips siltstone	Slightly calcareous	None

68	69		105-1110	5Y 4/1, 5GY 4/1	Silty shale	With sparse clay	None
69	70		105-1110	5Y 4/1, 5GY 4/1	Silty shale		None
70	71		105-1110	5Y 4/1, 5Y 2/1	Shale	Silty, slightly calcareous	None
71	72		105-1110	N4, 5Y 4/1	Siltstone		None
72	73		105-1111	5GY 4/1	Clay with rock chips shale	Silty, slightly calcareous	None
73	74		105-1111	5GY 4/1	Shale with clay	Silty, slightly calcareous	None
74	75		105-1111	N3-N4	Shale		None
75	76		105-1111	5GY 4/1	Shale	Silty	None
76	77		105-1111	N4, 5GY 4/1	Shale	Silty	None
77	78		105-1111	N4, 5Y 4/1	Shale	Silty	None
78	79		105-1111	N4, 5GY 4/1	Shale	Silty with sparse clay	None
79	80		105-1112	N4	Clay with rock fragments siltstone		None
80	81		105-1112	N3, 5GY 4/1	Shale	Slightly calcareous	None
81	82		105-1112	N4- N5	Siltstone and clay	Slightly calcareous	None
82	83		105-1112	N4, 5Y4/1	Shale	Slightly calcareous	None

83	84		105-1112	N3- N4	Shale	Silty	None
84	85		105-1113	N3- N4	Shale	Silty, with sparse clay, slightly calcareous	None
85	86		105-1113	5 YR 4/1, 5YR 3/2	Shale	Slightly silty, slightly calcareous	None
86	87		105-1113	5 YR 4/1, 5YR 3/2, 5GY4/1	Shale	Slightly silty, slightly calcareous	None
87	88		105-1113	5GY 4/1	Shale	Silty with sparse clay, calcareous	None
88	89		105-1113	5Y 4/1, 5GY 4/1	Siltstone	Calcareous	None
89	90		105-1114	N7; 5GY4/1, N4	Very fine grained sandstone and siltstone	Vf sst N7 (89- 89.5m) and siltstone 5GY 4/1, N4 (89.5-90m), calcareous	None
90	91		105-1114	N4, 5GY 4/1; 5R 2/2, 5YR 2/2	Siltstone and shale	N4 siltstone (90- 90.5m); 5R 2/2, 5YR 2/2 shale (90.5-91m); slightly calcareous	None
91	92		105-1114	N7; N4	Fine grained sandstone and siltstone	Slightly calcareous, N7 fg sst (91.5- 92m); N4 siltstone	None
92	93		105-1114	5GY 4/1; N7	Siltstone and fine grained sandstone	5GY 4/1 slt (92.5- 93m) and N7 fg sst (92- 92.5m)	None
93	94		105-1114	5GY 4/1, 5YR 2/1, 5YR 2/2	Siltstone an shale	Slt (93- 93.5m), calcareous; shale silty	None

94	95		105-1115	5R 4/2, 5YR 3/2, 5YR 2/2	Shale	Silty, slightly calcareous	None
95	96		105-1115	N4- N5	Siltstone	Slightly calcareous	None
96	97		105-1115	N4- N5	Siltstone	Slightly calcareous	None
97	98		105-1115	N4- N5	Very fine grained sandstone	Slightly calcareous	None
98	99		105-1115	N4; N7	Very fine grained sandstone	Calcareous	None
99	100		105-1116	N4	Very fine grained sandstone	Calcareous	None
100	101		105-1116	N4-N5	Very fine to fine grained sandstone	Calcareous	None
101	102		105-1116	N4	Very fine grained sandstone	Calcareous	None
102	103		105-1116	N5- N6; N7	Very fine grained sandstone	Slightly calcareous	None
103	104		105-1116	N4- N5	Very fine to fine grained sandstone	Calcareous	None
104	105		105-1116	N4- N5; N7	Sparse clay and rock chips	Sandstone N4-N5, very fine grained sandstone N7, calcareous	None
105	106		105-1116	N4- N5; N7	Very fine to fine grained sandstone and fine grained	Slightly calcareous, N4- N5 vf to fg sandstone, N7 fg sandstone	None
106	107		105-1116	N5; N7	Very fine to fine grained sandstone and fine grained	Calcareous, N5, vf to fg sandstone, N7, fg sandstone	None

107	108		105-1116	N4- N5; N7	Fine grained sandstone	N7, fg sst, calcareous	None
108	109		105-1117	N7; N4	Fine grained sandstone and siltstone	Calcareous	None
109	110		105-1117	N4, 5GY 4/1	Siltstone	Slightly calcareous	None
110	111		105-1117	N3- N4; 5YR 3/2	Siltstone to fine grained sandstone and shale	N3- N4 siltstone and fg sandstone, shale 5YR 3/2	None
111	112		105-1117	N3- N4; N3, 5GY 4/1	Very fine grained sandstone and siltstone	Vfg sandstone N3- N4; N3,5GY 4/1 siltstone	None
112	113		105-1117	N4, 5GY 4/1	Siltstone	Slightly calcareous	None
113	114		105-1117	N4; N3-N4	Siltstone and silty shale		None
114	115		105-1118	5GY 4/1, N4	Siltstone to fine grained sandstone	Calcareous	None
115	116		105-1118	N4- N5; 5YR 2/2	Siltstone and shale	Calcareous	None
116	117		105-1118	5GY 4/1, N4; 5YR 3/2, 5YR 2/2	Siltstone and shale	Calcareous	None
117	118		105-1118	5Y4/1, N4	Siltstone	Calcareous	None
118	119		105-1118	5YR 2/2, 5YR 3/2;	Shale and silty shale	Calcareous	None

				5GY4/1, N3			
119	120		105-1119	N4	Siltstone	Slightly calcareous	None
120	121		105-1119	N3-N4	Siltstone	Slightly calcareous, sub-ordinate clay, slightly calcareous	None
121	122		105-1119	N3- N4, 5GY 4/1	Siltstone	Slightly calcareous	None
122	123		105-1119	N7; N3-N4; 5YR 3/2	Very fine grained sandstone; siltstone; silty shale	Slightly calcareous	None
123	124		105-1119	5GY4/1, N4, 5YR 4/1	Silty shale		None
124	125		105-1120	N4, 5GY4/1	Siltstone		None
125	126		105-1120	N4	Siltstone		None
126	127		105-1120	N4, 5YR 3/2	Silty shale		None
127	128		105-1120	5GY 4/1, N4	Siltstone	Sparse clay, slightly calcareous	None
128	129		105-1120	N4	Very fine grained sandstone	Sparse clay, calcareous	None
129	130		105-1121	N4, 5GY 4/1	Clay with rock fragments	Siltstone, calcareous	None
130	131		105-1121	N4- N5	Clay with rock fragments	Very fine siltstone	None

131	132	WATER STRIKE	105-1121	N4	Clay with rock fragments	Siltstone, slightly calcareous	None
132	133		105-1121	5YR 4/1; 5GY 4/1, N4	Clay with rock fragments	5YR 4/1 silty shale; 5GY 4/1, N4 siltstone; slightly calcareous, calcite present, fractured zone?	None
133	134		105-1121	5YR 3/4, 5YR 3/2; N3- N4	Clay with rock fragments	5YR 3/4, 5YR 3/2 shale; N3-N4, siltstone	None
134	135		105-1122	N4; N5	Rock fragments with sparse clay	N4 shale; N5 very fine grained sandstone	None
135	136		105-1122	5YR 4/1, 5YR 3/2, 5Y4/1, 5GY 4/1	Rock fragments with sparse clay	5YR 4/1, 5YR 3/2, 5Y4/1, 5GY 4/1 shale	None
136	137		105-1122	5YR 4/1; N4- N5	Rock fragments with sparse clay	5YR 4/1 shale; N4-N5 siltstone	None
137	138		105-1122	5YR 3/2,5YR 3/4; 5GY 4/1, N4	Rock fragments, minor clay	5YR 3/2, 5YR 3/4 shale; 5GY 4/1, N4 siltstone	None
138	139		105-1122	5YR 4/1; N4- N5	Rock fragments, minor clay	5YR 4/1, silty shale; N4-N5 siltstone	None
139	140		105-1123	N4	Rock fragments with sparse clay	N4 siltstone	None
140	141		105-1123	5GY 4/1, N4	Rock fragments with sparse clay	5GY 4/1, N4 siltstone	None
141	142		105-1123	N4, 5GY 4/1	Rock fragments with sparse clay	N4, 5GY 4/1 siltstone	None

142	143		105-1123	N4	Rock fragments with sparse clay	N4, siltstone	None
143	144		105-1123	5GY 4/1, N4	Rock fragments with sparse clay	5GY 4/1, N4 siltstone	None
144	145		105-1124	5YR 4/1, 5YR 3/2; 5GY 4/1	Rock fragments with sparse clay	5YR 4/1, 5YR 3/2 shale; 5GY 4/1 silty shale; slightly calcareous	None
145	146		105-1124	N3- N4	Rock fragments with sparse clay	N3- N4 silty shale	None
146	147		105-1124	5YR 4/1, 5YR 3/2, 5YR 3/4	Rock fragments with sparse clay	5YR 4/1, 5YR 3/2, 5YR 3/4 silty shale, shaley morphology	None
147	148		105-1124	5GY 4/1; 5YR 3/2, 5YR 3/4	Rock fragments with sparse clay	5GY 4/1 silty shale; 5YR 3/2, 5YR 3/4 shale	None
148	149		105-1124	5GY 4/1, 5YR 4/1	Silty shale		None
149	150		105-1125	N4	Silty shale		None
150	151		105-1125	5YR 4/1, 5GY 4/1, N4	Rock fragments with sparse clay	5YR 4/1, 5GY 4/1, N4 silty shale; slightly calcareous	None
151	152		105-1125	5GY 4/1; 5YR 4/1, 5YR 3/4, 5YR 3/2	Siltstone and sub-ordinate shale	5GY 4/1 siltstone (predom); 5YR 4/1, 5YR 3/4, 5YR 3/2 shale	None
152	153		105-1125	5GY 4/1; 5YR 4/1, 5YR 3/4	Siltstone and sub-ordinate shale	5GY 4/1 siltstone (predom); 5YR 4/1, 5YR 3/4 shale	None

153	154		105-1125	N4, 5Y 4/1; 5YR 4/1, 5YR 3/4	Siltstone and sub-ordinate shale	N4, 5Y 4/1 siltstone; 5YR 4/1, 5YR 3/4 shale	None
154	155		105-1126	5G 4/1, 5GY 4/1; 5YR 4/1, 5YR 3/2	Silty shale and sub-ordinate shale	Slightly calcareous; 5G 4/1, 5GY 4/1 silty shale (predom); 5YR 4/1, 5YR 3/2 shale	None
155	156		105-1126	5GY 4/1; 5R 4/2	Silty shale and sub-ordinate shale	Slightly calcareous; 5GY 4/1 silty shale (predom); 5R 4/2 shale	None
156	157		105-1126	5GY 4/1; 5R 4/2	Rock fragments with sparse clay	Calcareous; 5GY 4/1 silty shale (predom); 5R 4/2 shale	None
157	158		105-1126	5GY 4/1; 5R 4/2	Rock fragments with sparse clay	5GY 4/1 silty shale (predom); 5R 4/2 shale	None
158	159		105-1126	5YR 3/4, 5R 4/2; 5GY 4/1	Silty shale and sub-ordinate shale	5YR 3/4, 5R 4/2 shale; 5GY 4/1 silty shale (predom)	None
159	160		105-1127	5YR 3/2, 5R 4/2; 5GY 4/, 5Y 4/1	Silty shale and sub-ordinate shale	5YR 3/2, 5R 4/2 shale; 5GY 4/, 5Y 4/1 silty shale (predom)	None
160	161		105-1127	5GY 4/1; 5R 4/2	Rock fragments with sparse clay	5GY 4/1 silty shale (predom); 5R 4/2 shale	None
161	162		105-1127	5GY 4/1; 5R 4/2	Rock fragments with sparse clay	5GY 4/1 silty shale (predominantly); 5R 4/2 shale	None
162	163		105-1127	N4	Very fine grained sandstone		None

163	164		105-1127	N4-N5	Very fine grained sandstone		None
164	165		105-1129	N4-N5	Very fine grained sandstone		None
165	166		105-1129	N4-N5	Very fine grained sandstone		None
166	167		105-1129	N4-N5	Very fine grained sandstone		None
167	168		105-1129	N4-N5	Very fine grained sandstone		None
168	169		105-1129	5Y 4/1; 5YR 3/4	Siltstone and shale	Equal siltstone and shale. 5Y 4/1 siltstone; 5YR 3/4 shale	None
169	170		105-1130	5Y 4/1, N4; 5YR 4/1	Siltstone and shale	Equal siltstone and shale. 5Y 4/1, N4 siltstone; 5YR 4/1 shale	None
170	171		105-1130	5Y 4/1, N4; 5YR 4/1	Siltstone and shale	Equal siltstone and shale. 5Y 4/1, N4 siltstone; 5YR 4/1 shale	None
171	172		105-1130	5Y 4/1, N4; 5YR 4/1	Siltstone and shale	Equal siltstone and shale. 5Y 4/1, N4 siltstone; 5YR 4/1 shale	None
172	173		105-1130	5Y 4/1, N4; 5YR 4/1	Siltstone and shale	Equal siltstone and shale. 5Y 4/1, N4 siltstone; 5YR 4/1 shale	None
173	174		105-1130	N5, 5YR 4/1	Rock fragments with sparse clay	N5, 5YR 4/1 siltstone	None
174	175		105-1131	5Y 4/1, N4; 5YR	Siltstone and shale	Equal siltstone and shale. 5Y 4/1, N4 siltstone; 5YR 4/1, 5YR 3/2 shale	None

				4/1, 5YR 3/2			
175	176		105-1131	5Y 4/1, N4; 5YR 4/1, 5YR 3/2	Siltstone and shale	Equal siltstone and shale. 5Y 4/1, N4 siltstone; 5YR 4/1, 5YR 3/2 shale	None
176	177		105-1131	5Y 4/1, N4; 5YR 4/1, 5YR 3/2	Siltstone and shale	Equal siltstone and shale. 5Y 4/1, N4 siltstone; 5YR 4/1, 5YR 3/2 shale	None
177	178		105-1131	5Y 4/1, N4; 5YR 4/1, 5YR 3/2	Siltstone and shale	Equal siltstone and shale. 5Y 4/1, N4 siltstone; 5YR 4/1, 5YR 3/2 shale	None
178	179		105-1131	5Y 4/1, N4; 5YR 4/1, 5YR 3/2	Siltstone and shale	Equal siltstone and shale. 5Y 4/1, N4 siltstone; 5YR 4/1, 5YR 3/2 shale	None
179	180		105-1131	5 GY 4/1	Rock fragments with sparse clay	5GY 4/1 siltstone	None
180	181		105-1132	5YR 4/1, N4	Siltstone		None
181	182		105-1132	5YR 3/4, 5YR 3/2, 5R 4/2; 5Y 4/1, N4	Shale and sub-ordinate siltstone	Slightly calcareous; dominantly shale; 5YR 3/4, 5YR 3/2, 5R 4/2 shale; 5Y 4/1, N4	None

						sub-ordinate siltstone	
182	183		105-1132	5YR 3/4, 5YR 3/2, 5R 4/2; 5Y 4/1, N4	Shale and sub-ordinate siltstone	Slightly calcareous; dominantly shale; 5YR 3/4, 5YR 3/2, 5R 4/2 shale; 5Y 4/1, N4 Sub-ordinate siltstone	NONE
183	184		105-1132	5Y 4/1, N4; 5YR 3/4, 5R 4/2	Shale and siltstone	Equal siltstone and shale. 5Y 4/1, N4 siltstone; 5YR 3/4, 5R 4/2 shale	None
184	185		105-1134	5Y 4/1, N4; 5YR 3/4, 5R 4/2	Shale and siltstone	Equal siltstone and shale. 5Y 4/1, N4 siltstone; 5YR 3/4, 5R 4/2 shale	None
185	186		105-1134	5Y 4/1, N4; 5YR 3/4, 5R 4/2	Shale and siltstone	Equal siltstone and shale. 5Y 4/1, N4 siltstone; 5YR 3/4, 5R 4/2 shale	None
186	187		105-1134	5Y 4/1, N4; 5YR 3/4, 5R 4/2	Shale and siltstone	Equal siltstone and shale. 5Y 4/1, N4 siltstone; 5YR 3/4, 5R 4/2 shale	None
187	188		105-1134	5Y 4/1, N4; 5YR 3/4, 5R 4/2	Shale and siltstone	Equal siltstone and shale. 5Y 4/1, N4 siltstone; 5YR 3/4, 5R 4/2 shale	None

188	189		105-1134	5Y 4/1, N4; 5YR 3/4, 5R 4/2	Shale and siltstone	Equal siltstone and shale. 5Y 4/1, N4 siltstone; 5YR 3/4, 5R 4/2 shale	None
189	190		105-1135	5GY 4/1, N4; 5YR 3/2	Siltstone and sub-ordinate shale	5GY 4/1, N4 siltstone; 5YR 3/2 shale	None
190	191		105-1135	5GY 4/1, N4; 5YR 3/2	Siltstone and sub-ordinate shale	5GY 4/1, N4 SILTSTONE; 5YR 3/2 shale	None
191	192		105-1135	N4, 5GY 4/1	Very fine grained sandstone		None
192	193		105-1135	N4	Very fine grained sandstone		None
193	194		105-1135	N4	Very fine grained sandstone		None
194	195		105-1136	N4	Very fine grained sandstone		None
195	196		105-1136	N4	Very fine grained sandstone		None
196	197		105-1136	5Y 4/1, 5YR 4/1; 5YR 3/4	Shale and siltstone	Equal siltstone and shale. 5Y 4/1, 5YR 4/1 siltstone; 5YR 3/4 shale	None
197	198		105-1136	5YR 2/1; 5YR 4/1	Very fine grained sandstone and siltstone	5YR 2/1 very fine grained sandstone; 5YR 4/1 siltstone	None
198	199		105-1136	5R 4/2; 5GY 4/1	Shale and sub-ordinate silty shale	5R 4/2 shale; 5GY 4/1 silty shale	None

199	200		105-1138	5Y 4/1, N4; 5YR 3/2, 5YR 2/2	Siltstone and shale	Equal siltstone and shale. 5Y 4/1, N4 siltstone; 5YR 3/2, 5YR 2/2 shale	None
200	201		105-1138	5Y 4/1, N4; 5YR 3/2, 5YR 2/2	Siltstone and shale	Equal siltstone and shale. 5Y 4/1, N4 siltstone; 5YR 3/2, 5YR 2/2 shale	None
201	202		105-1138	5Y 4/1, N4; 5YR 3/2, 5YR 2/2	Siltstone and shale	Equal siltstone and shale. 5Y 4/1, N4 siltstone; 5YR 3/2, 5YR 2/2 shale	None
202	203		105-1138	5Y 4/1, N4; 5YR 3/4, 5R 4/2	Siltstone and sub-ordinate shale	5Y 4/1, N4 siltstone; 5YR 3/4, 5R 4/2 shale	None
203	204		105-1138	5Y 4/1, N4; 5YR 3/4, 5R 4/2	Siltstone and sub-ordinate shale	5Y 4/1, N4 siltstone; 5YR 3/4, 5R 4/2 shale	None
204	205		105-1139	5Y 4/1, N4; 5YR 3/4, 5R 4/2	Siltstone and sub-ordinate shale	5Y 4/1, N4 siltstone; 5YR 3/4, 5R 4/2 shale	None
205	206		105-1139	N4	Rock fragments with sparse clay	N4 siltstone	None
206	207		105-1139	N4-N5	Siltstone		None
207	208		105-1139	N4-N5	Siltstone		None

208	209		105-1139	N4-N5	Siltstone		None
209	210		105-1140	N4-N5	Siltstone		None
210	211		105-1140	N4-N5	Siltstone		None
211	212		105-1140	5Y 4/1, N4; 5 YR 3/2, 5YR ¾	Silty shale and sub-ordinate shale	Possible brecciated zone? 5Y 4/1, N4 silty shale; 5YR 3/2, 5YR 3/4 shale	None
212	213.5		105-1140	5Y 4/1, N4; 5 YR 3/2, 5YR ¾	Silty shale and sub-ordinate shale	Possible brecciated zone? 5Y 4/1, N4 silty shale; 5YR 3/2, 5YR 3/4 shale	None
213.5	214		105-1140	5GY 4/1, N4	Siltstone		None
214	215		105-1140	5GY 4/1, N4	Siltstone		None
215	216		105-1140	5GY 4/1, N4	Siltstone		None
216	217		105-1140	5Y 4/1, N4; 5YR 3/2, 5YR ¾	Siltstone and shale	Equal siltstone and shale. 5Y 4/1, N4 siltstone; 5YR 3/2, 5YR 3/4 shale	None
217	218		105-1141	5Y 4/1, N4; 5YR 3/2, 5YR ¾	Siltstone and shale	Equal siltstone and shale. 5Y 4/1, N4 siltstone; 5YR 3/2, 5YR 3/4 shale	None
218	219		105-1141	5Y 4/1, 5GY 4/1	Silty shale	5Y 4/1, 5GY 4/1; 5YR 4/1 sparse shale	None

219	220		105-1141	5Y 4/1, 5GY 4/1	Silty shale	5Y 4/1, 5GY 4/1; 5YR 4/1 sparse shale	None
220	221		105-1156	5Y 4/1, 5GY 4/1	Silty shale	5Y 4/1, 5GY 4/1; 5YR 4/1 sparse shale	None
221	222	WATER STRIKE	105-1156	N4	Very fine to fine grained sandstone	Sparse clay; slightly calcareous	None
222	223		105-1156	N4	Very fine to fine grained sandstone	Sparse clay; slightly calcareous	None
223	224		105-1156	N4	Very fine grained sandstone	Slightly clayey	None
224	225		105-1156	N4	Very fine grained sandstone	Slightly clayey	None
225	226		105-1157	N4	Very fine grained sandstone	Slightly clayey	None
226	227		105-1157	N4	Very fine grained sandstone		None
227	228		105-1157	N4	Very fine grained sandstone		None
228	229		105-1157	N4	Very fine grained sandstone		None
229	230		105-1157	N3-N4	Siltstone	Clayey, slightly calcareous	None
230	231		105-1158	5G4/1, N4; 5YR 3/2, 5YR 2/2	Siltstone and shale	Slightly clayey; 5G 4/1, N4 siltstone; 5YR 3/2, 5YR 2/2 shale	None
231	232		105-1158	5GY 4/1, N4; 5YR 3/2, 5YR 2/2	Siltstone and shale	5GY4/1, N4 siltstone; 5YR 3/2, 5YR 2/2 shale	None

232	233		105-1158	5GY 4/1, N4; 5YR 3/2, 5YR 2/2	Siltstone and shale	5GY4/1, N4 siltstone; 5YR 3/2, 5YR 2/2 shale	None
233	234		105-1158	5Y 4/1, N4; 5YR 3/2, 5YR 2/2	Siltstone and silty shale	N4, 5Y 4/1 siltstone; 5YR 3/2, 5YR 2/2 silty shale	None
234	235		105-1158	N3; N3, 5YR 2/1	Siltstone and silty shale	Calcareous; N3, siltstone; N3, 5YR 2/1 silty shale	None
235	236		105-1159	N3; N3, 5YR 2/1	Siltstone and silty shale	Calcareous; N3, siltstone; N3, 5YR 2/1 silty shale	None
236	237		105-1159	5Y4/1, N4; 5YR 2/2, 5YR 3/2	Siltstone and silty shale	Calcareous; 5Y 4/1, N4 siltstone; 5YR 2/2, 5YR 3/2 silty shale	None
237	238		105-1159	N3; N4	Siltstone and very fine grained sandstone	Calcareous; N3 siltstone; N4 very fine grained sandstone	None
238	239		105-1159	N3; N4	Siltstone and very fine grained sandstone	Calcareous; N3 siltstone; N4 very fine grained sandstone	None
239	240		105-1159	N3; N4	Siltstone and very fine grained sandstone	N3 siltstone; N4 very fine grained sandstone	None
240	241		105-1160	N3; N4	Siltstone and very fine grained sandstone	Calcareous; N3 siltstone; N4 very fine grained sandstone	None

241	242		105-1160	N3; N4	Siltstone and very fine grained sandstone	Calcareous; N3 siltstone; N4 very fine grained sandstone	None
242	243		105-1160	N4	Very fine to fine sandstone grained	Slightly calcareous; N4	None
243	244		105-1160	N4	Very fine to fine sandstone grained	Slightly calcareous; N4	None
244	245		105-1161	5YR 2/1, N3	Siltstone		None
245	246		105-1161	5YR 2/1, N3	Siltstone		None
246	247		105-1161	5Y 4/1, 5GY 4/1; 5YR 4/1, 5YR 3/2, 5YR 2/2	Siltstone and shale	Slightly calcareous; 5Y 4/1, 5GY 4/1 siltstone; 5YR 4/1, 5YR 3/2, 5YR 2/2 shale	None
247	248		105-1161	5Y 4/1, 5GY 4/1; 5YR 4/1, 5YR 3/2, 5YR 2/2	Siltstone and shale	Slightly calcareous; 5Y 4/1, 5GY 4/1 siltstone; 5YR 4/1, 5YR 3/2, 5YR 2/2 shale	None
248	249		105-1161	5Y 4/1, 5GY 4/1; 5YR 4/1, 5YR 3/2, 5YR 2/2	Siltstone and shale	Slightly calcareous; 5Y 4/1, 5GY 4/1 siltstone; 5YR 4/1, 5YR 3/2, 5YR 2/2 shale	None
249	250		105-1161	5GY 4/1, N4	Siltstone		None
250	251		105-1162	5GY 4/1, N4	Siltstone		None

251	252		105-1162	N4	Very fine grained sandstone		None
252	253	WATER STRIKE	105-1162	5GY 4/1, N3- 4	Siltstone	Sparse clay, slightly calcareous	None
253	254		105-1162	N4	Clay with rock fragments	Calcareous, N4 very fine grained sandstone	None
254	255		105-1162	5Y 4/1; N4	Siltstone and very fine grained sandstone	Slightly calcareous; 5Y 4/1 siltstone; N4 very fine grained sandstone	None
255	256		105-1163	5Y 4/1; N4	Siltstone and very fine grained sandstone	Slightly calcareous; 5Y 4/1 siltstone; N4 very fine grained sandstone	None
256	257		105-1163	N4, 5Y 4/1	Siltstone		None
257	258		105-1163	N4, 5Y 4/1, 5GY 4/1	Siltstone	Calcareous	None
258	259		105-1163	5Y 4/1, 5GY 4/1	Siltstone	5Y 4/1, 5GY 4/1 siltstone	None
259	260		105-1163	5Y 4/1, 5GY 4/1	Siltstone	5Y 4/1, 5GY 4/1 siltstone	None
260	261		105-1164	5Y 4/1, 5GY 4/1	Siltstone	5Y 4/1, 5GY 4/1 siltstone	None
261	262		105-1164	5GY 4/1, N3; N4, 5GY 4/1	Silty shale and siltstone	Slightly calcareous; 5GY 4/1, N3 silty shale; N4, 5GY 4/1, siltstone	None
262	263		105-1164	5GY 4/1, N3; N4, 5GY 4/1	Silty shale and siltstone	Slightly calcareous; 5GY 4/1, N3 silty shale; N4, 5GY 4/1, siltstone	None

263	264		105-1164	5GY 4/1, N3; N4, 5GY 4/1	Silty shale and siltstone	Slightly calcareous; 5GY 4/1, N3 silty shale; N4, 5GY 4/1, siltstone	None
264	265		105-1164	N4, 5GY 4/1; N3	Siltstone and silty shale	Slightly calcareous; N4, 5GY 4/1 siltstone; N3 silty shale	None
265	266		105-1165	N4, 5GY 4/1; N3	Siltstone and silty shale	Slightly calcareous; N4, 5Gy 4/1 siltstone; N3 silty shale	None
266	267		105-1165	5YR 4/1; 5YR 3/4	Silty shale	Slightly calcareous; 5YR 4/1 silty shale; 5YR 3/4 shale	None
267	268		105-1165	5YR 4/1; 5YR 3/4	Silty shale	Slightly calcareous; 5YR 4/1 silty shale; 5YR 3/4 shale	None
268	269		105-1165	5GY 4/1	Siltstone	Calcareous	None
269	270		105-1165	N3, 5GY 4/1	Silty shale	Calcareous	None
270	271		105-1168	5YR 6/1, 5YR 2/2, 5YR 3/2; N3, 5GY 4/1	Silty shale and siltstone	Slightly calcareous; 5YR 6/1, 5YR 2/2, 5YR 3/2 silty shale; N3, 5GY 4/1 siltstone	None
271	272		105-1168	N3- N4, 5GY 4/1	Silty shale	Calcareous; N3-N4, 5GY 4/1	None
272	273		105-1168	N3- N4, 5GY 4/1	Silty shale	Calcareous; N3-N4, 5GY 4/1	None
273	274		105-1169	N4; N4, 5Y 4/1	Clay with rock fragments	N4 siltstone; N4, 5Y 4/1 very fine grained sandstone	None
274	275		105-1169	N4, 5GY 4/1	Siltstone	Sparse clay; N4, 5GY 4/1 siltstone; slightly calcareous	None

275	276		105-1169	N4, 5GY 4/1	Siltstone	Sparse clay; N4, 5GY 4/1 siltstone; slightly calcareous	None
276	278		105-1169	5GY 4/1; N5	Siltstone and very fine grained sandstone	Calcareous; 5GY 4/1 siltstone; N5 very fine grained sandstone	None
278	279		105-1169	5GY 4/1; N5	Siltstone and very fine grained sandstone	Calcareous; 5GY 4/1 siltstone; N5 very fine grained sandstone	None
279	280		105-1169	5GY 4/1; N5	Siltstone and very fine grained sandstone	Calcareous; 5GY 4/1 siltstone; N5 very fine grained sandstone	None
280	281		105-1170	N4, 5GY 4/1; 5YR 2/2, 5YR 3/2	Siltstone and shale	Slightly calcareous; N4, 5GY 4/1 siltstone; 5YR 2/2, 5YR 3/2 shale	None
281	282		105-1170	5GY 4/1; 5YR 2/2, 5YR 3/2	Siltstone and shale	5Gy 4/1 siltstone; 5YR 2/2, 5YR 3/2 shale	None
282	283	WATER STRIKE	105-1170	N3-N4	Silty shale		None
283	284		105-1170	N3-N4	Silty shale		None
284	285		105-1170	N4-N5, 5GY 4/1	Siltstone	Slightly calcareous	None
285	286		105-1171	N5; 5YR 3/2, 5YR ¾	Very fine to fine grained sandstone and shale	Slightly calcareous; N5 very fine to fine grained sandstone; 5YR 3/2, 5YR 3/4 shale	None

286	287		105-1171	N5; 5YR 3/2, 5YR ¾	Very fine to fine grained sandstone and shale	Slightly calcareous; N5 very fine to fine grained sandstone; 5YR 3/2, 5YR 3/4 shale	None
287	288		105-1171	N4, 5GY 4/1	Siltstone		None
288	289		105-1171	N4, 5GY 4/1	Siltstone		None
289	290		105-1171	N4, 5GY 4/1	Siltstone		None
290	291		105-1172	5Y 4/1; N3- N4	Siltstone and very fine grained sandstone	Calcareous; 5Y 4/1 siltstone; N3-N4 very fine grained sandstone	None
291	292		105-1172	5Y 4/1	Siltstone		None
292	293		105-1172	N3; N4, 5Y 4/1	Siltstone and very fine grained sandstone	N3 siltstone; N4, 5Y 4/1 very fine grained sandstone	None
293	294		105-1172	N3; N4, 5Y 4/1	Siltstone and very fine grained sandstone	N3 siltstone; N4, 5Y 4/1 very fine grained sandstone	None
294	295		105-1172	N4-N5; N3- N4	Very fine grained sandstone and silty shale	Calcareous; N4- N5 very fine grained sandstone; N3-N4 silty shale	None
295	296		105-1173	N4-N5; N3- N4	Very fine grained sandstone and silty shale	Calcareous; N4- N5 very fine grained sandstone; N3-N4 silty shale	None
296	297		105-1173	N4-N5; N3- N4	Very fine grained sandstone and silty shale	Calcareous; N4- N5 very fine grained sandstone; N3-N4 silty shale	None

297	298		105-1173	N4-N5; N3- N4	Very fine grained sandstone and silty shale	Calcareous; N4- N5 very fine grained sandstone; N3-N4 silty shale	None
298	299		105-1173	N4- N5	Siltstone		None
299	300		105-1173	N4- N5	Siltstone		None
300	301		105-1173	5Y 4/1; N5; 5YR 2/2	Siltstone; very fine grained sandstone and silty shale	Slightly calcareous; 5Y 4/1 siltstone; N5 very fine grained sandstone; 5YR 2/2 silly shale	None
301	302		105-1174	5Y 4/1; N5; 5YR 2/2	Siltstone; very fine grained sandstone and silty shale	Slightly calcareous; 5Y 4/1 siltstone; N5 very fine grained sandstone; 5YR 2/2 silty shale	None
302	303		105-1174	5Y 4/1; N5; 5YR 2/2	Siltstone; very fine grained sandstone and silty shale	Slightly calcareous; 5Y 4/1 siltstone; N5 very fine grained sandstone; 5YR 2/2 silty shale	None
303	304		105-1174	N5- N6	Very fine to fine grained sandstone		None
304	305		105-1174	N5- N6	Very fine to fine grained sandstone		None
305	306		105-1174	N4, 5Y4/1	Siltstone to very fine grained sandstone		None
306	307		105-1174	5GY 4/1, N4	Siltstone		None
307	308		105-1174	5GY 4/1, N4	Siltstone		None

308	309		105-1174	5GY 4/1, N4	Siltstone		None
309	310		105-1174	N5	Very fine to fine grained sandstone		None
310	311		105-1176	N6, 5GY 6/1; 5YR 6/1	Very fine grained sandstone and silty shale	N6, 5GY 6/1 very fine grained sandstone; 5YR 6/1 silty shale	None
311	312		105-1176	N6, 5GY 6/1; 5YR 6/1	Very fine grained sandstone and silty shale	N6, 5GY 6/1 very fine grained sandstone; 5YR 6/1 silty shale	None
312	313		105-1176	N6; 5Y 4/1, 5; 5YR 3/4, 5YR 3/2	Very fine to fine grained sandstone, siltstone, shale	N6 very fine to fine grained sandstone; 5Y 4/1, N5 siltstone; 5YR 3/4, 5YR 3/2 shale	None
313	314		105-1176	N6; 5Y 4/1, 5; 5YR 3/4, 5YR 3/2	Very fine to fine grained sandstone, siltstone, shale	N6 very fine to fine grained sandstone; 5Y 4/1, N5 siltstone; 5YR 3/4, 5YR 3/2 shale	None
314	315		105-1176	N6; 5Y 4/1, 5; 5YR 3/4, 5YR 3/2	Very fine to fine grained sandstone, siltstone, shale	N6 very fine to fine grained sandstone; 5Y 4/1, N5 siltstone; 5YR 3/4, 5YR 3/2 shale	None
315	316		105-1177	5GY 4/1; 5YR 3/4, 5YR 3/2	Siltstone and shale	5GY 4/1 siltstone; 5YR 3/4, 5YR 3/2 shale	None
316	317		105-1177	N6; 5YR 4/1	Very fine to fine grained sandstone and sub-ordinate siltstone	N6 very fine to fine grained sandstone; 5YR 4/1 siltstone (sub-ordinate)	None

317	318		105-1177	N6; 5YR 4/1	Very fine to fine grained sandstone and sub-ordinate siltstone	N6 very fine to fine grained sandstone; 5YR 4/1 siltstone (sub-ordinate)	None
318	319		105-1177	N6; 5YR 4/1	Very fine to fine grained sandstone and sub-ordinate siltstone	N6 very fine to fine grained sandstone; 5YR 4/1 siltstone (sub-ordinate)	None
319	320		105-1177	N6; 5YR 4/1	Very fine to fine grained sandstone and sub-ordinate siltstone	N6 very fine to fine grained sandstone; 5YR 4/1 siltstone (sub-ordinate)	None
320	321		105-1178	N6; 5YR 4/1	Very fine to fine grained sandstone and sub-ordinate siltstone	N6 very fine to fine grained sandstone; 5YR 4/1 siltstone (sub-ordinate)	None
321	322		105-1178	5Y 4/1; 5YR 3/2, 5YR 3/4	Siltstone and silty shale	5Y 4/1 siltstone; 5YR 3/2, 5YR 3/4 silty shale	None
322	323		105-1178	5Y 4/1, 5GY 4/1, 5YR 4/1	Siltstone	5Y 4/1, 5GY 4/1, 5YR 4/1 siltstone	None
323	324		105-1178	5Y 4/1, 5GY 4/1, 5YR 4/1	Siltstone	5Y 4/1, 5GY 4/1, 5YR 4/1 siltstone	None
324	325		105-1178	N4, 5Y 4/1, 5YR 3/4, 5YR 4/1	Siltstone		None

325	326		105-1179	N4, 5Y 4/1, 5YR 3/4, 5YR 4/1	Siltstone		None
326	327		105-1179	N4, 5Y 4/1, 5YR 3/4, 5YR 4/1	Siltstone		None
327	328		105-1179	N4, 5Y 4/1, 5YR 3/4, 5YR 4/1	Siltstone		None
328	329		105-1179	5YR 4/1; 5YR 3/4, 5YR 3/2	Siltstone and silty shale	Slightly calcareous; 5YR 4/1 siltstone; 5YR 3/4, 5YR 3/2 silty shale	None
329	330		105-1179	5YR 4/1; 5YR 3/4, 5YR 3/2	Siltstone and silty shale	Slightly calcareous; 5YR 4/1 siltstone; 5YR 3/4, 5YR 3/2 silty shale	None
330	331		105-1180	N3- N4	Very fine grained sandstone		None
331	332		105-1180	N3-N4	Siltstone to very fine grained sandstone		None
332	333		105-1180	N4	Very fine to fine grained sandstone		None
333	334		105-1180	N4- N5, 5GY 4/1	Very fine to fine grained sandstone		None
334	335		105-1180	N4- N5, 5GY 4/1	Very fine to fine grained sandstone		None
335	336		105-1181	N4- N5, 5GY 4/1	Very fine to fine grained sandstone		None

336	337		105-1181	N3- N4, 5GY 4/1	Very fine grained sandstone		None
337	338		105-1181	N3- N4, 5GY 4/1	Very fine grained sandstone		None
338	339		105-1181	N3- N4, 5GY 4/1	Very fine grained sandstone		None
339	340		105-1181	N3- N4, 5GY 4/1	Very fine grained sandstone		None
340	341		105-1182	N3- N4, 5GY 4/1	Very fine grained sandstone		None
341	342		105-1182	N4	Very fine grained sandstone	Slightly calcareous	None
342	343		105-1182	5YR 2/1, 5YR 2/2; N4, 5Y 4/1	Silty shale and very fine grained sandstone	Slightly calcareous; 5YR 2/1,5YR 2/2 silty shale; N4, 5y 4/1 very fine grained sandstone	None
343	344		105-1182	5YR 2/1, 5YR 2/2; N4, 5Y 4/1	Silty shale and very fine grained sandstone	Slightly calcareous; 5YR 2/1,5YR 2/2 silty shale; N4, 5Y 4/1 very fine grained sandstone	None
344	345		105-1182	5YR 2/1, 5YR 2/2; N4, 5Y 4/1	Silty shale and very fine grained sandstone	Slightly calcareous; 5YR 2/1,5YR 2/2 silty shale; N4, 5Y 4/1 very fine grained sandstone	None
345	346		105-1183	N4	Very fine to fine grained sandstone		None
346	347		105-1183	N4	Very fine to fine grained sandstone	Slightly calcareous	None

347	348		105-1183	N4; 5Y 2/1, 5YR 2/2, 5YR 3/2	Very fine grained sandstone and silty shale	Slightly calcareous; N4 very fine grained sandstone; 5Y 2/1, 5YR 2/2, 5YR 3/2 silty shale	None
348	349		105-1183	N4, 5GY 4/1	Siltstone		None
349	350		105-1183	N4, 5GY 4/1	Siltstone		None
350	351		105-1184	N5- N6	Very fine to fine grained sandstone		None
351	352		105-1184	N5- N6	Very fine to fine grained sandstone		None
352	353		105-1184	N4- N5	Very fine grained		None
353	354		105-1184	N4- N5	Very fine grained		None
354	355		105-1184	N4- N5, 5GY 4/1	Siltstone		None
355	356		105-1185	N4- N5, 5GY 4/1	Siltstone		None
356	357		105-1185	N6; N4, 5GY 4/1	Very fine to fine grained sandstone; siltstone to very fine grained sandstone	N6 very fine to fine grained sandstone; N4, 5GY 4/1 siltstone to very fine grained sandstone	None
357	358		105-1185	N6; N4, 5GY 4/1	Very fine to fine grained sandstone; siltstone to very fine grained sandstone	N6 very fine to fine grained sandstone; N4, 5GY 4/1 siltstone to very fine grained sandstone	None
358	359		105-1185	N6; N4, 5GY 4/1	Very fine to fine grained sandstone;	N6 very fine to fine grained sandstone; N4, 5GY 4/1	None

					siltstone to very fine grained sandstone	siltstone to very fine grained sandstone	
359	360		105-1186	N4	Very fine to fine grained sandstone		None
360	361		105-1186	5Y 4/1, N3; N4-N5	Siltstone and fine grained sandstone	5Y 4/1, N3 siltstone; N4-N5 fine grained sandstone	None
361	362		105-1186	5Y 4/1, N3; N4-N5	Siltstone and fine grained sandstone	5Y 4/1, N3 siltstone; N4-N5 fine grained sandstone	None
362	363		105-1186	N3; 5GY 4/1, N4	Fine grained sandstone and siltstone to very fine grained sandstone	N3 fine grained sandstone; 5GY 4/1, N4 siltstone to very fine grained sandstone	None
363	364		105-1186	N4; 5Y 4/1	Very fine to fine grained sandstone and siltstone	N4, very fine to fine grained sandstone; 5Y 4/1 siltstone	None
364	365		105-1186	N4; 5Y 4/1	Very fine to fine grained sandstone and siltstone	N4, very fine to fine grained sandstone; 5Y 4/1 siltstone	None
365	366		105-1187	N4; 5Y 4/1	Very fine to fine grained sandstone and siltstone	N4, very fine to fine grained sandstone; 5Y 4/1 siltstone	None
366	367		105-1187	N5, 5GY 4/1; N4	Very fine to fine grained sandstone and very fine grained sandstone	N5, 5GY 4/1 very fine to fine grained sandstone; N4 very fine grained sandstone	None
367	368		105-1187	N4- N5	Very fine grained sandstone		None

368	369		105-1187	N4- N5	Very fine grained sandstone		None
369	370		105-1187	5Y 4/1, N4- N6	Very fine to fine grained sandstone		None
370	371		105-1188	5Y 4/1, N4- N6	Very fine to fine grained sandstone		None
371	372		105-1188	5Y 4/1, N4- N6	Very fine to fine grained sandstone		None
372	373		105-1188	5GY 4/1, N4; 5R 2/2, 5YR 3/2	Clay with rock fragments	Calcareous; 5GY 4/1, N4 siltstone; 5R 2/2, 5YR 3/2 silty shale	None
373	374	WATER STRIKE	105-1188	5GY 4/1, N4; 5R 2/2, 5YR 3/2	Clay with rock fragments	Calcareous; 5GY 4/1, N4 siltstone; 5R 2/2, 5YR 3/2 silty shale	None
374	375		105-1188	N4- N5; 5YR 2/2, 5YR 3/2	Siltstone and silty shale	Sparse clay, slightly calcareous; N4-N5 siltstone;5YR 2/2, 5YR 3/2 silty shale	None
375	376		105-1190	N4- N5; 5YR 2/2, 5YR 3/2	Siltstone and silty shale	Sparse clay, slightly calcareous; N4-N5 siltstone;5YR 2/2, 5YR 3/2 silty shale	None
376	377		105-1190	N4- N5; 5YR 2/2, 5YR 3/2	Siltstone and silty shale	Sparse clay, slightly calcareous; N4-N5 siltstone;5YR 2/2, 5YR 3/2 silty shale	None
377	378		105-1190	N4- N5	Siltstone	Sparse clay	None

378	379		105-1190	5G 4/1, N4	Clay with rock fragments	5G 4/1, N4 fine grained sandstone	None
379	380		105-1190	N4-N5	Very fine to fine grained sandstone	Sparse clay; slightly calcareous	None
380	381		105-1191	N4-N5	Very fine to fine grained sandstone	Sparse clay; slightly calcareous	None
381	382		105-1191	N4-N5	Very fine to fine grained sandstone	Sparse clay; slightly calcareous	None
382	382		105-1191	N4-N5	Very fine to fine grained sandstone	Sparse clay; slightly calcareous	None
382	384		105-1191	N4-N5	Very fine to fine grained sandstone	Sparse clay; slightly calcareous	None
384	385		105-1191	N4, 5GY 4/1	Very fine grained sandstone	Slightly calcareous	None
385	386		105-1192	N4, 5GY 4/1	Very fine grained sandstone	Slightly calcareous	None
386	387		105-1192	5GY 4/1, N4	Siltstone to very fine grained sandstone	Calcareous	None
387	388		105-1192	5GY 4/1, N4	Siltstone to very fine grained sandstone	Calcareous	None
388	389		105-1192	N4- N5	Very fine grained sandstone	Calcareous	None
389	390		105-1193	N3- N4	Siltstone	Sparse clay	None
390	391		105-1193	N4-N5, 5GY 4/1	Very fine to fine grained sandstone	Sparse clay, calcareous; N4-N5, 5GY 4/1 very fine to fine grained sandstone	None
391	392		105-1193	N4-N5, 5GY 4/1	Very fine to fine grained sandstone	Sparse clay, calcareous; N4-N5, 5GY 4/1 very fine to fine grained sandstone	None

392	393		105-1193	N4-N5, 5GY 4/1	Very fine to fine grained sandstone	Sparse clay, calcareous; N4-N5, 5GY 4/1 very fine to fine grained sandstone	None
393	394		105-1193	N4-N5, 5GY 4/1	Very fine to fine grained sandstone	Sparse clay, calcareous; N4-N5, 5GY 4/1 very fine to fine grained sandstone	None
394	395		105-1193	N4- N6	Very fine to fine grained sandstone	Calcareous	None
395	396		105-1194	N4- N6	Clay with rock fragments	Calcareous; N4-N6 very fine to fine grained sandstone	None
396	397		105-1194	N4- N6	Clay with rock fragments	Calcareous; N4-N6 very fine to fine grained sandstone	None
397	398		105-1194	N4- N6	Clay with rock fragments	Calcareous; N4-N6 very fine to fine grained sandstone	None
398	399		105-1194	N4- N6	Clay with rock fragments	Calcareous; N4-N6 very fine to fine grained sandstone	None
399	400		105-1194	N4- N6	Very fine to fine grained sandstone	Sparse clay, calcareous; N4-N6 Very fine to fine grained sandstone	None
400	401		105-1195	N4- N6	Very fine to fine grained sandstone	Sparse clay, calcareous; N4-N6 very fine to fine grained sandstone	None
401	402		105-1195	N4- N6	Very fine to fine grained sandstone	Sparse clay, calcareous; N4-N6 very fine to fine grained sandstone	None
402	403		105-1195	N4-N5; N4	Very fine grained sandstone and siltstone	Calcareous; N4- N5 very fine grained sandstone; N4 siltstone	None

403	404		105-1195	N4-N5; N4	Very fine grained sandstone and siltstone	Calcareous; N4-N5 very fine grained sandstone; N4 siltstone	None
404	405		105-1195	N4-N5; N4	Very fine grained sandstone and siltstone	Calcareous; N4-N5 very fine grained sandstone; N4 siltstone	None
405	406		105-1196	N4-N5; N4	Very fine grained sandstone and siltstone	Calcareous; N4- N5 very fine grained sandstone; N4 siltstone	None
406	407		105-1196	5GY 4/1, N3	Siltstone	Slightly calcareous	None
407	408		105-1196	5GY 4/1, N3	Siltstone	Slightly calcareous	None
408	409		105-1196	5GY 4/1; N6	Siltstone and very fine to fine grained sandstone	Slightly calcareous; 5GY 4/1 siltstone; N6 very fine to fine grained sandstone	None
409	410		105-1196	5GY 4/1; N6	Siltstone and very fine to fine grained sandstone	Slightly calcareous; 5GY 4/1 siltstone; N6 very fine to fine grained sandstone	None
410	411		105-1197	N4; N3, 5GY 4/1	Very fine to fine grained sandstone and siltstone	Slightly calcareous; N4 very fine to fine grained sandstone; N3, 5GY 4/1 siltstone	None
411	412		105-1197	N4; N3, 5GY 4/1	Very fine to fine grained sandstone and siltstone	Slightly calcareous; N4 very fine to fine grained sandstone; N3, 5GY 4/1 siltstone	None
412	413		105-1197	N4	Very fine grained sandstone	Slightly calcareous; N4 very fine grained sandstone	None

413	414		105-1197	N4	Very fine grained sandstone	Slightly calcareous; N4 very fine grained sandstone	None
414	415		105-1197	N4, 5Y4/1; N3	Very fine grained sandstone and siltstone	Calcareous; N4, 5Y 4/1 very fine grained sandstone; N3 siltstone	None
415	416		105-1197	N4, 5Y4/1; N3	Very fine grained sandstone and siltstone	Calcareous; N4, 5Y 4/1 very fine grained sandstone; N3 siltstone	None
416	417		105-1197	N4, 5Y4/1; N3	Very fine grained sandstone and siltstone	Calcareous; N4, 5Y 4/1 very fine grained sandstone; N3 siltstone	None
417	418		105-1198	N4- N6; 5YR 3/2	Very fine grained sandstone and silty shale	Calcareous; N4-N6 very fine grained sandstone; 5YR 3/2 silty shale	None
418	419		105-1198	N4- N6; 5YR 3/2	Very fine grained sandstone and silty shale	Calcareous; N4-N6 very fine grained sandstone; 5YR 3/2 silty shale	None
419	420		105-1198	N4- N5, 5GY 4/1	Siltstone to very fine grained sandstone	Slightly calcareous	None
420	421		105-1199	N3- N4, 5Y 4/1; N5- N6	Siltstone and sub-ordinate very fine grained sandstone	Calcareous; N3-N4, 5Y 4/1 siltstone; N5- N6 very fine grained sandstone	None
421	422		105-1199	N3- N4, 5Y 4/1; N5- N6	Siltstone and sub-ordinate very fine grained sandstone	Calcareous; N3-N4, 5Y 4/1 siltstone; N5- N6 very fine grained sandstone	None
422	423		105-1199	N3- N4, 5Y 4/1; N5- N6	Siltstone and sub-ordinate very fine grained sandstone	Calcareous; N3-N4, 5Y 4/1 siltstone; N5- N6 very fine grained sandstone	None

423	424		105-1199	N3- N4, 5Y 4/1; N5- N6	Siltstone and sub-ordinate very fine grained sandstone	Calcareous; N3-N4, 5Y 4/1 siltstone; N5- N6 very fine grained sandstone	None
424	425		105-1199	N3- N4, 5Y 4/1; N5- N6	Siltstone and sub-ordinate very fine grained sandstone	Calcareous; N3-N4, 5Y 4/1 siltstone; N5- N6 very fine grained sandstone	None
425	426		105-1200	N3- N4, 5Y 4/1; N5- N6	Siltstone and sub-ordinate very fine grained sandstone	Calcareous; N3-N4, 5Y 4/1 siltstone; N5- N6 very fine grained sandstone	None
426	427		105-1200	N3- N4, 5GY 4/1, 5YR 4/1	Very fine grained sandstone	Calcareous	None
427	428		105-1200	N3- N4, 5GY 4/1, 5YR 4/1	Very fine grained sandstone	Calcareous	None
428	429		105-1200	N3- N4, 5GY 4/1, 5YR 4/1	Very fine grained sandstone	Calcareous	None
429	430		105-1200	5YR 4/1	Silty shale	Slightly calcareous	None
430	431		105-1201	5YR 4/1, N4	Siltstone to very fine grained sandstone	Slightly calcareous	None
431	432		105-1201	5 Y 4/1, N3- N4	Siltstone to very fine grained sandstone	Slightly calcareous	None
432	433		105-1201	N4, 5GY 4/1; 5Y 2/2, N3	Siltstone and silty shale	Slightly calcareous; N4, 5GY 4/1 siltstone; 5Y 2/2, N3 silty shale	None
433	434		105-1201	N3- N4, 5GY 4/1	Siltstone	Slightly calcareous	None

434	435		105-1201	5GY 4/1, N3- N4	Siltstone	Slightly calcareous	None
435	436		105-1202	5GY 4/1, N3- N4	Siltstone	Slightly calcareous	None
436	437		105-1202	5GY 4/1, N4	Very fine grained sandstone	Slightly calcareous	None
437	438		105-1202	5GY 4/1, N4	Very fine grained sandstone	Slightly calcareous	None
438	439		105-1202	5GY 4/1, N4; 5YR 2/2, 5YR 3/2	Siltstone and silty shale	Slightly calcareous; 5GY 4/1, N4 siltstone; 5YR 2/2, 5YR 3/2 silty shale	None
439	440		105-1202	5GY 4/1, 5YR 4/1, N3- N4	Siltstone		None
440	441		105-1203	5GY 4/1, 5YR 4/1, N3- N4	Siltstone		None
441	442		105-1203	5GY 4/1, 5YR 4/1, N3- N4	Siltstone		None
442	443		105-1203	5GY 4/1, 5YR 4/1, N3- N4	Siltstone		None
443	444		105-1203	N4- N6	Very fine grained sandstone		None
444	445		105-1203	5GY 4/1	Siltstone		None
445	446		105-1204	N3, 5Y 4/1	Silty shale		None

446	447		105-1204	N4, 5GY 4/1	Siltstone		None
447	448		105-1204	N4, 5GY 4/1	Siltstone		None
448	449		105-1204	5GY 4/1	Siltstone to very fine grained sandstone	Slightly calcareous	None
449	450		105-1204	N3, 5GY 4/1; N3-N3, 5GY 4/1	Siltstone; siltstone to very fine grained sandstone	N3, 5GY 4/1 siltstone; N3-N4, 5GY4/1 siltstone to very fine grained sandstone	None
450	451		105-1205	N3, 5GY 4/1; N3-N3, 5GY 4/1	Siltstone; siltstone to very fine grained sandstone	N3, 5GY 4/1 siltstone; N3-N4, 5GY4/1 siltstone to very fine grained sandstone	None
451	452		105-1205	N3, 5GY 4/1; N3-N3, 5GY 4/1	Siltstone; siltstone to very fine grained sandstone	N3, 5GY 4/1 siltstone; N3-N4, 5GY4/1 siltstone to very fine grained sandstone	None
452	453		105-1205	N3, 5GY 4/1; N3-N3, 5GY 4/1	Siltstone; siltstone to very fine grained sandstone	N3, 5GY 4/1 siltstone; N3-N4, 5GY4/1 siltstone to very fine grained sandstone	None
453	454		105-1205	N3, 5GY 4/1; N3-N3, 5GY 4/1	Siltstone; siltstone to very fine grained sandstone	N3, 5GY 4/1 siltstone; N3-N4, 5GY4/1 siltstone to very fine grained sandstone	None
454	455		105-1205	5GY 4/1, 5YR 3/2; 5GY 4/1,	Silty shale, siltstone to very fine grained sandstone and siltstone	5GY 4/1, 5YR 3/2 silty shale (predominant); 5GY 4/1, N4 siltstone to very fine	NONE

				N4; 5GY 4/1		grained sandstone; 5GY 4/1 siltstone	
455	456		105-1206	5GY 4/1, N4; 5YR 2/1, N3	Very fine grained sandstone and silty shale	5GY 4/1, N4 very fine grained sandstone; 5YR 2/1, N3 silty shale	None
456	457		105-1206	N4, 5GY 4/1	Very fine grained sandstone		None
457	458		105-1206	N4-N5	Very fine to fine grained sandstone		None
458	459		105-1206	N4-N5	Very fine to fine grained sandstone		None
459	460		105-1206	N4-N5	Very fine to fine grained sandstone		None
460	461		105-1207	N3, 5Y 2/1	Silty shale	Calcite vein	None
461	462		105-1207	N3- N5, 5GY 4/1	Very fine to fine grained sandstone		None
462	463		105-1207	N3- N5, 5GY 4/1	Very fine to fine grained sandstone		None
463	464		105-1207	N3- N5, 5GY 4/1	Very fine to fine grained sandstone		None
464	465		105-1207	N4- N5, 5GY 4/1	Very fine to fine grained sandstone		None
465	466		105-1208	N4- N5, 5GY 4/1	Very fine to fine grained sandstone		None
466	467		105-1208	N4- N5, 5GY 4/1	Very fine to fine grained sandstone		None
467	468		105-1208	N4	Fine grained sandstone	Mudstone clasts (5YR 3/4) present within sandstone	None

468	469		105-1208	N4	Very fine to fine grained sandstone		None
469	470		105-1208	N4	Very fine to fine grained sandstone		None
470	471		105-1208	N4; N3	Very fine to fine grained sandstone and siltstone	N4, very fine to fine grained sandstone; N3 siltstone	None
471	472		105-1209	N4	Very fine grained sandstone		None
472	473		105-1209	N4	Very fine grained sandstone		None
473	474		105-1209	N4	Siltstone		None
474	475		105-1209	N4	Very fine to fine grained sandstone		None
475	476		105-1209	N4	Very fine to fine grained sandstone		None
476	477		105-1209	N4- N5	Very fine grained sandstone		None
477	478		105-1209	N3- N4	Siltstone		None
478	479		105-1209	N4, 5GY 4/1	Very fine to fine grained sandstone		None
479	480		105-1209	N4, 5GY 4/1	Very fine to fine grained sandstone		None
480	481		105-1210	N4, 5GY 4/1	Very fine grained sandstone		None
481	482		105-1210	N4	Siltstone to very fine grained sandstone		None

482	483		105-1210	N5- N5	Very fine to fine grained sandstone		None
483	484		105-1210	N5- N5	Very fine to fine grained sandstone		None
484	485		105-1210	N5- N6	Very fine grained sandstone		None
485	486		105-1211	N5- N6	Very fine grained sandstone	Calcareous	None
486	487		105-1211	5GY 4/1, N3- N4	Siltstone		None
487	488		105-1211	N5-N6	Siltstone to very fine grained sandstone	Slightly calcareous	None
488	489		105-1211	N5- N6	Very fine grained sandstone	Calcareous	None
489	490		105-1211	N5- N6	Very fine grained sandstone		None
490	491		105-1212	N3- N5	Very fine grained sandstone		None
491	492		105-1212	N3- N5	Very fine grained sandstone		None
492	493		105-1212	N2-N3	Dolerite	Crystalline, fine to medium grained	None
493	494		105-1212	N2-N3	Dolerite	Crystalline, fine to medium grained	None
494	495		105-1212	N2-N3	Dolerite	Crystalline, fine to medium grained	None
495	496		105-1212	N2-N3	Dolerite	Crystalline, fine to medium grained	None
496	497		105-1212	N2-N3	Dolerite	Crystalline, fine to medium grained	None

497	498		105-1213	N2-N3	Dolerite	Crystalline, fine to medium grained	None
498	499		105-1213	N2-N3	Dolerite	Crystalline, fine to medium grained	None
499	500		105-1213	N2-N3	Dolerite	Crystalline, fine to medium grained	None
500	501		105-1214	N2-N3	Dolerite	Crystalline, fine to medium grained	None
501	502		105-1214	N2-N3	Dolerite	Crystalline, fine to medium grained	None
502	503		105-1214	N2-N3	Dolerite	Crystalline, fine to medium grained	None
503	504	WATER STRIKE	105-1214	N2-N3	Dolerite	Crystalline, fine to medium grained	None
504	505		105-1214	N2-N3	Dolerite	Crystalline, fine to medium grained	None
505	506		105-1216	N2-N3	Dolerite	Crystalline, fine to medium grained; clayey	None
506	507		105-1216	N2-N3	Dolerite	Crystalline, fine to medium grained; clayey	None
507	508		105-1216	N2- N3; N4	Dolerite and siltstone	Crystalline, N2-N3 fine to medium grained dolerite ;N4 siltstone	None
508	509		105-1216	N2- N3; N3	Dolerite and siltstone	Crystalline, N2-N3 fine to medium grained dolerite ;N3 siltstone	None
509	510		105-1216	N4	Siltstone		None
510	511		105-1217	N3- N4, 5GY 4/1	Silty shale	Baked	None

511	512		105-1217	N3- N4, 5GY 4/1	Silty shale	Baked	None
512	513		105-1217	N3- N4, 5GY 4/1	Silty shale	Slightly calcareous, baked	None
513	514		105-1217	N4	Very fine grained sandstone		None
514	515		105-1217	N4-N5	Very fine grained sandstone	Slightly calcareous; clayey	None
515	516		105-1218	5YR 2/1, N3	Silty shale		None
516	517		105-1218	N3- N4	Very fine grained sandstone		None
517	518		105-1218	N3- N4	Very fine grained sandstone		None
518	519		105-1218	N3- N4	Silty shale	Sparse clay	None
519	520		105-1218	N3- N4	Silty shale	Sparse clay	None
520	521		105-1219	N4	Siltstone	Sparse clay	None
521	522		105-1219	N3, 5GY 4/1; N5	Siltstone; very fine to fine grained sandstone	Clayey, slightly calcareous; N3, 5GY 4/1 siltstone; N5 very fine to fine grained sandstone	None
522	523		105-1219	N3- N5	Siltstone and very fine grained sandstone		None
523	524		105-1220	N3- 4	Very fine grained sandstone	Sparse clay	None

524	525		105-1220	N3- 4	Very fine grained sandstone	Sparse clay	None
525	526		105-1220	N4, 5GY 4/1, 5YR 2/2	Silty shale	Sparse clay	None
526	527		105-1220	N3- N4	Siltstone		None
527	528		105-1220	N3- N4	Siltstone		None
528	529		105-1220	N3- N4	Siltstone		None
529	530		105-1220	N3- N4	Siltstone		None
530	531		105-1221	N4- N5; N6	Siltstone and very fine grained sandstone	N4-N5 siltstone; N6 very fine grained sandstone	None
531	532		105-1221	N4- N5; N6	Siltstone and very fine grained sandstone	N4-N5 siltstone; N6 very fine grained sandstone	None
532	533		105-1221	5GY 4/1, N4; 5YR 3/4, 5YR 3/2	Siltstone and shale	5GY 4/1, N4 siltstone; 5YR 3/4, 5YR 3/2 shale	None
533	534		105-1221	5GY 4/1, N3; 5YR 2/2	Siltstone and silty shale	5GY 4/1, N3 siltstone; 5YR 2/2 silty shale	None
534	535		105-1221	5GY 4/1, N4	Siltstone to very fine grained sandstone		None
535	536		105-1222	N4	Very fine grained sandstone		None

536	537		105-1222	5YR 4/1, 5Y 2/1, 5YR 2/2	Shale		None
537	538		105-1222	5GY 4/1, 5Y 4/1	Siltstone		None
538	539		105-1222	N5- N6	Very fine grained sandstone	Slightly calcareous	None
539	540		105-1222	5YR 3/4, 5YR 3/2	Shale	Slightly calcareous	None
540	541		105-1223	5GY 4/1, N4	Very fine grained sandstone	Slightly calcareous	None
541	542		105-1223	N4	Very fine grained sandstone		None
542	543		105-1223	N3-N4	Very fine grained sandstone	Slightly calcareous	None
543	544		105-1223	N4	Siltstone	Slightly calcareous	None
544	545		105-1223	5GY 6/1, N5	Very fine grained sandstone	Slightly calcareous	None
545	546		105-1224	N4, 5GY 4/1	Very fine grained sandstone	Slightly calcareous	None
546	547		105-1224	N4- N5	Very fine to fine grained sandstone		None
547	548		105-1224	N4- N5	Very fine to fine grained sandstone		None
548	549		105-1224	N4, 5GY 4/1	Very fine grained sandstone	Slightly calcareous	None
549	550		105-1224	5GY 4/1, N4	Siltstone to very fine grained sandstone	Slightly calcareous	None

550	551		105-1224	N4- N5, 5GY 4/1	Very fine grained sandstone	Calcareous	None
551	552		105-1234	5GY 4/1	Siltstone to very fine grained sandstone		None
552	553		105-1234	N3- N4, 5GY 4/1	Siltstone	Slightly calcareous	None
553	554		105-1234	N3- N4, 5GY 4/1	Siltstone	Slightly calcareous	None
554	555		105-1234	N4; N3, 5GY 4/1	Very fine to fine grained sandstone and siltstone	N4 very fine to fine grained sandstone; N3, 5GY 4/1 siltstone	None
555	556		105-1235	N5- N6	Very fine to fine grained sandstone	Slightly calcareous	None
556	557		105-1235	N5- N6	Very fine to fine grained sandstone	Slightly calcareous	None
557	558		105-1235	N5- N6, 5GY 4/1	Very fine to fine grained sandstone		None
558	559		105-1235	N5- N6, 5GY 4/1	Very fine to fine grained sandstone		None
559	560		105-1236	5GY 4/1, N5	Very fine to fine grained sandstone		None
560	561		105-1236	5GY 4/1, N5	Very fine to fine grained sandstone		None
561	562		105-1236	N5	Very fine to fine grained sandstone		None
562	563		105-1236	N5	Very fine to fine grained sandstone		None
563	564		105-1236	N5	Very fine grained sandstone	Calcareous	None

564	565		105-1237	N4- N6	Very fine to fine grained sandstone		None
565	566		105-1237	N5	Very fine to fine grained sandstone	Sparse clay	None
566	567		105-1237	N5-N6	Clay with rock fragments	Calcareous; N5-N6 very fine to fine grained sandstone	None
567	568		105-1237	N4- N5	Very fine to fine grained sandstone		None
568	569		105-1237	N4- N6	Very fine to fine grained sandstone	Sparse clay	None
569	570		105-1238	N4- N6	Very fine to fine grained sandstone	Sparse clay	None
570	571		105-1238	5GY 4/1, 5G 4/1, N4	Siltstone	Clayey, slightly calcareous	None
571	572		105-1238	N4- N5	Very fine to fine grained sandstone	Sparse clay; slightly calcareous	None
572	573		105-1238	N4- N5	Very fine to fine grained sandstone	Sparse clay; slightly calcareous	None
573	574		105-1238	N5- N6	Very fine to fine grained sandstone	Sparse clay; slightly calcareous	None
574	575		105-1239	5GY 4/1	Siltstone to very fine grained sandstone	Sparse clay; slightly calcareous	None
575	576		105-1239	N4	Very fine grained sandstone	Sparse clay; slightly calcareous	None
576	577		105-1239	5GY 4/1; N4- N5	Siltstone and very fine to fine grained sandstone	Slightly calcareous; 5GY 4/1 siltstone; N4-N5 very fine to fine grained sandstone	None

577	578		105-1239	5GY 4/1; N4- N5	Siltstone and very fine to fine grained sandstone	Slightly calcareous; 5GY 4/1 siltstone; N4-N5 very fine to fine grained sandstone	None
578	579		105-1239	N4- N5	Very fine grained sandstone	Slightly calcareous	None
579	580		105-1240	N4, 5GY 4/1	Very fine grained sandstone	Slightly calcareous	None
580	581		105-1240	5GY 4/1, N4	Siltstone	Slightly calcareous	None
581	582		105-1240	5GY 4/1, N4	Siltstone	Slightly calcareous	None
582	583		105-1240	5GY 4/1, N4; 5YR 3/2, 5YR ¾	Siltstone to very fine grained sandstone and sub-ordinate silty shale	5GY 4/1, N4 siltstone to very fine grained sandstone; 5YR 3/2, 5YR 3/4 silty shale	None
583	584		105-1240	N4- N5	Siltstone		None
584	585		105-1241	N5	Very fine grained sandstone		None
585	586		105-1241	5GY 4/1, N4	Siltstone to very fine grained sandstone		None
586	587		105-1241	N4- N5	Siltstone to very fine grained sandstone	Slightly calcareous	None
587	588		105-1241	N5, 5GY 4/1	Very fine grained sandstone	Slightly calcareous	None
588	589		105-1241	N5	Very fine to fine grained sandstone		None
589	590		105-1242	5GY 4/1, N4	Very fine grained sandstone		None

590	591		105-1242	N6- N7; N3- N4	Very fine to fine grained sandstone and siltstone	N6-N7 very fine to fine grained sandstone; N3-N4 siltstone	None
591	592		105-1242	N3- N4	Siltstone		None
592	593		105-1242	N5- N6	Very fine to fine grained sandstone	Slightly calcareous	None
593	594		105-1242	5GY 4/1, N4- N5	Siltstone		None
594	595		105-1243	5GY 4/1, N4- N5	Siltstone		None
595	596		105-1243	5GY 4/1; N6	Siltstone to very fine grained sandstone and very fine to fine grained sandstone	5GY 4/1 siltstone to very fine grained sandstone; N6 very fine to fine grained sandstone	None
596	597		105-1243	5GY 4/1, N4	Siltstone to very fine grained sandstone		None
597	598		105-1243	N4	Siltstone to very fine grained sandstone	Calcareous	None
598	599		105-1243	N4; N6	Siltstone and very fine to fine grained sandstone	N4 siltstone; N6 very fine to fine grained sandstone; calcareous	None
599	600		105-1244	N5	Very fine to fine grained sandstone	Calcareous	None
600	601		105-1244	N5- N6	Very fine to fine grained sandstone		None
601	602		105-1244	N5- N6	Very fine to fine grained sandstone	Slightly calcareous	None
602	603		105-1244	N5- N6	Very fine to fine grained sandstone	Slightly calcareous	None

603	604		105-1244	N6	Very fine to fine grained sandstone	Calcareous	None
604	605		105-1245	5GY 4/1, N4	Siltstone	Slightly calcareous	None
605	606		105-1245	N4- N5	Siltstone	Slightly calcareous	None
606	607		105-1245	N4- N5, 5GY 4/1	Very fine grained sandstone	Calcareous; slightly clayey	None
607	608		105-1245	5GY 4/1, N5- N6	Siltstone to very fine grained sandstone	Calcareous	None
608	609		105-1245	N4	Silty shale		None
609	610		105-1246	N3- N4	Silty shale		None
610	611		105-1246	N4	Silty shale		None
611	612		105-1246	N4; N5-N6	Siltstone and very fine to fine grained sandstone	N4 siltstone; N5-N6 very fine to fine grained sandstone	None
612	613		105-1246	N3- N4	Silty shale	Slightly calcareous	None
613	614		105-1246	5GY 4/1, N4	Siltstone	Slightly calcareous	None
614	615		105-1247	5GY 4/1,N3-N4	Silty shale		None
615	616		105-1247	N4- N5, 5GY 4/1	Siltstone		None
616	617		105-1247	5GY 4/1	Siltstone	Slightly clayey; calcareous	None

617	618		105-1247	5GY 4/1; N4	Siltstone and silty shale	Slightly clayey; calcareous; 5GY 4/1 siltstone, N4 silty shale	None
618	619		105-1247	5GY 4/1, N4	Very fine grained sandstone	Slightly clayey; calcareous	None
619	620		105-1248	5GY 4/1, N4- N5	Siltstone	Calcareous	None
620	621		105-1248	5GY 4/1, N5	Siltstone to very fine grained sandstone	Clayey; calcareous	None
621	622		105-1248	5 G 4/1, N6	Very fine to fine grained sandstone	Slightly calcareous	None
622	623		105-1248	N5, 5G 4/1	Very fine to fine grained sandstone	Clayey; calcareous	None
623	624		105-1248	N5- N6, 5G 4/1	Very fine to fine grained sandstone	Clayey; calcareous	None
624	625		105-1249	N5, 5 G 4/1	Very fine to fine grained sandstone	Slightly clayey; slightly calcareous	None
625	626		105-1249	N5, 5 G 4/1	Very fine to fine grained sandstone	Slightly clayey; slightly calcareous	None
626	627		105-1249	N5- N6	Very fine to fine grained sandstone	Slightly calcareous	None
627	628		105-1249	5G 4/1, N5- N6	Very fine to fine grained sandstone	Slightly calcareous	None
628	629		105-1249	N5- N6	Very fine to fine grained sandstone	Slightly calcareous	None
629	630		105-1249	N5- N6	Very fine to fine grained sandstone	Slightly calcareous	None
630	631		105-1250	5 G 4/1, N5- N6	Very fine to fine grained sandstone	Calcareous	None

631	632		105-1250	5YR 3/2, 5YR 2/2; 5GY 4/1,N4	Shale and siltstone	Slightly calcareous; 5YR 3/2, 5YR 2/2 shale; 5 GY 4/1, N4 siltstone	None
632	633		105-1250	5YR 3/2, 5YR 2/2; 5GY 4/1,N4	Shale and siltstone	Slightly calcareous; 5YR 3/2, 5YR 2/2 shale; 5 GY 4/1, N4 siltstone	None
633	634		105-1250	5 G 4/1, N4- N5	Very fine grained sandstone	Clayey; calcareous	None
634	635		105-1250	N5, 5 G 4/1	Siltstone to very fine grained sandstone	Slightly clayey; slightly calcareous	None
635	636		105-1251	5 GY 4/1, N4	Siltstone to very fine grained sandstone		None
636	637		105-1251	5GY 4/1, N4 ; 5Y 4/1, N4	Siltstone and siltstone to very fine grained sandstone	Slightly clayey; slightly calcareous; 5GY 4/1, N4 siltstone; 5Y 4/1, N4 siltstone to very fine grained sandstone	NONE
637	638		105-1251	N4	Very fine grained sandstone		None
638	639		105-1251	5 G 4/1, 5 GY 4/1, N4	Siltstone		None
639	640		105-1251	N4, 5 Y 4/1	Siltstone to very fine grained sandstone	Slightly clayey	None
640	641		105-1252	N4, 5 Y 4/1	Siltstone to very fine grained sandstone	Slightly clayey	None
641	642		105-1252	N4- N5	Very fine grained sandstone		None

642	643		105-1252	N3- N4	Very fine grained sandstone		None
643	644		105-1252	N3- N4	Siltstone		None
644	645		105-1252	N3- N4	Siltstone	Slightly clayey	None
645	646		105-1253	N4	Siltstone		None
646	647		105-1253	N4- N5	Very fine grained sandstone		None
647	648		105-1253	N4- N5	Very fine grained sandstone		None
648	649		105-1253	N4- N5	Very fine grained sandstone		None
649	650		105-1253	5GY 4/1, N3	Siltstone		None
650	651		105-1253	N3- N4, 5GY 4/1	Siltstone to very fine grained sandstone		None
651	652		105-1253	N4	Very fine grained sandstone		None
652	653		105-1254	N3- N4	Siltstone	Slightly clayey; slightly calcareous	None
653	654		105-1254	N3- N4	Siltstone	Slightly clayey; slightly calcareous	None
654	655		105-1254	N4	Siltstone	Slightly clayey	None
655	656		105-1254	N5	Very fine to fine grained sandstone	Slightly clayey; slightly calcareous	None
656	657		105-1254	N4, 5GY 4/1	Siltstone	Slightly clayey; slightly calcareous	None

657	658		105-1254	N3-N 4	Siltstone to very fine grained sandstone		None
658	659		105-1254	N3	Silty shale	Slightly clayey; slightly calcareous	None
659	660		105-1254	N3; N4	Silty shale and siltstone	Slightly clayey; slightly calcareous; N3 silty shale; N4 siltstone	None
660	661		105-1255	N3- N4	Siltstone	Slightly clayey	None
661	662		105-1255	N3	Silty shale	Slightly clayey; slightly calcareous	None
662	663		105-1255	N3, 5GY 4/1	Silty shale	Slightly clayey	None
663	664		105-1255	N3, 5GY 4/1; N4, 5GY 4/1	Silty shale and siltstone	Slightly clayey; N3, 5GY 4/1 silty shale; N4, 5GY 4/1 siltstone	None
664	665		105-1255	N4- N5; N3	Very fine to fine grained sandstone and siltstone	Slightly calcareous; N4-N5 very fine to fine grained sandstone; N3 siltstone	None
665	666		105-1256	N5; N4	Very fine to fine grained sandstone and siltstone	N5 very fine to fine grained sandstone; N4 siltstone	None
666	667		105-1256	N5; N4	Very fine to fine grained sandstone and siltstone	N5 very fine to fine grained sandstone; N4 siltstone	None
667	668		105-1256	N5	Very fine grained sandstone		None
668	669		105-1256	N4	Siltstone		None

669	670		105-1256	N3- N4	Silty shale		None
670	671		105-1257	N3; N4-N5	Siltstone and very fine grained sandstone	Slightly clayey; N3 siltstone; N4- N5 very fine grained sandstone	None
671	672		105-1257	N3	Siltstone	Slightly clayey	None
672	673		105-1257	N4	Very fine grained sandstone	Slightly clayey; slightly calcareous	None
673	674		105-1257	N3	Silty shale	Slightly clayey; slightly calcareous	None
674	675		105-1257	N3	Silty shale	Slightly clayey; slightly calcareous	None
675	676		105-1258	N4, 5GY 4/1	Siltstone	Slightly calcareous	None
676	677		105-1258	N3- N4	Siltstone	Slightly clayey; slightly calcareous	None
677	678		105-1258	N3- N4	Siltstone	Slightly clayey; slightly calcareous	None
678	679		105-1258	N3- N4, 5GY 4/1	Siltstone	Slightly clayey	None
679	680		105-1258	N3- N4, 5GY 4/1	Siltstone	Slightly clayey	None
680	681		105-1259	N2- N3	Silty shale	Slightly clayey; slightly calcareous	None
681	682		105-1259	N2- N3	Silty shale	Slightly clayey; slightly calcareous	None
682	683		105-1259	N2; N3, 5GY 4/1	Silty shale and siltstone	N2 silty shale; N3, 5GY 4/1 siltstone	None

683	684		105-1259	N4	Very fine grained sandstone	Slightly clayey	None
684	685		105-1259	N5- N6; N3, 5GY 6/1	Very fine to fine grained sandstone and siltstone	Slightly clayey; N5- N6 very fine to fine grained sandstone; N3, 5GY 6/1 siltstone	None
685	686		105-1260	N4, 5 GY 4/1	Siltstone	Slightly clayey	None
686	687		105-1260	N3	Siltstone	Slightly clayey	None
687	688		105-1260	N3	Siltstone	Slightly clayey	None
688	689		105-1261	N4- N5	Siltstone to very fine grained sandstone	Slightly calcareous; possible calcite vein?	None
689	690		105-1261	N3	Silty shale	Slightly clayey; slightly calcareous	None
690	691		105-1261	5YR 3/2, 5YR 2/2; 5GY 4/1,N4	Silty shale and siltstone	Clayey; slightly calcareous; 5 YR 3/2, 5YR 2/2 silty shale; 5 GY 4/1, N4 siltstone	None
691	692		105-1261	N3; N5-N6	Silty shale and siltstone	N3 silty shale; N5-N6 siltstone	None
692	693		105-1261	5 GY 4/1, N4	Siltstone	Slightly clayey; slightly calcareous	None
693	694		105-1261	N3	Siltstone	Slightly clayey; slightly calcareous	None
694	695		105-1261	5GY 2/1; N4	Siltstone and silty shale	Slightly clayey; slightly calcareous; 5GY 2/1 silty shale; N4 siltstone	None

695	696		105-1262	N4	Siltstone	Slightly clayey; slightly calcareous;	None
696	697		105-1262	N3- N4	Siltstone		None
697	698		105-1262	N3	Silty shale	Calcareous; clayey	None
698	699		105-1262	N3- N4	Siltstone	Slightly clayey; slightly calcareous	None
699	700		105-1262	N3- N4	Siltstone	Slightly clayey; slightly calcareous	None
700	701		105-1263	N6	Very fine grained sandstone	Slightly clayey; slightly calcareous	None
701	702		105-1263	N6; N4	Very fine to fine grained sandstone and siltstone	Slightly clayey; slightly calcareous; N6 very fine to fine grained sandstone; N4 siltstone	None
702	703		105-1263	N4- N5	Very fine to fine grained sandstone	Slightly clayey; slightly calcareous	None
703	704		105-1263	N4, 5GY 4/1; N5	Siltstone and very fine grained sandstone	Calcareous; clayey; N4, 5GY 4/1 siltstone; N5 very fine grained sandstone	None
704	705		105-1263	N3, 5YR 3/2; N3-N4	Silty shale and siltstone	Slightly calcareous; N3, 5YR 3/2 silty shale; N3-N4 siltstone	None
705	706		105-1263	N2- N3	Silty shale	Calcareous; clayey	None
706	707		106-1343	N5, 5GY 4/1; N4	Very fine to fine grained sandstone and silty shale	Calcareous; N5, 5GY 4/1 very fine to fine grained sandstone; N4 silty shale	None

707	708		106-1343	N5, 5G4/1	Very fine grained sandstone	Slightly calcareous	None
708	709		106-1343	5G 4/1; 5GY 4/1, N5	Siltstone and very fine grained sandstone	Slightly calcareous; 5G 4/1 siltstone; 5GY 4/1, N5 very fine grained sandstone	None
709	710		106-1343	5Y4/1; N5- N6, 5GY 4/1; 5G4/1	Siltstone, very fine to fine grained sandstone and shale	5Y 4/1 siltstone, N5-N6, 5GY 4/1 very fine to fine grained sandstone and 5G4/1, N3 shale	None
710	711		106-1343	5G 4/1; N4- N5, 5G 5/1; N4	Siltstone, very fine to fine grained sandstone and shale	5G 4/1 siltstone; N4-N5, 5G 5/1 most numerous fine to fine grained sandstone and N4 silty shale	None
711	712		106-1343	N4, 5B 5/1; 5G 4/1, 5B 5/1 ; N6	Silty shale, siltstone and very fine to fine grained	Slightly calcareous; N4, 5B 5/1 silty shale predominant; 5G 4/1, 5B 5/1 siltstone; N6 very fine to fine grained	NONE
712	713		106-1344	N4 , 5GY 4/1 ; N5, 5B4/1	Very fine grained sandstone; siltstone	N4 , 5GY 4/1 very fine grained sandstone; N5, 5B 4/1 siltstone dominant	None
713	714		106-1344	N5, 5GY 4/1; 5GY 4/1, 5G4/1, N4	Very fine to fine grained sandstone and very fine grained sandstone	N5, 5GY 4/1 very fine to fine grained sandstone and 5GY 4/1, 5G4/1, N4 very fine grained sandstone	NONE
714	715		106-1344	N4, 5 B 5/1; N4	Siltstone and subordinate very fine to fine grained sandstone	Slightly calcareous; N4, 5 B 5/1 siltstone dominant; N4 very fine to fine grained subordinate sandstone	NONE

715	716		106-1344	N4- N5; N3- N4	Siltstone and silty shale	Slightly calcareous; N4-N5 siltstone; N3-N4 silty shale	None
716	717		106-1344	N3- N4; N5, 5GY 4/1, 5YR 4/1, 5R ¾	Silty shale and siltstone	N3-N4 silty shale; N5, 5GY 4/1, 5YR 4/1, 5R 3/4 siltstone	None
717	718		106-1344	N3- N4; N4, 5Y 4/1	Silty shale and siltstone	N3-N4 silty shale; N4, 5Y 4/1 siltstone	None
718	719		106-1344	N3- N4; N5	Silty shale and siltstone	N3-N4 silty shale; N5 siltstone	None
719	720		106-1344	N3; N5	Silty shale and siltstone	N3 silty shale; N5 siltstone	None
720	721		106-1344	N4; N3; N4, 5GY 4/1	Very fine grained sandstone, silty shale and siltstone	N4 very fine grained sandstone, N3 silty shale and N4, 5GY 4/1 siltstone	None
721	722		106-1345	N4- N5; 5G 4/1	Very fine to fine grained sandstone and siltstone	Slightly calcareous; N4-N5 very fine to fine grained sandstone; 5G 4/1 siltstone	None
722	723		106-1345	5GY 4/1, 5G 4/1, N4 ; N6, 5GY 4/1	Siltstone and very fine grained sandstone	5GY 4/1, 5G 4/1, N4 siltstone; N6, 5GY 4/1 very fine grained sandstone	None
723	724		106-1345	5Y 4/1, 5G 4/1, 5GY 4/1; N2- N3	Siltstone and shale	5Y 4/1, 5G 4/1, 5GY 4/1 siltstone; N2-N3 shale	None
724	725		106-1345	N3- N4; N4- N5, 5GY 4/1	Silty shale and siltstone	N3-N4 silty shale and N4-N5, 5GY 4/1 siltstone	None

725	726		106-1345	5GY 4/1, N4; N4; 5GY 4/1	Very fine grained sandstone, silty shale and siltstone	5GY 4/1, N4 very fine grained sandstone, N4 silty shale and 5G 4/1 predominant siltstone	None
726	727		106-1346	N3- N4	Silty shale		None
727	728		106-1346	N4,5GY 4.1; 4-N5	Siltstone and silty shale	N5, 5GY 4/1 siltstone; N4-N5 silty shale	None
728	729		106-1346	N4, 5GY 4/1	Siltstone	Slightly calcareous; N4, 5GY 4/1 siltstone	None
729	730		106-1346	N4- N5, 5GY 4/1; N3- N4, 5GY 4/1	Siltstone and a silty shale	N4-N5, 5GY 4/1 siltstone; N3-N4, 5GY 4/1 silty shale; gas emission?	None
730	731		106-1347	N4, 5GY 4/1	Silty shale		None
731	732		106-1347	N5; 3-N4; N4, 5B 5/1	Very fine to fine grained sandstone, silty shale and a siltstone	N5 very fine to fine grained sandstone, N3-N4 silty shale and N4, 5B 5/1 siltstone	None
732	733		106-1347	5GY 4/1; N3	Siltstone and silty shale	5GY 4/1 siltstone and N3 silty shale	None
733	734		106-1347	N4; N5, 5B 5/1	Siltstone and very fine grained sandstone	N4 siltstone; N5, 5 B 5/1 very fine grained sandstone	None
734	735		106-1347	N4- N5; N5- N6; 10YR 8/2	Siltstone , very fine grained sandstone and chert	Slightly calcareous; N4-N5 siltstone; N5-N6 very fine grained sandstone; 10YR 8/2 chert	None

735	736		106-1347	N4- N5, 5GY 4/1	Siltstone		None
736	737		106-1348	N4, 5G 4/1; N5-N6; N4-N5, 5GY 4/1	Siltstone , very fine to fine grained sandstone and very fine grained sandstone	Slightly calcareous; N4, 5G 4/1 siltstone; N5-N6 very fine to fine grained sandstone; N4-N5, 5GY 4/1 very fine grained sandstone	NONE
737	738		106-1348	N4- N5, 5GY 4/1	Siltstone	Calcareous	None
738	739		106-1348	N4; N4, 5GY 4/1	Silty shale and siltstone	N4 silty shale and N4, 5GY 4/1 siltstone	None
739	740		106-1348	N3; N5-N6	Silty shale and very fine grained sandstone	Calcareous; N3 silty shale and N5-N6 very fine grained sandstone	None
740	741		106-1349	5GY 4/1, N4 ;N4-N5; N3-N4	Siltstone; very fine grained sandstone and silty shale	Slightly calcareous; 5GY 4/1, N4 siltstone; N4-N5 very fine grained sandstone; N3-N4 silty shale	None
741	742		106-1349	N4- N5; N4	Siltstone and silty shale	Calcareous; N4-N5 siltstone dominant; N4 silty shale	None
742	743		106-1349	N3- N4, 5G 4/1	Silty shale	Slightly calcareous	None
743	744		106-1349	N5, 5GY 4/1; 5YR 4/1, 10R 2/2, 5YR 3/2, N4	Very fine grained sandstone and silty shale	Slightly calcareous; N5, 5GY 4/1 very fine grained sandstone and 5YR 4/1, 10R 2/2, 5YR 3/2, N4 silty shale	NONE

744	745		106-1349	N4, 5G 4/1; N5	Siltstone and very fine grained sandstone	Slightly calcareous;N4, 5G 4/1 siltstone; N5 very fine grained sandstone	None
745	746		106-1350	N5; N4-N6	Siltstone and very fine to fine grained sandstone	Calcareous; N5 siltstone dominant and N4-N6 very fine to fine grained sandstone	None
746	747		106-1350	N5- N6; N5- N6, 5G 4/1	Very fine grained sandstone and siltstone	Slightly calcareous; N5-N6 very fine grained sandstone and N5-N6 , 5G4/1 siltstone	None
747	748		106-1350	5G 4/1; N4, 5GY 4/1, 5G 4/1	Very fine grained sandstone and silty shale	Slightly calcareous; 5G 4/1 very fine grained sandstone and N4, 5GY 4/1, 5G 4/1 silty shale dominant	NONE
748	749		106-1350	N4- N5; N3	Siltstone and silty shale	Slightly calcareous;N4- N5 siltstone; N3 silty shale dominant	None
749	750		106-1350	N4- N5; N4- N5, 5G4/1	Very fine grained sandstone and siltstone	Slightly calcareous; N4-N5 very fine grained sandstone and N4-N5 , 5G4/1 siltstone	None
750	751		106-1350	N3- N6, 5GY 4/1; N4, 5G4/1	Very fine to fine grained sandstone and siltstone	Slightly calcareous; N3-N6, 5GY 4/1 very fine to fine grained sandstone and N4, 5G4/1 siltstone	None
751	752		106-1351	N6; N4	Very fine to fine grained sandstone and siltstone	N6 very fine to fine grained sandstone and N4 siltstone	None
752	753		106-1351	N4- N5; N3, 5 G 4/1; N6	Very fine grained sandstone; silty shale; very fine to	Slightly calcareous; N4-N5 very fine grained sandstone; N3, 5G 4/1 silty	NONE

					fine grained sandstone	shale; N6 very fine to fine grained sandstone	
753	754		106-1351	N4; N5, 5G 4/1	Silty shale and very fine grained sandstone	Slightly calcareous; N4 silty shale; N5, 5G 4/1 very fine grained sandstone	None
754	755		106-1351	N4- N5; N5- N6	Very fine grained sandstone and very fine to fine grained sandstone	N4-N5 very fine grained sandstone and N5-N6 very fine to fine grained sandstone	None
755	756		106-1352	N5- N6; N5, 5B 5/1	Very fine to fine grained sandstone and siltstone	Slightly calcareous; N5-N6 very fine to fine grained sandstone; N5 , 5B 5/1 siltstone	None
756	757		106-1352	N4, 5GY 4/1; N5-N6	Siltstone and very fine grained sandstone	Calcareous; N4, 5GY 4/1 siltstone; N5-N6 very fine grained sandstone	None
757	758		106-1352	N5; N4	Siltstone and very fine grained sandstone	Slightly calcareous; N5 siltstone; N4 very fine grained sandstone	None
758	759		106-1352	N4- N5; 5G 4/1, N5	Siltstone and very fine grained sandstone	Slightly calcareous; N4-N5 siltstone; 5G 4/1, N5 very fine grained sandstone	None
759	760		106-1352	N4- N5, 5G 4/1; N5	Siltstone and very fine grained sandstone	Calcareous; N4-N5, 5G 4/1 siltstone; N5 very fine grained sandstone	None
760	761		106-1353	N4, 5GY 4/1; N4, 5GY 4/1; 5GY 4/1	Siltstone, very fine grained sandstone and silty shale	Calcareous; N4, 5GY 4/1 siltstone; N4, 5G4 /1 very fine grained sandstone; 5G4/1 silty shale	None

761	762		106-1353	5G 4/1, 5GY 4/1; N6	Siltstone and very fine to fine grained sandstone	Calcareous; 5G4/1, 5GY 4/1 siltstone; N6 very fine to fine grained sandstone	None
762	763		106-1353	N3- N4; N4- N5	Siltstone and very fine grained sandstone	Calcareous; N3-N4 siltstone; N4-N5 very fine sandstone	None
763	764		106-1353	N6; N4	Very fine to fine grained sandstone and fine grained sandstone	Calcareous; N6 very fine to fine sandstone; N4 very fine sandstone	None
764	765		106-1353	5GY 4/1; N5, 5B 5/1; N5	Siltstone , very fine to fine grained sandstone and fine grained sandstone	Slightly calcareous; 5GY4/1 siltstone; N5, 5B 5/1 very fine to fine sandstone; N5 very fine sandstone	NONE
765	766		106-1353	N4; N5	Siltstone and very fine grained sandstone	Slightly calcareous; N4 siltstone; N5 very fine grained sandstone	None
766	767		106-1354	N4; N4-N5, 5GY 4/1; N3	Siltstone , very fine grained sandstone and shale	Calcareous; N4 siltstone; N4-N5, 5GY 4/1 very fine grained sandstone; N3 shale	None
767	768		106-1354	N4- N5	Siltstone	Slightly calcareous	None
768	769		106-1354	N4- N5; N4- N5, 5GY 4/1	Siltstone and very fine grained sandstone	Slightly calcareous; N4-N5 siltstone; N4-N5, 5GY 4/1 very fine grained sandstone	None
769	770		106-1354	N5- N6; N5- N6	Very fine grained sandstone and very fine to fine grained sandstone	Slightly calcareous; N5-N6 very fine grained sandstone; N5-N6 very fine to fine grained sandstone	NONE

770	771		106-1355	N5; N4, 5G 4/1	Siltstone and silty shale	Slightly calcareous; N5 siltstone; N4, 5G 4/1 silty shale	None
771	772		106-1355	N5; N5-N6; N4	Siltstone , very fine grained sandstone and silty shale	Calcareous; N5 siltstone; N5-N6 very fine grained sandstone; N4 silty shale	None
772	773		106-1355	N4-N5; N5- N6	Siltstone and very fine grained sandstone	Calcareous; N4-N5 siltstone; N5-N6 very fine grained sandstone	None
773	774		106-1355	5G 4/1,N4; N4- N5, 5 G4/1	Siltstone and very fine grained sandstone	5G 4/1, N4 siltstone; N4-N5, 5G 4/1 very fine grained sandstone	None
774	775		106-1355	N4; 5 Y 5/2	Siltstone and very fine grained sandstone	Slightly calcareous; N4 siltstone; 5Y 5/2 very fine grained sandstone	None
775	776		106-1356	N4, 5GY 4/1; N5; N3, 5GY 4/1	Siltstone , very fine grained sandstone and silty shale	Slightly calcareous; N4, 5GY 4/1 siltstone; N5 very fine grained sandstone; N3, 5GY 4/1 silty shale	None
776	777		106-1356	N4, 5G 4/1	Siltstone	Slightly calcareous	None
777	778		106-1356	N4- N5	Siltstone and very fine grained sandstone	Slightly calcareous; N4-N5 siltstone; N4-N5 very fine grained sandstone	None
778	779		106-1356	N4; N4-N5; N3	Siltstone , very fine grained sandstone and shale	Slightly calcareous; N4 siltstone; N4-N5 very fine grained sandstone; N3 shale	None

779	780		106-1356	N4- N5	Very fine grained sandstone		None
780	781		106-1356	N4- N5, 5G 4/1	Siltstone	Slightly calcareous	None
781	782		106-1357	N4- N5;N6	Very fine grained sandstone and very fine to fine grained sandstone	Slightly calcareous; N4-N5 very fine grained sandstone; N6 very fine to fine grained sandstone	None
782	783		106-1357	N4- N5; N6	Very fine grained sandstone and very fine to fine grained sandstone	N4-N5 very fine grained sandstone; N6 very fine to fine grained sandstone	None
783	784		106-1357	N4- N5	Siltstone	Slightly calcareous; N4-N5 siltstone	None
784	785		106-1357	N4; N4; N4- N5	Siltstone, very fine grained sandstone and very fine to fine grained sandstone	Slightly calcareous; N4 siltstone; N4 very fine grained sandstone; N4-N5 very fine to fine grained sandstone	NONE
785	786		106-1358	5Y 4/1; N6	Siltstone and very fine grained sandstone	Slightly calcareous; 5Y 4/1 siltstone; N6 very fine grained sandstone	None
786	787		106-1358	N4, 5G 4/1, 5GY 4/1; N5	Siltstone and very fine grained sandstone	Slightly calcareous; N4, 5G 4/1, 5GY4/1 siltstone; N5 very fine grained sandstone	None
787	788		106-1358	N4- N5; N5- N6, 5B 5/1	Siltstone and very fine grained sandstone	N4- N5 siltstone; N5-N6, 5B 5/1 very fine grained sandstone	None
788	789		106-1358	N4, 5G 4/1; N4	Siltstone and shale	Calcareous; N4, 5G 4/1 siltstone; N4 silty shale	None

789	790		106-1358	N4- N5, 5G 4/1; N3- N4	Siltstone and shale	Calcareous; N4-N5, 5G 4/1 siltstone; N3-N4 silty shale	None
790	791		106-1359	N4- N5; N6- N7	Siltstone and very fine to fine grained sandstone	Slightly calcareous; N4-N5 siltstone; N6-N7 very fine to fine grained sandstone	None
791	792		106-1359	N4- N5; 5YR 4/1	Siltstone and very fine grained sandstone	Calcareous; N4-N5 siltstone; 5YR 4/1 very fine grained sandstone	None
792	793		106-1359	N4; N3	Siltstone and shale	Slightly calcareous; N4 siltstone; N3 silty shale	None
793	794		106-1359	N3- N4	Silty shale	Slightly calcareous	None
794	795		106-1359	N4, 5GY 4/1, 5B 5/1;N5-N6	Silty shale and very fine grained sandstone	Slightly calcareous; N4, 5GY 4/1, 5B 5/1 silty shale; N5-N6 very fine grained sandstone	None
795	796		106-1359	N3-N4; N5	Silty shale and subordinate very fine grained sandstone	Slightly calcareous; N3-N4 silty shale dominant; N5 subordinate very fine grained sandstone	None
796	797		106-1360	N3- N4	Silty shale		None
797	798		106-1360	N4; N4-N5, 5Y 4/1; 5YR 4/1, 5YR ¾	Siltstone , very fine grained sandstone and silty shale	N4 siltstone; N4-N5, 5Y 4/1 very fine grained sandstone; 5YR 4/1, 5YR 3/4 silty shale	None

798	799		106-1360	N4- N5, 5GY 4/1; N3- N4	Siltstone and silty shale	N4-N5, 5GY 4/1 siltstone; N3-N4 silty shale	None
799	800		106-1360	5GY 4/1, N4	Siltstone	Slightly calcareous; 5GY 4/1, N4 siltstone	None
800	801		106-1361	N4, 5GY 4/1; N5; N3	Siltstone, siltstone to very fine grained sandstone and silty shale	N4, 5GY 4/1 siltstone; N5 siltstone to very fine grained sandstone; N3 silty shale	None
801	802		106-1361	N4, 5GY 4/1; N3-N4, 5B 5/1	Siltstone and silty shale	Calcareous; N4, 5GY 4/1 siltstone; N3 N4, 5B 5/1 silty shale	None
802	803		106-1361	N4; N3-N4	Siltstone and silty shale	Calcareous; N4 siltstone; N3-N4 silty shale	None
803	804		106-1361	N4- N5; 5Y 4/1, N4	Siltstone and silty shale	Calcareous; N4-N5 siltstone; 5Y 4/1, N4 silty shale	None
804	805		106-1361	N4- N5; N4, 5G 4/1	Siltstone and silty shale	Slightly calcareous; N4-N5 siltstone; N4, 5G 4/1 silty shale	None
805	806		106-1362	N5- N6; N3- N4	Very fine grained sandstone and silty shale	N5- N6 very fine grained sandstone; N3-N4 silty shale	None
806	807		106-1362	N3-N4, 5G 4/1	Silty shale	Slightly calcareous; N3-N4, 5G 4/1 silty shale	None
807	808		106-1362	N4- N5; N3, 5GY 4/1	Siltstone and silty shale	Slightly calcareous; N4-N5 siltstone; N3, 5GY 4/1 silty shale	None

808	809		106-1362	N4- N5	Siltstone		None
809	810		106-1362	N4- N5	Siltstone	Slightly calcareous	None
810	811		106-1362	N5- N6; N4, 5GY 4/1	Very fine to fine grained sandstone and siltstone	Calcareous; N5-N6 very fine to fine grained sandstone; N4, 5GY 4/1 siltstone	None
811	812		106-1363	N5- N6; N4	Very fine grained sandstone and siltstone	Calcareous; N5-N6 very fine grained sandstone; N4 siltstone	None
812	813		106-1363	N4, 5G 4/1	Siltstone	Slightly calcareous	None
813	814		106-1363	N4; N5	Siltstone and very fine grained sandstone	Slightly calcareous; N4 siltstone; N5 very fine grained sandstone	None
814	815		106-1363	N3, 5GY 4/1	Silty shale	Slightly calcareous	None
815	816		106-1364	N3; N4; N5	Silty shale, siltstone and very fine grained sandstone	Slightly calcareous N3 silty shale ; N4 siltstone; N5 very fine grained sandstone	None
816	817		106-1364	N5; N5-N6	Siltstone and very fine to fine grained sandstone	Slightly calcareous; N5 siltstone; N5-N6 very fine to fine grained sandstone	None
817	818		106-1364	N3; N4, 5GY 4/1	Silty shale and siltstone	Slightly calcareous; N3 silty shale; N4, 5GY 4/1 siltstone	None
818	819		106-1364	N4; N6	Siltstone and very fine grained sandstone	Slightly calcareous; N4 siltstone; N6 very fine grained sandstone	None

819	820		106-1364	N5- N6; N3- N5	Siltstone to very fine grained sandstone and siltstone	Calcareous; N5-N6 siltstone to very fine grained sandstone; N3-N5 siltstone	None
820	821		106-1365	N4; N3; N4- N5	Siltstone , silty shale and siltstone to very fine grained sandstone	Slightly calcareous; N4 siltstone; N3 silty shale; N4-N5 siltstone to very fine grained sandstone	None
821	822		106-1365	N4; N5	Siltstone and very fine grained sandstone	Slightly calcareous; N4 siltstone; N5 very fine grained sandstone	None
822	823		106-1365	N4; N5; N4, 5GY 4/1	Very fine to fine grained sandstone, very fine grained sandstone and siltstone	N4 very fine to fine grained sandstone; N5 very fine grained sandstone; N4, 5GY 4/1 siltstone	None
823	824		106-1365	N4- N5; N3- N4	Siltstone and shale	Calcareous; N4-N5 siltstone; N3-N4 shale	None
824	825		106-1365	N4; N3-N4	Siltstone and silty shale	N4 siltstone; N3- N4 silty shale	None
825	826		106-1365	N4- N5	Siltstone		None
826	827		106-1366	N4; 5G 4/1	Siltstone and silty shale	N4 siltstone; 5G4/1 silty shale	None
827	828		106-1366	N4; N3	Siltstone and shale	N4 siltstone; N3 shale	None
828	829		106-1366	N4	Siltstone		None
829	830		106-1366	N4; N3	Siltstone and silty shale	Slightly calcareous; N4 siltstone; N3 silty shale	None

830	831		106-1367	N6; N4; N3	Very fine grained sandstone, siltstone and silty shale	Slightly calcareous; N6 very fine grained sandstone; N4 siltstone; N3 silty shale	None
831	832		106-1367	5 Y6/1; N4- N5	Siltstone to very fine grained sandstone and siltstone	Calcareous;5Y 6/1 siltstone to very fine grained sandstone; N4-N5 siltstone	None
832	833		106-1367	N4-N5; N4;N3	Very fine grained sandstone, siltstone and silty shale	Calcareous; N4- N5 very fine grained sandstone; N4 siltstone; N3 silty shale	None
833	834		106-1367	N4	Siltstone	Slightly calcareous; N4 siltstone	None
834	835		106-1367	N4	Siltstone	Calcareous; N4 siltstone	None
835	836		106-1368	N4- N6; N3	Very fine grained sandstone and silty shale	Calcareous;N4- N6 very fine grained sandstone; N3 silty shale	None
836	837		106-1368	N4- N5; N3- N4; N4	Siltstone, shale and silty shale	Calcareous; N4-N5 siltstone; N3-N4 shale; N4 silty shale	None
837	838		106-1368	N5; N4-N5; N3-N4	Very fine grained sandstone, siltstone and silty shale	Slightly calcareous; N5 very fine grained sandstone; N4-N5 siltstone; N3- N4 silty shale	None
838	839		106-1368	N4- N5; N4; N3	Very fine grained sandstone, siltstone and silty shale	Calcareous;N4-N5 very fine grained sandstone; N4 siltstone; N3 silty shale	None
839	840		106-1368	N5; N3-N4	Very fine grained sandstone and silty shale	Calcareous; N5 very fine grained sandstone; N3-N4 silty shale	None

840	841		106-1368	N5, 5 GY 4/1; N4; N3- N4	Very fine grained sandstone, siltstone and shale	Calcareous; N5, 5GY 4/1 very fine grained sandstone; N4 siltstone; N3- N4 shale	None
841	842		106-1369	N5; N4	Very fine grained sandstone and siltstone	Calcareous; N5 very fine grained sandstone; N4 siltstone	None
842	843		106-1369	N5-N6;N4	Very fine grained sandstone and siltstone	Calcareous; N5- N6 very fine grained sandstone; N4 siltstone	None
843	844		106-1369	N6; N4-N5	Very fine to fine grained sandstone and siltstone	Calcareous; N6 very fine to fine grained sandstone; N4-N5 siltstone	None
844	845		106-1369	N4- N5; N4, 5G 4/1	Siltstone to very fine grained sandstone and siltstone	Calcareous; N4-N5 siltstone to very fine grained sandstone; N4, 5G 4/1 siltstone	None
845	846		106-1370	N5; N4	Very fine grained sandstone and siltstone	Calcareous; N5 very fine grained sandstone; N4 siltstone	None
846	847		106-1370	N5; N3	Very fine grained sandstone and silty shale	Calcareous; N5 very fine grained sandstone; N3 silty shale	None
847	848		106-1370	N6; N6; N5	Very fine grained sandstone, very fine to fine grained sandstone and siltstone	Calcareous; N6 very fine grained sandstone; N6 very fine to fine grained sandstone; N5 siltstone	None

848	849		106-1370	N5- N6; N4	Very fine to fine grained sandstone and siltstone	Calcareous; N5-N6 very fine to fine grained sandstone; N4 Siltstone	None
849	850		106-1370	N6; N4; N3	Very fine grained sandstone, siltstone and shale	Calcareous; N6 very fine grained sandstone; N4 siltstone; N3 silty shale	None
850	851		106-1371	N5- N6; 5G 4/1, N4	Siltstone to very fine grained sandstone and siltstone	Calcareous; N5-N6 siltstone to very fine grained sandstone; 5G 4/1, N4 siltstone	None
851	852		106-1371	5B 5/1, N6; N3-N4	Siltstone and silty shale	Slightly calcareous; 5B 5/1, N6 siltstone; N3-N4 silty shale	None
852	853		106-1371	N4; N4, 5GY 4/1	Siltstone to very fine grained sandstone and siltstone	Slightly calcareous; N4 siltstone to very fine grained sandstone; N4, 5GY 4/1 siltstone	None
853	854		106-1371	N4; N5; N4	Siltstone to very fine grained sandstone, very fine to fine grained sandstone and siltstone	Calcareous; N4 siltstone to very fine grained sandstone; N5 very fine to fine grained sandstone; N4 siltstone	None
854	855		106-1371	N5; N3	Very fine grained sandstone and silty shale	Slightly calcareous; N5 very fine grained sandstone; N3 silty shale	None
855	856		106-1371	N4, 5G 4/1; N3-N4	Siltstone and silty shale	Calcareous; glossopteris leave? N4, 5G 4/1 siltstone; N3-N4 silty shale	None

856	857		106-1372	N5- N6; N4- N5; N4	Very fine grained sandstone, siltstone and silty shale	Slightly calcareous; N5-N6 very fine grained sandstone; N4-N5 siltstone; N4 silty shale	None
857	858		106-1372	N4; N3	Siltstone and silty shale	Calcareous; N4 siltstone; N3 silty shale	None
858	859		106-1372	N5; N4-N5	Very fine grained sandstone and siltstone	Calcareous; N5 very fine grained sandstone; N4-N5 siltstone	None
859	860		106-1372	N6, 5B 5/1; N4	Very fine grained sandstone and siltstone	Calcareous; N6, 5 B 5/1 very fine grained sandstone; N4 siltstone	None
860	861		106-1373	N6; N4-N5	Very fine grained sandstone and siltstone	Calcareous; N6 very fine grained sandstone; N4-N5 siltstone	None
861	862		106-1373	N4, 5G 4/1; N6; N4	Siltstone to very fine grained sandstone, very fine to fine grained sandstone and siltstone	Slightly calcareous; N4, 5G4/1 siltstone to very fine grained sandstone; N6 very fine grained sandstone; N4 siltstone	None
862	863		106-1373	N4; N4, 5GY 4/1	Siltstone and silty shale	Calcareous N4 siltstone; N4, 5G 4/1 silty shale	None
863	864		106-1373	N7; N5; N5	Very fine to fine grained sandstone, siltstone to very fine grained sandstone and siltstone	Calcareous; N7 very fine to fine grained sandstone; N5 siltstone to very fine grained sandstone; N5 siltstone	None
864	865		106-1374	N5-N6; N4	Very fine grained sandstone and siltstone	Slightly calcareous; N5-N6 very fine grained sandstone; N4 siltstone	None

865	866		106-1374	N5; N4; N3	Very fine grained sandstone, siltstone and silty shale	Slightly calcareous; N5 very fine grained sandstone; N4 siltstone; N3 silty shale	None
866	867		106-1374	N5; N4; N3	Siltstone to very fine grained sandstone, siltstone and silty shale	Slightly calcareous; N5 siltstone to very fine grained sandstone; N4 siltstone; N3 silty shale	None
867	868		106-1374	N4; N3-N4	Siltstone and silty shale	Calcareous; N4 siltstone; N3-N4 silty shale	None
868	869		106-1374	N4- N5, 5G 4/1; N4	Very fine grained sandstone and siltstone	Calcareous; N4-N5, 5G 4/1 very fine grained sandstone; N4 siltstone	None
869	870		106-1374	N4; N3	Siltstone and silty shale	Slightly calcareous; N4 siltstone; N3 silty shale	None
870	871		106-1374	N5; N4	Very fine grained sandstone and siltstone	Slightly calcareous; N5 very fine grained sandstone; N4 siltstone	None
871	872		106-1375	N5; N4-N5; N4	Siltstone to very fine grained sandstone, siltstone and silty shale	Slightly calcareous; N5 siltstone to very fine grained sandstone; N4-N5 siltstone; N4 silty shale	None
872	873		106-1375	N4- N5	Siltstone	Slightly calcareous; N4-N5 siltstone	None
873	874		106-1375	N4; N3	Siltstone and silty shale	Slightly calcareous; N4 siltstone; N3 silty shale	None
874	875		106-1375	N4; N3	Siltstone and silty shale	Slightly calcareous; N4 siltstone; N3 silty shale	None
875	876		106-1376	N4; N3	Siltstone and silty shale	Slightly calcareous; N4 siltstone; N3 silty shale	None

876	877		106-1376	N4- N5; N3	Siltstone and silty shale	Slightly calcareous; N4-N5 siltstone; N3 silty shale	None
877	878		106-1376	N4- N5	Siltstone	Slightly calcareous; N4-N5 siltstone	None
878	879		106-1376	N4; N5-N6	Siltstone and very fine grained sandstone	Slightly calcareous; N4 siltstone; N5- N6 very fine grained sandstone	None
879	880		106-1376	N4- N5; 5GY 4/1, N3	Siltstone and silty shale	Slightly calcareous; N4-N5 siltstone; 5GY 4/1, N3 silty shale	None
880	881		106-1377	N5- N6; N4	Siltstone to very fine grained sandstone and siltstone	Slightly calcareous; N5-N6 siltstone to very fine grained sandstone; N4 siltstone	None
881	882		106-1377	N5; N5	Siltstone to very fine grained sandstone and siltstone	Calcareous; N5 siltstone to very fine grained sandstone; N5 siltstone	None
882	883		106-1377	N4- N5; N3- N4	Siltstone and silty shale	N4- N5 siltstone; N3-N4 silty shale	None
883	884		106-1377	N4; N5; N2- N3	Siltstone, very fine to fine grained sandstone and silty shale	Slightly calcareous; N4 siltstone; N5 very fine to fine grained sandstone; N2-N3 silty shale	None
884	885		106-1377	N4; N5	Siltstone and very fine grained sandstone	Slightly calcareous; N4 siltstone; N5 very fine grained sandstone	None
885	886		106-1377	N4- N5; N5- N6	Siltstone to very fine grained sandstone and very fine grained sandstone	Slightly calcareous; N4-N5 siltstone to very fine grained sandstone; N5-N6 very fine grained sandstone	None

886	887		106-1378	N4; N3	Siltstone and silty shale	Slightly calcareous; N4 siltstone; N3 silty shale	None
887	888		106-1378	N4; N3-N4	Siltstone and silty shale	Slightly calcareous; N4 siltstone; N3-N4 silty shale	None
888	889		106-1378	N5- N6; N3; N4	Very fine grained sandstone, silty shale and siltstone	Calcareous; N5-N6 very fine grained sandstone; N3 silty shale; N4 siltstone	None
889	890		106-1378	N4; N3, 5GY 4/1	Siltstone and silty shale	Slightly calcareous; N4 siltstone; N3, 5GY 4/1 silty shale	None
890	891		106-1379	N4- N5; N3	Siltstone and silty shale	Slightly calcareous; N4-N5 siltstone; N3 silty shale	None
891	892		106-1379	N4- N5	Siltstone	Calcareous; N4-N5 siltstone	None
892	893		106-1379	N5	Very fine grained sandstone	Slightly calcareous; N5 very fine grained sandstone	None
893	894		106-1379	N5, 5B 5/1; N6; N5	Siltstone, very fine to fine grained sandstone and very fine grained sandstone	Slightly calcareous; N5, 5B 5/1 siltstone; N6 very fine to fine grained sandstone; N5 very fine grained sandstone	None
894	895		106-1379	N5; N5	Siltstone to very fine grained sandstone and very fine grained sandstone	Slightly calcareous; N5 siltstone very fine grained sandstone; N5 very fine grained sandstone	None
895	896		106-1379	N4; N4-N5; N3	Siltstone, very fine grained sandstone and silty shale	Slightly calcareous; N4 siltstone; N4-N5 very fine grained sandstone; N3 silty shale	None

896	897		106-1380	N4; N5	Siltstone and very fine grained sandstone	Slightly calcareous; N4 siltstone; N5 very fine grained sandstone	None
897	898		106-1380	N5; N3	Very fine grained sandstone and silty shale	N5 very fine grained sandstone; N3 silty shale	None
898	899		106-1380	N4, 5GY 4/1; N5; N3- N4	Siltstone, very fine grained sandstone and silty shale	N4, 5GY 4/1 siltstone; N5 very fine grained sandstone; N3- N4 silty shale	None
899	900		106-1380	N4; N5-N6; N3	Siltstone, very fine grained sandstone and silty shale	N4 siltstone; N5- N6 very fine grained sandstone; N3 silty shale	None
900	901		106-1380	N4, 5B 5/1; N3	Siltstone and silty shale	N4, 5B 5/1 siltstone; N3 silty shale	None
901	902		106-1381	N4; N3	Siltstone and silty shale	N4 siltstone; N3 silty shale	None
902	903		106-1381	N4; N3	Siltstone and silty shale	N4 siltstone; N3 silty shale	None
903	904		106-1381	N4; N4	Siltstone and silty shale	N4 siltstone; N4 silty shale	None
904	905		106-1381	N3	Silty shale	N3 silty shale	None
905	906		106-1382	N4; N3	Siltstone and silty shale	N4 siltstone; N3 silty shale	None
906	907		106-1382	N4- N5	Siltstone	Slightly calcareous; N4-N5 siltstone	None
907	908		106-1382	N4; N5-N6; N3	Siltstone, siltstone to very fine grained	Slightly calcareous; N4 siltstone; N5- N6 siltstone	None

					sandstone and silty shale	to very fine grained sandstone; N3 silty shale	
908	909		106-1382	N5- N6; N5- N6	Siltstone to very fine grained sandstone, very fine grained sandstone and silty shale	Slightly calcareous; N5-N6 siltstone to very fine grained sandstone; N5-N6 very fine grained sandstone; N3 silty shale	None
909	910		106-1382	N4	Siltstone	Slightly calcareous; N4 siltstone	None
910	911		106-1383	N4	Siltstone		None
911	912		106-1383	N4; N3-N4	Siltstone and silty shale	Slightly calcareous; N4 siltstone; N3-N4 silty shale	None
912	913		106-1383	N4; N3	Siltstone and silty shale	N4 siltstone; N3 silty shale	None
913	914		106-1383	N4- N6; N5	Siltstone and siltstone to very fine grained sandstone	N4-N6 siltstone; N5 siltstone to very fine grained sandstone	None
914	915		106-1383	N4; N5-N6; N3	Siltstone , siltstone to very fine grained sandstone and silty shale	N4 siltstone; N5- N6 siltstone to very fine grained sandstone;N3 silty shale	None
915	916		106-1383	N4; N5-N6; N3	Siltstone , very fine grained sandstone and silty shale	N4 siltstone; N5-N6 very fine grained sandstone;N3 silty shale	None
916	917		106-1384	N4; N4-N5; N3	Siltstone , very fine grained sandstone and silty shale	N4 siltstone; N4-N5 very fine grained sandstone;N3 silty shale	None
917	918		106-1384	N4, 5GY 4/1; N3	Siltstone and silty shale	N4, 5GY 4/1 siltstone; N3 silty shale	None

918	919		106-1384	N4; N5	Siltstone and siltstone to very fine grained sandstone	N4 siltstone; N5 siltstone to very fine grained sandstone	None
919	920		106-1384	N4; N3	Siltstone and silty shale	N4 siltstone; N3 silty shale	None
920	921		106-1385	N4	Siltstone		None
921	922		106-1385	N4; N3	Siltstone and silty shale	N4 siltstone and N3 silty shale	None
922	923		106-1385	N4	Siltstone		None
923	924		106-1385	N4	Siltstone		None
924	925		106-1385	N4; N3	Siltstone and silty shale	N4 siltstone and N3 silty shale	None
925	926		106-1386	N4; N3	Siltstone and silty shale	N4 siltstone and N3 silty shale	None
926	927		106-1386	N5	Very fine grained sandstone	Slightly calcareous; N5 very fine grained sandstone	None
927	928		106-1386	N4- N5; N3	Siltstone and silty shale	N4- N5 siltstone and N3 silty shale	None
928	929		106-1386	N4- N6; N3- N4	Siltstone and silty shale	Slightly calcareous; N4-N6 siltstone; N3-N4 silty shale	None
929	930		106-1386	N3- N4; N2- N3	Siltstone and silty shale	Slightly calcareous; N3-N4 siltstone; N2-N3 silty shale	None
930	931		106-1386	N4; N3	Siltstone and silty shale	N4 siltstone and N3 silty shale	None
931	932		106-1387	N4, 5GY 4/1	Siltstone		None

932	933		106-1387	N4- N5	Siltstone		None
933	934		106-1387	N4- N5	Siltstone		None
934	935		106-1387	N4- N5; N3	Siltstone and silty shale	N4-N5 siltstone and N3 silty shale	None
935	936		106-1388	N4; N3	Siltstone and silty shale	N4 siltstone and N3 silty shale	None
936	937		106-1388	N4- N5	Siltstone		None
937	938		106-1388	N6; N3-N4, 5G 2/1	Very fine grained sandstone and silty shale	N6 very fine grained sandstone; N3-N4, 5G 2/1 silty shale	None
938	939		106-1388	N4; N5	Siltstone and very fine grained sandstone	N4 siltstone; N5 very fine grained sandstone	None
939	940		106-1388	N4- N5	Siltstone		None
940	941		106-1389	N4, 5GY 4/1; N5-N6	Siltstone and siltstone to very fine grained sandstone	N4, 5GY 4/1 siltstone; N5-N6 siltstone to very fine grained sandstone	None
941	942		106-1389	N4- N5; N3	Siltstone and silty shale	N4-N5 siltstone; N3 silty shale	None
942	943		106-1389	N4	Siltstone		None
943	944		106-1389	N5; N3	Siltstone to very fine grained sandstone and silty shale	N5 siltstone to very fine grained sandstone; N3 silty shale	None
944	945		106-1389	N5; N3-N4	Siltstone and silty shale	Slightly calcareous; N5 siltstone; N3-N4 silty shale	None

945	946		106-1389	N4- N5	Siltstone		None
946	947		106-1390	N4- N5	Siltstone		None
947	948		106-1390	N4- N5; N3, 5GY 4/1	Siltstone and silty shale	N4-N5 siltstone; N3, 5GY 4/1 silty shale	None
948	949		106-1390	N4; N7	Siltstone and very fine grained sandstone	N4 siltstone; N7 very fine grained sandstone	None
949	950		106-1390	N4- N5; N3	Siltstone and silty shale	N4-N5 siltstone; N3 silty shale	None
950	951		106-1391	N5; N6	Siltstone and very fine grained sandstone	N5 siltstone; N6 very fine grained sandstone	None
951	952		106-1391	N4- N5, 5GY 4/1; N5	Siltstone and very fine grained sandstone	N4-N5, 5GY 4/1 siltstone; N5 very fine grained sandstone	None
952	953		106-1391	N4- N5	Siltstone		None
953	954		106-1391	N4- N5; N3	Siltstone and silty shale	N4-N5 siltstone; N3 silty shale	None
954	955		106-1391	N4; N5; N3	Siltstone, very fine grained sandstone and silty shale	N4 siltstone; N5 very fine grained sandstone; N3 silty shale	None
955	956		106-1392	N4; N5	Siltstone and very fine grained sandstone	N4 siltstone; N5 very fine grained sandstone	None
956	957		106-1392	N5; N3	Siltstone and silty shale	N5 siltstone; N3 silty shale	None

957	958		106-1392	N4- N5	Siltstone		None
958	959		106-1392	N3- N4; N3	Siltstone and silty shale	N3-N4 siltstone; N3 silty shale	None
959	960		106-1392	N4- N5	Siltstone		None
960	961		106-1392	N4; N3	Siltstone and silty shale	N4 siltstone; N3 silty shale	None
961	962		106-1393	N4; N3	Siltstone and silty shale	N4 siltstone; N3 silty shale	None
962	963		106-1393	N4; N2-N3	Siltstone and silty shale	N4 siltstone; N2-N3 silty shale	None
963	964		106-1393	N3	Silty shale		None
964	965		106-1393	N4; N3	Siltstone and silty shale	N4 siltstone; N3 silty shale	None
965	966		106-1394	N4- N5; N2- N3	Siltstone and silty shale	N4-N5 siltstone; N2-N3 silty shale	None
966	967		106-1394	N4- N5; N3	Siltstone and silty shale	N4-N5 siltstone; N3 silty shale	None
967	968		106-1394	N4; N3	Siltstone and silty shale	N4 siltstone; N3 silty shale	None
968	969		106-1394	N4- N5; N3	Siltstone and silty shale	N4- N5 siltstone; N3 silty shale	None
969	970		106-1394	N4- N5	Siltstone		None
970	971		106-1395	N4- N5; N3	Siltstone and silty shale	N4-N5 siltstone; N3 silty shale	None
971	972		106-1395	N4- N5; N3	Siltstone and silty shale	N4-N5 siltstone; N3 silty shale	None

972	973		106-1395	N4- N5, 5G 4/1	Siltstone		None
973	974		106-1395	N4; N3, 5GY 4/1	Siltstone and silty shale	N4 siltstone; N3, 5GY 4/1 silty shale	None
974	975		106-1395	N4; N3	Siltstone and silty shale	N4 siltstone; N3 silty shale	None
975	976		106-1395	N4- N5; N5; N3	Siltstone, very fine grained sandstone and silty shale	N4-N5 siltstone; N5 very fine grained sandstone; N3 silty shale	None
976	977		106-1396	N4; N5	Siltstone and siltstone to very fine grained sandstone	N4 siltstone; N5 siltstone to very fine grained sandstone	None
977	978		106-1396	N4; N5; N3	Siltstone, very fine grained sandstone and silty shale	N4 siltstone; N5 very fine grained sandstone; N3 silty shale	None
978	979		106-1396	N4; N6	Siltstone and very fine to fine grained sandstone	N4 siltstone; N6 very fine to fine grained sandstone	None
979	980		106-1396	N4; N5-N6	Siltstone and very fine grained sandstone	N4 siltstone; N5- N6 very fine grained sandstone	None
980	981		106-1397	N4; N5	Siltstone and siltstone to very fine grained sandstone	N4 siltstone; N5 siltstone to very fine grained sandstone	None
981	982		106-1397	N4- N5	Siltstone		None
982	983		106-1397	N4; N5-N6; N3	Siltstone, very fine grained sandstone and silty shale	N4 siltstone; N5- N6 very fine grained sandstone; N3 silty shale	None

983	984		106-1397	N4- N5; N3	Siltstone and silty shale	N4-N5 siltstone; N3 silty shale	None
984	985		106-1397	N4- N5; N3	Siltstone and silty shale	N4-N5 siltstone; N3 silty shale	None
985	986		106-1398	N4- N5; N3- N4	Siltstone and silty shale	N4-N5 siltstone; N3-N4 silty shale	None
986	987		106-1398	N4; N3	Siltstone and silty shale	N4 siltstone; N3 silty shale	None
987	988		106-1398	N4- N5; N3	Siltstone and silty shale	N4-N5 siltstone; N3 silty shale	None
988	989		106-1398	N6; N3, 5Y 2/1	Very fine grained sandstone and silty shale	N6 very fine grained sandstone ; N3, 5Y 2/1 silty shale	None
989	990		106-1398	N4; N3	Siltstone and silty shale	N4 siltstone; N3 silty shale	None
990	991		106-1398	N4- N5	Siltstone		None
991	992		106-1399	N4- N5; N5- N6	Siltstone and very fine grained sandstone	N4- N5 siltstone; N5-N6 very fine grained sandstone	None
992	993		106-1399	N4; N3, 5Y 2/1	Siltstone and silty shale	N4 siltstone; N3, 5Y 2/1 silty shale	None
993	994		106-1399	N4- N5; N5- N6	Siltstone and very fine grained sandstone	N4-N5 siltstone; N5-N6 very fine grained sandstone	None
994	995		106-1399	N5; N5-N6; N3	Siltstone, siltstone to very fine grained sandstone and silty shale	N5 siltstone; N5-N6 siltstone to very fine grained sandstone; N3 silty shale	None

995	996		106-1400	N4- N5; N5- N6	Siltstone and very fine to fine grained sandstone	N4-N5 siltstone; N5-N6 very fine to fine grained sandstone	None
996	997		106-1400	N4; N5	Siltstone and very fine grained sandstone	N4 siltstone; N5 very fine grained sandstone together with a calcite vein	None
997	998		106-1400	N4; N5	Siltstone and siltstone to very fine grained sandstone	N4 siltstone; N5 siltstone to very fine grained sandstone	None
998	999		106-1400	N4; N6	Siltstone and very fine grained sandstone	N4 siltstone; N6 very fine grained sandstone	None
999	1000		106-1400	N4; N6; N3	Siltstone, very fine grained sandstone and silty shale	N4 siltstone; N6 very fine grained sandstone; N3 silty shale	None
1000	1001		106-1401	N5; N3	Siltstone and silty shale	N5 siltstone; N3 silty shale	None
1001	1002		106-1401	N4; N6; N3	Siltstone, very fine to fine grained sandstone and silty shale	N4 siltstone; N6 very fine to fine grained sandstone; N3 silty shale	None
1002	1003		106-1401	N4- N5	Siltstone		None
1003	1004		106-1401	N4; N6; N3	Siltstone, siltstone to very fine grained sandstone and silty shale	N4 siltstone; N6 siltstone to very fine grained sandstone; N3 silty shale	None
1004	1005		106-1401	N2- N3	Shale		None

1005	1006		106-1401	N4- N5; N3	Siltstone and silty shale	N4-N5 siltstone; N3 silty shale	None
1006	1007		106-1403	N4- N5; N3	Siltstone and silty shale	N4-N5 siltstone; N3 silty shale	None
1007	1008		106-1403	N6; N3-N4	Very fine grained sandstone and silty shale	N6 very fine grained sandstone; N3-N4 silty shale	None
1008	1009		106-1403	N6; N6; N3	Siltstone to very fine grained sandstone, very fine to fine grained sandstone and silty shale	N6 siltstone to very fine grained sandstone; N6 very fine to fine grained sandstone; N3 silty shale	None
1009	1010		106-1403	N4; N2-N3	Siltstone and silty shale	N4 siltstone; N2-N3 silty shale	None
1010	1011		106-1405	N4; N6; N3, 5Y 2/1	Siltstone, very fine grained sandstone and silty shale	N4 siltstone; N6 very fine grained sandstone; N3, 5Y 2/1 silty shale	None
1011	1012		106-1405	N5- N6; N6; N3	Very fine grained sandstone, very fine to fine grained sandstone and silty shale	N5-N6 very fine grained sandstone; N6 very fine to fine grained sandstone; N3 silty shale	None
1012	1013		106-1405	N4- N5; N6	Siltstone and very fine grained sandstone	N4-N5 siltstone; N6 very fine grained sandstone	None
1013	1014		106-1405	N4- N5	Siltstone		None
1014	1015		106-1405	N5; N6; N3	Siltstone, very fine grained sandstone and silty shale	N5 siltstone; N6 very fine grained sandstone; N3 silty shale	None

1015	1016		106-1406	N2- N3	Silty shale		None
1016	1017		106-1406	N4- N5; N3	Siltstone and silty shale	N4-N5 siltstone; N3 silty shale	None
1017	1018		106-1406	N3	Silty shale		None
1018	1019		106-1406	N3	Silty shale		None
1019	1020		106-1406	N4; N3	Siltstone and silty shale	N4 siltstone; N3 silty shale	None
1020	1021		106-1406	5YR 2/1, N3	Silty shale		None
1021	1022		106-1407	N4- N5; N3, 5YR 2/1	Siltstone and silty shale	N4-N5 siltstone; N3, 5YR 2/1 silty shale	None
1022	1023		106-1407	N2- N3, 5YR 2/1	Silty shale		None
1023	1024		106-1407	N2- N3, 5YR 2/1	Silty shale		None
1024	1025		106-1407	N2- N3, 5YR 2/1	Shale		None
1025	1026		106-1408	N4; N2, 5YR 2/1	Siltstone and shale	N4 siltstone; N2, 5YR 2/1 shale	None
1026	1027		106-1408	N4; N3	Siltstone and silty shale	N4 siltstone; N3 silty shale	None
1027	1028		106-1408	N4; N3	Siltstone and silty shale	Calcareous; N4 siltstone; N3 silty shale	None
1028	1029		106-1408	N5; N3	Siltstone and silty shale	N5 siltstone; N3 silty shale	None

1029	1030		106-1408	N4; N3	Siltstone and silty shale	N4 siltstone; N3 silty shale	None
1030	1031		106-1409	N5- N6; N3	Very fine grained sandstone and silty shale	N5-N6 very fine grained sandstone; N3 silty shale	None
1031	1032		106-1409	N4; N2	Siltstone and shale	N4 siltstone; N2 shale	None
1032	1033		106-1409	N5; N6; N2	Siltstone to very fine grained sandstone, very fine to fine grained sandstone and shale	N5 siltstone to very fine grained sandstone; N6 very fine grained sandstone; N2 shale	None
1033	1034		106-1409	N5; N5-N6; N3	Siltstone, very fine grained sandstone and silty shale	N5 siltstone; N5-N6 very fine grained sandstone; N3 silty shale	None
1034	1035		106-1409	N4- N5; N3, 5YR 2/1	Siltstone and shale	N4-N5 siltstone; N3, 5YR 2/1 shale	None
1035	1036		106-1409	N4; N3; 5YR 2/1	Siltstone, silty shale and shale	N4 siltstone; N3 silty shale; 5YR 2/1 shale	None
1036	1037		106-1410	N4- N5; N2	Siltstone and shale	N4-N5 siltstone; N2 shale	None
1037	1038		106-1410	N3; N2	Silty shale and shale	N3 silty shale; N2 shale	None
1038	1039		106-1410	N4; 5YR 2/1	Siltstone and shale	N4 siltstone; 5YR 2/1 shale	None
1039	1040		106-1410	N3; 5YR 2/1	Silty shale and shale	N3 silty shale; 5YR 2/1 shale	None
1040	1041		106-1411	N3; N2	Silty shale and shale	N3 silty shale; N2 shale	None

1041	1042		106-1411	N3; N2	Silty shale and shale	N3 silty shale; N2 shale	None
1042	1043		106-1411	N4; N3	Siltstone and silty shale	N4 siltstone; N3 silty shale	None
1043	1044		106-1411	N4- N5; N3	Siltstone and silty shale	N4-N5 siltstone; N3 silty shale	None
1044	1045		106-1411	N4; N3	Siltstone and silty shale	N4 siltstone; N3 silty shale	None
1045	1046		106-1412	N4; N3	Siltstone and silty shale	N4 siltstone; N3 silty shale	None
1046	1047		106-1412	N4- N5; N3; 5YR 2/1	Siltstone, silty shale and shale	N4-N5 siltstone; N3 silty shale; 5YR 2/1 shale	None
1047	1048		106-1412	N3; 5YR 2/1	Silty shale and shale	N3 silty shale; 5YR 2/1 shale	None
1048	1049		106-1412	N4; N3	Siltstone and silty shale	N4 siltstone; N3 silty shale	None
1049	1050		106-1412	N4; N6; N3	Siltstone, very fine to fine grained sandstone and silty shale	N4 siltstone; N6 very fine to fine grained sandstone; N3 silty shale	None
1050	1051		106-1412	N6	Very fine grained sandstone		None
1051	1052		106-1413	N5; N6; 5YR 2/1	Very fine grained sandstone, very fine to fine grained sandstone and shale	Slightly clayey; N5 very fine grained sandstone; N6 very fine to fine grained sandstone; 5YR 2/1 shale	None
1052	1053		106-1413	N5; N6	Siltstone and very fine to fine grained sandstone	Slightly clayey; N5 siltstone; N6 very fine to fine grained sandstone	None

1053	1054		106-1413	N5- N6; N3	Very fine grained sandstone and silty shale	Slightly clayey; N5-N6 very fine grained sandstone; N3 silty shale	None
1054	1055		106-1413	N4- N5; N5- N6	Clay with sparse rock fragments	N4-N5 siltstone; N5-N6 very fine to fine grained sandstone	None
1055	1056		106-1414	N6; 5YR 2/1	Clay with sparse rock fragments	N6 very fine grained sandstone; 5YR 2/1 shale	None
1056	1057		106-1414	N4; 5YR 2/1	Clay with sparse rock fragments	N4 siltstone; 5YR 2/1 shale	None
1057	1058		106-1414	N6; N3	Clay with sparse rock fragments	N6 very fine grained sandstone; N3 silty shale	None
1058	1059		106-1414	N4; N5-N6	Clay with sparse rock fragments	N4 siltstone; N5-N6 very fine to fine grained sandstone	None
1059	1060		106-1414	N6; N5	Clay with sparse rock fragments	N6 very fine to fine grained sandstone; N5 very fine grained sandstone	None
1060	1061		106-1415	N4- N5; N3	Slightly clayey with sparse rock fragments	N4-N5 Siltstone; N3 silty shale	None
1061	1062		106-1415	N2, 5YR 2/1; N3	Slightly clayey with sparse rock fragments	N2, 5YR 2/1 shale; N3 silty shale	None
1062	1063		106-1415	N4; N3; N6	Slightly clayey with sparse rock fragments	N4 siltstone; N3 silty shale; N6 very fine grained sandstone	None
1063	1064		106-1415	N3	Silty shale		None

1064	1065		106-1415	5YR 2/1; N3	Shale and silty shale	5YR 2/1 shale; N3 silty shale	None
1065	1066		106-1415	N3	Silty shale		None
1066	1067		106-1416	N4; N3; N2	Siltstone, silty shale and shale	N4 siltstone; N3 silty shale; N2 shale	None
1067	1068		106-1416	N4; N3; 5YR 2/1	Siltstone, silty shale and shale	N4 siltstone; N3 silty shale; 5YR 2/1 shale	None
1068	1069		106-1416	N3; N2	Silty shale and shale	N3 silty shale; N2 shale	None
1069	1070		106-1416	N3; 5YR 2/1	Silty shale and shale	N3 silty shale; 5YR 2/1 shale	None
1070	1071		106-1417	N4; N3	Siltstone and silty shale	N4 siltstone; N3 silty shale	None
1071	1072		106-1417	N4; N3	Siltstone and silty shale	N4 siltstone; N3 silty shale	None
1072	1073		106-1417	N3; N2	Silty shale and shale	N3 silty shale; N2 shale	None
1073	1074		106-1417	N3; 5YR 2/1	Silty shale and shale	N3 silty shale; 5YR 2/1 shale	None
1074	1075		106-1417	N5; 5YR 2/1	Siltstone and shale	N5 siltstone; 5YR 2/1 shale	None
1075	1076		106-1418	N1; N2	Carbonaceous shale and shale	N1 carbonaceous shale; N2 shale	None
1076	1077		106-1418	N1; N5	Carbonaceous shale and siltstone	N1 carbonaceous shale; N5 siltstone	None
1077	1078		106-1418	N1; 5YR 2/1; N5	Carbonaceous shale, shale and siltstone	N1 carbonaceous shale; 5YR 2/1 shale; N5 siltstone	None

1078	1079		106-1418	N1; N5	Carbonaceous shale and very fine grained sandstone	N1 carbonaceous shale; N5 very fine grained sandstone	None
1079	1080		106-1418	N1; N4	Carbonaceous shale and siltstone	N1 carbonaceous shale; N4 siltstone	None
1080	1081		106-1418	N1; N3; N6	Carbonaceous shale, silty shale and very fine grained sandstone	N1 carbonaceous shale; N3 silty shale; N6 very fine grained sandstone	None
1081	1082		106-1419	N4; N6	Siltstone and very fine grained sandstone	N4 siltstone; N6 very fine grained sandstone	None
1082	1083		106-1419	N1; N4; N5	Carbonaceous shale, siltstone and very fine grained sandstone	N1 carbonaceous shale; N4 siltstone; N5 very fine grained sandstone	None
1083	1084		106-1419	N3; 5YR 2/1	Clay with sparse rock fragments	N3 silty shale; 5YR 2/1 shale	None
1084	1085		106-1419	N4- N5; N3	Siltstone and silty shale	N4- N5 siltstone; N3 silty shale	None
1085	1086		106-1420	N5; N3	Siltstone and silty shale	N5 siltstone; N3 silty shale	None
1086	1087		106-1420	N1, 5YR 2/1; N2	Carbonaceous shale and silty shale	N1, 5YR 2/1 carbonaceous shale; N2 silty shale	None
1087	1088		106-1420	N1; N5; 5YR 2/1	Carbonaceous shale , siltstone and shale	N1 carbonaceous shale; N5 siltstone; 5YR 2/1 shale	None
1088	1089		106-1420	N1- N2; N6	Carbonaceous shale and very fine grained sandstone	N1- N2 carbonaceous shale; N6 very fine grained sandstone	None

1089	1090		106-1420	N6; N3; N4	Very fine grained sandstone, silty shale and siltstone	N6 very fine grained sandstone; N3 silty shale; N4 siltstone	None
1090	1091		106-1421	N3; N4	Silty shale and siltstone	N3 silty shale; N4 siltstone	None
1091	1092		106-1421	N4- N5	Siltstone		None
1092	1093		106-1421	N4- N5	Siltstone		None
1093	1094		106-1421	N3; N4	Silty shale and siltstone	N3 silty shale; N4 siltstone	None
1094	1095		106-1421	N3; N4	Silty shale and siltstone	N3 silty shale; N4 siltstone	None
1095	1096		106-1421	N3; N4	Silty shale and siltstone	N3 silty shale; N4 siltstone	None
1096	1097		106-1422	N3; N4; N2	Silty shale, siltstone and shale	N3 silty shale; N4 siltstone; N2 shale	None
1097	1098		106-1422	N1- N2; N4	Carbonaceous shale and siltstone	N1-N2 carbonaceous shale; N4 siltstone	None
1098	1099		106-1422	N4- N5; N2	Siltstone and shale	N4- N5 siltstone; N2 shale	None
1099	1100		106-1422	N3; N2	Silty shale and shale	N3 silty shale; N2 shale	None
1100	1101		106-1423	N3; N5	Silty shale and siltstone	N3 silty shale; N5 siltstone	None
1101	1102		106-1423	N1; N4; N3	Carbonaceous shale, siltstone and silty shale	N1 carbonaceous shale; N4 siltstone; N3 silty shale	None
1102	1103		106-1423	N3; N4	Silty shale and siltstone	N3 silty shale; N4 siltstone	None

1103	1104		106-1423	N3; N4	Silty shale and siltstone	N3 silty shale; N4 siltstone	None
1104	1105		106-1423	N3; N4; N6	Silty shale, siltstone and very fine grained sandstone	N3 silty shale; N4 siltstone; N6 very fine grained sandstone	None
1105	1106		106-1424	N3; N4-N5	Silty shale and siltstone	N3 silty shale; N4- N5 siltstone	None
1106	1107		106-1424	N4	Siltstone		None
1107	1108		106-1424	N4- N5	Siltstone		None
1108	1109		106-1424	N3	Silty shale		None
1109	1110		106-1424	N3; N2	Silty shale and shale	N3 silty shale; N2 shale	None
1110	1111		106-1424	N3; N4-N5	Silty shale and siltstone	N3 silty shale; N4- N5 siltstone	None
1111	1112		106-1425	N3; N4	Silty shale and siltstone	N3 silty shale; N4 siltstone	None
1112	1113		106-1425	N3; N4; N2	Silty shale, siltstone and shale	N3 silty shale; N4 siltstone; N2 shale	None
1113	1114		106-1425	N4- N5	Siltstone		None
1114	1115		106-1425	N3; N4; N2	Silty shale, siltstone and shale	N3 silty shale; N4 siltstone; N2 shale	None
1115	1116		106-1426	N3; N4	Silty shale and siltstone	N3 silty shale; N4 siltstone	None
1116	1117		106-1426	N3; N4; N2	Silty shale, siltstone and shale	N3 silty shale; N4 siltstone; N2 shale	None

1117	1118		106-1426	5Y 4/1, N4- N5	Siltstone		None
1118	1119		106-1426	N5- N6	Very fine grained sandstone		None
1119	1120		106-1426	N5; N5; N6	Siltstone, siltstone to very fine grained sandstone and very fine grained sandstone	N5 siltstone; N5 siltstone to very fine grained sandstone; N6 very fine grained sandstone	None
1120	1121		106-1427	N5; N6	Siltstone and very fine grained sandstone	N5 siltstone; N6 very fine grained sandstone	None
1121	1122		106-1427	N6; N2	Very fine to fine grained sandstone and shale	N6 very fine to fine grained sandstone; N2 shale	None
1122	1123		106-1427	N4- N5; N5- N6	Siltstone and very fine grained sandstone	N4-N5 Siltstone; N5- N6 very fine grained sandstone	None
1123	1124		106-1427	N4; N5	Siltstone and very fine grained sandstone	N4 siltstone; N5 very fine grained sandstone	None
1124	1125		106-1427	N4; N3	Siltstone and silty shale	N4 siltstone;N3 silty shale	None
1125	1126		106-1427	N4- N5; N3	Siltstone and silty shale	N4-N5 siltstone;N3 silty shale	None
1126	1127		106-1428	N4; N5-N6; N3	Siltstone, very fine grained sandstone and silty shale	N4 siltstone; N5-N6 very fine grained sandstone; N3 silty shale	None

1127	1128		106-1428	N5; N6	Siltstone and very fine grained sandstone	N5 siltstone; N6 very fine grained sandstone	None
1128	1129		106-1428	N6; N5; N3	Very fine to fine grained sandstone, siltstone and silty shale	N6 very fine to fine grained sandstone; N5 siltstone; N3 silty shale	None
1129	1130		106-1428	N4- N5; N3	Siltstone and silty shale	N4-N5 siltstone; N3 silty shale	None
1130	1131		106-1429	N4; N5-N6; N3	Siltstone, very fine grained sandstone and silty shale	N4 siltstone; N5- N6 very fine grained sandstone; N3 silty shale	None
1131	1132		106-1429	N5	Siltstone		None
1132	1133		106-1429	N4; N3	Siltstone and silty shale	N4 siltstone; N3 silty shale	None
1133	1134		106-1429	N4- N5; N5- N6	Siltstone and very fine grained sandstone	N4-N5 siltstone; N5-N6 very fine grained sandstone	None
1134	1135		106-1429	N4; N6	Siltstone and very fine to fine grained sandstone	N4 siltstone; N6 very fine to fine grained sandstone	None
1135	1136		106-1430	N4; N5-N6; N3	Siltstone, siltstone to very fine grained sandstone and silty shale	N4 siltstone; N5-N6 siltstone to very fine grained sandstone; N3 silty shale	None
1136	1137		106-1430	N3, 5Y 4/1	Silty shale		None
1137	1138		106-1430	N4; N3	Siltstone and silty shale	N4 siltstone; N3 silty shale	None

1138	1139		106-1430	N4; N3	Siltstone, silty shale and shale	N4 siltstone; N3 silty shale ; N2 shale	None
1139	1140		106-1430	N4- N5; N3	Siltstone and silty shale	N4-N5 siltstone; N3 silty shale	None
1140	1141		106-1430	N4; N3	Siltstone and silty shale	N4 siltstone; N3 silty shale	None
1141	1142		106-1431	N4; N6; N2	Siltstone, very fine grained sandstone and shale	N4 siltstone; N6 very fine grained sandstone ; N2 shale	None
1142	1143		106-1431	N4; 5GY 4/1	Siltstone and silty shale	N4 siltstone; 5GY 4/1 silty shale	None
1143	1144		106-1431	N4; N3	Siltstone and silty shale	N4 siltstone; N3 silty shale	None
1144	1145		106-1431	N4; N3	Siltstone and silty shale	N4 siltstone; N3 silty shale	None
1145	1146		106-1432	N4- N5; N5; N3	Siltstone, very fine grained sandstone and silty shale	N4-N5 siltstone; N5 very fine grained sandstone ; N3 silty shale	None
1146	1147		106-1432	N5; N3	Siltstone and silty shale	N5 siltstone ; N3 silty shale	None
1147	1148		106-1432	N4- N5; N6; N3	Siltstone, very fine grained sandstone and silty shale	N4-N5 siltstone; N6 very fine grained sandstone ; N3 silty shale	None
1148	1149		106-1432	N4- N5; N2; N3	Siltstone, shale and silty shale	N4-N5 siltstone ; N2 shale; N3 Silty shale	None
1149	1150		106-1432	N3	Silty shale		None
1150	1151		106-1433	5YR 2/1; N3	Shale and silty shale	5YR 2/1 shale; N3 silty shale	None

1151	1152		106-1433	N4; N2; N3	Siltstone, shale and silty shale	N4 siltstone; N2 shale; N3 silty shale	None
1152	1153		106-1433	N4; N3	Siltstone and silty shale	N4 siltstone; N3 silty shale	None
1153	1154		106-1433	N4- N5; N3	Siltstone and silty shale	N4-N5 siltstone; N3 silty shale	None
1154	1155		106-1433	N2; N3	Shale and silty shale	N2 shale; N3 silty shale	None
1155	1156		106-1433	N4; N2, 5YR 2/1	Siltstone and shale	N4 siltstone; N2, 5YR 2/1 shale	None
1156	1157		106-1434	N4; N3	Siltstone and silty shale	N4 siltstone; N3 silty shale	None
1157	1158		106-1434	N4; N3	Siltstone and silty shale	N4 siltstone; N3 silty shale	None
1158	1159		106-1434	N4- N5	Siltstone		None
1159	1160		106-1434	N4; N3	Siltstone and silty shale	N4 siltstone; N3 silty shale	None
1160	1161		106-1435	N4; N5	Siltstone and very fine grained sandstone	N4 siltstone; N5 very fine grained sandstone	None
1161	1162		106-1435	N4- N5	Siltstone		None
1162	1163		106-1435	N5; N3	Siltstone and silty shale	N5 siltstone; N3 silty shale	None
1163	1164		106-1435	N4- N5; N3	Siltstone and silty shale	N4- N5 siltstone; N3 silty shale	None
1164	1165		106-1435	N4; N3	Siltstone and silty shale	N4 siltstone; N3 silty shale	None

1165	1166		106-1436	N2, 5YR 2/1; N3	Shale and silty shale	N2, 5YR 2/1 shale; N3 silty shale	None
1166	1167		106-1436	N4; N2	Siltstone and shale	N4 siltstone; N2 shale	None
1167	1168		106-1436	N4; N2, 5YR 2/1	Siltstone and shale	N4 siltstone; N2, 5YR 2/1 shale	None
1168	1169		106-1436	N4; N2, 5YR 2/1	Siltstone and shale	N4 siltstone; N2, 5YR 2/1 shale	None
1169	1170		106-1436	N4; N1; N3	Siltstone, shale and silty shale	N4 siltstone; N1 Shale; N3 silty shale	None
1170	1171		106-1436	N5; N3	Siltstone and silty shale	N5 siltstone; N3 silty shale	None
1171	1172		106-1437	N4; N3	Siltstone and silty shale	Calcite crystal; N4 siltstone; N3 silty shale	None
1172	1173		106-1437	N4; N3	Siltstone and silty shale	N4 siltstone; N3 silty shale	None
1173	1174		106-1437	N4; N3	Siltstone and silty shale	N4 siltstone; N3 silty shale	None
1174	1175		106-1437	N5; N3	Siltstone and silty shale	N5 siltstone; N3 silty shale	None
1175	1176		106-1438	N4; N5	Siltstone and very fine grained sandstone	N4 siltstone; N5 very fine grained sandstone	None
1176	1177		106-1438	N4- N5	Siltstone		None
1177	1178		106-1438	N4; N3	Siltstone and silty shale	N4 siltstone; N3 silty shale	None
1178	1179		106-1438	N2; N3	Carbonaceous shale and silty shale	N2 carbonaceous shale; N3 silty shale	None

1179	1180		106-1438	N4; 5YR 2/1	Siltstone and shale	N4 siltstone; 5YR 2/1 shale	None
1180	1181		106-1439	N3; N2, 5YR 2/1	Silty shale and shale	N3 silty shale; N2, 5YR 2/1 shale	None
1181	1182		106-1439	N3; N2, 5YR 2/1	Silty shale and shale	N3 silty shale; 5YR 2/1 shale	None
1182	1183		106-1439	N3; 5YR 2/1	Silty shale and shale	N3 silty shale; 5YR 2/1 shale	None
1183	1184		106-1439	N4; N3	Siltstone and silty shale	N4 siltstone; N3 silty shale	None
1184	1185		106-1439	N4; 5YR 2/1, N2	Siltstone and shale	N4 siltstone; 5YR 2/1, N2 shale	None
1185	1186		106-1439	N4; N5; 5YR 2/1	Siltstone, very fine grained sandstone and shale	N4 siltstone; N5 very fine grained sandstone; 5YR 2/1 shale	None
1186	1187		106-1440	N4; N5; N3	Siltstone, very fine grained sandstone and silty shale	N4 siltstone; N5 very fine grained sandstone; N3 silty shale	None
1187	1188		106-1440	N;, N6; N3	Siltstone, very fine to fine grained sandstone and silty shale	N4 siltstone; N6 very fine to fine grained sandstone; N3 silty shale	None
1188	1189		106-1440	N6; 5YR 2/1; N5-N6	Very fine to fine grained sandstone, shale and very fine grained sandstone	N6 very fine to fine grained sandstone; 5YR 2/1 shale; N5-N6 very fine grained sandstone	None
1189	1190		106-1440	N4; N6; N3	Siltstone, very fine grained sandstone and silty shale	N4 siltstone; N6 very fine grained sandstone; N3 silty shale	None

1190	1191		106-1441	N4; N2; N3	Siltstone, shale and silty shale	N4 siltstone; N2 shale; N3 silty shale	None
1191	1192		106-1441	N4; N6; N3	Siltstone, very fine grained sandstone and silty shale	N4 siltstone; N6 very fine grained sandstone; N3 silty shale	None
1192	1193		106-1441	N3	Silty shale		None
1193	1194		106-1441	N4; N3	Siltstone and silty shale	N4 siltstone; N3 silty shale	None
1194	1195		106-1441	N2, 5YR 2/1	Shale		None
1195	1196		106-1442	N5; N3	Siltstone and silty shale	N5 siltstone; N3 silty shale	None
1196	1197		106-1442	N4; N2, 5YR 2/1	Siltstone and shale	N4 siltstone; N2, 5YR 2/1 shale	None
1197	1198		106-1442	N4; N3	Siltstone and silty shale	N4 siltstone; N3 Silty shale	None
1198	1199		106-1442	N4; N3	Siltstone and silty shale	N4 siltstone; N3 silty shale	None
1199	1200		106-1442	N4; N3	Siltstone and silty shale	N4 siltstone; N3 silty shale	None
1200	1201		106-1442	N4- N5; N3	Siltstone and silty shale	N4-N5 siltstone; n3 silty shale	None
1201	1202		106-1443	N3- N4	Siltstone		None
1202	1203		106-1443	N4; N3	Siltstone and silty shale	N4 siltstone; N3 silty shale	None
1203	1204		106-1443	N4- N5; N3	Siltstone and silty shale	N4-N5 siltstone; N3 silty shale	None

1204	1205		106-1443	N4- N5	Siltstone		None
1205	1206		106-1444	N4; N6	Siltstone and very fine grained sandstone	N4 siltstone; N6 very fine grained sandstone	None
1206	1207		106-1444	N4- N5	Siltstone		None
1207	1208		106-1444	N4- N5; N6	Siltstone and very fine to fine grained sandstone	N4-N5 siltstone; N6 very fine to fine grained sandstone	None
1208	1209		106-1444	N4; N6	Siltstone and very fine grained sandstone	N4 siltstone; N6 very fine grained sandstone	None
1209	1210		106-1444	N4- N5; N3	Siltstone and silty shale	N4-N5 siltstone; N3 silty shale	None
1210	1211		106-1445	N4	Siltstone		None
1211	1212		106-1445	N4; N3	Siltstone and silty shale	N4 siltstone; N3 silty shale	None
1212	1213		106-1445	N4; N3	Siltstone and silty shale	N4 siltstone; N3 silty shale	None
1213	1214		106-1445	N4; N3; N5	Siltstone, silty shale and very fine grained sandstone	N4 siltstone; N3 silty shale; N5 very fine grained sandstone	None
1214	1215		106-1445	N4; N3; N5	Siltstone, silty shale and very fine grained sandstone	N4 siltstone; N3 silty shale; N5 very fine grained sandstone	None
1215	1216		106-1445	N4- N5; 5YR2/1	Siltstone and shale	N4- N5 siltstone; 5YR 2/1 shale	None

1216	1217		106-1446	N4; N3	Siltstone and silty shale	Calcite crystal; N4 siltstone; N3 silty shale	None
1217	1218		106-1446	N4- N5; N3	Siltstone and silty shale	N4-N5 siltstone; N3 silty shale	None
1218	1219		106-1446	N4; N3	Siltstone and silty shale	N4 siltstone; N3 silty shale	None
1219	1220		106-1446	N4; N3	Siltstone and silty shale	N4 siltstone; N3 silty shale	None
1220	1221		106-1447	N3	Silty shale		None
1221	1222		106-1447	N4; N3	Siltstone and silty shale	N4 siltstone; N3 silty shale	None
1222	1223		106-1447	N4; N3	Siltstone and silty shale	N4 siltstone; N3 silty shale	None
1223	1224		106-1447	N4; N3	Siltstone and silty shale	N4 siltstone; N3 silty shale	None
1224	1225		106-1447	N4; N3	Siltstone and silty shale	N4 siltstone; N3 silty shale	None
1225	1226		106-1448	N4; 5YR 2/1, N2	Siltstone and shale	N4 siltstone; 5YR 2/1, N2 shale	None
1226	1227		106-1448	N4; 5YR 2/1	Siltstone and shale	N4 siltstone; 5YR 2/1 shale	None
1227	1228		106-1448	N4	Siltstone		None
1228	1229		106-1448	N5; N3; N6	Siltstone, silty shale and very fine to fine grained sandstone	N5 siltstone; N3 silty shale; N6 very fine to fine grained sandstone	None
1229	1230		106-1448	N3; N5	Silty shale and very fine grained sandstone	N3 silty shale; N5 very fine grained sandstone	None

1230	1231		106-1448	N3; N6; N5	Silty shale, very fine to fine grained sandstone and very fine grained sandstone	N3 silty shale; N6 very fine to fine grained sandstone; N5 very fine grained sandstone	None
1231	1232		106-1449	N4; N3	Siltstone and silty shale	N4 siltstone; N3 silty shale	None
1232	1233		106-1449	N3; N2; N5	Silty shale, shale and very fine grained sandstone	N3 silty shale; N2 shale; N5 very fine grained sandstone	None
1233	1234		106-1449	N2; N4	Shale and siltstone to very fine grained sandstone	N2 shale; N4 siltstone to very fine grained sandstone	None
1234	1235		106-1449	N6; N4-N5	Very fine to fine grained sandstone and siltstone to very fine grained sandstone	N6 very fine to fine grained sandstone; N4-N5 siltstone to very fine grained sandstone	None
1235	1236		106-1450	N2; N4-N5	Shale and siltstone	N2 shale; N4-N5 siltstone	None
1236	1237		106-1450	5YR 2/1; N3	Shale and silty shale	5YR 2/1 shale; N3 silty shale	None
1237	1238		106-1450	N2, 5YR 2/1; N5	Shale and siltstone	N2, 5YR 2/1 shale; N5 siltstone	None
1238	1239		106-1450	N2, 5YR 2/1; N5	Shale and siltstone	N2, 5YR 2/1 shale; N5 siltstone	None
1239	1240		106-1450	5YR 2/1; N3; N4	Shale, silty shale and siltstone	5YR 2/1 shale; N3 silty shale; N4 siltstone	None
1240	1241		106-1451	N3; N4	Silty shale and siltstone	N3 silty shale; N4 Siltstone	None

1241	1242		106-1451	N1; N4	Shale and siltstone	N1 shale; N4 siltstone	None
1242	1243		106-1451	N3; N4	Silty shale and siltstone	N3 silty shale; N4 siltstone	None
1243	1244		106-1451	5YR 2/1; N3; N4-N5	Shale, silty shale and siltstone	5YR 2/1 shale; N3 silty shale; N4-N5 siltstone	None
1244	1245		106-1451	N6; N5; N4	Very fine to fine grained sandstone, very fine grained sandstone and siltstone	N6 very fine to fine grained sandstone; N5 very fine grained sandstone; N4 siltstone	None
1245	1246		106-1451	5YR 2/1; N4	Shale and siltstone	5YR 2/1 shale; N4 siltstone	None
1246	1247		106-1452	N2, 5YR 2/1; N3	Shale and silty shale	N2, 5YR 2/1 shale; N3 silty shale	None
1247	1248		106-1452	N3; N4	Silty shale and siltstone	N3 silty shale; N4 siltstone	None
1248	1249		106-1452	5YR 2/1; N3; N4	Shale, silty shale and siltstone	5YR 2/1 shale; N3 silty shale; N4 siltstone	None
1249	1250		106-1452	N3; N4	Silty shale and siltstone	N3 silty shale; N4 siltstone	None
1250	1251		106-1453	N3; N4	Silty shale and siltstone	N3 silty shale; N4 siltstone	None
1251	1252		106-1453	N3; N4	Silty shale and siltstone	N3 silty shale; N4 siltstone	None
1252	1253		106-1453	N3; N4	Silty shale and siltstone	N3 silty shale; N4 siltstone	None
1253	1254		106-1453	N2; N3; N4	Shale, silty shale and siltstone	N2 shale; N3 silty shale; N4 siltstone	None

1254	1255		106-1453	N3; N4	Silty shale and siltstone	N3 silty shale; N4 siltstone	None
1255	1256		106-1454	5YR 2/1; N4	Shale and siltstone	5YR 2/1 shale; N4 siltstone	None
1256	1257		106-1454	N6; N4	Very fine grained sandstone and siltstone	N6 very fine grained sandstone; N4 siltstone	None
1257	1258		106-1454	N4-N5	Siltstone		None
1258	1259		106-1454	N5; N3; N2	Very fine grained sandstone, silty shale and shale	N5 very fine grained sandstone; N3 silty shale; N2 shale	None
1259	1260		106-1454	N3; N4	Silty shale and siltstone	N3 silty shale; N4 siltstone	None
1260	1261		106-1454	N3; N4	Silty shale and siltstone	N3 silty shale; N4 siltstone	None
1261	1262		106-1455	N3; N4	Silty shale and siltstone	N3 silty shale; N4 siltstone	None
1262	1263		106-1455	N3; N4	Silty shale and siltstone	Slightly clayey; N3 silty shale; N4 siltstone	None
1263	1264		106-1455	N3; N4	Silty shale and siltstone	Slightly clayey; N3 silty shale; N4 siltstone	None
1264	1265		106-1455	N4	Siltstone		None
1265	1266		106-1456	N3; N4-N5	Silty shale and siltstone	N3 silty shale; N4-N5 siltstone	None
1266	1267		106-1456	N6; N5; N4	Very fine to fine grained sandstone, very fine grained	N6 very fine to fine grained sandstone; N5 very fine grained sandstone; N4 siltstone	None

					sandstone and siltstone		
1267	1268		106-1456	N5- N6; N4- N5	Very fine grained sandstone and siltstone	N5-N6 very fine grained sandstone; N4-N5 siltstone	None
1268	1269		106-1456	N6; N4	Very fine to fine grained sandstone and siltstone	N6 very fine to fine grained sandstone; N4 siltstone	None
1269	1270		106-1456	N4	Siltstone		None
1270	1271		106-1457	N4	Siltstone		None
1271	1272		106-1457	N5- N6; N5	Very fine grained sandstone and siltstone	N5-N6 very fine grained sandstone; N5 siltstone	None
1272	1273		106-1457	N3; N4-N5	Silty shale and siltstone	N3 silty shale; N4-N5 siltstone	None
1273	1274		106-1457	N3; N4-N5	Silty shale and siltstone	N3 silty shale; N4-N5 siltstone	None
1274	1275		106-1457	N3; N4	Silty shale and siltstone	N3 silty shale; N4 siltstone	None
1275	1276		106-1457	N3; N4-N5	Silty shale and siltstone	N3 silty shale; N4-N5 siltstone	None
1276	1277		106-1458	N3; N4	Silty shale and siltstone	N3 silty shale; N4 siltstone	None
1277	1278		106-1458	N4	Siltstone		None
1278	1279		106-1458	N5; N4	Very fine grained sandstone and siltstone	N5 very fine grained sandstone; N4 siltstone	None

1279	1280		106-1458	N3; N2	Silty shale and shale	N3 silty shale; N2 shale	None
1280	1281		106-1459	N4	Siltstone		None
1281	1282		106-1459	N5- N6; N4; N3	Mudstone tuffaceous? Siltstone and silty shale	N5-N6 mudstone tuffaceous? None calcareous, hardness less than 7; N4 siltstone; N3 silty shale	None
1282	1283		106-1459	N4- N5; N3	Very fine grained sandstone and silty shale	N4-N5 very fine grained sandstone; N3 silty shale	None
1283	1284		106-1459	N3; N4	Silty shale and siltstone	N3 silty shale; N4 siltstone	None
1284	1285		106-1459	N3; N5; N4	Silty shale, siltstone to very fine grained sandstone and siltstone	N3 silty shale; N5 siltstone to very fine grained sandstone; N4 siltstone	None
1285	1286		106-1460	N4	Siltstone		None
1286	1287		106-1460	5YR 2/1; N4- N5	Shale and siltstone	5YR 2/1 shale; N4-N5 siltstone	None
1287	1288		106-1460	N3; N4	Silty shale and siltstone	N3 silty shale; N4 siltstone	None
1288	1289		106-1460	N3; N4-N5	Silty shale and siltstone	N3 silty shale; N4-N5 siltstone	None
1289	1290		106-1460	N3; N4	Silty shale and siltstone	N3 silty shale; N4 siltstone	None
1290	1291		106-1460	N3; N4	Silty shale and siltstone	N3 silty shale; N4 siltstone	None

1291	1292		106-1461	N5- N6; N4- N5	Mudstone tuffaceous and siltstone	Slightly clayey; N5-N6 mudstone tuffaceous? N4-N5 siltstone	None
1292	1293		106-1461	N4- N5	Siltstone	Slightly clayey	None
1293	1294		106-1461	N5; N4	Clayey with sparse rock fragments	N5 very fine grained sandstone; N4 Siltstone to very fine grained sandstone	None
1294	1295		106-1461	N4; N4	Siltstone and silty shale	Slightly clayey; N4 siltstone; N4 silty shale	None
1295	1296		106-1463	N6; N3	Very fine grained sandstone and silty shale	N6 very fine grained sandstone; N3 silty shale	None
1296	1297		106-1463	N4- N5	Siltstone	Slightly clayey	None
1297	1298		106-1463	N3; N4-N5	Clayey with sparse rock fragments	N3 silty shale; N4-N5 siltstone	None
1298	1299		106-1463	N3; N5	Silty shale and siltstone to very fine grained sandstone	Slightly clayey; N3 silty shale; N5 siltstone to very fine grained sandstone	None
1299	1300		106-1463	N4	Siltstone		None
1300	1301		106-1464	N4- N5	Siltstone		None
1301	1302		106-1464	N3; N4; N5- N6	Silty shale, siltstone and mudstone tuffaceous?	N3 silty shale; N4 siltstone; N5-N6 mudstone tuffaceous?	None
1302	1303		106-1464	N4; N5; N3	Siltstone, siltstone to very fine grained	Calcite crystal; N4 siltstone; N5 siltstone to very fine	None

					sandstone and silty shale	grained sandstone; N3 silty shale	
1303	1304		106-1464	N5; N6	Very fine grained sandstone and very fine to fine grained sandstone	N5 very fine grained sandstone; N6 very fine to fine grained sandstone	None
1304	1305		106-1464	N4; N5	Siltstone and siltstone to very fine grained sandstone	N4 siltstone; N5 siltstone to very fine grained sandstone	None
1305	1306		106-1464	N5- N6; N5	Very fine grained sandstone and siltstone to very fine grained sandstone	N5-N6 very fine grained sandstone; N5 siltstone to very fine grained sandstone	None
1306	1307		106-1465	N4- N5; N5; N3	Siltstone, siltstone to very fine grained sandstone and silty shale	Calcite crystal; N4-N5 siltstone; N5 siltstone to very fine grained sandstone; N3 silty shale	None
1307	1308		106-1465	N4; N5	Siltstone and siltstone to very fine grained sandstone	N4 siltstone; N5 siltstone to very fine grained sandstone	None
1308	1309		106-1465	N4- N5; N3	Siltstone and silty shale	N4-N5 siltstone; N3 silty shale	None
1309	1310		106-1465	N4; N6; N3	Siltstone, very fine grained sandstone and silty shale	N4 siltstone; N6 very fine grained sandstone; N3 silty shale	None
1310	1311		106-1466	N5; N4	Very fine grained sandstone and siltstone	N5 very fine grained sandstone; N4 siltstone	None

1311	1312		106-1466	N4; N5	Siltstone, siltstone to very fine grained sandstone and silty shale	N4 siltstone; N5 siltstone to very fine grained sandstone; N3 silty shale	None
1312	1313		106-1466	N3; N4	Silty shale and siltstone	Slightly clayey; N3 silty shale; N4 siltstone	None
1313	1314		106-1466	N4; N3	Siltstone and silty shale	N4 siltstone; N3 silty shale	None
1314	1315		106-1466	N4; 5YR 2/1; N3	Siltstone, carbonaceous shale and silty shale	N4 siltstone; 5YR 2/1 carbonaceous shale; N3 silty shale	None
1315	1316		106-1467	N4; N4-N5; N3	Siltstone, siltstone to very fine grained sandstone and silty shale	N4 siltstone; N4-N5 siltstone to very fine grained sandstone; N3 silty shale	None
1316	1317		106-1467	N4; N3	Siltstone and silty shale	N4 siltstone; N3 silty shale	None
1317	1318		106-1467	N4; N5; N3	Siltstone, siltstone to very fine grained sandstone and silty shale	N4 siltstone; N5 siltstone to very fine grained sandstone; N3 silty shale	None
1318	1319		106-1467	N4- N5; N6	Siltstone and siltstone to very fine grained sandstone	N4-N5 siltstone; N6 siltstone to very fine grained sandstone	None
1319	1320		106-1467	N4- N5	Siltstone		None
1320	1321		106-1467	N4; N3	Siltstone and silty shale	N4 siltstone; N3 silty shale	None
1321	1322		106-1468	N4- N5; N3	Siltstone and silty shale	Calcite crystals; N4-N5 siltstone; N3 silty shale	None

1322	1323		106-1468	N4	Siltstone		None
1323	1324		106-1468	N4; N5-N6	Siltstone and siltstone to very fine grained sandstone	N4 siltstone; N5-N6 siltstone to very fine grained sandstone	None
1324	1325		106-1468	N4; N3	Siltstone and silty shale	N4 siltstone; N3 silty shale	None
1325	1326		106-1469	N5; N3	Siltstone to very fine grained sandstone and silty shale	N5 siltstone to very fine grained sandstone; N3 silty shale	None
1326	1327		106-1469	N4; N3	Siltstone and silty shale	N4 siltstone; N3 silty shale	None
1327	1328		106-1469	N4- N5; N3	Siltstone and silty shale	Calcite crystals; N4- N5 siltstone; N3 silty shale	None
1328	1329		106-1469	N4; N3; N2	Siltstone, silty shale and shale	N4 siltstone; N3 silty shale; N2 shale	None
1329	1330		106-1469	N4; N3	Siltstone and silty shale	N4 siltstone; N3 silty shale	None
1330	1331		106-1470	N4; N3	Siltstone and silty shale	N4 siltstone; N3 silty shale	None
1331	1332		106-1470	N5; N3	Siltstone and silty shale	N5 siltstone; N3 silty shale	None
1332	1333		106-1470	N3; N2	Silty shale and shale	N3 silty shale; N2 shale	None
1333	1334		106-1470	N4- N5; N3	Siltstone and silty shale	N4-N5 siltstone; N3 silty shale	None
1334	1335		106-1470	N3; N5; N5- N6	Silty shale, siltstone and very fine grained sandstone	Slightly clayey; N3 silty shale; N5 siltstone; N5-N6 very fine grained sandstone	None

1335	1336		106-1470	N3; N4	Silty shale and siltstone	Slightly clayey; N3 silty shale; N4 siltstone	None
1336	1337		106-1471	N3; 5YR 2/1	Silty shale and shale	Calcite crystals; N3 silty shale; 5YR 2/1 shale	None
1337	1338		106-1471	N4; N2, 5YR 2/1	Siltstone and shale	N4 siltstone; N2, 5YR 2/1 shale	None
1338	1339		106-1471	N4; N2	Siltstone and shale	N4 siltstone; N2 shale	None
1339	1340		106-1471	N3	Silty shale	Calcite crystals	None
1340	1341		106-1472	N3	Silty shale		None
1341	1342		106-1472	N3	Silty shale		None
1342	1343		106-1472	N3	Silty shale		None
1343	1344		106-1472	N3; N4; N6	Silty shale, siltstone and siltstone to very fine grained sandstone	N3 silty shale; N4 siltstone; N6 siltstone to very fine grained sandstone	None
1344	1345		106-1472	N3; N4	Silty shale and siltstone	N3 silty shale; N4 siltstone	None
1345	1346		106-1473	N3; N4-N5	Silty shale and siltstone	N3 silty shale; N4-N5 siltstone	None
1346	1347		106-1473	N3; 5Y 4/1, N4	Silty shale and siltstone	N3 silty shale; 5Y 4/1, N4 siltstone	None
1347	1348		106-1473	N3; N4	Silty shale and siltstone	N3 silty shale; N4 siltstone	None
1348	1349		106-1473	N3; N6; N6	Silty shale, very fine grained sandstone	Calcite crystals; N3 silty shale; N6 very fine grained	None

					and very fine to fine grained sandstone	sandstone; N6 very fine to fine grained sandstone	
1349	1350		106-1473	N3; N4	Silty shale and siltstone	N3 silty shale; N4 siltstone	None
1350	1351		106-1473	N4- N5	Siltstone		None
1351	1352		106-1474	N3; N4	Silty shale and siltstone	Calcite crystals; N3 silty shale; N4 siltstone	None
1352	1353		106-1474	N3; N4	Silty shale and siltstone	N3 silty shale; N4 siltstone	None
1353	1354		106-1474	N3; N4	Silty shale and siltstone	N3 silty shale; N4 siltstone	None
1354	1355		106-1474	N3; N4	Silty shale and siltstone	N3 silty shale; N4 siltstone	None
1355	1356		106-1475	N3; N4	Silty shale and siltstone	N3 silty shale; N4 siltstone	None
1356	1357		106-1475	N3; N4	Silty shale and siltstone	N3 silty shale; N4 siltstone	None
1357	1358		106-1475	N3; N4	Silty shale and siltstone	Calcite crystals; N3 silty shale; N4 siltstone	None
1358	1359		106-1475	N5- N6; N4- N5	Very fine grained sandstone and siltstone	N5-N6 very fine grained sandstone; N4-N5 siltstone	None
1359	1360		106-1475	N5; N4	Very fine grained sandstone and siltstone	N5 very fine grained sandstone; N4 siltstone	None
1360	1361		106-1476	N3; N4	Silty shale and siltstone	N3 silty shale; N4 siltstone	None
1361	1362		106-1476	N3; N4	Silty shale and siltstone	N3 silty shale; N4 siltstone	None

1362	1363		106-1476	N3; N6	Silty shale and very fine to fine grained sandstone	N3 silty shale; N6 very fine to fine grained sandstone	None
1363	1364		106-1476	N3; N4	Silty shale and siltstone	N3 silty shale; N4 siltstone	None
1364	1365		106-1476	N3; N5; N1	Silty shale, siltstone to very fine grained sandstone and carbonaceous shale	N3 silty shale; N5 siltstone to very fine grained sandstone; N1 carbonaceous shale	None
1365	1366		106-1476	N3; N4	Silty shale and siltstone	N3 silty shale; N4 siltstone	None
1366	1367		106-1477	N5; N5	Siltstone to very fine grained sandstone and very fine grained sandstone	N5 siltstone to very fine grained sandstone; N5 very fine grained sandstone	None
1367	1368		106-1477	N3; N5-N6	Silty shale and very fine grained sandstone	N3 silty shale; N5-N6 very fine grained sandstone	None
1368	1369		106-1477	N3; N5	Silty shale and siltstone to very fine grained sandstone	N3 silty shale; N5 siltstone to very fine grained sandstone	None
1369	1370		106-1477	N5; 5YR 2/1	Siltstone and shale	N5 siltstone; 5YR 2/1 shale	None
1370	1371		106-1478	N3; N4	Silty shale and siltstone	N3 silty shale; N4 siltstone	None
1371	1372		106-1478	N3; N5	Silty shale and siltstone	N3 silty shale; N5 siltstone	None
1372	1373		106-1478	N4; 5YR 2/1; N5	Siltstone, shale and siltstone to very fine grained sandstone	N4 siltstone; 5YR 2/1 shale; N5 siltstone to very fine grained sandstone	None

1373	1374		106-1478	N3; 5YR 2/1; N6	Silty shale, shale and siltstone	Slightly clayey; N3 silty shale; 5YR 2/1 shale; N6 siltstone	None
1374	1375		106-1478	N3; N4; N6	Silty shale, siltstone and tuffaceous? Mudstone	N3 silty shale; N4 siltstone; N6 tuffaceous? Mudstone	None
1375	1376		106-1479	N3; N5; N4; 5B 7/1	Silty shale, siltstone to very fine grained sandstone, siltstone and tuffaceous? Mudstone	N3 silty shale; N5 siltstone to very fine grained sandstone; N4 siltstone; 5B 7/1 tuffaceous? Mudstone , soapy texture	None
1376	1377		106-1479	N3; N4; 5B 7/1	Silty shale, siltstone and tuff?	N3 silty shale; N4 siltstone; 5B 7/1tuff? With mudstone clasts	None
1377	1378		106-1479	N3; N4; 5B 7/1	Silty shale, siltstone and tuff?	N3 silty shale; N4 siltstone; 5B 7/1tuff? With mudstone clasts	None
1378	1379		106-1479	N3; N4-N5	Silty shale and siltstone	Calcite crystals; N3 silty shale; N4- N5 siltstone	None
1379	1380		106-1479	N3; N4	Silty shale and siltstone	N3 silty shale; N4 siltstone	None
1380	1381		106-1479	N3; N4	Silty shale and siltstone	N3 silty shale; N4 siltstone	None
1381	1382		106-1480	5YR 2/1; N5- N6; N4	Shale, very fine grained sandstone and siltstone	Calcite crystals; 5YR 2/1 shale; N5-N6 very fine grained sandstone; N4 siltstone	None
1382	1383		106-1480	N5; N4; 5B 7/1	Very fine grained sandstone, siltstone and tuff?	N5 very fine grained sandstone; N4 siltstone; 5B 7/1tuff?	None

1383	1384		106-1480	N5; N4	Very fine grained sandstone and siltstone	N5 very fine grained sandstone; N4 siltstone	None
1384	1385		106-1480	N3; N5-N6	Silty shale and siltstone to very fine grained sandstone	N3 silty shale; N5-N6 siltstone to very fine grained sandstone	None
1385	1386		106-1481	N3; N4-N5	Silty shale and siltstone	N3 silty shale; N4- N5 siltstone	None
1386	1387		106-1481	N4; N3; 5B 7/1, N6	Siltstone, silty shale and tuff?	N4 siltstone; N3 silty shale; 5B 7/1, N6 tuff?	None
1387	1388		106-1481	N6; N5; N3	Very fine to fine grained sandstone, siltstone and silty shale	N6 very fine to fine grained sandstone; N5 siltstone; N3 silty shale	None
1388	1389		106-1481	N6; N4	Siltstone to very fine grained sandstone and siltstone	N6 siltstone to very fine grained sandstone; N4 siltstone	None
1389	1390		106-1481	N3; N4	Silty shale and siltstone	Calcite crystals; N3 silty shale; N4 siltstone	None
1390	1391		106-1482	N3; N4	Silty shale and siltstone	Slightly clayey; N3 silty shale; N4 siltstone	None
1391	1392		106-1482	N3; N5	Silty shale and siltstone	N3 silty shale; N5 siltstone	None
1392	1393		106-1482	N3; N4-N5	Silty shale and siltstone	N3 silty shale; N4-N5 siltstone	None
1393	1394		106-1482	N3; 5YR 2/1; N4	Silty shale, shale and siltstone	Calcite crystals; N3 silty shale; 5YR 2/1 shale; N4 siltstone	None

1394	1395		106-1482	N3; N4	Silty shale and siltstone	N3 silty shale; N4 siltstone	None
1395	1396		106-1482	N3; N2; N4	Silty shale, shale and siltstone	N3 silty shale; N2 shale; N4 siltstone	None
1396	1397		106-1483	N3; N5; N6	Silty shale, siltstone to very fine grained sandstone and very fine to fine grained sandstone	Calcite crystals; N3 silty shale; N5 siltstone to very fine grained; N6 very fine to fine grained sandstone	None
1397	1398		106-1483	N4- N5	Siltstone		None
1398	1399		106-1483	N3; N4-N5	Silty shale and siltstone	Slightly clayey; N3 silty shale; N4-N5 siltstone	None
1399	1400		106-1483	N3; N4-N5	Silty shale and siltstone	Slightly clayey; N3 silty shale; N4-N5 siltstone	None
1400	1401		106-1483	N3; N4-N5	Silty shale and siltstone	Slightly clayey; N3 silty shale; N4-N5 siltstone	None
1401	1402		106-1483	N3; N4	Silty shale and siltstone	Slightly clayey; calcite crystal; N3 silty shale; N4 siltstone	None

Appendix 11: XRD mineralogical results from Laingsburg, Tankwa and Prince Albert outcrops.

Sample	Locality	Calcite	Goethite	Hematite	Plagioclase	Quartz	Chlorite	Kaolinite	Mica	Apatite	Chloitoid/I/S
HM1	Witbergs River, Laingsburg	5	-	-	14	51	20	-	6	-	3
HM2	Witbergs River, Laingsburg	-	-	-	12	46	23	-	12	-	7
HM3	Witbergs River, Laingsburg	-	-	-	11	54	13	-	19	-	4
HM4	Witbergs River, Laingsburg	-	-	-	9	58	22	-	5	-	5
HM5	Witbergs River, Laingsburg	2	-	-	7	52	30	-	6	-	3
HM6	Witbergs River, Laingsburg	-	-	-	4	58	29	-	5	-	4
HM7	Witbergs River, Laingsburg	-	-	-	5	64	15	-	9	-	7
HM8	Witbergs River, Laingsburg	-	-	-	4	77	11	-	5	-	3
HM9	Witbergs River, Laingsburg	-	-	-	3	54	35	-	5	-	3
HM10	Witbergs River, Laingsburg	-	-	-	3	54	37	-	3	-	3
HM11	Witbergs River, Laingsburg	-	-	-	5	41	41	-	8	-	5

HM12	Witbergs River, Laingsburg	-	-	-	9	48	40	-	4	-	-
HM13	Witbergs River, Laingsburg	-	-	-	6	65	16	-	7	-	6
HM14	Witbergs River, Laingsburg	-	-	-	3	55	21	-	11	-	9
HM15	Witbergs River, Laingsburg	8	-	-	-	49	31	-	4	-	7
HM16	Witbergs River, Laingsburg	-	-	-	4	54	31	-	6	-	5
HM17	Witbergs River, Laingsburg	-	-	-	6	63	14	-	9	-	8
HM18	Witbergs River, Laingsburg	-	-	-	5	75	9	-	4	-	6
HM19	Laingsburg	-	-	-	2	82	3	-	5	-	8
HM20	Tankwa	-	-	-	18	44	25	-	8	-	4
HM21	Tankwa	-	-	-	17	57	13	-	6	-	7
HM22	Tankwa	-	-	-	7	60	7	-	15	-	10
HM23	Tankwa	2	-	-	12	56	23	-	4	-	3
HM24	Tankwa	-	-	-	16	53	6	-	15	-	10
HM25	Tankwa	-	-	-	-	38	3	-	6	53	-
HM26	Tankwa	-	-	-	13	68	4	-	8	-	7
HM27	Tankwa	-	-	-	7	71	14	-	4	-	4
HM28	Tankwa	-	-	-	6	84	4	-	2	-	4
HM29	Tankwa	-	-	-	10	74	4	-	6	-	6
HM30	Tankwa	-	-	-	9	80	2	-	3	-	5
HM31	Tankwa	-	-	-	5	74	17	-	2	-	2
HM32	Tankwa	-	-	-	10	60	20	-	4	-	5
HM33	Tankwa	-	46	25	-	16	-	13	-	-	-

HM34	Tankwa	-	-	-	9	71	6	-	5	-	10
HM35	Tankwa	-	-	-	12	55	19	-	6	-	8
HM36	Tankwa	-	-	-	12	64	14	-	5	-	5
HM37	Tankwa	-	-	-	12	60	12	-	8	-	8
HM38	Tankwa	-	-	-	12	68	5	-	8	-	7
HM39	Tankwa	-	-	-	13	67	-	-	12	-	7
HM40	Gamka River, Prince Albert	2	-	-	12	72	5	-	5	-	4
HM41	Gamka River, Prince Albert	-	-	-	6	54	14	-	15	-	11
HM42	Gamka River, Prince Albert	-	-	-	2	73	16	-	5	-	4
HM43	Gamka River, Prince Albert	-	-	-	3	60	27	-	5	-	5
HM44	Gamka River, Prince Albert	-	-	-	-	17	-	-	-	80	3
HM45	Gamka River, Prince Albert	-	-	-	3	69	8	-	10	-	10
HM46	Gamka River, Prince Albert	-	-	-	2	61	16	-	10	-	11
HM47	Gamka River, Prince Albert	12	-	-	-	53	-	4	-	28	-
HM48	Gamka River, Prince Albert	-	-	-	-	68	9	-	-	-	-
HM49	Gamka River, Prince Albert	-	-	-	-	71	17	-	5	-	6
HM50	Gamka River, Prince Albert	-	-	-	-	60	23	-	9	-	8
HM51	Gamka River, Prince Albert	-	-	-	-	60	26	-	8	-	6

HM52	Gamka River, Prince Albert	-	-	-	4	61	23	-	6	-	6
HM53	Gamka River, Prince Albert	15	-	-	-	66	15	-	2	-	2
HM54	Gamka River, Prince Albert	-	-	-	-	56	30	-	6	-	8
HM55	Gamka River, Prince Albert	-	-	-	-	81	6	-	7	-	7
HM56	Gamka River, Prince Albert	95	-	-	-	3	-	-	-	-	-

Appendix 12: XRD mineralogical results from boreholes KZF-01 and KWV-01.

Sample	Locality	Dolomite	Pyrrhotite		Pyrite	Plagioclase	Quartz	Chlorite	Mica	K-Feldspar	Chloitoid/I/S
HM57	Borehole KZF-01	-	-		6	16	44	2	27	-	6
HM58	Borehole KZF-01	88	-		1	-	5	-	3	-	2
HM59	Borehole KZF-01	-	-		11	20	36	2	19	-	11
HM60	Borehole KZF-01	44	-		3	10	15	24	3	-	1
HM61	Borehole KZF-01	-	-		20	-	45	13	19	-	3
HM62	Borehole KZF-01	-	-		25	12	42	6	11	-	4
HM63	Borehole KZF-01	-	-		6	17	36	21	17	-	3
HM64	Borehole KZF-01	-	-		7	18	43	15	12	-	6
HM65	Borehole KZF-01	-	-		-	11	47	23	12	-	7
HM66	Borehole KZF-01	-	-		-	11	50	22	10	-	7
HM67	Borehole KZF-01	-	-		-	12	47	24	11	-	7

HM68	Borehole KZF-01	-	-		-	13	47	19	11	-	10
HM69	Borehole KZF-01	-	-		-	6	59	20	10	-	6
HM70	Borehole KZF-01	-	-		-	13	47	23	11	-	7
HM71	Borehole KZF-01	-	-		-	13	45	19	14	-	10
HM72	Borehole KZF-01	-	-		-	16	43	24	10	-	7
HM73	Borehole KZF-01	-	-		-	11	39	26	15	-	9
HM74	Borehole KZF-01	-	-		-	14	49	15	14	-	8
HM75	Borehole KZF-01	-	-		-	13	44	21	13	-	8
HM76	Borehole KZF-01	-	-		-	10	40	30	12	-	8
HM77	Borehole KZF-01	-	-		-	10	54	25	7	-	4
HM78	Borehole KZF-01	-	-		-	9	46	34	7	-	4
HM79	Borehole KZF-01	-	-		-	14	44	25	12	-	5
HM80	Borehole KZF-01	-	-		-	7	48	34	7	-	4
HM81	Borehole KZF-01	-	-		-	10	37	26	18	-	9
HM82	Borehole KZF-01	-	-		-	6	55	25	11	-	4

HM83	Borehole KZF-01	-	-		-	7	46	30	13	-	4
HM84	Borehole KZF-01	-	-		-	7	44	33	12	-	4
HM85	Borehole KZF-01	-	-		-	6	42	30	12	-	9
HM86	Borehole KZF-01	-	-		-	5	44	33	12	-	6
HM87	Borehole KZF-01	-	-		-	6	44	31	14	-	5
HM88	Borehole KZF-01	-	-		-	6	57	25	9	-	4
HM89	Borehole KZF-01	-	-		-	7	47	30	13	-	3
HM90	Borehole KZF-01	-	-		-	4	39	42	13	-	2
HM91	Borehole KZF-01	-	-		-	9	45	34	11	-	2
HM92	Borehole KZF-01	-	-		-	8	41	33	15	-	3
HM93	Borehole KWV-01	-	10		2	10	37	-	37	-	4
HM94	Borehole KWV-01	-	16		-	4	52	8	18	-	2
HM95	Borehole KWV-01	-	-		-	7	48	28	15	-	3
HM96	Borehole KWV-01	-	-		-	-	38	42	16	-	4
HM97	Borehole KWV-01	-	-		-	-	36	39	21	1	3

HM98	Borehole KWV-01	-	-		-	-	36	42	18	1	3
HM99	Borehole KWV-01	-	-		-	-	40	40	17	-	3
HM100	Borehole KWV-01	-	-		2	-	25	53	18	-	2
HM101	Borehole KWV-01	-	-		-	-	33	48	16	1	1
HM102	Borehole KWV-01	-	-		-	-	35	40	23	-	2
HM103	Borehole KWV-01	-	-		-	-	28	32	38	-	2
HM104	Borehole KWV-01	-	-		-	-	62	16	21	-	1

Appendix 13: XRD mineralogical results from Debruinspoort, Ecca Pass, Pluto's Vale and borehole SA 1/66.

Sample	Locality	Dolomite	Gypsum		Calcite	Plagioclase	Quartz	Kaolinite/ Clinochlore	Ilmenite	Mica	Hematite/ Goethite
HM105	Debruinspoort	-	-		-	21	65	7	-	7	-
HM106	Debruinspoort	-	-		40	-	34	11	-	6	9
HM107	Debruinspoort	-	-		-	-	82	4	-	14	-
HM108	Debruinspoort	-	-		-	-	86	5	-	9	-
HM109	Debruinspoort	-	-		-	-	89	-	-	11	-
HM110	Ecca Pass	-	-		-	-	60	17	-	23	-
HM111	Ecca Pass	-	-		-	-	88	-	-	12	-
HM112	Ecca Pass	-	-		-	-	75	8	-	17	-
HM113	Ecca Pass	-	-		-	-	75	12	-	13	-
HM114	Ecca Pass	-	-		-	-	88	4	-	8	-
HM115	Ecca Pass	-	-		-	-	84	-	-	16	-
HM116	Ecca Pass	-	-		-	45	42	9	-	4	-
HM117	Pluto's Vale	-	-		-	-	71	16	-	13	-
HM118	Pluto's Vale	-	-		-	-	56	30	-	14	-
HM119	Pluto's Vale	-	-		-	-	80	-	-	20	-
HM120	Pluto's Vale	-	-		-	-	71	12	-	17	-
HM121	Pluto's Vale	-	-		-	-	79	7	-	14	-
HM122	Pluto's Vale	-	-		-	-	77	11	-	12	-
HM123	Pluto's Vale	-	-		-	-	79	10	-	11	-
HM124	Pluto's Vale	-	-		-	-	74	12	-	14	-
HM125	Borehole SA 1/66	-	7		3	18	40	12	8	12	-

HM126	Borehole SA 1/66	-	-		2	22	44	12	5	15	-
HM127	Borehole SA 1/66	-	8		4	6	47	18	-	17	-
HM128	Borehole SA 1/66	12	7		13	-	41	13	-	14	-
HM129	Borehole SA 1/66	-	-		28	-	50	10	-	12	-
HM130	Borehole SA 1/66	20	4		3	-	38	22	-	13	-
HM131	Borehole SA 1/66	-	-		-	11	56	16	-	17	-
HM132	Borehole SA 1/66	-	9		-	9	53	14	-	15	-
HM133	Borehole SA 1/66	-	-		-	-	53	35	-	12	-
HM134	Borehole SA 1/66	-	-		-	-	47	31	-	22	-
HM135	Borehole SA 1/66	-	-		-	-	47	35	-	18	-
HM136	Borehole SA 1/66	-	-		-	-	49	30	-	21	-
HM137	Borehole SA 1/66	-	-		-	-	37	40	-	23	-
HM138	Borehole SA 1/66	-	-		-	-	50	29	-	21	-
HM139	Borehole SA 1/66	-	-		-	23	44	24	-	9	-

Appendix 14: Results of major elements (wt%) analysed by XRF spectrometry.

Sample	SiO_2	TiO_2	Al_2O_3	Fe_2O_3 (t)	MnO	MgO	CaO	Na_2O	K_2O	P_2O_5	Cr_2O_3	LOI	H_2O^-
HM1	68.67	0.60	12.19	6.00	0.277	1.77	2.75	1.87	1.82	0.172	0.019	3.99	0.5
HM2	63.38	0.72	16.56	7.81	0.215	2.46	0.36	1.27	3.41	0.145	0.023	3.76	0.96
HM3	61.9	0.69	18.67	7.00	0.128	1.80	0.41	0.75	4.46	0.101	0.014	4.14	1.34
HM4	58.86	0.65	15.63	12.97	0.341	2.49	1.15	1.43	2.03	0.155	0.014	4.45	1.1
HM5	68.57	0.66	12.60	8.45	0.204	1.59	1.17	1.03	2.01	0.242	0.020	3.46	0.54
HM6	72.65	0.30	12.03	8.52	0.121	1.22	0.11	0.39	1.99	0.065	0.008	2.79	0.52
HM7	73.84	0.49	13.65	3.67	0.062	0.80	0.17	0.51	3.21	0.098	0.008	3.07	0.58
HM8	84.43	0.23	8.36	2.89	0.038	0.50	0.07	0.40	1.59	0.058	0.011	1.77	0.39
HM9	70.01	0.36	11.89	10.67	0.122	1.59	0.08	0.35	1.49	0.058	0.008	3.15	0.46
HM10	71.54	0.32	10.73	11.30	0.149	1.60	0.11	0.34	0.98	0.057	0.008	3.01	0.39
HM11	60.84	0.65	17.44	11.65	0.178	1.65	0.16	0.74	2.35	0.102	0.011	4.27	0.96
HM12	35.3	0.13	5.35	27.12	13.25	1.24	4.46	0.19	0.16	1.91	0.003	10.83	1.01
HM13	68.57	0.48	14.23	8.58	0.120	1.40	0.30	0.56	1.99	0.088	0.007	3.83	1.04
HM14	62.41	0.55	16.55	9.66	0.216	1.70	0.85	0.24	2.69	0.194	0.011	4.91	1.12
HM15	54.55	0.33	10.79	18.60	1.53	1.91	3.56	0.11	1.10	0.194	0.007	7.43	0.75
HM16	67.85	0.43	13.48	7.94	0.087	1.78	0.64	0.61	2.15	0.383	0.018	3.63	0.64
HM17	68.22	0.50	14.07	7.64	0.031	1.63	0.17	0.76	2.26	0.124	0.013	4.26	1.07
HM18	66.44	0.43	12.58	10.80	0.089	1.76	0.62	0.26	1.34	0.119	0.010	5.04	1.77
HM19	73.8	0.41	12.33	6.24	0.006	0.50	0.32	0.15	1.65	0.121	0.008	4.43	1.81
HM20	65.69	0.68	15.08	7.03	0.093	2.04	0.71	2.47	2.92	0.169	0.018	3.11	0.45
HM21	65.19	0.60	14.58	9.42	0.081	1.93	0.58	1.35	2.37	0.180	0.017	3.91	1.13
HM22	61.7	0.87	15.90	9.55	0.078	1.80	0.95	0.57	3.33	0.448	0.016	4.85	1.63
HM23	70.18	0.52	11.35	8.42	0.242	1.78	1.24	1.17	1.40	0.237	0.011	3.54	0.44
HM24	62.65	0.88	17.23	7.03	0.063	1.65	0.94	1.32	3.46	0.521	0.016	4.29	1.08
HM25	42.09	0.22	9.15	4.17	0.352	0.73	21.39	0.49	1.74	16.06	0.015	3.87	0.75

HM26	71.28	0.55	13.91	5.43	0.047	1.04	0.31	1.24	2.44	0.090	0.015	3.71	0.86
HM27	78.11	0.25	9.36	6.75	0.052	0.86	0.17	0.70	1.15	0.061	0.014	2.65	0.49
HM28	79.79	0.24	8.15	6.82	0.036	0.54	0.11	0.55	0.90	0.068	0.007	2.91	0.77
HM29	72.29	0.41	12.19	7.46	0.158	0.83	0.24	1.05	1.60	0.084	0.009	3.76	1.01
HM30	77.6	0.39	10.85	4.50	0.026	0.72	0.20	1.08	1.58	0.082	0.011	2.95	0.82
HM31	79.24	0.29	7.63	7.79	0.072	0.74	0.13	0.72	0.53	0.043	0.005	2.86	0.52
HM32	71.72	0.53	13.81	6.31	0.052	0.88	0.33	1.37	1.74	0.125	0.007	3.21	1.12
HM33	14.24	0.11	3.66	58.53	10.24	0.64	1.09	0.25	0.51	1.13	0.007	9.63	1.28
HM34	73.13	0.38	13.56	5.13	0.033	1.06	0.37	0.87	2.07	0.086	0.007	3.43	1.37
HM35	72.45	0.41	13.42	5.88	0.030	1.24	0.23	1.20	2.03	0.087	0.007	3.04	0.93
HM36	76.09	0.36	12.05	4.57	0.024	1.00	0.22	1.22	1.80	0.086	0.007	2.65	0.77
HM37	72.69	0.46	14.69	3.74	0.020	1.04	0.30	1.24	2.68	0.112	0.008	3.10	1.06
HM38	74.67	0.44	12.78	4.31	0.038	1.01	0.23	1.23	2.19	0.111	0.009	3.04	1.03
HM39	75.1	0.43	13.20	3.85	0.028	0.46	0.17	1.46	2.45	0.096	0.011	2.93	0.95
HM40	74.15	0.55	11.91	4.85	0.158	1.02	1.04	1.46	2.12	0.176	0.019	2.74	0.58
HM41	63.33	0.81	17.53	6.97	0.173	1.75	0.49	0.49	4.07	0.171	0.102	4.25	0.77
HM42	82.16	0.28	8.54	4.16	0.092	0.68	0.12	0.29	1.62	0.052	0.032	2.06	0.45
HM43	72.78	0.38	11.46	8.50	0.166	1.25	0.19	0.19	1.89	0.059	0.029	3.02	0.49
HM44	20.99	0.15	3.82	0.94	1.650	0.20	38.13	0.23	0.82	28.28	0.005	4.06	0.3
HM45	69.47	0.45	14.88	3.5	0.136	0.83	2.38	0.19	3.42	1.59	0.014	3.35	0.76
HM46	61.41	0.49	18.01	9.40	0.129	1.69	0.45	0.20	3.28	0.085	0.008	4.99	1.16
HM47	52.28	0.12	3.72	1.90	0.821	0.25	21.67	0.10	0.60	11.89	0.005	6.74	0.36
HM48	65.12	0.49	17.25	6.81	0.091	1.39	0.62	0.26	3.06	0.085	0.024	4.87	1.18
HM49	75.8	0.37	11.44	5.74	0.130	1.02	0.34	0.22	1.76	0.091	0.009	3.23	0.76
HM50	59.07	0.52	14.73	15.80	0.307	2.17	0.42	.08	1.80	0.167	0.013	4.98	0.74
HM51	57.83	0.52	14.94	16.76	0.37	2.36	0.36	0.08	1.7	0.146	0.014	4.99	0.6
HM52	53.98	0.53	14.70	17.20	0.389	2.45	2.22	0.10	1.49	1.39	0.011	5.64	0.81
HM53	61.35	0.16	6.41	8.99	1.30	1.39	9.62	0.01	0.40	0.239	0.008	10.08	0.38
HM54	49.46	0.44	16.43	18.91	0.204	3.16	2.16	0.05	1.44	1.40	0.013	6.38	0.99

HM55	77.39	0.40	11.04	4.60	0.041	0.92	0.24	0.15	1.90	0.124	0.008	3.13	0.77
HM56	5.65	0.02	1.50	0.78	0.510	0.54	50.00	<0.01	0.04	0.027	0.003	40.81	0.26
HM57	62.24	0.62	17.26	3.68	0.010	1.22	0.32	1.77	3.89	0.210	0.030	8.76	0.8
HM58	9.45	0.11	2.88	1.61	0.113	17.43	26.80	0.23	0.47	0.722	0.033	40.09	0.26
HM59	59.82	0.55	17.51	8.03	0.010	0.91	0.27	1.88	3.21	0.184	0.010	7.59	0.77
HM60	25.33	0.24	6.53	12.73	5.390	6.40	16.45	0.17	0.66	0.228	0.017	25.56	0.27
HM61	58.75	0.49	16.06	10.64	0.102	1.05	0.21	1.57	2.94	0.143	0.010	7.96	0.6
HM62	59.59	0.44	12.86	13.12	0.070	0.64	0.17	1.79	2.32	0.100	0.010	8.85	0.5
HM63	61.29	0.67	18.52	6.66	0.031	1.43	0.30	2.27	3.18	0.157	0.010	5.40	0.74
HM64	62.59	0.53	16.45	7.03	0.064	1.28	1.04	2.11	2.75	0.502	0.011	5.39	0.72
HM65	67.86	0.51	17.02	5.32	0.053	1.29	0.22	1.47	2.77	0.106	0.011	3.41	0.79
HM66	69.25	0.56	15.96	4.97	0.053	1.24	0.35	1.36	2.75	0.116	0.011	3.44	0.69
HM67	66.65	0.63	16.74	5.13	0.064	1.48	0.48	1.56	3.00	0.118	0.011	3.97	0.74
HM68	66.11	0.52	18.64	4.40	0.064	1.18	0.45	1.46	3.23	0.128	0.011	3.70	1.04
HM69	72.97	0.49	14.30	4.75	0.064	1.00	0.17	0.87	2.46	0.064	0.011	2.91	0.63
HM70	67.76	0.44	17.16	5.83	0.086	0.98	0.20	1.62	2.53	0.075	0.011	3.26	0.72
HM71	65.76	0.51	19.22	4.71	0.065	0.88	0.27	1.70	3.12	0.140	0.011	3.49	0.84
HM72	65.58	0.65	18.09	6.09	0.096	0.95	0.39	1.89	2.63	0.235	0.011	3.36	0.64
HM73	62.17	0.74	20.54	6.14	0.095	1.06	0.24	1.54	3.36	0.106	0.011	3.96	0.91
HM74	67.13	0.60	17.98	4.89	0.075	0.90	0.18	1.71	2.73	0.086	0.011	3.60	0.69
HM75	66.11	0.72	18.82	4.56	0.074	0.81	0.23	1.87	2.81	0.106	0.011	3.84	0.82
HM76	62.19	0.73	19.86	6.92	0.126	1.16	0.27	1.45	3.00	0.116	0.011	4.18	1.01
HM77	71.02	0.49	14.19	6.49	0.131	0.83	0.16	1.57	1.69	0.076	0.011	3.09	0.53
HM78	67.31	0.71	15.34	8.34	0.192	1.05	0.23	1.43	1.68	0.117	0.011	3.54	0.6
HM79	63.74	0.78	19.41	5.43	0.133	0.71	0.31	2.33	2.50	0.122	0.011	4.05	1.06
HM80	67.48	0.56	13.81	9.60	0.271	1.26	0.49	1.05	1.62	0.097	0.011	3.55	0.42
HM81	62.63	0.69	21.88	4.01	0.094	0.69	0.29	1.90	3.29	0.105	0.010	4.44	1.26
HM82	70.13	0.60	15.05	6.23	0.149	0.88	0.19	0.88	2.34	0.096	0.021	3.42	0.57
HM83	65.67	0.73	16.81	6.64	0.178	1.07	0.23	1.21	2.62	0.115	0.010	4.75	0.59

HM84	64.44	0.71	17.19	6.94	0.285	1.06	0.26	1.12	2.79	0.116	0.011	5.00	0.63
HM85	61.49	0.78	19.47	7.07	0.211	0.97	0.55	0.93	3.46	0.359	0.011	4.63	0.79
HM86	63.2	0.70	18.77	7.20	0.169	0.93	0.28	0.72	3.48	0.148	0.011	4.36	0.73
HM87	63.7	0.69	19.08	6.27	0.126	1.00	0.22	0.76	3.80	0.095	0.011	4.28	0.85
HM88	69.86	0.49	15.23	5.89	0.107	0.97	0.17	0.77	2.92	0.064	0.021	3.47	0.68
HM89	64.16	0.58	17.40	7.99	0.160	1.54	0.23	0.82	3.55	0.085	0.011	3.45	0.72
HM90	60.76	0.73	17.37	9.88	0.205	2.15	0.26	0.76	3.66	0.119	0.022	3.89	0.75
HM91	65.17	0.72	15.09	8.65	0.171	2.36	0.43	1.26	2.71	0.150	0.021	3.21	0.45
HM92	63.43	0.84	16.50	7.98	0.148	2.41	0.48	1.25	3.42	0.191	0.021	3.36	0.56
HM93	48.71	0.71	18.63	10.93	0.223	1.86	3.46	0.35	3.36	0.466	0.010	11.33	0.5
HM94	56.52	0.43	14.27	16.40	0.175	0.94	1.02	0.30	2.67	0.093	0.010	7.12	0.31
HM95	63.76	0.58	17.53	8.14	0.298	1.30	2.49	0.35	2.49	0.128	0.011	2.94	0.3
HM96	61.42	0.62	18.39	10.02	0.235	1.31	0.70	0.15	3.29	0.128	0.011	3.66	0.43
HM97	60.36	0.71	19.04	9.12	0.297	1.39	0.86	0.20	3.79	0.149	0.011	4.01	0.45
HM98	60.4	0.69	18.68	10.15	0.245	1.43	0.64	0.17	3.70	0.160	0.011	3.68	0.42
HM99	60.67	0.71	18.39	10.35	0.223	1.27	0.69	0.14	3.74	0.148	0.011	3.65	0.42
HM100	50.48	0.55	21.84	11.98	0.217	1.29	3.18	0.26	4.20	1.610	0.022	4.11	0.29
HM101	64.07	0.63	16.86	9.81	0.140	1.08	0.64	0.13	3.20	0.097	0.011	3.23	0.23
HM102	59.97	0.54	20.68	8.90	0.097	1.00	0.52	0.18	4.33	0.086	0.011	3.50	0.29
HM103	58.13	0.60	23.99	6.50	0.064	0.79	0.36	0.22	5.48	0.096	0.011	3.70	0.29
HM104	71.54	0.62	15.43	4.73	0.064	0.71	0.43	0.17	3.89	0.064	0.011	2.38	0.31
HM105	67.81	0.65	13.00	5.87	0.259	1.57	2.26	1.09	2.49	0.198	0.023	4.12	0.87
HM106	32.29	0.12	3.71	23.23	7.160	0.92	15.43	0.07	0.20	0.298	0.005	16.13	1.34
HM107	66.42	0.54	16.03	7.97	0.118	0.92	0.36	0.11	2.62	0.096	0.025	4.27	1.75
HM108	68.27	0.49	14.50	8.35	0.152	1.14	0.33	0.12	2.29	0.081	0.007	3.89	1.33
HM109	76.45	0.33	11.11	4.17	0.037	0.77	0.22	0.90	2.14	0.084	0.016	3.26	1.09
HM110	61.52	0.76	18.08	7.15	0.071	1.86	0.92	1.54	3.77	0.209	0.016	3.80	1.24
HM111	67.43	0.57	14.28	8.31	0.045	1.31	1.02	0.12	2.14	0.153	0.011	4.57	2.14
HM112	59.56	0.53	18.82	10.00	0.108	1.05	0.41	0.29	2.83	0.496	0.011	5.45	3.00

HM113	58.66	0.54	16.90	13.16	0.071	1.54	0.45	0.16	2.18	0.396	0.013	5.59	3.20
HM114	71.78	0.43	11.53	8.78	0.042	1.18	0.19	0.06	1.59	0.132	0.012	3.97	1.37
HM115	72.31	0.50	14.67	4.51	0.011	0.73	0.17	0.13	2.44	0.163	0.010	3.98	2.08
HM116	71.06	0.59	12.55	4.31	0.092	1.41	1.68	3.32	1.88	0.169	0.015	2.23	0.40
HM117	63.71	0.75	16.71	6.27	0.185	1.46	1.69	0.66	3.43	0.204	0.017	4.43	1.06
HM118	60.45	0.88	17.25	10.37	0.122	1.34	0.93	0.16	3.51	0.654	0.038	3.89	1.19
HM119	58.12	0.71	19.87	10.09	0.107	1.02	0.15	0.24	4.10	0.152	0.012	4.97	2.34
HM120	62.27	0.63	18.82	8.27	0.088	1.06	0.20	0.18	3.66	0.099	0.009	4.38	1.67
HM121	66.66	0.45	15.62	8.66	0.100	0.92	0.11	0.17	2.76	0.062	0.009	3.99	1.62
HM122	61.74	0.55	17.50	10.54	0.190	1.14	0.22	0.17	2.95	0.069	0.008	4.55	1.82
HM123	64.71	0.60	16.23	8.98	0.154	1.07	0.19	0.20	2.55	0.071	0.011	4.83	1.92
HM124	64.16	0.59	16.74	9.00	0.153	1.13	0.24	0.22	2.67	0.072	0.010	4.72	1.89
HM125	52.37	0.57	15.79	8.10	0.027	1.68	1.52	0.90	3.56	0.479	0.016	14.31	2.48
HM126	55.99	0.57	15.34	7.80	0.030	1.54	1.10	1.11	3.27	0.212	0.017	12.60	1.97
HM127	52.01	0.61	16.65	6.02	0.190	2.99	3.49	0.08	3.77	0.291	0.016	13.45	2.48
HM128	49.83	0.52	13.42	5.95	0.359	3.88	8.31	<0.01	3.06	0.276	0.013	13.59	1.35
HM129	58.88	0.54	14.70	4.75	0.121	1.48	4.76	0.29	3.37	0.154	0.010	10.27	2.54
HM130	46.60	0.42	11.79	4.43	0.132	7.70	9.21	0.29	2.38	0.250	0.008	16.18	1.60
HM131	55.08	0.72	17.33	6.90	0.050	1.41	0.82	0.42	3.81	0.217	0.013	12.63	3.73
HM132	53.02	0.61	15.22	7.40	0.038	1.85	1.39	0.28	3.42	0.248	0.025	16.13	3.92
HM133	64.30	0.57	17.21	7.96	0.175	1.24	0.21	0.42	3.23	0.110	0.010	3.83	0.78
HM134	61.49	0.73	20.81	5.97	0.116	0.96	0.28	0.46	4.32	0.148	0.012	4.18	1.02
HM135	60.97	0.66	17.97	6.11	0.152	1.01	2.44	0.56	3.99	1.460	0.009	4.21	0.89
HM136	60.00	0.95	20.68	6.24	0.131	1.45	0.32	0.56	5.02	0.126	0.013	4.13	1.03
HM137	57.56	0.86	20.28	8.31	0.190	1.78	0.45	0.51	5.02	0.141	0.023	4.38	0.97
HM138	62.65	0.72	18.41	6.41	0.155	1.52	0.60	0.60	4.63	0.184	0.024	3.76	0.97
HM139	66.41	0.71	14.52	5.74	0.225	1.54	2.00	1.39	3.02	0.200	0.017	3.87	0.68

Appendix 15: Results of trace elements (ppm) analysed by XRF spectrometry.

Sample	**Ag**	**As**	**Ba**	**Bi**	**Br**	**Cd**	**Ce**	**Co**	**Cr**	**Cu**	**Ga**	**Ge**	**Hf**	**La**	**Mo**	**Nb**	**Nd**	**Ni**
HM 1	<2	4.8	301	<5	<3	<4	48	7.9	69	73	15	<2	7.2	29	<2	9.9	19	27
HM 2	<2	14	457	<5	<3	<4	68	16	107	23	25	<2	5.6	37	<2	12	23	46
HM 3	<2	39	571	<5	<3	<4	82	12	49	60	25	3	6.7	51	<2	13	38	39
HM 4	<2	<3	352	<5	<3	<4	66	9.3	79	45	20	<2	4.9	38	<2	9.6	31	38
HM 5	<2	<3	321	<5	<3	<4	82	7.8	73	30	15	<2	6.2	35	<2	10	42	27
HM 6	<2	<3	343	<5	<3	<4	59	9.2	12	47	17	<2	5.1	28	<2	7.7	28	20
HM 7	<2	<3	450	<5	<3	<4	72	3.9	28	64	18	<2	5.4	44	<2	11	31	12
HM 8	<2	<3	296	<5	<3	<4	39	2.9	24	36	10	<2	<2	25	<2	6.4	16	8
HM 9	<2	5.4	322	<5	<3	<4	63	14	30	38	16	<2	<2	37	<2	7.4	28	15
HM 10	<2	14	261	<5	<3	<4	56	9.4	30	24	16	<2	<2	29	<2	7.2	22	15
HM 11	<2	42	601	<5	<3	<4	64	26	26	46	24	<2	6.4	36	<2	13	31	26
HM 12	<2	8.8	361	<5	4.4	<4	37	7.2	15	7.3	7	2.1	3.2	25	4.3	2.6	8	11
HM 13	<2	38	595	<5	<3	<4	60	20	22	51	19	<2	2.8	31	<2	8.5	21	22
HM 14	<2	23	622	<5	<3	<4	83	12	42	46	22	<2	3.5	40	2.1	9.8	36	16
HM 15	<2	7.7	555	<5	<3	<4	61	4.2	32	34	16	2.9	13.0	28	4.1	6.3	21	5.7
HM 16	<2	4.0	444	<5	<3	<4	66	<2	30	46	16	<2	2.1	31	<2	9.2	28	6.5
HM 17	<2	204	634	<5	<3	<4	80	15	33	71	19	<2	2.5	41	3.1	12	35	17
HM 18	<2	56	500	<5	<3	<4	90	15	35	43	16	<2	5.3	41	<2	8.2	42	28
HM 19	<2	12	595	<5	<3	<4	76	<2	26	37	17	<2	3.1	33	3.4	9.1	33	8.6
HM 20	<2	15	501	<5	<3	<4	126	20	91	35	19	<2	3.5	58	<2	11	67	47
HM 21	<2	<3	358	<5	<3	<4	67	5.2	60	41	19	<2	2.6	35	<2	9.8	35	34
HM 22	<2	92	458	<5	<3	<4	116	14	77	40	23	2.5	<2	67	<2	14	49	53
HM 23	<2	3.1	340	<5	<3	<4	50	5.3	71	23	14	<2	4.7	29	<2	8.3	26	23
HM 24	<2	47	551	<5	<3	<4	115	26	74	35	25	<2	2.1	59	2.2	16	49	48
HM 25	<2	7.9	679	<5	<3	<4	154	2.7	44	37	14	<2	<2	99	<2	4.9	121	20
HM 26	<2	<3	531	<5	<3	<4	68	7.2	27	63	19	<2	5.6	41	<2	10	35	25

HM 27	<2	<3	372	<5	<3	<4	37	4.9	29	29	13	<2	4.4	22	<2	5	14	22
HM 28	<2	3.3	305	<5	<3	<4	35	6.1	14	38	11	<2	<2	21	<2	5.5	14	21
HM 29	<2	3.5	453	<5	<3	<4	57	6	36	48	17	<2	2.4	30	<2	8.6	30	19
HM 30	2.7	3	1428	<5	<3	<4	45	6	15	36	16	<2	4.7	24	2.3	6.2	19	10
HM 31	<2	<3	240	<5	<3	<4	15	5.4	17	28	11	2	4.9	12	<2	4.6	4.6	12
HM 32	<2	<3	497	<5	<3	<4	84	4	19	47	18	<2	2.1	43	<2	14	36	11
HM 33	<2	<3	2215	10	<3	<4	48	7.5	7.9	<5	<2	<2	<2	34	2.2	<2	<2	<4
HM 34	<2	4.4	550	<5	<3	<4	44	2.3	19	32	19	<2	5.5	27	<2	12	23	5.8
HM 35	<2	4.6	605	<5	<3	<4	68	2.3	19	40	18	2	<2	39	<2	9.6	33	13
HM 36	<2	13	477	<5	<3	<4	91	3.3	20	35	16	2.1	<2	48	<2	9.1	42	11
HM 37	<2	22	569	<5	<3	<4	69	5.2	34	36	20	<2	6.3	38	<2	14	32	13
HM 38	2.5	117	447	<5	<3	<4	65	12	27	41	18	2.1	6.5	35	<2	9.3	34	24
HM 39	<2	14	464	<5	<3	<4	57	<2	28	21	18	<2	<2	28	<2	9.1	24	<4
HM 40	<2	3.2	356	<5	<3	<4	83	8.1	41	20	15	<2	6.9	43	<2	8.1	29	17
HM 41	<2	8	566	<5	<3	<4	84	19	68	44	25	<2	4.2	42	<2	13	40	58
HM 42	<2	<3	343	<5	<3	<4	46	7.5	18	32	12	<2	<2	29	<2	7	17	12
HM 43	<2	<3	509	<5	<3	<4	60	10	21	36	16	<2	<2	34	<2	8.7	26	18
HM 44	<2	5.5	859	<5	<3	<4	370	<2	16	9	5.4	<2	<2	123	5.4	2.2	340	6.8
HM 45	<2	12	593	<5	<3	<4	107	6.7	17	26	20	2.3	4.5	54	<2	13	47	13
HM 46	<2	7.5	655	<5	4.3	<4	82	9.8	21	29	25	2.3	3.4	36	<2	14	35	22
HM 47	2.9	12	703	<5	<3	<4	95	6.4	18	7.6	4.8	<2	<2	48	2.9	3	55	6.1
HM 48	<2	6.6	745	<5	<3	<4	87	5.7	19	53	24	<2	5.2	46	<2	12	36	15
HM 49	<2	<3	591	<5	3	<4	89	3	18	28	16	2.2	2.0	48	<2	7.4	38	5.1
HM 50	<2	<3	462	<5	<3	<4	42	8	35	62	20	<2	4.3	23	<2	8.3	13	14
HM 51	<2	10	424	<5	<3	<4	73	14	42	34	20	<2	6.1	40	<2	8.6	27	19
HM 52	<2	44	298	<5	<3	<4	101	23	38	59	17	2.5	8.0	41	2.1	8.3	45	21
HM 53	<2	34	316	<5	<3	<4	29	12	19	17	8.6	<2	9.1	14	<2	3.6	16	12
HM 54	<2	<3	462	<5	<3	<4	109	5	34	49	20	2.3	7.5	42	3.9	8.6	63	14
HM 55	<2	73	663	<5	<3	<4	111	10	22	49	16	<2	2.6	55	<2	8.2	43	13

HM 56	<2	<3	136	<5	<3	<4	30	<2	3.2	<5	<2	<2	<2	30	<2	<2	12	<4
HM57	<2	24	700	<5	<3	<4	76	18	44	48	25	<2	6.3	40	5.8	13	32	37
HM58	<2	5.3	202	<5	<3	<4	13	<2	6.8	<5	4.3	<2	3.1	14	12	<2	6.0	<4
HM59	2.2	28	994	<5	<3	<4	108	5.5	20	48	27	<2	13	60	8.6	16	46	6.0
HM60	<2	126	253	<5	<3	<4	25	4.2	23	11	8.8	<2	6.0	24	47	5.7	5.2	10
HM61	<2	375	872	<5	<3	<4	119	10	40	73	23	2.0	12	64	12	12	53	19
HM62	<2	151	666	<5	<3	<4	84	10	36	50	17	<2	8.9	51	<2	11	41	18
HM63	<2	105	798	<5	<3	<4	96	9.8	47	62	25	<2	10	51	3.2	12	47	21
HM64	<2	100	780	<5	<3	<4	86	10	32	41	21	2.2	9.8	55	3.1	10	49	13
HM65	<2	4.7	676	<5	<3	<4	91	2.8	19	46	22	2.0	10	47	<2	12	38	10
HM66	<2	<3	658	<5	<3	<4	71	4.1	37	64	23	2.5	10	37	<2	12	30	10
HM67	<2	36	686	<5	<3	<4	93	13	46	54	23	<2	11	44	<2	12	42	21
HM68	<2	6.7	825	<5	<3	<4	105	4.3	17	37	25	2.3	13	55	<2	23	43	9.0
HM69	<2	18	634	<5	<3	<4	63	19	30	34	19	3.0	7.2	32	<2	11	27	22
HM70	<2	3.2	702	<5	<3	<4	100	3.7	18	39	25	2.8	13	45	<2	20	43	4.5
HM71	<2	3.8	807	<5	<3	<4	141	2.7	18	42	26	2.8	13	75	<2	16	61	5.1
HM72	<2	7.1	692	<5	<3	<4	96	14	24	39	24	2.2	10	50	<2	15	46	13
HM73	<2	4.0	908	<5	<3	<4	73	4.4	26	34	28	<2	9.9	36	<2	14	31	10
HM74	<2	<3	744	<5	<3	<4	85	2.2	25	38	24	<2	10	48	<2	13	38	8.2
HM75	<2	8.7	784	<5	<3	<4	96	5.3	29	41	23	2.2	8.9	49	<2	15	41	8.5
HM76	<2	6.7	851	<5	<3	<4	100	6.8	34	45	28	3.4	13	43	<2	15	44	12
HM77	<2	<3	499	<5	<3	<4	74	4.5	23	44	19	2.8	10	42	<2	12	30	9.5
HM78	<2	5.5	528	<5	<3	<4	68	11	27	50	20	3.1	11	37	3.0	10	33	17
HM79	<2	41	708	<5	<3	<4	91	22	26	66	24	<2	12	50	6.4	13	40	20
HM80	<2	9.7	437	<5	<3	<4	63	8.2	28	43	19	2.8	9.3	30	<2	9.4	31	13
HM81	<2	8.2	871	<5	<3	<4	110	6.8	33	68	29	2.1	12.0	60	3.5	17	49	11
HM82	<2	36	608	<5	<3	<4	83	13	28	51	20	<2	9.2	49	<2	12	38	27
HM83	<2	12	666	<5	<3	<4	93	12	45	66	23	2.6	12	57	2.8	14	45	24
HM84	<2	5.8	694	<5	<3	<4	100	12	44	63	24	3.8	14	50	3.6	15	46	31

HM85	<2	12	817	<5	<3	<4	130	12	31	56	25	2.4	12	73	3.6	14	67	27
HM86	<2	71	787	<5	<3	<4	96	28	33	66	25	2.6	13	54	3.8	15	44	44
HM87	<2	<3	752	<5	<3	<4	91	7.9	35	74	23	3.4	11	54	3.6	15	44	23
HM88	<2	4.7	559	<5	<3	<4	74	7.2	33	59	20	<2	9.2	47	4.9	12	29	24
HM89	<2	17	641	<5	<3	<4	72	10	58	38	24	<2	6.8	42	<2	10	33	34
HM90	<2	18	622	<5	<3	<4	67	12	83	49	24	<2	9.9	34	<2	11	26	44
HM91	<2	12	489	<5	<3	<4	50	14	83	17	22	<2	6.2	31	<2	12	20	35
HM92	<2	9.3	593	<5	<3	<4	91	14	94	35	25	<2	9.4	43	<2	13	34	35
HM93	<2	<3	834	<5	<3	<4	93	11	63	37	25	2.2	6.9	45	6.5	13	38	40
HM94	<2	80	629	<5	<3	<4	69	15	30	58	18	2.9	13	42	24	9.2	24	31
HM95	<2	9.7	643	<5	<3	<4	106	6.9	36	45	23	2.0	12	53	<2	12	47	12
HM96	2.0	18	594	<5	<3	<4	86	12	44	57	24	2.4	10	45	<2	11	43	15
HM97	<2	43	613	<5	<3	<4	89	27	53	64	25	2.7	9.2	45	2	11	41	31
HM98	<2	43	562	<5	<3	<4	85	22	52	54	25	<2	7.6	39	<2	11	41	23
HM99	<2	69	616	<5	<3	<4	76	54	45	62	25	<2	8.7	34	<2	12	32	54
HM100	<2	<3	695	<5	<3	<4	168	14	26	68	26	2.5	13	80	<2	12	91	18
HM101	<2	<3	517	<5	<3	<4	91	12	37	64	21	2.7	8.7	48	<2	11	40	17
HM102	<2	<3	772	<5	<3	<4	104	9.7	24	87	26	2.7	12	61	5.7	17	36	16
HM103	2.1	<3	776	<5	<3	<4	95	9.1	18	77	30	2.7	16	41	3.3	19	46	22
HM104	<2	<3	428	<5	<3	<4	104	9.6	38	59	19	2.6	13	67	<2	9.8	49	25
HM105	<3	4.2	428	<2	<2	<3	68	9.9	55	20	18	<2	<6	43	<2	11	40	31
HM106	<3	4.9	140	<2	<2	<3	13	8.1	13	9.5	3.4	<2	<6	10	2.8	4.4	<3	9.3
HM107	<3	12	649	2.3	<2	<3	84	12	29	29	21	<2	<6	50	<2	12	40	26
HM108	<3	15	534	2.3	<2	<3	53	12	26	27	20	<2	<6	28	<2	12	24	22
HM109	<3	20	393	<2	<2	<3	87	6.9	14	39	14	<2	<6	50	2.9	13	40	15
HM110	<3	12	631	<2	5.4	<3	58	11	61	34	24	<2	<6	38	2.2	14	36	27
HM111	<3	102	550	<2	3.4	<3	125	12	36	59	21	<2	<6	64	2.7	13	61	25
HM112	<3	27	798	2	2.1	<3	137	8.4	32	93	24	<2	8.9	72	<2	14	69	13
HM113	<3	28	540	2.9	2.5	<3	123	10	46	66	21	<2	<6	64	<2	13	61	26

HM114	<3	60	435	<2	2.1	<3	77	9.2	27	57	17	<2	<6	41	2.2	13	35	15
HM115	<3	64	669	<2	2.9	<3	113	3.3	28	63	19	<2	6.9	67	<2	13	46	18
HM116	<3	<4	361	<2	<2	<3	69	8.8	59	15	16	<2	7.8	40	<2	11	35	25
HM117	<3	13	572	<2	<2	<3	48	18	66	37	23	<2	6.8	22	2.3	14	28	44
HM118	<3	<4	657	<2	<2	<3	115	11	61	71	24	2	<6	65	<2	16	59	25
HM119	<3	<4	754	<2	<2	<3	92	9.9	42	21	29	2.4	6.6	49	<2	16	47	34
HM120	<3	<4	711	<2	<2	<3	101	12	29	31	23	<2	7.2	47	<2	17	50	19
HM121	<3	<4	671	<2	<2	<3	63	8.8	16	20	23	<2	8	31	<2	16	24	16
HM122	<3	<4	660	2.3	<2	<3	54	11	20	49	22	<2	<6	33	<2	15	17	15
HM123	<3	15	636	<2	3.4	<3	70	14	37	50	19	<2	<6	36	6.4	11	34	24
HM124	<3	11	631	<2	<2	<3	70	16	37	40	20	<2	6.4	42	2.3	12	36	21
HM 125	<3	23	659	<2	2.5	<3	45	5.8	39	43	22	<2	6	22	9.7	13	26	17
HM 126	<3	22	630	<2	<2	<3	45	5.7	41	43	23	<2	<6	19	6.7	14	22	17
HM 127	<3	28	767	<2	2.1	<3	39	11	47	34	22	<2	<6	20	6.7	13	18	22
HM 128	<3	31	681	<2	2.1	<3	28	9.7	38	37	19	<2	<6	21	4.4	11	14	27
HM 129	<3	27	670	<2	2	<3	36	4.1	38	36	21	<2	<6	18	6.6	14	15	14
HM 130	<3	13	545	<2	<2	<3	25	6.8	31	27	17	<2	<6	17	22	11	10	14
HM 131	<3	17	727	<2	<2	<3	45	13	44	51	24	<2	6.4	32	5.2	17	20	22
HM 132	<3	41	641	<2	<2	<3	31	11	45	48	21	<2	<6	18	23	14	16	25
HM 133	<3	13	786	<2	<2	<3	30	21	31	34	23	<2	<6	26	2.1	17	11	28
HM 134	<3	11	1019	<2	<2	<3	47	11	33	50	25	<2	<6	29	<2	19	22	17
HM 135	<3	15	792	<2	<2	<3	70	12	34	56	25	<2	<6	49	<2	17	42	24
HM 136	<3	14	832	<2	<2	<3	93	11	51	43	27	<2	8	49	<2	19	48	26
HM 137	<3	16	821	<2	<2	<3	47	16	81	43	28	<2	<6	30	<2	15	23	39
HM 138	<3	<4	818	<2	<2	<3	68	8.5	62	62	25	<2	<6	37	<2	15	32	31
HM 139	<3	<4	536	<2	<2	<3	69	9.7	76	18	20	<2	<6	38	<2	13	38	33

Appendix 16: Results of trace elements (ppm) analysed by XRF spectrometry (continued).

Sample	Pb	Rb	Sb	Sc	Se	Sm	Sn	Sr	Ta	Th	Tl	U	V	W	Y	Yb	Zn	Zr
HM1	21	79	<2	12	<2	<2	<3	114	<2	13	<4	3.5	81	<4	29	<4	77	241
HM2	20	150	<2	13	<2	<2	3.6	43	<2	19	<4	3.9	110	<4	19	<4	100	110
HM3	27	196	<2	15	<2	5.8	5	43	<2	21	<4	6.1	89	4.7	32	<4	118	187
HM4	12	85	<2	8.8	<2	<2	4.9	65	<2	14	<4	3.2	79	<4	23	<4	186	140
HM5	7.7	85	<2	9.6	<2	2.1	3.6	48	2.4	15	<4	2.8	76	<4	33	<4	139	183
HM6	16	81	<2	7.9	<2	<2	<3	27	<2	10	<4	4.2	41	<4	52	4.2	146	122
HM7	17	125	<2	11	<2	6.2	<3	36	<2	15	<4	4.2	55	<4	32	<4	57	164
HM8	9.1	67	<2	5.3	<2	<2	<3	30	<2	8.9	<4	2.3	30	<4	14	<4	36	76
HM9	13	66	<2	8.4	<2	<2	4.3	35	<2	11	<4	3.5	56	<4	26	<4	67	110
HM10	14	50	<2	7.3	<2	<2	5.3	40	<2	12	<4	<2	39	<4	21	<4	87	120
HM11	42	121	2.6	15	<2	<2	7.8	62	2.2	15	<4	4	94	4.9	30	<4	113	170
HM12	12	3.1	<2	8.3	<2	38	10	454	<2	5.5	<4	3.7	66	<4	37	<4	48	43
HM13	42	104	2.2	12	<2	<2	3.9	70	<2	15	<4	3.7	93	<4	25	<4	45	140
HM14	33	138	<2	14	<2	<2	4.6	74	<2	17	<4	3.8	152	<4	28	5.1	171	141
HM15	8.6	52	<2	12	<2	<2	4.9	117	2.8	11	<4	2.9	139	6.3	38	<4	101	153
HM16	6.1	99	<2	9	<2	<2	3.6	57	2.2	14	<4	5.1	103	<4	22	<4	44	120
HM17	73	110	<2	12	<2	3.8	3.1	73	<2	14	<4	5.5	106	4.4	26	<4	53	147
HM18	54	64	<2	9.7	<2	<2	3.6	76	2.6	14	<4	6	109	5.8	48	4.2	87	149
HM19	8.5	84	<2	9.1	<2	<2	<3	124	<2	13	<4	6.8	83	<4	23	<4	35	138
HM20	35	117	<2	13	<2	16	3.5	85	<2	17	<4	5.6	101	<4	32	<4	101	143
HM21	14	99	<2	9.7	<2	<2	4.4	67	<2	16	<4	4.7	87	<4	25	<4	148	107
HM22	28	152	<2	14	<2	3.3	5.0	49	<2	28	<4	5.9	114	4.9	26	<4	118	108
HM23	10	56	<2	8.6	<2	<2	3.3	53	<2	12	<4	2.6	65	<4	19	<4	103	137
HM24	33	148	<2	15	<2	<2	4	82	<2	30	<4	5.2	127	4.6	33	<4	160	106
HM25	6	79	<2	17	<2	45	4.7	798	<2	11	<4	8.8	53	7.7	166	6.5	68	37
HM26	18	100	<2	12	<2	2.3	3.6	84	2.1	12	<4	3.9	63	4.1	29	<4	84	143

HM27	16	50	<2	6.1	<2	<2	<3	45	5	7.7	<4	2.7	37	<4	19	<4	55	86
HM28	16	37	<2	5.6	<2	<2	<3	39	<2	7.1	<4	2.9	34	<4	22	<4	69	80
HM29	12	73	<2	8.9	<2	3.4	4.9	78	<2	13	<4	3.6	57	<4	27	<4	61	136
HM30	11	69	<2	9.3	<2	<2	<3	87	<2	11	<4	2.1	60	<4	22	<4	61	119
HM31	7.1	23	<2	6.6	<2	<2	<3	34	<2	7.7	<4	<2	45	<4	7.4	<4	88	83
HM32	5.4	89	<2	9.4	<2	2.6	<3	98	<2	14	<4	4.4	63	<4	23	<4	96	169
HM33	28	17	<2	6.1	2.1	<2	13	941	<2	5	<4	7.3	52	<4	27	<4	165	53
HM34	16	116	<2	8.8	<2	<2	3.8	50	2.1	18	<4	3.8	53	4.6	32	<4	68	163
HM35	11	109	<2	11	<2	<2	<3	65	<2	12	<4	3.7	60	<4	31	<4	88	138
HM36	22	98	<2	8.2	<2	2.6	<3	65	<2	14	<4	4	54	<4	25	<4	91	123
HM37	25	152	<2	10	<2	4.3	3.3	63	<2	15	<4	7.9	92	<4	34	4.4	39	161
HM38	71	117	<2	8.7	<2	5.1	<3	59	<2	15	<4	6	82	4	30	<4	61	149
HM39	13	125	<2	8.1	<2	8.2	3.3	95	<2	12	<4	3.4	77	4	23	<4	31	109
HM40	12	100	<2	9	<2	7.4	<3	45	<2	9.7	<4	<2	58	<4	25	<4	63	235
HM41	14	189	<2	13	<2	7.9	3.4	43	<2	21	<4	2.6	100	<4	28	<4	95	171
HM42	14	74	<2	4.8	<2	4.6	<3	28	<2	9	<4	<2	36	<4	18	<4	79	88
HM43	12	91	<2	9	<2	<2	<3	37	<2	13	<4	2.6	51	<4	21	<4	115	121
HM44	128	41	<2	14	<2	162	5.4	1086	<2	2.9	<4	19	36	14	489	10	60	62
HM45	44	164	<2	12	<2	13	3.2	102	<2	18	<4	4.7	45	4.5	60	4.9	56	202
HM46	23	159	<2	14	<2	3.9	5.5	92	<2	22	<4	6	61	4.2	33	<4	99	197
HM47	46	29	<2	11	<2	20	<3	616	<2	5.2	<4	3.5	16	7.1	104	<4	28	51
HM48	25	148	<2	12	<2	3.7	6.8	105	<2	15	<4	4.4	72	<4	35	4.3	94	200
HM49	20	93	<2	6.3	<2	4.9	<3	109	<2	11	<4	3.1	64	<4	24	<4	83	132
HM50	19	90	<2	11	<2	<2	5.7	82	<2	13	<4	2.9	89	4.2	14	4.7	158	120
HM51	9.8	77	<2	12	<2	<2	5.4	96	<2	13	<4	2.6	118	5.5	15	<4	99	115
HM52	39	61	<2	13	<2	<2	6.2	121	2.3	15	<4	4.3	149	8.9	33	<4	90	125
HM53	13	18	<2	13	<2	8.4	<3	184	<2	4.8	<4	3.3	91	5.7	62	<4	58	175
HM54	8.2	63	<2	13	<2	<2	6.5	117	<2	18	<4	5.4	147	6.4	53	<4	119	143
HM55	63	103	<2	9.4	<2	4	<3	113	<2	12	<4	2.8	79	4.6	24	<4	52	132

HM56	<2	8.9	<2	<3	<2	3.5	4.1	3343	<2	6.1	<4	13	<2	<4	17	<4	7.1	19
HM57	48	196	<2	11	<2	3.6	<3	136	<2	19	<4	4.2	88	5.1	26	<4	106	131
HM58	<2	30	<2	<3	<2	<2	<3	1556	<2	4.7	<4	5.4	31	<4	5	<4	12	57
HM59	49	158	<2	14	<2	<2	4.4	153	<2	24	<4	8.0	64	<4	39	<4	73	201
HM60	12	35	<2	5.9	<2	6.8	6.6	463	<2	7.4	<4	5.9	91	7.9	17	<4	32	100
HM61	60	153	3.9	10	<2	<2	6.4	111	<2	19	<4	7.8	110	6.5	28	<4	88	152
HM62	38	121	<2	8	<2	<2	5.0	92	<2	17	<4	5.4	90	<4	24	<4	52	109
HM63	38	168	<2	14	<2	<2	3.2	135	<2	23	<4	7.3	130	5.3	34	<4	91	168
HM64	22	138	2.7	12	<2	13	5.3	169	<2	21	<4	6.7	100	<4	49	<4	87	153
HM65	18	155	<2	12	<2	8.3	<3	146	<2	21	<4	7.1	69	<4	36	<4	53	177
HM66	14	161	<2	13	<2	8.0	<3	130	<2	18	<4	5.8	94	<4	32	<4	39	173
HM67	53	169	<2	17	<2	4.0	<3	140	<2	20	<4	4.3	144	6.7	41	<4	38	207
HM68	28	183	<2	12	<2	12	5.0	187	<2	28	<4	7.8	60	<4	56	6.4	78	291
HM69	8	154	<2	10	<2	2.3	<3	115	<2	15	<4	2.5	68	<4	29	<4	42	157
HM70	15	144	<2	13	<2	5.6	5.3	155	<2	29	<4	6.7	74	4.4	43	<4	65	214
HM71	13	171	<2	17	<2	11	5.5	185	<2	24	<4	7.0	76	6.5	70	5.0	47	284
HM72	14	152	<2	15	<2	5.3	4.7	156	<2	20	<4	6.1	82	4.6	47	<4	114	229
HM73	9.3	192	<2	15	<2	<2	3.7	178	2.6	25	<4	5.7	95	<4	36	<4	42	222
HM74	27	154	<2	12	<2	10	3.4	158	<2	20	<4	5.2	75	4.5	35	<4	77	210
HM75	21	160	<2	14	<2	7.2	4.1	181	2.9	21	<4	5.8	96	5.9	39	<4	55	228
HM76	27	175	<2	15	<2	4	4.9	205	2.5	24	<4	6.3	101	7.6	40	4.4	84	225
HM77	17	90	<2	9.9	<2	<2	<3	132	<2	15	<4	3.5	65	4.1	34	<4	40	160
HM78	21	92	<2	12	<2	3.7	<3	144	<2	16	<4	4	90	<4	33	<4	81	177
HM79	26	122	3.1	15	<2	5.9	4.6	241	<2	22	<4	6.2	93	6	46	4.5	54	238
HM80	21	80	<2	11	<2	<2	<3	103	<2	14	<4	2.8	80	<4	32	<4	56	147
HM81	26	163	<2	15	<2	12	4.0	257	<2	28	<4	7.1	88	4.4	39	<4	76	277
HM82	18	121	<2	13	<2	<2	3.2	123	<2	16	<4	4.1	72	4.3	36	<4	50	170
HM83	25	127	<2	14	<2	4.1	4.7	128	<2	19	<4	6.1	95	<4	45	<4	100	212
HM84	28	130	<2	14	<2	<2	4.1	127	<2	21	<4	5.0	90	5	44	<4	105	215

HM85	31	143	<2	15	<2	9.9	4.9	146	<2	19	<4	6.0	87	<4	60	7.6	132	295
HM86	38	145	<2	16	<2	5.7	4.5	136	<2	21	<4	5.2	89	6.4	56	4.2	112	227
HM87	40	159	<2	16	<2	4.8	3.5	127	<2	20	<4	5.9	89	7.8	47	4.1	125	222
HM88	30	120	<2	9.7	<2	2.6	3.5	100	<2	20	<4	6.9	53	<4	31	<4	72	163
HM89	19	159	<2	13	<2	<2	4.9	104	<2	19	<4	4.9	90	<4	28	<4	51	138
HM90	18	164	<2	14	<2	<2	4.1	101	<2	23	<4	4.7	110	<4	12	<4	111	98
HM91	20	127	<2	11	<2	<2	3.8	77	<2	21	<4	2.4	100	<4	17	<4	90	115
HM92	20	163	<2	15	<2	<2	5.0	90	<2	25	<4	3.8	124	<4	23	<4	87	130
HM93	35	191	<2	15	<2	<2	5.0	246	<2	21	5.8	5.9	125	4.9	33	<4	153	141
HM94	35	140	3.8	12	3.1	<2	4.5	187	<2	18	<4	10	116	<4	27	<4	92	151
HM95	29	140	<2	13	<2	3.8	<3	283	<2	24	<4	8.7	128	4.9	37	4.2	86	191
HM96	27	176	2.6	15	<2	<2	5.3	158	<2	21	<4	3.7	165	<4	34	<4	91	165
HM97	30	186	<2	18	<2	4.4	5.2	117	<2	21	<4	4.9	173	4.3	37	<4	102	175
HM98	31	184	<2	16	<2	<2	5.9	97	<2	19	<4	3.8	157	<4	33	<4	92	151
HM99	22	187	5.3	14	<2	<2	7.1	95	<2	19	<4	3.4	132	<4	29	<4	105	167
HM100	34	200	<2	14	<2	4.2	7.8	194	<2	44	<4	22	97	6.9	84	<4	126	234
HM101	23	152	<2	17	<2	<2	6.5	84	<2	18	<4	2.8	113	<4	36	<4	108	177
HM102	77	224	<2	15	<2	<2	7.3	129	<2	28	<4	8.5	79	5.9	44	4.7	102	233
HM103	34	307	<2	14	<2	<2	6.1	186	<2	39	<4	18	87	6.4	51	4.8	96	349
HM104	12	230	<2	8.7	<2	7.5	<3	75	<2	15	<4	3.6	64	<4	23	<4	83	261
HM105	22	101	<3	13	<2	5.3	3.9	71	<3	12	2.1	<2	76	<4	35	<4	77	225
HM106	9	3.6	<3	12	2.7	<5	7.7	419	4.9	6.5	3.7	3.3	44	<4	21	<4	194	107
HM107	39	136	<3	15.0	<2	<5	4.7	85	<3	15	<2	5.3	100	<4	34	6.2	90	186
HM108	18	117	<3	14	<2	<5	3.8	73	<3	15	<2	3.9	69	<4	24	<4	88	182
HM109	27	92	<3	8.7	<2	9.4	4.4	76	<3	13	<2	5.5	35	<4	31	<4	96	173
HM110	30	175	<3	17	<2	<5	6.6	92	<3	18	<2	3.4	109	<4	30	<4	128	143
HM111	51	118	<3	16	2.1	10	4.3	88	<3	18	2	8.7	140	4.8	37	<4	87	194
HM112	56	150	<3	16	2.6	18	5.1	510	<3	22	2.5	16	115	4.2	51	<4	75	195
HM113	12	118	3.9	17	4.9	19	6.2	184	<3	19	<2	6	186	<4	57	7.6	93	170

HM114	39	87	3.6	12	3.2	<5	3.8	55	<3	14	<2	8.6	111	4.4	30	<4	91	160
HM115	41	138	<3	11	3.3	8.6	3.8	106	<3	19	<2	6.8	93	<4	29	<4	27	161
HM116	22	79	<3	11	<2	<5	<3	153	<3	12	<2	2.1	68	<4	29	<4	59	241
HM117	78	150	<3	16.0	<2	7	5	48	<3	17	2.7	6.4	96	<4	37	<4	125	224
HM118	20	175	<3	16	<2	9.6	6.1	36	<3	24	<2	5.8	86	4.8	50	<4	102	158
HM119	<3	208	<3	16	<2	12	6.9	25	5.5	22	<2	4.8	85	<4	47	<4	107	244
HM120	4.5	183	<3	14.0	<2	9.3	5.3	48	<3	20	<2	4.8	60	4.6	42	4.3	144	222
HM121	7.8	136	<3	14	<2	<5	5.8	33	<3	18	<2	4.2	54	<4	29	<4	118	166
HM122	51	155	<3	14.0	<2	<5	7.1	43	<3	22	<2	3.4	68	<4	29	<4	148	221
HM123	18	133	<3	15	<2	<5	3.1	63	<3	16	2.6	3.4	122	4	31	<4	92	159
HM124	15	143	<3	14.0	<2	<5	5.2	68	<3	18	<2	3.9	117	<4	30	4.1	118	178
HM125	44	170	<3	15	3.8	9	5.5	187	4.6	17	2.4	4.6	95	<4	30	<4	1584	164
HM126	47	163	<3	15	2.6	5.4	5.5	200	<3	18	<2	4.9	97	<4	27	<4	626	151
HM127	27	180	<3	17.0	<2	<5	6	233	<3	19	<2	5	107	<4	25	<4	342	139
HM128	31	147	<3	16	<2	<5	4.8	401	<3	14	<2	3.3	94	<4	22	<4	167	108
HM129	42	169	<3	14.0	2.2	<5	4.3	309	<3	16	<2	4.6	85	5	34	4.8	212	159
HM130	27	117	<3	14	2.1	<5	3.7	463	<3	12	<2	4.1	80	<4	25	<4	195	122
HM131	45	189	3.3	15	2	<5	7.6	131	<3	19	<2	7.7	100	<4	39	<4	409	199
HM132	48	176	4.0	13	3.1	5.1	3.7	145	<3	17	2.4	4.3	104	<4	25	<4	409	136
HM133	15	162	3.2	15	<2	<5	5.5	109	<3	19	<2	5.6	87	<4	35	<4	76	207
HM134	26	203	<3	17	<2	<5	6.3	139	3.5	24	<2	8.2	88	6.6	48	4.7	108	273
HM135	24	183	<3	18	<2	7.4	5.4	191	<3	17	<2	6.2	82	4.4	54	6.5	83	231
HM136	23	223	<3	18	<2	8.1	6.5	129	<3	22	<2	8	108	4	44	<4	127	243
HM137	25	236	<3	19.0	<2	<5	6.1	113	<3	24	<2	5.3	138	<4	24	4	85	153
HM138	36	230	<3	15	<2	<5	4.9	124	<3	21	<2	3.8	95	<4	32	<4	112	201
HM139	19	142	<3	14	<2	7.2	3.2	122	3.8	15	<2	<2	89	<4	28	<4	75	221

Appendix 17: Geochemical proxies taken from the Prince Albert outcrop, Ecca Pass, Debruinspoort, Pluto's Vale, Laingsburg, Tankwa, and boreholes KZF-01, KWV-01 and SA 1/66. WHF= Whitehill Formation, PAF= Prince Albert Formation, DWY= Dwyka Group.

Locality	Stratigraphy	Sample	SiO_2/Al_2O_3	CIA	P_2O_5/Al_2O_3	Sr/Cu	V/(V+Ni)	V/CR	Rb/K
Laingsburg outcrop	WHF	19	5.99	85.33	0.01	3.35	0.91	3.19	0.0061
Laingsburg outcrop	PAF	18	5.28	85.00	0.01	1.77	0.80	3.11	0.0058
Laingsburg outcrop	PAF	17	4.85	81.52	0.01	1.03	0.86	3.21	0.0059
Laingsburg outcrop	PAF	16	5.03	79.86	0.03	1.24	0.94	3.43	0.0055
Laingsburg outcrop	PAF	15	5.06	69.34	0.02	3.44	0.96	4.34	0.0057
Laingsburg outcrop	PAF	14	3.77	81.41	0.01	1.61	0.90	3.62	0.0062
Laingsburg outcrop	PAF	13	4.82	83.31	0.01	1.37	0.81	4.23	0.0063
Laingsburg outcrop	PAF	12	6.60	52.66	0.36	62.19	0.86	4.40	0.0023
Laingsburg outcrop	PAF	11	3.49	84.29	0.01	1.35	0.78	3.62	0.0062
Laingsburg outcrop	PAF	10	6.67	88.24	0.01	1.67	0.72	1.30	0.0061
Laingsburg outcrop	PAF	9	5.89	86.10	0.00	0.92	0.79	1.87	0.0053
Laingsburg outcrop	PAF	8	10.10	80.23	0.01	0.83	0.79	1.25	0.0051

Laingsburg outcrop	PAF	7	5.41	77.82	0.01	0.56	0.82	1.96	0.0047
Laingsburg outcrop	PAF	6	6.04	82.85	0.01	0.57	0.67	3.42	0.0049
Laingsburg outcrop	PAF	5	5.44	74.96	0.02	1.60	0.74	1.04	0.0051
Laingsburg outcrop	PAF	4	3.77	77.22	0.01	1.44	0.68	1.00	0.0050
Laingsburg outcrop	PAF	3	3.32	76.86	0.01	0.72	0.70	1.82	0.0053
Laingsburg outcrop	PAF	2	3.83	76.67	0.01	1.87	0.71	1.03	0.0053
Laingsburg outcrop	DWY	1	5.63	65.43	0.01	1.56	0.75	1.17	0.0052
Tankwa outcrop	WHF	39	5.69	76.39	0.01	4.52	0.95	2.75	0.0061
Tankwa outcrop	PAF	38	5.84	77.78	0.01	1.44	0.77	3.04	0.0064
Tankwa outcrop	PAF	37	4.95	77.68	0.01	1.75	0.88	2.71	0.0068
Tankwa outcrop	PAF	36	6.31	78.81	0.01	1.86	0.83	2.70	0.0066
Tankwa outcrop	PAF	35	5.40	79.50	0.01	1.63	0.82	3.16	0.0065
Tankwa outcrop	PAF	34	5.39	80.38	0.01	1.56	0.90	2.79	0.0068
Tankwa outcrop	PAF	33	3.89	66.42	0.31	188.20	0.93	6.58	0.0040
Tankwa outcrop	PAF	32	5.19	80.06	0.01	2.09	0.85	3.32	0.0062

Tankwa outcrop	PAF	31	10.39	84.68	0.01	1.21	0.79	2.65	0.0052
Tankwa outcrop	PAF	30	7.15	79.14	0.01	2.42	0.86	4.00	0.0053
Tankwa outcrop	PAF	29	5.93	80.84	0.01	1.63	0.75	1.58	0.0055
Tankwa outcrop	PAF	28	9.79	83.93	0.01	1.03	0.62	2.43	0.0050
Tankwa outcrop	PAF	27	8.35	82.25	0.01	1.55	0.63	1.28	0.0052
Tankwa outcrop	PAF	26	5.12	77.71	0.01	1.33	0.72	2.33	0.0049
Tankwa outcrop	PAF	25	4.60	27.92	1.76	21.57	0.73	1.20	0.0055
Tankwa outcrop	PAF	24	3.64	75.08	0.03	2.34	0.73	1.72	0.0052
Tankwa outcrop	PAF	23	6.18	74.87	0.02	2.30	0.74	0.92	0.0048
Tankwa outcrop	PAF	22	3.88	76.63	0.03	1.23	0.68	1.48	0.0055
Tankwa outcrop	PAF	21	4.47	77.22	0.01	1.63	0.72	1.45	0.0050
Tankwa outcrop	DWY	20	4.36	71.20	0.01	2.43	0.68	1.11	0.0048
Prince Albert outcrop	WHF	56	3.77	2.91	0.02	668.60	0.33	0.63	0.0268
Prince Albert outcrop	PAF	55	7.01	82.82	0.01	2.31	0.86	3.59	0.0065
Prince Albert outcrop	PAF	54	3.01	81.82	0.09	2.39	0.91	4.32	0.0053

Prince Albert outcrop	PAF	53	9.57	38.99	0.04	10.82	0.88	4.79	0.0054
Prince Albert outcrop	PAF	52	3.67	79.42	0.09	2.05	0.88	3.92	0.0049
Prince Albert outcrop	PAF	51	3.87	87.47	0.01	2.82	0.86	2.81	0.0055
Prince Albert outcrop	PAF	50	4.01	86.49	0.01	1.32	0.86	2.54	0.0060
Prince Albert outcrop	PAF	49	6.63	83.14	0.01	3.89	0.93	3.56	0.0064
Prince Albert outcrop	PAF	48	3.78	81.41	0.00	1.98	0.83	3.79	0.0058
Prince Albert outcrop	PAF	47	14.05	14.26	3.20	81.05	0.72	0.89	0.0058
Prince Albert outcrop	PAF	46	3.41	82.09	0.00	3.17	0.73	2.90	0.0058
Prince Albert outcrop	PAF	45	4.67	71.30	0.11	3.92	0.78	2.65	0.0058
Prince Albert outcrop	PAF	44	5.49	8.88	7.40	120.67	0.84	2.25	0.0060
Prince Albert outcrop	PAF	43	6.35	83.47	0.01	1.03	0.74	2.43	0.0058
Prince Albert outcrop	PAF	42	9.62	80.79	0.01	0.88	0.75	2.00	0.0055
Prince Albert outcrop	PAF	41	3.61	77.64	0.01	0.98	0.63	1.47	0.0056
Prince Albert outcrop	DWY	40	6.23	72.05	0.01	2.25	0.77	1.41	0.0057
Debruinspoort outcrop	WHF	109	6.88	77.31	0.01	1.95	0.70	2.50	0.0052

Debruinspoort outcrop	PAF	108	4.71	84.11	0.01	2.70	0.76	2.65	0.0062
Debruinspoort outcrop	PAF	107	4.14	83.84	0.01	2.93	0.79	3.45	0.0063
Debruinspoort outcrop	PAF	106	8.70	19.11	0.08	44.11	0.83	3.38	0.0022
Debruinspoort outcrop	DWY	105	5.22	69.00	0.02	3.55	0.71	1.38	0.0049
Ecca Pass outcrop	PAF	115	4.93	84.26	0.01	1.68	0.84	3.32	0.0068
Ecca Pass outcrop	PAF	114	6.23	86.24	0.01	0.96	0.88	4.11	0.0066
Ecca Pass outcrop	PAF	113	3.47	85.83	0.02	2.79	0.88	4.04	0.0065
Ecca Pass outcrop	PAF	112	3.16	84.21	0.03	5.48	0.90	3.59	0.0064
Ecca Pass outcrop	PAF	111	4.72	81.32	0.01	1.49	0.85	3.89	0.0066
Ecca Pass outcrop	PAF	110	3.40	74.37	0.01	2.71	0.80	1.79	0.0056
Ecca Pass outcrop	DWY	116	5.66	64.59	0.01	10.20	0.73	1.15	0.0051
Pluto's Vale outcrop	PAF	124	3.83	84.25	0.00	1.70	0.85	3.16	0.0065
Pluto's Vale outcrop	PAF	123	3.99	84.66	0.00	1.26	0.84	3.30	0.0063
Pluto's Vale outcrop	PAF	122	3.53	83.97	0.00	0.88	0.82	3.40	0.0063
Pluto's Vale outcrop	PAF	121	4.27	83.71	0.00	1.65	0.77	3.38	0.0059

Pluto's Vale outcrop	PAF	120	3.31	82.33	0.01	1.55	0.76	2.07	0.0060
Pluto's Vale outcrop	PAF	119	2.93	81.57	0.01	1.19	0.71	2.02	0.0061
Pluto's Vale outcrop	PAF	118	3.50	78.95	0.04	0.51	0.77	1.41	0.0060
Pluto's Vale outcrop	DWY	117	3.81	74.30	0.01	1.30	0.69	1.45	0.0053
Borehole KZF-01	WHF	57	3.61	74.27	0.01	2.83	0.70	2.00	0.0061
Borehole KZF-01	PAF	58	3.28	9.48	0.25	311.20	0.89	4.56	0.0077
Borehole KZF-01	PAF	59	3.42	76.56	0.01	3.19	0.91	3.20	0.0059
Borehole KZF-01	PAF	60	3.88	27.43	0.03	42.09	0.90	3.96	0.0064
Borehole KZF-01	PAF	61	3.66	77.29	0.01	1.52	0.85	2.75	0.0063
Borehole KZF-01	PAF	62	4.63	75.03	0.01	1.84	0.83	2.50	0.0063
Borehole KZF-01	PAF	63	3.31	76.31	0.01	2.18	0.86	2.77	0.0064
Borehole KZF-01	PAF	64	3.80	73.60	0.03	4.12	0.88	3.13	0.0060
Borehole KZF-01	PAF	65	3.99	79.24	0.01	3.17	0.87	3.63	0.0067
Borehole KZF-01	PAF	66	4.34	78.16	0.01	2.03	0.90	2.54	0.0071
Borehole KZF-01	PAF	67	3.98	76.86	0.01	2.59	0.87	3.13	0.0068

Borehole KZF-01	PAF	68	3.55	78.39	0.01	5.05	0.87	3.53	0.0068
Borehole KZF-01	PAF	69	5.10	80.34	0.00	3.38	0.76	2.27	0.0075
Borehole KZF-01	PAF	70	3.95	79.78	0.00	3.97	0.94	4.11	0.0069
Borehole KZF-01	PAF	71	3.42	79.06	0.01	4.40	0.94	4.22	0.0066
Borehole KZF-01	PAF	72	3.63	78.65	0.01	4.00	0.86	3.42	0.0070
Borehole KZF-01	PAF	73	3.03	79.98	0.01	5.24	0.90	3.65	0.0069
Borehole KZF-01	PAF	74	3.73	79.56	0.00	4.16	0.90	3.00	0.0068
Borehole KZF-01	PAF	75	3.51	79.31	0.01	4.41	0.92	3.31	0.0069
Borehole KZF-01	PAF	76	3.13	80.80	0.01	4.56	0.89	2.97	0.0070
Borehole KZF-01	PAF	77	5.00	80.58	0.01	3.00	0.87	2.83	0.0064
Borehole KZF-01	PAF	78	4.39	82.12	0.01	2.88	0.84	3.33	0.0066
Borehole KZF-01	PAF	79	3.28	79.06	0.01	3.65	0.82	3.58	0.0059
Borehole KZF-01	PAF	80	4.89	81.38	0.01	2.40	0.86	2.86	0.0059
Borehole KZF-01	PAF	81	2.86	79.97	0.00	3.78	0.89	2.67	0.0060
Borehole KZF-01	PAF	82	4.66	81.53	0.01	2.41	0.73	2.57	0.0062

Borehole KZF-01	PAF	83	3.91	80.55	0.01	1.94	0.80	2.11	0.0058
Borehole KZF-01	PAF	84	3.75	80.48	0.01	2.02	0.74	2.05	0.0056
Borehole KZF-01	PAF	85	3.16	79.76	0.02	2.61	0.76	2.81	0.0050
Borehole KZF-01	PAF	86	3.37	80.73	0.01	2.06	0.67	2.70	0.0050
Borehole KZF-01	PAF	87	3.34	79.97	0.00	1.72	0.79	2.54	0.0050
Borehole KZF-01	PAF	88	4.59	79.78	0.00	1.69	0.69	1.61	0.0050
Borehole KZF-01	PAF	89	3.69	79.09	0.00	2.74	0.73	1.55	0.0054
Borehole KZF-01	PAF	90	3.50	78.78	0.01	2.06	0.71	1.33	0.0054
Borehole KZF-01	PAF	91	4.32	77.42	0.01	4.53	0.74	1.20	0.0056
Borehole KZF-01	DWY	92	3.84	76.21	0.01	2.57	0.78	1.32	0.0057
Borehole KWV-01	WHF	93	2.61	72.21	0.03	6.65	0.76	1.98	0.0068
Borehole KWV-01	PAF	94	3.96	78.15	0.01	3.22	0.79	3.87	0.0063
Borehole KWV-01	PAF	95	3.64	76.68	0.01	6.29	0.91	3.56	0.0068
Borehole KWV-01	PAF	96	3.34	81.62	0.01	2.77	0.92	3.75	0.0064
Borehole KWV-01	PAF	97	3.17	79.70	0.01	1.83	0.85	3.26	0.0059

Borehole KWV-01	PAF	98	3.23	80.55	0.01	1.80	0.87	3.02	0.0060
Borehole KWV-01	PAF	99	3.30	80.10	0.01	1.53	0.71	2.93	0.0060
Borehole KWV-01	PAF	100	2.31	74.08	0.07	2.85	0.84	3.73	0.0057
Borehole KWV-01	PAF	101	3.80	80.94	0.01	1.31	0.87	3.05	0.0057
Borehole KWV-01	PAF	102	2.90	80.44	0.00	1.48	0.83	3.29	0.0062
Borehole KWV-01	PAF	103	2.42	79.83	0.00	2.42	0.80	4.83	0.0067
Borehole KWV-01	DWY	104	4.64	77.46	0.00	1.27	0.72	1.68	0.0071
Borehole SA1/66	WHF	125	3.32	72.53	0.03	4.35	0.85	2.44	0.0058
Borehole SA1/66	WHF	126	3.65	73.68	0.01	4.65	0.85	2.37	0.0060
Borehole SA1/66	PAF	127	3.12	69.40	0.02	6.85	0.83	2.28	0.0058
Borehole SA1/66	PAF	128	3.71	54.11	0.02	10.84	0.78	2.47	0.0058
Borehole SA1/66	PAF	129	4.01	63.58	0.01	8.58	0.86	2.24	0.0060
Borehole SA1/66	PAF	130	3.95	49.81	0.02	17.15	0.85	2.58	0.0059
Borehole SA1/66	PAF	131	3.18	77.44	0.01	2.57	0.82	2.27	0.0060
Borehole SA1/66	PAF	132	3.48	74.94	0.02	3.02	0.81	2.31	0.0062

Borehole SA1/66	PAF	133	3.74	81.68	0.01	3.21	0.76	2.81	0.0060
Borehole SA1/66	PAF	134	2.95	80.44	0.01	2.78	0.84	2.67	0.0057
Borehole SA1/66	PAF	135	3.39	72.00	0.08	3.41	0.77	2.41	0.0055
Borehole SA1/66	PAF	136	2.90	77.80	0.01	3.00	0.81	2.12	0.0054
Borehole SA1/66	PAF	137	2.84	77.23	0.01	2.63	0.78	1.70	0.0057
Borehole SA1/66	PAF	138	3.40	75.95	0.01	2.00	0.75	1.53	0.0060
Borehole SA1/66	DWY	139	4.57	69.37	0.01	6.78	0.73	1.17	0.0057